

Andrew Jonathan Sheehan

2005

Report Documentation Page				Form Approved OMB No. 0704-0188	
Public reporting burden for the collection of information is estimated to average 1 hour per response, including the time for reviewing instructions, searching existing data sources, gathering and maintaining the data needed, and completing and reviewing the collection of information. Send comments regarding this burden estimate or any other aspect of this collection of information, including suggestions for reducing this burden, to Washington Headquarters Services, Directorate for Information Operations and Reports, 1215 Jefferson Davis Highway, Suite 1204, Arlington VA 22202-4302. Respondents should be aware that notwithstanding any other provision of law, no person shall be subject to a penalty for failing to comply with a collection of information if it does not display a currently valid OMB control number.					
1. REPORT DATE <b>01 DEC 2005</b>		2. REPORT TYPE <b>N/A</b>		3. DATES COVERED <b>-</b>	
4. TITLE AND SUBTITLE <b>Prediction Of Shallow Footing Settlements On Cohesionless Materials From Seismic Testing</b>				5a. CONTRACT NUMBER	
				5b. GRANT NUMBER	
				5c. PROGRAM ELEMENT NUMBER	
6. AUTHOR(S)				5d. PROJECT NUMBER	
				5e. TASK NUMBER	
				5f. WORK UNIT NUMBER	
7. PERFORMING ORGANIZATION NAME(S) AND ADDRESS(ES) <b>The University of Texas at Austin</b>				8. PERFORMING ORGANIZATION REPORT NUMBER	
9. SPONSORING/MONITORING AGENCY NAME(S) AND ADDRESS(ES)				10. SPONSOR/MONITOR'S ACRONYM(S)	
				11. SPONSOR/MONITOR'S REPORT NUMBER(S)	
12. DISTRIBUTION/AVAILABILITY STATEMENT <b>Approved for public release, distribution unlimited</b>					
13. SUPPLEMENTARY NOTES <b>The original document contains color images.</b>					
14. ABSTRACT					
15. SUBJECT TERMS					
16. SECURITY CLASSIFICATION OF:			17. LIMITATION OF ABSTRACT <b>UU</b>	18. NUMBER OF PAGES <b>269</b>	19a. NAME OF RESPONSIBLE PERSON
a. REPORT <b>unclassified</b>	b. ABSTRACT <b>unclassified</b>	c. THIS PAGE <b>unclassified</b>			

**PREDICTION OF SHALLOW FOOTING  
SETTLEMENTS ON COHESIONLESS MATERIALS  
FROM SEISMIC TESTING**

**by**

**Andrew Jonathan Sheehan, B.S.**

**Thesis**

Presented to the Faculty of the Graduate School of  
The University of Texas at Austin  
in Partial Fulfillment  
of the Requirements  
for the Degree of

**Master of Science in Engineering**

**The University of Texas at Austin  
December, 2005**

**PREDICTION OF SHALLOW FOOTING  
SETTLEMENTS ON COHESIONLESS MATERIALS  
FROM SEISMIC TESTING**

**Approved by  
Supervising Committee:**

---

---



## **Acknowledgement**

Many thanks to my wonderful wife who supported and encouraged me throughout this project.

I would like to thank my supervisor Dr. Kenneth H. Stokoe, II for his guidance, advice, and support. His enthusiasm was instrumental to the successful completion of this study.

To the rest of the faculty in the Geotechnical Engineering Department at the University of Texas, I extend my sincere thanks and appreciation for your dedication to the students in this program.

## **Abstract**

# **PREDICTION OF SHALLOW FOOTING SETTLEMENTS ON COHESIONLESS MATERIALS FROM SEISMIC TESTING**

Andrew Jonathan Sheehan, MSE.

The University of Texas at Austin, 2005

Supervisor: Kenneth H. Stokoe, II

The practice of predicting settlements of shallow foundations has evolved in the past 50 years, but the basic principles and obstacles in making such predictions remain the same. First, the engineer must accurately characterize the soil beneath the proposed foundation. Second, the engineer must choose an analytical technique to model the behavior of that soil under the load. Since settlement, rather than bearing capacity, is most often the controlling design factor (Schmertmann, 1970), the accuracy with which an engineer estimates the settlement directly bear on the design and cost of the foundation. The practice of

estimating settlements of shallow footings on cohesionless soils has historically been over-conservative.

The goal of this study is to investigate how well measured soil stiffnesses determined by field and laboratory dynamic tests predict the settlement of a shallow footing on a granular soil. The stiffness, or modulus, of the soil was estimated based on SPT tests, field seismic tests (SASW and crosshole tests), and dynamic laboratory tests (torsional resonant column tests). The moduli from these tests were then used in two different settlement analysis techniques, Schmertmann's method and a finite element analysis, to predict the settlement of the footing and the soil mass beneath it. A series of field load tests were performed and settlements were measured at the top of the footing and at several depths beneath it. These field measurements are compared to the predicted values.

The results indicate that seismic field and dynamic laboratory tests can be effectively used to conduct a site investigation for the purposes of predicting the settlement potential of this shallow footing on the nonplastic sandy silt. Very importantly for working load levels, the seismic-based settlement predictions were more accurate than the SPT-based predictions.

## Table of Contents

List of Tables.....	xii
List of Figures .....	xiv
<b>CHAPTER 1 INTRODUCTION</b>	<b>1</b>
<i>1.1 Problem Significance</i> .....	1
<i>1.2 Research Objectives</i> .....	3
<i>1.3 Thesis Organization</i> .....	3
<b>CHAPTER 2 LITERATURE REVIEW</b>	<b>6</b>
<i>2.1 Introduction</i> .....	6
<i>2.2 Historical and Current Settlement Prediction Methods</i> .....	6
<i>2.3 Case Histories of Settlement Predictions Based on Dynamic Moduli</i> .....	7
<i>2.4 Case Study: Texas A&amp;M Prediction Symposium</i> .....	8
<i>2.5 Back-Analysis Evaluation of In-Situ Dynamic Moduli</i> .....	8
<i>2.6 Summary</i> .....	11
<b>CHAPTER 3 FIELD SITE CONDITIONS</b>	<b>12</b>
<i>3.1 Introduction</i> .....	12
<i>3.2 Site Location</i> .....	12
<i>3.3 Disturbed and Undisturbed Samples</i> .....	14
<i>3.4 Standard Penetration Tests</i> .....	16
<i>3.5 Spectral Analysis of Surface Waves (SASW) Tests</i> .....	18
<i>3.6 Crosshole Seismic Tests</i> .....	20
<i>3.7 Torsional Resonant Column Tests</i> .....	22

3.8 Summary .....	27
<b>CHAPTER 4 EXPERIMENTAL FIELD SET-UP</b>	<b>28</b>
4.1 Introduction .....	28
4.2 Footing Design and Construction .....	28
4.2.1 Construction Details of the Telltales .....	34
4.3 Loading Systems .....	37
4.3.1 Vibroseis Truck (Thumper) .....	38
4.3.2 Vibroseis Truck (T-Rex) .....	39
4.4 Instrumentation .....	40
4.4.1 Linear Potentiometers .....	41
4.4.2 Reference Frame .....	43
4.4.3 Load Cell .....	46
4.4.4 VXI Multi-Channel Analyzer .....	46
4.5 Summary .....	47
<b>CHAPTER 5 FIELD LOAD TESTS</b>	<b>48</b>
5.1 Introduction .....	48
5.2 Field Testing Procedure .....	48
5.3 Measurements .....	51
5.4 History of Testing .....	52
5.5 Loading Sequence .....	53
5.6 Loading Levels .....	54
5.7 Field Test Results .....	56
5.7.1 Tabulated Measured Settlements .....	57
5.7.2 Typical Load-Settlement Curve .....	57
5.7.3 Peak Settlements .....	64

5.7.4 Measured Vertical Strain Distribution .....	67
5.7.5 Comparison of Measured Settlements at Each Depth .....	69
5.8 Summary .....	72
<b>CHAPTER 6 SETTLEMENT PREDICTIONS OF THE CENTER OF THE FOOTING</b>	<b>73</b>
6.1 Introduction .....	73
6.2 Schmertmann's (1970) Settlement Analysis .....	74
6.3 Burland and Burbidge's Settlement Method .....	81
6.4 Settlement Analysis Using Finite Element Code .....	81
6.4.1 Soil Behavior Model .....	82
6.4.2 Finite Element Model Input Parameters .....	83
6.5 Summary .....	94
<b>CHAPTER 7 COMPARISON OF PREDICTED AND MEASURED SETTLEMENTS</b>	<b>95</b>
7.1 Introduction .....	95
7.2 Total Settlement of the Center of the Footing .....	95
7.3 Settlements of the Footing and the Soil Mass .....	96
7.4 Strain Distribution with Depth .....	99
7.5 Simplified Settlement Prediction from SASW Tests .....	101
7.6 Summary .....	102
<b>CHAPTER 8 SUMMARY, CONCLUSIONS AND RECOMMENDATIONS</b>	<b>104</b>
8.1 Summary .....	104
8.2 Conclusions .....	104
8.3 Recommendations .....	105

<b>APPENDIX A FIELD MEASUREMENTS</b>	<b>107</b>
<b>APPENDIX B INSTRUMENT CALIBRATION DATA</b>	<b>171</b>
<b>APPENDIX C SITE CHARACTERIZATION STUDY</b>	<b>202</b>
<b>REFERENCES</b>	<b>250</b>
<b>VITA</b>	<b>253</b>

## List of Tables

Table 2.1 – Factors of Safety $F = Q_f/Q_d$ (measured design load*/predicted design load) [*ultimate with FS = 3] (from Briaud and Gibbens, 1994).....	9
Table 3.1 – USCS Soil Classification of Top 14 ft of Soil Material at Capitol Aggregates Field Site (from Kurtulus, 2006).....	15
Table 3.2 – Summary of Soil Index Properties Determined from Undisturbed Samples (from Kurtulus, 2006).....	15
Table 3.3 – SPT Test Results from Capitol Aggregate Field Site, Dec, 2004 (from Kurtulus, 2006).....	16
Table 3.4 – Tabulated Values of Best-Fit Wave Velocity Profile from SASW Testing at Capitol Aggregates Field Site; SASW-Line A (from Kurtulus, 2006).....	19
Table 3.5 – Tabulated Values of Best-Fit Wave Velocity Profile from SASW Testing at Capitol Aggregates Field Site; SASW-Line B (from Kurtulus, 2006).....	19
Table 3.6 – Summary of Soil Characteristics at the Capitol Aggregates Field Site.....	27
Table 5.1 – History of the Load Tests at the Capitol Aggregates Field Site.....	52
Table 5.2 – Tabulated Results From Field Load Test #3.....	58
Table 5.3 – Measured Vertical Strain Beneath the Footing During Test #3.....	67
Table 6.1 – Schmertmann's Method using SPT Test Data.....	78
Table 6.2 – Schmertmann's Method using SASW Test Data.....	78
Table 6.3 – Schmertmann's Method using Crosshole Test Data.....	79
Table 6.4 – Schmertmann's Method using Resonant Column Test Data.....	79
Table 6.5 – Results of the Finite Element Method Using SPT Test Data.....	86
Table 6.6 – Results of the Finite Element Method Using SASW Test Data.....	86
Table 6.7 – Results of the Finite Element Method Using Crosshole Test Data.....	87



Table 6.8 – Results of the Finite Element Method Using Resonant Column Test Data .....	87
Table 7.1 – Summary of Total-Settlement Predictions for the Center of a 3-ft Diameter Footing Under a Static Load of 20,000 lb .....	96

## List of Figures

Figure 2.1 – Comparison of Stiffness Profiles from Laboratory Tests, Back-Analysis and Seismic Crosshole Surveys at Various Sites on London Clay (Menzies, 2001) .....	10
Figure 3.1 – Location of Capitol Aggregates Field Site in Austin, Texas (from Kurtulus, 2006) .....	13
Figure 3.2 – Plan View of Capitol Aggregates Field Site (after Kurtulus, 2006) .....	13
Figure 3.3 – Picture of Field Site Prior to Construction of the 3-ft Diameter Footing .....	14
Figure 3.4 – Variation of Corrected SPT Blow Count with Depth at Capitol Aggregates Field Site (from Kurtulus, 2006) .....	17
Figure 3.5 – Theoretical Dispersion Curve Fit to the Composite Experimental Dispersion Curve at SASW Line A (from Kurtulus, 2006) .....	18
Figure 3.6 – Shear Wave Velocity Profiles Determined from SASW Testing at Capitol Aggregates Field Site on February 3, 2005 (from Kurtulus, 2006) .....	20
Figure 3.7 – Installed Locations and Depths of Geophones Under 3-ft Diameter Footing at the Capital Aggregates Field Site (from Park, 2007) .....	21
Figure 3.8 – Results of Crosshole Tests Conducted Under the 3-ft Diameter Footing at the Capital Aggregates Field Site in August 2005 (from Park, 2007) .....	22
Figure 3.9 – Variation of Low-Amplitude Shear Wave Velocity with Isotropic Confining Pressure from Resonant Column Tests (from Kurtulus, 2006) .....	23
Figure 3.10 – Variation of Low-Amplitude Shear Wave Velocity with Isotropic Confining Pressure from Resonant Column Tests (from Kurtulus, 2006) .....	24
Figure 3.11 – Comparison of the Variation in Normalized Shear Modulus with Shearing Strain at Isotropic Confining Pressure of 6 psi (0.86 ksf = 41.37 kPa) from the Resonant Column Tests with Modulus Reduction Curves proposed by Seed et al. (1986) and Darendeli (2001) (from Kurtulus, 2006) .....	25

Figure 3.12 – Comparison of the Variation in Normalized Shear Modulus with Shearing Strain at Isotropic Confining Pressure of 24 psi (3.46 ksf = 165.48kPa) from the Resonant Column Tests with Modulus Reduction Curves proposed by Seed et al. (1986) and Darendeli (2001) (from Kurtulus, 2006) .....	26
Figure 4.1 – Design of Reinforced Concrete Footing .....	29
Figure 4.2 – Excavation and Leveling of the Footing Location.....	30
Figure 4.3 – Augering 2-in. boreholes for Telltale Installation .....	30
Figure 4.4 – Footing Excavation After Installation of the Telltales and Geophones .....	32
Figure 4.5 – First Stage of Rebar Cage Installation .....	32
Figure 4.6 – Second Stage of Rebar Cage Installation.....	33
Figure 4.7 – Finished Footing Construction.....	33
Figure 4.8 – Field Site During Footing Curing and Between Test Days .....	34
Figure 4.9 – Detailed Telltale Picture .....	35
Figure 4.10 – Footing Plan View Showing Telltale Locations .....	36
Figure 4.11 – Section A-A from Figure 4.10: Depths of Telltales Beneath the Footing .....	37
Figure 4.12 – Static Vertical Loading Applied to Footing using a Vibroseis System.....	38
Figure 4.13 – Arrangement Used to Load the Footing with Thumper.....	39
Figure 4.14 – Arrangement Used to Load the Footing With the Hydraulic Ram on the Back of T-Rex.....	40
Figure 4.15 – Schematic of Linear Potentiometer.....	41
Figure 4.16 – 2-inch Linear Potentiometer Used in this Study .....	42
Figure 4.17 – Typical Calibration Curve of a Linear Potentiometer for a Calibration Range of 60 to 90% of Full Compression .....	43
Figure 4.18 – Arrangement of Reference Frame and Linear Potentiometers .....	44
Figure 4.19 – Pictures of Linear Potentiometers Supported by the Reference Frame .....	44

Figure 4.20 – Plan View of Reference Frame over Footing and 3-Point Loading Frame .....	45
Figure 4.21 – Arrangement of the Footing Instrumentation and Loading System.....	45
Figure 4.22 – Arrangement of Recording Instruments in the Field .....	46
Figure 5.1 – Typical Load vs. Time Measurement During an Individual Test.....	55
Figure 5.2 – Typical Settlement Measurements During an Individual Test .....	55
Figure 5.3 – Typical Settlement Measurements of the Top of the Footing near the Center .....	60
Figure 5.4 – Typical Settlement Measurements of Telltale at 6 in. Beneath the Center of the Footing.....	60
Figure 5.5 – Typical Settlement Measurements of Telltale at 12 in. Beneath the Center of the Footing.....	61
Figure 5.6 – Typical Settlement Measurements of Telltale at 18 in. Beneath the Center of the Footing.....	61
Figure 5.7 – Typical Settlement Measurements of Telltale at 30 in. Beneath the Center of the Footing.....	62
Figure 5.8 – Comparison of Typical Settlement Measurements of the Surface and the Telltales Beneath the Center of the Footing .....	62
Figure 5.9 – Comparison of Peak Measured Settlements Near the Center of the Footing Under a Static Load of 20,000 lb .....	65
Figure 5.10 – Comparison of Peak Measured Settlements Near the Perimeter of the Footing Under a Static Load of 20,000 lb .....	65
Figure 5.11 – Measured Variation of Vertical Strain with Depth Beneath the Footing .....	67
Figure 5.12 – Measured Settlements of the Top of the Footing for Four Tests .....	70
Figure 5.13 – Measured Settlements at 6 in. Beneath the Footing for Four Tests .....	70
Figure 5.14 – Measured Settlements at 12 in Beneath the Footing for Four Tests.....	71

Figure 5.15 – Measured Settlements at 18 in. Beneath the Footing for Four Tests .....	71
Figure 5.16 – Measured Settlements at 30 in. Beneath the Footing for Four Tests .....	72
Figure 6.1 – Schmertmann’s Zone of Strain Influence for a 3-ft Diameter Footing Under a Uniform Pressure of 2800psf (Schmertmann, 1970) .....	75
Figure 6.2 – Predicted Variation of Settlement with Depth Using Schmertmann’s Method .....	80
Figure 6.3 – Predicted Variation of Vertical Strain with Depth Using Schmertmann’s Method -- (Expanded Scale) .....	80
Figure 6.4 – Deformed Finite Element Mesh Constructed from the SPT Test Data.....	88
Figure 6.5 – Deformed Finite Element Mesh Constructed from the SASW Test Data .....	89
Figure 6.6 – Deformed Finite Element Mesh Constructed from the Crosshole Test Data .....	90
Figure 6.7 – Deformed Finite Element Mesh Constructed from the Resonant Column Test Data.....	91
Figure 6.8 – Finite Element Method- Predicted Variation of Settlement with Depth .....	92
Figure 6.9 – Finite Element Method- Predicted Variation of Settlement with Depth (Expanded Scale).....	92
Figure 6.10 – Finite Element Method- Predicted Variation of Strain with Depth .....	93
Figure 6.11 – Finite Element Method- Predicted Variation of Strain with Depth (Expanded Scale).....	93
Figure 7.1 – Comparison of Measured and Predicted Settlements, Based on Dynamic Moduli Measured in the Field and the Laboratory, Beneath the Footing Under a Static Load of 20,000 lb.....	97
Figure 7.2 – Comparison of Measured and Predicted Settlements, Based on Dynamic Moduli Measured in the Field and the Laboratory, Beneath the Footing Under a Static Load of 20,000 lb. (Expanded Scale) .....	98

Figure 7.3 – Comparison of Calculated and Predicted Strains Beneath the Footing Under a Static Load of 20,000 lb .....	100
Figure 7.4 – Comparison of Calculated and Predicted Strain Beneath the Footing Under a Static Load of 20,000 lb (Expanded Scale) .....	100

# **CHAPTER 1**

## **INTRODUCTION**

### **1.1 PROBLEM SIGNIFICANCE**

In the design of shallow foundations, permissible settlement is often the controlling design criterion. Numerous methods have been developed over the years to estimate the settlement of shallow foundations (Peck et al., 1974, Schmertmann, 1970 and Burland and Burbidge, 1985). These methods all require a certain amount of field and/or laboratory testing to determine the soil parameters required for use in each method. In granular soils (sands, silty sands, silty sands, and gravelly sands), problems associated with sample disturbance have generally caused engineers to use in-situ tests such as the Standard Penetration Test (SPT) or Cone Penetrometer Test (CPT) to estimate the strength parameters of the soil. These strength parameters are then empirically correlated to stiffness parameters based on a history of experimentation, case studies, and laboratory tests.

It should be noted that the stiffness of the soil is strongly influenced by the strain level beneath the foundation, which is not directly considered when implicit or explicit correlations between the strength and stiffness of the material are used. Additionally, parameters such as stress history, degree of saturation, relative density, cementation, etc. can affect the stiffness to different levels than strength. Given the difficulty and cost of obtaining the effects of these parameters on strength-stiffness correlations and the general non-use by the profession of methods to measure directly the soil stiffness in situ, settlement prediction models for shallow foundations have

continued to be based on information commonly measured in the field by large strain penetration tests. The engineer using these models must understand the limitations of the methods and the general tendency to overestimate shallow foundation movement.

In the past few decades, seismic wave velocity measurements have been used to characterize in-situ soil and rock stiffnesses for use in the evaluation of the response of geotechnical sites to earthquake loading and machine vibrations. Some examples of this type of field seismic testing include crosshole, downhole, suspension logging, and spectral analysis of surface waves (SASW) testing methods (Stokoe and Santamarina, 2000). These in situ seismic tests are used to measure the shear wave velocity ( $V_s$ ) of the soil from which one can directly calculate the shear modulus ( $G_{\max}$ ) in the small-strain (linear) range by :

$$G_{\max} = \rho * V_s^2 \quad (1.1)$$

where:  $\rho$  = mass density of the soil.

With a known shear modulus, the value of Young's modulus at small strains ( $E_{\max}$ ) of the soil is obtained from:

$$E_{\max} = 2*(1+\nu)*G_{\max} \quad (1.2)$$

where:  $\nu$  = Poisson's ratio (0.15-0.35 for unsaturated cohesionless soils).

As outlined above, soil stiffness can be directly evaluated in situ. These moduli ( $G_{\max}$  and  $E_{\max}$ ) are the stiffnesses at strains  $< 10^{-3}\%$  where the values are independent of strain amplitude. By contrast, traditional triaxial testing generally results in measurement of the modulus of the soil in the strain range of 0.1% and



greater. It has been shown that the working strain range for many shallow foundations on cohesionless soils is in the strain range of 0.01 to 0.1% (Menzies et al., 2001).

## **1.2. RESEARCH STATEMENT**

The goal of this study is to demonstrate that measured in-situ soil stiffnesses gathered from field and laboratory dynamic testing methods can be used in static applications to predict the settlement of shallow foundations on granular soils. In this study, the granular soil is a predominantly nonplastic sandy silt. Field seismic testing involved the crosshole and SASW testing methods to characterize the stiffness of the sandy silt. Laboratory testing involved the torsional resonant column test. For the purposes of comparison to traditional methods, a site investigation using SPT testing was also conducted. Based on these field and laboratory methods of characterizing the soil, the settlement of a 3-ft diameter concrete footing constructed at the site was predicted. The footing was loaded and unloaded statically over short periods of time (3 to 4 minutes), and settlements of the surface of the footing and at various depths beneath the footing were measured. The measured settlements are then compared to predicted settlements derived from the SPT, seismic field, and dynamic laboratory tests.

## **1.3 THESIS ORGANIZATION**

In Chapter 2, a few case studies are discussed where soil moduli determined by seismic measurements were used to predict the settlement of foundations on granular soils. In some studies, the dynamic moduli were determined with laboratory testing of samples taken from the field. Other studies used dynamic moduli derived from empirical correlations to non-seismic field tests such as SPT or CPT tests. Very

few of these studies were conducted in sands. A more extensive review of similar case histories can be found in Smith, 2004.

In Chapter 3, the material properties of the Capitol Aggregates field site are described. The location of the footing is presented with maps and photos. A summary of the initial site investigation is discussed.

In Chapter 4, the test layout at the Capitol Aggregates field site is described. This description includes the design and installation of the circular footing and the locations and depths of the subsurface instrumentation. Two different loading systems were used to statically load the footing. These loading systems are described and illustrated. Finally, a brief description of the data acquisition hardware and test instrumentation is presented.

In Chapter 5, the field load tests are described. The procedures and loading sequence are described in detail. Settlements measured at the top of the footing and within the soil mass at various depths beneath the footing are presented.

In Chapter 6, the analytical and numerical models used to calculate settlements are presented. Settlements were predicted using two different analytical models and one finite element model. The analytical models used were Schmertmann's method (1970) and the Burland and Burbidge method (1985). The input parameters for the analytical models were derived from traditional SPT testing. The numerical model used was a finite element software package (PLAXIS) in which the soil was modeled with linear soil moduli and the Mohr-Coulomb failure criterion. The input parameters for the numerical analysis were obtained from field seismic testing and dynamic laboratory testing.

In Chapter 7, the predicted settlements are compared to the field measurements. The differences between the models are discussed and the likely sources of error are suggested.

In Chapter 8, the conclusions of this study are presented. Recommendations for further studies are also made.

Appendix A contains a complete set of data gathered in the field during testing on 11 Nov 2005. Three series of five tests were conducted on that day. The data is presented in tabular form for use or evaluation in further studies. Load-settlement curves for each series of tests are presented.

Appendix B contains the calibration curves of the instruments used in the field.

Appendix C contains a copy of the Site Characterization study conducted by Asli Kurtulus which will be published as part of her Ph.D. dissertation in 2006.

## **CHAPTER 2**

### **LITERATURE REVIEW**

#### **2.1 INTRODUCTION**

In this chapter, a brief review of the historical and current practices of predicting settlement is given, followed by a few case studies dealing with granular soils in which “dynamic” moduli were used to predict settlement. A more comprehensive review of similar case studies can be found in Smith, 2004. It is shown that dynamic moduli determined by field seismic testing are more accurate in settlement predictions than stiffness (moduli) estimates based on conventional laboratory test methods such as oedometer or triaxial tests. A case study is presented in which computed stiffnesses from back analyses of ground deformations measured in the field are compared to stiffnesses predicted by in-situ seismic tests and stiffnesses predicted by oedometer tests.

#### **2.2 HISTORICAL AND CURRENT SETTLEMENT PREDICTION METHODS**

The practice of predicting settlements of shallow foundations has evolved in the past 50 years, but the basic principles and obstacles in making such predictions remain the same. First, the engineer must accurately characterize the soil beneath the proposed foundation. Second, the engineer must choose an analytical technique to model the behavior of that soil under the load. Since settlement, rather than bearing capacity, is most often the controlling design factor (Schmertmann, 1970), the accuracy with which an engineer estimates the settlement will bear directly on the design and cost of the foundation.

Characterizing the soil properties is the difficult element in this process and the source of greatest error. In sands, it is extremely difficult and generally very costly to obtain undisturbed samples. Hence, the use of in-situ tests is preferred by most engineers. Many field tests, however, only measure strength or are correlated with strength parameters of the soil rather than the stiffness (modulus), of the soil, even though the material property of interest is stiffness (Menzies, 2001). To obtain the stiffness of the soil, the strength parameters measured by field tests, such as the SPT, CPT or plate load tests, are empirically correlated to the stiffness of the soil. This empirical correlation between the strength and stiffness is the source of the significant error in accurately estimating the settlement of footings on sand.

Several settlement analytical techniques are available, depending on the soil type and the method of characterizing the soil. For sands and other cohesionless materials, the settlement analysis technique proposed by Schmertmann (1970) is among the most commonly used techniques (Briaud and Gibbens, 1994). A numerical model such as a finite element code is another emerging analytical technique. Both of these techniques are discussed further in Chapter 6.

### **2.3 CASE HISTORIES OF SETTLEMENT PREDICTIONS BASED ON DYNAMIC MODULI**

In May 2005, Ryan Smith compiled a review of 41 case histories in which dynamic moduli were used to predict static ground deformations (Smith, 2005). These case histories involved many different types of foundations and soil types. The dynamic moduli were determined by laboratory resonant column tests, in-situ crosshole or downhole tests, or by empirical correlations with penetration tests such as the SPT or CPT. Of these cases, the projects which used field seismic testing to predict foundation and ground movements showed the greatest accuracy when

compared to actual movements in the field. No instances of using spectral-analysis-of-surface-waves (SASW) testing to measure the stiffness used to predict settlement was noted in his review.

#### **2.4 CASE STUDY: TEXAS A&M PREDICTION SYMPOSIUM**

In 1994, ASCE hosted a specialty conference at Texas A&M University (Briaud and Gibbens, 1994). Five, full-scale, reinforced concrete footings of different sizes were constructed on a site composed of medium dense silty sand 11 ft deep. Each footing was loaded to failure and detailed load-settlement measurements were recorded. Thirty-one participants submitted settlement predictions. Three of the 31 participants used dynamic moduli to estimate the settlement of each footing. Table 1 below illustrates the results of the symposium. One participant (#23) used dynamic moduli determined from an empirical correlation to CPT data. The other two (#22 & #28) used dynamic moduli determined from crosshole testing. Both predictors using in situ seismic the crosshole data performed better than the mean of their peers for every footing. Participant #23 outperformed his peers on 3 of the 5 footings. It should also be noted that the mean prediction for each footing ranged from 160-220% of the measured value. This illustrates the over-conservative state of the practice.

#### **2.5 BACK-ANALYSIS EVALUATION OF IN-SITU DYNAMIC MODULI**

As one would expect, the values of stiffness measured by in-situ dynamic tests have been shown to represent the soil conditions much more correctly than stiffnesses estimated from correlations with traditional laboratory and in-situ techniques used today. Laboratory methods such as oedometer and triaxial tests, as well as penetration testing, have been shown to often give poor estimates of stiffness (Burland and Hancock, 1977; Izumi et al., 1997). This concept was illustrated by a

back-analysis study completed in London (Menzies et al., 2001). The ground movements

Table 2.1: Factors of Safety  $F = Q_f/Q_d$  (measured design load\*/predicted design load)  
[\*ultimate with  $FS = 3$ ] (from Briaud and Gibbens, 1994)

No.	Authors	$Q_f/Q_d$ 1m	$Q_f/Q_d$ 1.5m	$Q_f/Q_d$ 2.5m	$Q_f/Q_d$ 3.0m(s)	$Q_f/Q_d$ 3.0m(n)
1	Wiseman	4.66	3.92	2.70	2.39	2.72
2	Poulos	4.66	0.90	2.77	3.23	2.78
3	Siddiquee	29.49	29.31	24.07	22.11	24.70
4	Silvestri	4.81	4.76	4.77	4.67	5.31
5	Horvath	3.16	2.43	2.27	2.00	2.28
6	Thomas	11.42	15.69	7.28	16.53	6.34
7	Surendra	6.53	3.86	4.54	1.93	2.20
8	Chang	11.60	20.40	8.19	7.50	6.15
9	Brahma	4.75	5.13	3.84	5.81	3.39
10	Floess	5.22	4.25	2.77	2.35	2.65
11	Boone	6.87	4.74	3.04	5.14	3.42
12	Cooksey	5.80	5.10	3.38	3.00	3.42
13	Scott	6.14	4.25	2.98	3.00	3.11
14	Townsend	4.31	1.62	2.03	1.67	1.69
15	Foshee	4.11	6.03	5.97	13.74	5.58
16	Mesri	1.88	2.31	2.56	2.71	3.08
17	Ariemma	1.58	2.92	1.89	7.20	1.87
18	Tand	5.44	4.70	3.54	3.06	3.52
19	Funegard	5.44	4.70	3.54	3.06	3.52
20	Deschamps	3.48	3.00	3.94	2.50	2.85
21	Altaee	2.90	3.09	3.74	3.91	4.46
22	Decourt	2.23	2.63	2.59	1.93	2.39
23	Mayne	13.22	8.10	4.14	3.20	3.64
24	Kuo	12.43	10.52	6.09	5.00	5.59
25	Shahrour	6.33	7.56	9.59	5.88	6.70
26	Abid	3.26	3.40	2.73	2.50	3.11
27	Utah State	5.80	4.81	2.89	1.87	2.21
28	Gottardi	4.78	3.25	1.95	1.63	1.88
29	Chua	10.42	10.89	8.83	8.13	9.19
30	Bhowmik	4.75	4.25	3.55	3.21	3.42
31	Diyaljee	8.52	6.47	4.03	3.70	4.26
Mean		6.64	6.29	4.72	4.99	4.43
Standard Deviation		5.23	5.90	4.12	4.63	4.13
Measured Value		3	3	3	3	3

of several major structures in the London area were used to back-calculate the stiffness of the soil below. This back-calculated stiffness was then compared to stiffnesses determined from crosshole field tests and laboratory triaxial and oedometer tests of the same soil. Figure 2.1 illustrates the results. It can be seen that the back-calculated stiffness is approximately an order of magnitude higher than the stiffness measured in

the laboratory. By contrast, stiffness from the crosshole tests are generally above, but much closer to, those values derived through back analysis.

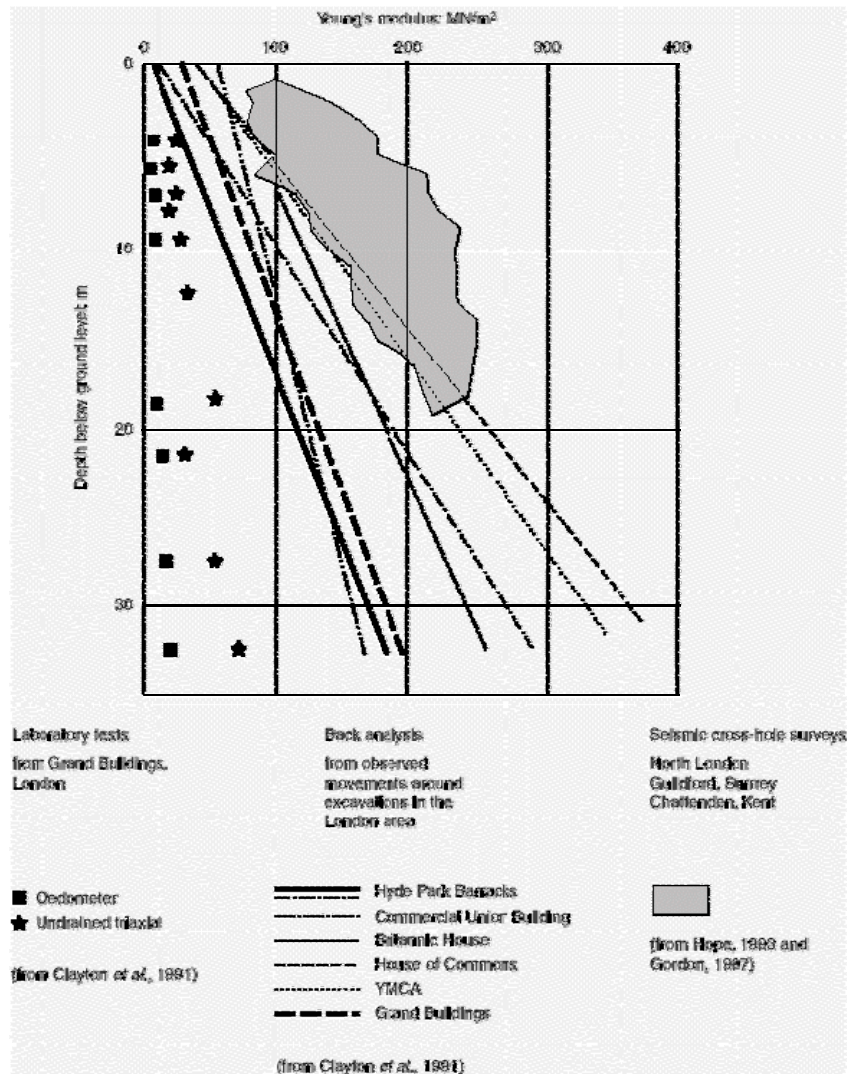


Figure 2.1: Comparison of Stiffness Profiles from Laboratory Tests, Back-Analysis and Seismic Crosshole Surveys at Various Sites on London Clay (Menzies, 2001)



## **2.6 SUMMARY**

Case histories suggest that conventional approaches to settlement prediction over-estimate the ground movement. One significant source of error in this procedure is the mischaracterization of the soil stiffness in situ by traditional field tests such as the SPT and CPT which involve empirical correlations.

Dynamic moduli offer an alternative method to estimating the in-situ stiffness of soil. The use of these moduli obtained from in-situ tests have been shown to reasonably predict the settlement of foundations on sand. It is expected that SASW testing will also yield accurate estimates of the soil stiffness for predicting foundation settlements under working loads.

## **CHAPTER 3**

### **FIELD SITE CONDITIONS**

#### **3.1 INTRODUCTION**

In December 2004 thru February 2005, a detailed site characterization study was performed at the Capital Aggregates field site by Kurtulus, 2006. As part of the study, disturbed and undisturbed samples were collected, two borings with Standard Penetration Tests (SPT) were conducted, and Spectral Analysis of Surface Waves (SASW) seismic tests were performed. In August, 2005, crosshole and downhole seismic tests were conducted by Mr. Kwangsoo Park as part of his Ph.D. dissertation research (Park, 2007). In this chapter, a summary of the results from these studies are presented. The detailed site report can be found in Ms. Asli Kurtulus's Ph.D. dissertation (Kurtulus, 2006).

#### **3.2 SITE LOCATION**

The location of the field site relative to the location of the University of Texas is shown in Figure 3.1. A plan view of the Capitol Aggregates field site is shown in Figure 3.2. In this figure, the location of the footing is shown. In addition, the locations of other small-scale foundations that are being tested on another project are shown. The foundations are four drilled shafts and two bridge bents which are being tested on a project sponsored by the National Science Foundation (Wood et al, 2006). A picture of the test site before the footing was constructed is shown in Figure 3.3.

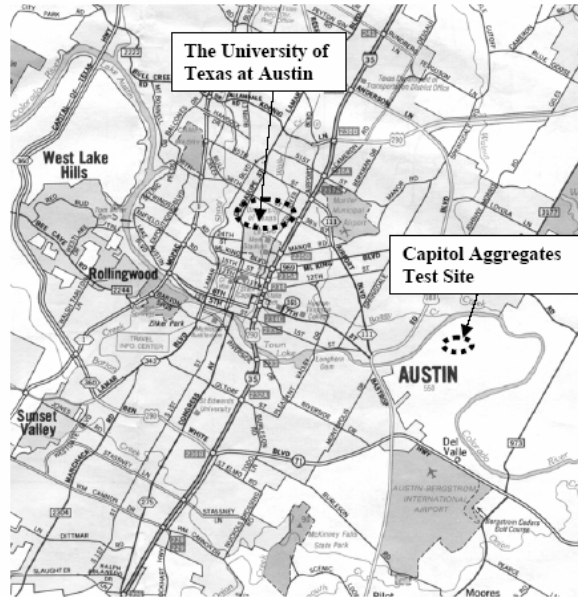


Figure 3.1: Location of Capitol Aggregates Field Site in Austin, Texas (from Kurtulus, 2006)

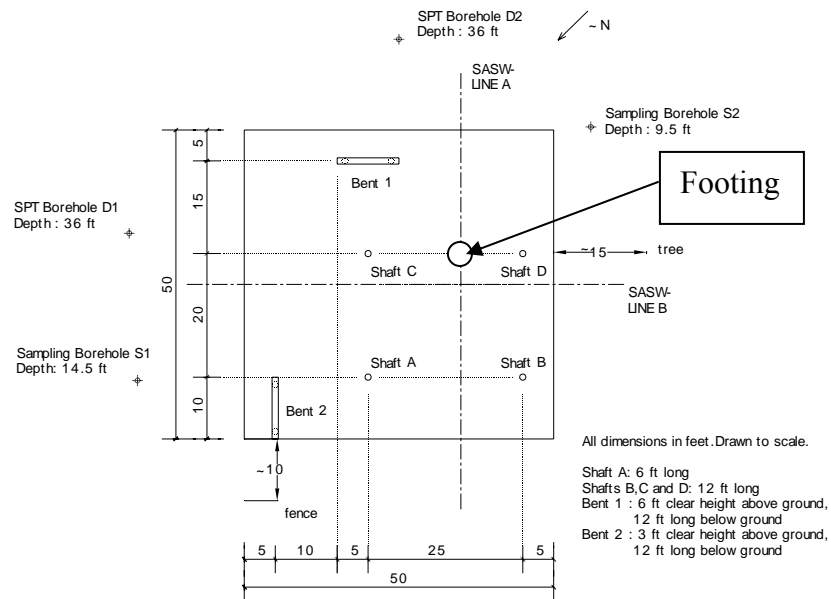


Figure 3.2: Plan View of Capitol Aggregates Field Site (after Kurtulus, 2006)

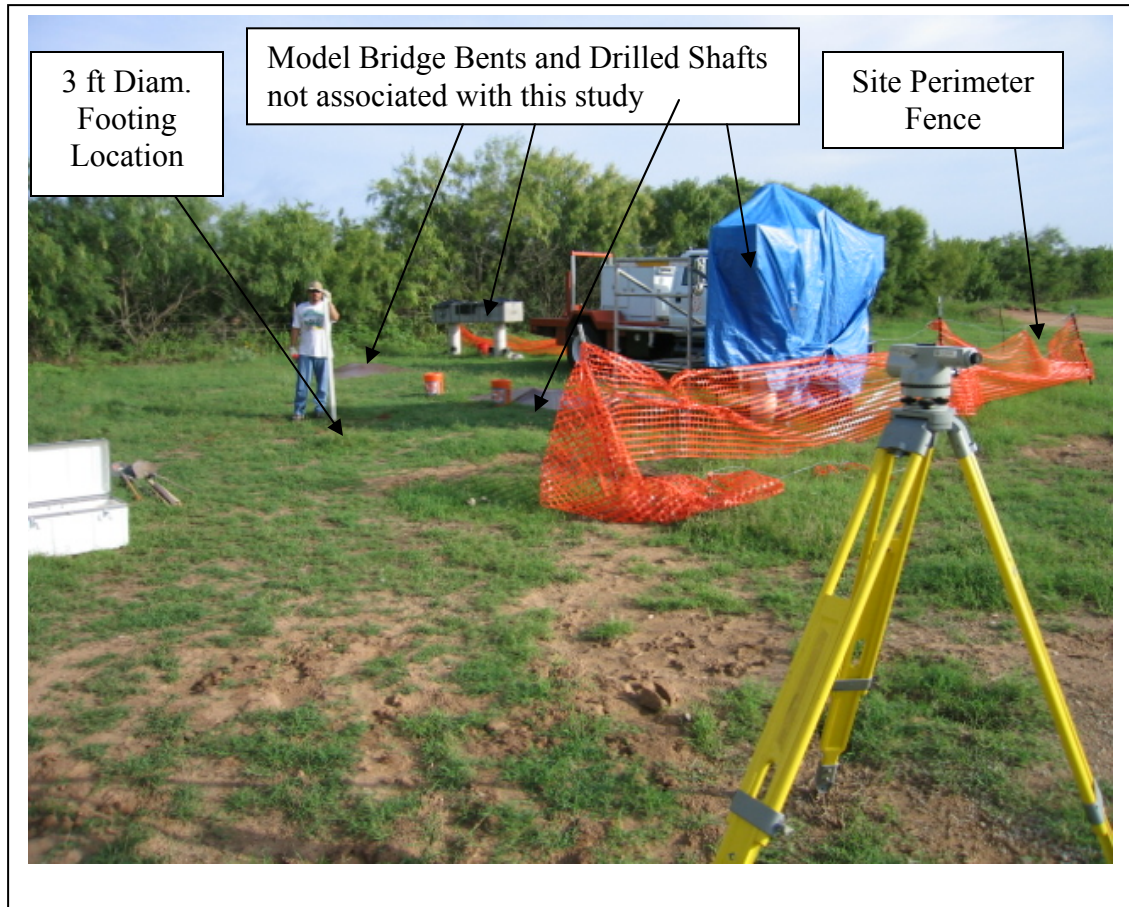


Figure 3.3: Picture of Field Site Prior to Construction of the 3-ft Diameter Footing.

### 3.3 DISTURBED AND UNDISTURBED SAMPLES

Disturbed and undisturbed samples were obtained at the site (Kurtulus, 2006). From the disturbed samples taken during the SPT tests, grain size analyses and Atterberg limit tests were conducted in accordance with ASTM D 2217 and ASTM D 4318, respectively. The top 14 ft of soil was classified per ASTM D 2487. The results are presented in Table 3.1. In terms of this study, the site is composed of 1.5 ft of silty sand (SM) underlain by 10 ft of nonplastic silt (ML).

The undisturbed samples were obtained from two sampling boreholes using 3-in. O.D. ASTM thin-walled Shelby tubes (Kurtulus, 2006). The undisturbed samples were used to determine soil index properties for the top 12 ft of soil. These properties are presented in Table 3.2. The undisturbed samples were used to carve intact specimens that were tested in the torsional resonant column test to evaluate dynamically the variation in shear modulus with shear strain. These results are discussed in Section 3.7.

Table 3.1: USCS Soil Classification of Top 14 ft of Soil Material at Capitol Aggregates Field Site (from Kurtulus, 2006)

Borehole No.	Depth Range, ft	Fines Content, %	Soil Classification, USCS
<b>D1</b>	0- 1.5	28	SM
	2.5-4.0	58	ML
	5.0- 6.5	65	ML
	7.5- 9.0	82	ML
	10.0- 11.5	83	ML
	12.5- 14.0	25	SM
<b>D2</b>	0- 1.5	14	SM
	2.5-4.0	51	ML
	5.0- 6.5	61	ML
	7.5- 9.0	84	ML
	10.0- 11.5	80	ML
	12.5- 14.0	23	SM

Table 3.2: Summary of Soil Index Properties Determined from Undisturbed Samples (from Kurtulus, 2006)

Depth, ft	Water Content, %	Total Unit Weight, pcf	Dry Unit Weight, pcf	Void Ratio*	Degree of Saturation*, %
5.6	8	NA	NA	NA	NA
6.0	16	131.1	113.0	0.5	89
6.5	NA	112.3	NA	NA	NA
8.4	22	118.3	97.1	0.7	81
8.8	25	110.7	88.6	0.9	75
9.2	24	122.7	99.1	0.7	93
10.6	18	107.3	90.9	0.8	57
11.1	8	96.1	89.1	0.9	24
11.6	10	99.7	90.7	0.8	31

\*Specific Gravity,  $G_s$ , is assumed to be 2.68.

### 3.4 STANDARD PENETRATION TESTS

Two boreholes with SPT tests were conducted on the test site at the locations indicated in Figure 3.2. The SPT blow counts were obtained at 2.5-ft intervals. The results of the tests are presented in Table 3.3 and Figure 3.4. In terms of the 3-ft diameter footing in this study, the depth-corrected blow counts between depths of 1 to 7 ft (within 2B of the base of the footing) range from 13 to 29 and average 17.

Table 3.3: SPT Test Results from Capitol Aggregate Field Site, Dec, 2004 (from Kurtulus, 2006)

Borehole No.	Depth, ft	Field N, bpf	N <sub>60</sub> , bpf	N <sub>1,60</sub> , bpf
<b>D1</b>	1.0	13	15	29
	3.5	8	9	18
	6.0	8	9	16
	8.5	14	16	24
	11.0	12	15	20
	13.5	19	24	29
	16.0	19	27	30
	18.5	6	9	9
	21.0	2	3	3
	23.5	22	31	28
	26.0	11	16	13
	31.0	13	19	15
	36.0	100	shale	shale
<b>D2</b>	1.0	12	13	27
	3.5	6	7	13
	6.0	8	9	16
	8.5	5	6	8
	11.0	10	13	17
	13.5	13	17	20
	16.0	9	13	14
	18.5	8	11	12
	21.0	10	14	14
	23.5	14	20	18
	26.0	6	9	7
	31.0	18	27	21
	36.0	100	shale	shale

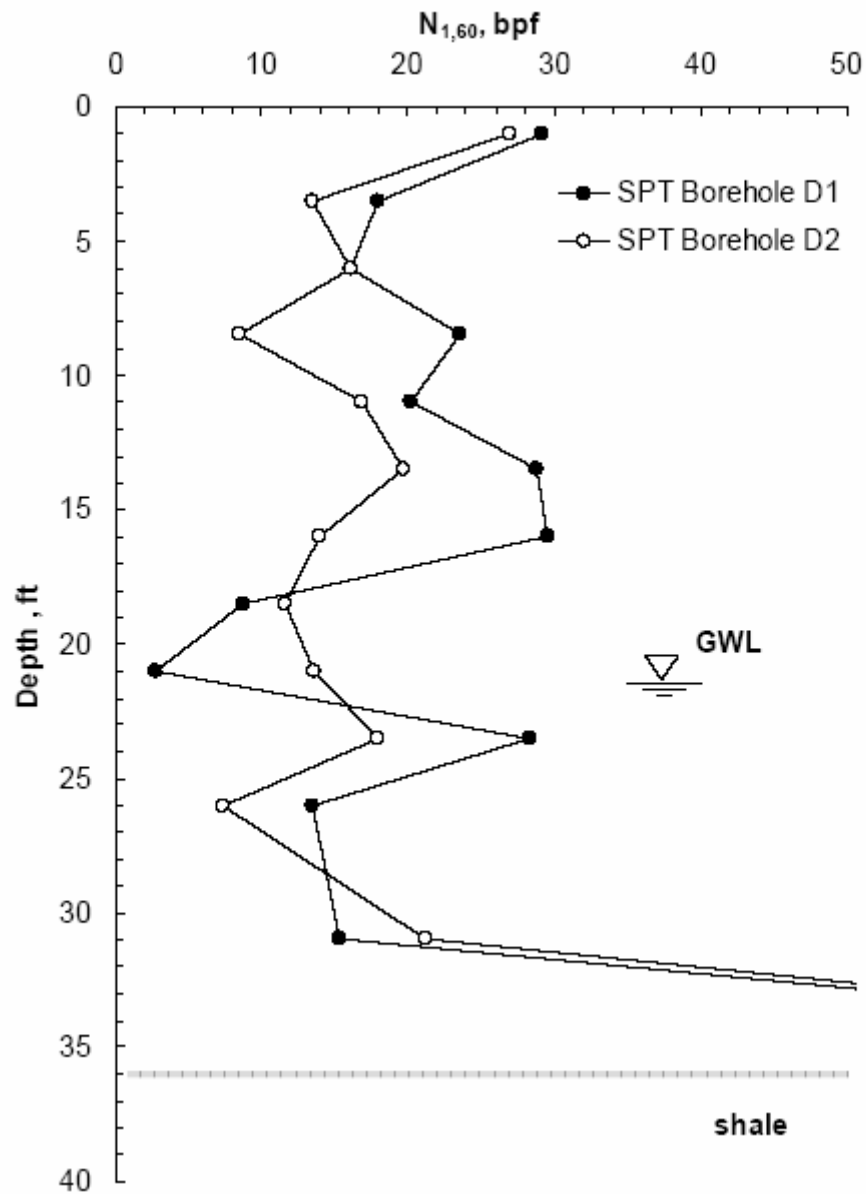


Figure 3.4: Variation of Corrected SPT Blow Count with Depth at Capitol Aggregates Field Site (from Kurtulus, 2006)

### 3.5 SPECTRAL ANALYSIS OF SURFACE WAVES (SASW) TESTS

Shear wave velocity profiles of the Capitol Aggregates field site were evaluated using the SASW seismic method in February of 2005. Two perpendicular arrays were measured. The locations of the arrays are shown in Figure 3.2. The field dispersion curve obtained during SASW testing is presented in Figure 3.5. The shear wave velocity profiles generated from the SASW tests are presented Figure 3.6. The tabular results from each array are presented in Tables 3.4 and 3.5. In terms of this study, the shear wave velocity measured between the surface and a depth of 7 ft ranged from 320 ft/s to 540 ft/s.

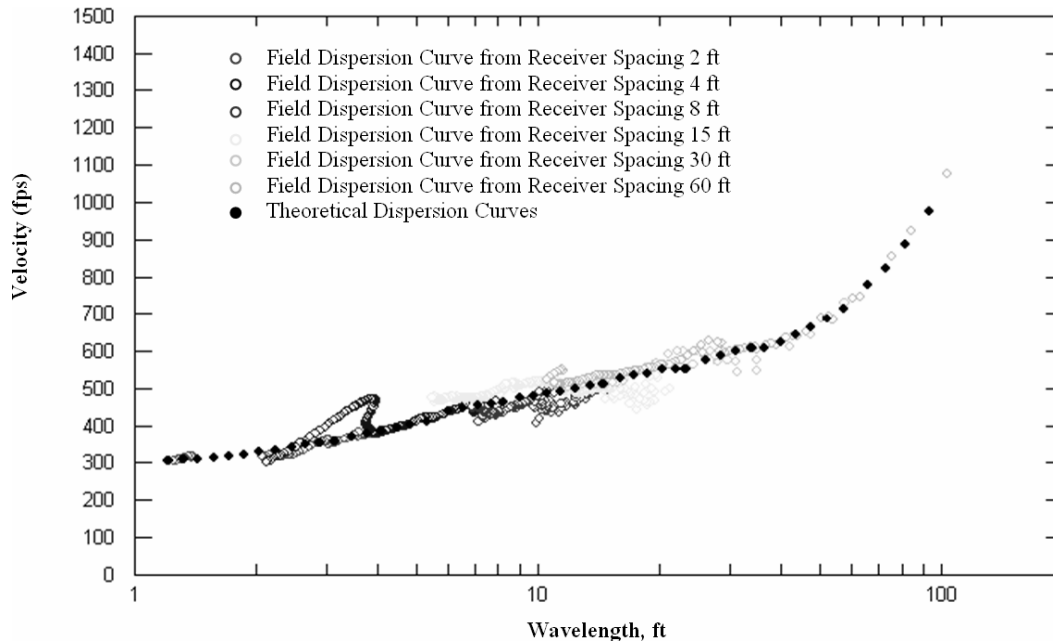


Figure 3.5: Theoretical Dispersion Curve Fit to the Composite Experimental Dispersion Curve at SASW Line A (from Kurtulus, 2006)



Table 3.4: Tabulated Values of Best-Fit Wave Velocity Profile from SASW Testing at Capitol Aggregates Field Site; SASW- Line A (from Kurtulus, 2006)

Depth to Top of Layer, ft	Layer Thickness, ft	Compression Wave Velocity* , fps	Shear Wave Velocity, fps	Assumed Poisson's Ratio	Assumed Total Unit Weight, pcf
0	1	635	320	0.33	110
1	1.5	834	420	0.33	110
2.5	4.5	1072	540	0.33	110
7	7	1310	660	0.33	110
14	7.5	1390	700	0.33	110
21.5	17	5000	750	0.49	125
38.5	half-space	5000	2200	0.38	125

\*Based on the shear wave velocity and assumed value of Poisson's ratio above the water table. Below the water table,  $V_p$  was assumed equal to 5000 fps.

Table 3.5: Tabulated Values of Best-Fit Wave Velocity Profile from SASW Testing at Capitol Aggregates Field Site; SASW- Line B (from Kurtulus, 2006)

Depth to Top of Layer, ft	Layer Thickness, ft	Compression Wave Velocity* , fps	Shear Wave Velocity, fps	Assumed Poisson's Ratio	Assumed Total Unit Weight, pcf
0	1	675	340	0.33	110
1	1.5	953	480	0.33	110
2.5	4.5	1013	510	0.33	110
7	7	1310	660	0.33	110
14	7.5	1390	700	0.33	110
21.5	17	5000	750	0.49	125
38.5	half-space	5000	2200	0.38	125

\*Based on the shear wave velocity and assumed value of Poisson's ratio above the water table. Below the water table,  $V_p$  was assumed equal to 5000 fps.

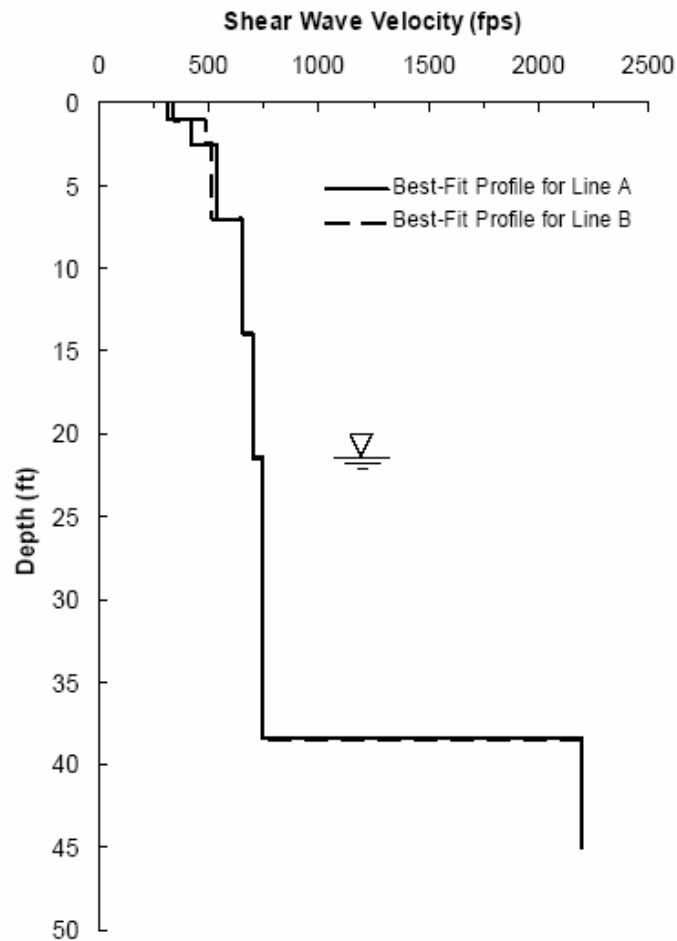


Figure 3.6: Shear Wave Velocity Profiles Determined from SASW Testing at Capitol Aggregates Field Site on February 3, 2005 (from Kurtulus, 2006)

### 3.6 CROSSHOLE SEISMIC TESTS

During construction of the footing used in this study, geophones were placed below the surface of the footing as part of Mr. Kwangsoo Park's Ph.D. dissertation research. The exact location and orientation of these geophones is shown in Figure 3.7. The details of the footing's design, construction and instrumentation will be discussed further in Chapter 4. Crosshole testing was conducted using the

horizontally oriented geophones below the footing. The crosshole source was generated in an adjacent borehole located approximately 12 in. from the edge of the footing as shown in Figure 3.7.

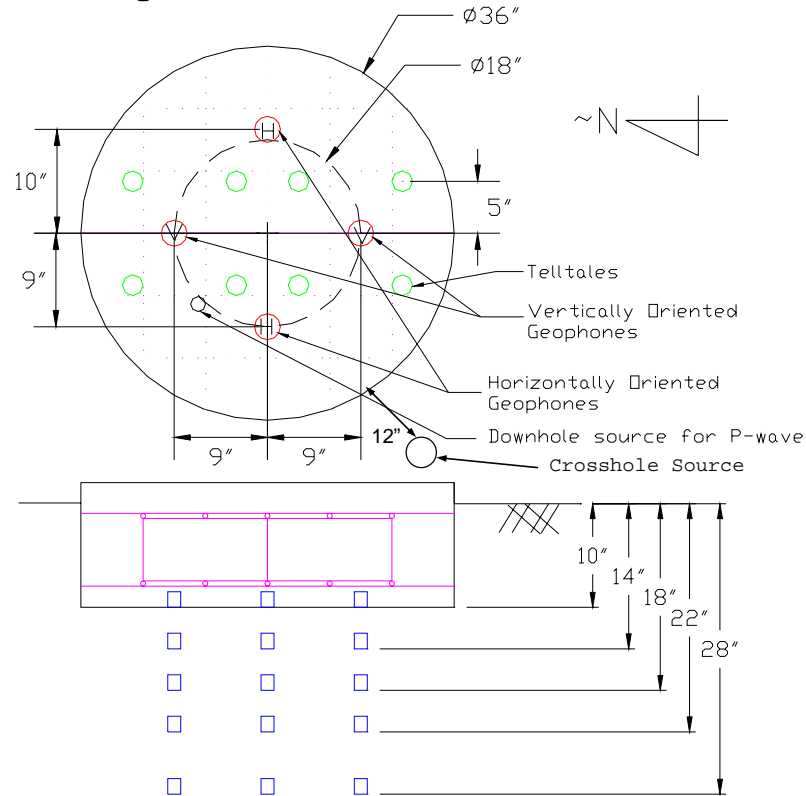


Figure 3.7: Locations and Depths of Embedded Geophones Under 3-ft Diameter Footing at the Capital Aggregates Field Site (from Park, 2007)

The results of the crosshole tests are plotted in Figure 3.7. These results are shown with the shear wave velocity profile determined from the SASW testing conducted by Kurtulus (2006). A good comparison is shown considering the SASW measurements are global in nature and the crosshole and downhole measurements are very localized in the soil beneath the footing.

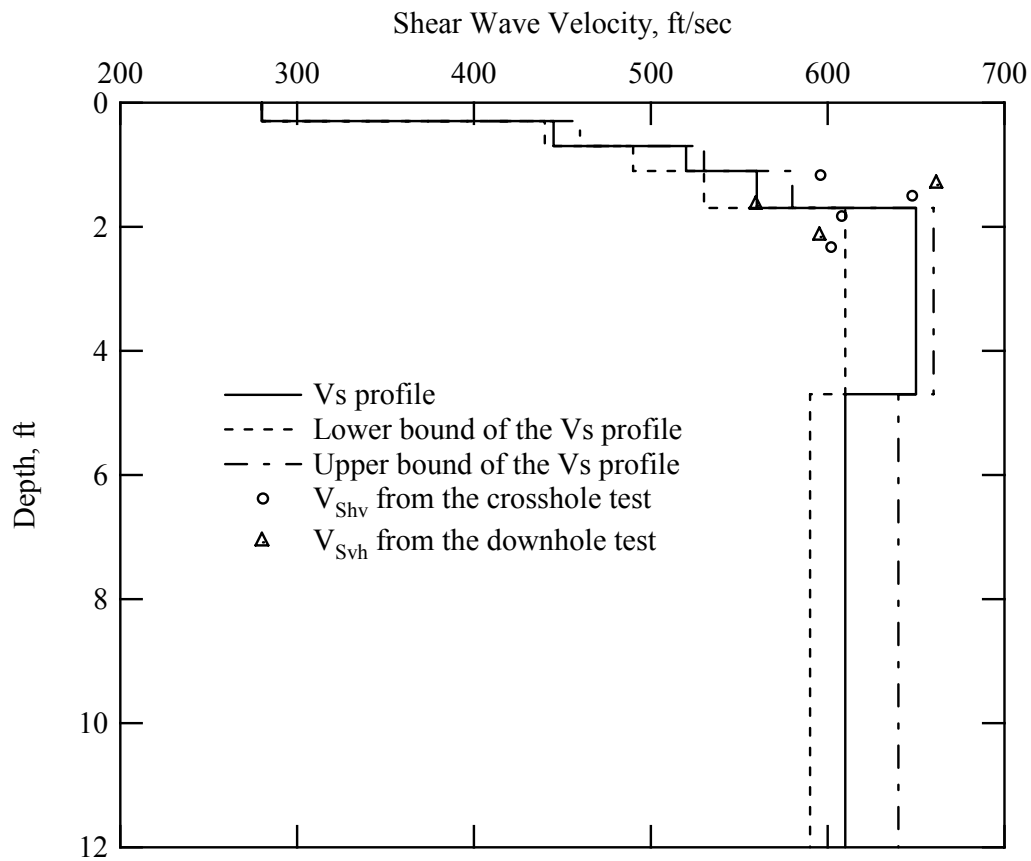


Figure 3.8: Results of Crosshole Tests Conducted Under the 3-ft Diameter Footing at the Capital Aggregates Field Site in August 2005 (from Park, 2007).

### 3.7 TORSIONAL RESONANT COLUMN TESTS

Torsional Resonant column tests were performed on two specimens taken from undisturbed samples at 6.0 and 9.2 ft below the surface. Each sample was tested at five isotropic confining pressures (1.5, 3, 6, 12, and 24 psi) at very low strains ( $\gamma < 0.001\%$ ) to determine the variation of shear wave velocity with confining pressure. The results of these tests are presented in Figure 3.9. Then, the samples were tested at higher amplitude strains under confining pressures of 6 and 24 psi to determine the

nonlinear behavior of the soil. The variation in shear modulus with shearing strain for each sample at each confining pressure is plotted in Figure 3.10. The normalized modulus reduction curves for isotropic confining pressures of 6 and 24 psi are presented in Figures 3.11 and 3.12, respectively.

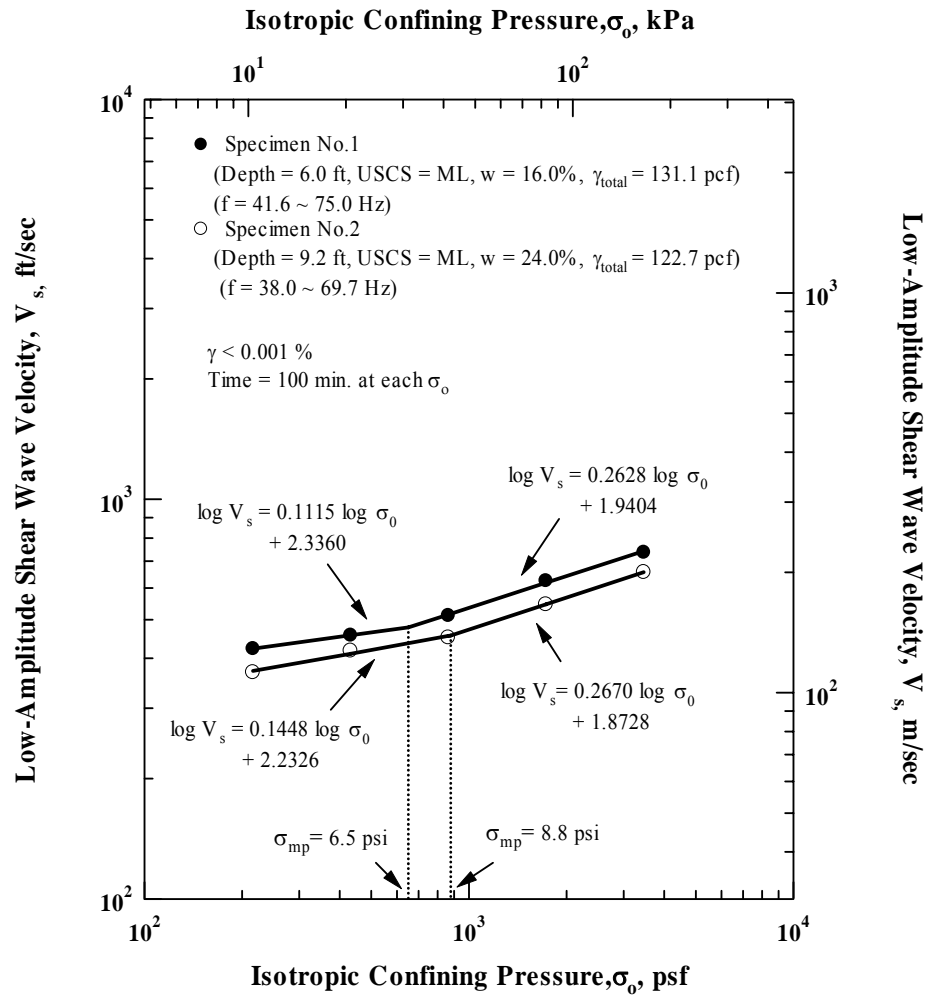


Figure 3.9: Variation of Low-Amplitude Shear Wave Velocity with Isotropic Confining Pressure from Resonant Column Tests (from Kurtulus, 2006).

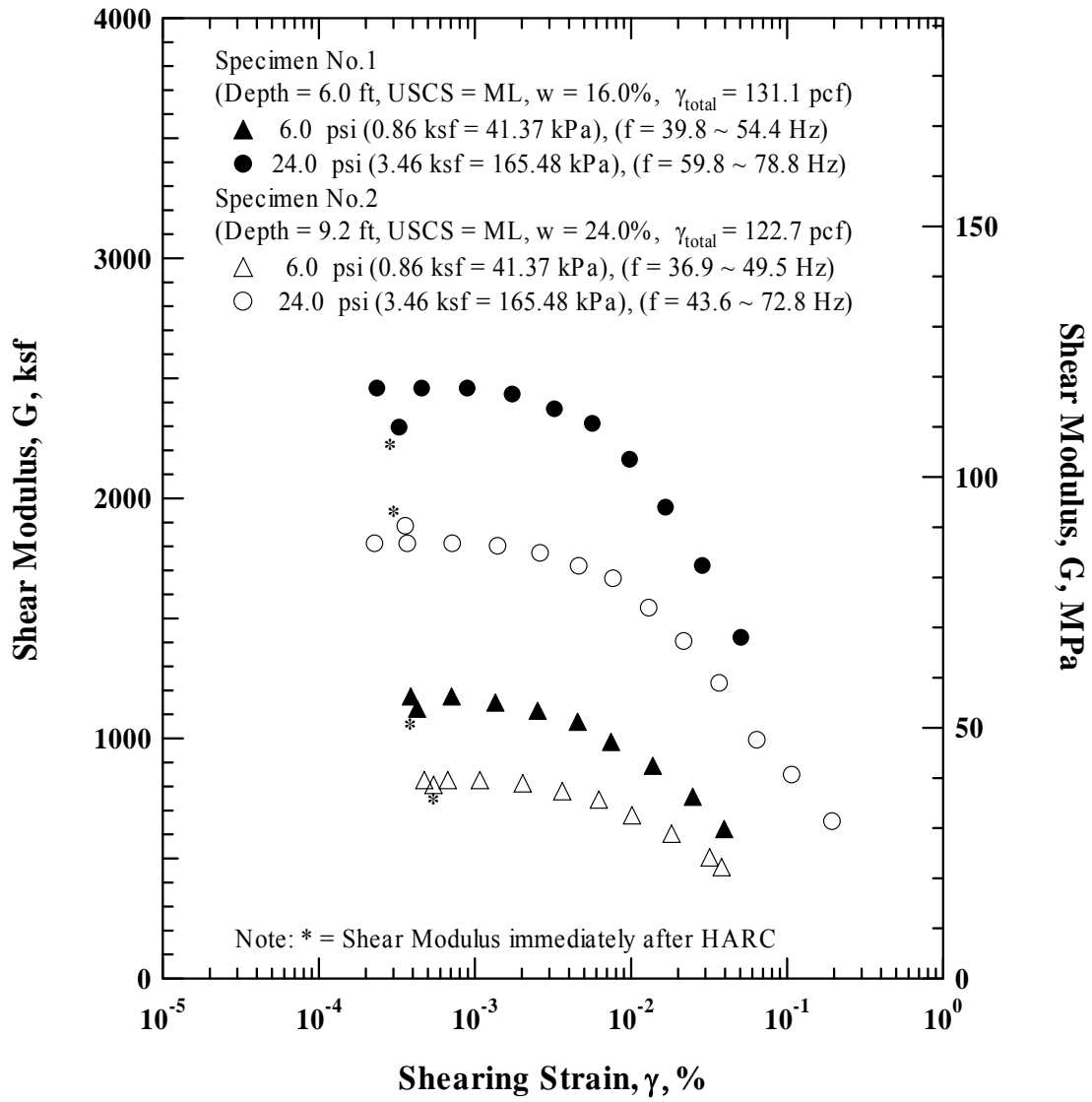


Figure 3.10: Comparison of the Variation in Shear Modulus with Shearing Strain at Two Isotropic Confining Pressures from the Resonant Column Tests (from Kurtulus, 2006).

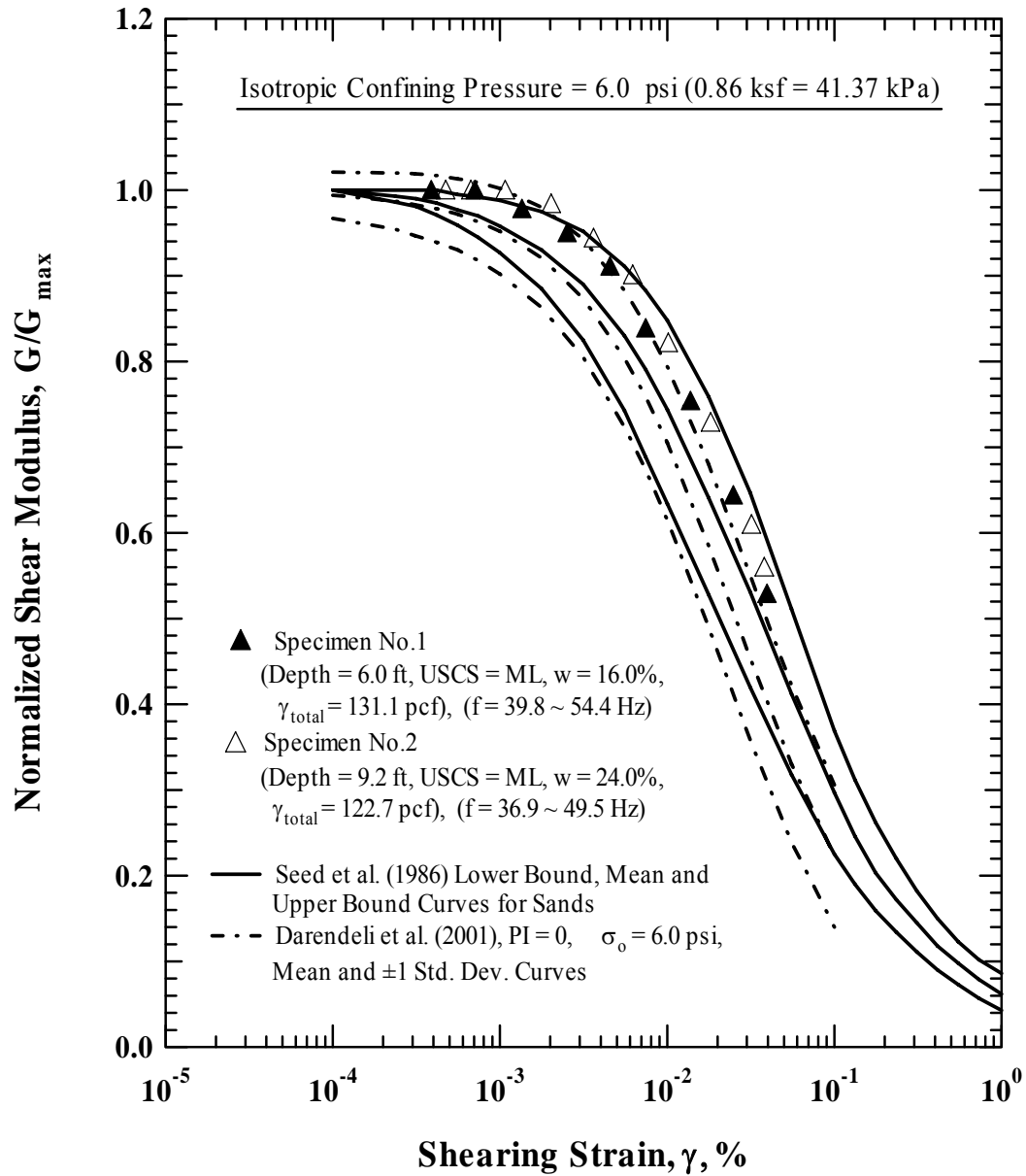


Figure 3.11: Comparison of the Variation in Normalized Shear Modulus with Shearing Strain at Isotropic Confining Pressure of 6 psi (0.86 ksf = 41.37 kPa) from the Resonant Column Tests with Modulus Reduction Curves proposed by Seed et al. (1986) and Darendeli (2001) (from Kurtulus, 2006).

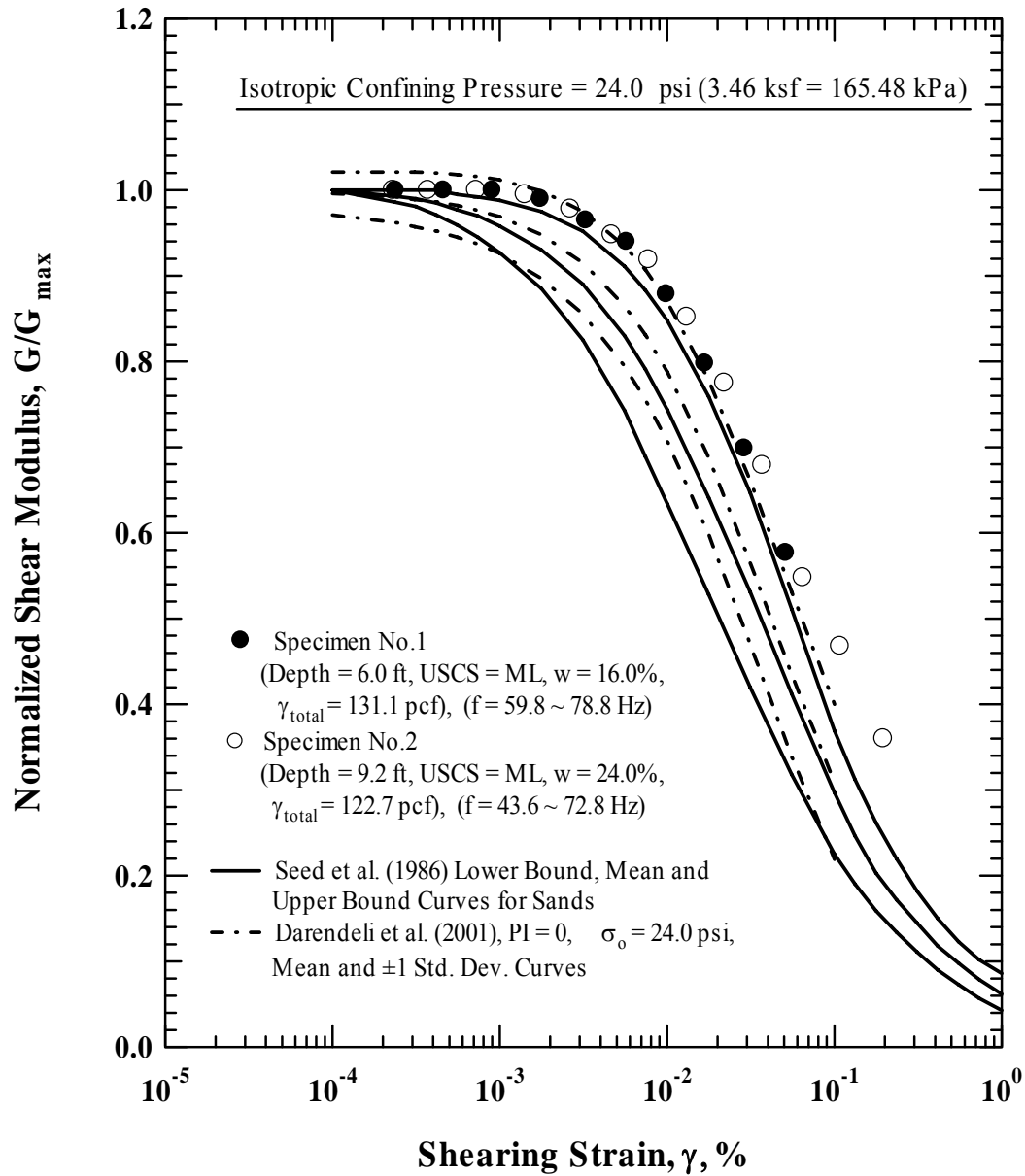


Figure 3.12: Comparison of the Variation in Normalized Shear Modulus with Shearing Strain at Isotropic Confining Pressure of 24 psi (3.46 ksf = 165.48kPa) from the Resonant Column Tests with Modulus Reduction Curves proposed by Seed et al. (1986) and Darendeli (2001) (from Kurtulus, 2006).



### 3.8 SUMMARY

A number of field characterization measurements were performed at the Capitol Aggregates field site by Kurtulus, 2006 and Park, 2007. Some of these results were used in this study. In terms of the soil within 2B (B= 3ft) of the footing base, the soil profile is:

1. 8 in. of silty sand (SM), and
2. 10 ft of nonplastic silt (ML).

The average characteristics of the soil are summarized in Table 3.6

Table 3.6: Summary of Soil Characteristics at the Capitol Aggregates Field Site

Soil Property	Range	Average
Total Unit Weight (pcf)	112 -131	121.5
Dry Unit Weight (pcf)	113	113
Water content (%)	8 -16	12
Void Ratio	0.5	0.5
Fines Content (%)	14 - 65	50
Degree of Saturation (%)	89	89
SPT Blow Count	13 - 29	17
Shear Wave Velocity (fps) <sup>1</sup>	420 - 540	508
Shear Wave Velocity (fps) <sup>2</sup>	550 - 670	600
Notes: 1. Vs from SASW tests 2. Vs from crosshole and downhole tests		

## **CHAPTER 4**

### **EXPERIMENTAL FIELD SET-UP**

#### **4.1 INTRODUCTION**

In this chapter, the test layout at the Capitol Aggregates field site is described. This description includes the design and installation of the circular footing and the locations and depths of the subsurface instrumentation. Two different loading systems were used to statically load the footing. These loading systems are described and illustrated. During each test, the footing was loaded and unloaded over a period of about 3-4 minutes. The details of this testing procedure are outlined in the next chapter, Chapter 5. A brief description of the data acquisition hardware and test instrumentation is presented.

#### **4.2 FOOTING DESIGN AND CONSTRUCTION**

The circular footing was a reinforced concrete footing that was 3 ft in diameter and 1 ft thick. The design of the footing is shown in Figure 4.1. To construct the footing, an excavation was first made with small hand tools. Great care was taken to ensure that the bottom surface of the excavation was disturbed as little as possible. A surveyor's level was used to ensure that an excavation of uniform depth was made and that the bottom was level (see Figure 4.2). A 2-in. hand auger was used to bore holes in the soil so that telltales and geophones could be placed beneath the footing. The holes were carefully augered for this purpose. The soil removed from the holes was retained in plastic bags and used to backfill the holes after

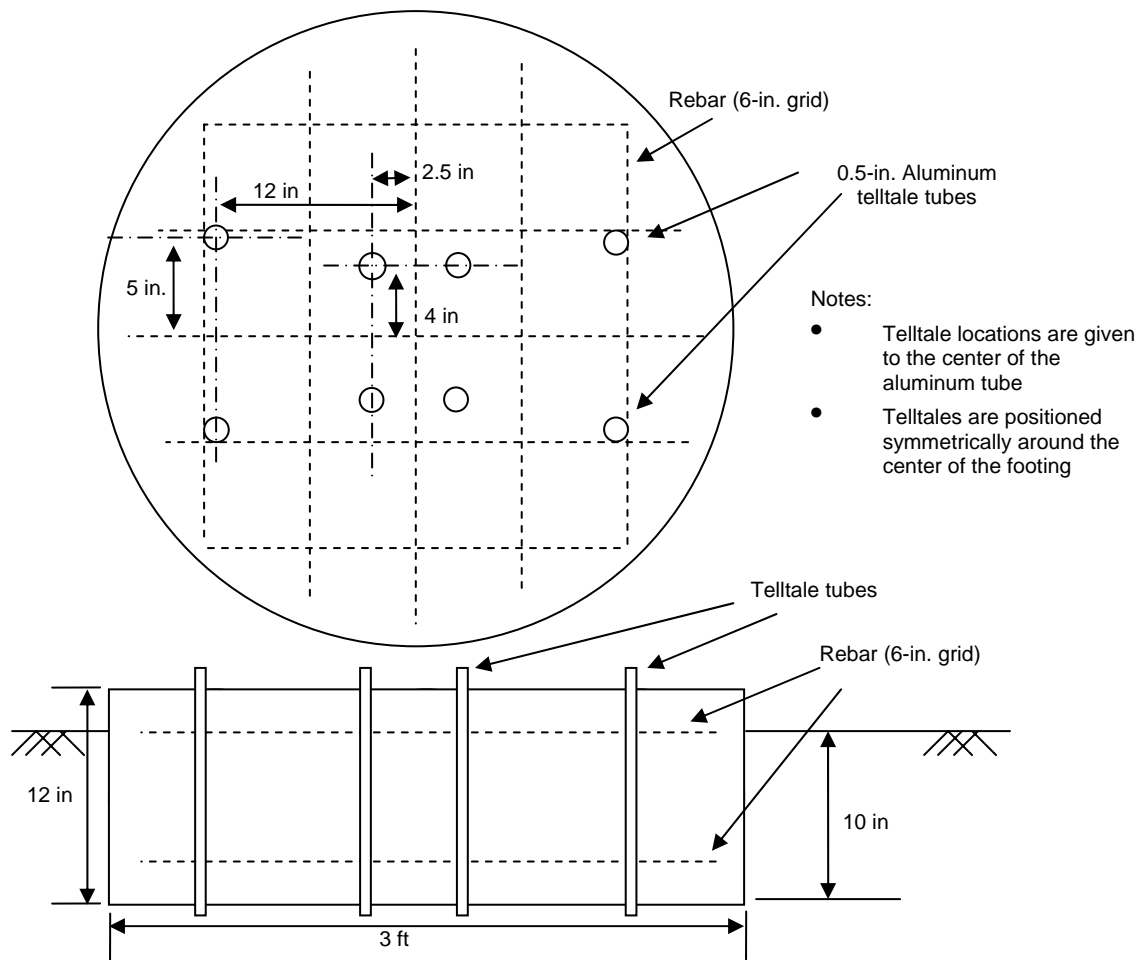


Figure 4.1: Design of Reinforced Concrete Footing

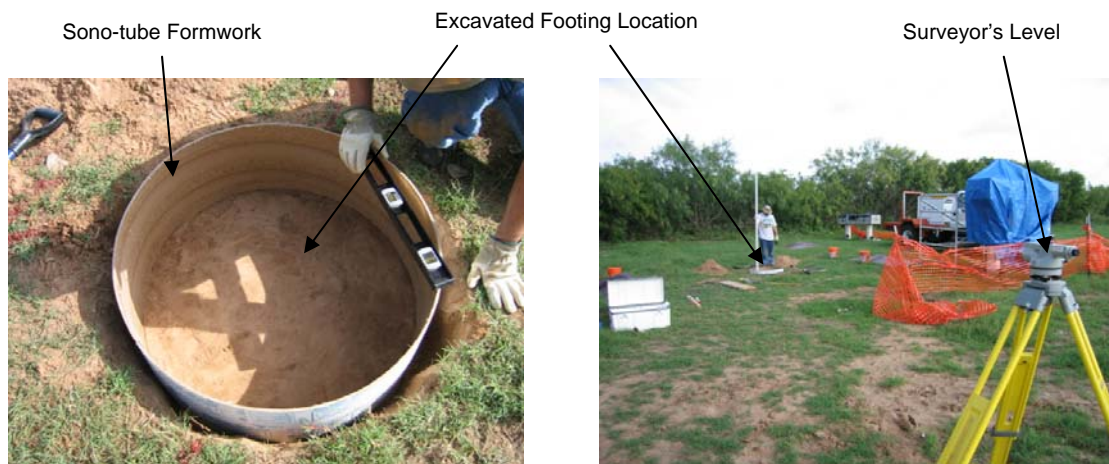


Figure 4.2: Excavation and Leveling of the Footing Location

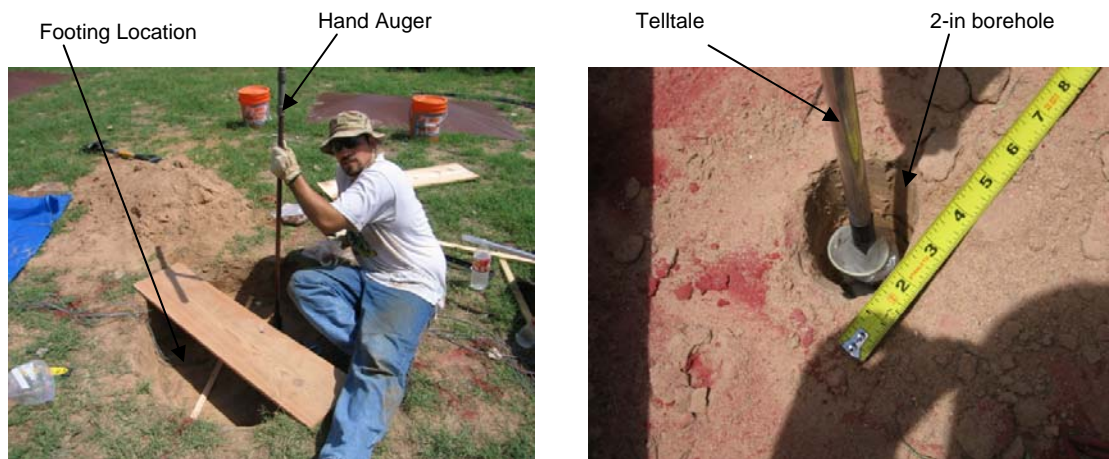


Figure 4.3: Augering 2-in. Boreholes for Telltale Installation

placement of the instrumentation. During the entire excavation and instrumentation installation process, the surface of the soil beneath the footing was never stepped on or loaded in any way. A wooden plank was used to bridge across the open excavation while installing telltales, thus minimizing disturbance of the soil to be tested (see Figure 4.3). The telltales in place are shown in Figure 4.4.

Once the subsurface instrumentation was installed, a circular sono-tube form was placed in the open hole as shown in Figure 4.5. Next, the steel rebar cage was placed. The rebar cage was constructed of two horizontal layers with #4 bars in a 6-in. grid pattern. The vertical stabilizing bars were #5 bars. Next, the aluminum tubes encasing the telltales, with their ends covered with duct tape, were zip-tied in place to ensure their position during concrete pouring (see Figure 4.6). A downhole seismic wave source was also installed in the footing as a part of an associated research project (Park, 2007). The position of the downhole source is noted in Figures 4.5 and 4.6.

To construct the footing,  $7 \text{ ft}^3$  ( $0.26 \text{ yd}^3$ ) of concrete were used. The concrete was a 3,000-psi mix, with a maximum aggregate size of 0.75 in. It was delivered by a ready-mix truck from Capitol Aggregates Co. The concrete was poured, rodded to eliminate any air voids, and finished within approximately 30 minutes after the pour started. The footing cured for three weeks under a protective cover as shown in Figure 4.8. Then, the sono-tubeform was removed and the area between the footing and natural soil was backfilled.

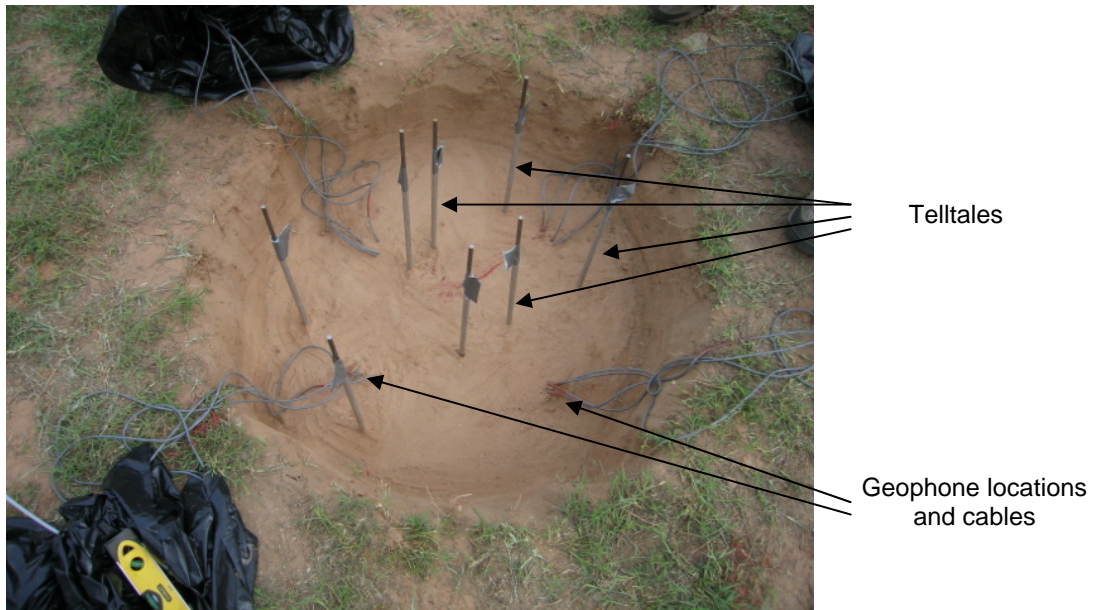


Figure 4.4: Footing Excavation After Installation of the Telltales and Geophones

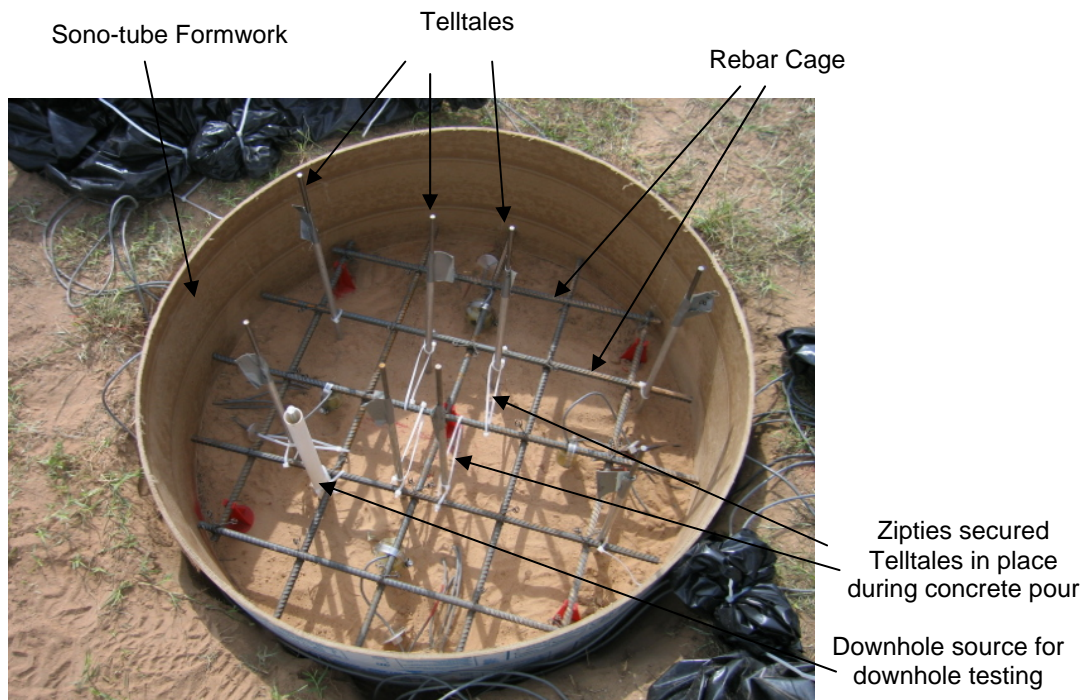


Figure 4.5: First Stage of Rebar Cage Installation



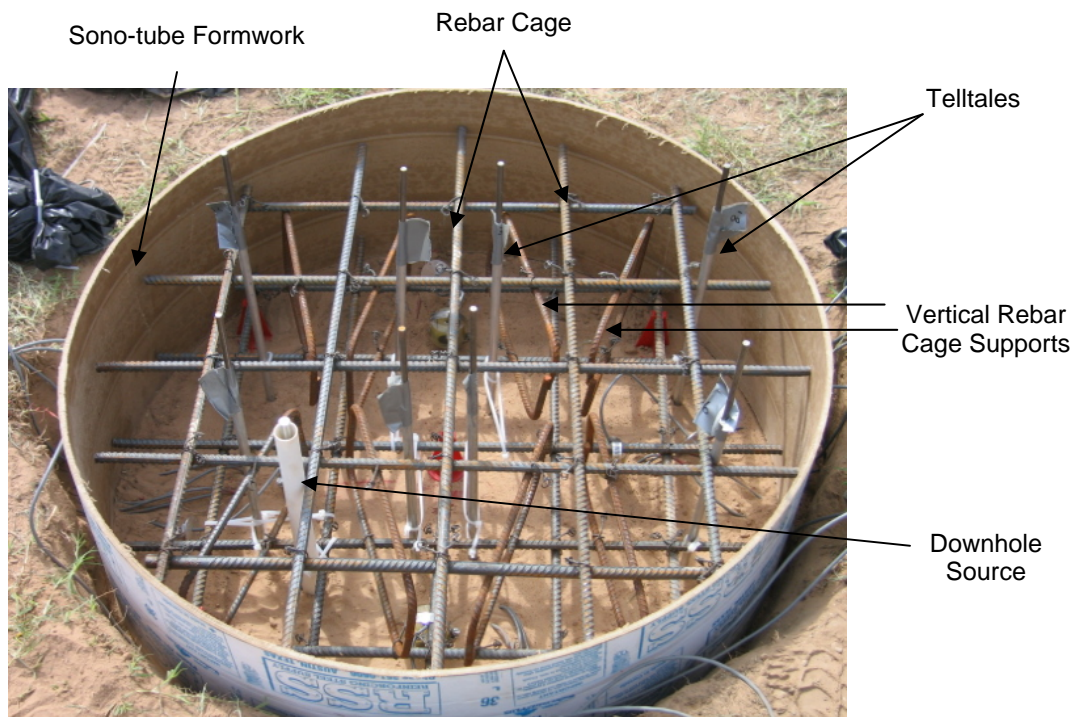


Figure 4.6: Second Stage of Rebar Cage Installation

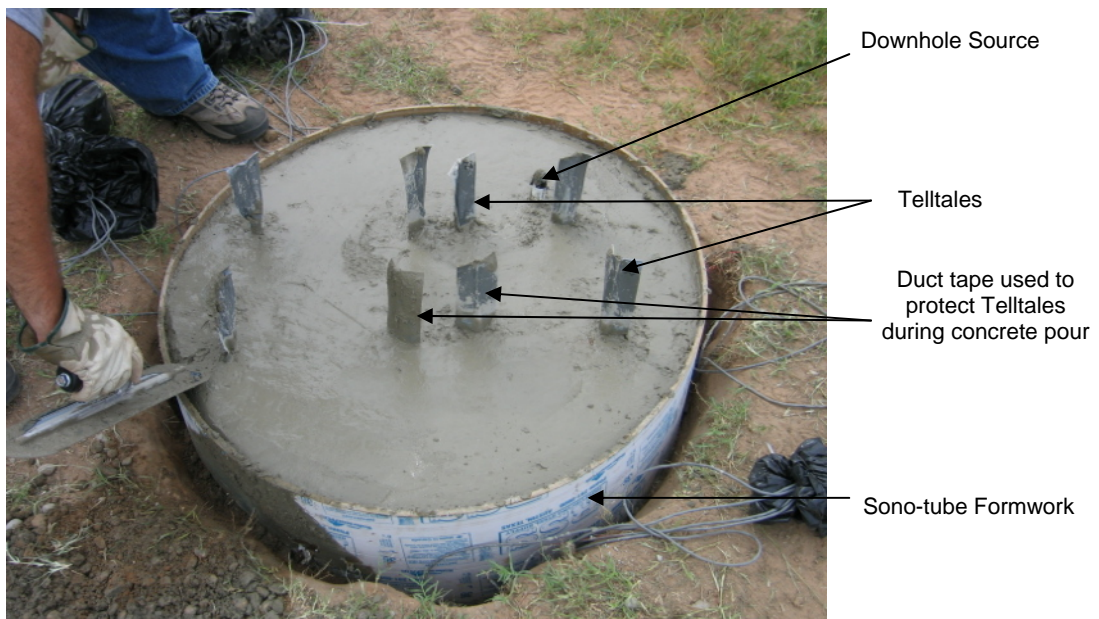


Figure 4.7: Finished Footing Construction



Figure 4.8: Field Site During Footing Curing and Between Test Days

#### 4.2.1 CONSTRUCTION DETAILS OF THE TELLTALLES

The telltales were used to measure settlement at various depths beneath the footing. The telltales were built with a 0.25-in. steel rod with a square steel plate, 1.4 in. on a side, welded to the bottom. Each telltale rod was placed in a 0.5-in. outside diameter aluminum tube, with 0.375-in. inside diameter. The purpose of the aluminum tubes was to prevent side shear or loading of each rod of the telltales from the surrounding soil. The aluminum tube was segmented into pieces that were 5.5-in. long to allow axial movement of the sleeve without influencing the inner telltale rod. The connection between segments of the aluminum tubing was constructed with standard electrical tape to prevent soil intrusion into the tube while allowing axial compression. The sticky side of the tape exposed to the telltale rod was covered with another reversed piece of tape to ensure that the tape did not interfere with the movement of the telltale rod. Finally, a rubber membrane was secured to the bottom



of the telltale with a rubber o-ring to ensure no soil intrusion between the aluminum tube and the rod at the base of the instrument. An example telltale is shown in Figure 4.9.

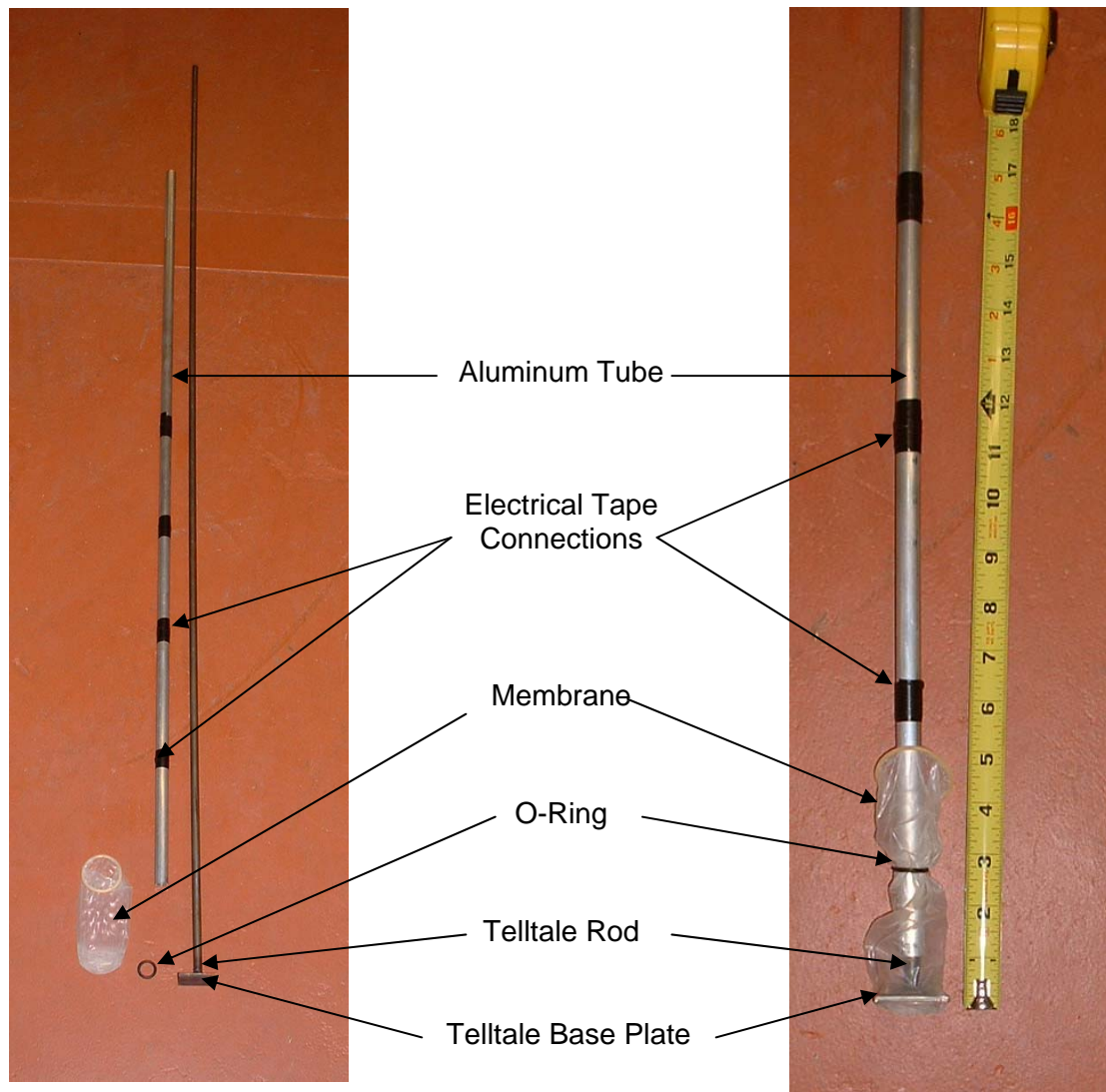


Figure 4.9: Detailed Telltale Picture

Telltales were placed at depths of 6, 12, 18, and 30 in. below the base of the footing. Two telltales were placed at each depth. Four of these telltales were placed

~4 in. from the center of the footing and the other four telltales were placed ~13 in. from the center. For each depth below the footing, the settlement was measured with two telltales, one near the center of the footing and one near the edge of the footing. The depths of each telltale are shown in Figure 4.10. A cross-sectional view of the telltales and footing are shown in Figure 4.11.

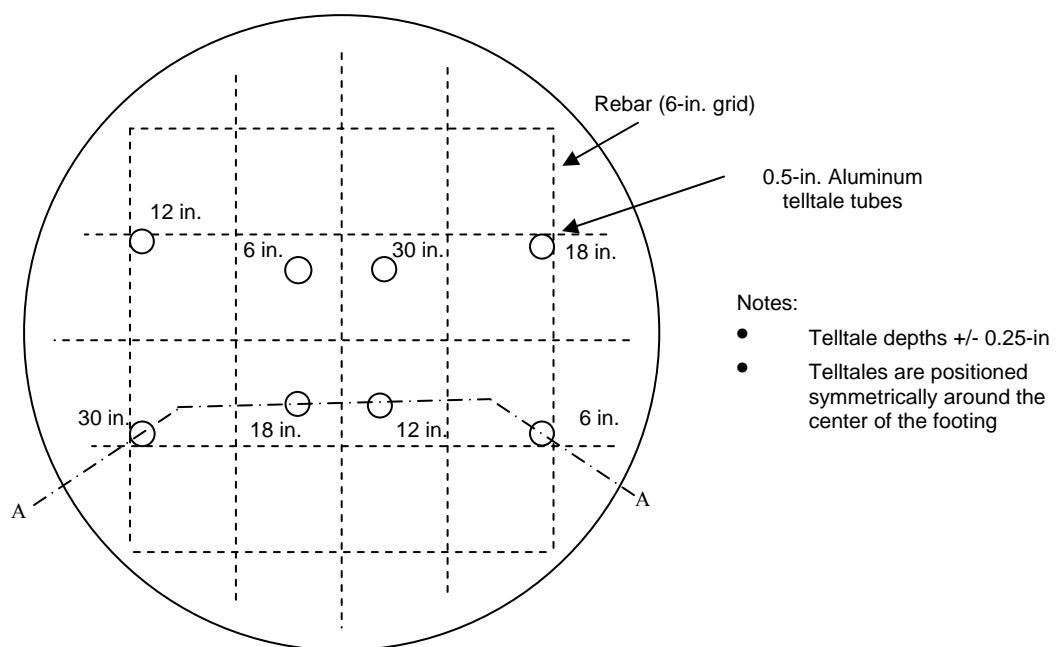


Figure 4.10: Footing Plan View Showing Telltale Locations

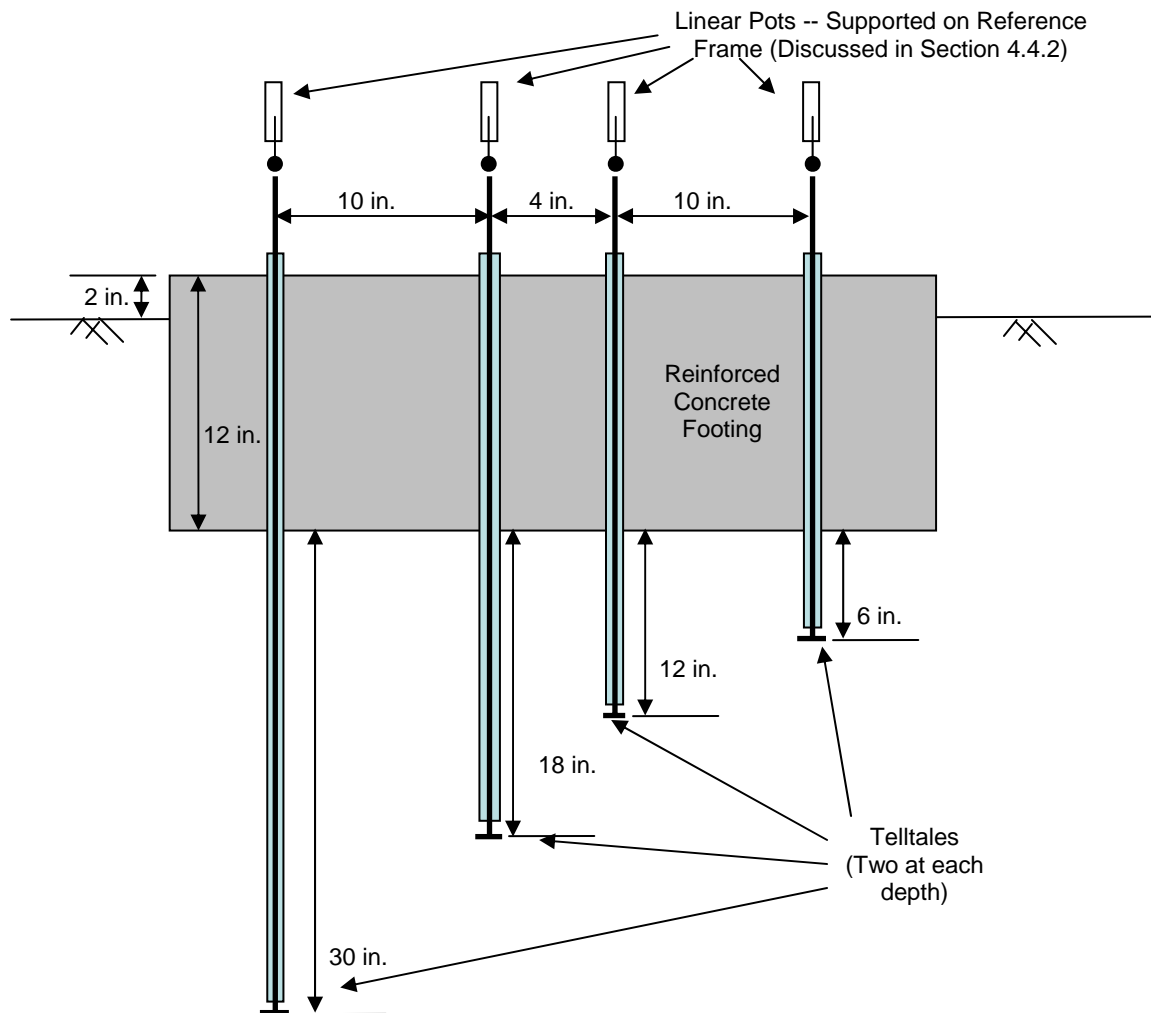


Figure 4.11 Section A-A from Figure 4.10: Depths of Telltales Beneath the Footing

### 4.3 LOADING SYSTEMS

Vertical static loads were applied to the footing using two different vibroseis systems as illustrated in Figure 4.12. The two vibroseis systems were a smaller one, called “Thumper,” and a larger one, called “T-Rex”. Thumper loading the footing is shown in Figure 4.13. T-Rex loading the footing is shown in Figure 4.14. Both systems essentially operate in the same fashion; a hydraulic ram pushes a large plate

downward. The magnitude of the reaction force in Thumper is significantly smaller than the reaction force of T-Rex. The load between the hydraulic ram was transferred through a load cell to a three point loading frame that was centrally located on top of the footing as illustrated in Figure 4.12. The loading frame serves to distribute the point load from the truck into three evenly distributed load points on top of the footing. This arrangement minimizes any unwanted movement that might occur from an off-center, single point load at the top of the footing.

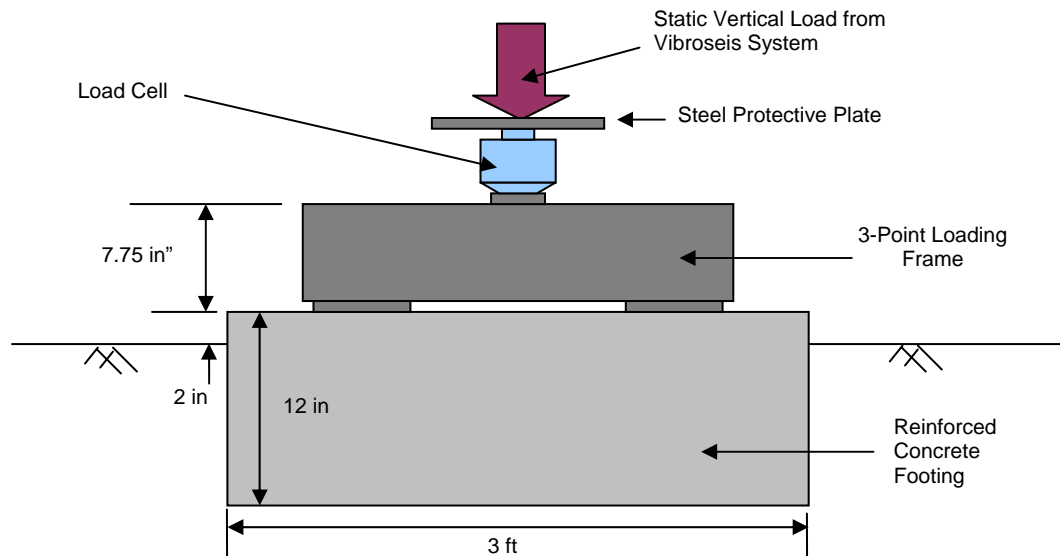


Figure 4.12: Static Vertical Loading Applied to Footing using a Vibroseis System

#### 4.3.1 VIBROSEIS TRUCK (THUMPER)

The small vibroseis truck (a.k.a Thumper) was used to load the footing and measure the response of the soil in the linear range. This arrangement is shown in Figure 4.13. This vehicle applied vertical static loads to the footing through a hydraulic ram mounted on the rear of the vehicle using the vehicle weight as the

resisting force. The maximum static load that could be applied with Thumper was 10,000 lb. This load created an equivalent vertical pressure at the base of the footing equal to 1400psf.



Figure 4.13: Arrangement Used to Load the Footing with Thumper.

#### 4.3.2 VIBROSEIS TRUCK (T-REX)

The large vibroseis truck (T-Rex) was used to apply larger loads to the top of the footing and thus induce higher pressures in the soil mass below the footing than was possible with Thumper. These larger loads were used to measure the soil response in the linear and mildly non-linear strain ranges. This vehicle applied loads to the footing through a hydraulic ram mounted on the rear of the vehicle using the vehicle weight as the resisting force. The maximum static load T-Rex could achieve

was 23,000 lb. This load created an equivalent, uniform vertical pressure at the base of the footing equal to 3300 psf.

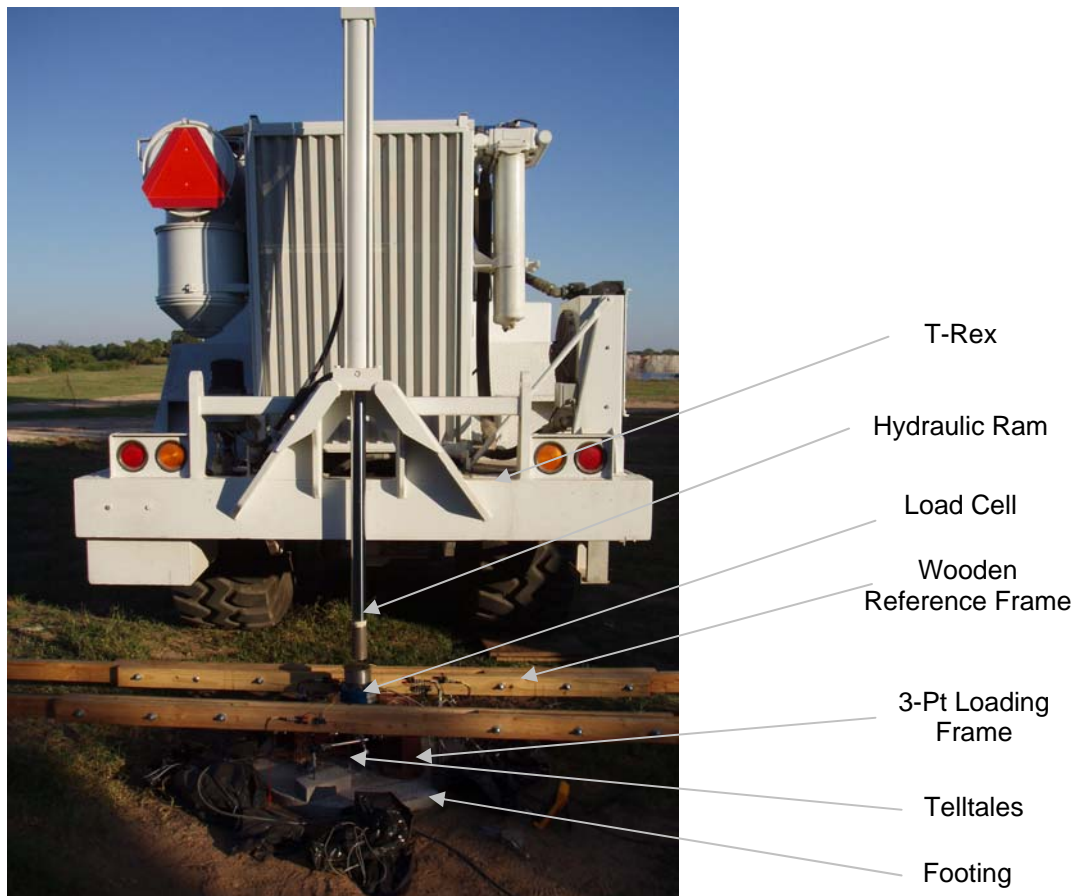


Figure 4.14: Arrangement Used to Load the Footing With the Hydraulic Ram on the Back of T-Rex

#### 4.4 INSTRUMENTATION

The instrumentation used to measure and record the settlements of the footing and the soil at various depths beneath the footing are discussed below.

#### 4.4.1 LINEAR POTENTIOMETERS

A linear potentiometer is essentially a variable resistor. The resistance output is proportional to the position of the wiper within the range of the circuit. Figure 4.15 illustrates the basic operation of a linear potentiometer. One linear potentiometer (pot) used in this study is pictured in Figure 4.16.

##### *Linear potentiometer construction*

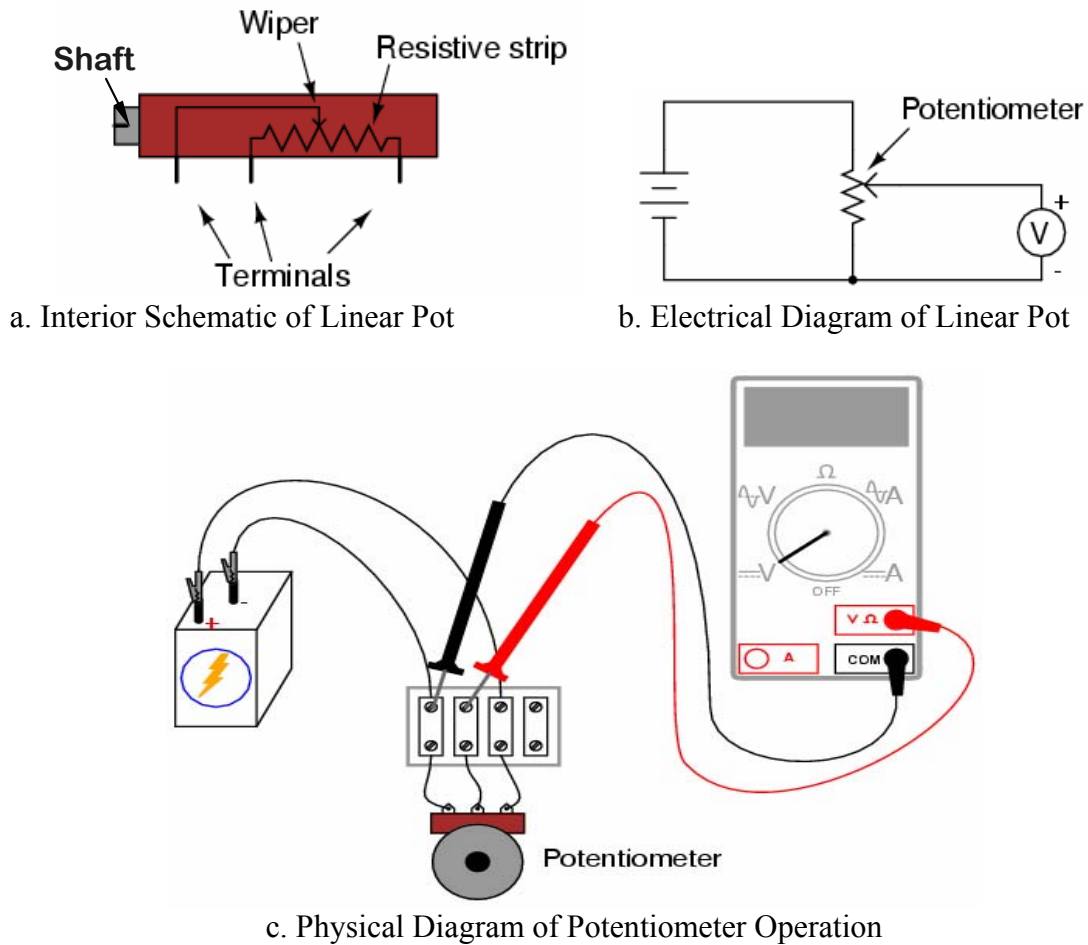


Figure 4.15: Schematic of Linear Potentiometer  
([http://www.allaboutcircuits.com/vol\\_6/chpt\\_3/6.html](http://www.allaboutcircuits.com/vol_6/chpt_3/6.html))



The wiper in contact with the resistor inside the linear potentiometer is fixed to the shaft. Thus, any displacement of the shaft will reduce or increase the resistance over the measured circuit. A 10-V DC power source was supplied to each linear pot, and the voltage passing through the variable resistor was measured. Therefore, in principle, when the shaft is fully extended, the output voltage is zero volts; and when the shaft is fully compressed, the output voltage is 10 volts.

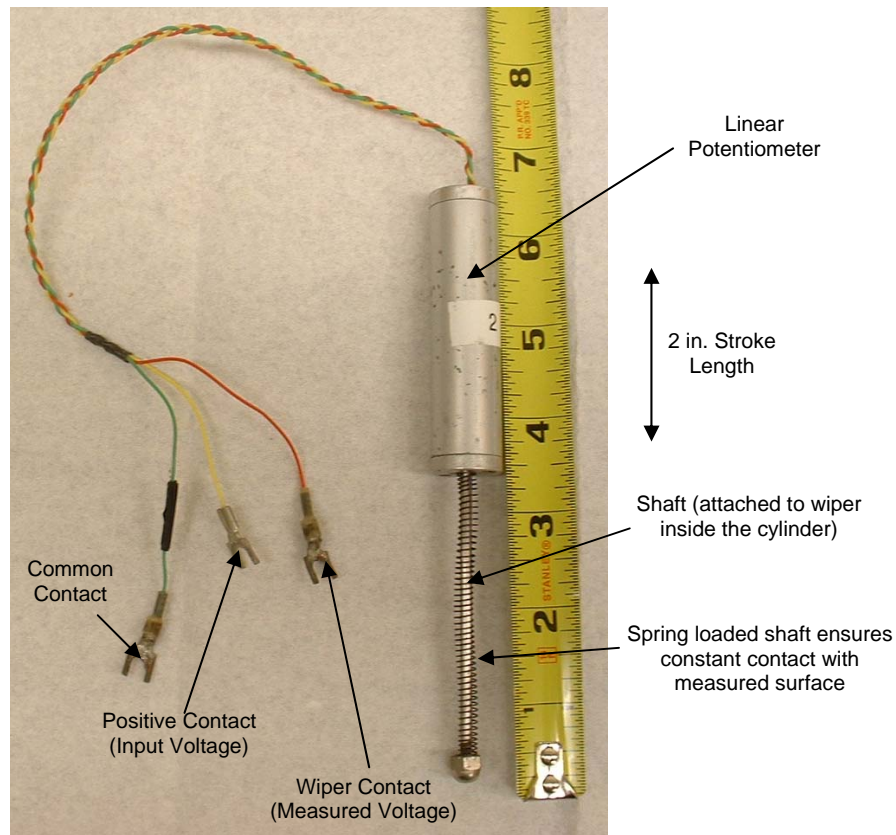


Figure 4.16: 2-inch Linear Potentiometer Used in this Study

Each linear pot was individually calibrated to determine the precise operating range and to check linearity within that range. During calibration, measurements were taken each 0.01 in. over the stroke length from 60 to 90% of full compression. This stroke was the range in which the each linear pot was used in the field. The linear pots used had a 2-in. range of motion and measured displacements with a precision of  $\pm 0.025\%FS$ , or  $\pm 0.0005$  in. An example calibration curve from one



linear potentiometer is presented in Figure 4.17. Calibration data from each linear potentiometer are presented in Appendix B.

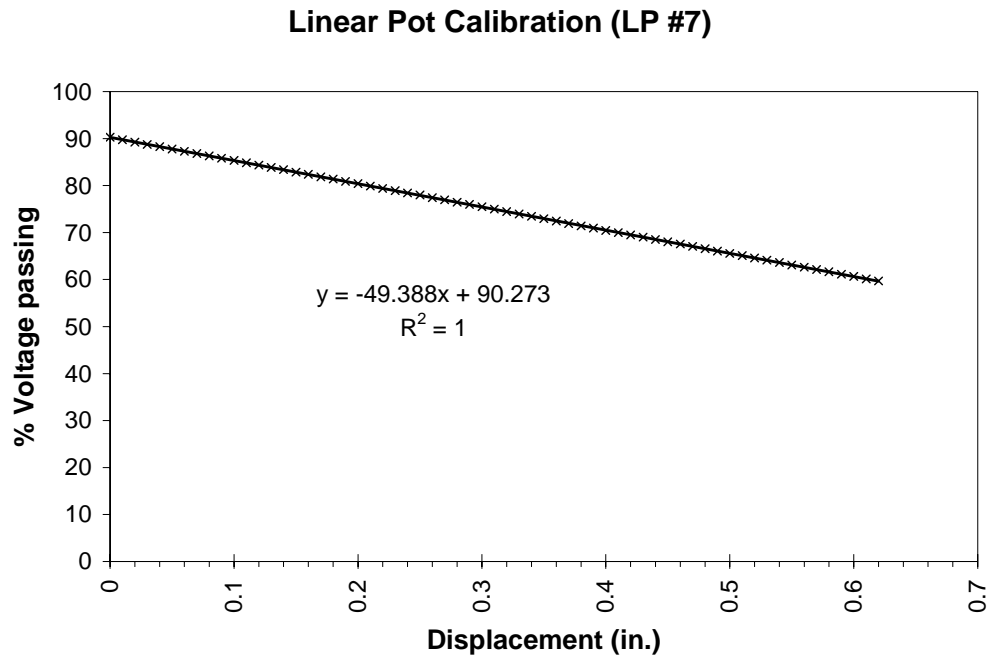


Figure 4.17: Typical Calibration Curve of a Linear Potentiometer for a Calibration Range of 60 to 90% of Full Compression

#### 4.4.2 REFERENCE FRAME

To measure the settlement of the foundation under each load and to measure the resulting settlement of the individual telltales, a reference frame was constructed in accordance with ASTM D 1194-94, “Bearing Capacity for Static Load on Spread Footings.” The frame was constructed of wooden 2 in. x 4 in. beams and was supported by steel stakes driven 20 in. into the ground. The steel stakes were located 8 ft from the center of the foundation as shown in Figure 4.18. The reference frame supported the linear potentiometers (linear pots) and the electrical circuits, as shown in Figures 4.19, 4.20 and 4.21.

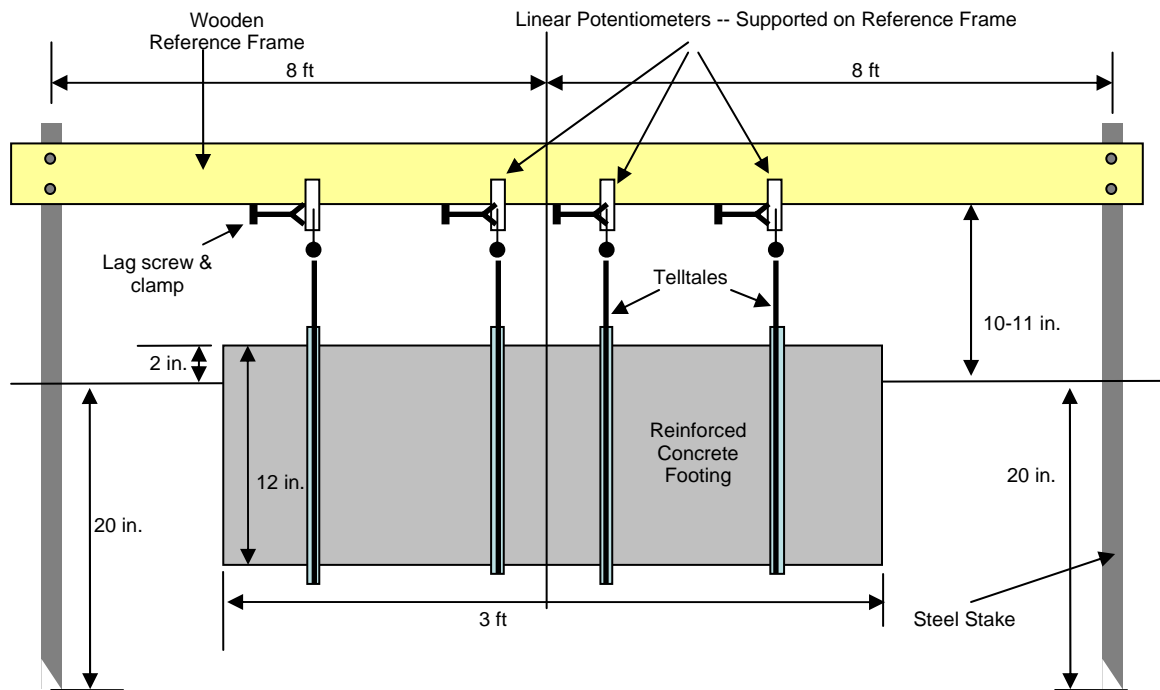


Figure 4.18: Arrangement of Reference Frame and Linear Potentiometers (not to scale)

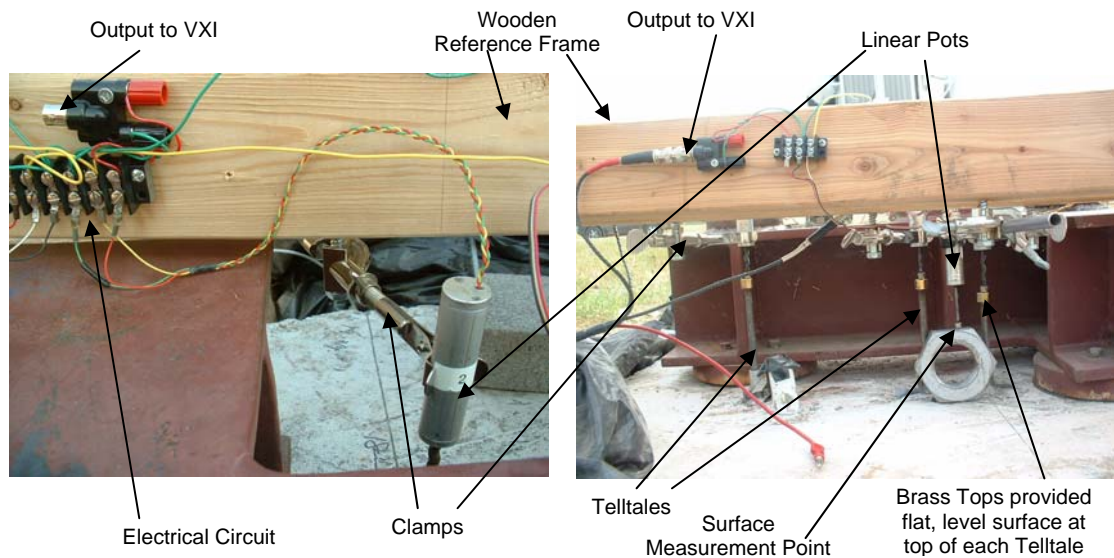


Figure 4.19: Pictures of Linear Potentiometers Supported by the Reference Frame

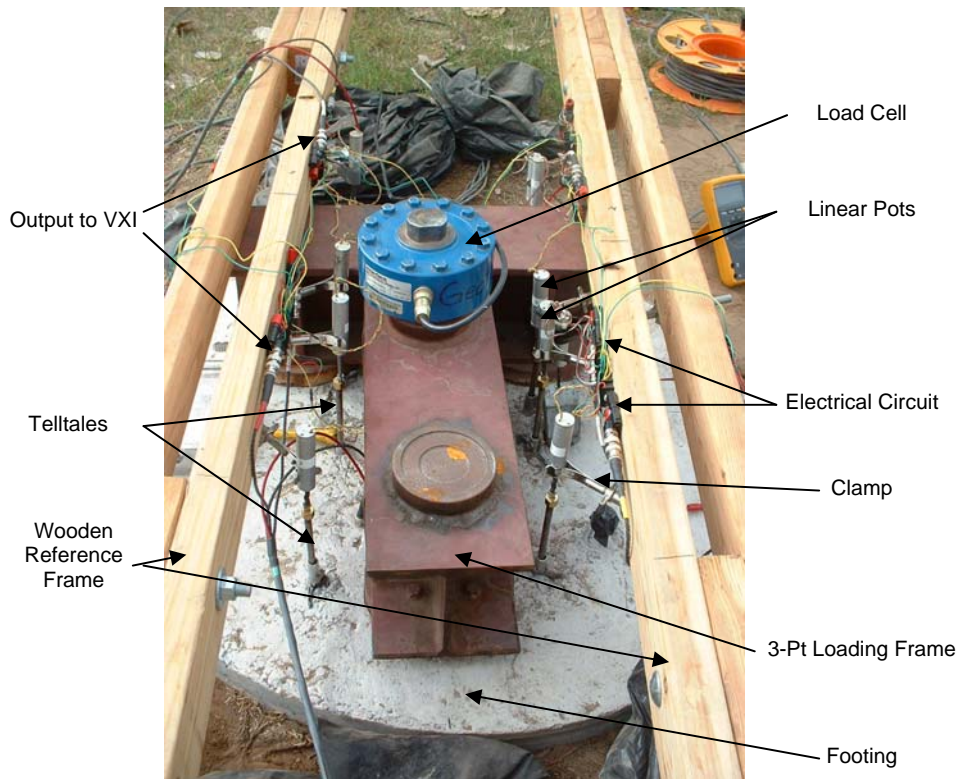


Figure 4.20: Plan View of Reference Frame over Footing and 3-Point Loading Frame

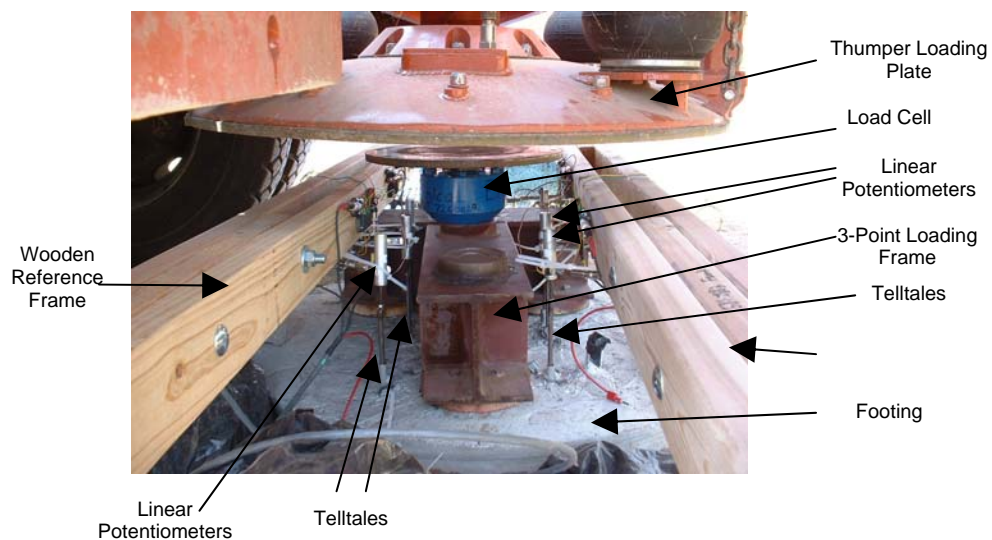


Figure 4.21: Arrangement of the Footing Instrumentation and Loading System

#### 4.4.3 LOAD CELL

A single, 50-kip (222 kN) load cell was used to measure the force applied to the footing. The load cell sensed the load by measuring the strain in a piece of precisely machined metal. The strain is measured using strain gauges bonded to metal beams within the load cell. The voltage drop across the circuit within the strain gauge is related to the strain in the metal which is in turn proportional to the load applied. The load cell was calibrated by the manufacturer, Interface Force.

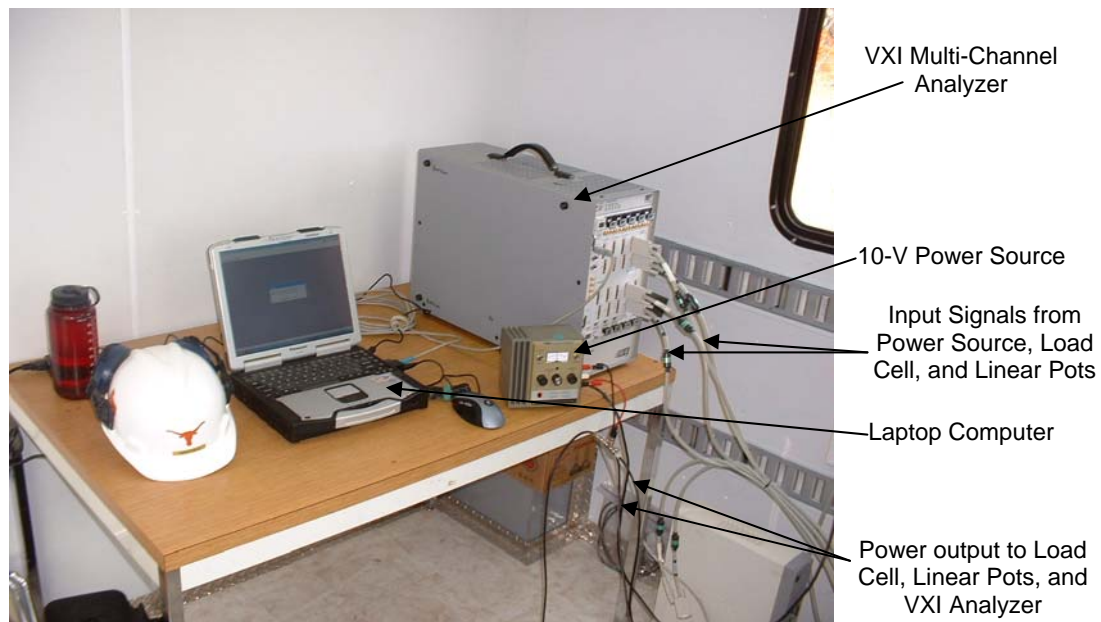


Figure 4.22: Arrangement of Recording Instruments in the Field

#### 4.4.4 VXI- MULTI-CHANNEL ANALYZER

A VXI Multi Channel Analyzer was used to measure and record the voltage output of each linear pot, the load cell, and the input voltage produced by the power source. The VXI is a 72-channel dynamic signal analyzer designed to record

extremely small variations in voltage rapidly and with precision. The VXI recorded voltage to the nearest 0.0001 volt at a rate of 32 readings per second, approximately 2000 readings per minute. This analyzer was selected because it had the capability to record multiple channels simultaneously, with tremendous accuracy.

#### **4.5 SUMMARY**

The experimental set-up in the field used to perform load tests on a small shallow footing is described in this chapter. A 3-ft diameter reinforced concrete footing was designed and constructed with telltales installed at four different depths beneath the footing. A load was applied using either T-Rex or Thumper. The load was directed through a load cell and a 3-point loading frame to the footing. The loading sequence occurred over a period of 3-4 minutes as further described in Chapter 5. The settlements of the footing and the soil mass beneath the footing were measured by linear potentiometers and recorded at a rate of about 2000 readings per minute on a VXI Multi-Channel Analyzer.

## **CHAPTER 5**

### **FIELD LOAD TESTS**

#### **5.1 INTRODUCTION**

In this chapter, the footing load tests conducted at the Capital Aggregates field site are discussed. The goal of these tests was to measure vertical settlements of the top of the footing and within the soil mass at various depths below the footing. These measurements are later used to assess the accuracy of various models that are used to predict the vertical settlement of shallow foundations on granular soils.

Several days of testing were required over a period of two months. For the tests discussed in this chapter, the footing was loaded to a maximum load of 20,000 lb, resulting in a maximum average footing pressure of 2800 psf. This load is estimated to be 35% of the ultimate bearing capacity of the footing. Under this load, the maximum measured settlement of the footing was very small (0.016 in.).

#### **5.2 FIELD TESTING PROCEDURE**

The testing procedure used to load and measure settlements of the footing and soil mass was modeled after the procedure outlined in ASTM D1194-94, "Bearing Capacity on Soil for Static Load on Spread Footings". This procedure was modified where necessary to improve the accuracy of the vertical settlement measurements.

Each day that testing was conducted, the following procedure was followed.

1. Remove the protective cover over the footing and adjacent soil. The footing was covered with two layers of tarps to protect the footing, telltales, and surrounding soil from foul weather.
2. Place the loading frame on the center of the footing. When possible, the loading frame was left in place between testing days so that it did not have to be reset.
3. Erect the reference frame by bolting it to the stakes driven in the ground. When possible, the reference frame was left in place between testing days. Hence, it was not required to reset it each testing day.
4. Connect the linear potentiometers to the reference frame.
5. Run twisted, shielded, BNC cables between the linear pots and the VXI dynamic signal analyzer.
6. Set-up the VXI analyzer, laptop computer, and power source.
7. Set the load cell on the 3-point loading frame.
8. Check the location (and center if necessary) of the 3-point loading frame.
9. Connect the load cell to the power source and the VXI analyzer.
10. Connect all linear pots to the power source and the VXI analyzer.
11. Connect the power source to the VXI analyzer.
12. Position the linear pots in place to record settlement.
13. Conduct an electronics check to ensure each linear pot was functioning and properly recording on the assigned channel.

14. Check to ensure each linear pot was set at an initial position between 50 to 90% of the fully compressed position. This check is done by reading the initial voltage of each linear pot which should be between 5 and 9 volts.
15. Take an initial record of the telltale positions using the linear pots.
16. Position the loading vehicle with the loading apparatus centered over the load cell.
17. Take a second record of telltale positions. This record indicates any movement of the footing due to movement of the loading vehicle close to the footing. Note: This step was eliminated after repeated measurements revealed that the placement of the loading vehicle had no effect on the initial position of the telltales.
18. Prepare the VXI to make measurements for 256 seconds at a rate of 32 measurements/sec (approximately 2000 measurements/min).
19. Initiate the recording. The load and displacement were equal to zero at the initiation of each test.
20. Initiate loading immediately after initiating recording. The loading was controlled by an operator increasing and decreasing the hydraulic pressure in the loading system. The operator monitored the load applied on a multi-meter throughout the test.
21. Complete the loading sequence which took approximately 4 minutes. This short time was selected for several reasons:
  - a) to minimize the influence of temperature on the reference frame and telltales,



- b) to minimize the influence of foundation/ground vibrations caused by truck traffic on the loading frame and reference frame, and
  - c) to avoid the influence of wind on the reference frame
22. Complete the recording.
  23. Repeat steps 18-22 for all desired load sequences.
  24. Upon completion of testing for the day, the loading system was removed from the site.
  25. Disconnect and remove all linear potentiometers and the load cell from the footing.
  26. Replace the protective cover over the footing.

### **5.3 MEASUREMENTS**

Measurements of the applied vertical load and resulting vertical settlement of the telltales and footing were taken throughout the time period of the test. Measurements were taken at a rate of about 2000 records per min. The VXI Analyzer was used to measure and record the voltage to the nearest 0.0001 Volt. The calibrated precision of each measurement was  $\pm 0.0005$  in. The following list details each measurement taken and its impact on the data analysis.

1. The voltage of the power supply was recorded. The power source was used to provide a 10V DC power supply to the linear pots and the load cell. It was important to know the precise input voltage because the output voltage of the linear pots and the load cell are a function of the input voltage provided by the power source.

2. The output voltage of the load cell was recorded. The output voltage was used to calculate the applied load on the footing. During each test, the load measured at any time ( $t$ ) was equal to the difference between the load recorded at time  $t$  and the load recorded at time  $t = 0$ . Thus, any background voltage in the strain gauge of the load cell was eliminated.
3. The output voltage of each linear potentiometer was recorded. This output voltage of each linear potentiometer was used to measure the movement of each telltale and the surface of the footing. During each test, the settlement measured at any time ( $t$ ) was equal to the difference between the position of the linear potentiometer recorded at time  $t$  and the position of the linear potentiometer recorded at time  $t = 0$ . Thus, the zero position was reset for each linear potentiometer for each test.

## 5.4 HISTORY OF TESTING

Table 5.1 presents the complete history of testing conducted in this study.

Table 5.1: History of the Load Tests at the Capitol Aggregates Field Site

Date	Purpose	# of tests	Peak load	Vibroseis	Remarks
9-Sep	Initial tests	1	9,000	Thumper	Data suggested footing rose from the ground
16-Sep	Temperature Tests	1	0	N/A	Tested reference apparatus to evaluate the impact of changing temperature over time.
30-Sep	Test	2	9,000	Thumper	Truck Traffic impact noted
18-Oct	Test	1	9,000	T-Rex	Good data, but only 1 test at each load and missing some data points
		1	18,000		
25-Oct	Test	4	5,000	T-Rex	Good data, but missing several important data points.
		4	20,000		
		4	23,000		
11-Nov	Final Tests	15	20,000	T-Rex	Complete data set

## **5.5 LOADING SEQUENCE**

The total testing time was determined from the results of a set of initial tests. During the initial tests on 9 Sep 2005, an incremental load was applied at 15-minute increments, per ASTM D1194-94. Settlement measurements were taken at each load step. The results of these initial tests indicated that the temperature change in ambient air temperature was sufficient to move the reference frame and thus negatively impact the measured settlements which were very small. Thus, the total time of the load sequence was reduced to eliminate or minimize the effects of temperature change. Since the measured settlements are essentially in the linear range and the soil is less than saturated, the reduction in testing time should not have an effect on the measured settlement of the footing or soil mass, other than any creep effect which was ignored in this study.

The second day of testing, 30 Sep 2005, revealed the influence of passing truck traffic on the recorded measurements. During load tests, it was visually observed that passing trucks crossing a cattle guard next to the site caused the reference frame to vibrate. The data collected also showed a clear spike in the measurements when trucks passed. Even though the influence of the truck traffic lasted only a few seconds, the zero position of the reference frame was disturbed and therefore the remainder of the test data was useless. The remainder of the tests were conducted only during periods of no traffic. However, traffic did pass in between tests. Thus, it was still required to reset the initial position of the linear pots at the beginning of each test.

Each test was conducted over a period of 256 seconds. However, the Load was applied and released in about 210 sec. During this time, the load was gradually applied for approximately 60 seconds, then it was held as close to constant as possible

for 30-90 seconds, then gradually removed over approximately 60 seconds. A typical record of the applied load versus time is shown in Figure 5.1.

The effect of this loading rate on pore pressures was also considered. Undisturbed soil samples were taken as part of the site characterization study of the Capitol Aggregates field site (Appendix C). Within the zone of influence, a depth of about 7 ft, the measured degree of saturation was  $< 90\%$  and the void ratio was approximately 0.5. Given this level of saturation and void ratio, it was assumed that no significant pore pressure changes occurred due to loading the footing.

## **5.6 LOADING LEVELS**

The focus of this study was on settlement in the linear and mildly nonlinear ranges that would be associated with working (not failure) load levels. Hence, it was important to ensure that much of the measured settlements were recovered during the unloading portion of each test. During the initial tests on the footing, the maximum load level was 5,000 lb, resulting in an average vertical stress of about 700 psf. The data from those tests indicated that the soil was within the elastic range at this load level. The maximum load applied was subsequently increased to 10,000 lb (~1400 psf) and a second series of tests was conducted. Again, the settlement measurements indicated that the soil remained in the elastic range. Finally, the maximum applied load was increased to 20,000 lb (~2800 psf). During the tests where this peak load was induced, the settlement measurements indicate nearly complete recovery of the induced settlements. The typical movements of four telltales measured during the loading illustrated in Figure 5.1 are shown in Figure 5.2.

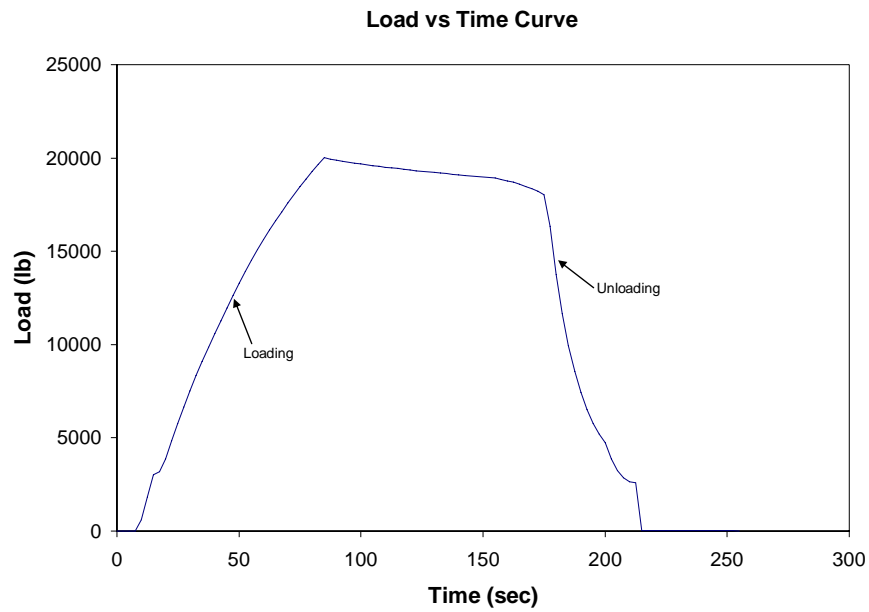


Figure 5.1: Typical Load vs. Time Measurement During an Individual Test.

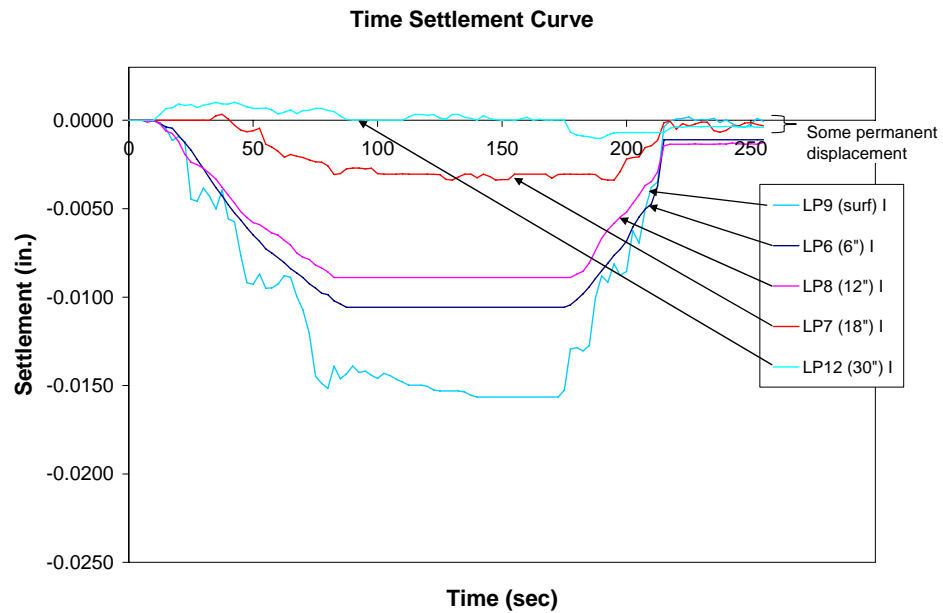


Figure 5.2: Typical Settlement Measurements During an Individual Test

## 5.7 FIELD TEST RESULTS

The results presented and discussed in this section were obtained from a series of five tests in which the footing was loaded to 20,000 lb and then completely unloaded in each test. The results from tests performed at lower loads show the same trends, although the movements of the footing and telltales under the lower peak loads are very small. The main conclusion that can be drawn from the earlier tests is that the footing settled no more than 0.001 in. under 10,000 lb and the data suggest that most of the deformation was recovered during unloading.

At a peak load of 20,000 lb, the bearing capacity analysis reveals that this load is still only about 40% of the estimated ultimate bearing capacity of the footing. The bearing capacity was calculated at 56,000 lb (8,000 psf) using Meyerhoff's equation (Meyerhoff, 1951) (Equation 5.1) for ultimate bearing capacity and neglecting the cohesion and surcharge terms. The 20,000-lb load level can be considered a reasonable "working load" that a geotechnical engineer might expect to be applied in the field. Thus, the footing was loaded to a factor of safety in the range of 2 to 2.5.

$$p_f = c N_c f_c + q N_q f_q + 0.5 B \gamma N_\gamma f_\gamma \quad (5.1)$$

where:  $p_f$  = bearing capacity at failure as a pressure,

$N_c$ ,  $N_q$ , and  $N_\gamma$  are dimensionless factors that depend on  $\phi$ ,

$c$  = soil cohesion,

$f_c$ ,  $f_q$ , and  $f_\gamma$  are correction factors,

$q$  = surcharge pressure at footing depth, and

$\gamma$  = unit weight.

The  $N_\gamma$  term was computed assuming  $\phi = 35$  degrees and using Ingra and Beacher's equation:

$$N_\gamma = \exp(-1.646 + 0.173\phi). \quad (5.2)$$

The result was  $N_\gamma = 82$ .

### **5.7.1 TABULATED MEASURED SETTLEMENTS**

The maximum load achieved in these tests was 20,000 lb +/-1%. In each test, over 8,000 data points were recorded. To present a useful data set, the data were averaged over 2.5 seconds which resulted in about 100 data points per test per measurement point. The results from one load test conducted as described above are presented in Table 5.2. The results from all the load tests conducted in this study, on 11 Nov 05, can be found in Appendix A. Each of the figures presented in this section were generated from the data in Table 5.2 and the tables in Appendix A.

### **5.7.2 TYPICAL LOAD-SETTLEMENT CURVE**

In Figures 5.3 through 5.8, typical load-settlement curves obtained from the measurements of settlement near the center of the footing during a single load-unload test are shown. The general response of the footing and soil can be observed in these plots. The notation of each telltale indicates the number of the linear potentiometer used (LP 1), the vertical position of the telltale (i.e. surface, 6, 12, 18, 30 in.), and the radial position of the telltale (I= interior, near the center of the footing, O = outer perimeter of the footing). As an example, LP6 (6")I is linear pot number 6 which is measuring the telltale at a depth of 6 in. at the interior of the footing.

Consider Figure 5.4 as an example. First, the potentiometer shows a general trend of increasing settlement nearly linearly with increasing load. Note the sign convention used in this study. Settlement was recorded as negative motion in the vertical direction.

Table 5.2: Tabulated Results From Field Load Test #3

Test # 3		Notes: -- Linear Pot #3 was determined to be damaged at the outset of these tests -- Linear Pot #4 failed to function properly during this test -- Each Telltale is labeled by the same notation: (LP# (Depth) I/O)									
Date: 11-Nov-05		Interior Telltales (I)					Perimeter Telltales (O)				
Time (sec)	Load (lbs)	LP9 (surf) I (in)	LP6 (6") I (in)	LP8 (12") I (in)	LP7 (18") I (in)	LP12 (30") I (in)	LP1 (surf) O (in)	LP3 (6") O (in)	LP2 (12") O (in)	LP4 (18") O (in)	LP10 (30") O (in)
MAX	19983	-0.0157	-0.0106	-0.0089	-0.0034	-0.0010	-0.0142	0.0000	-0.0073	-0.0056	-0.0010
0	0	0.0000	0.0000	0.0000	0.0000	0.0000	0.0000	0.0000	0.0000	0.0000	0.0000
2.5	-29	0.0000	0.0000	0.0000	0.0000	0.0000	0.0000	0.0000	0.0000	0.0000	0.0000
5	2	0.0000	0.0000	0.0000	0.0000	0.0000	0.0000	0.0000	0.0000	0.0000	0.0000
7.5	134	0.0000	0.0000	-0.0001	0.0000	0.0000	0.0000	0.0000	0.0000	0.0000	0.0000
10	1220	0.0000	0.0000	0.0000	0.0000	0.0000	0.0000	0.0000	0.0000	0.0000	0.0000
12.5	2417	-0.0001	-0.0002	-0.0002	0.0000	0.0003	-0.0009	0.0000	-0.0001	0.0001	0.0000
15	3076	-0.0005	-0.0004	-0.0006	0.0000	0.0007	-0.0016	0.0000	-0.0005	0.0002	0.0000
17.5	3460	-0.0011	-0.0005	-0.0007	0.0000	0.0007	-0.0020	0.0000	-0.0003	0.0003	0.0001
20	4347	-0.0009	-0.0009	-0.0012	0.0000	0.0009	-0.0028	0.0000	0.0000	0.0000	0.0005
22.5	5296	-0.0012	-0.0013	-0.0019	0.0000	0.0008	-0.0033	0.0000	0.0000	0.0003	0.0007
25	6208	-0.0045	-0.0017	-0.0024	0.0000	0.0009	-0.0038	0.0000	-0.0003	0.0000	0.0007
27.5	7079	-0.0046	-0.0022	-0.0025	0.0000	0.0007	-0.0048	0.0000	-0.0007	0.0003	0.0007
30	7915	-0.0038	-0.0027	-0.0027	0.0000	0.0009	-0.0059	0.0000	-0.0011	0.0011	0.0007
32.5	8712	-0.0043	-0.0033	-0.0030	0.0000	0.0009	-0.0062	0.0000	-0.0014	0.0003	0.0007
35	9477	-0.0050	-0.0038	-0.0033	0.0003	0.0010	-0.0070	0.0000	-0.0018	0.0010	0.0007
37.5	10217	-0.0039	-0.0043	-0.0038	0.0003	0.0009	-0.0078	0.0000	-0.0020	0.0000	0.0007
40	10934	-0.0056	-0.0048	-0.0042	0.0001	0.0009	-0.0082	0.0000	-0.0020	0.0000	0.0007
42.5	11626	-0.0058	-0.0052	-0.0047	-0.0003	0.0010	-0.0089	0.0000	-0.0023	0.0000	0.0007
45	12294	-0.0077	-0.0056	-0.0052	-0.0006	0.0009	-0.0091	0.0000	-0.0026	0.0000	0.0007
47.5	12962	-0.0092	-0.0061	-0.0055	-0.0006	0.0008	-0.0092	0.0000	-0.0030	0.0000	0.0007
50	13606	-0.0093	-0.0065	-0.0058	-0.0006	0.0007	-0.0089	0.0000	-0.0035	0.0000	0.0007
52.5	14217	-0.0087	-0.0068	-0.0059	-0.0005	0.0007	-0.0099	0.0000	-0.0042	0.0000	0.0007
55	14799	-0.0095	-0.0073	-0.0061	-0.0014	0.0007	-0.0104	0.0000	-0.0047	0.0000	0.0007
57.5	15352	-0.0095	-0.0075	-0.0064	-0.0015	0.0006	-0.0111	0.0000	-0.0050	0.0000	0.0007
60	15884	-0.0093	-0.0078	-0.0065	-0.0017	0.0004	-0.0118	0.0000	-0.0052	0.0000	0.0007
62.5	16389	-0.0088	-0.0080	-0.0068	-0.0021	0.0004	-0.0120	0.0000	-0.0054	0.0000	0.0007
65	16879	-0.0089	-0.0084	-0.0071	-0.0019	0.0006	-0.0126	0.0000	-0.0057	0.0000	0.0007
67.5	17351	-0.0099	-0.0086	-0.0075	-0.0020	0.0004	-0.0129	0.0000	-0.0057	0.0000	0.0006
70	17806	-0.0107	-0.0089	-0.0077	-0.0021	0.0005	-0.0129	0.0000	-0.0060	0.0000	0.0004
72.5	18241	-0.0121	-0.0092	-0.0079	-0.0022	0.0006	-0.0130	0.0000	-0.0062	0.0000	0.0003
75	18663	-0.0145	-0.0095	-0.0082	-0.0023	0.0007	-0.0132	0.0000	-0.0063	0.0000	0.0003
77.5	19069	-0.0149	-0.0098	-0.0083	-0.0024	0.0007	-0.0138	0.0000	-0.0065	0.0000	0.0003
80	19461	-0.0152	-0.0099	-0.0086	-0.0026	0.0006	-0.0140	0.0000	-0.0067	0.0000	0.0003
82.5	19833	-0.0139	-0.0102	-0.0089	-0.0031	0.0005	-0.0140	0.0000	-0.0067	0.0000	0.0003
85	19983	-0.0146	-0.0104	-0.0089	-0.0030	0.0002	-0.0141	0.0000	-0.0070	0.0000	0.0003
87.5	19914	-0.0143	-0.0106	-0.0089	-0.0028	0.0000	-0.0141	0.0000	-0.0070	0.0000	0.0003
90	19856	-0.0139	-0.0106	-0.0089	-0.0027	0.0000	-0.0142	0.0000	-0.0070	0.0000	0.0003
92.5	19799	-0.0143	-0.0106	-0.0089	-0.0027	0.0000	-0.0142	0.0000	-0.0070	0.0000	0.0003
95	19745	-0.0142	-0.0106	-0.0089	-0.0028	0.0000	-0.0142	0.0000	-0.0070	0.0000	0.0003
97.5	19700	-0.0144	-0.0106	-0.0089	-0.0027	0.0000	-0.0142	0.0000	-0.0070	0.0000	0.0003
100	19656	-0.0146	-0.0106	-0.0089	-0.0030	0.0000	-0.0142	0.0000	-0.0070	0.0000	0.0003
102.5	19613	-0.0143	-0.0106	-0.0089	-0.0030	0.0000	-0.0142	0.0000	-0.0070	0.0000	0.0003
105	19574	-0.0144	-0.0106	-0.0089	-0.0030	0.0000	-0.0142	0.0000	-0.0070	0.0000	0.0003
107.5	19535	-0.0146	-0.0106	-0.0089	-0.0030	0.0000	-0.0142	0.0000	-0.0070	0.0000	0.0003
110	19495	-0.0148	-0.0106	-0.0089	-0.0030	0.0000	-0.0142	0.0000	-0.0070	0.0000	0.0003
112.5	19455	-0.0150	-0.0106	-0.0089	-0.0030	0.0002	-0.0142	0.0000	-0.0070	0.0000	0.0003
115	19419	-0.0150	-0.0106	-0.0089	-0.0030	0.0003	-0.0142	0.0000	-0.0070	0.0000	0.0003
117.5	19382	-0.0150	-0.0106	-0.0089	-0.0030	0.0003	-0.0142	0.0000	-0.0070	0.0000	0.0003
120	19347	-0.0151	-0.0106	-0.0089	-0.0030	0.0003	-0.0142	0.0000	-0.0070	0.0000	0.0003
122.5	19312	-0.0152	-0.0106	-0.0089	-0.0031	0.0003	-0.0142	0.0000	-0.0070	0.0000	0.0003
125	19278	-0.0153	-0.0106	-0.0089	-0.0031	0.0001	-0.0142	0.0000	-0.0070	0.0000	0.0003
127.5	19246	-0.0153	-0.0106	-0.0089	-0.0033	0.0001	-0.0142	0.0000	-0.0070	0.0000	0.0003
130	19214	-0.0153	-0.0106	-0.0089	-0.0034	0.0003	-0.0142	0.0000	-0.0070	0.0000	0.0003
132.5	19184	-0.0153	-0.0106	-0.0089	-0.0032	0.0003	-0.0142	0.0000	-0.0070	0.0000	0.0003
135	19150	-0.0154	-0.0106	-0.0089	-0.0030	0.0002	-0.0142	0.0000	-0.0070	0.0000	0.0003



Table 5.2: Tabulated Results from Field Load Test #3 (continued)

Test # 3		Notes: -- Linear Pot #3 was determined to be damaged at the outset of these tests -- Linear Pot #4 failed to function properly during this test -- Each Telltale is labeled by the same notation: (LP# (Depth) I/O)									
Date: 11-Nov-05		Interior Telltales (I)					Perimeter Telltales (O)				
Time (sec)	Load (lbs)	LP9 (surf) I (in)	LP6 (6") I (in)	LP8 (12") I (in)	LP7 (18") I (in)	LP12 (30") I (in)	LP1 (surf) O (in)	LP3 (6") O (in)	LP2 (12") O (in)	LP4 (18") O (in)	LP10 (30") O (in)
137.5	19119	-0.0155	-0.0106	-0.0089	-0.0030	0.0001	-0.0142	0.0000	-0.0070	0.0019	0.0003
140	19089	-0.0157	-0.0106	-0.0089	-0.0032	0.0000	-0.0141	0.0000	-0.0070	0.0019	0.0003
142.5	19057	-0.0157	-0.0106	-0.0089	-0.0030	0.0003	-0.0140	0.0000	-0.0070	0.0019	0.0003
145	19026	-0.0157	-0.0106	-0.0089	-0.0032	0.0001	-0.0140	0.0000	-0.0070	0.0018	0.0003
147.5	18994	-0.0157	-0.0106	-0.0089	-0.0034	0.0000	-0.0139	0.0000	-0.0070	0.0018	0.0003
150	18974	-0.0157	-0.0106	-0.0089	-0.0034	0.0000	-0.0140	0.0000	-0.0070	0.0018	0.0003
152.5	18946	-0.0157	-0.0106	-0.0089	-0.0034	0.0000	-0.0141	0.0000	-0.0070	0.0017	0.0003
155	18890	-0.0157	-0.0106	-0.0089	-0.0030	0.0000	-0.0139	0.0000	-0.0070	0.0018	0.0003
157.5	18811	-0.0157	-0.0106	-0.0089	-0.0030	0.0001	-0.0139	0.0000	-0.0070	0.0017	0.0003
160	18738	-0.0157	-0.0106	-0.0089	-0.0030	0.0002	-0.0140	0.0000	-0.0070	0.0017	0.0003
162.5	18644	-0.0157	-0.0106	-0.0089	-0.0030	0.0000	-0.0139	0.0000	-0.0070	0.0017	0.0003
165	18532	-0.0157	-0.0106	-0.0089	-0.0030	0.0001	-0.0139	0.0000	-0.0071	0.0017	0.0003
167.5	18410	-0.0157	-0.0106	-0.0089	-0.0030	0.0000	-0.0139	0.0000	-0.0073	0.0017	0.0003
170	18295	-0.0157	-0.0106	-0.0089	-0.0033	0.0000	-0.0139	0.0000	-0.0073	0.0017	0.0003
172.5	18144	-0.0157	-0.0106	-0.0089	-0.0031	0.0000	-0.0139	0.0000	-0.0073	0.0017	0.0003
175	17460	-0.0153	-0.0106	-0.0089	-0.0030	0.0000	-0.0139	0.0000	-0.0073	0.0017	0.0002
177.5	14990	-0.0129	-0.0104	-0.0089	-0.0030	-0.0007	-0.0139	0.0000	-0.0073	0.0017	-0.0001
180	12682	-0.0129	-0.0101	-0.0087	-0.0031	-0.0008	-0.0130	0.0000	-0.0070	0.0017	-0.0006
182.5	10789	-0.0131	-0.0098	-0.0085	-0.0031	-0.0009	-0.0126	0.0000	-0.0069	0.0017	-0.0009
185	9236	-0.0127	-0.0094	-0.0081	-0.0031	-0.0009	-0.0120	0.0000	-0.0067	0.0017	-0.0010
187.5	7979	-0.0101	-0.0090	-0.0074	-0.0031	-0.0010	-0.0109	0.0000	-0.0067	0.0017	-0.0010
190	6953	-0.0088	-0.0085	-0.0067	-0.0033	-0.0010	-0.0100	0.0000	-0.0064	0.0018	-0.0010
192.5	6134	-0.0092	-0.0081	-0.0062	-0.0034	-0.0008	-0.0089	0.0000	-0.0063	0.0018	-0.0010
195	5479	-0.0081	-0.0076	-0.0058	-0.0034	-0.0007	-0.0088	0.0000	-0.0060	0.0018	-0.0010
197.5	4962	-0.0088	-0.0073	-0.0055	-0.0029	-0.0007	-0.0086	0.0000	-0.0058	0.0008	-0.0010
200	4377	-0.0085	-0.0068	-0.0052	-0.0022	-0.0007	-0.0084	0.0000	-0.0055	0.0009	-0.0010
202.5	3512	-0.0062	-0.0060	-0.0047	-0.0021	-0.0007	-0.0071	0.0000	-0.0048	0.0000	-0.0010
205	3046	-0.0069	-0.0055	-0.0042	-0.0021	-0.0007	-0.0064	0.0000	-0.0042	0.0001	-0.0009
207.5	2720	-0.0051	-0.0050	-0.0037	-0.0016	-0.0007	-0.0057	0.0000	-0.0035	0.0010	-0.0010
210	2606	-0.0038	-0.0047	-0.0035	-0.0014	-0.0007	-0.0057	0.0000	-0.0032	0.0005	-0.0010
212.5	1715	-0.0035	-0.0037	-0.0029	-0.0011	-0.0007	-0.0042	0.0000	-0.0024	0.0012	-0.0009
215	28	-0.0004	-0.0011	-0.0014	-0.0001	-0.0007	-0.0010	0.0000	-0.0007	0.0026	-0.0007
217.5	30	0.0000	-0.0011	-0.0014	0.0000	-0.0004	-0.0010	0.0000	-0.0007	0.0013	-0.0007
220	31	0.0001	-0.0011	-0.0014	-0.0005	-0.0004	-0.0010	0.0000	-0.0007	0.0020	-0.0007
222.5	31	0.0001	-0.0011	-0.0014	-0.0002	-0.0004	-0.0010	0.0000	-0.0007	0.0028	-0.0007
225	30	0.0002	-0.0011	-0.0014	-0.0003	-0.0003	-0.0010	0.0000	-0.0007	0.0026	-0.0007
227.5	33	0.0000	-0.0011	-0.0013	-0.0002	-0.0003	-0.0010	0.0000	-0.0007	0.0027	-0.0007
230	30	0.0001	-0.0011	-0.0014	-0.0001	-0.0004	-0.0010	0.0000	-0.0007	0.0027	-0.0007
232.5	30	0.0000	-0.0011	-0.0014	-0.0001	-0.0003	-0.0009	0.0000	-0.0007	0.0030	-0.0007
235	29	0.0001	-0.0011	-0.0014	-0.0006	-0.0004	-0.0010	0.0000	-0.0007	0.0031	-0.0007
237.5	24	-0.0001	-0.0011	-0.0013	-0.0007	-0.0004	-0.0009	0.0000	-0.0007	0.0031	-0.0007
240	23	0.0000	-0.0011	-0.0013	-0.0006	-0.0003	-0.0010	0.0000	-0.0007	0.0031	-0.0007
242.5	25	-0.0002	-0.0011	-0.0013	-0.0003	-0.0003	-0.0010	0.0000	-0.0007	0.0031	-0.0007
245	20	-0.0003	-0.0011	-0.0013	-0.0003	-0.0004	-0.0009	0.0000	-0.0007	0.0031	-0.0007
247.5	20	-0.0004	-0.0011	-0.0014	-0.0002	-0.0004	-0.0010	0.0000	-0.0007	0.0031	-0.0007
250	17	-0.0002	-0.0011	-0.0013	-0.0001	-0.0004	-0.0009	0.0000	-0.0007	0.0032	-0.0007
252.5	16	0.0001	-0.0011	-0.0014	-0.0002	-0.0004	-0.0007	0.0000	-0.0007	0.0031	-0.0007
255	12	-0.0001	-0.0011	-0.0013	-0.0003	-0.0004	-0.0007	0.0000	-0.0007	0.0032	-0.0007

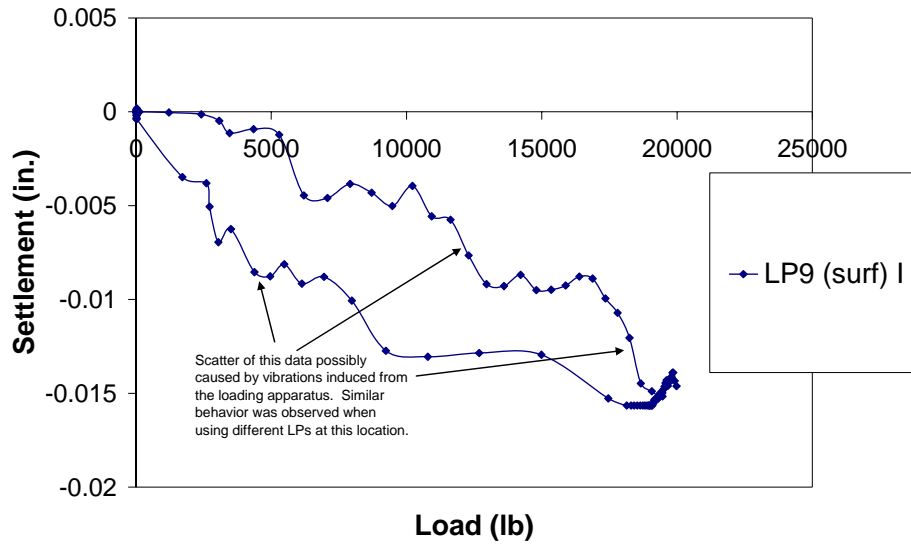


Figure 5.3: Typical Settlement Measurements of the Top of the Footing near the Center

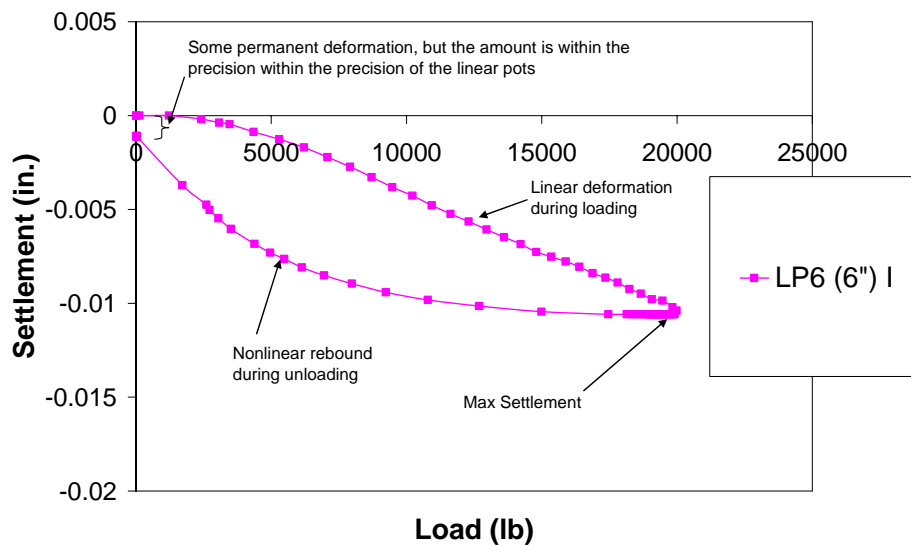


Figure 5.4: Typical Settlement Measurements of Telltale at 6 in. Beneath the Center of the Footing

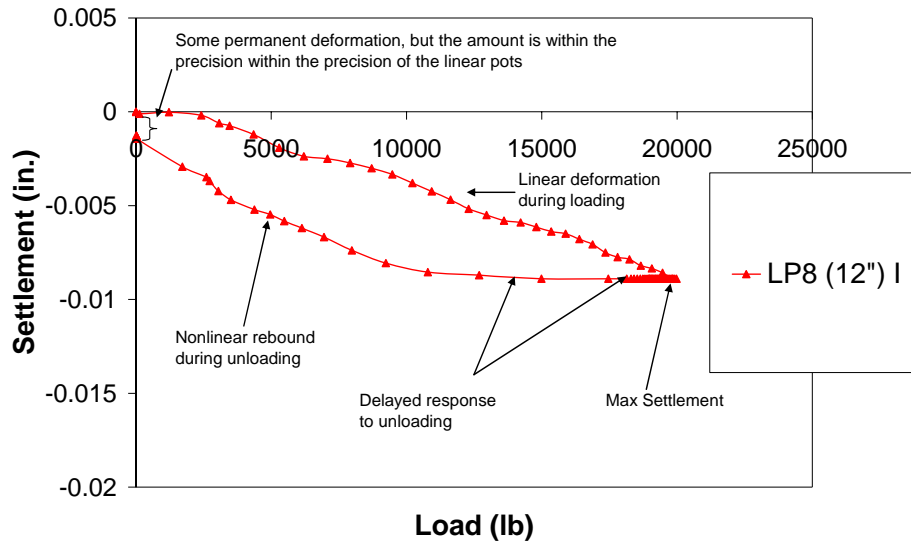


Figure 5.5: Typical Settlement Measurements of Telltale at 12 in. Beneath the Center of the Footing

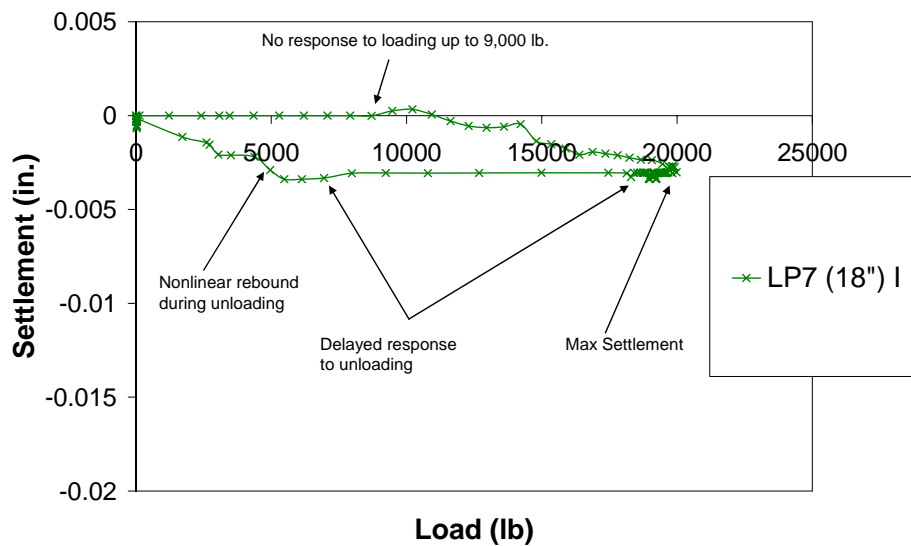


Figure 5.6: Typical Settlement Measurements of Telltale at 18 in. Beneath the Center of the Footing

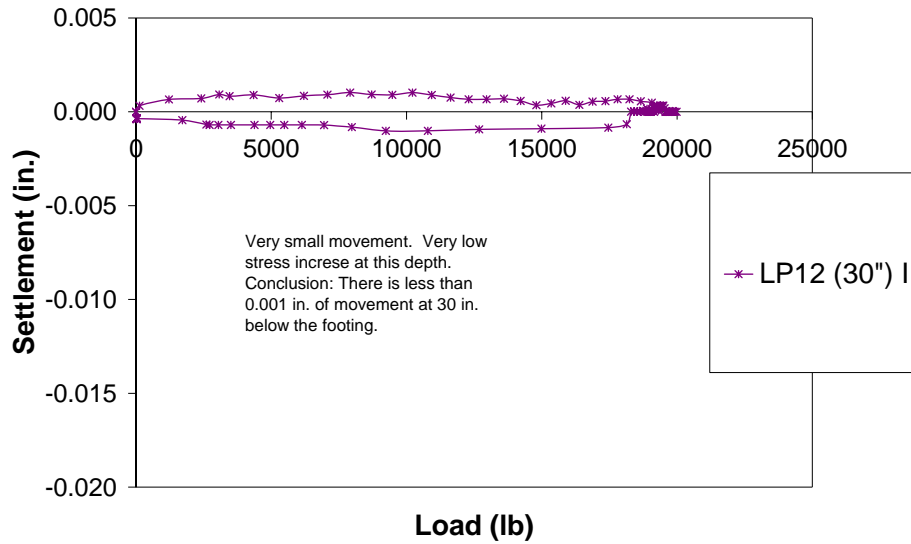


Figure 5.7: Typical Settlement Measurements of Telltale at 30 in. Beneath the Center of the Footing

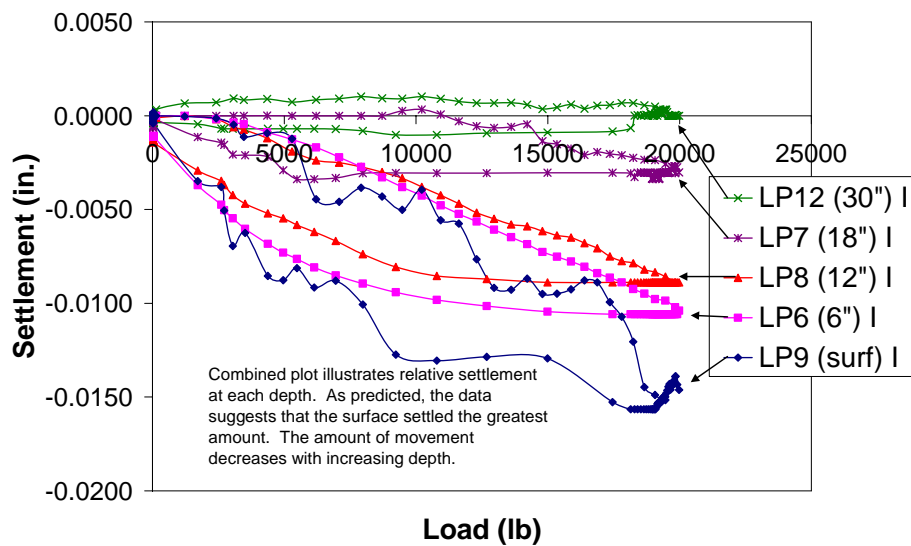


Figure 5.8: Comparison of Typical Settlement Measurements of the Surface and the Telltales Beneath the Center of the Footing

Second, during the unload phase of the test, the soil did not rebound on the same curve recorded during loading. These data suggest slight non-linear behavior of the soil mass. It should be noted in the test presented in Figure 5.4, the total permanent settlement after unloading was less than 0.002 in. This amount of permanent settlement was not recorded for all tests during this study. The final position of telltales varied from zero to -0.010 in. from the telltales' original position with an average of approximately -0.004 in. Some of this apparent permanent deformation may be due to movement of the reference frame in the wind. However, given the very small deformations and the relative precision of the linear potentiometers, it was difficult to distinguish actual non-linearity of the soil from movement in the measurement apparatus.

Third, each telltale begins to move at a slightly different load. The measured settlement at the surface and 6 in. below the surface show movement at approximately 1000 lb. On the other hand, the telltales at depths of 12 in. and 18 in. do not record any settlement until loads of about 3000 lb and 9000 lb, respectively. The telltale at 30 in. indicates almost no response to the loading or unloading. This observation confirms the expectation that greater loads are required to induce measurable settlements at greater depths (as expected due to stress distribution). This observation also indicates that the telltales are indeed moving independently from one another as designed.

Fourth, the maximum settlement of each point under the footing can be determined. The maximum settlement of each point was expected to decrease with increasing depth. In all of these tests, the data show the expected trend. The measured settlement of the surface of the footing shows the greatest movement while

the telltale at 30 in. below the footing shows very little movement. This point is illustrated in Figure 5.8 in which all the load-settlement curves are placed on the same graph.

### **5.7.3 PEAK SETTLEMENTS**

As noted previously, each test reached a peak load of about 20,000 lb and the induced settlement was nearly completely recovered during each test. Thus a comparison can be made of the peak measured settlements at each location for these tests. In Figures 5.9 and 5.10, the peak measured settlements of each telltale near the center and perimeter of the footing are shown, respectively. This figure illustrates several important points as discussed below.

First, the initial test during this series of tests showed the highest settlements for each measurement point. On the days in which multiple load tests were run with the same peak load, 25 Oct and 11 Nov, the tests were run in a series of four or five tests. Between series of tests, the data was analyzed and linear pots were repositioned. Typically, the time between series of tests was no more than one hour. It was recognized that the first test in each series, consistently showed greater settlement and less rebound, for all measurement points, than the following tests. It is believed that the measured settlements during the first test in each series reflect an unknown amount of seating which occurred in response to the applied load. The tests which followed the initial “seating” test reflect a more accurate description of the soil behavior under loading and unloading. So, the first test in each series was discarded from further analysis.

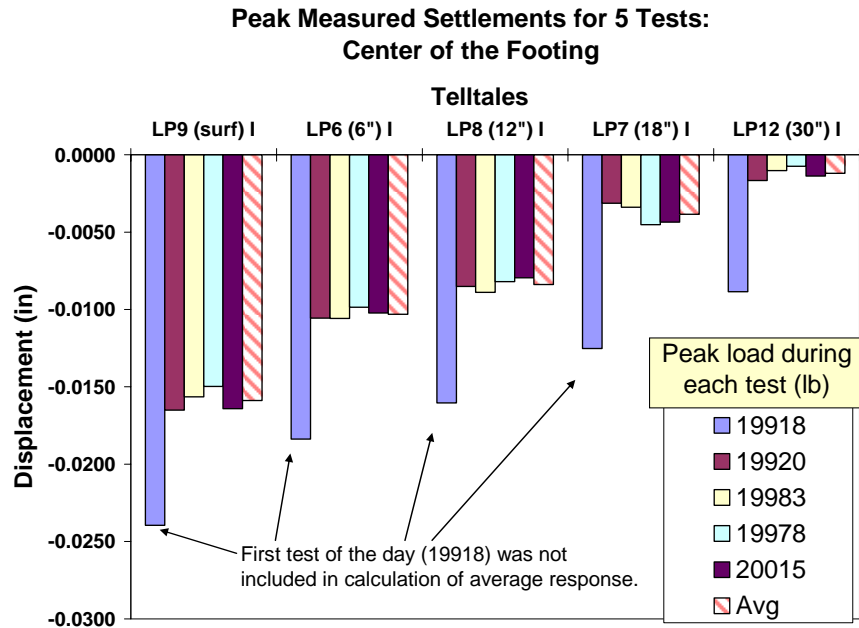


Figure 5.9: Comparison of Peak Measured Settlements Near the Center of the Footing Under a Static Load of 20,000 lb

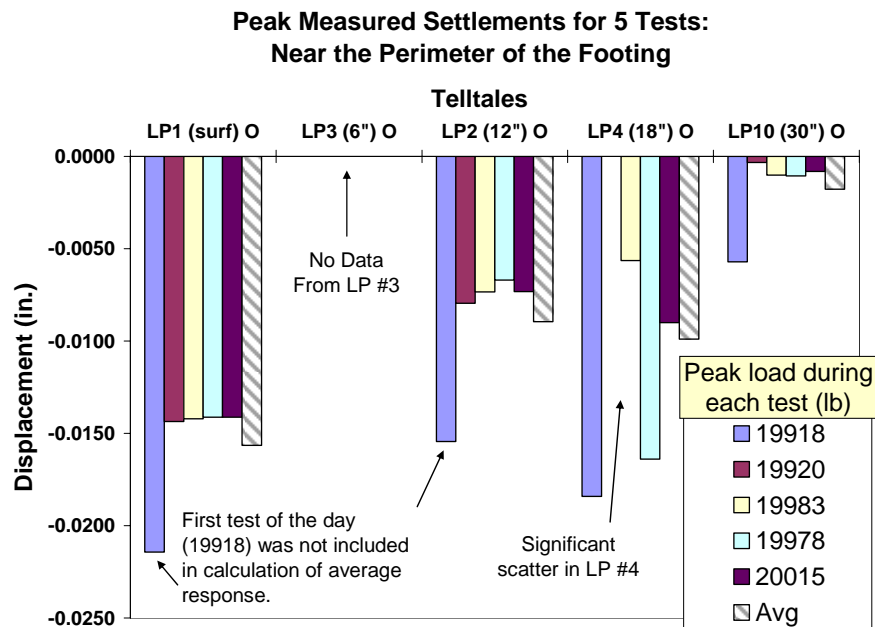


Figure 5.10: Comparison of Peak Measured Settlements Near the Perimeter of the Footing Under a Static Load of 20,000 lb

Second, the precision of the measurement technique appears very good. Nearly the same peak settlement was measured during each test, with the exception of the first test which was discarded.

Third, no apparent correlation can be seen between the slight differences in load and the slight differences in measured settlement. This observation gives further credit to the idea that the source of the differences in measured settlements is influenced more by random variability than differences in load. A certain amount of random variability was expected from uncontrollable variables at the site.

Fourth, by averaging the measured settlements during each test, the random variability within each measurement can be reduced. Further analysis using the averaged settlements yield a more accurate picture of the behavior of the soil under this load as discussed subsequently.

Fifth, the measured settlements of telltales near the center of the footing are very similar in magnitude to the settlements measured of telltales near the perimeter of the footing. As can be seen in Table 5.2 and Figure 5.10, two of the linear potentiometers failed during testing. Thus, a complete set of data points for the telltales near the perimeter was not recorded for any single series of tests. The linear potentiometers were moved from point to point between series of tests to obtain a full record of the behavior of each point during loading and unloading. Henceforth, the measured settlements near the center of the footing were selected for discussion, since a measurement was made for each of the five interior measurement points during each of the 15 tests conducted. The full record of record measurements near the perimeter of the footing is presented in Appendix A.



#### 5.7.4 MEASURED VERTICAL STRAIN DISTRIBUTION

The settlement measurements were also used to calculate the vertical strain at various depths beneath the footing. The vertical strain was calculated by dividing the difference in settlement between adjacent telltales by the original vertical distance between the telltales ( $\epsilon_v = \Delta \ell / \ell$ ). This vertical strain was plotted at a depth equal to the midpoint between the telltales. The calculated vertical strains are presented in Table 5.3. The measured vertical strain distribution with depth is shown in Figure 5.11. The measured data indicate that the peak strain amplitude occurs at a higher elevation than predicted by Schmertmann (1970), who predicted a peak strain amplitude at a depth of  $B/2$ . The shape of the measured strain distribution does not match Schmertmann's theoretical curve. Schmertmann's strain distribution curve is discussed further in Chapter 6. This difference may be due to the fact that the upper material is a silty sand (SM) while the soil below is a sandy silt (ML).

Table 5.3: Measured Vertical Strain Beneath the Footing During Test #3

<b>Telltale Depths</b>	<b>Layer Midpoints</b>	<b>Total Measured Movement</b>	<b>Compression of Each Layer</b>	<b>Strain in each Layer</b>
<b>Depth, z ft</b>	<b>Depth ft</b>	<b><math>\Delta z</math> in.</b>	<b>in.</b>	<b>%</b>
0	0.25	0.0159	0.00558	0.09302
0.5	0.75	0.0103	0.00192	0.03197
1	1.25	0.0084	0.00454	0.07572
1.5	2	0.0038	0.00265	0.02209
2.5	4.25	0.0012	0.00119	0.00284
6				
* The settlement at 6 ft beneath the footing was assumed to be zero.				

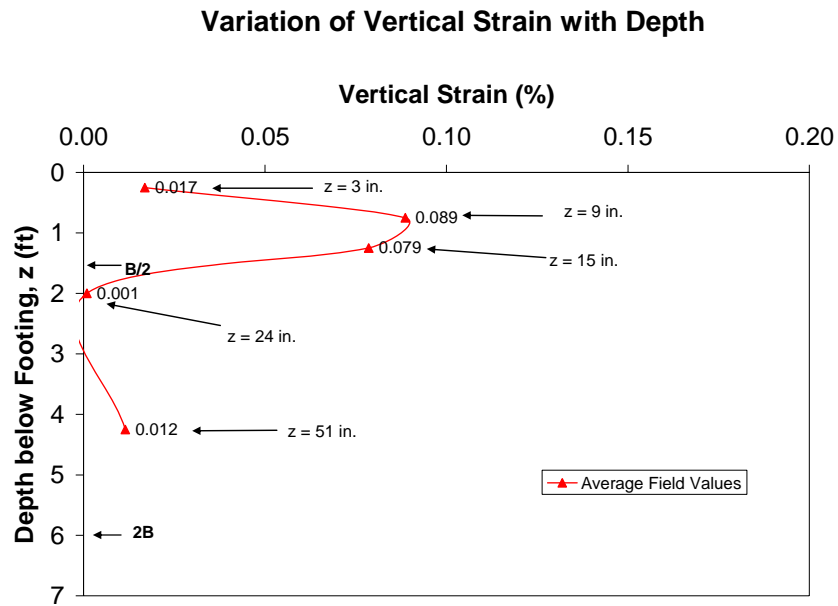


Figure 5.11: Measured Variation of Vertical Strain with Depth Beneath the Footing

It is difficult to compare calculated vertical strains in this study because the movements recorded were very small (maximum settlement  $< 0.02$  in.) and thus the difference between adjacent points beneath the footing was even smaller ( $\sim 0.001$  to  $0.01$  in.). Since the precision of the linear potentiometers was only  $\pm 0.0005$  in., one must be careful in drawing conclusions about the relative vertical strain distribution beneath the footing. The data suggest that the strain distribution generally follows the theoretical distribution proposed by Schmertmann, but the precision of the linear pots preclude any strong conclusions. One important point that can be concluded is that the maximum induced vertical strains below the foundation, under a load of 2800 psf, is less than 0.1%.

### **5.7.5 COMPARISON OF MEASURED SETTLEMENTS AT EACH DEPTH**

Settlements were measured at two radial distances away from the center of the footing. At each radial distance, measurements of the surface of the footing and at each depth below the footing were recorded. At each elevation, one measurement was taken approximately 4 in. from the center of the footing and another measurement was taken approximately 13 in. from the center. The discussion below focuses on the telltales closer to the center of the footing. The plots of the telltales at 13 in. from the center of the footing can be found in Appendix A.

In Figure 5.12, the measured settlements of the surface during each of the four tests are presented. The data indicate that the settlement of the surface is fairly consistent for each test. The measurement record appears to be adversely impacted by outside vibrations throughout the test. This same pattern is not seen in the records of settlements below the surface of the footing. A closer look at the time records of each test revealed that the vibration noise was not recorded until the hydraulic ram made contact with the load cell during each test. So, this noise seems to originate from the motor on the Vibroseis truck operating the hydraulic ram.

In Figures 5.13 to 5.16, the measured settlements of the telltales at depths of 6, 12, 18, and 30 in. beneath the footing during each of the four tests are presented, respectively. The data indicates that the behavior of the soil beneath the footing was the same during each load and unload cycle. For each depth, the telltales show the same response to the load and unload cycle.

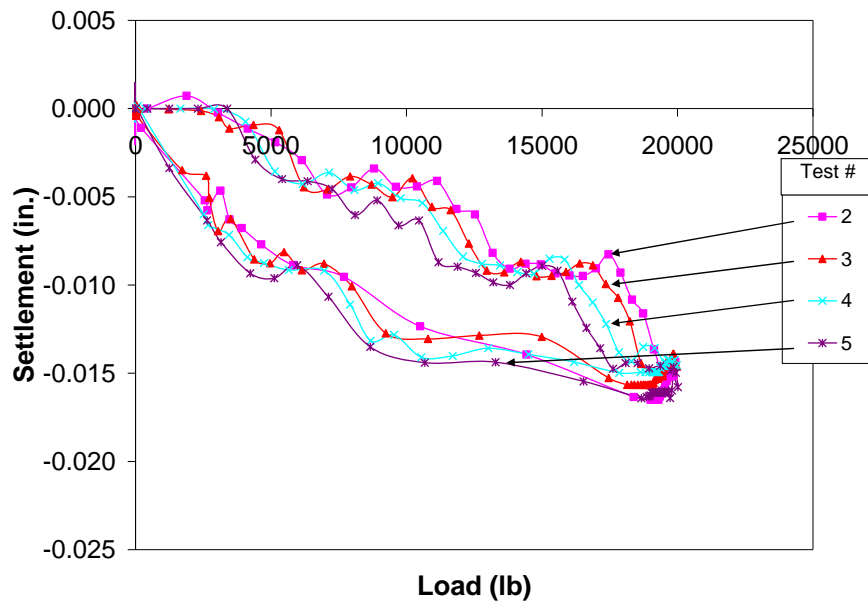


Figure 5.12: Measured Settlements of the Top of the Footing for Four Tests

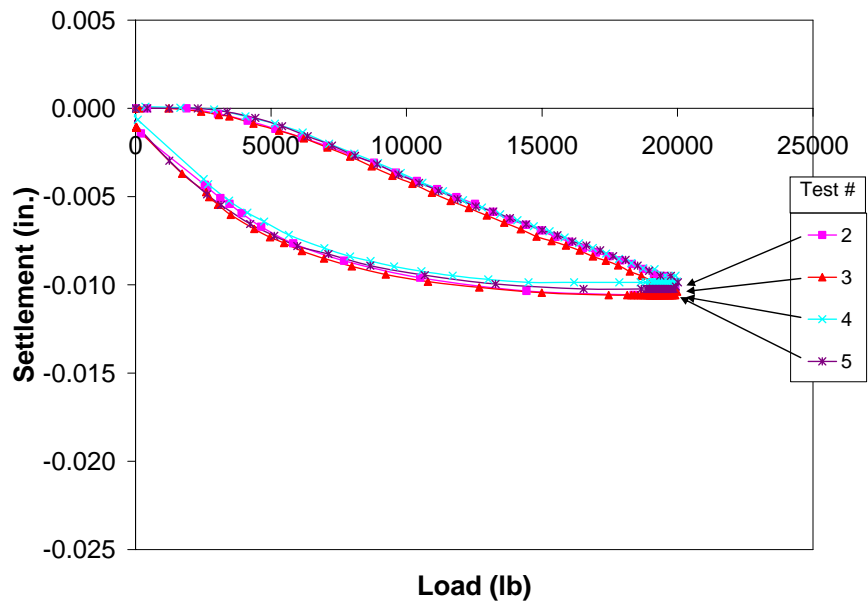


Figure 5.13: Measured Settlements at 6 in. Beneath the Footing for Four Tests

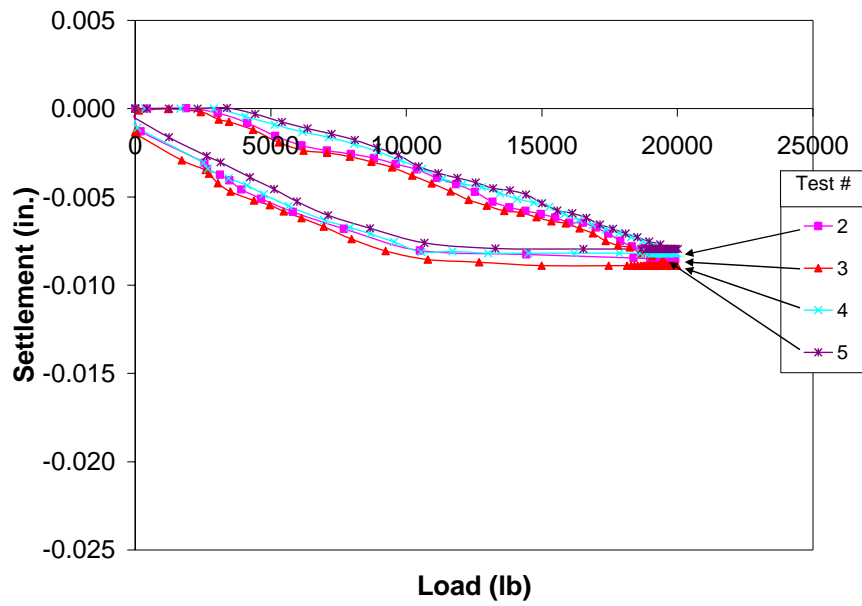


Figure 5.14: Measured Settlements at 12 in Beneath the Footing for Four Tests

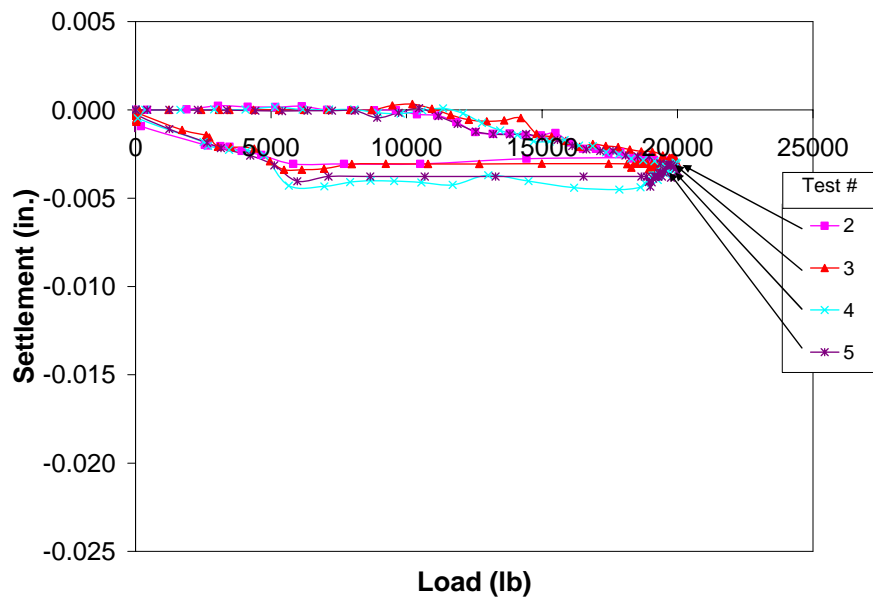


Figure 5.15: Measured Settlements at 18 in. Beneath the Footing for Four Tests

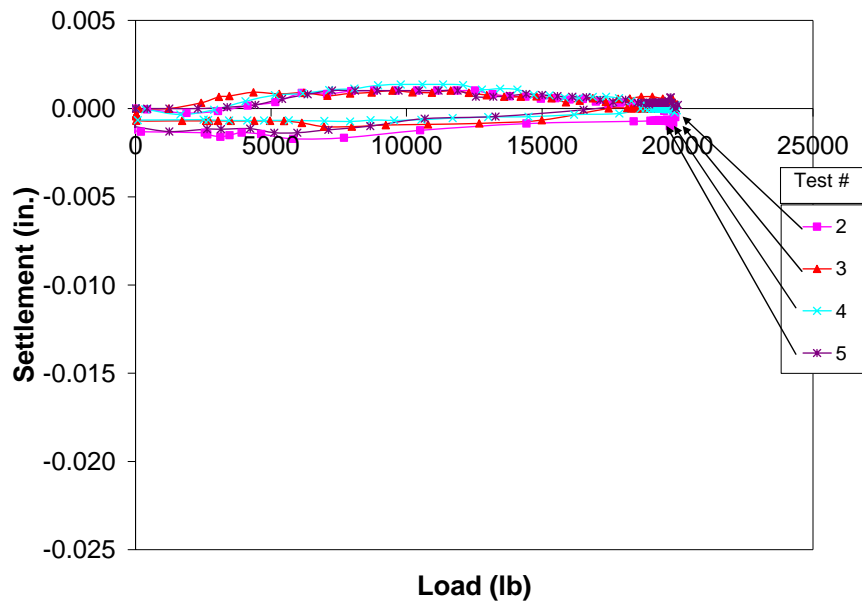


Figure 5.16: Measured Settlements at 30 in. Beneath the Footing for Four Tests

## 5.8 SUMMARY

A series of load tests was conducted on a 3-ft diameter footing at the Capitol Aggregates field site to measure the settlement of the footing and the soil mass beneath it. A series of initial tests refined the test procedure and eliminated several sources of variability. The final set of tests is discussed in this chapter. These results are compared to predicted settlements in Chapter 7. The measured response of the soil was shown to be very consistent over a series of tests with a peak load of 20,000 lb.

## **CHAPTER 6**

### **SETTLEMENT PREDICTIONS OF THE CENTER OF THE FOOTING**

#### **6.1 INTRODUCTION**

Over the years, several analytical and empirical techniques have been developed to predict the settlement of shallow foundations. In sandy soils, due to the difficulty in obtaining undisturbed samples, these analytical techniques primarily use data from in-situ tests such as the SPT or CPT. In recent years, the improvement in finite element analysis software and its widespread usage have enabled engineers to employ numerical analytical techniques to these types of problems as well. However, these numerical techniques do not solve the problems associated with estimating the material properties of soil. Nonetheless, they can assist the engineer in conducting a more robust analysis of complicated geometry or layered systems which previously were evaluated analytically with various simplifying assumptions.

In this chapter, two semi-empirical models and one numerical model are used to predict the deformation of the soil mass beneath the 3-ft diameter prototype footing. The first semi-empirical model is the method of settlement prediction originally proposed by Schmertmann in 1970. This model, as used in this study, is based on correlating the stiffness of each layer with the SPT blow count. The second semi-empirical model used is the method proposed by Burland and Burbidge, 1985. This model is based purely on the SPT blow count. The numerical model involves using the finite element program, PLAXIS. Where possible, the variation in vertical

movements with depth beneath the footing are predicted. Also, strain distribution with depth are illustrated and compared.

To compare the site characterization techniques used in this study, Schmertmann's method was applied with two different sets of data; once using the data gathered from the SPT tests and then again using the results of SASW testing. Similarly, the finite element analysis was performed three times using moduli from field SASW, field crosshole tests and laboratory RC tests. In this way, the influence of the in situ test could be distinguished from the other assumptions of each analytical technique. Additionally, the difference between global dynamic moduli (from SASW testing), local dynamic moduli (from crosshole testing), and laboratory moduli (from resonant column testing) could be shown.

## **6.2 SCHMERTMANN'S (1970) SETTLEMENT ANALYSIS**

The Schmertmann method is based on a physical model of settlement which has been calibrated by empirical data (Coduto, 2001). The method requires the following information from in-situ tests: (1) the layered structure of the soil deposit (layer thickness and unit weight of soil) and (2) an estimation of the equivalent modulus of elasticity,  $E_s$ , for each soil layer. Schmertmann conducted extensive research on the vertical distribution of strain with depth (Schmertmann et al., 1978). For square and circular footings, an assumed distribution of strain with depth (to a depth of  $2B$ ) is used to estimate the compression of each layer under the design load. This assumed distribution is shown in Figure 6.1.



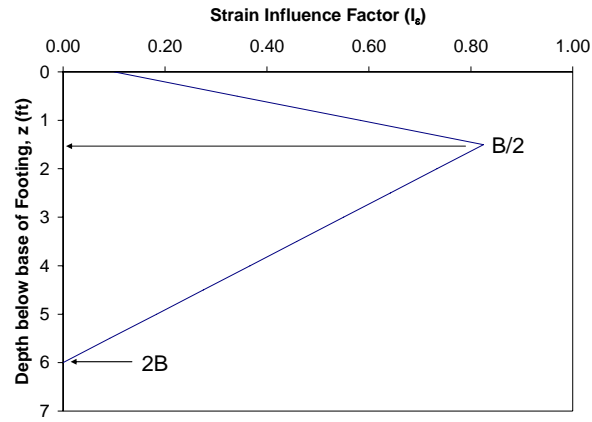


Figure 6.1: Schmertmann's Zone of Strain Influence for a 3-ft Diameter Footing Under a Uniform Pressure of 2800psf (Schmertmann, 1970)

The peak value of the strain influence factor,  $I_{ep}$ , is:

$$I_{ep} = 0.5 + 0.1 \cdot \sqrt{\frac{q - \sigma_{zD}}{\sigma_{zp}}} \quad (6.1)$$

where:

- $q$  = bearing pressure at the base of the footing,
- $\sigma_{zD}$  = effective vertical stress at a depth  $D$  below the ground surface, and
- $\sigma_{zp}$  = initial effective vertical stress at depth of peak strain influence factor.

The compression of each layer is totaled to compute the total settlement of the footing. The general form of Schmertmann's expression is:

$$\delta = C_1 \cdot C_2 \cdot C_3 \cdot (q - \sigma_{zD}) \cdot \sum \frac{I_z \cdot H}{E_s} \quad (6.2)$$

where:

- $\delta$  = total settlement,
- $C_1$  = depth factor ( $C_1 = 1$  for this study),
- $C_2$  = secondary creep factor ( $C_2 = 1$  for this study),

$C_3$  = shape factor ( $C_3 = 1$  for square and circular footings),  
 $q$  = bearing pressure,  
 $\sigma_{zD}$  = effective vertical stress at a depth,  $D$  below the ground surface,  
 $D$  = depth of the base of the footing below the ground surface (10 in.),  
 $I_\varepsilon$  = Strain Influence Factor for layer  $i$ ,  
 $H$  = thickness of soil layer  $i$ , and  
 $E_s$  = equivalent modulus of elasticity of soil in layer  $i$ .

The Strain Influence Factor ( $I_\varepsilon$ ) for circular footings is given as:

$$\text{For } z_f = 0 \text{ to } B/2: \quad I_\varepsilon = 0.1 + (z_f/B)(2(I_{\varepsilon p} - 0.2)) \quad (6.3)$$

$$\text{For } z_f = B/2 \text{ to } 2B: \quad I_\varepsilon = 0.667I_{\varepsilon p} (2 - z_f/B) \quad (6.4)$$

where  $z_f$  = depth below the base of the footing, and  
 $I_{\varepsilon p}$  = peak  $I_\varepsilon$  given from Equation 6.1.

The equivalent modulus of elasticity was determined differently for each analysis using Schmertmann's method depending on the in-situ test used. For the SPT tests, the equivalent modulus of elasticity was based on the correlation between  $E_s$  and  $N_{60}$  suggested by Coduto, 2001 for silty sands as:

$$E_s = 50,000 \frac{\text{lbs}}{\text{ft}^2} \cdot \sqrt{\text{OCR}} + 12,000 \frac{\text{lbs}}{\text{ft}^2} \cdot N_{60} \quad (6.5)$$

where:

$\text{OCR}$  = overconsolidation ratio, and  
 $N_{60}$  = SPT blow count corrected for field procedures

The OCR used over the depth of the influence was 2-4, based on a study of the Capitol Aggregates field site study conducted in 2002 (Axtell, 2002). For SASW testing, the modulus of elasticity was determined from the theoretical relationship

between Young's modulus (E) and the shear modulus (G) using an assumed Poisson's ratio ( $\nu$ ) of 0.33. Young's Modulus can be calculated as:

$$E = 2 \cdot G(1 + \nu) \quad (6.6)$$

The results of the settlement analyses conducted using Schmertmann's method are presented in Tables 6.1, 6.2, and 6.3. The layers analyzed were selected from the strain distribution in Figure 6.1. Note that the primary differences between the SPT input parameters and the SASW and crosshole input parameters are the elastic moduli estimated through a correlation in the SPT test (Table 6.1) and evaluated from the measured  $V_s$  values in the SASW (Table 6.2) and crosshole (Table 6.3) tests. These differences were expected given the nature of the test methods and the strain magnitude induced by each test. These differences between the in-situ tests and their relative value to the engineer are explored in Chapter 7.

For the three analyses using Schmertmann's method, the predicted variation in total settlements with depth are presented in Figure 6.2. The predicted variation in strain with depth is presented in Figure 6.3. Note that the predicted total settlement of the footing differs, depending on the in-situ test used. In fact, the difference in the predictions is essentially an order of magnitude with the SPT based modulus predicting about 10 times more settlement than either the SASW or crosshole moduli. The total settlement predicted with the SASW moduli is about 50% greater than the settlement predicted with the crosshole-determined moduli. However, both field seismic tests predict very small settlements which is in fact true. The difference between these two seismic based predictions is attributed to the difference between the global (SASW) and localized (crosshole) measurements.

Table 6.1: Schmertmann's Method using SPT Test Data

	SPT Obtained Values							SPT Modulus Based Prediction						
Layer #	Depth		Thickness of Layer	Footing to Midpt of Layer	SPT		Elastic Modulus	Strain Influence Factor		Compression of each layer	Vertical Strain in each Layer	Total movement predicted		
					N <sub>60</sub>	N <sub>1,60</sub>								
	Top of Layer ft	Bottom of Layer ft	(H) ft	(z) ft	# blows/ft	# blows/ft	E <sub>s</sub> psf	I <sub>ε</sub>	I <sub>ε</sub> H/Es ft^3/lb	q-σ <sub>zd</sub> psf	ft	in.	%	in.
0	0.00	0.83												
1	0.83	1.50	0.67	0.33	15	29	280000	0.261	6.22E-07	2708	0.0017	0.0202	0.2525	0.3911
2	1.50	2.33	0.83	1.08	9	18	208000	0.623	2.48E-06	2708	0.0067	0.0808	0.8108	0.3709
3	2.33	4.00	1.67	2.33	9	18	208000	0.673	5.40E-06	2708	0.0146	0.1755	0.8760	0.2901
4	4.00	6.50	2.50	4.42	9	16	208000	0.290	3.49E-06	2708	0.0095	0.1134	0.3781	0.1146
5	6.50	6.83	0.33	5.83	16	24	292000	0.031	3.49E-08	2708	0.0001	0.0011	0.0286	0.0011

Total Settlement (ft, in) =

**0.0326 0.3911**

Table 6.2: Schmertmann's Method using SASW Test Data

	SASW Obtained Values							SASW Modulus Based Prediction						
Layer #	Depth		Thickness of Layer	Footing to Midpt of Layer	SASW		Elastic Modulus	Strain influence		Compression of each layer	Vertical Strain in each Layer	Total movement predicted		
	Top of Layer	Bottom of Layer			V <sub>s</sub>	G								
	ft	ft	(H)	(z)			psf	E	$I_{\epsilon}$	$I_{\epsilon}H/E_s$	q- $\sigma_{zd}$	ft	in.	%
0	0.00	0.83												
1	0.83	1.00	0.17	0.08	320	349814	815066	0.140	2.87E-08	2708	0.0001	0.0009	0.0466	0.0437
2	1.00	2.33	1.33	0.83	420	602609	1404078	0.502	4.75E-07	2708	0.0013	0.0155	0.0968	0.0427
3	2.33	2.50	0.17	1.58	420	602609	1404078	0.810	9.81E-08	2708	0.0003	0.0032	0.1563	0.0273
4	2.50	6.83	4.33	3.83	540	996149	2321027	0.398	7.42E-07	2708	0.0020	0.0241	0.0464	0.0241

Total Settlement (ft, in) =

**0.0036 0.0437**

Table 6.3: Schmertmann's Method using Crosshole Test Data

Layer #	Crosshole Test Obtained Values							Crosshole Test Modulus Based Prediction						
	Depth		Thkness of Layer	Footing to Midpt of Layer	SASW		Elastic Modulus	Strain influence			Compression of each layer		Vertical Strain in each Layer	Total movement predicted
	Top of Layer ft	Bottom of Layer ft	(H) ft	(z) ft	V <sub>s</sub> ft/s	G psf	E psf	I <sub>ε</sub>	I <sub>ε</sub> H/E <sub>s</sub> ft <sup>3</sup> /lb	q-σ <sub>zd</sub> psf	ft	in.	%	in.
0	0.00	0.83												
1	0.83	1.00	0.17	0.08	600	1229814	2865466	0.140	8.16E-09	2708	0.0000	0.0003	0.0133	0.0289
2	1.00	2.33	1.33	0.83	600	1229814	2865466	0.502	2.33E-07	2708	0.0006	0.0076	0.0474	0.0287
3	2.33	2.50	0.17	1.58	600	1229814	2865466	0.810	4.81E-08	2708	0.0001	0.0016	0.0766	0.0211
4	2.50	6.83	4.33	3.83	600	1229814	2865466	0.398	6.01E-07	2708	0.0016	0.0195	0.0376	0.0195

Total Settlement (ft, in) =

**0.0024    0.0289**

Table 6.4: Schmertmann's Method using Resonant Column Test Data

Layer #	Resonant Column Test Obtained Values							Resonant Column Test Modulus Based Prediction						
	Depth		Thkness of Layer	Footing to Midpt of Layer	SASW		Elastic Modulus	Strain influence			Compression of each layer		Vertical Strain in each Layer	Total movement predicted
	Top of Layer ft	Bottom of Layer ft	(H) ft	(z) ft	V <sub>s</sub> ft/s	G psf	E psf	I <sub>ε</sub>	I <sub>ε</sub> H/E <sub>s</sub> ft <sup>3</sup> /lb	q-σ <sub>zd</sub> psf	ft	in.	%	in.
0	0.00	0.83												
1	0.83	1.00	0.17	0.08	420	602609	1404078	0.140	1.67E-08	2708	0.0000	0.0005	0.0271	0.0381
2	1.00	2.33	1.33	0.83	460	722857	1684257	0.502	3.96E-07	2708	0.0011	0.0129	0.0807	0.0375
3	2.33	2.50	0.17	1.58	500	854037	1989907	0.810	6.92E-08	2708	0.0002	0.0022	0.1103	0.0247
4	2.50	6.83	4.33	3.83	560	1071304	2496139	0.398	6.90E-07	2708	0.0019	0.0224	0.0431	0.0224

Total Settlement (ft, in) =

**0.0032    0.0381**

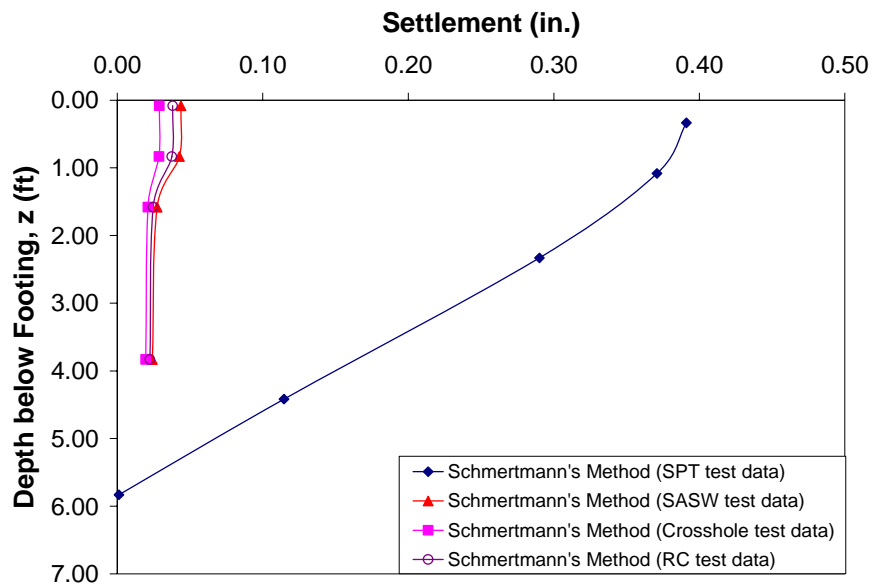


Figure 6.2: Predicted Variation of Settlement with Depth Using Schmertmann's Method

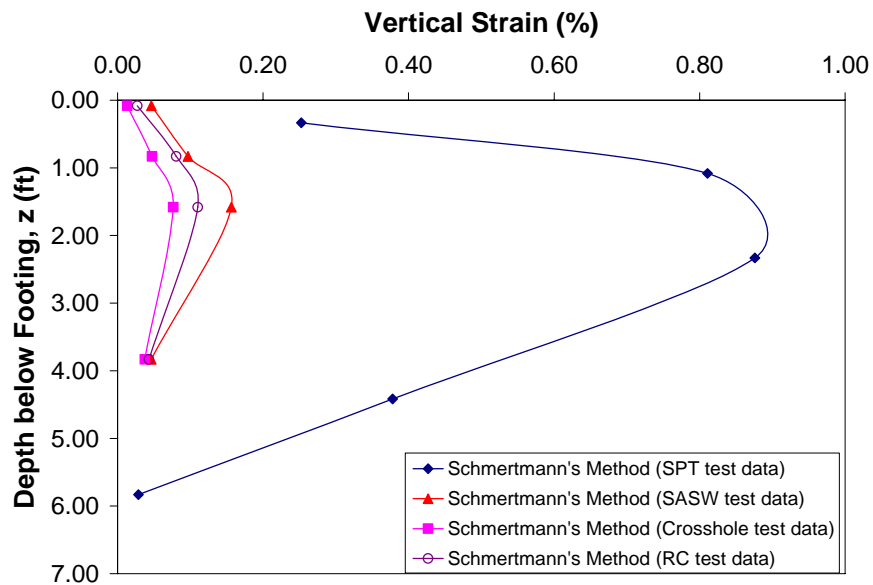


Figure 6.3: Predicted Variation of Vertical Strain with Depth Using Schmertmann's Method – (Expanded Scale)

### 6.3 BURLAND AND BURBIDGE'S SETTLEMENT METHOD

Burland and Burbidge (1985) suggested the following empirical relationship for predicting the settlement of a footing underlain by sand as:

$$S_i = \frac{1.71q \cdot B^{0.7}}{N^{1.4}} \quad (6.7)$$

where:

$S_i$  = immediate settlement (mm),  
 $q$  = bearing pressure (kPa),  
 $B$  = footing width (m), and  
 $N$  = SPT blow count uncorrected for overburden pressure.

This empirical correlation was based on a statistical analysis of over 200 settlement records of foundations on sands and gravels. This relationship does not attempt to estimate the modulus of the soil or the relative influence of each layer on overall settlement. The bearing pressure on the footing is 2800 psf (134 kPa). The footing is 3 ft (0.914 m) in diameter ( $B$ ). An average SPT blow count (10 bpf) is used over the depth of influence suggested by Schmertmann (over  $2B$  beneath the footing). Thus, the total settlement computed using Burland and Burbidge's method is 0.34 in. (8.57 mm).

### 6.4 SETTLEMENT ANALYSIS USING FINITE ELEMENT CODE

Accurately estimating the in-situ material properties and modeling the nonlinear behavior of soil have always been limiting factors in the use of numerical models in geotechnical applications. Most in-situ tests involve some measure of a strength parameter (SPT blow count or CPT tip resistance) and empirically relate it to the stiffness of the soil. In this study, the shear wave velocity of the soil was

measured in-situ by field SASW, field crosshole, and laboratory resonant column tests. A few undisturbed samples were also required to estimate the unit weight of the soil. As noted earlier, the shear wave velocity can be directly related to the stiffness of the soil, which is the material property of interest in the calculation of settlements of a footing on granular soil.

The Plaxis finite element software package was used to predict the settlement of the footing using a numerical method. Plaxis was the finite element program selected because it was developed primarily for geotechnical applications and offers several constitutive models for soil behavior.

#### **6.4.1 SOIL BEHAVIOR MODEL**

The soil model selected in Plaxis was the Mohr-Coulomb model. While this model is an elasto-plastic model and does not model softening of the soil after yielding, it can be used to deliver reasonable results at low ( $< 0.01\%$ ) to moderate ( $< 0.1\%$ ) strain levels. The use of a more complicated soil model requires additional parameters derived from additional laboratory testing. Further, the value of using a more complicated, nonlinear model, such as the Duncan hyperbolic model, is questionable since it is designed to match the nonlinear behavior of soil at high strain levels ( $> 1\%$ ), rather than at small to moderate strains.

The stiffness of the soil changes with changes in confining pressure and strain amplitude. During loading of the footing, the confining pressure (expressed as the mean stress assuming a  $K_o$  of 1.5) increased from  $\sim 166$  psf to  $\sim 2000$  psf. Since  $G_{\max}$  is nearly proportional to the square root of the isotropic confining pressure, the expected change in  $G_{\max}$  during loading, at a depth of 3 in. beneath the center of the footing, is increased by a factor of  $\sim 3.4$ . At a strain amplitude of 0.1, the shear



modulus can be taken as  $\sim 0.3G_{\max}$  (Idriss, 1970; Darendeli, 2001). This relationship was also shown by the laboratory resonant column tests (Figures 3.10 and 3.11) conducted during the site characterization study (Kurtulus, 2006).

Near the base of the footing, the increase in  $G_{\max}$  due to an increase in confining pressure and the decrease in  $G_{\max}$  due to an increase in strain amplitude are approximately equal to the values discussed above. The shear modulus representative of the soil behavior should be increased by a factor of  $\sim 4$  and then decreased by a factor of 0.3 which approximately equals the original value of shear modulus estimated in the field with SASW testing.

At greater depths below the footing, the change in isotropic confining pressure and the increase in strain amplitude are smaller and thus the modulus of the soil changes very little. So, the stress dependency and nonlinear effects of strain amplitude on shear modulus were considered to cancel each other out. Thus, the stiffness of the soil was taken as the small-strain modulus measured by seismic testing.

#### **6.4.2 FINITE ELEMENT MODEL INPUT PARAMETERS**

In this study, a two-dimensional, axi-symmetrical, finite element mesh of 15-node triangles was used to model the area of soil beneath the footing (see Figure 6.5). The boundary conditions imposed in the model included a rigid layer at a depth of 10 ft below the ground surface and horizontal fixity at 10 ft from the central axis of the footing. The layered soil system, determined during in-situ testing, was modeled to a depth of 10 ft. The results of the finite element simulation indicate no strain at the boundaries of the model, which indicates that the fixed boundaries had no impact on the strain induced at any point under the footing.

The concrete footing was modeled as a linear elastic material with  $E = 6 \times 10^8$  psf ( $V_s = 4128$  fps) and Poisson's ratio = 0.15. The Mohr-Coulomb soil model requires 4 parameters ( 2 elastic constants, the angle of internal friction ( $\phi$ ), and a cohesion value) to model the soil behavior. The properties assigned to each soil layer were derived from the in-situ tests performed on site or estimated from reasonable correlations based on the soil material. The first elastic constant which was used for all layers in all analyses was the Poisson's ratio, which was taken as 0.33. The second elastic constant used was Young's Modulus determined from the shear wave velocity of the material. Plaxis offers a feature in which the shear wave and compression wave velocities can be input directly to define the elastic parameters of the soil. Plaxis automatically computes the Young's modulus and Poisson's ratio from these velocities. Based on correlations with SPT blow count of 18 bpf, each sand and silt layer was assigned an angle of internal friction,  $\phi$  equal to 31 degrees. The cohesion of each layer was estimated as 1 psf.

The finite element analysis was conducted once using the field data obtained from the SPT tests, once using the data obtained from the SASW testing, and once using the data obtained during crosshole tests, and again using the data obtained during resonant column tests. The results of the settlement analyses conducted using the finite element method are presented in Tables 6.5 through 6.8. The predicted movements were taken from points under the center of the footing. The predicted variation in total settlement with depth is presented in Figures 6.8 and 6.9. The predicted variation in strain with depth is presented in Figure 6.10 and 6.11.

The figures below suggest several items which should be noted. First, the primary difference between the in-situ test methods is the estimation of stiffness. The

layer breaks determined by each test are comparable and do not have a significant effect on the total settlement of the footing. Second, at low values of strain amplitude, the shape of the strain distribution predicted by the finite element method does not agree with Schmertmann's theoretical distribution of strain. However, as the strain magnitude increases, the predicted variation of strain appears to be similar to Schmertmann's theoretical strain distribution. Third, the settlement predicted using the moduli estimated from the SPT tests (Equation 6.5) is much higher than the settlement estimated based on the SASW, crosshole, and laboratory resonant column testing. Further, when using the SPT test data, the settlement predicted by the finite element method was higher than the settlement predicted by Schmertmann's method. Each of these observations will be discussed further in Chapter 7 where the settlement prediction methods are compared to the settlement measured in the field.

Table 6.5: Results of the Finite Element Method Using SPT Test Data

Layer #	SPT Obtained Values							F.E.M. Predictions			
	Depth		Thickness of Layer	Footing to Midpt of Layer	SPT		Elastic Modulus	Depth Below Footing	Total Movement of Point at Depth (i) Predicted		Vertical Strain
	Top of Layer ft	Bottom of Layer ft	(H) ft	(z) ft	N <sub>60</sub> # blows/ft	N <sub>1,60</sub> # blows/ft	E psf	ft	ft	in.	(%)
0	0.00	0.83						0.0	0.0630	0.7560	0.7190
1	0.83	1.50	0.67	0.33	15	29	330000	0.5	0.0600	0.7200	0.8050
2	1.50	2.33	0.83	1.08	9	18	258000	1.0	0.0540	0.6480	1.2000
3	2.33	4.00	1.67	2.33	9	18	258000	1.5	0.0480	0.5760	1.2000
4	4.00	6.50	2.50	4.42	9	16	258000	2.5	0.0360	0.4320	2.0000
5	6.50	6.83	0.33	5.83	16	24	342000	4.0	0.0130	0.1560	0.8430
								5.0	0.0055	0.0659	0.5760

Table 6.6: Results of the Finite Element Method Using SASW Test Data

Layer #	SASW Obtained Values							F.E.M. Predictions			
	Depth		Thkness of Layer	Footing to Midpt of Layer	SASW		Elastic Modulus	Depth Below Footing	Total Movement of Point at Depth (i) Predicted		Vertical Strain
	Top of Layer ft	Bottom of Layer ft	(H) ft	(z) ft	Vs ft/s	G psf	E psf	ft	ft	in.	(%)
0	0.00	0.83						0.0	0.0016	0.0187	0.0341
1	0.83	1.00	0.17	0.08	320	349814	815066	0.5	0.0014	0.0171	0.0383
2	1.00	2.33	1.33	0.83	420	602609	1404078	1.0	0.0012	0.0144	0.0403
3	2.33	2.50	0.17	1.58	420	602609	1404078	1.5	0.0010	0.0118	0.0382
4	2.50	6.83	4.33	3.83	540	996149	2321027	2.5	0.0008	0.0090	0.0303
								4.0	0.0003	0.0041	0.0002
								5.0	0.0001	0.0016	0.0002

Table 6.7: Results of the Finite Element Method Using Crosshole Test Data

Layer #	Crosshole Obtained Values							F.E.M. Predictions			
	Depth		Thkness of Layer	Footing to Midpt of Layer	SASW		Elastic Modulus	Depth Below Footing	Total Movement of Point at Depth (i) Predicted		Vertical Strain
	Top of Layer ft	Bottom of Layer ft	(H) ft	(z) ft	Vs ft/s	G psf	E psf	ft	ft	in.	(%)
0	0.00	0.83						0.0	0.0011	0.0129	0.0168
1	0.83	1.00	0.17	0.08	600	1229814	2865466	0.5	0.0010	0.0117	0.0187
2	1.00	2.33	1.33	0.83	600	1229814	2865466	1.0	0.0009	0.0109	0.0197
3	2.33	2.50	0.17	1.58	600	1229814	2865466	1.5	0.0008	0.0096	0.0192
4	2.50	6.83	4.33	3.83	660	1488075	3467214	2.5	0.0006	0.0073	0.0217
								4.0	0.0003	0.0034	0.0198
								5.0	0.0001	0.0015	0.0157

Table 6.8: Results of the Finite Element Method Using Resonant Column Test Data

Layer #	Resonant Column Obtained Values							F.E.M. Predictions			
	Depth		Thkness of Layer	Footing to Midpt of Layer	SASW		Elastic Modulus	Depth Below Footing	Total Movement of Point at Depth (i) Predicted		Vertical Strain
	Top of Layer ft	Bottom of Layer ft	(H) ft	(z) ft	Vs ft/s	G psf	E psf	ft	ft	in.	(%)
0	0.00	0.83						0.0	0.0019	0.0229	0.0058
1	0.83	1.00	0.17	0.08	420	602609	1404078	0.5	0.0017	0.0201	0.0657
2	1.00	2.33	1.33	0.83	420	602609	1404078	1.0	0.0013	0.0156	0.0700
3	2.33	2.50	0.17	1.58	420	602609	1404078	1.5	0.0009	0.0110	0.0651
4	2.50	6.83	4.33	3.83	420	602609	1404078	2.5	0.0007	0.0084	0.0233
								4.0	0.0003	0.0041	0.0219
								5.0	0.0001	0.0018	0.0188

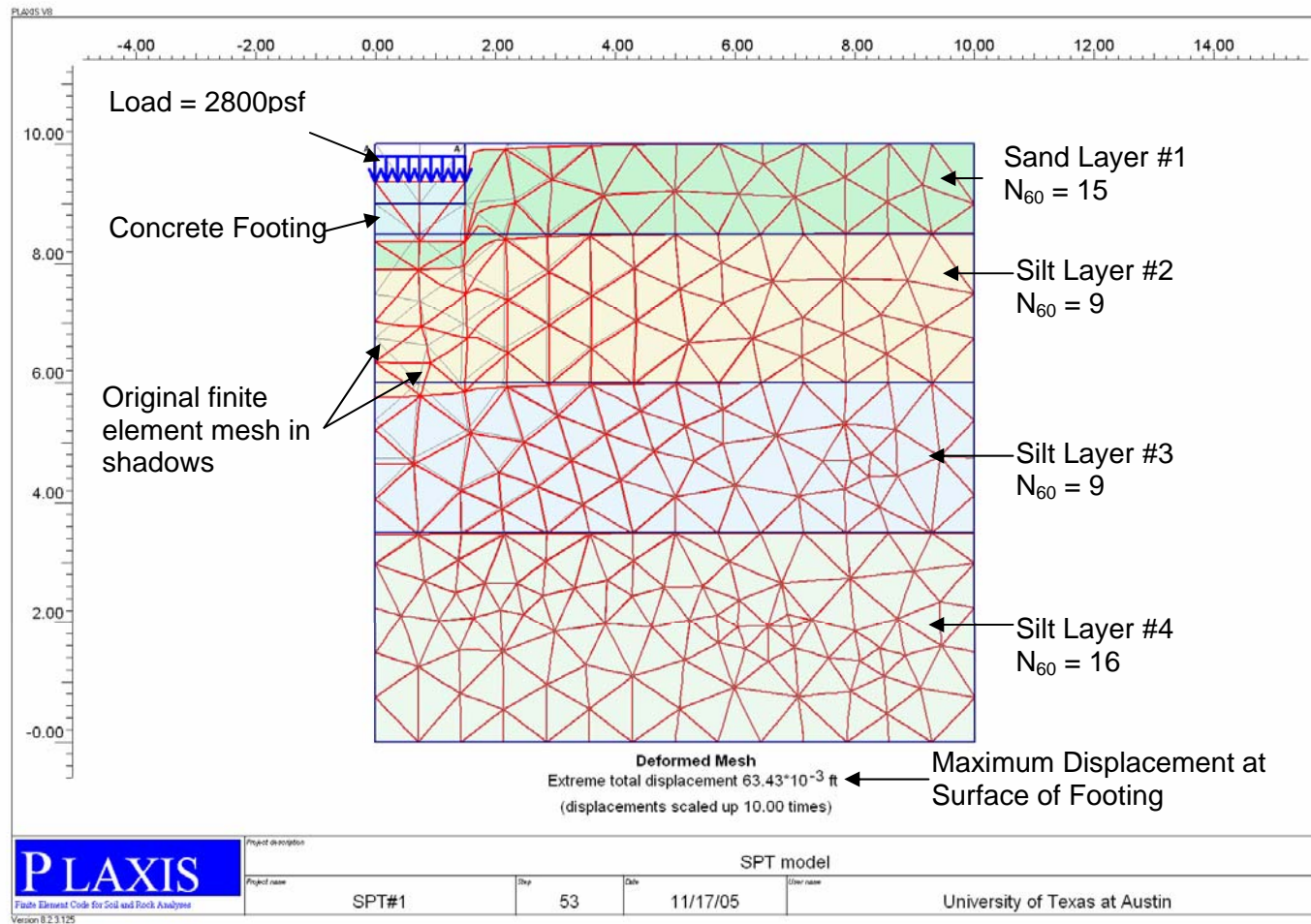


Figure 6.4: Deformed Finite Element Mesh Constructed from the SPT Test Data

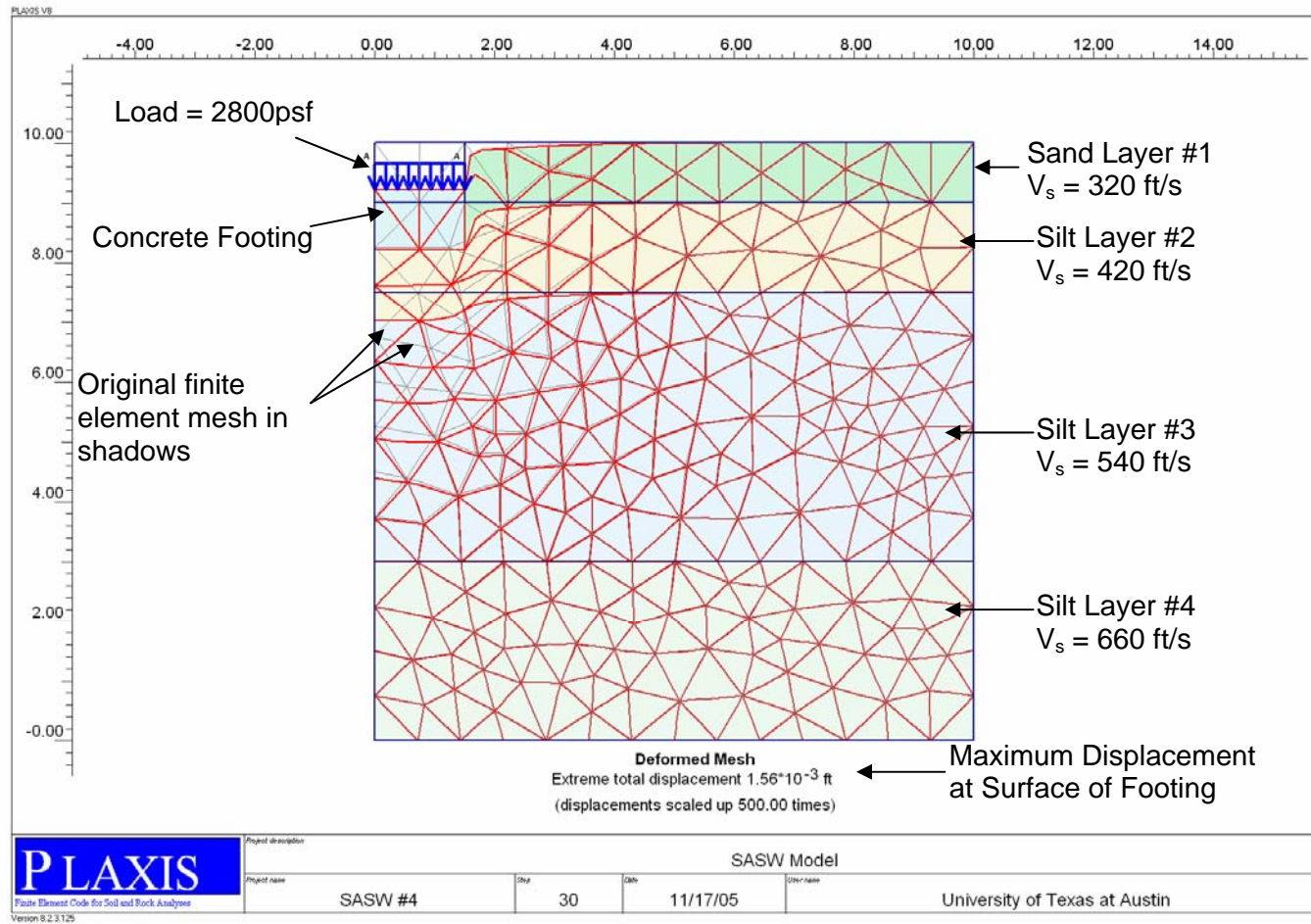


Figure 6.5: Deformed Finite Element Mesh Constructed from the SASW Test Data

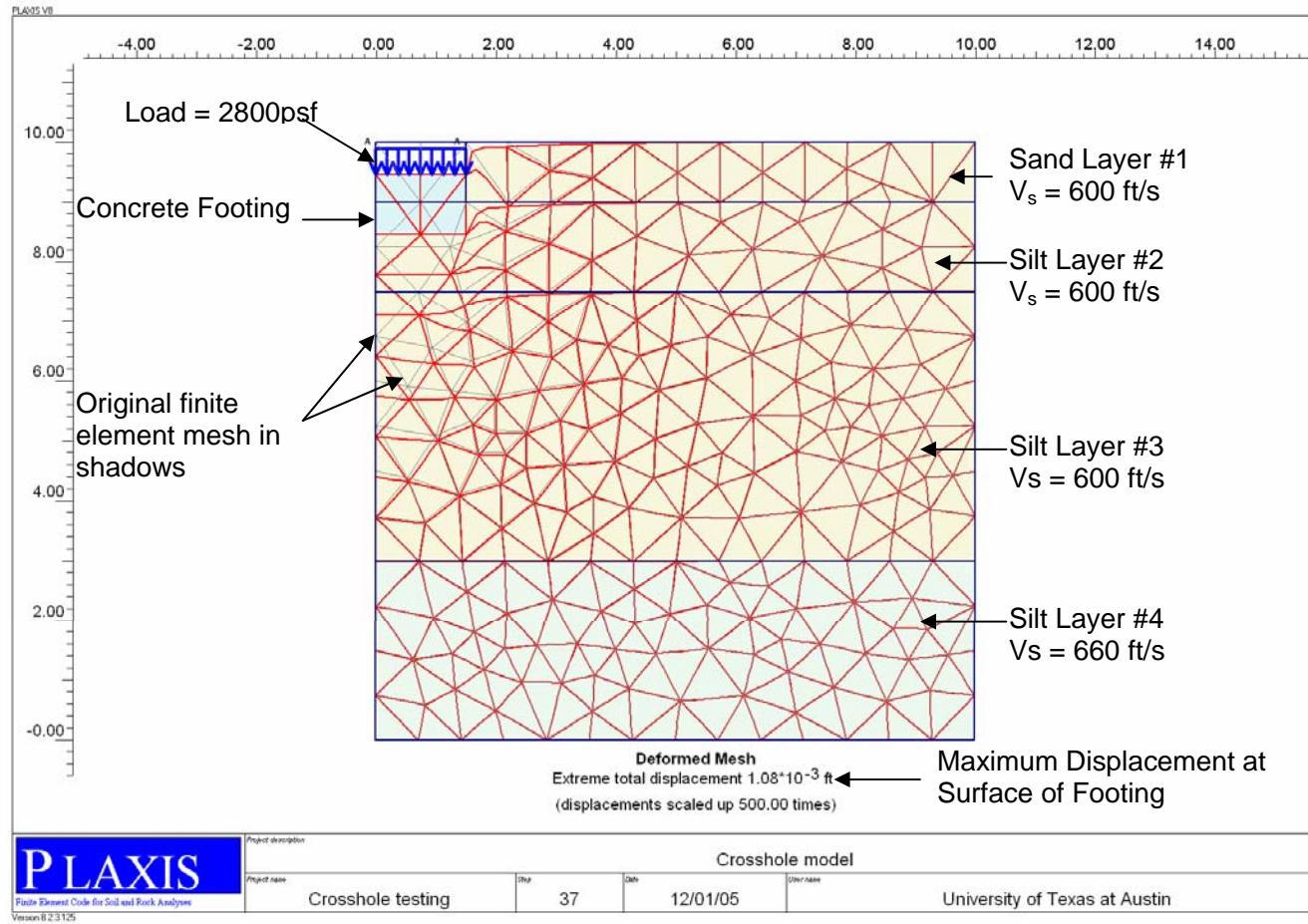


Figure 6.6: Deformed Finite Element Mesh Constructed from the Crosshole Test Data



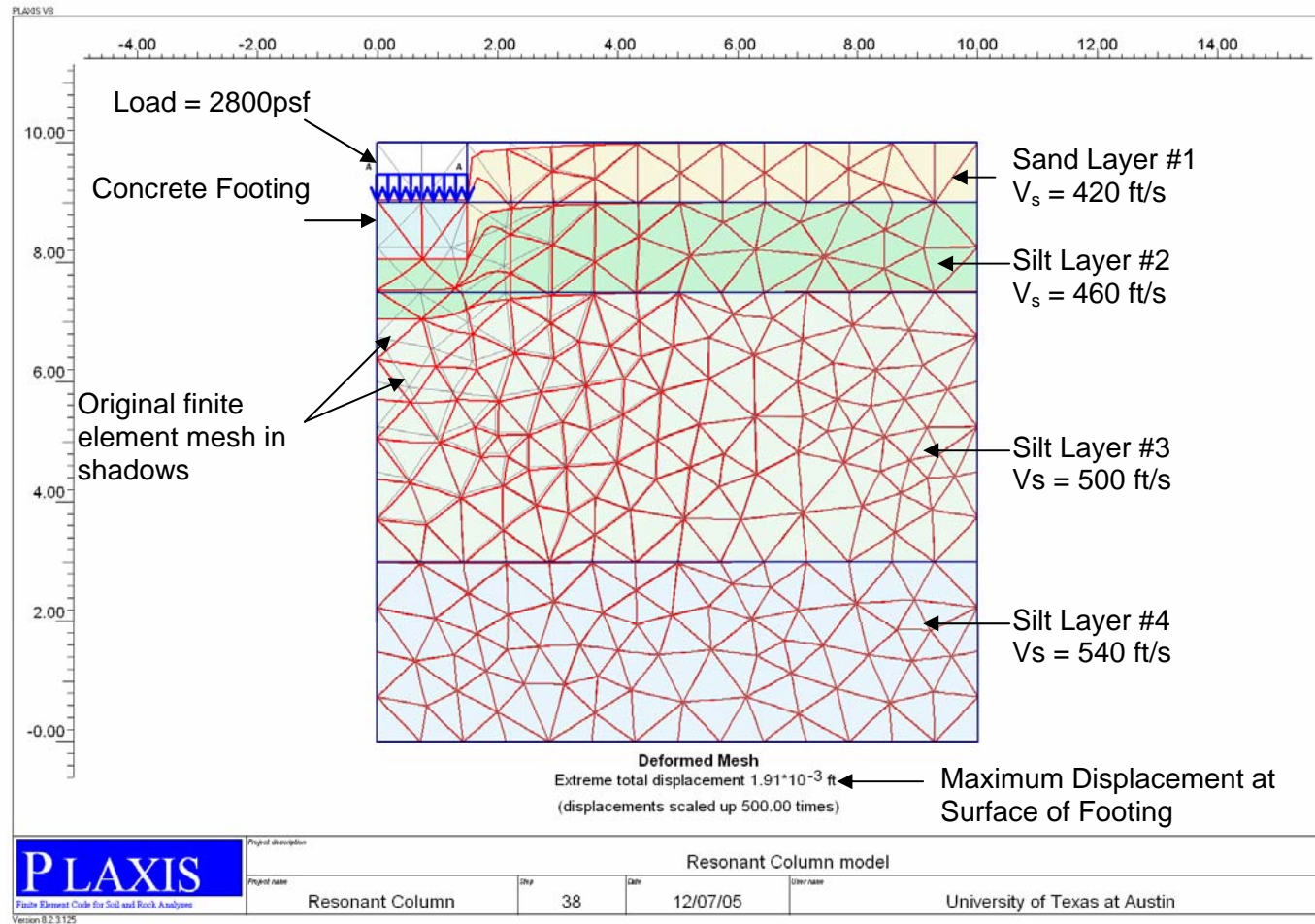


Figure 6.7: Deformed Finite Element Mesh Constructed from the Resonant Column Test Data

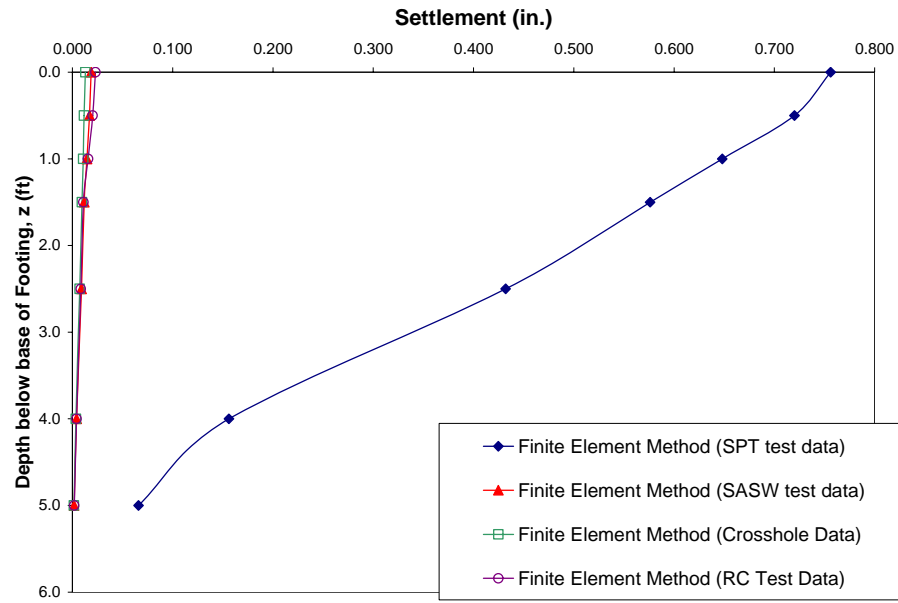


Figure 6.8: Finite Element Method- Predicted Variation of Settlement with Depth

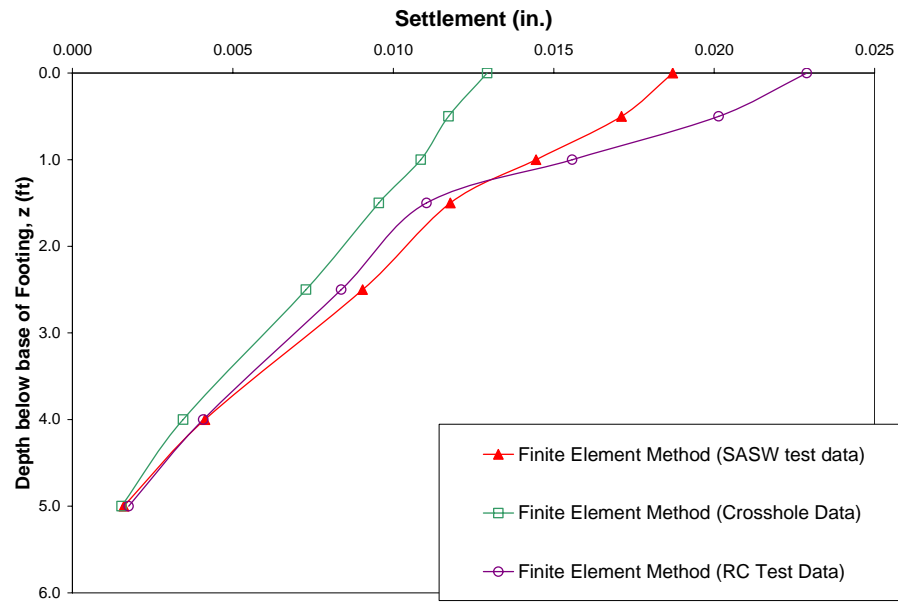


Figure 6.9: Finite Element Method- Predicted Variation of Settlement with Depth (Expanded Scale)

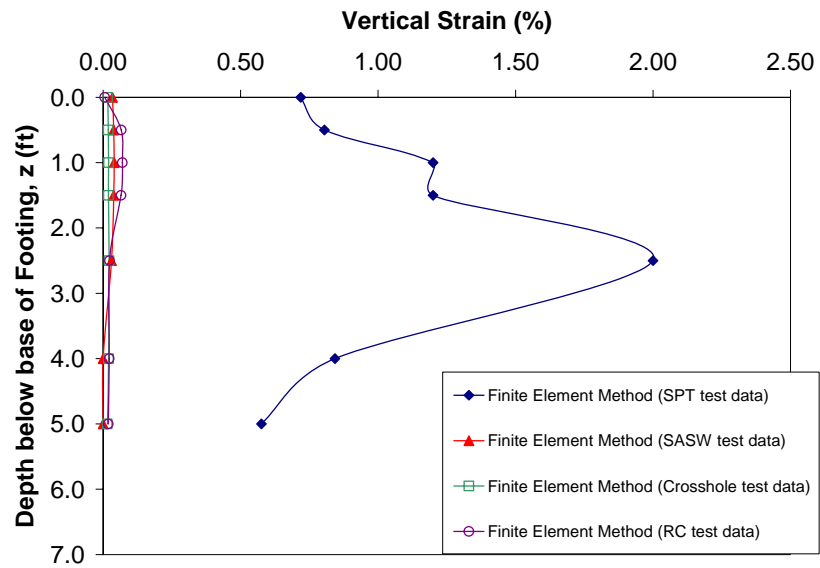


Figure 6.10: Finite Element Method- Predicted Variation of Strain with Depth

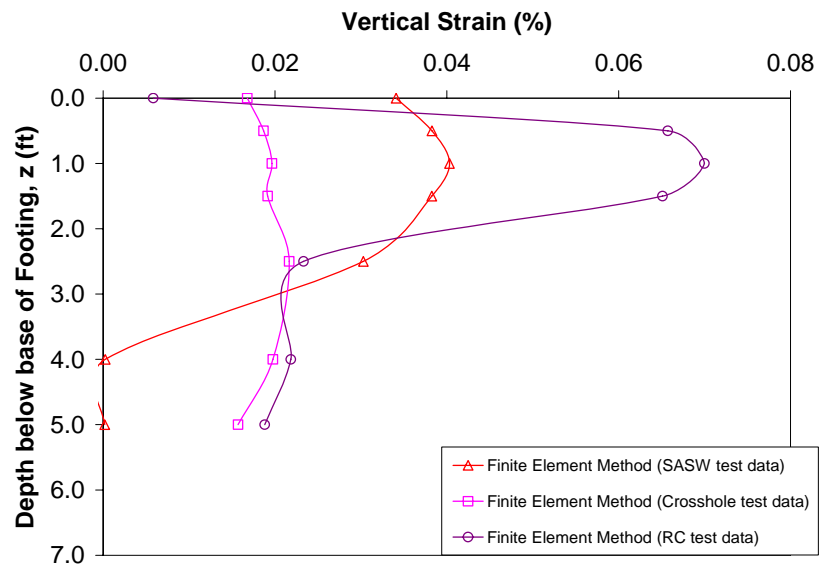


Figure 6.11: Finite Element Method- Predicted Variation of Strain with Depth (Expanded Scale)

## **6.5 SUMMARY**

The settlement of the 3-ft diameter footing under a load of 20,000 lb was predicted using three different analytical techniques. The source information used in the analytical techniques came from three different field characterization studies, SPT testing and SASW testing, conducted prior to construction of the footing, and crosshole testing after footing construction. In the laboratory, resonant column testing conducted on undisturbed samples was used to generate a fourth estimate of the site shear wave velocity profile. The settlement predictions based on dynamic moduli determined from field seismic testing consistently predict total settlements of an order of magnitude less than predictions based on an SPT-modulus correlation. The layered structure of the site determined by both characterization methods was effectively the same. The principal difference between the site characterization results is the estimation of the stiffness of each layer. In Chapter 7, the predictions of all studies are compared to measured settlements in the field.

## **CHAPTER 7**

### **COMPARISON OF PREDICTED AND MEASURED SETTLEMENTS**

#### **7.1 INTRODUCTION**

In this chapter, the settlements measured in the field are compared to predicted settlements of the soil beneath the footing under a load of 20,000 lb. First, the total settlement of the footing is compared to the predicted total settlements by the methods outlined in Chapter 6. Second, the predicted settlements at each depth beneath the footing are compared to the measured field data from each depth. Third, the calculated strain distribution with depth is compared to the predicted strain distribution. Finally, the total settlement is compared to a simplified prediction method based on the SASW results.

#### **7.2 TOTAL SETTLEMENT OF THE CENTER OF THE FOOTING**

In Chapter 6, the total settlement caused by a vertical static load of 20,000 lb on the footing located at the Capitol Aggregates field site was predicted by various methods. A summary of the results from the various prediction models and the average settlement measured in the field are presented in Table 7.1. The measured settlement was smaller than all predicted settlements. Given the very small movement of the footing ( $\sim 0.016$  in.), predicted settlements within a factor of three times measured settlements were considered very good. Settlement predictions based on the SPT test data were consistently more than an order of magnitude larger than

the measured settlements in the field. Settlement predictions based on SASW, crosshole of resonant column test data were all within a factor of three of the measured settlements. Note that both Schmertmann's method and the finite element analysis gave good predictions when the soil stiffness was accurately characterized. The prediction using the SASW data and the finite element analysis differed from the measured field settlements by only 17%. These limited results suggest that the most accurate method of predicting the total settlements of a shallow footing on this sandy silt is to conduct field seismic testing and analyze the settlement with a finite element code. It is only prudent to incorporate non-linear soil behavior. However, for these tests, the very small movements resulted in non-linearity having a minor impact on the predictions. As outlined in Chapter 6, it is likely that the decrease in modulus due to nonlinearity was compensated for by the increase in modulus due to the increase in confining pressure.

Table 7.1: Summary of Total-Settlement Predictions for the Center of a 3-ft Diameter Footing Under a Static Load of 20,000 lb.

Analysis Technique	Burland & Burbridge Method	Schmertmann's Method				Finite Element Method				Measured Settlement
Test Data	SPT	SPT	SASW	Crosshole Testing	Resonant Column	SPT	SASW	Crosshole Testing	Resonant Column	
Total Settlement (in.)	0.340	0.391	0.044	0.029	0.038	0.756	0.019	0.013	0.023	0.016
Predicted/Measured	21	24	2.7	1.81	2.38	47	1.17	0.81	1.43	1.00

### 7.3 SETTLEMENTS OF THE FOOTING AND THE SOIL MASS

In Figure 7.1, measured and predicted settlements at each depth below the footing are plotted. The predictions based on the SPT test data consistently overestimate the settlement at any given point beneath the footing. In practice,

settlement predictions based on SPT blow count or SPT-modulus correlations have historically over-predicted settlements in sand (Gibbens and Briaud, 1994). So, it was not surprising to find this phenomenon again during this study. The likely cause of this overprediction is the method in which the soil strength is empirically correlated to the stiffness of the soil. During an SPT test, the soil in the immediate vicinity of the split-spoon sampler undergoes very large strains. This strain level is unrelated to the strain level beneath a footing under “working loads.” The result is that the modulus of the soil is underestimated.

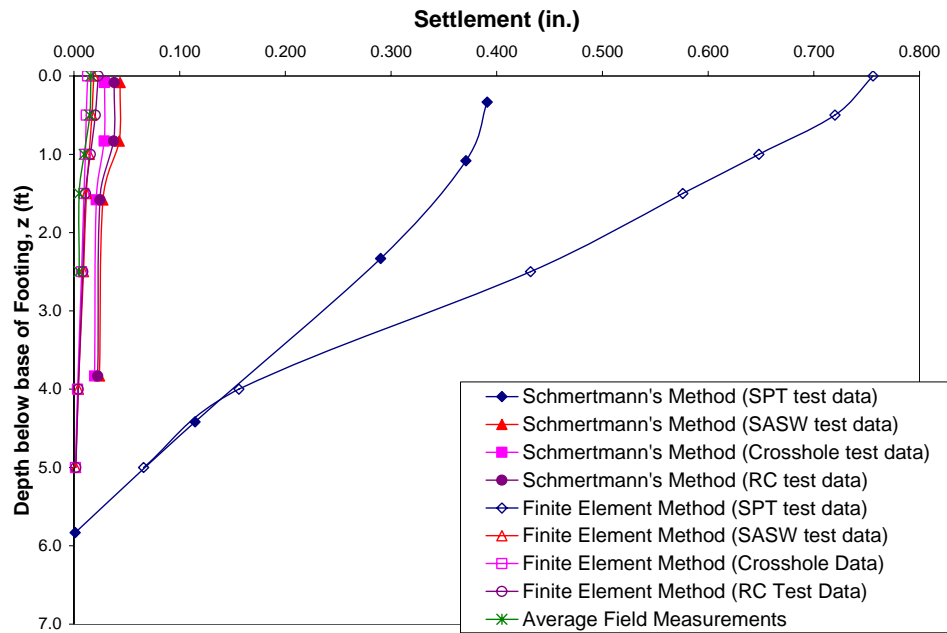


Figure 7.1: Comparison of Measured and Predicted Settlements, Based on Dynamic Moduli Measured in the Field and the Laboratory, Beneath the Footing Under a Static Load of 20,000 lb.

The results in Figure 7.1 also suggest that the settlement predictions based on SASW, crosshole, and resonant column tests, are in close agreement with the field measurements, throughout the depth of influence. To further evaluate and compare

this phenomenon, the settlement predictions based on SASW, crosshole, and resonant column data are plotted with the measured settlements in Figure 7.2. In this figure, the shape of the settlement distribution predicted by Schmertmann's method is similar to the measured field data. The cause of this similarity is assumed to be that the strain distribution predicted by Schmertmann is a good representation of the actual strain distribution. His strain distribution is the primary mechanism by which non-linear behavior is introduced into the settlement analysis.

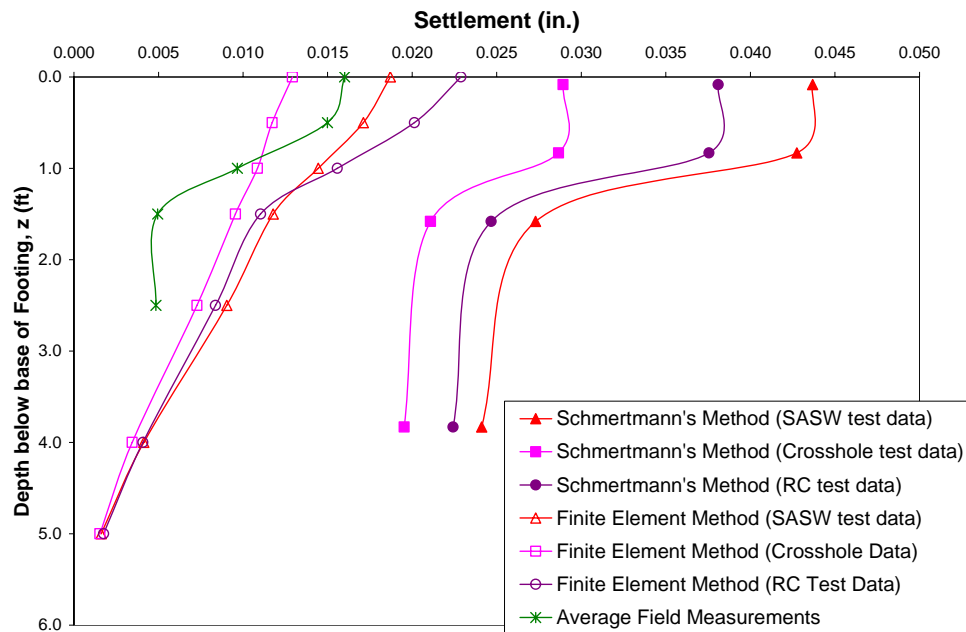


Figure 7.2: Comparison of Measured and Predicted Settlements, Based on Dynamic Moduli Measured in the Field and the Laboratory, Beneath the Footing Under a Static Load of 20,000 lb. (expanded scale)

By contrast, the finite element model (FEM) used in this study is an elasto-plastic (Mohr-Coulomb) soil model. It does not model the change in stiffness due to increasing confining pressure or strain amplitude. Since these effects largely compensate for one another, the total settlements can still be estimated with an elasto-



plastic model. However, the shape of the settlement distribution in the FEM with depth does not incorporate the basic mechanism that is occurring in the field. It is possible that a more advanced soil model could be used to model the strain softening of the soil beneath the footing, but that analysis would require additional parameters beyond the scope of this study. Further, current models of strain softening are focused on matching the soil behavior at strains closer to failure, rather than “working” strains.

The results of this study suggest that the settlement at depth below a footing on a sandy silt can be estimated using SASW, crosshole, or resonant column test results. The analytical technique selected seems to be less important than accurately estimating the modulus of the soil. Settlement predictions using either Schmertmann’s method or a finite element code will give reasonable results, within a factor of three to four times the measured settlement using Schmertmann’s method and less than two times if seismically measured field moduli or dynamically measured laboratory moduli (with high-quality intact specimens) are used in a finite element code.

#### **7.4 STRAIN DISTRIBUTION WITH DEPTH**

The calculated and predicted distributions of strain are presented in Figure 7.3. The results show that both predictions based on the SPT test data overestimate the strain calculated from the field measurements by an order of magnitude. This overestimation in strain is caused mainly by errors in the estimation of the stiffness of the soil. However, the strain calculated from field measurements appears to closely follow the predictions based on SASW, crosshole, and resonant column tests.

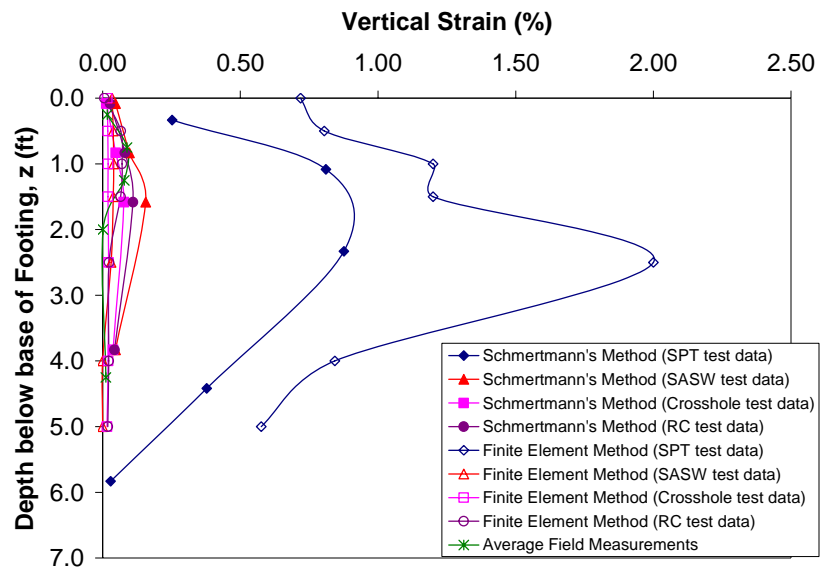


Figure 7.3: Comparison of Calculated and Predicted Strains Beneath the Footing Under a Static Load of 20,000 lb.

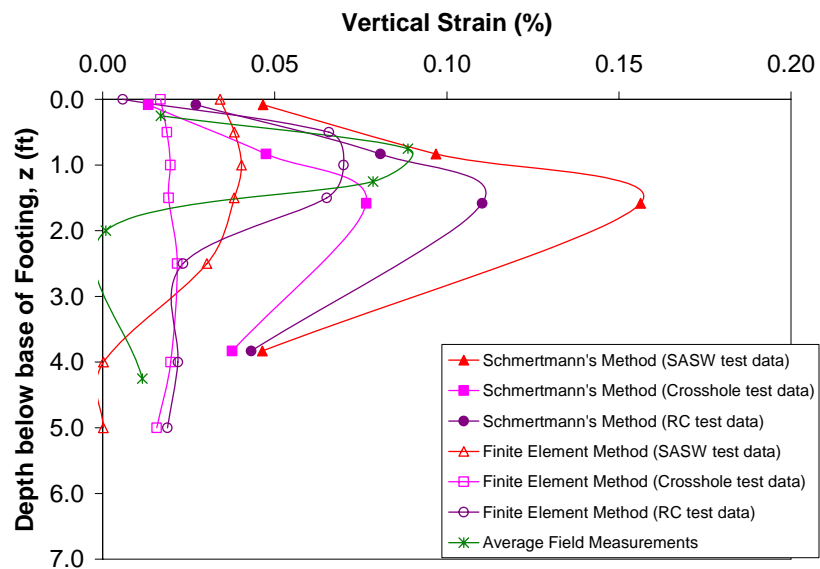


Figure 7.4: Comparison of Calculated and Predicted Strain Beneath the Footing Under a Static Load of 20,000 lb (Expanded Scale)

Figure 7.4 presents the calculated strains from field measurements and the predicted strains based on SASW, crosshole, and resonant column tests at an enlarged scale so it is easier to see the differences. The difference between the elasto-plastic finite element model and Schmertmann's method are clear in Figure 7.4. Schmertmann's method consistently predicts strains along the controlled distribution in which the peak strain occurs at  $B/2$  and the strain at  $2B$  is zero. On the other hand, the strains predicted by the finite element program are a function of the stiffness of each layer with no controlling strain distribution.

The strains predicted with the finite element model are below the measured strains at depths of 0.5 to 1.5 ft. It is difficult to ascertain the reason for this difference. However, given the extremely small measured settlements, it is difficult to conclude much about the distribution of strain beneath the footing. The data do suggest, however, that Schmertmann's strain distribution is indeed correct at this very low strain range.

## **7.5 SETTLEMENT PREDICTIONS WITH OTHER DYNAMIC MODULI**

For all methods of dynamic testing (SASW, crosshole, downhole, resonant column tests), the range of the measured shear wave velocity in the zone of influence under the footing was 420-600 ft/s. The resonant column tests in the lab measured shear wave velocities at the low end of this range. The crosshole tests gave velocities at the high end of this range.

Another possible method to characterize the soil in the field comes from the field dispersion curve generated during SASW testing. The field dispersion curve is a plot of measured Rayleigh wave velocities at various frequencies. Rayleigh waves are influenced by the relative stiffness of the soil layers. The shape of the Rayleigh

wave closely mimics the strain distribution proposed by Schmertmann. So, the Rayleigh wave velocity at a frequency equal to the depth of influence (2B) may be a good estimation of the material stiffness for settlement predictions. The shear wave velocity can be computed from the Rayleigh wave velocity by:

$$V_s = 1.1 * V_R \quad (7.1)$$

where:  $V_s$  = shear wave velocity and

$V_R$  = Rayleigh wave velocity (Richart, Hall and Woods, 197?)

For example, in this study, the field dispersion curve is shown in Figure 3.5. The Rayleigh wave velocity at a wavelength of 6 ft (2B) is approximately 450 ft/s. Thus the shear wave velocity of this material is estimated at 495 ft/s. This value is in the middle of the range of shear wave velocities determined by other dynamic tests. Thus, settlement predictions based on this estimate will yield similar results.

Use of any of these values to estimate the total settlement of the footing gave a good prediction of the settlement. Thus, it should be recognized that shear wave velocity measurements accurately characterize the stiffness of the soil and can be used to estimate settlements of foundations.

## **7.6 SUMMARY**

In this chapter, measured settlements at the center of the footing, gathered in the field, are compared to predicted settlements. It is found that the field seismic and laboratory dynamic test data can be used to accurately estimate the settlement of a footing on a nonplastic sandy silt. When compared to settlement predictions based on SPT test data, the predictions based on the SASW, crosshole, or resonant column tests

more closely match the measured settlement in the field. The data from this study suggests that Schmertmann's strain distribution accurately reflects the behavior of this sandy silt at very low strain ranges.

## **CHAPTER 8**

### **SUMMARY, CONCLUSIONS AND RECOMMENDATIONS**

#### **8.1 SUMMARY**

The goal of this study was to investigate how well measured soil stiffnesses determined by field and laboratory dynamic tests with intact specimens predict the settlement of shallow footings on granular materials. The stiffness, or modulus, of the soil was estimated based on SPT tests, field seismic tests(SASW and crosshole tests), and dynamic laboratory tests (torsional resonant column tests). The moduli from these tests were then used in two different settlement analysis techniques, Schmertmann's method and a finite element analysis, to predict the settlement of the footing surface and the soil mass beneath it. A series of field load tests were performed and settlements were measured at the top of a footing and at depth beneath it. These field measurements were compared to the predicted values. The results indicate that seismic field and dynamic laboratory tests can be effectively used to conduct a site investigation for the purposes of predicting the settlement potential of shallow footings on this nonplastic sandy silt.

#### **8.2 CONCLUSIONS**

1. The in-situ stiffness of the soil system is more accurately represented by moduli determined from seismic tests such as SASW, crosshole and laboratory resonant column tests than estimated by SPT based correlations.
2. The total settlement under working loads (strain < 0.1%) of a shallow footing on cohesionless material can be accurately predicted using field seismic

testing to characterize the site. Both methods of settlement analysis (Schmertmann's method and the finite element method) yielded reasonable results when applying the stiffnesses and layer structure derived from field seismic tests.

3. The distribution of settlement beneath the center of the footing closely followed the shape predicted by Schmertmann's semi-empirical technique.

4. The instrumentation technique used to measure settlements beneath the foundation worked well and could be used in future studies.

5. The magnitude of the strains generated beneath the footing can be estimated using Schmertmann's analysis and field seismic derived moduli.

6. The settlement of a footing on cohesionless soil can be quickly estimated from the field dispersion curve obtained during SASW testing. At a wavelength equal to  $2B$ , the shear wave velocity can be used to roughly estimate the stiffness of the soil to a depth of  $2B$ . Settlement predictions based on this stiffness were shown to be accurate within a factor of three

### **8.3 RECOMMENDATIONS**

1. The Capitol Aggregates field site should be characterized by a cone penetrometer test. Many modulus correlations are based on cone-tip resistance. It will be valuable to compare these estimates of modulus and the settlement predictions based on them to the data in this study.

2. In the future, any footing should also be tested to failure. This process will show the non-linear behavior of the soil during failure. As was done thus far, the settlements at higher and higher loads can be predicted and compared to the measured settlements.

3. The strain distribution with depth below the center of the footing requires further study. Schmertmann's strain influence curve appears to be accurate, but the physics behind this behavior are still yet unknown. Several factors may have an impact on the strain distribution including the stress dependency of the modulus, stress history, soil type, effective stress, etc.

4. The zone of influence in this study was only approximately 6 ft below the surface. To verify the ability of field seismic testing to predict the modulus at deeper depths, a series of plate load tests could be conducted at various deeper depths.

5. Theoretically, these site characterization techniques can also be used in saturated sands and clays. The settlement prediction technique is more complex when the effects of consolidation are considered, but the estimate of stiffness based on shear wave velocity should still be a valid method. A similar study to the study presented here, will yield insight to the application of the seismic wave testing in saturated soils.

6. This study was limited to one foundation on one site. Additional studies of other cohesionless soils with different sized footings are recommended.



## **APPENDIX A**

### **FIELD MEASUREMENTS**

#### **INTRODUCTION**

In this appendix, the field test data recorded during tests on 11 Nov 05 is presented in three sections.

#### **SECTION 1**

The data is presented in tabular form. The time, applied load, and settlement of each measured point are given. There were over 8000 data points recorded during each test. The tables consist of the average values of load and settlement every 2.5 seconds.

#### **SECTION 2**

The load-settlement curves for each individual test are presented. Thus, the relative settlement of each point beneath the footing during a single test can be observed. A total of two plots for each test are presented. The first plot shows the settlement measurements near the center of the footing. The second plot shows the settlements measured near the perimeter of the footing.

#### **SECTION 3**

The load-settlement curves at each depth, for each series of tests, are presented. Thus, the behavior of a single point beneath the footing can be observed over a series of tests. This is a total of 10 plots for each series of tests. Each plot shows the behavior of the one telltale for a series of tests.

**APPENDIX A**  
**SECTION 1**

Table A.1: Tabulated Results from 11 Nov 2005, Field Load Test #1

Test # 1		Notes:									
Date: 11-Nov-05		-- Linear Pot #3 did not successfully record during this test -- Data from Linear Pot #4 was discarded due to excessive scatter -- Each Telltale is labeled by the same notation: (LP# (Depth) I/O)									
Time (sec)	Load (lbs)	Interior Telltales (I)					Perimeter Telltales (O)				
		LP9 (surf) I (in)	LP6 (6") I (in)	LP8 (12") I (in)	LP7 (18") I (in)	LP12 (30") I (in)	LP1 (surf) O (in)	LP3 (6") O (in)	LP2 (12") O (in)	LP4 (18") O (in)	LP10 (30") O (in)
MAX	19918	-0.0240	-0.0184	-0.0160	-0.0125	-0.0088	-0.0214	0.0000	-0.0154	-0.0184	-0.0057
0	-3	0.0000	0.0000	0.0000	0.0000	0.0000	0.0000	0.0000	0.0000	0.0000	0.0000
2.5	-3	0.0000	0.0000	0.0000	0.0000	0.0000	0.0000	0.0000	0.0000	0.0000	0.0000
5	470	0.0000	0.0000	-0.0002	-0.0002	0.0000	-0.0003	0.0000	0.0000	-0.0004	0.0000
7.5	1637	0.0001	0.0000	-0.0001	-0.0004	0.0001	-0.0006	0.0000	0.0000	-0.0000	0.0001
10	2698	-0.0025	-0.0009	-0.0006	-0.0010	0.0001	-0.0014	0.0000	-0.0003	-0.0007	0.0001
12.5	3701	-0.0036	-0.0017	-0.0015	-0.0011	0.0001	-0.0021	0.0000	-0.0009	-0.0005	0.0001
15	4643	-0.0036	-0.0025	-0.0023	-0.0014	0.0000	-0.0042	0.0000	-0.0014	-0.0006	-0.0003
17.5	5541	-0.0065	-0.0033	-0.0033	-0.0024	-0.0003	-0.0062	0.0000	-0.0018	-0.0006	-0.0002
20	6397	-0.0090	-0.0041	-0.0042	-0.0034	-0.0004	-0.0064	0.0000	-0.0027	-0.0009	0.0000
22.5	7218	-0.0098	-0.0051	-0.0052	-0.0042	-0.0009	-0.0072	0.0000	-0.0041	-0.0009	-0.0006
25	8010	-0.0099	-0.0059	-0.0059	-0.0043	-0.0011	-0.0082	0.0000	-0.0050	-0.0009	-0.0018
27.5	8767	-0.0107	-0.0069	-0.0066	-0.0047	-0.0019	-0.0094	0.0000	-0.0054	-0.0016	-0.0024
30	9490	-0.0108	-0.0076	-0.0071	-0.0051	-0.0023	-0.0105	0.0000	-0.0058	-0.0016	-0.0027
32.5	10187	-0.0123	-0.0083	-0.0078	-0.0056	-0.0029	-0.0113	0.0000	-0.0064	-0.0025	-0.0032
35	10860	-0.0131	-0.0089	-0.0087	-0.0067	-0.0041	-0.0119	0.0000	-0.0069	-0.0028	-0.0036
37.5	11511	-0.0136	-0.0097	-0.0092	-0.0073	-0.0044	-0.0124	0.0000	-0.0073	-0.0030	-0.0036
40	12134	-0.0133	-0.0103	-0.0097	-0.0080	-0.0048	-0.0132	0.0000	-0.0079	-0.0035	-0.0038
42.5	12734	-0.0129	-0.0109	-0.0102	-0.0082	-0.0053	-0.0144	0.0000	-0.0087	-0.0043	-0.0039
45	13308	-0.0130	-0.0114	-0.0104	-0.0085	-0.0058	-0.0149	0.0000	-0.0095	-0.0046	-0.0042
47.5	13851	-0.0131	-0.0119	-0.0108	-0.0089	-0.0063	-0.0152	0.0000	-0.0103	-0.0054	-0.0043
50	14369	-0.0126	-0.0125	-0.0110	-0.0092	-0.0063	-0.0160	0.0000	-0.0106	-0.0056	-0.0043
52.5	14866	-0.0137	-0.0130	-0.0113	-0.0097	-0.0065	-0.0164	0.0000	-0.0108	-0.0058	-0.0045
55	15345	-0.0143	-0.0134	-0.0118	-0.0098	-0.0064	-0.0169	0.0000	-0.0112	-0.0061	-0.0046
57.5	15804	-0.0147	-0.0138	-0.0122	-0.0102	-0.0065	-0.0172	0.0000	-0.0115	-0.0064	-0.0046
60	16248	-0.0156	-0.0142	-0.0125	-0.0106	-0.0072	-0.0175	0.0000	-0.0115	-0.0066	-0.0048
62.5	16678	-0.0186	-0.0146	-0.0130	-0.0108	-0.0073	-0.0176	0.0000	-0.0118	-0.0069	-0.0049
65	17091	-0.0180	-0.0151	-0.0135	-0.0110	-0.0074	-0.0176	0.0000	-0.0119	-0.0070	-0.0049
67.5	17490	-0.0175	-0.0154	-0.0137	-0.0110	-0.0074	-0.0183	0.0000	-0.0123	-0.0073	-0.0048
70	17874	-0.0181	-0.0158	-0.0140	-0.0108	-0.0071	-0.0191	0.0000	-0.0125	-0.0075	-0.0038
72.5	18246	-0.0182	-0.0162	-0.0141	-0.0111	-0.0074	-0.0191	0.0000	-0.0128	-0.0076	-0.0027
75	18603	-0.0189	-0.0165	-0.0143	-0.0111	-0.0079	-0.0200	0.0000	-0.0133	-0.0078	-0.0028
77.5	18948	-0.0187	-0.0168	-0.0146	-0.0116	-0.0080	-0.0206	0.0000	-0.0138	-0.0081	-0.0028
80	19279	-0.0176	-0.0171	-0.0148	-0.0118	-0.0083	-0.0208	0.0000	-0.0140	-0.0083	-0.0031
82.5	19599	-0.0193	-0.0175	-0.0153	-0.0121	-0.0082	-0.0213	0.0000	-0.0146	-0.0086	-0.0045
85	19893	-0.0218	-0.0177	-0.0156	-0.0119	-0.0082	-0.0214	0.0000	-0.0148	-0.0087	-0.0049
87.5	19918	-0.0226	-0.0180	-0.0160	-0.0120	-0.0084	-0.0214	0.0000	-0.0151	-0.0089	-0.0053
90	19849	-0.0225	-0.0184	-0.0160	-0.0120	-0.0088	-0.0213	0.0000	-0.0154	-0.0091	-0.0056
92.5	19785	-0.0230	-0.0184	-0.0160	-0.0118	-0.0087	-0.0213	0.0000	-0.0154	-0.0092	-0.0056
95	19722	-0.0229	-0.0184	-0.0160	-0.0117	-0.0084	-0.0213	0.0000	-0.0154	-0.0094	-0.0056
97.5	19656	-0.0238	-0.0184	-0.0160	-0.0118	-0.0084	-0.0213	0.0000	-0.0154	-0.0095	-0.0056
100	19591	-0.0239	-0.0184	-0.0160	-0.0118	-0.0084	-0.0213	0.0000	-0.0154	-0.0096	-0.0056
102.5	19520	-0.0239	-0.0184	-0.0160	-0.0118	-0.0084	-0.0213	0.0000	-0.0154	-0.0097	-0.0056
105	19440	-0.0240	-0.0184	-0.0160	-0.0118	-0.0084	-0.0213	0.0000	-0.0154	-0.0098	-0.0056
107.5	19353	-0.0239	-0.0184	-0.0160	-0.0118	-0.0084	-0.0213	0.0000	-0.0154	-0.0099	-0.0056
110	19254	-0.0239	-0.0184	-0.0160	-0.0118	-0.0084	-0.0213	0.0000	-0.0154	-0.0100	-0.0056
112.5	19152	-0.0239	-0.0184	-0.0160	-0.0118	-0.0084	-0.0213	0.0000	-0.0154	-0.0101	-0.0056
115	19050	-0.0239	-0.0184	-0.0160	-0.0118	-0.0084	-0.0213	0.0000	-0.0154	-0.0102	-0.0056
117.5	18938	-0.0239	-0.0184	-0.0160	-0.0118	-0.0084	-0.0213	0.0000	-0.0154	-0.0103	-0.0056
120	18774	-0.0239	-0.0184	-0.0160	-0.0121	-0.0084	-0.0213	0.0000	-0.0154	-0.0104	-0.0056
122.5	18445	-0.0239	-0.0184	-0.0160	-0.0125	-0.0084	-0.0213	0.0000	-0.0154	-0.0105	-0.0056
125	18039	-0.0239	-0.0184	-0.0160	-0.0125	-0.0085	-0.0213	0.0000	-0.0154	-0.0106	-0.0056
127.5	17619	-0.0237	-0.0184	-0.0160	-0.0124	-0.0088	-0.0213	0.0000	-0.0154	-0.0107	-0.0057
130	17195	-0.0234	-0.0184	-0.0160	-0.0122	-0.0089	-0.0213	0.0000	-0.0154	-0.0108	-0.0058
132.5	16778	-0.0235	-0.0184	-0.0160	-0.0122	-0.0091	-0.0213	0.0000	-0.0154	-0.0109	-0.0060
135	16377	-0.0230	-0.0184	-0.0160	-0.0124	-0.0090	-0.0213	0.0000	-0.0155	-0.0110	-0.0062

Table A.1: Tabulated Results from 11 Nov 2005, Field Load Test #3 (continued)

Test # 1		Notes: -- Linear Pot #3 did not successfully record during this test -- Data from Linear Pot #4 was discarded due to excessive scatter -- Each Telltale is labeled by the same notation: (LP# (Depth) I/O)									
Date: 11-Nov-05		Interior Telltales (I)					Perimeter Telltales (O)				
Time (sec)	Load (lbs)	LP9 (surf) I (in)	LP6 (6") I (in)	LP8 (12") I (in)	LP7 (18") I (in)	LP12 (30") I (in)	LP1 (surf) O (in)	LP3 (6") O (in)	LP2 (12") O (in)	LP4 (18") O (in)	LP10 (30") O (in)
137.5	15997	-0.0226	-0.0184	-0.0160	-0.0125	-0.0091	-0.0213	0.0000	-0.0155	-0.0180	-0.0062
140	15632	-0.0221	-0.0184	-0.0160	-0.0124	-0.0092	-0.0213	0.0000	-0.0155	-0.0182	-0.0065
142.5	15274	-0.0218	-0.0184	-0.0160	-0.0122	-0.0094	-0.0214	0.0000	-0.0156	-0.0186	-0.0064
145	14761	-0.0215	-0.0184	-0.0160	-0.0125	-0.0094	-0.0214	0.0000	-0.0157	-0.0186	-0.0066
147.5	14066	-0.0209	-0.0183	-0.0160	-0.0124	-0.0096	-0.0215	0.0000	-0.0158	-0.0186	-0.0069
150	13375	-0.0207	-0.0180	-0.0158	-0.0125	-0.0096	-0.0214	0.0000	-0.0158	-0.0186	-0.0070
152.5	12655	-0.0207	-0.0180	-0.0157	-0.0126	-0.0095	-0.0211	0.0000	-0.0155	-0.0183	-0.0070
155	11020	-0.0204	-0.0178	-0.0157	-0.0128	-0.0097	-0.0206	0.0000	-0.0153	-0.0186	-0.0073
157.5	8785	-0.0185	-0.0171	-0.0151	-0.0125	-0.0101	-0.0190	0.0000	-0.0150	-0.0208	-0.0073
160	7129	-0.0183	-0.0164	-0.0142	-0.0125	-0.0099	-0.0177	0.0000	-0.0147	-0.0181	-0.0073
162.5	5921	-0.0178	-0.0158	-0.0136	-0.0128	-0.0098	-0.0172	0.0000	-0.0141	-0.0148	-0.0073
165	5064	-0.0170	-0.0151	-0.0132	-0.0128	-0.0097	-0.0168	0.0000	-0.0135	-0.0166	-0.0073
167.5	4427	-0.0151	-0.0145	-0.0128	-0.0128	-0.0097	-0.0160	0.0000	-0.0130	-0.0173	-0.0073
170	3861	-0.0153	-0.0140	-0.0123	-0.0128	-0.0097	-0.0153	0.0000	-0.0125	-0.0158	-0.0073
172.5	3425	-0.0142	-0.0135	-0.0120	-0.0128	-0.0097	-0.0148	0.0000	-0.0118	-0.0158	-0.0073
175	2900	-0.0135	-0.0129	-0.0116	-0.0123	-0.0097	-0.0144	0.0000	-0.0117	-0.0163	-0.0073
177.5	2662	-0.0140	-0.0125	-0.0113	-0.0115	-0.0097	-0.0137	0.0000	-0.0115	-0.0164	-0.0073
180	87	-0.0106	-0.0094	-0.0090	-0.0109	-0.0098	-0.0087	0.0000	-0.0090	-0.0146	-0.0073
182.5	0	-0.0104	-0.0090	-0.0088	-0.0107	-0.0097	-0.0082	0.0000	-0.0088	-0.0151	-0.0073
185	0	-0.0104	-0.0089	-0.0085	-0.0107	-0.0097	-0.0082	0.0000	-0.0088	-0.0140	-0.0073
187.5	0	-0.0101	-0.0089	-0.0085	-0.0108	-0.0097	-0.0082	0.0000	-0.0088	-0.0136	-0.0073
190	0	-0.0098	-0.0089	-0.0085	-0.0108	-0.0097	-0.0082	0.0000	-0.0088	-0.0144	-0.0073
192.5	7	-0.0105	-0.0089	-0.0085	-0.0106	-0.0097	-0.0082	0.0000	-0.0088	-0.0135	-0.0073
195	8	-0.0103	-0.0089	-0.0085	-0.0107	-0.0097	-0.0082	0.0000	-0.0086	-0.0130	-0.0073
197.5	6	-0.0105	-0.0089	-0.0085	-0.0108	-0.0097	-0.0082	0.0000	-0.0085	-0.0141	-0.0073
200	8	-0.0102	-0.0089	-0.0085	-0.0106	-0.0097	-0.0082	0.0000	-0.0085	-0.0143	-0.0073
202.5	8	-0.0097	-0.0089	-0.0085	-0.0106	-0.0097	-0.0082	0.0000	-0.0086	-0.0145	-0.0073
205	9	-0.0101	-0.0089	-0.0085	-0.0106	-0.0097	-0.0082	0.0000	-0.0087	-0.0144	-0.0073
207.5	10	-0.0102	-0.0089	-0.0085	-0.0106	-0.0097	-0.0082	0.0000	-0.0087	-0.0140	-0.0073
210	8	-0.0101	-0.0089	-0.0085	-0.0105	-0.0097	-0.0082	0.0000	-0.0087	-0.0141	-0.0073
212.5	3	-0.0105	-0.0089	-0.0085	-0.0105	-0.0097	-0.0082	0.0000	-0.0085	-0.0140	-0.0073
215	3	-0.0110	-0.0089	-0.0085	-0.0105	-0.0097	-0.0082	0.0000	-0.0086	-0.0155	-0.0073
217.5	5	-0.0101	-0.0089	-0.0085	-0.0105	-0.0097	-0.0082	0.0000	-0.0085	-0.0140	-0.0073
220	10	-0.0106	-0.0089	-0.0085	-0.0106	-0.0097	-0.0082	0.0000	-0.0085	-0.0140	-0.0073
222.5	9	-0.0106	-0.0089	-0.0085	-0.0107	-0.0097	-0.0082	0.0000	-0.0085	-0.0152	-0.0073
225	8	-0.0105	-0.0089	-0.0085	-0.0106	-0.0097	-0.0082	0.0000	-0.0087	-0.0154	-0.0073
227.5	10	-0.0102	-0.0089	-0.0085	-0.0106	-0.0097	-0.0082	0.0000	-0.0085	-0.0158	-0.0073
230	10	-0.0104	-0.0089	-0.0085	-0.0107	-0.0097	-0.0082	0.0000	-0.0085	-0.0152	-0.0072
232.5	10	-0.0109	-0.0089	-0.0085	-0.0107	-0.0097	-0.0082	0.0000	-0.0085	-0.0150	-0.0072
235	10	-0.0103	-0.0089	-0.0085	-0.0106	-0.0097	-0.0082	0.0000	-0.0085	-0.0151	-0.0071
237.5	10	-0.0100	-0.0089	-0.0085	-0.0105	-0.0096	-0.0081	0.0000	-0.0085	-0.0152	-0.0071
240	10	-0.0101	-0.0089	-0.0085	-0.0105	-0.0094	-0.0081	0.0000	-0.0085	-0.0152	-0.0070
242.5	12	-0.0108	-0.0089	-0.0085	-0.0105	-0.0094	-0.0082	0.0000	-0.0086	-0.0151	-0.0070
245	14	-0.0109	-0.0089	-0.0085	-0.0105	-0.0094	-0.0082	0.0000	-0.0085	-0.0153	-0.0070
247.5	13	-0.0109	-0.0089	-0.0085	-0.0105	-0.0094	-0.0082	0.0000	-0.0085	-0.0151	-0.0070
250	12	-0.0113	-0.0089	-0.0085	-0.0105	-0.0094	-0.0081	0.0000	-0.0085	-0.0152	-0.0070
252.5	12	-0.0119	-0.0089	-0.0085	-0.0105	-0.0094	-0.0081	0.0000	-0.0085	-0.0151	-0.0070
255	14	-0.0120	-0.0089	-0.0085	-0.0105	-0.0094	-0.0081	0.0000	-0.0085	-0.0152	-0.0070

Table A.2: Tabulated Results from 11 Nov 2005, Field Load Test #2

Test # 2		Notes:									
Date: 11-Nov-05		-- Linear Pot #3 did not successfully record during this test -- Data from Linear Pot #4 was discarded due to excessive scatter -- Each Telltale is labeled by the same notation: (LP# (Depth) I/O)									
Time (sec)	Load (lbs)	Interior Telltales (I)					Perimeter Telltales (O)				
		LP9 (surf) I (in)	LP6 (6") I (in)	LP8 (12") I (in)	LP7 (18") I (in)	LP12 (30") I (in)	LP1 (surf) O (in)	LP3 (6") O (in)	LP2 (12") O (in)	LP4 (18") O (in)	LP10 (30") O (in)
MAX	19920	-0.0165	-0.0106	-0.0085	-0.0031	-0.0017	-0.0144	0.0000	-0.0079	-0.0612	-0.0003
0	-7	0.0000	0.0000	0.0000	0.0000	0.0000	0.0000	0.0000	0.0000	0.0000	0.0000
2.5	-2	0.0000	0.0000	0.0000	0.0000	0.0000	0.0000	0.0000	0.0000	0.0000	0.0000
5	424	0.0000	0.0000	0.0000	0.0000	0.0000	0.0000	0.0000	0.0000	0.0000	0.0000
7.5	1881	0.0007	0.0000	0.0000	0.0000	-0.0003	0.0000	0.0000	0.0000	0.0000	0.0000
10	3042	-0.0002	-0.0003	-0.0002	0.0002	-0.0001	-0.0011	0.0000	0.0000	0.0000	0.0001
12.5	4134	-0.0011	-0.0007	-0.0008	0.0002	0.0002	-0.0021	0.0000	-0.0002	0.0000	0.0004
15	5163	-0.0019	-0.0012	-0.0016	0.0002	0.0004	-0.0031	0.0000	-0.0003	0.0000	0.0005
17.5	6139	-0.0029	-0.0017	-0.0021	0.0002	0.0009	-0.0035	0.0000	-0.0005	0.0000	0.0006
20	7069	-0.0049	-0.0021	-0.0024	0.0000	0.0008	-0.0043	0.0000	-0.0013	0.0000	0.0007
22.5	7960	-0.0045	-0.0026	-0.0026	0.0000	0.0010	-0.0052	0.0000	-0.0018	0.0000	0.0007
25	8806	-0.0034	-0.0031	-0.0028	0.0000	0.0010	-0.0063	0.0000	-0.0022	0.0000	0.0007
27.5	9612	-0.0044	-0.0036	-0.0031	0.0000	0.0010	-0.0066	0.0000	-0.0025	0.0000	0.0007
30	10387	-0.0044	-0.0041	-0.0034	-0.0003	0.0010	-0.0074	0.0000	-0.0029	0.0000	0.0007
32.5	11129	-0.0041	-0.0046	-0.0039	-0.0003	0.0010	-0.0080	0.0000	-0.0030	0.0000	0.0007
35	11842	-0.0057	-0.0050	-0.0043	-0.0007	0.0010	-0.0085	0.0000	-0.0033	0.0000	0.0007
37.5	12525	-0.0060	-0.0054	-0.0047	-0.0013	0.0010	-0.0088	0.0000	-0.0033	0.0000	0.0007
40	13180	-0.0082	-0.0059	-0.0053	-0.0014	0.0008	-0.0090	0.0000	-0.0035	0.0000	0.0007
42.5	13802	-0.0091	-0.0063	-0.0056	-0.0013	0.0007	-0.0094	0.0000	-0.0040	0.0000	0.0007
45	14396	-0.0088	-0.0066	-0.0058	-0.0014	0.0007	-0.0092	0.0000	-0.0043	0.0000	0.0007
47.5	14958	-0.0088	-0.0069	-0.0060	-0.0014	0.0006	-0.0102	0.0000	-0.0045	0.0000	0.0007
50	15496	-0.0093	-0.0073	-0.0062	-0.0013	0.0006	-0.0106	0.0000	-0.0049	0.0000	0.0007
52.5	16014	-0.0095	-0.0076	-0.0065	-0.0018	0.0005	-0.0112	0.0000	-0.0054	0.0000	0.0006
55	16511	-0.0095	-0.0079	-0.0065	-0.0022	0.0005	-0.0119	0.0000	-0.0057	0.0000	0.0005
57.5	16989	-0.0091	-0.0082	-0.0067	-0.0022	0.0004	-0.0121	0.0000	-0.0062	0.0000	0.0004
60	17449	-0.0083	-0.0084	-0.0071	-0.0024	0.0003	-0.0126	0.0000	-0.0063	0.0000	0.0004
62.5	17894	-0.0093	-0.0086	-0.0075	-0.0024	0.0003	-0.0131	0.0000	-0.0066	0.0000	0.0004
65	18320	-0.0108	-0.0088	-0.0078	-0.0028	0.0003	-0.0131	0.0000	-0.0067	0.0000	0.0004
67.5	18734	-0.0116	-0.0091	-0.0079	-0.0027	0.0001	-0.0131	0.0000	-0.0070	0.0000	0.0004
70	19132	-0.0137	-0.0094	-0.0082	-0.0028	0.0002	-0.0131	0.0000	-0.0070	0.0000	0.0004
72.5	19508	-0.0152	-0.0095	-0.0082	-0.0029	-0.0001	-0.0135	0.0000	-0.0071	0.0000	0.0004
75	19855	-0.0151	-0.0098	-0.0083	-0.0029	-0.0003	-0.0140	0.0000	-0.0074	0.0000	0.0004
77.5	19920	-0.0144	-0.0102	-0.0085	-0.0031	-0.0005	-0.0141	0.0000	-0.0076	0.0000	0.0004
80	19845	-0.0151	-0.0102	-0.0085	-0.0030	-0.0008	-0.0141	0.0000	-0.0079	0.0000	0.0004
82.5	19777	-0.0152	-0.0105	-0.0085	-0.0030	-0.0009	-0.0142	0.0000	-0.0079	0.0000	0.0004
85	19716	-0.0151	-0.0106	-0.0085	-0.0031	-0.0010	-0.0144	0.0000	-0.0079	0.0000	0.0004
87.5	19656	-0.0153	-0.0106	-0.0085	-0.0031	-0.0007	-0.0143	0.0000	-0.0079	0.0000	0.0004
90	19601	-0.0154	-0.0106	-0.0085	-0.0031	-0.0006	-0.0141	0.0000	-0.0079	0.0000	0.0004
92.5	19546	-0.0158	-0.0106	-0.0085	-0.0030	-0.0007	-0.0141	0.0000	-0.0079	0.0000	0.0004
95	19494	-0.0160	-0.0106	-0.0085	-0.0030	-0.0007	-0.0141	0.0000	-0.0079	0.0000	0.0004
97.5	19441	-0.0162	-0.0106	-0.0085	-0.0031	-0.0007	-0.0141	0.0000	-0.0079	0.0000	0.0004
100	19392	-0.0162	-0.0106	-0.0085	-0.0031	-0.0007	-0.0141	0.0000	-0.0079	0.0000	0.0004
102.5	19345	-0.0163	-0.0106	-0.0085	-0.0030	-0.0007	-0.0142	0.0000	-0.0079	0.0000	0.0004
105	19299	-0.0165	-0.0106	-0.0085	-0.0031	-0.0007	-0.0142	0.0000	-0.0079	0.0000	0.0004
107.5	19251	-0.0165	-0.0106	-0.0085	-0.0031	-0.0007	-0.0141	0.0000	-0.0079	0.0000	0.0004
110	19204	-0.0165	-0.0106	-0.0085	-0.0031	-0.0007	-0.0141	0.0000	-0.0079	0.0000	0.0004
112.5	19157	-0.0165	-0.0106	-0.0085	-0.0031	-0.0007	-0.0141	0.0000	-0.0079	0.0000	0.0004
115	19107	-0.0165	-0.0106	-0.0085	-0.0030	-0.0007	-0.0141	0.0000	-0.0079	0.0000	0.0004
117.5	18999	-0.0165	-0.0106	-0.0085	-0.0028	-0.0007	-0.0141	0.0000	-0.0079	0.0000	0.0004
120	18381	-0.0163	-0.0106	-0.0085	-0.0027	-0.0007	-0.0141	0.0000	-0.0079	0.0000	0.0004
122.5	14426	-0.0139	-0.0104	-0.0083	-0.0028	-0.0008	-0.0132	0.0000	-0.0079	0.0000	0.0000
125	10501	-0.0123	-0.0096	-0.0080	-0.0031	-0.0012	-0.0122	0.0000	-0.0077	0.0000	-0.0003
127.5	7694	-0.0095	-0.0086	-0.0068	-0.0031	-0.0017	-0.0100	0.0000	-0.0073	0.0000	-0.0003
130	5815	-0.0089	-0.0076	-0.0059	-0.0031	-0.0017	-0.0089	0.0000	-0.0067	0.0000	-0.0003
132.5	4638	-0.0077	-0.0067	-0.0051	-0.0025	-0.0014	-0.0082	0.0000	-0.0059	0.0000	-0.0003
135	3917	-0.0068	-0.0059	-0.0046	-0.0023	-0.0014	-0.0071	0.0000	-0.0047	0.0000	-0.0003



Table A.2: Tabulated Results from 11 Nov 2005, Field Load Test #2 (continued)

Test # 2		Notes: -- Linear Pot #3 did not successfully record during this test -- Data from Linear Pot #4 was discarded due to excessive scatter -- Each Telltale is labeled by the same notation: (LP# (Depth) I/O)									
Date: 11-Nov-05		Interior Telltales (I)					Perimeter Telltales (O)				
Time (sec)	Load (lbs)	LP9 (surf) I	LP6 (6") I	LP8 (12") I	LP7 (18") I	LP12 (30") I	LP1 (surf) O	LP3 (6") O	LP2 (12") O	LP4 (18") O	LP10 (30") O
		(in)	(in)	(in)	(in)	(in)	(in)	(in)	(in)	(in)	(in)
137.5	3470	-0.0063	-0.0054	-0.0041	-0.0021	-0.0015	-0.0067	0.0000	-0.0044	-0.0028	-0.0003
140	3128	-0.0047	-0.0051	-0.0037	-0.0021	-0.0016	-0.0061	0.0000	-0.0040	-0.0015	-0.0003
142.5	2650	-0.0058	-0.0045	-0.0034	-0.0020	-0.0015	-0.0053	0.0000	-0.0034	-0.0018	-0.0003
145	2557	-0.0052	-0.0043	-0.0031	-0.0020	-0.0014	-0.0050	0.0000	-0.0033	-0.0017	-0.0003
147.5	198	-0.0011	-0.0014	-0.0013	-0.0009	-0.0013	-0.0009	0.0000	-0.0016	-0.0011	-0.0003
150	-10	-0.0006	-0.0008	-0.0007	-0.0004	-0.0013	-0.0002	0.0000	-0.0010	-0.0020	-0.0003
152.5	-10	-0.0012	-0.0007	-0.0007	-0.0005	-0.0014	-0.0001	0.0000	-0.0010	-0.0020	-0.0003
155	-10	-0.0008	-0.0007	-0.0007	-0.0007	-0.0014	0.0000	0.0000	-0.0010	-0.0020	-0.0003
157.5	-10	-0.0007	-0.0007	-0.0007	-0.0006	-0.0014	0.0000	0.0000	-0.0010	-0.0018	-0.0003
160	-9	-0.0006	-0.0007	-0.0007	-0.0004	-0.0014	0.0000	0.0000	-0.0010	-0.0017	-0.0003
162.5	-10	-0.0008	-0.0007	-0.0007	-0.0005	-0.0014	0.0000	0.0000	-0.0010	-0.0020	-0.0003
165	-10	-0.0008	-0.0007	-0.0007	-0.0003	-0.0014	0.0000	0.0000	-0.0010	-0.0021	-0.0003
167.5	-9	-0.0010	-0.0007	-0.0007	-0.0003	-0.0014	0.0000	0.0000	-0.0010	-0.0021	-0.0003
170	-9	-0.0009	-0.0007	-0.0007	-0.0003	-0.0014	0.0000	0.0000	-0.0010	-0.0021	-0.0003
172.5	-10	-0.0009	-0.0007	-0.0007	-0.0006	-0.0014	0.0000	0.0000	-0.0010	-0.0021	-0.0003
175	-10	-0.0012	-0.0007	-0.0007	-0.0004	-0.0014	0.0000	0.0000	-0.0010	-0.0021	-0.0003
177.5	-10	-0.0012	-0.0007	-0.0007	-0.0003	-0.0014	0.0000	0.0000	-0.0010	-0.0021	-0.0003
180	-10	-0.0010	-0.0007	-0.0007	-0.0003	-0.0014	0.0000	0.0000	-0.0010	-0.0021	-0.0003
182.5	-10	-0.0013	-0.0007	-0.0007	-0.0005	-0.0014	0.0000	0.0000	-0.0010	-0.0021	-0.0003
185	-9	-0.0012	-0.0007	-0.0007	-0.0004	-0.0014	0.0000	0.0000	-0.0010	-0.0021	-0.0003
187.5	-9	-0.0013	-0.0007	-0.0007	-0.0003	-0.0014	0.0000	0.0000	-0.0010	-0.0021	-0.0003
190	-9	-0.0013	-0.0007	-0.0007	-0.0004	-0.0013	0.0000	0.0000	-0.0010	-0.0021	-0.0003
192.5	-6	-0.0013	-0.0007	-0.0007	-0.0006	-0.0013	0.0000	0.0000	-0.0010	-0.0021	-0.0003
195	-5	-0.0013	-0.0007	-0.0007	-0.0007	-0.0014	0.0000	0.0000	-0.0010	-0.0022	-0.0003
197.5	-3	-0.0016	-0.0007	-0.0007	-0.0004	-0.0014	0.0000	0.0000	-0.0010	-0.0023	-0.0003
200	-8	-0.0017	-0.0007	-0.0007	-0.0003	-0.0014	0.0000	0.0000	-0.0010	-0.0023	-0.0003
202.5	-9	-0.0014	-0.0007	-0.0006	-0.0004	-0.0014	0.0000	0.0000	-0.0010	-0.0021	-0.0003
205	-8	-0.0014	-0.0007	-0.0006	-0.0003	-0.0014	0.0000	0.0000	-0.0010	-0.0022	-0.0003
207.5	-7	-0.0016	-0.0007	-0.0005	-0.0003	-0.0014	0.0000	0.0000	-0.0010	-0.0023	-0.0003
210	-8	-0.0016	-0.0007	-0.0006	-0.0003	-0.0014	0.0000	0.0000	-0.0010	-0.0024	-0.0003
212.5	-9	-0.0018	-0.0007	-0.0006	-0.0004	-0.0014	0.0000	0.0000	-0.0010	-0.0024	-0.0003
215	-9	-0.0020	-0.0007	-0.0005	-0.0006	-0.0014	0.0000	0.0000	-0.0010	-0.0024	-0.0003
217.5	-10	-0.0020	-0.0007	-0.0006	-0.0007	-0.0014	0.0000	0.0000	-0.0010	-0.0024	-0.0003
220	-10	-0.0020	-0.0007	-0.0006	-0.0007	-0.0014	0.0000	0.0000	-0.0010	-0.0024	-0.0003
222.5	-10	-0.0020	-0.0007	-0.0006	-0.0007	-0.0014	0.0000	0.0000	-0.0010	-0.0024	-0.0003
225	-10	-0.0020	-0.0007	-0.0006	-0.0007	-0.0014	0.0000	0.0000	-0.0010	-0.0024	-0.0003
227.5	-10	-0.0020	-0.0007	-0.0006	-0.0007	-0.0014	0.0000	0.0000	-0.0010	-0.0025	-0.0003
230	-11	-0.0020	-0.0007	-0.0006	-0.0007	-0.0014	0.0000	0.0000	-0.0010	-0.0022	-0.0003
232.5	-10	-0.0016	-0.0007	-0.0006	-0.0007	-0.0014	0.0000	0.0000	-0.0010	-0.0021	-0.0003
235	-10	-0.0010	-0.0007	-0.0006	-0.0006	-0.0014	0.0000	0.0000	-0.0010	-0.0021	-0.0002
237.5	-10	-0.0009	-0.0007	-0.0006	-0.0003	-0.0014	0.0000	0.0000	-0.0010	-0.0022	-0.0001
240	-11	-0.0006	-0.0007	-0.0006	-0.0003	-0.0014	0.0000	0.0000	-0.0010	-0.0030	-0.0001
242.5	-11	-0.0012	-0.0007	-0.0005	-0.0003	-0.0014	0.0000	0.0000	-0.0010	-0.0031	0.0000
245	-10	-0.0015	-0.0007	-0.0005	-0.0003	-0.0014	0.0000	0.0000	-0.0010	-0.0030	0.0000
247.5	-11	-0.0017	-0.0007	-0.0005	-0.0003	-0.0013	0.0000	0.0000	-0.0010	-0.0030	0.0000
250	-10	-0.0018	-0.0007	-0.0004	-0.0003	-0.0011	0.0000	0.0000	-0.0010	-0.0028	0.0000
252.5	-10	-0.0018	-0.0007	-0.0003	-0.0003	-0.0013	0.0000	0.0000	-0.0010	-0.0027	0.0000
255	-10	-0.0020	-0.0007	-0.0004	-0.0003	-0.0014	0.0000	0.0000	-0.0010	-0.0027	0.0000

Table A.3: Tabulated Results from 11 Nov 2005, Field Load Test #3

Test # 3		Notes:									
Date: 11-Nov-05		-- Linear Pot #3 was determined to be damaged at the outset of these tests -- Linear Pot #4 failed to function properly during this test -- Each Telltale is labeled by the same notation: (LP# (Depth) I/O)									
Time (sec)	Load (lbs)	Interior Telltales (I)					Perimeter Telltales (O)				
		LP9 (surf) I (in)	LP6 (6") I (in)	LP8 (12") I (in)	LP7 (18") I (in)	LP12 (30") I (in)	LP1 (surf) O (in)	LP3 (6") O (in)	LP2 (12") O (in)	LP4 (18") O (in)	LP10 (30") O (in)
MAX	19983	-0.0157	-0.0106	-0.0089	-0.0034	-0.0010	-0.0142	0.0000	-0.0073	-0.0056	-0.0010
0	0	0.0000	0.0000	0.0000	0.0000	0.0000	0.0000	0.0000	0.0000	0.0000	0.0000
2.5	-29	0.0000	0.0000	0.0000	0.0000	0.0000	0.0000	0.0000	0.0000	0.0000	0.0000
5	2	0.0000	0.0000	0.0000	0.0000	0.0000	0.0000	0.0000	0.0000	0.0000	0.0000
7.5	134	0.0000	0.0000	-0.0001	0.0000	0.0000	0.0000	0.0000	0.0000	0.0000	0.0000
10	1220	0.0000	0.0000	0.0000	0.0000	0.0000	0.0000	0.0000	0.0000	0.0000	0.0000
12.5	2417	-0.0001	-0.0002	-0.0002	0.0000	0.0003	-0.0009	0.0000	-0.0001	0.0000	0.0000
15	3076	-0.0005	-0.0004	-0.0006	0.0000	0.0007	-0.0016	0.0000	-0.0005	0.0000	0.0000
17.5	3460	-0.0011	-0.0005	-0.0007	0.0000	0.0007	-0.0020	0.0000	-0.0003	0.0000	0.0001
20	4347	-0.0009	-0.0009	-0.0012	0.0000	0.0009	-0.0028	0.0000	0.0000	0.0000	0.0005
22.5	5296	-0.0012	-0.0013	-0.0019	0.0000	0.0008	-0.0033	0.0000	0.0000	0.0000	0.0007
25	6208	-0.0045	-0.0017	-0.0024	0.0000	0.0009	-0.0038	0.0000	-0.0003	0.0000	0.0007
27.5	7079	-0.0046	-0.0022	-0.0025	0.0000	0.0007	-0.0048	0.0000	-0.0007	0.0000	0.0007
30	7915	-0.0038	-0.0027	-0.0027	0.0000	0.0009	-0.0059	0.0000	-0.0011	0.0000	0.0007
32.5	8712	-0.0043	-0.0033	-0.0030	0.0000	0.0009	-0.0062	0.0000	-0.0014	0.0000	0.0007
35	9477	-0.0050	-0.0038	-0.0033	0.0003	0.0010	-0.0070	0.0000	-0.0018	0.0000	0.0007
37.5	10217	-0.0039	-0.0043	-0.0038	0.0003	0.0009	-0.0078	0.0000	-0.0020	0.0000	0.0007
40	10934	-0.0056	-0.0048	-0.0042	0.0001	0.0009	-0.0082	0.0000	-0.0020	0.0000	0.0007
42.5	11626	-0.0058	-0.0052	-0.0047	-0.0003	0.0010	-0.0089	0.0000	-0.0023	0.0000	0.0007
45	12294	-0.0077	-0.0056	-0.0052	-0.0006	0.0009	-0.0091	0.0000	-0.0026	0.0000	0.0007
47.5	12962	-0.0092	-0.0061	-0.0055	-0.0006	0.0008	-0.0092	0.0000	-0.0030	0.0000	0.0007
50	13606	-0.0093	-0.0065	-0.0058	-0.0006	0.0007	-0.0089	0.0000	-0.0035	0.0000	0.0007
52.5	14217	-0.0087	-0.0068	-0.0059	-0.0005	0.0007	-0.0099	0.0000	-0.0042	0.0000	0.0007
55	14799	-0.0095	-0.0073	-0.0061	-0.0014	0.0007	-0.0104	0.0000	-0.0047	0.0000	0.0007
57.5	15352	-0.0095	-0.0075	-0.0064	-0.0015	0.0006	-0.0111	0.0000	-0.0050	0.0000	0.0007
60	15884	-0.0093	-0.0078	-0.0065	-0.0017	0.0004	-0.0118	0.0000	-0.0052	0.0000	0.0007
62.5	16389	-0.0088	-0.0080	-0.0068	-0.0021	0.0004	-0.0120	0.0000	-0.0054	0.0000	0.0007
65	16879	-0.0089	-0.0084	-0.0071	-0.0019	0.0006	-0.0126	0.0000	-0.0057	0.0000	0.0007
67.5	17351	-0.0099	-0.0086	-0.0075	-0.0020	0.0004	-0.0129	0.0000	-0.0057	0.0000	0.0006
70	17806	-0.0107	-0.0089	-0.0077	-0.0021	0.0005	-0.0129	0.0000	-0.0060	0.0000	0.0004
72.5	18241	-0.0121	-0.0092	-0.0079	-0.0022	0.0006	-0.0130	0.0000	-0.0062	0.0000	0.0003
75	18663	-0.0145	-0.0095	-0.0082	-0.0023	0.0007	-0.0132	0.0000	-0.0063	0.0000	0.0003
77.5	19069	-0.0149	-0.0098	-0.0083	-0.0024	0.0007	-0.0138	0.0000	-0.0065	0.0000	0.0003
80	19461	-0.0152	-0.0099	-0.0086	-0.0026	0.0006	-0.0140	0.0000	-0.0067	0.0000	0.0003
82.5	19833	-0.0139	-0.0102	-0.0089	-0.0031	0.0005	-0.0140	0.0000	-0.0067	0.0000	0.0003
85	19983	-0.0146	-0.0104	-0.0089	-0.0030	0.0002	-0.0141	0.0000	-0.0070	0.0000	0.0003
87.5	19914	-0.0143	-0.0106	-0.0089	-0.0028	0.0000	-0.0141	0.0000	-0.0070	0.0000	0.0003
90	19856	-0.0139	-0.0106	-0.0089	-0.0027	0.0000	-0.0142	0.0000	-0.0070	0.0000	0.0003
92.5	19799	-0.0143	-0.0106	-0.0089	-0.0027	0.0000	-0.0142	0.0000	-0.0070	0.0000	0.0003
95	19745	-0.0142	-0.0106	-0.0089	-0.0028	0.0000	-0.0142	0.0000	-0.0070	0.0000	0.0003
97.5	19700	-0.0144	-0.0106	-0.0089	-0.0027	0.0000	-0.0142	0.0000	-0.0070	0.0000	0.0003
100	19656	-0.0146	-0.0106	-0.0089	-0.0030	0.0000	-0.0142	0.0000	-0.0070	0.0000	0.0003
102.5	19613	-0.0143	-0.0106	-0.0089	-0.0030	0.0000	-0.0142	0.0000	-0.0070	0.0000	0.0003
105	19574	-0.0144	-0.0106	-0.0089	-0.0030	0.0000	-0.0142	0.0000	-0.0070	0.0000	0.0003
107.5	19535	-0.0146	-0.0106	-0.0089	-0.0030	0.0000	-0.0142	0.0000	-0.0070	0.0000	0.0003
110	19495	-0.0148	-0.0106	-0.0089	-0.0030	0.0000	-0.0142	0.0000	-0.0070	0.0000	0.0003
112.5	19455	-0.0150	-0.0106	-0.0089	-0.0030	0.0002	-0.0142	0.0000	-0.0070	0.0000	0.0003
115	19419	-0.0150	-0.0106	-0.0089	-0.0030	0.0003	-0.0142	0.0000	-0.0070	0.0000	0.0003
117.5	19382	-0.0150	-0.0106	-0.0089	-0.0030	0.0003	-0.0142	0.0000	-0.0070	0.0000	0.0003
120	19347	-0.0151	-0.0106	-0.0089	-0.0030	0.0003	-0.0142	0.0000	-0.0070	0.0000	0.0003
122.5	19312	-0.0152	-0.0106	-0.0089	-0.0031	0.0003	-0.0142	0.0000	-0.0070	0.0000	0.0003
125	19278	-0.0153	-0.0106	-0.0089	-0.0031	0.0001	-0.0142	0.0000	-0.0070	0.0000	0.0003
127.5	19246	-0.0153	-0.0106	-0.0089	-0.0033	0.0001	-0.0142	0.0000	-0.0070	0.0000	0.0003
130	19214	-0.0153	-0.0106	-0.0089	-0.0034	0.0003	-0.0142	0.0000	-0.0070	0.0000	0.0003
132.5	19184	-0.0153	-0.0106	-0.0089	-0.0032	0.0003	-0.0142	0.0000	-0.0070	0.0000	0.0003
135	19150	-0.0154	-0.0106	-0.0089	-0.0030	0.0002	-0.0142	0.0000	-0.0070	0.0000	0.0003

Table A.3: Tabulated Results from 11 Nov 2005, Field Load Test #3 (continued)

Test # 3		Notes:									
Date: 11-Nov-05		-- Linear Pot #3 was determined to be damaged at the outset of these tests -- Linear Pot #4 failed to function properly during this test -- Each Telltale is labeled by the same notation: (LP# (Depth) I/O)									
Time (sec)	Load (lbs)	Interior Telltales (I)					Perimeter Telltales (O)				
		LP9 (surf) I (in)	LP6 (6") I (in)	LP8 (12") I (in)	LP7 (18") I (in)	LP12 (30") I (in)	LP1 (surf) O (in)	LP3 (6") O (in)	LP2 (12") O (in)	LP4 (18") O (in)	LP10 (30") O (in)
137.5	19119	-0.0155	-0.0106	-0.0089	-0.0030	0.0001	-0.0142	0.0000	-0.0070	0.0019	0.0003
140	19089	-0.0157	-0.0106	-0.0089	-0.0032	0.0000	-0.0141	0.0000	-0.0070	0.0019	0.0003
142.5	19057	-0.0157	-0.0106	-0.0089	-0.0030	0.0003	-0.0140	0.0000	-0.0070	0.0019	0.0003
145	19026	-0.0157	-0.0106	-0.0089	-0.0032	0.0001	-0.0140	0.0000	-0.0070	0.0019	0.0003
147.5	18994	-0.0157	-0.0106	-0.0089	-0.0034	0.0000	-0.0139	0.0000	-0.0070	0.0019	0.0003
150	18974	-0.0157	-0.0106	-0.0089	-0.0034	0.0000	-0.0140	0.0000	-0.0070	0.0019	0.0003
152.5	18946	-0.0157	-0.0106	-0.0089	-0.0034	0.0000	-0.0141	0.0000	-0.0070	0.0017	0.0003
155	18890	-0.0157	-0.0106	-0.0089	-0.0030	0.0000	-0.0139	0.0000	-0.0070	0.0019	0.0003
157.5	18811	-0.0157	-0.0106	-0.0089	-0.0030	0.0001	-0.0139	0.0000	-0.0070	0.0017	0.0003
160	18738	-0.0157	-0.0106	-0.0089	-0.0030	0.0002	-0.0140	0.0000	-0.0070	0.0017	0.0003
162.5	18644	-0.0157	-0.0106	-0.0089	-0.0030	0.0000	-0.0139	0.0000	-0.0070	0.0017	0.0003
165	18532	-0.0157	-0.0106	-0.0089	-0.0030	0.0001	-0.0139	0.0000	-0.0071	0.0017	0.0003
167.5	18410	-0.0157	-0.0106	-0.0089	-0.0030	0.0000	-0.0139	0.0000	-0.0073	0.0017	0.0003
170	18295	-0.0157	-0.0106	-0.0089	-0.0033	0.0000	-0.0139	0.0000	-0.0073	0.0017	0.0003
172.5	18144	-0.0157	-0.0106	-0.0089	-0.0031	0.0000	-0.0139	0.0000	-0.0073	0.0017	0.0003
175	17460	-0.0153	-0.0106	-0.0089	-0.0030	0.0000	-0.0139	0.0000	-0.0073	0.0017	0.0002
177.5	14990	-0.0129	-0.0104	-0.0089	-0.0030	-0.0007	-0.0139	0.0000	-0.0073	0.0017	-0.0001
180	12682	-0.0129	-0.0101	-0.0087	-0.0031	-0.0008	-0.0130	0.0000	-0.0070	0.0017	-0.0006
182.5	10789	-0.0131	-0.0098	-0.0085	-0.0031	-0.0009	-0.0126	0.0000	-0.0069	0.0017	-0.0009
185	9236	-0.0127	-0.0094	-0.0081	-0.0031	-0.0009	-0.0120	0.0000	-0.0067	0.0017	-0.0010
187.5	7979	-0.0101	-0.0090	-0.0074	-0.0031	-0.0010	-0.0109	0.0000	-0.0067	0.0017	-0.0010
190	6953	-0.0088	-0.0085	-0.0067	-0.0033	-0.0010	-0.0100	0.0000	-0.0064	0.0016	-0.0010
192.5	6134	-0.0092	-0.0081	-0.0062	-0.0034	-0.0008	-0.0089	0.0000	-0.0063	0.0019	-0.0010
195	5479	-0.0081	-0.0076	-0.0058	-0.0034	-0.0007	-0.0088	0.0000	-0.0060	0.0019	-0.0010
197.5	4962	-0.0088	-0.0073	-0.0055	-0.0029	-0.0007	-0.0086	0.0000	-0.0058	0.0020	-0.0010
200	4377	-0.0085	-0.0068	-0.0052	-0.0022	-0.0007	-0.0084	0.0000	-0.0055	0.0020	-0.0010
202.5	3512	-0.0062	-0.0060	-0.0047	-0.0021	-0.0007	-0.0071	0.0000	-0.0048	0.0020	-0.0010
205	3046	-0.0069	-0.0055	-0.0042	-0.0021	-0.0007	-0.0064	0.0000	-0.0042	0.0021	-0.0009
207.5	2720	-0.0051	-0.0050	-0.0037	-0.0016	-0.0007	-0.0057	0.0000	-0.0035	0.0019	-0.0010
210	2606	-0.0038	-0.0047	-0.0035	-0.0014	-0.0007	-0.0057	0.0000	-0.0032	0.0020	-0.0010
212.5	1715	-0.0035	-0.0037	-0.0029	-0.0011	-0.0007	-0.0042	0.0000	-0.0024	0.0019	-0.0009
215	28	-0.0004	-0.0011	-0.0014	-0.0001	-0.0007	-0.0010	0.0000	-0.0007	0.0020	-0.0007
217.5	30	0.0000	-0.0011	-0.0014	0.0000	-0.0004	-0.0010	0.0000	-0.0007	0.0019	-0.0007
220	31	0.0001	-0.0011	-0.0014	-0.0005	-0.0004	-0.0010	0.0000	-0.0007	0.0020	-0.0007
222.5	31	0.0001	-0.0011	-0.0014	-0.0002	-0.0004	-0.0010	0.0000	-0.0007	0.0020	-0.0007
225	30	0.0002	-0.0011	-0.0014	-0.0003	-0.0003	-0.0010	0.0000	-0.0007	0.0020	-0.0007
227.5	33	0.0000	-0.0011	-0.0013	-0.0002	-0.0003	-0.0010	0.0000	-0.0007	0.0021	-0.0007
230	30	0.0001	-0.0011	-0.0014	-0.0001	-0.0004	-0.0010	0.0000	-0.0007	0.0021	-0.0007
232.5	30	0.0000	-0.0011	-0.0014	-0.0001	-0.0003	-0.0009	0.0000	-0.0007	0.0020	-0.0007
235	29	0.0001	-0.0011	-0.0014	-0.0006	-0.0004	-0.0010	0.0000	-0.0007	0.0021	-0.0007
237.5	24	-0.0001	-0.0011	-0.0013	-0.0007	-0.0004	-0.0009	0.0000	-0.0007	0.0021	-0.0007
240	23	0.0000	-0.0011	-0.0013	-0.0006	-0.0003	-0.0010	0.0000	-0.0007	0.0021	-0.0007
242.5	25	-0.0002	-0.0011	-0.0013	-0.0003	-0.0003	-0.0010	0.0000	-0.0007	0.0021	-0.0007
245	20	-0.0003	-0.0011	-0.0013	-0.0003	-0.0004	-0.0009	0.0000	-0.0007	0.0021	-0.0007
247.5	20	-0.0004	-0.0011	-0.0014	-0.0002	-0.0004	-0.0010	0.0000	-0.0007	0.0021	-0.0007
250	17	-0.0002	-0.0011	-0.0013	-0.0001	-0.0004	-0.0009	0.0000	-0.0007	0.0022	-0.0007
252.5	16	0.0001	-0.0011	-0.0014	-0.0002	-0.0004	-0.0007	0.0000	-0.0007	0.0021	-0.0007
255	12	-0.0001	-0.0011	-0.0013	-0.0003	-0.0004	-0.0007	0.0000	-0.0007	0.0022	-0.0007



Table A.4: Tabulated Results from 11 Nov 2005, Field Load Test #4

Test # 4		Notes:									
Date: 11-Nov-05		-- Linear Pot #3 was determined to be damaged at the outset of these tests -- The data gathered from Linear Pot #4 was discarded due to excessive scatter -- Each Telltale is labeled by the same notation: (LP# (Depth) I/O)									
Time (sec)	Load (lbs)	Interior Telltales (I)					Perimeter Telltales (O)				
		LP9 (surf) I (in)	LP6 (6") I (in)	LP8 (12") I (in)	LP7 (18") I (in)	LP12 (30") I (in)	LP1 (surf) O (in)	LP3 (6") O (in)	LP2 (12") O (in)	LP4 (18") O (in)	LP10 (30") O (in)
MAX	19978	-0.0150	-0.0099	-0.0082	-0.0045	-0.0007	-0.0141	0.0000	-0.0067	-0.0164	-0.0011
0	0	0.0000	0.0000	0.0000	0.0000	0.0000	0.0000	0.0000	0.0000	0.0000	0.0000
2.5	-3	0.0000	0.0000	0.0000	0.0000	0.0000	0.0000	0.0000	0.0001	0.0000	0.0000
5	0	0.0000	0.0000	0.0000	0.0000	0.0000	0.0000	0.0000	0.0002	0.0000	0.0000
7.5	-1	0.0000	0.0000	0.0000	0.0000	0.0000	0.0000	0.0000	0.0000	0.0000	0.0000
10	-6	0.0000	0.0001	0.0000	0.0000	0.0000	0.0000	0.0000	0.0000	0.0000	0.0000
12.5	360	0.0000	0.0001	0.0000	0.0000	0.0000	0.0000	0.0000	0.0000	0.0000	0.0000
15	1659	0.0000	0.0000	0.0000	0.0000	-0.0003	-0.0005	0.0000	0.0000	0.0000	0.0000
17.5	2899	0.0000	-0.0001	0.0000	0.0000	-0.0001	-0.0016	0.0000	0.0000	0.0000	0.0000
20	4057	-0.0007	-0.0005	-0.0004	0.0000	0.0004	-0.0024	0.0000	-0.0002	0.0000	0.0005
22.5	5143	-0.0036	-0.0009	-0.0009	0.0002	0.0008	-0.0028	0.0000	0.0000	0.0000	0.0006
25	6169	-0.0043	-0.0014	-0.0013	0.0000	0.0009	-0.0039	0.0000	-0.0002	0.0000	0.0006
27.5	7144	-0.0036	-0.0020	-0.0016	0.0000	0.0011	-0.0052	0.0000	-0.0006	0.0000	0.0006
30	8071	-0.0046	-0.0026	-0.0020	0.0000	0.0011	-0.0056	0.0000	-0.0010	0.0000	0.0006
32.5	8949	-0.0042	-0.0031	-0.0024	-0.0002	0.0013	-0.0066	0.0000	-0.0013	0.0000	0.0006
35	9786	-0.0051	-0.0037	-0.0029	-0.0002	0.0014	-0.0073	0.0000	-0.0013	0.0000	0.0006
37.5	10587	-0.0053	-0.0042	-0.0034	0.0000	0.0014	-0.0080	0.0000	-0.0015	0.0000	0.0006
40	11350	-0.0069	-0.0047	-0.0040	0.0001	0.0014	-0.0082	0.0000	-0.0021	0.0000	0.0006
42.5	12082	-0.0084	-0.0052	-0.0043	-0.0002	0.0013	-0.0084	0.0000	-0.0028	0.0000	0.0006
45	12785	-0.0088	-0.0056	-0.0045	-0.0007	0.0011	-0.0082	0.0000	-0.0034	0.0000	0.0006
47.5	13453	-0.0089	-0.0060	-0.0048	-0.0012	0.0011	-0.0093	0.0000	-0.0040	0.0000	0.0006
50	14090	-0.0093	-0.0063	-0.0051	-0.0014	0.0011	-0.0098	0.0000	-0.0043	0.0000	0.0006
52.5	14696	-0.0094	-0.0067	-0.0053	-0.0018	0.0008	-0.0108	0.0000	-0.0045	0.0000	0.0006
55	15276	-0.0085	-0.0070	-0.0056	-0.0018	0.0008	-0.0111	0.0000	-0.0047	0.0000	0.0006
57.5	15831	-0.0086	-0.0073	-0.0060	-0.0017	0.0006	-0.0118	0.0000	-0.0049	0.0000	0.0006
60	16363	-0.0100	-0.0076	-0.0063	-0.0020	0.0006	-0.0121	0.0000	-0.0053	0.0000	0.0006
62.5	16873	-0.0110	-0.0079	-0.0066	-0.0020	0.0007	-0.0120	0.0000	-0.0054	0.0000	0.0006
65	17366	-0.0122	-0.0082	-0.0068	-0.0024	0.0007	-0.0121	0.0000	-0.0056	0.0000	0.0006
67.5	17841	-0.0138	-0.0085	-0.0070	-0.0025	0.0006	-0.0127	0.0000	-0.0058	0.0000	0.0006
70	18295	-0.0143	-0.0088	-0.0073	-0.0028	0.0004	-0.0131	0.0000	-0.0060	0.0000	0.0006
72.5	18731	-0.0135	-0.0091	-0.0075	-0.0028	0.0003	-0.0133	0.0000	-0.0060	0.0000	0.0006
75	19150	-0.0136	-0.0091	-0.0078	-0.0029	0.0003	-0.0133	0.0000	-0.0062	0.0000	0.0003
77.5	19553	-0.0144	-0.0095	-0.0080	-0.0032	0.0003	-0.0136	0.0000	-0.0063	0.0000	0.0003
80	19925	-0.0146	-0.0095	-0.0082	-0.0030	0.0002	-0.0141	0.0000	-0.0064	0.0000	0.0003
82.5	19978	-0.0145	-0.0098	-0.0082	-0.0030	-0.0001	-0.0141	0.0000	-0.0067	0.0000	0.0003
85	19894	-0.0142	-0.0099	-0.0082	-0.0033	-0.0002	-0.0141	0.0000	-0.0067	0.0000	0.0003
87.5	19823	-0.0143	-0.0099	-0.0082	-0.0034	-0.0001	-0.0141	0.0000	-0.0067	0.0000	0.0003
90	19756	-0.0145	-0.0099	-0.0082	-0.0031	-0.0001	-0.0141	0.0000	-0.0067	0.0000	0.0003
92.5	19696	-0.0142	-0.0099	-0.0082	-0.0031	-0.0001	-0.0141	0.0000	-0.0067	0.0000	0.0003
95	19638	-0.0142	-0.0099	-0.0082	-0.0034	0.0000	-0.0141	0.0000	-0.0067	0.0000	0.0003
97.5	19581	-0.0144	-0.0099	-0.0082	-0.0036	0.0000	-0.0141	0.0000	-0.0067	0.0000	0.0003
100	19527	-0.0146	-0.0099	-0.0082	-0.0033	0.0000	-0.0141	0.0000	-0.0067	0.0000	0.0003
102.5	19475	-0.0146	-0.0099	-0.0082	-0.0033	0.0000	-0.0141	0.0000	-0.0067	0.0000	0.0003
105	19420	-0.0146	-0.0099	-0.0082	-0.0031	0.0000	-0.0141	0.0000	-0.0067	0.0000	0.0003
107.5	19367	-0.0147	-0.0099	-0.0082	-0.0035	0.0000	-0.0141	0.0000	-0.0067	0.0000	0.0003
110	19319	-0.0149	-0.0099	-0.0082	-0.0037	0.0000	-0.0141	0.0000	-0.0067	0.0000	0.0003
112.5	19271	-0.0149	-0.0099	-0.0082	-0.0040	0.0000	-0.0141	0.0000	-0.0067	0.0000	0.0003
115	19225	-0.0149	-0.0099	-0.0082	-0.0037	0.0000	-0.0141	0.0000	-0.0067	0.0000	0.0003
117.5	19176	-0.0149	-0.0099	-0.0082	-0.0037	0.0000	-0.0141	0.0000	-0.0067	0.0000	0.0003
120	19127	-0.0149	-0.0099	-0.0082	-0.0037	0.0000	-0.0141	0.0000	-0.0067	0.0000	0.0003
122.5	19074	-0.0149	-0.0099	-0.0082	-0.0037	0.0000	-0.0141	0.0000	-0.0067	0.0000	0.0003
125	18958	-0.0149	-0.0099	-0.0082	-0.0039	0.0000	-0.0141	0.0000	-0.0067	0.0000	0.0003
127.5	18818	-0.0149	-0.0099	-0.0082	-0.0042	0.0000	-0.0141	0.0000	-0.0067	0.0000	0.0003
130	18631	-0.0149	-0.0099	-0.0082	-0.0044	0.0000	-0.0141	0.0000	-0.0067	0.0000	0.0003
132.5	17852	-0.0150	-0.0099	-0.0082	-0.0045	-0.0003	-0.0140	0.0000	-0.0067	0.0000	0.0002
135	16186	-0.0144	-0.0099	-0.0082	-0.0044	-0.0003	-0.0138	0.0000	-0.0067	0.0000	-0.0003

Table A.4: Tabulated Results from 11 Nov 2005, Field Load Test #4 (continued)

Test # 4		Notes:									
Date: 11-Nov-05		-- Linear Pot #3 was determined to be damaged at the outset of these tests -- The data gathered from Linear Pot #4 was discarded due to excessive scatter -- Each Telltale is labeled by the same notation: (LP# (Depth) I/O)									
Time (sec)	Load (lbs)	Interior Telltales (I)					Perimeter Telltales (O)				
		LP9 (surf) I	LP6 (6") I	LP8 (12") I	LP7 (18") I	LP12 (30") I	LP1 (surf) O	LP3 (6") O	LP2 (12") O	LP4 (18") O	LP10 (30") O
(in)	(in)	(in)	(in)	(in)	(in)	(in)	(in)	(in)	(in)	(in)	(in)
137.5	14504	-0.0139	-0.0099	-0.0082	-0.0040	-0.0005	-0.0134	0.0000	-0.0067	0.0064	-0.0004
140	13018	-0.0136	-0.0097	-0.0082	-0.0037	-0.0005	-0.0132	0.0000	-0.0066	0.0061	-0.0007
142.5	11702	-0.0140	-0.0095	-0.0081	-0.0042	-0.0005	-0.0128	0.0000	-0.0065	0.0060	-0.0008
145	10547	-0.0141	-0.0092	-0.0081	-0.0041	-0.0006	-0.0120	0.0000	-0.0064	0.0059	-0.0008
147.5	9541	-0.0128	-0.0090	-0.0076	-0.0040	-0.0007	-0.0119	0.0000	-0.0063	0.0058	-0.0009
150	8674	-0.0132	-0.0087	-0.0071	-0.0040	-0.0007	-0.0115	0.0000	-0.0063	0.0056	-0.0010
152.5	7917	-0.0111	-0.0084	-0.0067	-0.0041	-0.0007	-0.0110	0.0000	-0.0063	0.0060	-0.0009
155	6968	-0.0092	-0.0079	-0.0063	-0.0043	-0.0007	-0.0101	0.0000	-0.0060	0.0047	-0.0009
157.5	5654	-0.0091	-0.0072	-0.0055	-0.0043	-0.0007	-0.0086	0.0000	-0.0056	0.0031	-0.0010
160	4741	-0.0087	-0.0064	-0.0049	-0.0026	-0.0007	-0.0080	0.0000	-0.0052	0.0001	-0.0010
162.5	4121	-0.0084	-0.0059	-0.0043	-0.0023	-0.0007	-0.0079	0.0000	-0.0048	0.0051	-0.0010
165	3449	-0.0072	-0.0052	-0.0039	-0.0023	-0.0007	-0.0073	0.0000	-0.0042	0.0045	-0.0009
167.5	2681	-0.0066	-0.0043	-0.0034	-0.0020	-0.0006	-0.0058	0.0000	-0.0031	0.0043	-0.0010
170	2513	-0.0060	-0.0040	-0.0031	-0.0018	-0.0006	-0.0055	0.0000	-0.0026	0.0038	-0.0011
172.5	84	0.0001	-0.0006	-0.0011	-0.0005	-0.0007	-0.0014	0.0000	-0.0005	0.0025	-0.0008
175	-14	0.0009	-0.0004	-0.0009	0.0001	-0.0006	-0.0009	0.0000	-0.0003	0.0025	-0.0008
177.5	-18	0.0014	-0.0004	-0.0007	0.0000	-0.0004	-0.0009	0.0000	-0.0003	0.0026	-0.0008
180	-18	0.0010	-0.0004	-0.0007	-0.0002	-0.0003	-0.0007	0.0000	-0.0003	0.0024	-0.0008
182.5	-19	0.0003	-0.0004	-0.0007	-0.0003	-0.0003	-0.0006	0.0000	-0.0003	0.0024	-0.0008
185	-18	0.0004	-0.0004	-0.0007	-0.0005	-0.0003	-0.0006	0.0000	-0.0003	0.0024	-0.0008
187.5	-18	0.0005	-0.0004	-0.0007	-0.0007	-0.0003	-0.0006	0.0000	-0.0003	0.0024	-0.0008
190	-20	0.0006	-0.0004	-0.0007	-0.0007	-0.0003	-0.0006	0.0000	-0.0003	0.0023	-0.0009
192.5	-20	0.0004	-0.0004	-0.0007	-0.0005	-0.0003	-0.0006	0.0000	-0.0003	0.0020	-0.0008
195	-19	0.0004	-0.0004	-0.0007	-0.0006	-0.0003	-0.0006	0.0000	-0.0003	0.0020	-0.0008
197.5	-20	0.0005	-0.0004	-0.0007	-0.0007	-0.0003	-0.0006	0.0000	-0.0003	0.0018	-0.0008
200	-20	0.0005	-0.0004	-0.0007	-0.0007	-0.0003	-0.0006	0.0000	-0.0003	0.0017	-0.0008
202.5	-20	0.0000	-0.0004	-0.0007	-0.0007	-0.0003	-0.0006	0.0000	-0.0003	0.0017	-0.0009
205	-15	0.0002	-0.0004	-0.0007	-0.0007	-0.0003	-0.0006	0.0000	-0.0003	0.0017	-0.0008
207.5	-19	0.0002	-0.0004	-0.0007	-0.0007	-0.0003	-0.0006	0.0000	-0.0003	0.0017	-0.0008
210	-20	0.0000	-0.0004	-0.0007	-0.0006	-0.0003	-0.0006	0.0000	-0.0003	0.0017	-0.0009
212.5	-20	0.0002	-0.0004	-0.0007	-0.0005	-0.0003	-0.0006	0.0000	-0.0003	0.0017	-0.0008
215	-20	-0.0001	-0.0004	-0.0007	-0.0007	-0.0003	-0.0006	0.0000	-0.0003	0.0016	-0.0008
217.5	-20	0.0004	-0.0004	-0.0007	-0.0007	-0.0003	-0.0006	0.0000	-0.0003	0.0015	-0.0008
220	-19	0.0003	-0.0004	-0.0007	-0.0007	-0.0003	-0.0006	0.0000	-0.0003	0.0015	-0.0008
222.5	-19	0.0003	-0.0004	-0.0007	-0.0009	-0.0003	-0.0006	0.0000	-0.0003	0.0014	-0.0009
225	-19	0.0005	-0.0004	-0.0007	-0.0007	-0.0003	-0.0006	0.0000	-0.0003	0.0014	-0.0008
227.5	-20	0.0003	-0.0004	-0.0007	-0.0007	-0.0003	-0.0006	0.0000	-0.0003	0.0014	-0.0009
230	-20	-0.0001	-0.0004	-0.0007	-0.0007	-0.0003	-0.0006	0.0000	-0.0003	0.0014	-0.0009
232.5	-20	-0.0001	-0.0004	-0.0007	-0.0007	-0.0003	-0.0006	0.0000	-0.0003	0.0014	-0.0009
235	-20	-0.0001	-0.0004	-0.0007	-0.0008	-0.0003	-0.0006	0.0000	-0.0003	0.0014	-0.0009
237.5	-20	-0.0003	-0.0004	-0.0007	-0.0007	-0.0003	-0.0006	0.0000	-0.0003	0.0014	-0.0008
240	-20	-0.0004	-0.0004	-0.0007	-0.0007	-0.0003	-0.0006	0.0000	-0.0003	0.0014	-0.0009
242.5	-20	-0.0004	-0.0004	-0.0007	-0.0007	-0.0003	-0.0006	0.0000	-0.0003	0.0014	-0.0010
245	-20	-0.0004	-0.0004	-0.0007	-0.0007	-0.0003	-0.0006	0.0000	-0.0003	0.0014	-0.0009
247.5	-20	-0.0005	-0.0004	-0.0007	-0.0007	-0.0003	-0.0006	0.0000	-0.0003	0.0014	-0.0009
250	-20	-0.0007	-0.0004	-0.0007	-0.0007	-0.0004	-0.0006	0.0000	-0.0003	0.0014	-0.0008
252.5	-20	-0.0007	-0.0004	-0.0007	-0.0007	-0.0003	-0.0006	0.0000	-0.0003	0.0014	-0.0008
255	-20	-0.0007	-0.0004	-0.0007	-0.0007	-0.0003	-0.0006	0.0000	-0.0003	0.0014	-0.0008

Table A.5: Tabulated Results from 11 Nov 2005, Field Load Test #5

Test # 5		Notes:									
Date: 11-Nov-05		-- Linear Pot #3 was determined to be damaged at the outset of these tests -- The data gathered from Linear Pot #4 was discarded due to excessive scatter -- Each Telltale is labeled by the same notation: (LP# (Depth) I/O)									
Time (sec)	Load (lbs)	Interior Telltales (I)					Perimeter Telltales (O)				
		LP9 (surf) I (in)	LP6 (6") I (in)	LP8 (12") I (in)	LP7 (18") I (in)	LP12 (30") I (in)	LP1 (surf) O (in)	LP3 (6") O (in)	LP2 (12") O (in)	LP4 (18") O (in)	LP10 (30") O (in)
MAX	20015	-0.0164	-0.0102	-0.0080	-0.0043	-0.0014	-0.0141	0.0000	-0.0073	-0.0090	-0.0008
0	-1	0.0000	0.0000	0.0000	0.0000	0.0000	0.0000	0.0000	0.0000	0.0000	0.0000
2.5	-1	0.0000	0.0000	0.0000	0.0000	0.0000	0.0000	0.0000	0.0000	0.0000	0.0000
5	-3	0.0000	0.0000	0.0000	0.0000	0.0000	0.0000	0.0000	0.0000	0.0000	0.0000
7.5	431	0.0000	0.0000	0.0000	0.0000	0.0000	0.0000	0.0000	0.0000	0.0000	0.0000
10	1243	0.0000	0.0000	0.0000	0.0000	0.0000	-0.0002	0.0000	0.0000	0.0000	0.0000
12.5	2297	0.0000	0.0000	0.0000	0.0000	0.0000	-0.0011	0.0000	0.0000	0.0000	0.0000
15	3383	0.0000	-0.0002	0.0000	0.0000	0.0001	-0.0019	0.0000	0.0000	0.0000	0.0000
17.5	4420	-0.0029	-0.0005	-0.0003	0.0000	0.0002	-0.0021	0.0000	-0.0004	0.0000	0.0004
20	5407	-0.0040	-0.0010	-0.0008	-0.0001	0.0005	-0.0031	0.0000	-0.0003	0.0000	0.0005
22.5	6349	-0.0041	-0.0016	-0.0011	0.0000	0.0008	-0.0043	0.0000	-0.0003	0.0000	0.0005
25	7245	-0.0046	-0.0021	-0.0014	0.0000	0.0010	-0.0044	0.0000	-0.0007	0.0000	0.0005
27.5	8100	-0.0060	-0.0027	-0.0018	0.0000	0.0010	-0.0056	0.0000	-0.0010	0.0000	0.0005
30	8919	-0.0052	-0.0032	-0.0022	-0.0004	0.0010	-0.0066	0.0000	-0.0010	0.0000	0.0005
32.5	9704	-0.0066	-0.0037	-0.0026	-0.0002	0.0010	-0.0072	0.0000	-0.0012	0.0000	0.0005
35	10457	-0.0063	-0.0042	-0.0033	0.0001	0.0010	-0.0076	0.0000	-0.0018	0.0000	0.0005
37.5	11181	-0.0087	-0.0047	-0.0037	-0.0004	0.0010	-0.0076	0.0000	-0.0025	0.0000	0.0005
40	11884	-0.0090	-0.0051	-0.0039	-0.0008	0.0010	-0.0075	0.0000	-0.0032	0.0000	0.0005
42.5	12559	-0.0093	-0.0056	-0.0042	-0.0012	0.0007	-0.0085	0.0000	-0.0037	0.0000	0.0005
45	13203	-0.0098	-0.0058	-0.0045	-0.0014	0.0007	-0.0091	0.0000	-0.0040	0.0000	0.0005
47.5	13818	-0.0100	-0.0062	-0.0046	-0.0014	0.0007	-0.0099	0.0000	-0.0042	0.0000	0.0005
50	14413	-0.0093	-0.0066	-0.0049	-0.0014	0.0008	-0.0104	0.0000	-0.0044	0.0000	0.0005
52.5	15003	-0.0089	-0.0069	-0.0054	-0.0016	0.0008	-0.0111	0.0000	-0.0047	0.0000	0.0005
55	15572	-0.0092	-0.0072	-0.0058	-0.0017	0.0007	-0.0116	0.0000	-0.0050	0.0000	0.0005
57.5	16117	-0.0109	-0.0075	-0.0059	-0.0020	0.0007	-0.0116	0.0000	-0.0052	0.0000	0.0005
60	16641	-0.0124	-0.0078	-0.0062	-0.0022	0.0006	-0.0115	0.0000	-0.0053	0.0000	0.0005
62.5	17143	-0.0136	-0.0080	-0.0066	-0.0023	0.0005	-0.0121	0.0000	-0.0056	0.0000	0.0005
65	17623	-0.0148	-0.0084	-0.0068	-0.0023	0.0004	-0.0128	0.0000	-0.0056	0.0000	0.0005
67.5	18085	-0.0144	-0.0086	-0.0071	-0.0026	0.0005	-0.0128	0.0000	-0.0057	0.0000	0.0005
70	18526	-0.0144	-0.0089	-0.0073	-0.0026	0.0003	-0.0128	0.0000	-0.0060	0.0000	0.0003
72.5	18954	-0.0147	-0.0092	-0.0075	-0.0026	0.0002	-0.0130	0.0000	-0.0063	0.0000	0.0003
75	19364	-0.0146	-0.0095	-0.0077	-0.0030	0.0003	-0.0134	0.0000	-0.0066	0.0000	0.0002
77.5	19757	-0.0149	-0.0095	-0.0079	-0.0038	0.0006	-0.0136	0.0000	-0.0068	0.0000	0.0002
80	20015	-0.0158	-0.0099	-0.0080	-0.0035	0.0002	-0.0138	0.0000	-0.0070	0.0000	0.0002
82.5	19839	-0.0150	-0.0101	-0.0079	-0.0033	0.0000	-0.0140	0.0000	-0.0073	0.0000	0.0002
85	19859	-0.0146	-0.0102	-0.0079	-0.0032	0.0002	-0.0141	0.0000	-0.0073	0.0000	0.0002
87.5	19788	-0.0160	-0.0102	-0.0079	-0.0031	0.0003	-0.0141	0.0000	-0.0073	0.0000	0.0002
90	19724	-0.0164	-0.0102	-0.0079	-0.0031	0.0006	-0.0141	0.0000	-0.0072	0.0000	0.0002
92.5	19661	-0.0161	-0.0102	-0.0079	-0.0031	0.0004	-0.0141	0.0000	-0.0072	0.0000	0.0002
95	19601	-0.0161	-0.0102	-0.0079	-0.0031	0.0003	-0.0141	0.0000	-0.0070	0.0000	0.0002
97.5	19541	-0.0161	-0.0102	-0.0079	-0.0034	0.0003	-0.0141	0.0000	-0.0070	0.0000	0.0002
100	19484	-0.0161	-0.0102	-0.0079	-0.0035	0.0003	-0.0141	0.0000	-0.0070	0.0000	0.0002
102.5	19428	-0.0160	-0.0102	-0.0079	-0.0038	0.0003	-0.0141	0.0000	-0.0070	0.0000	0.0002
105	19372	-0.0161	-0.0102	-0.0079	-0.0035	0.0003	-0.0141	0.0000	-0.0070	0.0000	0.0002
107.5	19316	-0.0161	-0.0102	-0.0079	-0.0036	0.0003	-0.0140	0.0000	-0.0070	0.0000	0.0002
110	19262	-0.0161	-0.0102	-0.0079	-0.0038	0.0003	-0.0140	0.0000	-0.0070	0.0000	0.0001
112.5	19208	-0.0161	-0.0102	-0.0079	-0.0038	0.0003	-0.0139	0.0000	-0.0070	0.0000	0.0000
115	19157	-0.0161	-0.0102	-0.0079	-0.0038	0.0003	-0.0138	0.0000	-0.0070	0.0000	-0.0001
117.5	19104	-0.0161	-0.0102	-0.0079	-0.0039	0.0003	-0.0138	0.0000	-0.0070	0.0000	-0.0001
120	19048	-0.0161	-0.0102	-0.0079	-0.0041	0.0003	-0.0139	0.0000	-0.0070	0.0000	-0.0001
122.5	18997	-0.0163	-0.0102	-0.0079	-0.0043	0.0003	-0.0139	0.0000	-0.0070	0.0000	-0.0001
125	18948	-0.0163	-0.0102	-0.0079	-0.0041	0.0003	-0.0138	0.0000	-0.0070	0.0000	-0.0001
127.5	18856	-0.0163	-0.0102	-0.0079	-0.0038	0.0003	-0.0138	0.0000	-0.0070	0.0000	-0.0001
130	18665	-0.0164	-0.0102	-0.0079	-0.0038	0.0003	-0.0138	0.0000	-0.0070	0.0000	-0.0001
132.5	16530	-0.0155	-0.0102	-0.0079	-0.0038	-0.0001	-0.0137	0.0000	-0.0070	0.0000	-0.0003
135	13283	-0.0144	-0.0100	-0.0079	-0.0038	-0.0005	-0.0130	0.0000	-0.0070	0.0000	-0.0008



Table A.5: Tabulated Results from 11 Nov 2005, Field Load Test #5 (continued)

Test # 5		Notes: -- Linear Pot #3 was determined to be damaged at the outset of these tests -- The data gathered from Linear Pot #4 was discarded due to excessive scatter -- Each Telltale is labeled by the same notation: (LP# (Depth) I/O)									
Date: 11-Nov-05		Interior Telltales (I)					Perimeter Telltales (O)				
Time (sec)	Load (lbs)	LP9 (surf) I (in)	LP6 (6") I (in)	LP8 (12") I (in)	LP7 (18") I (in)	LP12 (30") I (in)	LP1 (surf) O (in)	LP3 (6") O (in)	LP2 (12") O (in)	LP4 (18") O (in)	LP10 (30") O (in)
137.5	10670	-0.0144	-0.0095	-0.0076	-0.0038	-0.0006	-0.0120	0.0000	-0.0070	-0.0061	-0.0008
140	8660	-0.0135	-0.0089	-0.0068	-0.0038	-0.0010	-0.0112	0.0000	-0.0069	-0.0061	-0.0008
142.5	7115	-0.0107	-0.0083	-0.0060	-0.0038	-0.0012	-0.0101	0.0000	-0.0064	-0.0062	-0.0008
145	5965	-0.0089	-0.0078	-0.0053	-0.0040	-0.0014	-0.0088	0.0000	-0.0060	-0.0065	-0.0008
147.5	5119	-0.0096	-0.0072	-0.0046	-0.0031	-0.0014	-0.0076	0.0000	-0.0058	-0.0061	-0.0008
150	4231	-0.0093	-0.0066	-0.0039	-0.0026	-0.0011	-0.0074	0.0000	-0.0054	-0.0066	-0.0008
152.5	3149	-0.0076	-0.0055	-0.0030	-0.0022	-0.0012	-0.0063	0.0000	-0.0048	-0.0067	-0.0008
155	2637	-0.0063	-0.0049	-0.0027	-0.0019	-0.0012	-0.0052	0.0000	-0.0042	-0.0062	-0.0008
157.5	1245	-0.0034	-0.0030	-0.0016	-0.0011	-0.0013	-0.0028	0.0000	-0.0026	-0.0060	-0.0008
160	-30	0.0003	-0.0008	-0.0005	-0.0002	-0.0010	-0.0006	0.0000	-0.0010	-0.0031	-0.0008
162.5	-30	0.0005	-0.0007	-0.0004	0.0002	-0.0010	-0.0006	0.0000	-0.0010	-0.0035	-0.0008
165	-30	0.0006	-0.0007	-0.0004	0.0002	-0.0010	-0.0004	0.0000	-0.0010	-0.0034	-0.0008
167.5	-30	0.0009	-0.0007	-0.0004	0.0001	-0.0010	-0.0003	0.0000	-0.0010	-0.0032	-0.0008
170	-30	0.0006	-0.0007	-0.0004	0.0000	-0.0010	-0.0003	0.0000	-0.0010	-0.0031	-0.0008
172.5	-27	0.0006	-0.0007	-0.0004	-0.0003	-0.0010	-0.0003	0.0000	-0.0010	-0.0031	-0.0008
175	-25	0.0004	-0.0007	-0.0004	-0.0005	-0.0010	-0.0003	0.0000	-0.0010	-0.0031	-0.0008
177.5	-29	0.0006	-0.0007	-0.0004	-0.0004	-0.0010	-0.0003	0.0000	-0.0010	-0.0031	-0.0008
180	-30	0.0004	-0.0007	-0.0004	-0.0005	-0.0010	-0.0003	0.0000	-0.0010	-0.0031	-0.0008
182.5	-30	0.0009	-0.0007	-0.0004	-0.0007	-0.0010	-0.0003	0.0000	-0.0010	-0.0031	-0.0008
185	-30	0.0007	-0.0007	-0.0004	-0.0007	-0.0010	-0.0003	0.0000	-0.0010	-0.0031	-0.0008
187.5	-30	0.0007	-0.0007	-0.0004	-0.0007	-0.0010	-0.0003	0.0000	-0.0009	-0.0031	-0.0008
190	-30	0.0005	-0.0007	-0.0004	-0.0007	-0.0010	-0.0003	0.0000	-0.0008	-0.0031	-0.0008
192.5	-30	0.0010	-0.0007	-0.0004	-0.0007	-0.0010	-0.0003	0.0000	-0.0007	-0.0031	-0.0008
195	-30	0.0007	-0.0007	-0.0004	-0.0007	-0.0010	-0.0003	0.0000	-0.0007	-0.0032	-0.0008
197.5	-30	0.0011	-0.0007	-0.0004	-0.0007	-0.0010	-0.0003	0.0000	-0.0007	-0.0032	-0.0008
200	-28	0.0013	-0.0007	-0.0004	-0.0007	-0.0010	-0.0003	0.0000	-0.0007	-0.0033	-0.0008
202.5	-29	0.0002	-0.0007	-0.0004	-0.0008	-0.0010	-0.0003	0.0000	-0.0007	-0.0034	-0.0008
205	-30	0.0011	-0.0007	-0.0004	-0.0012	-0.0010	-0.0003	0.0000	-0.0007	-0.0034	-0.0008
207.5	-29	0.0015	-0.0007	-0.0004	-0.0012	-0.0010	-0.0003	0.0000	-0.0007	-0.0034	-0.0008
210	-30	0.0010	-0.0007	-0.0004	-0.0003	-0.0010	-0.0003	0.0000	-0.0007	-0.0034	-0.0008
212.5	-30	0.0006	-0.0007	-0.0004	0.0000	-0.0010	-0.0003	0.0000	-0.0007	-0.0034	-0.0008
215	-28	0.0005	-0.0007	-0.0004	0.0000	-0.0010	-0.0003	0.0000	-0.0009	-0.0034	-0.0008
217.5	-27	0.0003	-0.0007	-0.0004	0.0000	-0.0010	-0.0003	0.0000	-0.0008	-0.0034	-0.0008
220	-22	0.0003	-0.0007	-0.0004	0.0000	-0.0010	-0.0003	0.0000	-0.0008	-0.0034	-0.0008
222.5	-20	-0.0002	-0.0007	-0.0003	0.0000	-0.0010	-0.0003	0.0000	-0.0008	-0.0034	-0.0008
225	-20	0.0005	-0.0007	-0.0002	0.0000	-0.0010	-0.0003	0.0000	-0.0010	-0.0034	-0.0008
227.5	-20	0.0001	-0.0007	-0.0001	0.0000	-0.0010	-0.0003	0.0000	-0.0010	-0.0034	-0.0008
230	-20	-0.0003	-0.0007	-0.0001	0.0000	-0.0010	-0.0003	0.0000	-0.0010	-0.0034	-0.0008
232.5	-20	-0.0005	-0.0007	-0.0001	0.0000	-0.0010	-0.0003	0.0000	-0.0010	-0.0034	-0.0008
235	-20	-0.0006	-0.0007	-0.0001	0.0000	-0.0010	-0.0003	0.0000	-0.0010	-0.0034	-0.0008
237.5	-20	-0.0006	-0.0007	-0.0001	0.0000	-0.0010	-0.0003	0.0000	-0.0010	-0.0034	-0.0008
240	-20	-0.0003	-0.0007	-0.0001	0.0000	-0.0008	-0.0003	0.0000	-0.0010	-0.0034	-0.0008
242.5	-20	0.0000	-0.0007	-0.0001	0.0000	-0.0007	-0.0003	0.0000	-0.0010	-0.0034	-0.0008
245	-14	-0.0002	-0.0007	-0.0001	0.0000	-0.0007	-0.0003	0.0000	-0.0010	-0.0034	-0.0008
247.5	-10	-0.0002	-0.0007	-0.0001	0.0000	-0.0007	-0.0002	0.0000	-0.0010	-0.0035	-0.0008
250	-10	-0.0002	-0.0007	-0.0001	0.0000	-0.0007	-0.0002	0.0000	-0.0010	-0.0035	-0.0008
252.5	-10	-0.0002	-0.0007	-0.0001	0.0000	-0.0007	-0.0002	0.0000	-0.0010	-0.0037	-0.0008
255	-16	-0.0002	-0.0007	-0.0001	0.0000	-0.0007	0.0000	0.0000	-0.0010	-0.0037	-0.0008

Table A.6: Tabulated Results from 11 Nov 2005, Field Load Test #6

Test # 6		Notes:									
Date: 11-Nov-05		-- Linear Pot #3 was determined to be damaged at the outset of these tests -- The data gathered from Linear Pot #4 was discarded due to excessive scatter -- Each Telltale is labeled by the same notation: (LP# (Depth) I/O)									
Time (sec)	Load (lbs)	Interior Telltales (I)					Perimeter Telltales (O)				
		LP10 (surf) I (in)	LP6 (6") I (in)	LP8 (12") I (in)	LP7 (18") I (in)	LP12 (30") I (in)	LP1 (surf) O (in)	LP9 (6") O (in)	LP3 (12") O (in)	LP4 (18") O (in)	LP2 (30") O (in)
MAX	19932	-0.0141	-0.0175	-0.0123	-0.0095	-0.0070	-0.0183	-0.0191	0.0000	-0.0328	-0.0070
0	-8	0.0000	0.0000	0.0000	0.0000	0.0000	0.0000	0.0000	0.0000	0.0000	0.0000
2.5	-10	0.0000	0.0000	0.0000	0.0000	0.0000	0.0000	0.0000	0.0000	0.0000	0.0000
5	-10	0.0000	0.0000	0.0000	0.0000	0.0000	0.0000	0.0000	0.0000	0.0000	0.0000
7.5	-4	0.0000	0.0000	0.0000	0.0000	0.0000	0.0000	0.0000	0.0000	0.0000	0.0000
10	428	0.0000	0.0000	0.0000	0.0000	0.0000	-0.0004	0.0000	0.0000	0.0000	-0.0002
12.5	931	-0.0001	-0.0001	-0.0001	0.0000	0.0000	-0.0007	-0.0002	0.0000	0.0000	-0.0003
15	1528	-0.0002	-0.0006	-0.0003	0.0001	0.0000	-0.0004	-0.0002	0.0000	0.0000	-0.0002
17.5	2546	-0.0012	-0.0014	-0.0004	-0.0001	-0.0002	-0.0006	-0.0011	0.0000	0.0000	0.0000
20	3637	-0.0021	-0.0024	-0.0007	-0.0005	-0.0006	-0.0017	-0.0025	0.0000	0.0000	0.0000
22.5	4685	-0.0029	-0.0037	-0.0014	-0.0010	-0.0017	-0.0036	-0.0043	0.0000	0.0000	0.0000
25	5624	-0.0019	-0.0048	-0.0022	-0.0018	-0.0024	-0.0046	-0.0055	0.0000	0.0000	-0.0001
27.5	6531	-0.0023	-0.0054	-0.0027	-0.0021	-0.0025	-0.0053	-0.0065	0.0000	0.0000	0.0000
30	7394	-0.0028	-0.0060	-0.0032	-0.0031	-0.0026	-0.0060	-0.0076	0.0000	0.0000	0.0000
32.5	8221	-0.0029	-0.0067	-0.0035	-0.0034	-0.0026	-0.0067	-0.0081	0.0000	0.0000	0.0000
35	9011	-0.0025	-0.0074	-0.0037	-0.0033	-0.0026	-0.0074	-0.0085	0.0000	0.0000	0.0000
37.5	9767	-0.0029	-0.0080	-0.0040	-0.0037	-0.0028	-0.0081	-0.0089	0.0000	0.0000	0.0000
40	10496	-0.0054	-0.0086	-0.0045	-0.0041	-0.0029	-0.0089	-0.0094	0.0000	0.0000	0.0000
42.5	11195	-0.0058	-0.0092	-0.0050	-0.0044	-0.0030	-0.0094	-0.0103	0.0000	0.0000	0.0000
45	11866	-0.0063	-0.0097	-0.0054	-0.0046	-0.0032	-0.0097	-0.0109	0.0000	0.0000	0.0000
47.5	12508	-0.0075	-0.0105	-0.0059	-0.0047	-0.0037	-0.0105	-0.0114	0.0000	0.0000	0.0000
50	13127	-0.0078	-0.0113	-0.0064	-0.0051	-0.0039	-0.0108	-0.0119	0.0000	0.0000	-0.0003
52.5	13720	-0.0066	-0.0120	-0.0068	-0.0058	-0.0040	-0.0111	-0.0122	0.0000	0.0000	-0.0006
55	14287	-0.0072	-0.0126	-0.0075	-0.0065	-0.0041	-0.0120	-0.0128	0.0000	0.0000	-0.0013
57.5	14830	-0.0068	-0.0128	-0.0085	-0.0068	-0.0041	-0.0138	-0.0138	0.0000	0.0000	-0.0023
60	15350	-0.0068	-0.0133	-0.0089	-0.0069	-0.0047	-0.0146	-0.0148	0.0000	0.0000	-0.0023
62.5	15850	-0.0061	-0.0137	-0.0091	-0.0068	-0.0051	-0.0149	-0.0155	0.0000	0.0000	-0.0023
65	16332	-0.0080	-0.0141	-0.0092	-0.0068	-0.0053	-0.0154	-0.0160	0.0000	0.0000	-0.0023
67.5	16795	-0.0083	-0.0144	-0.0094	-0.0068	-0.0053	-0.0155	-0.0164	0.0000	0.0000	-0.0023
70	17244	-0.0084	-0.0147	-0.0096	-0.0068	-0.0052	-0.0158	-0.0167	0.0000	0.0000	-0.0023
72.5	17676	-0.0086	-0.0150	-0.0098	-0.0069	-0.0054	-0.0160	-0.0171	0.0000	0.0000	-0.0023
75	18094	-0.0077	-0.0153	-0.0099	-0.0070	-0.0054	-0.0163	-0.0172	0.0000	0.0000	-0.0023
77.5	18499	-0.0074	-0.0157	-0.0102	-0.0072	-0.0055	-0.0163	-0.0175	0.0000	0.0000	-0.0023
80	18888	-0.0069	-0.0160	-0.0105	-0.0077	-0.0059	-0.0162	-0.0178	0.0000	0.0000	-0.0024
82.5	19261	-0.0064	-0.0163	-0.0106	-0.0078	-0.0061	-0.0163	-0.0181	0.0000	0.0000	-0.0023
85	19617	-0.0087	-0.0167	-0.0109	-0.0081	-0.0063	-0.0166	-0.0182	0.0000	0.0000	-0.0025
87.5	19924	-0.0106	-0.0171	-0.0111	-0.0083	-0.0066	-0.0168	-0.0186	0.0000	0.0000	-0.0029
90	19932	-0.0106	-0.0171	-0.0115	-0.0088	-0.0067	-0.0169	-0.0187	0.0000	0.0000	-0.0031
92.5	19862	-0.0118	-0.0174	-0.0118	-0.0092	-0.0068	-0.0171	-0.0188	0.0000	0.0000	-0.0034
95	19800	-0.0132	-0.0175	-0.0120	-0.0095	-0.0068	-0.0175	-0.0191	0.0000	0.0000	-0.0034
97.5	19743	-0.0132	-0.0175	-0.0120	-0.0094	-0.0067	-0.0177	-0.0191	0.0000	0.0000	-0.0036
100	19690	-0.0127	-0.0175	-0.0120	-0.0093	-0.0069	-0.0176	-0.0191	0.0000	0.0000	-0.0036
102.5	19637	-0.0129	-0.0175	-0.0120	-0.0094	-0.0070	-0.0177	-0.0191	0.0000	0.0000	-0.0037
105	19587	-0.0131	-0.0175	-0.0120	-0.0095	-0.0069	-0.0178	-0.0191	0.0000	0.0000	-0.0037
107.5	19541	-0.0130	-0.0175	-0.0120	-0.0095	-0.0068	-0.0181	-0.0191	0.0000	0.0000	-0.0036
110	19495	-0.0129	-0.0175	-0.0120	-0.0094	-0.0068	-0.0182	-0.0191	0.0000	0.0000	-0.0036
112.5	19450	-0.0136	-0.0175	-0.0120	-0.0094	-0.0068	-0.0182	-0.0191	0.0000	0.0000	-0.0037
115	19406	-0.0134	-0.0175	-0.0120	-0.0094	-0.0068	-0.0182	-0.0191	0.0000	0.0000	-0.0037
117.5	19362	-0.0131	-0.0175	-0.0120	-0.0094	-0.0068	-0.0182	-0.0191	0.0000	0.0000	-0.0037
120	19321	-0.0130	-0.0175	-0.0122	-0.0094	-0.0068	-0.0182	-0.0191	0.0000	0.0000	-0.0037
122.5	19278	-0.0133	-0.0175	-0.0123	-0.0095	-0.0068	-0.0182	-0.0191	0.0000	0.0000	-0.0037
125	19239	-0.0135	-0.0175	-0.0123	-0.0095	-0.0067	-0.0182	-0.0191	0.0000	0.0000	-0.0038
127.5	19197	-0.0136	-0.0175	-0.0123	-0.0095	-0.0067	-0.0183	-0.0191	0.0000	0.0000	-0.0040
130	19153	-0.0133	-0.0175	-0.0123	-0.0095	-0.0068	-0.0182	-0.0191	0.0000	0.0000	-0.0040
132.5	19113	-0.0134	-0.0175	-0.0123	-0.0095	-0.0068	-0.0182	-0.0191	0.0000	0.0000	-0.0040
135	19074	-0.0141	-0.0175	-0.0123	-0.0095	-0.0068	-0.0182	-0.0191	0.0000	0.0000	-0.0040

Table A.6: Tabulated Results from 11 Nov 2005, Field Load Test #6 (continued)

Test # 6		Notes:									
Date: 11-Nov-05		-- Linear Pot #3 was determined to be damaged at the outset of these tests -- The data gathered from Linear Pot #4 was discarded due to excessive scatter -- Each Telltale is labeled by the same notation: (LP# (Depth) I/O)									
Time (sec)	Load (lbs)	Interior Telltales (I)					Perimeter Telltales (O)				
		LP10 (surf) I (in)	LP6 (6") I (in)	LP8 (12") I (in)	LP7 (18") I (in)	LP12 (30") I (in)	LP1 (surf) O (in)	LP9 (6") O (in)	LP3 (12") O (in)	LP4 (18") O (in)	LP2 (30") O (in)
137.5	19033	-0.0134	-0.0175	-0.0123	-0.0095	-0.0068	-0.0182	-0.0191	0.0000	0.0073	-0.0040
140	18953	-0.0130	-0.0175	-0.0123	-0.0095	-0.0068	-0.0182	-0.0191	0.0000	0.0068	-0.0040
142.5	18803	-0.0132	-0.0175	-0.0123	-0.0095	-0.0068	-0.0182	-0.0191	0.0000	0.0042	-0.0040
145	18845	-0.0134	-0.0173	-0.0123	-0.0094	-0.0068	-0.0180	-0.0191	0.0000	0.0112	-0.0040
147.5	13718	-0.0135	-0.0164	-0.0123	-0.0095	-0.0065	-0.0170	-0.0191	0.0000	0.0141	-0.0042
150	11246	-0.0132	-0.0152	-0.0123	-0.0095	-0.0063	-0.0166	-0.0191	0.0000	0.0187	-0.0047
152.5	9314	-0.0130	-0.0139	-0.0123	-0.0094	-0.0062	-0.0160	-0.0191	0.0000	0.0153	-0.0055
155	7824	-0.0122	-0.0125	-0.0121	-0.0094	-0.0054	-0.0159	-0.0190	0.0000	0.0172	-0.0058
157.5	6681	-0.0115	-0.0115	-0.0118	-0.0094	-0.0050	-0.0155	-0.0188	0.0000	0.0075	-0.0062
160	5810	-0.0102	-0.0107	-0.0116	-0.0095	-0.0046	-0.0150	-0.0188	0.0000	0.0194	-0.0064
162.5	5140	-0.0098	-0.0100	-0.0113	-0.0095	-0.0043	-0.0143	-0.0187	0.0000	0.0034	-0.0066
165	4607	-0.0083	-0.0093	-0.0110	-0.0095	-0.0041	-0.0134	-0.0184	0.0000	0.0061	-0.0067
167.5	4121	-0.0081	-0.0086	-0.0108	-0.0095	-0.0043	-0.0124	-0.0183	0.0000	0.0087	-0.0066
170	3201	-0.0085	-0.0075	-0.0103	-0.0093	-0.0041	-0.0120	-0.0174	0.0000	0.0023	-0.0067
172.5	2740	-0.0081	-0.0068	-0.0098	-0.0089	-0.0039	-0.0110	-0.0167	0.0000	0.0017	-0.0069
175	1939	-0.0075	-0.0053	-0.0088	-0.0085	-0.0036	-0.0099	-0.0148	0.0000	0.0063	-0.0067
177.5	-1	-0.0064	-0.0016	-0.0069	-0.0070	-0.0020	-0.0060	-0.0111	0.0000	0.0022	-0.0067
180	-2	-0.0059	-0.0014	-0.0067	-0.0069	-0.0019	-0.0060	-0.0110	0.0000	0.0021	-0.0067
182.5	0	-0.0055	-0.0011	-0.0066	-0.0069	-0.0021	-0.0060	-0.0110	0.0000	0.0036	-0.0067
185	0	-0.0057	-0.0011	-0.0067	-0.0068	-0.0021	-0.0060	-0.0110	0.0000	0.0034	-0.0068
187.5	0	-0.0052	-0.0011	-0.0065	-0.0068	-0.0020	-0.0060	-0.0109	0.0000	0.0041	-0.0069
190	0	-0.0062	-0.0011	-0.0065	-0.0069	-0.0020	-0.0060	-0.0108	0.0000	0.0029	-0.0070
192.5	0	-0.0081	-0.0011	-0.0066	-0.0071	-0.0021	-0.0059	-0.0109	0.0000	0.0032	-0.0069
195	0	-0.0079	-0.0011	-0.0067	-0.0071	-0.0021	-0.0060	-0.0109	0.0000	0.0031	-0.0070
197.5	0	-0.0082	-0.0011	-0.0066	-0.0071	-0.0021	-0.0060	-0.0109	0.0000	0.0035	-0.0070
200	0	-0.0083	-0.0011	-0.0066	-0.0071	-0.0020	-0.0060	-0.0109	0.0000	0.0027	-0.0070
202.5	0	-0.0083	-0.0011	-0.0067	-0.0071	-0.0020	-0.0059	-0.0108	0.0000	0.0021	-0.0070
205	0	-0.0086	-0.0011	-0.0067	-0.0073	-0.0020	-0.0060	-0.0108	0.0000	0.0023	-0.0070
207.5	0	-0.0086	-0.0011	-0.0068	-0.0074	-0.0020	-0.0060	-0.0109	0.0000	0.0023	-0.0070
210	0	-0.0089	-0.0011	-0.0068	-0.0074	-0.0020	-0.0060	-0.0108	0.0000	0.0011	-0.0070
212.5	0	-0.0089	-0.0011	-0.0066	-0.0074	-0.0019	-0.0060	-0.0107	0.0000	0.0011	-0.0070
215	0	-0.0089	-0.0011	-0.0067	-0.0074	-0.0020	-0.0060	-0.0107	0.0000	0.0004	-0.0070
217.5	0	-0.0090	-0.0011	-0.0065	-0.0075	-0.0021	-0.0060	-0.0108	0.0000	0.0020	-0.0070
220	0	-0.0086	-0.0011	-0.0065	-0.0074	-0.0020	-0.0057	-0.0108	0.0000	0.0034	-0.0070
222.5	0	-0.0083	-0.0011	-0.0065	-0.0074	-0.0019	-0.0059	-0.0107	0.0000	0.0022	-0.0070
225	0	-0.0089	-0.0011	-0.0065	-0.0074	-0.0020	-0.0059	-0.0107	0.0000	0.0012	-0.0070
227.5	3	-0.0085	-0.0011	-0.0065	-0.0075	-0.0018	-0.0059	-0.0107	0.0000	0.0031	-0.0070
230	3	-0.0073	-0.0011	-0.0065	-0.0075	-0.0017	-0.0057	-0.0107	0.0000	0.0024	-0.0070
232.5	3	-0.0074	-0.0011	-0.0065	-0.0075	-0.0017	-0.0057	-0.0107	0.0000	0.0030	-0.0070
235	2	-0.0087	-0.0011	-0.0065	-0.0074	-0.0018	-0.0057	-0.0108	0.0000	0.0021	-0.0070
237.5	1	-0.0088	-0.0011	-0.0065	-0.0074	-0.0019	-0.0056	-0.0107	0.0000	0.0021	-0.0070
240	4	-0.0084	-0.0011	-0.0065	-0.0074	-0.0019	-0.0056	-0.0107	0.0000	0.0023	-0.0070
242.5	6	-0.0085	-0.0011	-0.0065	-0.0074	-0.0019	-0.0056	-0.0107	0.0000	0.0030	-0.0070
245	5	-0.0089	-0.0011	-0.0065	-0.0075	-0.0019	-0.0056	-0.0107	0.0000	0.0034	-0.0070
247.5	4	-0.0083	-0.0011	-0.0065	-0.0072	-0.0019	-0.0057	-0.0107	0.0000	0.0035	-0.0070
250	0	-0.0085	-0.0011	-0.0065	-0.0071	-0.0020	-0.0056	-0.0107	0.0000	0.0033	-0.0070
252.5	0	-0.0089	-0.0011	-0.0065	-0.0072	-0.0020	-0.0056	-0.0107	0.0000	0.0030	-0.0070
255	0	-0.0086	-0.0011	-0.0065	-0.0072	-0.0020	-0.0056	-0.0107	0.0000	0.0027	-0.0070



Table A.7: Tabulated Results from 11 Nov 2005, Field Load Test #7

Test # 7		Notes: -- The wind blew fast during this test. Possibly affected reference frame. -- Linear Pot #3 was determined to be damaged at the outset of these tests -- The data gathered from Linear Pot #4 was discarded due to excessive scatter -- Each Telltale is labeled by the same notation: (LP# (Depth) I/O)									
Date: 11-Nov-05		Interior Telltales (I)					Perimeter Telltales (O)				
Time (sec)	Load (lbs)	LP10 (surf) I (in)	LP6 (6") I (in)	LP8 (12") I (in)	LP7 (18") I (in)	LP12 (30") I (in)	LP1 (surf) O (in)	LP9 (6") O (in)	LP3 (12") O (in)	LP4 (18") O (in)	LP2 (30") O (in)
MAX	19947	-0.0087	-0.0173	-0.0073	-0.0041	-0.0069	-0.0132	-0.0100	0.0000	-0.0460	-0.0005
0	-6	0.0000	0.0000	-0.0003	-0.0002	-0.0003	0.0001	0.0000	0.0000	0.0000	0.0000
2.5	-8	0.0000	0.0000	-0.0003	-0.0001	-0.0001	0.0001	0.0000	0.0000	0.0000	0.0000
5	-3	0.0000	0.0000	-0.0002	0.0001	-0.0001	0.0001	0.0000	0.0000	0.0000	-0.0002
7.5	-8	0.0000	0.0000	-0.0001	0.0002	-0.0003	0.0002	0.0000	0.0000	0.0000	0.0000
10	-10	0.0000	0.0000	-0.0003	0.0001	-0.0002	0.0002	0.0000	0.0000	0.0000	0.0000
12.5	27	0.0000	-0.0001	-0.0003	-0.0001	-0.0002	0.0001	0.0000	0.0000	0.0000	-0.0003
15	865	-0.0004	-0.0003	-0.0001	0.0000	0.0001	0.0000	0.0000	0.0000	0.0000	-0.0001
17.5	1459	-0.0005	-0.0005	0.0000	0.0001	0.0002	-0.0003	0.0000	0.0000	0.0000	0.0002
20	2252	-0.0007	-0.0011	0.0000	0.0001	0.0001	-0.0007	0.0000	0.0000	0.0000	0.0002
22.5	3178	-0.0004	-0.0019	0.0000	0.0001	-0.0001	-0.0015	-0.0001	0.0000	0.0000	0.0006
25	4271	0.0003	-0.0029	-0.0001	-0.0001	-0.0006	-0.0022	-0.0003	0.0000	0.0000	0.0011
27.5	5311	0.0006	-0.0038	-0.0003	-0.0002	-0.0010	-0.0031	-0.0003	0.0000	0.0000	0.0019
30	6295	0.0008	-0.0047	-0.0003	-0.0003	-0.0015	-0.0035	-0.0003	0.0000	0.0000	0.0024
32.5	7227	0.0009	-0.0060	-0.0005	-0.0004	-0.0019	-0.0039	-0.0007	0.0000	0.0000	0.0025
35	8116	0.0007	-0.0067	-0.0007	-0.0003	-0.0020	-0.0046	-0.0012	0.0000	0.0000	0.0027
37.5	8959	0.0003	-0.0074	-0.0011	-0.0003	-0.0024	-0.0050	-0.0015	0.0000	0.0000	0.0026
40	9760	-0.0002	-0.0082	-0.0013	-0.0003	-0.0026	-0.0053	-0.0018	0.0000	0.0000	0.0025
42.5	10527	-0.0013	-0.0090	-0.0016	-0.0006	-0.0033	-0.0055	-0.0019	0.0000	0.0000	0.0025
45	11261	-0.0006	-0.0099	-0.0019	-0.0007	-0.0033	-0.0062	-0.0022	0.0000	0.0000	0.0028
47.5	11966	-0.0005	-0.0105	-0.0022	-0.0002	-0.0033	-0.0065	-0.0026	0.0000	0.0000	0.0029
50	12643	-0.0005	-0.0108	-0.0024	-0.0001	-0.0032	-0.0072	-0.0031	0.0000	0.0000	0.0028
52.5	13288	-0.0013	-0.0112	-0.0027	-0.0002	-0.0033	-0.0081	-0.0036	0.0000	0.0000	0.0026
55	13902	-0.0016	-0.0117	-0.0029	-0.0003	-0.0034	-0.0088	-0.0050	0.0000	0.0000	0.0026
57.5	14491	-0.0025	-0.0123	-0.0032	-0.0004	-0.0037	-0.0095	-0.0056	0.0000	0.0000	0.0026
60	15055	-0.0030	-0.0128	-0.0034	-0.0008	-0.0043	-0.0099	-0.0061	0.0000	0.0000	0.0026
62.5	15594	-0.0023	-0.0133	-0.0038	-0.0010	-0.0047	-0.0104	-0.0065	0.0000	0.0000	0.0026
65	16110	-0.0027	-0.0137	-0.0039	-0.0013	-0.0047	-0.0106	-0.0068	0.0000	0.0000	0.0026
67.5	16606	-0.0029	-0.0142	-0.0043	-0.0014	-0.0048	-0.0106	-0.0070	0.0000	0.0000	0.0026
70	17088	-0.0033	-0.0146	-0.0047	-0.0019	-0.0048	-0.0105	-0.0075	0.0000	0.0000	0.0026
72.5	17552	-0.0034	-0.0149	-0.0049	-0.0021	-0.0049	-0.0105	-0.0078	0.0000	0.0000	0.0026
75	17997	-0.0042	-0.0154	-0.0051	-0.0027	-0.0054	-0.0110	-0.0082	0.0000	0.0000	0.0027
77.5	18426	-0.0037	-0.0158	-0.0054	-0.0029	-0.0056	-0.0113	-0.0082	0.0000	0.0000	0.0026
80	18841	-0.0046	-0.0160	-0.0055	-0.0029	-0.0057	-0.0112	-0.0085	0.0000	0.0000	0.0026
82.5	19242	-0.0069	-0.0163	-0.0056	-0.0030	-0.0059	-0.0115	-0.0085	0.0000	0.0000	0.0026
85	19627	-0.0073	-0.0167	-0.0061	-0.0032	-0.0063	-0.0124	-0.0086	0.0000	0.0000	0.0026
87.5	19947	-0.0074	-0.0169	-0.0064	-0.0034	-0.0066	-0.0127	-0.0086	0.0000	0.0000	0.0026
90	19927	-0.0066	-0.0171	-0.0065	-0.0035	-0.0066	-0.0129	-0.0086	0.0000	0.0000	0.0026
92.5	19856	-0.0066	-0.0173	-0.0066	-0.0034	-0.0065	-0.0129	-0.0087	0.0000	0.0000	0.0025
95	19793	-0.0065	-0.0172	-0.0065	-0.0033	-0.0063	-0.0128	-0.0088	0.0000	0.0000	0.0026
97.5	19735	-0.0072	-0.0173	-0.0066	-0.0034	-0.0064	-0.0128	-0.0089	0.0000	0.0000	0.0026
100	19677	-0.0077	-0.0173	-0.0066	-0.0036	-0.0066	-0.0129	-0.0090	0.0000	0.0000	0.0025
102.5	19625	-0.0079	-0.0173	-0.0065	-0.0035	-0.0065	-0.0128	-0.0092	0.0000	0.0000	0.0026
105	19576	-0.0077	-0.0172	-0.0066	-0.0034	-0.0066	-0.0128	-0.0092	0.0000	0.0000	0.0026
107.5	19527	-0.0079	-0.0173	-0.0069	-0.0037	-0.0067	-0.0128	-0.0092	0.0000	0.0000	0.0023
110	19477	-0.0080	-0.0173	-0.0070	-0.0036	-0.0068	-0.0129	-0.0090	0.0000	0.0000	0.0021
112.5	19432	-0.0077	-0.0173	-0.0070	-0.0038	-0.0066	-0.0130	-0.0093	0.0000	0.0000	0.0021
115	19387	-0.0075	-0.0173	-0.0071	-0.0039	-0.0069	-0.0130	-0.0094	0.0000	0.0000	0.0019
117.5	19343	-0.0074	-0.0172	-0.0072	-0.0039	-0.0067	-0.0130	-0.0095	0.0000	0.0000	0.0020
120	19300	-0.0073	-0.0172	-0.0072	-0.0039	-0.0066	-0.0130	-0.0096	0.0000	0.0000	0.0020
122.5	19255	-0.0073	-0.0173	-0.0072	-0.0040	-0.0067	-0.0131	-0.0099	0.0000	0.0000	0.0019
125	19217	-0.0072	-0.0172	-0.0072	-0.0039	-0.0067	-0.0130	-0.0098	0.0000	0.0000	0.0020
127.5	19177	-0.0070	-0.0172	-0.0071	-0.0039	-0.0065	-0.0129	-0.0098	0.0000	0.0000	0.0020
130	19133	-0.0078	-0.0173	-0.0073	-0.0040	-0.0066	-0.0132	-0.0099	0.0000	0.0000	0.0019
132.5	19083	-0.0081	-0.0173	-0.0073	-0.0041	-0.0068	-0.0132	-0.0100	0.0000	0.0000	0.0018
135	18976	-0.0084	-0.0173	-0.0073	-0.0041	-0.0069	-0.0130	-0.0099	0.0000	0.0000	0.0018

Table A.7: Tabulated Results from 11 Nov 2005, Field Load Test #7 (continued)

Test # 7		Notes: -- The wind blew fast during this test. Possibly affected reference frame. -- Linear Pot #3 was determined to be damaged at the outset of these tests -- The data gathered from Linear Pot #4 was discarded due to excessive scatter -- Each Telltale is labeled by the same notation: (LP# (Depth) I/O)									
Date: 11-Nov-05											
Time (sec)	Load (lbs)	Interior Telltales (I)					Perimeter Telltales (O)				
		LP10 (surf) I	LP6 (6") I	LP8 (12") I	LP7 (18") I	LP12 (30") I	LP1 (surf) O	LP9 (6") O	LP3 (12") O	LP4 (18") O	LP2 (30") O
137.5	18838	-0.0086	-0.0173	-0.0073	-0.0041	-0.0066	-0.0129	-0.0097	0.0000	-0.0169	0.0019
140	17603	-0.0087	-0.0172	-0.0073	-0.0041	-0.0068	-0.0129	-0.0096	0.0000	-0.0168	0.0018
142.5	14225	-0.0074	-0.0166	-0.0073	-0.0041	-0.0066	-0.0128	-0.0096	0.0000	-0.0221	0.0015
145	11594	-0.0050	-0.0152	-0.0073	-0.0040	-0.0060	-0.0115	-0.0096	0.0000	-0.0363	0.0010
147.5	10324	-0.0050	-0.0143	-0.0070	-0.0040	-0.0059	-0.0111	-0.0096	0.0000	-0.0377	0.0006
150	9285	-0.0054	-0.0135	-0.0069	-0.0040	-0.0056	-0.0108	-0.0095	0.0000	-0.0362	0.0003
152.5	8379	-0.0057	-0.0128	-0.0068	-0.0040	-0.0052	-0.0104	-0.0092	0.0000	-0.0399	0.0002
155	7550	-0.0062	-0.0122	-0.0066	-0.0041	-0.0050	-0.0104	-0.0093	0.0000	-0.0215	0.0001
157.5	5945	-0.0066	-0.0106	-0.0062	-0.0040	-0.0043	-0.0101	-0.0089	0.0000	-0.0164	0.0001
160	4062	-0.0037	-0.0086	-0.0051	-0.0037	-0.0034	-0.0079	-0.0081	0.0000	-0.0101	-0.0001
162.5	3272	-0.0028	-0.0074	-0.0045	-0.0033	-0.0033	-0.0065	-0.0074	0.0000	-0.0113	-0.0001
165	2950	-0.0029	-0.0068	-0.0041	-0.0032	-0.0034	-0.0063	-0.0067	0.0000	-0.0197	-0.0002
167.5	2637	-0.0027	-0.0064	-0.0038	-0.0030	-0.0034	-0.0056	-0.0065	0.0000	-0.0116	-0.0002
170	2199	-0.0015	-0.0057	-0.0034	-0.0028	-0.0032	-0.0050	-0.0054	0.0000	-0.0255	-0.0002
172.5	4	-0.0006	-0.0020	-0.0016	-0.0014	-0.0019	-0.0014	-0.0009	0.0000	-0.0149	-0.0002
175	5	0.0001	-0.0016	-0.0015	-0.0014	-0.0018	-0.0009	-0.0006	0.0000	-0.0145	-0.0002
177.5	3	0.0004	-0.0013	-0.0014	-0.0013	-0.0017	-0.0009	-0.0004	0.0000	-0.0143	-0.0001
180	1	0.0003	-0.0013	-0.0015	-0.0014	-0.0015	-0.0007	-0.0005	0.0000	-0.0460	-0.0002
182.5	2	0.0007	-0.0012	-0.0011	-0.0011	-0.0013	-0.0006	-0.0004	0.0000	-0.0416	-0.0001
185	2	0.0002	-0.0013	-0.0011	-0.0011	-0.0014	-0.0006	-0.0006	0.0000	-0.0155	-0.0001
187.5	5	0.0005	-0.0013	-0.0011	-0.0010	-0.0015	-0.0004	-0.0007	0.0000	-0.0326	-0.0002
190	4	0.0013	-0.0013	-0.0011	-0.0010	-0.0014	-0.0003	-0.0005	0.0000	-0.0128	-0.0002
192.5	4	0.0012	-0.0013	-0.0012	-0.0011	-0.0014	-0.0004	-0.0005	0.0000	-0.0062	-0.0002
195	6	0.0013	-0.0013	-0.0012	-0.0011	-0.0014	-0.0004	-0.0005	0.0000	-0.0074	-0.0002
197.5	6	0.0013	-0.0013	-0.0009	-0.0011	-0.0012	-0.0003	-0.0005	0.0000	-0.0161	-0.0002
200	10	0.0010	-0.0013	-0.0009	-0.0010	-0.0012	-0.0003	-0.0005	0.0000	-0.0112	-0.0002
202.5	10	0.0012	-0.0013	-0.0008	-0.0011	-0.0014	-0.0003	-0.0005	0.0000	-0.0085	-0.0002
205	7	0.0015	-0.0013	-0.0008	-0.0010	-0.0015	-0.0003	-0.0005	0.0000	-0.0059	-0.0002
207.5	5	0.0011	-0.0011	-0.0009	-0.0010	-0.0014	-0.0003	-0.0005	0.0000	-0.0071	-0.0002
210	2	0.0009	-0.0010	-0.0008	-0.0009	-0.0015	-0.0003	-0.0005	0.0000	-0.0139	-0.0002
212.5	0	0.0008	-0.0010	-0.0008	-0.0010	-0.0013	-0.0004	-0.0005	0.0000	-0.0071	-0.0002
215	0	0.0008	-0.0010	-0.0008	-0.0008	-0.0012	-0.0004	-0.0005	0.0000	-0.0072	-0.0002
217.5	0	0.0005	-0.0010	-0.0008	-0.0009	-0.0013	-0.0004	-0.0005	0.0000	-0.0075	-0.0002
220	1	0.0001	-0.0010	-0.0008	-0.0010	-0.0013	-0.0004	-0.0005	0.0000	-0.0180	-0.0002
222.5	1	0.0000	-0.0010	-0.0008	-0.0011	-0.0012	-0.0004	-0.0005	0.0000	-0.0238	-0.0002
225	1	0.0000	-0.0010	-0.0008	-0.0011	-0.0014	-0.0004	-0.0005	0.0000	-0.0158	-0.0002
227.5	0	-0.0002	-0.0010	-0.0008	-0.0011	-0.0014	-0.0004	-0.0005	0.0000	-0.0133	-0.0002
230	0	-0.0002	-0.0010	-0.0008	-0.0010	-0.0015	-0.0004	-0.0005	0.0000	-0.0080	-0.0002
232.5	0	-0.0003	-0.0010	-0.0008	-0.0011	-0.0014	-0.0004	-0.0005	0.0000	-0.0045	-0.0002
235	0	-0.0009	-0.0010	-0.0008	-0.0010	-0.0015	-0.0004	-0.0005	0.0000	-0.0046	-0.0003
237.5	0	0.0004	-0.0010	-0.0008	-0.0007	-0.0015	-0.0004	-0.0005	0.0000	-0.0069	-0.0002
240	0	0.0004	-0.0010	-0.0008	-0.0008	-0.0012	-0.0004	-0.0005	0.0000	-0.0042	-0.0003
242.5	0	0.0001	-0.0009	-0.0008	-0.0009	-0.0012	-0.0004	-0.0005	0.0000	-0.0032	-0.0005
245	0	0.0012	-0.0009	-0.0008	-0.0007	-0.0012	-0.0003	-0.0005	0.0000	-0.0012	-0.0005
247.5	0	0.0016	-0.0009	-0.0008	-0.0005	-0.0012	-0.0003	-0.0005	0.0000	-0.0057	-0.0005
250	2	0.0017	-0.0010	-0.0008	-0.0007	-0.0012	-0.0004	-0.0005	0.0000	-0.0065	-0.0005
252.5	0	0.0008	-0.0009	-0.0008	-0.0006	-0.0012	-0.0004	-0.0005	0.0000	-0.0062	-0.0004
255	0	0.0006	-0.0009	-0.0008	-0.0005	-0.0012	-0.0004	-0.0005	0.0000	-0.0079	-0.0002



Table A.8: Tabulated Results from 11 Nov 2005, Field Load Test #8

Test # 8		Notes: -- The wind blew fast during this test. Possibly affected reference frame. -- Linear Pot #3 was determined to be damaged at the outset of these tests -- The data gathered from Linear Pot #4 was discarded due to excessive scatter -- Each Telltale is labeled by the same notation: (LP# (Depth) I/O)									
Date: 11-Nov-05											
Time (sec)	Load (lbs)	Interior Telltales (I)					Perimeter Telltales (O)				
		LP10 (surf) I (in)	LP6 (6") I (in)	LP8 (12") I (in)	LP7 (18") I (in)	LP12 (30") I (in)	LP1 (surf) O (in)	LP9 (6") O (in)	LP3 (12") O (in)	LP4 (18") O (in)	LP2 (30") O (in)
MAX	20032	-0.0138	-0.0169	-0.0089	-0.0047	-0.0057	-0.0146	-0.0112	0.0000	-0.0699	-0.0026
0	-1	0.0000	0.0001	0.0001	0.0002	-0.0003	0.0000	0.0001	0.0000	0.0000	-0.0001
2.5	-1	0.0000	0.0002	0.0000	0.0002	-0.0002	0.0001	0.0001	0.0000	0.0000	0.0000
5	-6	0.0000	0.0002	-0.0001	0.0002	0.0000	0.0000	0.0000	0.0000	0.0000	0.0000
7.5	-7	0.0000	0.0002	-0.0001	0.0002	-0.0001	0.0000	0.0001	0.0000	0.0000	0.0000
10	-9	0.0000	0.0002	0.0000	0.0003	0.0001	0.0001	0.0001	0.0000	0.0000	0.0001
12.5	-8	0.0001	0.0003	0.0000	0.0003	0.0001	0.0001	0.0003	0.0000	0.0000	0.0001
15	-9	0.0000	0.0003	0.0000	0.0000	0.0002	0.0001	0.0001	0.0000	0.0000	0.0001
17.5	654	0.0000	0.0000	0.0000	-0.0001	0.0002	-0.0003	0.0001	0.0000	0.0000	0.0001
20	1345	-0.0012	-0.0006	-0.0001	-0.0001	0.0001	-0.0010	0.0001	0.0000	0.0000	0.0001
22.5	2805	0.0000	-0.0016	-0.0004	-0.0001	-0.0002	-0.0017	0.0000	0.0000	-0.0018	0.0000
25	4329	-0.0009	-0.0029	-0.0004	-0.0001	-0.0001	-0.0024	0.0001	0.0000	-0.0029	0.0003
27.5	5753	-0.0031	-0.0041	-0.0008	-0.0001	-0.0004	-0.0034	-0.0001	0.0000	-0.0018	0.0004
30	7081	-0.0047	-0.0054	-0.0012	-0.0002	-0.0010	-0.0048	-0.0010	0.0000	-0.0024	0.0006
32.5	8338	-0.0054	-0.0067	-0.0016	-0.0002	-0.0011	-0.0054	-0.0017	0.0000	-0.0042	0.0009
35	9513	-0.0061	-0.0079	-0.0022	0.0002	-0.0018	-0.0064	-0.0025	0.0000	-0.0042	0.0011
37.5	10617	-0.0053	-0.0089	-0.0027	-0.0004	-0.0021	-0.0069	-0.0029	0.0000	-0.0042	0.0011
40	11660	-0.0053	-0.0099	-0.0034	-0.0005	-0.0022	-0.0077	-0.0035	0.0000	-0.0042	0.0010
42.5	12646	-0.0053	-0.0108	-0.0039	-0.0009	-0.0025	-0.0082	-0.0042	0.0000	-0.0042	0.0008
45	13572	-0.0053	-0.0116	-0.0045	-0.0009	-0.0027	-0.0100	-0.0058	0.0000	-0.0042	0.0005
47.5	14471	-0.0075	-0.0123	-0.0051	-0.0017	-0.0031	-0.0113	-0.0072	0.0000	-0.0042	0.0008
50	15390	-0.0074	-0.0127	-0.0055	-0.0018	-0.0034	-0.0118	-0.0078	0.0000	-0.0042	0.0008
52.5	16308	-0.0074	-0.0136	-0.0058	-0.0020	-0.0037	-0.0122	-0.0082	0.0000	-0.0042	0.0008
55	17165	-0.0075	-0.0144	-0.0062	-0.0022	-0.0040	-0.0123	-0.0088	0.0000	-0.0042	0.0007
57.5	17976	-0.0092	-0.0150	-0.0068	-0.0026	-0.0046	-0.0120	-0.0094	0.0000	-0.0042	0.0007
60	18739	-0.0102	-0.0156	-0.0071	-0.0030	-0.0046	-0.0125	-0.0097	0.0000	-0.0042	0.0007
62.5	19460	-0.0120	-0.0161	-0.0075	-0.0038	-0.0050	-0.0132	-0.0101	0.0000	-0.0042	0.0007
65	20032	-0.0122	-0.0164	-0.0077	-0.0037	-0.0050	-0.0141	-0.0099	0.0000	-0.0042	0.0007
67.5	20012	-0.0113	-0.0168	-0.0079	-0.0038	-0.0052	-0.0143	-0.0101	0.0000	-0.0042	0.0007
70	19919	-0.0104	-0.0169	-0.0079	-0.0038	-0.0049	-0.0143	-0.0101	0.0000	-0.0042	0.0006
72.5	19839	-0.0111	-0.0169	-0.0081	-0.0039	-0.0049	-0.0143	-0.0104	0.0000	-0.0042	0.0004
75	19767	-0.0112	-0.0169	-0.0083	-0.0042	-0.0053	-0.0143	-0.0105	0.0000	-0.0042	0.0004
77.5	19703	-0.0124	-0.0169	-0.0086	-0.0043	-0.0057	-0.0146	-0.0108	0.0000	-0.0042	0.0001
80	19640	-0.0114	-0.0169	-0.0086	-0.0042	-0.0054	-0.0146	-0.0110	0.0000	-0.0042	0.0001
82.5	19578	-0.0107	-0.0169	-0.0086	-0.0042	-0.0054	-0.0146	-0.0112	0.0000	-0.0042	0.0001
85	19519	-0.0115	-0.0169	-0.0086	-0.0043	-0.0055	-0.0146	-0.0111	0.0000	-0.0042	0.0001
87.5	19458	-0.0115	-0.0169	-0.0087	-0.0042	-0.0055	-0.0146	-0.0110	0.0000	-0.0042	0.0001
90	19400	-0.0128	-0.0169	-0.0089	-0.0041	-0.0054	-0.0146	-0.0110	0.0000	-0.0042	0.0001
92.5	19344	-0.0128	-0.0169	-0.0088	-0.0043	-0.0053	-0.0146	-0.0110	0.0000	-0.0042	0.0001
95	19286	-0.0120	-0.0169	-0.0088	-0.0044	-0.0053	-0.0146	-0.0110	0.0000	-0.0042	0.0001
97.5	19232	-0.0113	-0.0169	-0.0089	-0.0043	-0.0054	-0.0146	-0.0110	0.0000	-0.0042	-0.0001
100	19180	-0.0107	-0.0169	-0.0089	-0.0044	-0.0056	-0.0146	-0.0110	0.0000	-0.0042	-0.0002
102.5	19127	-0.0107	-0.0169	-0.0089	-0.0044	-0.0056	-0.0146	-0.0110	0.0000	-0.0042	-0.0002
105	19070	-0.0109	-0.0169	-0.0089	-0.0043	-0.0056	-0.0146	-0.0110	0.0000	-0.0042	-0.0002
107.5	19017	-0.0126	-0.0169	-0.0089	-0.0043	-0.0053	-0.0146	-0.0110	0.0000	-0.0042	-0.0002
110	18961	-0.0135	-0.0169	-0.0089	-0.0042	-0.0053	-0.0146	-0.0110	0.0000	-0.0042	0.0001
112.5	18880	-0.0135	-0.0169	-0.0089	-0.0042	-0.0053	-0.0146	-0.0111	0.0000	-0.0042	-0.0002
115	18745	-0.0135	-0.0169	-0.0089	-0.0042	-0.0054	-0.0146	-0.0111	0.0000	-0.0042	-0.0003
117.5	18578	-0.0135	-0.0169	-0.0089	-0.0044	-0.0056	-0.0146	-0.0111	0.0000	-0.0042	-0.0002
120	16932	-0.0138	-0.0168	-0.0089	-0.0043	-0.0057	-0.0144	-0.0110	0.0000	-0.0042	-0.0003
122.5	13765	-0.0125	-0.0160	-0.0089	-0.0041	-0.0054	-0.0141	-0.0110	0.0000	-0.0042	-0.0011
125	13158	-0.0121	-0.0158	-0.0089	-0.0044	-0.0052	-0.0140	-0.0110	0.0000	-0.0042	-0.0012
127.5	12545	-0.0112	-0.0155	-0.0089	-0.0044	-0.0049	-0.0138	-0.0110	0.0000	-0.0042	-0.0012
130	11858	-0.0095	-0.0151	-0.0089	-0.0045	-0.0049	-0.0131	-0.0110	0.0000	-0.0042	-0.0015
132.5	11195	-0.0094	-0.0148	-0.0089	-0.0044	-0.0050	-0.0128	-0.0110	0.0000	-0.0042	-0.0016
135	10585	-0.0097	-0.0145	-0.0089	-0.0044	-0.0049	-0.0127	-0.0110	0.0000	-0.0042	-0.0018

Table A.8: Tabulated Results from 11 Nov 2005, Field Load Test #8 (continued)

Test #		8		Notes: -- The wind blew fast during this test. Possibly affected reference frame. -- Linear Pot #3 was determined to be damaged at the outset of these tests -- The data gathered from Linear Pot #4 was discarded due to excessive scatter -- Each Telltale is labeled by the same notation: (LP# (Depth) I/O)									
Date:		11-Nov-05											
Time (sec)	Load (lbs)	Interior Telltales (I)					Perimeter Telltales (O)						
		LP10 (surf) I (in)	LP6 (6") I (in)	LP8 (12") I (in)	LP7 (18") I (in)	LP12 (30") I (in)	LP1 (surf) O (in)	LP9 (6") O (in)	LP3 (12") O (in)	LP4 (18") O (in)	LP2 (30") O (in)		
137.5	9409	-0.0102	-0.0138	-0.0089	-0.0044	-0.0050	-0.0126	-0.0110	0.0000	0.0000	-0.0021		
140	7771	-0.0105	-0.0127	-0.0086	-0.0044	-0.0048	-0.0120	-0.0107	0.0000	0.0000	-0.0022		
142.5	6544	-0.0098	-0.0115	-0.0084	-0.0044	-0.0041	-0.0119	-0.0106	0.0000	0.0000	-0.0022		
145	5630	-0.0114	-0.0106	-0.0079	-0.0045	-0.0038	-0.0117	-0.0102	0.0000	0.0000	-0.0025		
147.5	4948	-0.0108	-0.0099	-0.0076	-0.0045	-0.0036	-0.0112	-0.0097	0.0000	0.0000	-0.0026		
150	4426	-0.0094	-0.0091	-0.0073	-0.0047	-0.0032	-0.0103	-0.0096	0.0000	0.0000	-0.0026		
152.5	3203	-0.0078	-0.0077	-0.0068	-0.0044	-0.0025	-0.0081	-0.0092	0.0000	0.0000	-0.0026		
155	2611	-0.0077	-0.0063	-0.0060	-0.0041	-0.0023	-0.0074	-0.0082	0.0000	0.0000	-0.0026		
157.5	2499	-0.0075	-0.0059	-0.0057	-0.0038	-0.0021	-0.0074	-0.0080	0.0000	0.0000	-0.0026		
160	647	-0.0062	-0.0032	-0.0043	-0.0029	-0.0019	-0.0043	-0.0041	0.0000	0.0000	-0.0026		
162.5	-10	-0.0056	-0.0017	-0.0035	-0.0022	-0.0014	-0.0029	-0.0025	0.0000	0.0000	-0.0026		
165	-10	-0.0048	-0.0015	-0.0034	-0.0021	-0.0011	-0.0026	-0.0023	0.0000	0.0000	-0.0026		
167.5	-10	-0.0041	-0.0015	-0.0032	-0.0021	-0.0009	-0.0024	-0.0023	0.0000	0.0000	-0.0026		
170	-11	-0.0049	-0.0013	-0.0031	-0.0020	-0.0009	-0.0022	-0.0020	0.0000	0.0000	-0.0026		
172.5	-14	-0.0039	-0.0012	-0.0030	-0.0018	-0.0009	-0.0021	-0.0019	0.0000	0.0000	-0.0026		
175	-18	-0.0040	-0.0012	-0.0028	-0.0018	-0.0011	-0.0021	-0.0020	0.0000	0.0000	-0.0026		
177.5	-20	-0.0035	-0.0012	-0.0028	-0.0018	-0.0011	-0.0021	-0.0020	0.0000	0.0000	-0.0026		
180	-23	-0.0037	-0.0011	-0.0028	-0.0018	-0.0011	-0.0019	-0.0020	0.0000	0.0000	-0.0026		
182.5	-28	-0.0047	-0.0009	-0.0028	-0.0017	-0.0010	-0.0020	-0.0021	0.0000	0.0000	-0.0026		
185	-23	-0.0048	-0.0008	-0.0028	-0.0017	-0.0009	-0.0021	-0.0021	0.0000	0.0000	-0.0026		
187.5	-22	-0.0047	-0.0008	-0.0028	-0.0016	-0.0008	-0.0021	-0.0020	0.0000	0.0000	-0.0026		
190	-21	-0.0046	-0.0008	-0.0028	-0.0017	-0.0009	-0.0021	-0.0020	0.0000	0.0000	-0.0026		
192.5	-20	-0.0044	-0.0008	-0.0028	-0.0016	-0.0008	-0.0021	-0.0020	0.0000	0.0000	-0.0026		
195	-20	-0.0044	-0.0009	-0.0028	-0.0018	-0.0009	-0.0021	-0.0020	0.0000	0.0000	-0.0026		
197.5	-20	-0.0047	-0.0008	-0.0028	-0.0017	-0.0008	-0.0021	-0.0021	0.0000	0.0000	-0.0026		
200	-20	-0.0047	-0.0008	-0.0028	-0.0017	-0.0008	-0.0021	-0.0020	0.0000	0.0000	-0.0026		
202.5	-19	-0.0050	-0.0008	-0.0028	-0.0017	-0.0008	-0.0021	-0.0020	0.0000	0.0000	-0.0026		
205	-15	-0.0051	-0.0008	-0.0028	-0.0018	-0.0009	-0.0021	-0.0020	0.0000	0.0000	-0.0026		
207.5	-20	-0.0053	-0.0008	-0.0028	-0.0020	-0.0007	-0.0021	-0.0019	0.0000	0.0000	-0.0026		
210	-20	-0.0058	-0.0008	-0.0028	-0.0020	-0.0005	-0.0021	-0.0019	0.0000	0.0000	-0.0026		
212.5	-20	-0.0060	-0.0008	-0.0028	-0.0018	-0.0005	-0.0021	-0.0019	0.0000	0.0000	-0.0026		
215	-20	-0.0061	-0.0008	-0.0028	-0.0020	-0.0004	-0.0021	-0.0019	0.0000	0.0000	-0.0026		
217.5	-20	-0.0063	-0.0008	-0.0028	-0.0020	-0.0005	-0.0021	-0.0019	0.0000	0.0000	-0.0026		
220	-19	-0.0063	-0.0008	-0.0028	-0.0021	-0.0005	-0.0021	-0.0019	0.0000	0.0000	-0.0026		
222.5	-20	-0.0066	-0.0008	-0.0028	-0.0021	-0.0005	-0.0021	-0.0019	0.0000	0.0000	-0.0026		
225	-20	-0.0067	-0.0008	-0.0028	-0.0021	-0.0004	-0.0021	-0.0019	0.0000	0.0000	-0.0026		
227.5	-20	-0.0067	-0.0008	-0.0028	-0.0021	-0.0002	-0.0021	-0.0019	0.0000	0.0000	-0.0026		
230	-20	-0.0067	-0.0008	-0.0028	-0.0021	-0.0003	-0.0021	-0.0019	0.0000	0.0000	-0.0026		
232.5	-20	-0.0067	-0.0008	-0.0028	-0.0023	-0.0005	-0.0021	-0.0019	0.0000	0.0000	-0.0026		
235	-20	-0.0062	-0.0008	-0.0028	-0.0024	-0.0004	-0.0021	-0.0019	0.0000	0.0000	-0.0026		
237.5	-20	-0.0067	-0.0008	-0.0028	-0.0022	-0.0001	-0.0021	-0.0019	0.0000	0.0000	-0.0026		
240	-20	-0.0069	-0.0008	-0.0028	-0.0021	-0.0003	-0.0021	-0.0019	0.0000	0.0000	-0.0026		
242.5	-20	-0.0066	-0.0008	-0.0028	-0.0024	-0.0002	-0.0021	-0.0019	0.0000	0.0000	-0.0026		
245	-20	-0.0063	-0.0008	-0.0028	-0.0024	-0.0003	-0.0021	-0.0019	0.0000	0.0000	-0.0026		
247.5	-20	-0.0064	-0.0008	-0.0028	-0.0024	-0.0004	-0.0021	-0.0019	0.0000	0.0000	-0.0026		
250	-20	-0.0065	-0.0008	-0.0028	-0.0024	-0.0004	-0.0021	-0.0019	0.0000	0.0000	-0.0026		
252.5	-20	-0.0067	-0.0008	-0.0028	-0.0024	-0.0004	-0.0021	-0.0019	0.0000	0.0000	-0.0026		
255	-20	-0.0040	-0.0008	-0.0028	-0.0023	-0.0005	-0.0021	-0.0019	0.0000	0.0000	-0.0026		

Table A.9: Tabulated Results from 11 Nov 2005, Field Load Test #9

Test #		9	Notes: -- The wind blew fast during this test. Possibly affected reference frame. -- Linear Pot #3 was determined to be damaged at the outset of these tests -- The data gathered from Linear Pot #4 was discarded due to excessive scatter -- Each Telltale is labeled by the same notation: (LP# (Depth) I/O)									
Date:		11-Nov-05										
Time (sec)	Load (lbs)	Interior Telltales (I)					Perimeter Telltales (O)					
		LP10 (surf) I (in)	LP6 (6") I (in)	LP8 (12") I (in)	LP7 (18") I (in)	LP12 (30") I (in)	LP1 (surf) O (in)	LP9 (6") O (in)	LP3 (12") O (in)	LP4 (18") O (in)	LP2 (30") O (in)	
MAX	19933	-0.0085	-0.0164	-0.0068	-0.0046	-0.0059	-0.0132	-0.0098	0.0000	-0.0228	-0.0003	
0	1	0.0000	0.0001	0.0000	0.0000	0.0000	0.0000	0.0001	0.0000	0.0457	0.0000	
2.5	3	0.0000	0.0001	0.0000	0.0000	0.0000	0.0000	0.0001	0.0000	0.0111	0.0000	
5	2	0.0000	0.0001	0.0000	0.0000	0.0000	0.0000	0.0000	0.0000	0.1012	0.0000	
7.5	6	0.0000	0.0002	0.0000	0.0000	0.0000	0.0000	0.0000	0.0000	0.1002	0.0000	
10	1	0.0000	0.0002	0.0000	0.0000	0.0000	0.0000	0.0000	0.0000	0.0557	0.0000	
12.5	-27	0.0000	0.0001	0.0000	0.0000	0.0000	0.0000	0.0000	0.0000	0.0276	-0.0001	
15	4	0.0000	0.0001	0.0000	0.0000	0.0000	0.0000	0.0000	0.0000	0.1197	-0.0003	
17.5	3	0.0000	0.0001	0.0000	0.0000	0.0000	0.0000	0.0000	0.0000	0.1185	-0.0003	
20	494	-0.0003	0.0001	0.0000	0.0000	-0.0001	0.0000	0.0000	0.0000	0.0819	-0.0003	
22.5	1168	-0.0004	0.0000	0.0000	0.0000	0.0000	-0.0003	0.0002	0.0000	0.0886	-0.0003	
25	2675	-0.0003	-0.0013	0.0000	0.0000	-0.0003	-0.0016	0.0000	0.0000	0.1217	0.0007	
27.5	4560	0.0009	-0.0026	0.0000	0.0000	-0.0002	-0.0031	0.0000	0.0000	0.1266	0.0012	
30	6292	0.0024	-0.0039	-0.0001	0.0001	-0.0006	-0.0037	-0.0001	0.0000	0.1248	0.0019	
32.5	7877	0.0020	-0.0053	-0.0005	0.0000	-0.0009	-0.0047	-0.0008	0.0000	0.0860	0.0025	
35	9338	0.0016	-0.0068	-0.0009	0.0000	-0.0012	-0.0055	-0.0012	0.0000	0.0675	0.0028	
37.5	10687	0.0011	-0.0080	-0.0015	0.0000	-0.0019	-0.0059	-0.0018	0.0000	0.1061	0.0028	
40	11944	0.0005	-0.0093	-0.0019	-0.0002	-0.0021	-0.0074	-0.0033	0.0000	0.0981	0.0030	
42.5	13119	-0.0010	-0.0102	-0.0024	-0.0001	-0.0021	-0.0089	-0.0049	0.0000	0.0958	0.0030	
45	14209	-0.0018	-0.0110	-0.0028	-0.0001	-0.0024	-0.0098	-0.0056	0.0000	0.0981	0.0030	
47.5	15223	-0.0017	-0.0118	-0.0033	-0.0005	-0.0027	-0.0104	-0.0062	0.0000	0.0970	0.0030	
50	16166	-0.0025	-0.0125	-0.0039	-0.0010	-0.0034	-0.0103	-0.0069	0.0000	0.0944	0.0030	
52.5	17055	-0.0046	-0.0133	-0.0044	-0.0018	-0.0037	-0.0104	-0.0074	0.0000	0.0957	0.0030	
55	17894	-0.0050	-0.0140	-0.0048	-0.0021	-0.0039	-0.0109	-0.0078	0.0000	0.0925	0.0029	
57.5	18683	-0.0057	-0.0147	-0.0053	-0.0024	-0.0046	-0.0121	-0.0079	0.0000	0.0951	0.0028	
60	19420	-0.0053	-0.0153	-0.0057	-0.0027	-0.0048	-0.0126	-0.0085	0.0000	0.0986	0.0024	
62.5	19933	-0.0056	-0.0157	-0.0061	-0.0029	-0.0050	-0.0128	-0.0091	0.0000	0.1012	0.0024	
65	19862	-0.0070	-0.0159	-0.0061	-0.0032	-0.0054	-0.0129	-0.0091	0.0000	0.1043	0.0023	
67.5	19770	-0.0069	-0.0160	-0.0061	-0.0032	-0.0056	-0.0129	-0.0091	0.0000	0.0957	0.0023	
70	19692	-0.0063	-0.0160	-0.0062	-0.0033	-0.0055	-0.0129	-0.0091	0.0000	0.1043	0.0023	
72.5	19617	-0.0067	-0.0160	-0.0062	-0.0035	-0.0055	-0.0129	-0.0091	0.0000	0.1168	0.0023	
75	19552	-0.0067	-0.0160	-0.0063	-0.0034	-0.0055	-0.0129	-0.0091	0.0000	0.0977	0.0025	
77.5	19490	-0.0071	-0.0160	-0.0064	-0.0034	-0.0055	-0.0129	-0.0091	0.0000	0.0983	0.0026	
80	19424	-0.0071	-0.0160	-0.0064	-0.0035	-0.0055	-0.0129	-0.0091	0.0000	0.0938	0.0024	
82.5	19364	-0.0076	-0.0160	-0.0065	-0.0034	-0.0055	-0.0129	-0.0091	0.0000	0.0984	0.0024	
85	19303	-0.0073	-0.0160	-0.0065	-0.0037	-0.0055	-0.0129	-0.0091	0.0000	0.0974	0.0023	
87.5	19239	-0.0069	-0.0160	-0.0065	-0.0036	-0.0054	-0.0129	-0.0091	0.0000	0.0989	0.0023	
90	19184	-0.0075	-0.0160	-0.0065	-0.0037	-0.0054	-0.0129	-0.0091	0.0000	0.0968	0.0025	
92.5	19124	-0.0075	-0.0160	-0.0065	-0.0039	-0.0055	-0.0129	-0.0091	0.0000	0.1055	0.0024	
95	19062	-0.0077	-0.0160	-0.0065	-0.0039	-0.0055	-0.0129	-0.0091	0.0000	0.0971	0.0023	
97.5	19006	-0.0078	-0.0161	-0.0065	-0.0041	-0.0055	-0.0129	-0.0092	0.0000	0.1042	0.0023	
100	18949	-0.0078	-0.0160	-0.0065	-0.0043	-0.0054	-0.0129	-0.0091	0.0000	0.0984	0.0023	
102.5	18896	-0.0078	-0.0160	-0.0065	-0.0040	-0.0053	-0.0129	-0.0091	0.0000	0.0987	0.0025	
105	18838	-0.0078	-0.0160	-0.0065	-0.0038	-0.0054	-0.0129	-0.0091	0.0000	0.1009	0.0025	
107.5	18781	-0.0078	-0.0161	-0.0065	-0.0038	-0.0054	-0.0129	-0.0093	0.0000	0.0989	0.0023	
110	18736	-0.0078	-0.0160	-0.0065	-0.0037	-0.0055	-0.0129	-0.0095	0.0000	0.0986	0.0023	
112.5	18735	-0.0078	-0.0160	-0.0065	-0.0036	-0.0055	-0.0129	-0.0095	0.0000	0.0989	0.0023	
115	18963	-0.0084	-0.0161	-0.0065	-0.0040	-0.0053	-0.0129	-0.0095	0.0000	0.0982	0.0023	
117.5	19656	-0.0085	-0.0162	-0.0065	-0.0040	-0.0052	-0.0129	-0.0095	0.0000	0.0975	0.0023	
120	19820	-0.0078	-0.0164	-0.0065	-0.0040	-0.0054	-0.0132	-0.0095	0.0000	0.1159	0.0023	
122.5	19746	-0.0078	-0.0164	-0.0065	-0.0040	-0.0055	-0.0132	-0.0095	0.0000	0.1158	0.0023	
125	19676	-0.0082	-0.0164	-0.0065	-0.0040	-0.0055	-0.0132	-0.0095	0.0000	0.1154	0.0023	
127.5	19611	-0.0063	-0.0164	-0.0065	-0.0040	-0.0055	-0.0132	-0.0095	0.0000	0.1145	0.0022	
130	19545	-0.0062	-0.0164	-0.0065	-0.0037	-0.0055	-0.0132	-0.0095	0.0000	0.1094	0.0021	
132.5	19483	-0.0056	-0.0164	-0.0065	-0.0037	-0.0055	-0.0132	-0.0095	0.0000	0.0975	0.0020	
135	19426	-0.0063	-0.0164	-0.0065	-0.0038	-0.0055	-0.0132	-0.0095	0.0000	0.1070	0.0020	



Table A.9: Tabulated Results from 11 Nov 2005, Field Load Test #9 (continued)

Test # 9		Notes: -- The wind blew fast during this test. Possibly affected reference frame. -- Linear Pot #3 was determined to be damaged at the outset of these tests -- The data gathered from Linear Pot #4 was discarded due to excessive scatter -- Each Telltale is labeled by the same notation: (LP# (Depth) I/O)									
Date: 11-Nov-05											
Time (sec)	Load (lbs)	Interior Telltales (I)					Perimeter Telltales (O)				
		LP10 (surf) I (in)	LP6 (6") I (in)	LP8 (12") I (in)	LP7 (18") I (in)	LP12 (30") I (in)	LP1 (surf) O (in)	LP9 (6") O (in)	LP3 (12") O (in)	LP4 (18") O (in)	LP2 (30") O (in)
137.5	19366	-0.0073	-0.0164	-0.0065	-0.0038	-0.0055	-0.0132	-0.0095	0.0000	0.1052	0.0020
140	19305	-0.0076	-0.0164	-0.0065	-0.0039	-0.0055	-0.0132	-0.0095	0.0000	0.1180	0.0020
142.5	19237	-0.0072	-0.0164	-0.0065	-0.0040	-0.0055	-0.0132	-0.0095	0.0000	0.1128	0.0020
145	19117	-0.0074	-0.0164	-0.0065	-0.0044	-0.0055	-0.0132	-0.0095	0.0000	0.1234	0.0020
147.5	18963	-0.0072	-0.0164	-0.0065	-0.0043	-0.0055	-0.0132	-0.0095	0.0000	0.1236	0.0020
150	17976	-0.0074	-0.0164	-0.0067	-0.0040	-0.0058	-0.0132	-0.0095	0.0000	0.1234	0.0020
152.5	15234	-0.0075	-0.0163	-0.0068	-0.0043	-0.0059	-0.0131	-0.0097	0.0000	0.1188	0.0019
155	13410	-0.0070	-0.0159	-0.0068	-0.0044	-0.0058	-0.0129	-0.0098	0.0000	0.0952	0.0014
157.5	11844	-0.0059	-0.0152	-0.0068	-0.0045	-0.0056	-0.0126	-0.0098	0.0000	0.0082	0.0010
160	10548	-0.0054	-0.0145	-0.0068	-0.0041	-0.0054	-0.0120	-0.0098	0.0000	0.0296	0.0007
162.5	9449	-0.0056	-0.0138	-0.0068	-0.0044	-0.0054	-0.0112	-0.0096	0.0000	0.0524	0.0005
165	8503	-0.0052	-0.0129	-0.0067	-0.0044	-0.0051	-0.0111	-0.0095	0.0000	0.0667	0.0003
167.5	7679	-0.0054	-0.0123	-0.0065	-0.0045	-0.0052	-0.0108	-0.0095	0.0000	0.1183	0.0003
170	6974	-0.0046	-0.0118	-0.0065	-0.0046	-0.0050	-0.0103	-0.0095	0.0000	0.0861	0.0003
172.5	6380	-0.0053	-0.0112	-0.0063	-0.0042	-0.0047	-0.0103	-0.0095	0.0000	0.0072	0.0001
175	5811	-0.0049	-0.0108	-0.0061	-0.0041	-0.0044	-0.0103	-0.0094	0.0000	0.0371	0.0000
177.5	5146	-0.0056	-0.0101	-0.0058	-0.0042	-0.0043	-0.0103	-0.0090	0.0000	0.0908	0.0000
180	4479	-0.0062	-0.0091	-0.0055	-0.0044	-0.0038	-0.0097	-0.0084	0.0000	0.0054	-0.0001
182.5	2982	-0.0033	-0.0074	-0.0046	-0.0040	-0.0031	-0.0068	-0.0077	0.0000	0.1275	-0.0003
185	2539	-0.0020	-0.0064	-0.0042	-0.0032	-0.0026	-0.0066	-0.0073	0.0000	0.1288	-0.0003
187.5	174	0.0009	0.0025	0.0020	0.0020	0.0023	0.0026	0.0020	0.0000	0.1288	0.0003
190	0	0.0013	-0.0018	-0.0017	-0.0017	-0.0021	-0.0019	-0.0011	0.0000	0.1335	-0.0003
192.5	0	0.0012	-0.0018	-0.0017	-0.0017	-0.0022	-0.0019	-0.0011	0.0000	0.1335	-0.0003
195	0	0.0011	-0.0016	-0.0017	-0.0017	-0.0019	-0.0019	-0.0011	0.0000	0.1245	-0.0003
197.5	1	0.0015	-0.0013	-0.0014	-0.0016	-0.0016	-0.0016	-0.0010	0.0000	0.1136	-0.0003
200	2	0.0020	-0.0011	-0.0014	-0.0015	-0.0014	-0.0016	-0.0010	0.0000	0.1157	-0.0003
202.5	5	0.0020	-0.0011	-0.0014	-0.0014	-0.0012	-0.0016	-0.0010	0.0000	0.1136	-0.0003
205	3	0.0017	-0.0011	-0.0014	-0.0013	-0.0013	-0.0016	-0.0010	0.0000	0.1068	-0.0003
207.5	2	0.0009	-0.0011	-0.0014	-0.0013	-0.0014	-0.0016	-0.0010	0.0000	0.1004	-0.0003
210	6	0.0007	-0.0011	-0.0014	-0.0013	-0.0013	-0.0016	-0.0010	0.0000	0.1136	-0.0003
212.5	7	0.0014	-0.0011	-0.0014	-0.0012	-0.0011	-0.0016	-0.0010	0.0000	0.1180	-0.0003
215	10	0.0028	-0.0011	-0.0014	-0.0011	-0.0012	-0.0016	-0.0010	0.0000	0.1218	-0.0003
217.5	10	0.0024	-0.0011	-0.0013	-0.0011	-0.0011	-0.0016	-0.0010	0.0000	0.1263	-0.0003
220	10	0.0025	-0.0011	-0.0010	-0.0010	-0.0010	-0.0016	-0.0008	0.0000	0.1282	-0.0003
222.5	10	0.0022	-0.0011	-0.0010	-0.0010	-0.0010	-0.0015	-0.0007	0.0000	0.1275	-0.0003
225	10	0.0016	-0.0011	-0.0010	-0.0007	-0.0009	-0.0010	-0.0007	0.0000	0.1275	-0.0003
227.5	10	0.0019	-0.0011	-0.0007	-0.0006	-0.0010	-0.0009	-0.0007	0.0000	0.1284	-0.0001
230	10	0.0016	-0.0011	-0.0007	-0.0006	-0.0009	-0.0009	-0.0007	0.0000	0.1391	-0.0002
232.5	10	0.0018	-0.0011	-0.0007	-0.0005	-0.0007	-0.0007	-0.0007	0.0000	0.1288	-0.0003
235	10	0.0019	-0.0011	-0.0007	-0.0005	-0.0007	-0.0006	-0.0007	0.0000	0.1273	-0.0001
237.5	10	0.0017	-0.0011	-0.0007	-0.0004	-0.0007	-0.0006	-0.0007	0.0000	0.1285	0.0000
240	10	0.0014	-0.0011	-0.0007	-0.0004	-0.0007	-0.0006	-0.0007	0.0000	0.1257	0.0000
242.5	10	0.0014	-0.0011	-0.0007	-0.0004	-0.0007	-0.0007	-0.0007	0.0000	0.1258	-0.0001
245	8	0.0019	-0.0010	-0.0005	-0.0004	-0.0007	-0.0008	-0.0007	0.0000	0.1223	-0.0003
247.5	8	0.0015	-0.0007	-0.0006	-0.0003	-0.0008	-0.0006	-0.0007	0.0000	0.1297	-0.0003
250	10	0.0015	-0.0007	-0.0005	-0.0003	-0.0008	-0.0007	-0.0007	0.0000	0.1248	-0.0003
252.5	10	0.0016	-0.0007	-0.0004	-0.0003	-0.0009	-0.0006	-0.0007	0.0000	0.1246	-0.0001
255	10	0.0023	-0.0007	-0.0003	-0.0003	-0.0010	-0.0006	-0.0007	0.0000	0.1255	0.0000

Table A.10: Tabulated Results from 11 Nov 2005, Field Load Test #10

Test # 10		Notes:									
Date: 11-Nov-05		-- Linear Pot #3 was determined to be damaged at the outset of these tests -- The data gathered from Linear Pot #4 was discarded due to excessive scatter -- Each Telltale is labeled by the same notation: (LP# (Depth) I/O)									
Time (sec)	Load (lbs)	Interior Telltales (I)					Perimeter Telltales (O)				
		LP10 (surf) I (in)	LP6 (6") I (in)	LP8 (12") I (in)	LP7 (18") I (in)	LP12 (30") I (in)	LP1 (surf) O (in)	LP9 (6") O (in)	LP3 (12") O (in)	LP4 (18") O (in)	LP2 (30") O (in)
MAX	19989	-0.0096	-0.0180	-0.0111	-0.0063	-0.0077	-0.0159	-0.0135	0.0000	-0.0859	-0.0030
0	-1	-0.0015	0.0002	0.0001	0.0002	0.0001	0.0001	0.0000	0.0000	0.0016	0.0002
2.5	0	-0.0015	0.0002	0.0001	0.0002	0.0001	0.0001	0.0001	0.0000	0.0033	0.0000
5	0	-0.0015	0.0002	0.0001	0.0002	0.0001	0.0001	0.0001	0.0000	0.0063	0.0000
7.5	0	-0.0003	0.0002	0.0001	0.0005	0.0001	0.0001	0.0001	0.0000	0.0040	0.0000
10	0	-0.0004	0.0002	0.0001	0.0004	0.0001	0.0001	0.0001	0.0000	0.0106	0.0000
12.5	1	-0.0011	0.0002	0.0001	0.0001	0.0001	0.0001	0.0000	0.0000	0.0034	-0.0001
15	1	-0.0012	0.0001	0.0001	0.0002	0.0001	0.0001	0.0001	0.0000	0.0041	0.0000
17.5	23	-0.0006	0.0002	0.0001	0.0003	0.0003	0.0001	0.0001	0.0000	0.0093	0.0002
20	886	-0.0002	0.0000	0.0001	0.0002	0.0004	-0.0004	0.0001	0.0000	0.0005	0.0003
22.5	1422	-0.0001	-0.0002	0.0001	0.0002	0.0005	-0.0010	0.0001	0.0000	0.0017	0.0003
25	1877	0.0001	-0.0007	0.0001	0.0002	0.0004	-0.0012	0.0001	0.0000	0.0010	0.0005
27.5	2912	0.0007	-0.0015	-0.0002	0.0002	0.0005	-0.0020	0.0001	0.0000	0.0010	0.0006
30	4109	0.0011	-0.0026	-0.0002	0.0002	0.0002	-0.0028	0.0001	0.0000	0.0050	0.0010
32.5	5252	0.0014	-0.0034	-0.0005	0.0002	-0.0002	-0.0033	0.0000	0.0000	0.0057	0.0015
35	6326	0.0003	-0.0046	-0.0007	0.0001	-0.0007	-0.0040	-0.0003	0.0000	0.0015	0.0020
37.5	7340	-0.0005	-0.0056	-0.0010	-0.0001	-0.0013	-0.0046	-0.0008	0.0000	0.0037	0.0023
40	8302	-0.0006	-0.0064	-0.0013	-0.0001	-0.0015	-0.0053	-0.0010	0.0000	0.0042	0.0024
42.5	9211	-0.0001	-0.0073	-0.0016	-0.0001	-0.0016	-0.0059	-0.0014	0.0000	0.0044	0.0026
45	10074	-0.0007	-0.0081	-0.0018	-0.0003	-0.0015	-0.0062	-0.0017	0.0000	0.0055	0.0026
47.5	10903	-0.0008	-0.0088	-0.0021	0.0005	-0.0014	-0.0065	-0.0022	0.0000	0.0126	0.0026
50	11697	-0.0017	-0.0095	-0.0026	0.0001	-0.0019	-0.0080	-0.0036	0.0000	0.0154	0.0026
52.5	12458	-0.0041	-0.0103	-0.0031	-0.0004	-0.0022	-0.0093	-0.0049	0.0000	0.0099	0.0026
55	13182	-0.0036	-0.0109	-0.0035	-0.0007	-0.0027	-0.0100	-0.0054	0.0000	0.0215	0.0026
57.5	13872	-0.0036	-0.0114	-0.0037	-0.0008	-0.0030	-0.0106	-0.0058	0.0000	0.0554	0.0026
60	14547	-0.0036	-0.0118	-0.0040	-0.0011	-0.0033	-0.0106	-0.0062	0.0000	0.0559	0.0026
62.5	15427	-0.0046	-0.0125	-0.0044	-0.0014	-0.0034	-0.0104	-0.0066	0.0000	0.0156	0.0026
65	16350	-0.0062	-0.0135	-0.0050	-0.0021	-0.0038	-0.0104	-0.0072	0.0000	0.0136	0.0023
67.5	17231	-0.0072	-0.0143	-0.0057	-0.0026	-0.0042	-0.0112	-0.0078	0.0000	0.0005	0.0020
70	18062	-0.0073	-0.0149	-0.0062	-0.0028	-0.0049	-0.0123	-0.0078	0.0000	0.0023	0.0019
72.5	18840	-0.0072	-0.0154	-0.0070	-0.0034	-0.0056	-0.0128	-0.0088	0.0000	0.0108	0.0015
75	19579	-0.0072	-0.0163	-0.0074	-0.0039	-0.0059	-0.0132	-0.0094	0.0000	0.0038	0.0011
77.5	19989	-0.0083	-0.0171	-0.0080	-0.0038	-0.0064	-0.0132	-0.0096	0.0000	0.0031	0.0010
80	19887	-0.0096	-0.0175	-0.0086	-0.0040	-0.0064	-0.0136	-0.0099	0.0000	0.0023	0.0006
82.5	19802	-0.0088	-0.0176	-0.0089	-0.0044	-0.0064	-0.0142	-0.0102	0.0000	0.0022	0.0005
85	19719	-0.0093	-0.0175	-0.0093	-0.0050	-0.0065	-0.0150	-0.0105	0.0000	0.0065	0.0002
87.5	19645	-0.0064	-0.0177	-0.0097	-0.0058	-0.0071	-0.0149	-0.0112	0.0000	0.0005	-0.0005
90	19575	-0.0067	-0.0180	-0.0098	-0.0058	-0.0074	-0.0152	-0.0117	0.0000	0.0053	-0.0007
92.5	19505	-0.0071	-0.0180	-0.0098	-0.0059	-0.0074	-0.0152	-0.0118	0.0000	0.0031	-0.0007
95	19437	-0.0071	-0.0179	-0.0098	-0.0058	-0.0073	-0.0151	-0.0118	0.0000	0.0033	-0.0007
97.5	19379	-0.0077	-0.0180	-0.0098	-0.0058	-0.0073	-0.0151	-0.0118	0.0000	0.0051	-0.0008
100	19323	-0.0077	-0.0180	-0.0098	-0.0058	-0.0071	-0.0151	-0.0120	0.0000	0.0075	-0.0007
102.5	19265	-0.0081	-0.0180	-0.0098	-0.0056	-0.0068	-0.0151	-0.0121	0.0000	0.0059	-0.0007
105	19202	-0.0082	-0.0180	-0.0098	-0.0056	-0.0067	-0.0150	-0.0120	0.0000	0.0163	-0.0007
107.5	19146	-0.0080	-0.0180	-0.0098	-0.0058	-0.0070	-0.0152	-0.0121	0.0000	0.0043	-0.0008
110	19083	-0.0068	-0.0180	-0.0100	-0.0059	-0.0070	-0.0152	-0.0121	0.0000	0.0059	-0.0008
112.5	19019	-0.0070	-0.0180	-0.0099	-0.0059	-0.0069	-0.0152	-0.0121	0.0000	0.0044	-0.0007
115	18968	-0.0074	-0.0177	-0.0098	-0.0059	-0.0069	-0.0152	-0.0121	0.0000	0.0060	-0.0010
117.5	18976	-0.0076	-0.0179	-0.0099	-0.0059	-0.0070	-0.0152	-0.0121	0.0000	0.0018	-0.0010
120	19332	-0.0076	-0.0180	-0.0098	-0.0058	-0.0068	-0.0152	-0.0121	0.0000	0.0124	-0.0009
122.5	19891	-0.0076	-0.0180	-0.0099	-0.0059	-0.0067	-0.0152	-0.0121	0.0000	0.0183	-0.0009
125	19908	-0.0080	-0.0180	-0.0099	-0.0058	-0.0067	-0.0152	-0.0121	0.0000	0.0024	-0.0009
127.5	19826	-0.0081	-0.0180	-0.0098	-0.0059	-0.0067	-0.0152	-0.0121	0.0000	0.0116	-0.0010
130	19743	-0.0081	-0.0180	-0.0098	-0.0059	-0.0066	-0.0152	-0.0121	0.0000	0.0099	-0.0010
132.5	19676	-0.0075	-0.0180	-0.0100	-0.0059	-0.0065	-0.0152	-0.0121	0.0000	0.0019	-0.0010
135	19608	-0.0069	-0.0180	-0.0101	-0.0059	-0.0065	-0.0152	-0.0121	0.0000	0.0060	-0.0010

Table A.10: Tabulated Results from 11 Nov 2005, Field Load Test #10 (continued)

Test #		Notes:									
Date:		-- Linear Pot #3 was determined to be damaged at the outset of these tests -- The data gathered from Linear Pot #4 was discarded due to excessive scatter -- Each Telltale is labeled by the same notation: (LP# (Depth) I/O)									
Time (sec)	Load (lbs)	Interior Telltales (I)					Perimeter Telltales (O)				
		LP10 (surf) I	LP6 (6") I	LP8 (12") I	LP7 (18") I	LP12 (30") I	LP1 (surf) O	LP9 (6") O	LP3 (12") O	LP4 (18") O	LP2 (30") O
		(in)	(in)	(in)	(in)	(in)	(in)	(in)	(in)	(in)	(in)
137.5	19540	-0.0071	-0.0180	-0.0101	-0.0059	-0.0065	-0.0152	-0.0121	0.0000	0.0073	-0.0010
140	19475	-0.0078	-0.0180	-0.0101	-0.0060	-0.0067	-0.0152	-0.0122	0.0000	0.0096	-0.0010
142.5	19409	-0.0079	-0.0180	-0.0101	-0.0059	-0.0064	-0.0152	-0.0122	0.0000	0.0070	-0.0010
145	19323	-0.0082	-0.0180	-0.0101	-0.0059	-0.0064	-0.0152	-0.0124	0.0000	0.0043	-0.0010
147.5	19178	-0.0086	-0.0180	-0.0101	-0.0059	-0.0066	-0.0151	-0.0123	0.0000	0.0027	-0.0010
150	18947	-0.0079	-0.0179	-0.0103	-0.0060	-0.0074	-0.0152	-0.0124	0.0000	0.0019	-0.0013
152.5	17947	-0.0092	-0.0178	-0.0111	-0.0063	-0.0077	-0.0159	-0.0135	0.0000	0.0030	-0.0024
155	16321	-0.0091	-0.0173	-0.0111	-0.0063	-0.0074	-0.0156	-0.0134	0.0000	0.0067	-0.0026
157.5	14890	-0.0079	-0.0167	-0.0106	-0.0062	-0.0074	-0.0151	-0.0132	0.0000	0.0042	-0.0027
160	13613	-0.0077	-0.0162	-0.0104	-0.0062	-0.0072	-0.0149	-0.0131	0.0000	0.0045	-0.0027
162.5	12459	-0.0078	-0.0156	-0.0104	-0.0062	-0.0068	-0.0149	-0.0131	0.0000	0.0058	-0.0026
165	11420	-0.0072	-0.0150	-0.0104	-0.0062	-0.0062	-0.0145	-0.0131	0.0000	0.0083	-0.0027
167.5	10491	-0.0062	-0.0138	-0.0101	-0.0062	-0.0055	-0.0136	-0.0131	0.0000	0.0078	-0.0027
170	9667	-0.0063	-0.0128	-0.0094	-0.0062	-0.0047	-0.0134	-0.0131	0.0000	0.0044	-0.0027
172.5	8939	-0.0068	-0.0125	-0.0094	-0.0062	-0.0045	-0.0130	-0.0131	0.0000	0.0069	-0.0029
175	8293	-0.0070	-0.0123	-0.0092	-0.0062	-0.0042	-0.0129	-0.0129	0.0000	0.0074	-0.0030
177.5	7574	-0.0075	-0.0118	-0.0091	-0.0062	-0.0043	-0.0125	-0.0127	0.0000	0.0052	-0.0030
180	6556	-0.0086	-0.0110	-0.0089	-0.0062	-0.0042	-0.0121	-0.0124	0.0000	0.0033	-0.0030
182.5	5747	-0.0081	-0.0102	-0.0086	-0.0062	-0.0039	-0.0111	-0.0121	0.0000	0.0073	-0.0030
185	5120	-0.0086	-0.0094	-0.0081	-0.0059	-0.0032	-0.0107	-0.0110	0.0000	0.0078	-0.0030
187.5	4628	-0.0083	-0.0089	-0.0080	-0.0059	-0.0034	-0.0104	-0.0107	0.0000	0.0038	-0.0030
190	4189	-0.0076	-0.0083	-0.0077	-0.0059	-0.0030	-0.0102	-0.0105	0.0000	0.0080	-0.0030
192.5	3699	-0.0074	-0.0075	-0.0071	-0.0059	-0.0025	-0.0100	-0.0100	0.0000	0.0093	-0.0030
195	3177	-0.0082	-0.0069	-0.0067	-0.0057	-0.0020	-0.0097	-0.0095	0.0000	0.0099	-0.0030
197.5	2720	-0.0079	-0.0062	-0.0063	-0.0053	-0.0018	-0.0090	-0.0088	0.0000	0.0036	-0.0030
200	2532	-0.0074	-0.0056	-0.0060	-0.0045	-0.0018	-0.0080	-0.0082	0.0000	0.0026	-0.0030
202.5	205	-0.0040	-0.0025	-0.0039	-0.0033	-0.0017	-0.0039	-0.0040	0.0000	0.0030	-0.0030
205	10	-0.0030	-0.0016	-0.0033	-0.0032	-0.0014	-0.0032	-0.0028	0.0000	0.0014	-0.0029
207.5	10	-0.0029	-0.0013	-0.0032	-0.0032	-0.0014	-0.0030	-0.0026	0.0000	0.0012	-0.0027
210	10	-0.0023	-0.0009	-0.0029	-0.0031	-0.0013	-0.0028	-0.0024	0.0000	0.0086	-0.0027
212.5	13	-0.0024	-0.0009	-0.0029	-0.0029	-0.0013	-0.0027	-0.0023	0.0000	0.0005	-0.0027
215	12	-0.0033	-0.0009	-0.0029	-0.0028	-0.0011	-0.0027	-0.0023	0.0000	0.0084	-0.0027
217.5	10	-0.0041	-0.0009	-0.0029	-0.0029	-0.0010	-0.0027	-0.0023	0.0000	0.0035	-0.0027
220	9	-0.0048	-0.0009	-0.0029	-0.0031	-0.0010	-0.0027	-0.0023	0.0000	0.0063	-0.0027
222.5	8	-0.0049	-0.0009	-0.0029	-0.0031	-0.0009	-0.0027	-0.0023	0.0000	0.0042	-0.0027
225	10	-0.0058	-0.0009	-0.0029	-0.0031	-0.0009	-0.0027	-0.0023	0.0000	0.0103	-0.0027
227.5	10	-0.0056	-0.0009	-0.0029	-0.0029	-0.0009	-0.0027	-0.0023	0.0000	0.0062	-0.0027
230	12	-0.0056	-0.0009	-0.0029	-0.0029	-0.0009	-0.0027	-0.0023	0.0000	0.0003	-0.0027
232.5	10	-0.0040	-0.0009	-0.0029	-0.0028	-0.0008	-0.0026	-0.0023	0.0000	0.0078	-0.0027
235	10	-0.0022	-0.0009	-0.0028	-0.0028	-0.0006	-0.0025	-0.0023	0.0000	0.0047	-0.0027
237.5	17	-0.0024	-0.0007	-0.0028	-0.0028	-0.0005	-0.0026	-0.0023	0.0000	0.0094	-0.0027
240	14	-0.0015	-0.0005	-0.0026	-0.0028	-0.0005	-0.0027	-0.0023	0.0000	0.0034	-0.0027
242.5	10	-0.0013	-0.0005	-0.0026	-0.0025	-0.0005	-0.0028	-0.0023	0.0000	0.0018	-0.0027
245	10	-0.0005	-0.0002	-0.0024	-0.0024	-0.0003	-0.0024	-0.0019	0.0000	0.0073	-0.0023
247.5	10	0.0004	-0.0002	-0.0019	-0.0017	-0.0005	-0.0019	-0.0013	0.0000	0.0053	-0.0016
250	15	-0.0005	-0.0001	-0.0015	-0.0011	-0.0004	-0.0014	-0.0009	0.0000	0.0068	-0.0010
252.5	12	0.0003	0.0002	-0.0012	-0.0011	-0.0004	-0.0014	-0.0009	0.0000	0.0022	-0.0009
255	10	-0.0011	0.0001	-0.0008	-0.0006	-0.0005	-0.0005	-0.0006	0.0000	0.0050	-0.0004

Table A.11: Tabulated Results from 11 Nov 2005, Field Load Test #11

Test # 11		Notes: -- The wind blew fast during this test. Possibly affected reference frame. -- Linear Pot #3 was determined to be damaged at the outset of these tests -- The data gathered from Linear Pot #4 was discarded due to excessive scatter -- Each Telltale is labeled by the same notation: (LP# (Depth) I/O)									
Date: 11-Nov-05											
Time (sec)	Load (lbs)	Interior Telltales (I)					Perimeter Telltales (O)				
		LP7 (surf) I (in)	LP6 (6") I (in)	LP8 (12") I (in)	LP10 (18") I (in)	LP12 (30") I (in)	LP1 (surf) O (in)	LP4 (6") O (in)	LP3 (12") O (in)	LP9 (18") O (in)	LP2 (30") O (in)
MAX	20060	-0.0230	-0.0202	-0.0167	-0.0135	-0.0109	-0.0219	0.0000	0.0000	-0.0146	-0.0090
0	0	0.0000	0.0000	0.0000	0.0000	0.0000	0.0000	0.0000	0.0000	0.0000	0.0000
2.5	2	0.0000	0.0000	0.0000	0.0000	0.0000	0.0000	0.0000	0.0000	0.0000	0.0000
5	7	0.0000	0.0000	0.0000	0.0000	0.0000	0.0000	0.0000	0.0000	0.0000	0.0000
7.5	0	0.0000	0.0000	0.0000	0.0000	0.0000	0.0000	0.0000	0.0000	0.0000	0.0000
10	0	0.0000	0.0000	0.0000	0.0000	0.0000	0.0000	0.0000	0.0000	0.0000	0.0000
12.5	0	0.0000	0.0000	0.0000	0.0000	-0.0003	0.0000	0.0000	0.0000	0.0000	0.0001
15	837	-0.0001	-0.0001	-0.0001	0.0000	-0.0006	-0.0001	0.0000	0.0000	0.0001	0.0001
17.5	2334	-0.0015	-0.0012	-0.0008	0.0000	-0.0007	-0.0014	0.0000	0.0000	-0.0004	0.0000
20	3959	-0.0043	-0.0030	-0.0021	-0.0009	-0.0019	-0.0033	0.0000	0.0000	-0.0003	-0.0006
22.5	4586	-0.0051	-0.0039	-0.0024	-0.0012	-0.0029	-0.0032	0.0000	0.0000	-0.0011	-0.0007
25	5362	-0.0054	-0.0045	-0.0028	-0.0013	-0.0028	-0.0038	0.0000	0.0000	-0.0026	-0.0007
27.5	6130	-0.0064	-0.0051	-0.0034	-0.0013	-0.0027	-0.0049	0.0000	0.0000	-0.0033	-0.0007
30	6878	-0.0069	-0.0057	-0.0041	-0.0016	-0.0028	-0.0064	0.0000	0.0000	-0.0012	-0.0007
32.5	7744	-0.0075	-0.0067	-0.0044	-0.0019	-0.0032	-0.0073	0.0000	0.0000	-0.0006	-0.0007
35	9075	-0.0088	-0.0078	-0.0051	-0.0024	-0.0037	-0.0083	0.0000	0.0000	-0.0016	-0.0007
37.5	10390	-0.0099	-0.0087	-0.0059	-0.0034	-0.0038	-0.0096	0.0000	0.0000	-0.0029	-0.0008
40	11610	-0.0110	-0.0098	-0.0068	-0.0043	-0.0041	-0.0108	0.0000	0.0000	-0.0054	-0.0011
42.5	12743	-0.0117	-0.0110	-0.0075	-0.0047	-0.0040	-0.0116	0.0000	0.0000	-0.0064	-0.0014
45	13806	-0.0127	-0.0121	-0.0081	-0.0051	-0.0044	-0.0127	0.0000	0.0000	-0.0089	-0.0017
47.5	14799	-0.0135	-0.0131	-0.0086	-0.0056	-0.0055	-0.0132	0.0000	0.0000	-0.0081	-0.0018
50	15725	-0.0143	-0.0137	-0.0093	-0.0062	-0.0055	-0.0137	0.0000	0.0000	-0.0068	-0.0021
52.5	16594	-0.0153	-0.0144	-0.0102	-0.0071	-0.0058	-0.0148	0.0000	0.0000	-0.0088	-0.0029
55	17416	-0.0163	-0.0153	-0.0106	-0.0074	-0.0064	-0.0151	0.0000	0.0000	-0.0097	-0.0030
57.5	18195	-0.0171	-0.0160	-0.0111	-0.0079	-0.0067	-0.0158	0.0000	0.0000	-0.0089	-0.0031
60	18933	-0.0176	-0.0164	-0.0115	-0.0084	-0.0073	-0.0160	0.0000	0.0000	-0.0101	-0.0033
62.5	19614	-0.0185	-0.0169	-0.0120	-0.0089	-0.0076	-0.0175	0.0000	0.0000	-0.0123	-0.0036
65	19782	-0.0190	-0.0172	-0.0125	-0.0094	-0.0080	-0.0192	0.0000	0.0000	-0.0122	-0.0041
67.5	19991	-0.0190	-0.0176	-0.0125	-0.0094	-0.0083	-0.0193	0.0000	0.0000	-0.0113	-0.0043
70	20060	-0.0193	-0.0176	-0.0125	-0.0094	-0.0082	-0.0193	0.0000	0.0000	-0.0115	-0.0043
72.5	19957	-0.0193	-0.0176	-0.0127	-0.0097	-0.0082	-0.0195	0.0000	0.0000	-0.0113	-0.0045
75	19881	-0.0196	-0.0178	-0.0131	-0.0098	-0.0081	-0.0198	0.0000	0.0000	-0.0108	-0.0051
77.5	19810	-0.0197	-0.0180	-0.0136	-0.0104	-0.0080	-0.0198	0.0000	0.0000	-0.0111	-0.0057
80	19749	-0.0206	-0.0180	-0.0141	-0.0108	-0.0079	-0.0196	0.0000	0.0000	-0.0117	-0.0062
82.5	19683	-0.0206	-0.0183	-0.0144	-0.0110	-0.0090	-0.0196	0.0000	0.0000	-0.0117	-0.0061
85	19626	-0.0206	-0.0184	-0.0143	-0.0110	-0.0091	-0.0195	0.0000	0.0000	-0.0122	-0.0063
87.5	19579	-0.0207	-0.0184	-0.0143	-0.0111	-0.0091	-0.0196	0.0000	0.0000	-0.0120	-0.0063
90	19522	-0.0209	-0.0184	-0.0146	-0.0111	-0.0089	-0.0195	0.0000	0.0000	-0.0119	-0.0064
92.5	19475	-0.0208	-0.0184	-0.0146	-0.0112	-0.0089	-0.0196	0.0000	0.0000	-0.0129	-0.0063
95	19426	-0.0208	-0.0184	-0.0150	-0.0114	-0.0089	-0.0197	0.0000	0.0000	-0.0125	-0.0069
97.5	19385	-0.0210	-0.0185	-0.0156	-0.0115	-0.0093	-0.0201	0.0000	0.0000	-0.0122	-0.0074
100	19340	-0.0210	-0.0187	-0.0155	-0.0116	-0.0098	-0.0201	0.0000	0.0000	-0.0122	-0.0074
102.5	19299	-0.0217	-0.0191	-0.0162	-0.0124	-0.0102	-0.0205	0.0000	0.0000	-0.0124	-0.0082
105	19258	-0.0223	-0.0194	-0.0166	-0.0131	-0.0106	-0.0207	0.0000	0.0000	-0.0129	-0.0088
107.5	19218	-0.0223	-0.0198	-0.0165	-0.0132	-0.0108	-0.0209	0.0000	0.0000	-0.0135	-0.0087
110	19181	-0.0224	-0.0196	-0.0165	-0.0131	-0.0102	-0.0210	0.0000	0.0000	-0.0127	-0.0089
112.5	19143	-0.0224	-0.0197	-0.0163	-0.0131	-0.0107	-0.0209	0.0000	0.0000	-0.0138	-0.0089
115	19106	-0.0225	-0.0197	-0.0163	-0.0131	-0.0104	-0.0211	0.0000	0.0000	-0.0132	-0.0088
117.5	19077	-0.0227	-0.0198	-0.0163	-0.0131	-0.0107	-0.0212	0.0000	0.0000	-0.0133	-0.0088
120	19102	-0.0227	-0.0198	-0.0164	-0.0132	-0.0106	-0.0215	0.0000	0.0000	-0.0137	-0.0089
122.5	19281	-0.0226	-0.0197	-0.0165	-0.0132	-0.0103	-0.0215	0.0000	0.0000	-0.0143	-0.0089
125	19800	-0.0225	-0.0198	-0.0167	-0.0133	-0.0098	-0.0218	0.0000	0.0000	-0.0146	-0.0089
127.5	19933	-0.0227	-0.0200	-0.0165	-0.0132	-0.0105	-0.0216	0.0000	0.0000	-0.0143	-0.0089
130	19855	-0.0227	-0.0202	-0.0166	-0.0134	-0.0109	-0.0218	0.0000	0.0000	-0.0139	-0.0089
132.5	19786	-0.0228	-0.0202	-0.0167	-0.0134	-0.0109	-0.0219	0.0000	0.0000	-0.0137	-0.0090
135	19721	-0.0227	-0.0202	-0.0164	-0.0134	-0.0108	-0.0218	0.0000	0.0000	-0.0135	-0.0090



Table A.11: Tabulated Results from 11 Nov 2005, Field Load Test #11 (continued)

Test # 11		Notes: -- The wind blew fast during this test. Possibly affected reference frame. -- Linear Pot #3 was determined to be damaged at the outset of these tests -- The data gathered from Linear Pot #4 was discarded due to excessive scatter -- Each Telltale is labeled by the same notation: (LP# (Depth) I/O)									
Date: 11-Nov-05		Interior Telltales (I)					Perimeter Telltales (O)				
Time	Load	LP7 (surf) I	LP6 (6") I	LP8 (12") I	LP10 (18") I	LP12 (30") I	LP1 (surf) O	LP4 (6") O	LP3 (12") O	LP9 (18") O	LP2 (30") O
(sec)	(lbs)	(in)	(in)	(in)	(in)	(in)	(in)	(in)	(in)	(in)	(in)
137.5	19657	-0.0227	-0.0202	-0.0163	-0.0135	-0.0107	-0.0218	0.0000	0.0000	-0.0136	-0.0090
140	19598	-0.0227	-0.0202	-0.0163	-0.0135	-0.0107	-0.0218	0.0000	0.0000	-0.0136	-0.0090
142.5	19539	-0.0227	-0.0201	-0.0164	-0.0134	-0.0104	-0.0215	0.0000	0.0000	-0.0139	-0.0090
145	19487	-0.0228	-0.0199	-0.0166	-0.0134	-0.0107	-0.0216	0.0000	0.0000	-0.0139	-0.0089
147.5	19426	-0.0229	-0.0198	-0.0166	-0.0135	-0.0104	-0.0218	0.0000	0.0000	-0.0138	-0.0090
150	19313	-0.0230	-0.0198	-0.0166	-0.0135	-0.0103	-0.0218	0.0000	0.0000	-0.0140	-0.0090
152.5	19169	-0.0229	-0.0198	-0.0166	-0.0135	-0.0101	-0.0217	0.0000	0.0000	-0.0139	-0.0090
155	19011	-0.0226	-0.0198	-0.0163	-0.0135	-0.0102	-0.0213	0.0000	0.0000	-0.0136	-0.0090
157.5	18649	-0.0227	-0.0198	-0.0163	-0.0135	-0.0097	-0.0211	0.0000	0.0000	-0.0136	-0.0088
160	17488	-0.0224	-0.0195	-0.0160	-0.0135	-0.0097	-0.0207	0.0000	0.0000	-0.0133	-0.0089
162.5	16166	-0.0218	-0.0187	-0.0157	-0.0132	-0.0100	-0.0201	0.0000	0.0000	-0.0124	-0.0089
165	14974	-0.0210	-0.0181	-0.0156	-0.0125	-0.0100	-0.0195	0.0000	0.0000	-0.0113	-0.0084
167.5	13883	-0.0210	-0.0178	-0.0154	-0.0125	-0.0101	-0.0196	0.0000	0.0000	-0.0111	-0.0086
170	12893	-0.0200	-0.0170	-0.0147	-0.0122	-0.0097	-0.0195	0.0000	0.0000	-0.0115	-0.0082
172.5	11969	-0.0195	-0.0164	-0.0143	-0.0121	-0.0092	-0.0191	0.0000	0.0000	-0.0118	-0.0079
175	10251	-0.0189	-0.0158	-0.0136	-0.0118	-0.0090	-0.0177	0.0000	0.0000	-0.0115	-0.0080
177.5	4885	-0.0146	-0.0113	-0.0106	-0.0101	-0.0070	-0.0131	0.0000	0.0000	-0.0085	-0.0070
180	3350	-0.0125	-0.0091	-0.0089	-0.0085	-0.0057	-0.0106	0.0000	0.0000	-0.0081	-0.0061
182.5	2761	-0.0114	-0.0079	-0.0081	-0.0078	-0.0053	-0.0099	0.0000	0.0000	-0.0063	-0.0060
185	1401	-0.0092	-0.0060	-0.0069	-0.0071	-0.0049	-0.0074	0.0000	0.0000	-0.0049	-0.0060
187.5	29	-0.0064	-0.0035	-0.0052	-0.0061	-0.0039	-0.0034	0.0000	0.0000	-0.0023	-0.0057
190	30	-0.0060	-0.0033	-0.0047	-0.0058	-0.0040	-0.0031	0.0000	0.0000	-0.0005	-0.0055
192.5	29	-0.0053	-0.0027	-0.0042	-0.0056	-0.0038	-0.0034	0.0000	0.0000	0.0008	-0.0049
195	25	-0.0049	-0.0029	-0.0040	-0.0053	-0.0039	-0.0036	0.0000	0.0000	0.0009	-0.0046
197.5	26	-0.0047	-0.0027	-0.0038	-0.0053	-0.0040	-0.0035	0.0000	0.0000	0.0008	-0.0046
200	27	-0.0047	-0.0027	-0.0037	-0.0052	-0.0040	-0.0033	0.0000	0.0000	0.0005	-0.0046
202.5	29	-0.0047	-0.0027	-0.0037	-0.0050	-0.0039	-0.0033	0.0000	0.0000	0.0009	-0.0045
205	28	-0.0047	-0.0027	-0.0038	-0.0050	-0.0040	-0.0032	0.0000	0.0000	0.0010	-0.0044
207.5	30	-0.0047	-0.0024	-0.0039	-0.0050	-0.0042	-0.0030	0.0000	0.0000	0.0010	-0.0040
210	30	-0.0047	-0.0023	-0.0037	-0.0050	-0.0041	-0.0029	0.0000	0.0000	0.0011	-0.0040
212.5	30	-0.0047	-0.0023	-0.0037	-0.0050	-0.0041	-0.0029	0.0000	0.0000	0.0011	-0.0040
215	30	-0.0047	-0.0024	-0.0037	-0.0050	-0.0041	-0.0029	0.0000	0.0000	0.0011	-0.0040
217.5	30	-0.0044	-0.0024	-0.0037	-0.0050	-0.0040	-0.0029	0.0000	0.0000	0.0008	-0.0039
220	30	-0.0044	-0.0024	-0.0037	-0.0049	-0.0040	-0.0029	0.0000	0.0000	0.0002	-0.0038
222.5	21	-0.0044	-0.0023	-0.0037	-0.0049	-0.0040	-0.0029	0.0000	0.0000	0.0006	-0.0037
225	27	-0.0044	-0.0023	-0.0037	-0.0049	-0.0039	-0.0029	0.0000	0.0000	0.0001	-0.0037
227.5	30	-0.0044	-0.0023	-0.0037	-0.0048	-0.0039	-0.0029	0.0000	0.0000	-0.0003	-0.0037
230	30	-0.0044	-0.0023	-0.0037	-0.0049	-0.0037	-0.0029	0.0000	0.0000	0.0002	-0.0036
232.5	30	-0.0045	-0.0023	-0.0037	-0.0049	-0.0036	-0.0029	0.0000	0.0000	0.0001	-0.0036
235	30	-0.0044	-0.0023	-0.0037	-0.0047	-0.0034	-0.0029	0.0000	0.0000	-0.0004	-0.0036
237.5	22	-0.0044	-0.0023	-0.0037	-0.0049	-0.0037	-0.0029	0.0000	0.0000	0.0007	-0.0040
240	20	-0.0044	-0.0023	-0.0037	-0.0048	-0.0035	-0.0029	0.0000	0.0000	0.0007	-0.0040
242.5	20	-0.0045	-0.0023	-0.0037	-0.0050	-0.0034	-0.0029	0.0000	0.0000	0.0000	-0.0040
245	20	-0.0047	-0.0023	-0.0037	-0.0050	-0.0033	-0.0029	0.0000	0.0000	-0.0001	-0.0040
247.5	21	-0.0047	-0.0023	-0.0037	-0.0049	-0.0033	-0.0029	0.0000	0.0000	-0.0006	-0.0039
250	22	-0.0044	-0.0023	-0.0037	-0.0049	-0.0033	-0.0029	0.0000	0.0000	0.0001	-0.0039
252.5	24	-0.0044	-0.0023	-0.0037	-0.0049	-0.0033	-0.0029	0.0000	0.0000	0.0000	-0.0039
255	29	-0.0044	-0.0023	-0.0037	-0.0048	-0.0033	-0.0029	0.0000	0.0000	-0.0002	-0.0040



Table A.12: Tabulated Results from 11 Nov 2005, Field Load Test #12

Test # 12		Notes: -- The wind blew fast during this test. Possibly affected reference frame. -- Linear Pot #3 was determined to be damaged at the outset of these tests -- The data gathered from Linear Pot #4 was discarded due to excessive scatter -- Each Telltale is labeled by the same notation: (LP# (Depth) I/O)									
Date: 11-Nov-05											
Time	Load	Interior Telltales (I)					Perimeter Telltales (O)				
		LP7 (surf) I	LP6 (6") I	LP8 (12") I	LP10 (18") I	LP12 (30") I	LP1 (surf) O	LP4 (6") O	LP3 (12") O	LP9 (18") O	LP2 (30") O
(sec)	(lbs)	(in)	(in)	(in)	(in)	(in)	(in)	(in)	(in)	(in)	(in)
MAX	20002	-0.0162	-0.0171	-0.0111	-0.0065	-0.0069	-0.0176	0.0000	0.0000	-0.0141	-0.0027
0	0	0.0000	0.0000	0.0000	0.0000	-0.0001	0.0000	0.0000	0.0000	0.0001	0.0000
2.5	0	0.0000	0.0000	0.0000	0.0000	0.0000	0.0000	0.0000	0.0000	0.0002	0.0000
5	0	0.0000	0.0000	0.0000	0.0000	-0.0001	0.0000	0.0000	0.0000	0.0002	0.0000
7.5	0	0.0000	0.0001	0.0000	0.0000	0.0000	0.0000	0.0000	0.0000	0.0005	0.0000
10	0	0.0000	0.0000	0.0000	0.0000	0.0000	0.0000	0.0000	0.0000	0.0003	0.0000
12.5	-1	0.0000	0.0001	0.0000	0.0000	0.0000	0.0000	0.0000	0.0000	0.0000	0.0000
15	0	0.0000	0.0001	0.0000	0.0000	0.0000	0.0000	0.0000	0.0000	-0.0003	0.0000
17.5	231	0.0000	0.0001	0.0000	0.0000	0.0000	0.0000	0.0000	0.0000	0.0011	0.0000
20	1292	0.0000	-0.0003	-0.0001	0.0000	-0.0002	-0.0009	0.0000	0.0000	0.0018	0.0002
22.5	2230	-0.0003	-0.0009	-0.0004	0.0000	-0.0003	-0.0004	0.0000	0.0000	0.0015	0.0003
25	3948	-0.0018	-0.0022	-0.0014	0.0000	-0.0003	-0.0025	0.0000	0.0000	-0.0004	0.0003
27.5	5784	-0.0032	-0.0038	-0.0023	0.0000	-0.0007	-0.0047	0.0000	0.0000	-0.0039	0.0003
30	7459	-0.0049	-0.0056	-0.0032	-0.0001	-0.0012	-0.0063	0.0000	0.0000	-0.0046	0.0003
32.5	8947	-0.0061	-0.0068	-0.0040	-0.0009	-0.0011	-0.0077	0.0000	0.0000	-0.0067	0.0003
35	10078	-0.0068	-0.0078	-0.0045	-0.0011	-0.0014	-0.0084	0.0000	0.0000	-0.0069	0.0001
37.5	10947	-0.0078	-0.0089	-0.0051	-0.0013	-0.0021	-0.0095	0.0000	0.0000	-0.0067	0.0000
40	11729	-0.0084	-0.0098	-0.0055	-0.0014	-0.0028	-0.0099	0.0000	0.0000	-0.0077	0.0000
42.5	12473	-0.0090	-0.0103	-0.0061	-0.0018	-0.0027	-0.0102	0.0000	0.0000	-0.0081	-0.0001
45	13180	-0.0094	-0.0109	-0.0065	-0.0020	-0.0029	-0.0105	0.0000	0.0000	-0.0081	-0.0004
47.5	13858	-0.0099	-0.0115	-0.0068	-0.0023	-0.0033	-0.0113	0.0000	0.0000	-0.0080	-0.0005
50	14499	-0.0105	-0.0119	-0.0071	-0.0029	-0.0034	-0.0117	0.0000	0.0000	-0.0106	-0.0005
52.5	15109	-0.0114	-0.0124	-0.0077	-0.0035	-0.0034	-0.0123	0.0000	0.0000	-0.0121	-0.0007
55	15693	-0.0117	-0.0128	-0.0078	-0.0037	-0.0037	-0.0125	0.0000	0.0000	-0.0113	-0.0008
57.5	16294	-0.0122	-0.0133	-0.0080	-0.0040	-0.0045	-0.0131	0.0000	0.0000	-0.0112	-0.0007
60	16951	-0.0125	-0.0140	-0.0082	-0.0041	-0.0054	-0.0132	0.0000	0.0000	-0.0112	-0.0008
62.5	17682	-0.0130	-0.0145	-0.0086	-0.0044	-0.0053	-0.0138	0.0000	0.0000	-0.0108	-0.0008
65	18408	-0.0135	-0.0152	-0.0090	-0.0046	-0.0056	-0.0149	0.0000	0.0000	-0.0116	-0.0009
67.5	19099	-0.0138	-0.0156	-0.0092	-0.0047	-0.0058	-0.0159	0.0000	0.0000	-0.0109	-0.0010
70	19743	-0.0143	-0.0159	-0.0095	-0.0048	-0.0061	-0.0167	0.0000	0.0000	-0.0124	-0.0010
72.5	19960	-0.0145	-0.0162	-0.0096	-0.0051	-0.0060	-0.0172	0.0000	0.0000	-0.0125	-0.0009
75	19855	-0.0145	-0.0164	-0.0095	-0.0051	-0.0058	-0.0170	0.0000	0.0000	-0.0130	-0.0008
77.5	19772	-0.0145	-0.0164	-0.0095	-0.0051	-0.0058	-0.0171	0.0000	0.0000	-0.0130	-0.0009
80	19700	-0.0145	-0.0164	-0.0095	-0.0051	-0.0057	-0.0175	0.0000	0.0000	-0.0132	-0.0010
82.5	19632	-0.0145	-0.0164	-0.0097	-0.0051	-0.0056	-0.0174	0.0000	0.0000	-0.0131	-0.0010
85	19564	-0.0145	-0.0164	-0.0095	-0.0051	-0.0056	-0.0173	0.0000	0.0000	-0.0141	-0.0010
87.5	19502	-0.0145	-0.0164	-0.0095	-0.0051	-0.0057	-0.0174	0.0000	0.0000	-0.0133	-0.0010
90	19442	-0.0145	-0.0164	-0.0096	-0.0052	-0.0058	-0.0173	0.0000	0.0000	-0.0124	-0.0010
92.5	19382	-0.0145	-0.0164	-0.0099	-0.0054	-0.0058	-0.0175	0.0000	0.0000	-0.0132	-0.0010
95	19327	-0.0145	-0.0164	-0.0098	-0.0054	-0.0058	-0.0176	0.0000	0.0000	-0.0139	-0.0010
97.5	19278	-0.0145	-0.0164	-0.0098	-0.0054	-0.0057	-0.0176	0.0000	0.0000	-0.0133	-0.0010
100	19241	-0.0145	-0.0164	-0.0096	-0.0054	-0.0057	-0.0176	0.0000	0.0000	-0.0137	-0.0010
102.5	19270	-0.0145	-0.0164	-0.0095	-0.0054	-0.0058	-0.0176	0.0000	0.0000	-0.0133	-0.0010
105	19637	-0.0145	-0.0164	-0.0095	-0.0054	-0.0056	-0.0176	0.0000	0.0000	-0.0132	-0.0010
107.5	20002	-0.0145	-0.0165	-0.0097	-0.0054	-0.0057	-0.0175	0.0000	0.0000	-0.0130	-0.0010
110	19924	-0.0146	-0.0167	-0.0099	-0.0054	-0.0057	-0.0173	0.0000	0.0000	-0.0126	-0.0010
112.5	19852	-0.0147	-0.0168	-0.0099	-0.0055	-0.0058	-0.0173	0.0000	0.0000	-0.0124	-0.0012
115	19784	-0.0150	-0.0169	-0.0100	-0.0056	-0.0059	-0.0176	0.0000	0.0000	-0.0125	-0.0014
117.5	19717	-0.0150	-0.0170	-0.0101	-0.0056	-0.0060	-0.0175	0.0000	0.0000	-0.0127	-0.0015
120	19654	-0.0149	-0.0171	-0.0102	-0.0057	-0.0061	-0.0175	0.0000	0.0000	-0.0127	-0.0016
122.5	19592	-0.0150	-0.0171	-0.0102	-0.0058	-0.0062	-0.0176	0.0000	0.0000	-0.0125	-0.0016
125	19533	-0.0152	-0.0171	-0.0102	-0.0058	-0.0062	-0.0176	0.0000	0.0000	-0.0125	-0.0017
127.5	19463	-0.0150	-0.0170	-0.0100	-0.0058	-0.0062	-0.0176	0.0000	0.0000	-0.0130	-0.0017
130	19401	-0.0149	-0.0171	-0.0101	-0.0058	-0.0063	-0.0176	0.0000	0.0000	-0.0132	-0.0017
132.5	19351	-0.0149	-0.0171	-0.0102	-0.0058	-0.0062	-0.0176	0.0000	0.0000	-0.0124	-0.0017
135	19299	-0.0149	-0.0171	-0.0102	-0.0058	-0.0062	-0.0176	0.0000	0.0000	-0.0119	-0.0017

Table A.12: Tabulated Results from 11 Nov 2005, Field Load Test #12 (continued)

Test # 12		Notes: -- The wind blew fast during this test. Possibly affected reference frame. -- Linear Pot #3 was determined to be damaged at the outset of these tests -- The data gathered from Linear Pot #4 was discarded due to excessive scatter -- Each Telltale is labeled by the same notation: (LP# (Depth) I/O)									
Date: 11-Nov-05											
Time	Load	Interior Telltales (I)					Perimeter Telltales (O)				
		LP7 (surf) I	LP6 (6") I	LP8 (12") I	LP10 (18") I	LP12 (30") I	LP1 (surf) O	LP4 (6") O	LP3 (12") O	LP9 (18") O	LP2 (30") O
(sec)	(lbs)	(in)	(in)	(in)	(in)	(in)	(in)	(in)	(in)	(in)	(in)
137.5	19254	-0.0149	-0.0170	-0.0100	-0.0058	-0.0063	-0.0176	0.0000	0.0000	-0.0117	-0.0017
140	19202	-0.0149	-0.0170	-0.0100	-0.0058	-0.0063	-0.0176	0.0000	0.0000	-0.0117	-0.0015
142.5	19147	-0.0149	-0.0171	-0.0104	-0.0058	-0.0063	-0.0176	0.0000	0.0000	-0.0111	-0.0017
145	19093	-0.0156	-0.0171	-0.0109	-0.0063	-0.0067	-0.0173	0.0000	0.0000	-0.0123	-0.0021
147.5	19031	-0.0159	-0.0171	-0.0111	-0.0065	-0.0069	-0.0170	0.0000	0.0000	-0.0133	-0.0023
150	18924	-0.0159	-0.0171	-0.0109	-0.0065	-0.0066	-0.0170	0.0000	0.0000	-0.0133	-0.0023
152.5	18777	-0.0159	-0.0171	-0.0109	-0.0065	-0.0064	-0.0169	0.0000	0.0000	-0.0136	-0.0023
155	18601	-0.0159	-0.0171	-0.0109	-0.0064	-0.0062	-0.0169	0.0000	0.0000	-0.0137	-0.0023
157.5	18235	-0.0159	-0.0171	-0.0109	-0.0063	-0.0064	-0.0169	0.0000	0.0000	-0.0132	-0.0023
160	17684	-0.0160	-0.0168	-0.0109	-0.0062	-0.0062	-0.0169	0.0000	0.0000	-0.0136	-0.0023
162.5	15512	-0.0162	-0.0165	-0.0109	-0.0061	-0.0063	-0.0171	0.0000	0.0000	-0.0131	-0.0023
165	12703	-0.0151	-0.0157	-0.0105	-0.0061	-0.0064	-0.0166	0.0000	0.0000	-0.0121	-0.0023
167.5	11166	-0.0149	-0.0151	-0.0099	-0.0061	-0.0064	-0.0155	0.0000	0.0000	-0.0118	-0.0024
170	9879	-0.0144	-0.0143	-0.0095	-0.0061	-0.0063	-0.0138	0.0000	0.0000	-0.0109	-0.0025
172.5	8696	-0.0137	-0.0135	-0.0090	-0.0061	-0.0058	-0.0128	0.0000	0.0000	-0.0114	-0.0026
175	7690	-0.0129	-0.0128	-0.0088	-0.0060	-0.0060	-0.0125	0.0000	0.0000	-0.0111	-0.0024
177.5	6848	-0.0121	-0.0119	-0.0085	-0.0058	-0.0056	-0.0119	0.0000	0.0000	-0.0111	-0.0026
180	6152	-0.0114	-0.0109	-0.0080	-0.0057	-0.0045	-0.0116	0.0000	0.0000	-0.0113	-0.0025
182.5	5546	-0.0109	-0.0103	-0.0078	-0.0055	-0.0041	-0.0114	0.0000	0.0000	-0.0107	-0.0024
185	4998	-0.0106	-0.0097	-0.0076	-0.0053	-0.0037	-0.0107	0.0000	0.0000	-0.0080	-0.0024
187.5	4365	-0.0099	-0.0092	-0.0072	-0.0050	-0.0037	-0.0103	0.0000	0.0000	-0.0076	-0.0025
190	3843	-0.0094	-0.0086	-0.0069	-0.0048	-0.0037	-0.0100	0.0000	0.0000	-0.0077	-0.0026
192.5	3351	-0.0087	-0.0079	-0.0063	-0.0050	-0.0034	-0.0094	0.0000	0.0000	-0.0083	-0.0026
195	2824	-0.0081	-0.0072	-0.0061	-0.0047	-0.0029	-0.0085	0.0000	0.0000	-0.0072	-0.0026
197.5	2632	-0.0077	-0.0068	-0.0058	-0.0045	-0.0029	-0.0081	0.0000	0.0000	-0.0065	-0.0027
200	1527	-0.0059	-0.0051	-0.0049	-0.0038	-0.0025	-0.0062	0.0000	0.0000	-0.0064	-0.0027
202.5	0	-0.0027	-0.0020	-0.0031	-0.0024	-0.0013	-0.0028	0.0000	0.0000	-0.0047	-0.0026
205	1	-0.0027	-0.0018	-0.0030	-0.0024	-0.0014	-0.0025	0.0000	0.0000	-0.0043	-0.0023
207.5	4	-0.0027	-0.0018	-0.0030	-0.0024	-0.0014	-0.0025	0.0000	0.0000	-0.0044	-0.0023
210	0	-0.0027	-0.0018	-0.0030	-0.0023	-0.0014	-0.0025	0.0000	0.0000	-0.0045	-0.0023
212.5	0	-0.0027	-0.0016	-0.0030	-0.0023	-0.0014	-0.0024	0.0000	0.0000	-0.0045	-0.0023
215	0	-0.0027	-0.0015	-0.0030	-0.0023	-0.0012	-0.0023	0.0000	0.0000	-0.0047	-0.0023
217.5	0	-0.0026	-0.0015	-0.0030	-0.0022	-0.0013	-0.0023	0.0000	0.0000	-0.0049	-0.0023
220	0	-0.0024	-0.0015	-0.0030	-0.0020	-0.0013	-0.0022	0.0000	0.0000	-0.0051	-0.0023
222.5	0	-0.0026	-0.0015	-0.0030	-0.0020	-0.0011	-0.0022	0.0000	0.0000	-0.0053	-0.0023
225	0	-0.0024	-0.0015	-0.0030	-0.0020	-0.0010	-0.0022	0.0000	0.0000	-0.0057	-0.0023
227.5	0	-0.0024	-0.0015	-0.0030	-0.0020	-0.0011	-0.0022	0.0000	0.0000	-0.0059	-0.0023
230	0	-0.0024	-0.0015	-0.0030	-0.0020	-0.0010	-0.0022	0.0000	0.0000	-0.0057	-0.0023
232.5	0	-0.0024	-0.0015	-0.0030	-0.0020	-0.0011	-0.0022	0.0000	0.0000	-0.0055	-0.0023
235	1	-0.0024	-0.0015	-0.0029	-0.0020	-0.0014	-0.0022	0.0000	0.0000	-0.0054	-0.0023
237.5	1	-0.0024	-0.0015	-0.0028	-0.0019	-0.0014	-0.0022	0.0000	0.0000	-0.0050	-0.0023
240	0	-0.0024	-0.0015	-0.0029	-0.0020	-0.0016	-0.0021	0.0000	0.0000	-0.0047	-0.0023
242.5	3	-0.0024	-0.0015	-0.0027	-0.0020	-0.0015	-0.0020	0.0000	0.0000	-0.0047	-0.0024
245	5	-0.0024	-0.0014	-0.0027	-0.0020	-0.0016	-0.0020	0.0000	0.0000	-0.0049	-0.0025
247.5	4	-0.0024	-0.0014	-0.0027	-0.0019	-0.0015	-0.0022	0.0000	0.0000	-0.0050	-0.0023
250	8	-0.0024	-0.0013	-0.0027	-0.0020	-0.0016	-0.0019	0.0000	0.0000	-0.0045	-0.0023
252.5	8	-0.0024	-0.0011	-0.0027	-0.0020	-0.0016	-0.0019	0.0000	0.0000	-0.0049	-0.0023
255	9	-0.0023	-0.0011	-0.0027	-0.0020	-0.0016	-0.0018	0.0000	0.0000	-0.0050	-0.0023

Table A.13: Tabulated Results from 11 Nov 2005, Field Load Test #13

Test # 13		Notes:									
Date: 11-Nov-05		-- Linear Pot #3 was determined to be damaged at the outset of these tests -- The data gathered from Linear Pot #4 was discarded due to excessive scatter -- Each Telltale is labeled by the same notation: (LP# (Depth) I/O)									
Time (sec)	Load (lbs)	Interior Telltales (I)					Perimeter Telltales (O)				
		LP7 (surf) I	LP6 (6") I	LP8 (12") I	LP10 (18") I	LP12 (30") I	LP1 (surf) O	LP4 (6") O	LP3 (12") O	LP9 (18") O	LP2 (30") O
		(in)	(in)	(in)	(in)	(in)	(in)	(in)	(in)	(in)	(in)
MAX	19928	-0.0159	-0.0168	-0.0113	-0.0062	-0.0061	-0.0175	0.0000	0.0000	-0.0093	-0.0030
0	1	0.0000	0.0000	0.0000	-0.0001	0.0000	0.0000	0.0000	0.0000	0.0000	0.0000
2.5	0	0.0000	0.0000	0.0000	0.0000	0.0000	0.0000	0.0000	0.0000	0.0000	0.0000
5	0	0.0000	0.0000	0.0000	-0.0001	0.0000	0.0000	0.0000	0.0000	0.0000	0.0000
7.5	0	0.0000	0.0000	0.0000	-0.0001	0.0000	0.0000	0.0000	0.0000	0.0000	0.0000
10	-1	0.0000	0.0000	0.0000	-0.0001	0.0000	0.0000	0.0000	0.0000	0.0000	0.0000
12.5	-1	0.0000	0.0000	0.0000	-0.0001	0.0000	0.0000	0.0000	0.0000	0.0000	0.0000
15	0	0.0000	0.0000	0.0000	0.0000	0.0000	0.0000	0.0000	0.0000	0.0000	-0.0001
17.5	72	0.0000	0.0000	0.0000	0.0001	0.0000	0.0000	0.0000	0.0000	-0.0001	0.0000
20	1010	0.0000	-0.0002	0.0000	0.0000	-0.0001	-0.0006	0.0000	0.0000	0.0003	0.0000
22.5	2207	-0.0001	-0.0006	0.0000	0.0000	0.0002	-0.0014	0.0000	0.0000	0.0009	0.0002
25	3537	-0.0005	-0.0016	-0.0001	0.0001	0.0002	-0.0029	0.0000	0.0000	0.0020	0.0006
27.5	4817	-0.0022	-0.0026	-0.0011	0.0000	0.0003	-0.0040	0.0000	0.0000	0.0023	0.0007
30	6084	-0.0031	-0.0035	-0.0017	-0.0001	0.0002	-0.0052	0.0000	0.0000	0.0012	0.0007
32.5	7492	-0.0042	-0.0047	-0.0023	-0.0001	0.0000	-0.0067	0.0000	0.0000	-0.0003	0.0007
35	8884	-0.0051	-0.0061	-0.0029	-0.0001	0.0001	-0.0074	0.0000	0.0000	-0.0001	0.0007
37.5	10179	-0.0062	-0.0073	-0.0037	-0.0001	-0.0004	-0.0086	0.0000	0.0000	-0.0012	0.0007
40	11390	-0.0073	-0.0086	-0.0042	-0.0004	-0.0013	-0.0090	0.0000	0.0000	-0.0014	0.0006
42.5	12520	-0.0079	-0.0096	-0.0045	-0.0012	-0.0017	-0.0098	0.0000	0.0000	-0.0042	0.0006
45	13575	-0.0086	-0.0103	-0.0048	-0.0015	-0.0018	-0.0103	0.0000	0.0000	-0.0055	0.0006
47.5	14558	-0.0093	-0.0111	-0.0054	-0.0019	-0.0024	-0.0109	0.0000	0.0000	-0.0053	0.0006
50	15479	-0.0100	-0.0118	-0.0058	-0.0024	-0.0025	-0.0115	0.0000	0.0000	-0.0051	0.0005
52.5	16339	-0.0106	-0.0125	-0.0062	-0.0027	-0.0033	-0.0119	0.0000	0.0000	-0.0055	0.0004
55	17159	-0.0113	-0.0133	-0.0067	-0.0029	-0.0042	-0.0129	0.0000	0.0000	-0.0061	0.0003
57.5	17939	-0.0122	-0.0139	-0.0071	-0.0033	-0.0043	-0.0145	0.0000	0.0000	-0.0063	0.0003
60	18672	-0.0125	-0.0144	-0.0075	-0.0036	-0.0044	-0.0154	0.0000	0.0000	-0.0074	0.0003
62.5	19362	-0.0128	-0.0148	-0.0079	-0.0039	-0.0050	-0.0159	0.0000	0.0000	-0.0070	0.0003
65	19892	-0.0129	-0.0153	-0.0082	-0.0042	-0.0051	-0.0160	0.0000	0.0000	-0.0079	0.0005
67.5	19831	-0.0129	-0.0153	-0.0084	-0.0044	-0.0048	-0.0160	0.0000	0.0000	-0.0084	0.0005
70	19735	-0.0129	-0.0153	-0.0085	-0.0045	-0.0050	-0.0159	0.0000	0.0000	-0.0083	0.0003
72.5	19650	-0.0130	-0.0153	-0.0085	-0.0045	-0.0049	-0.0158	0.0000	0.0000	-0.0082	0.0003
75	19570	-0.0130	-0.0153	-0.0085	-0.0044	-0.0049	-0.0158	0.0000	0.0000	-0.0081	0.0003
77.5	19496	-0.0132	-0.0153	-0.0085	-0.0042	-0.0048	-0.0159	0.0000	0.0000	-0.0074	0.0003
80	19422	-0.0132	-0.0153	-0.0085	-0.0042	-0.0048	-0.0158	0.0000	0.0000	-0.0079	0.0003
82.5	19346	-0.0132	-0.0153	-0.0085	-0.0042	-0.0047	-0.0158	0.0000	0.0000	-0.0081	0.0003
85	19279	-0.0132	-0.0153	-0.0085	-0.0042	-0.0045	-0.0156	0.0000	0.0000	-0.0080	0.0003
87.5	19215	-0.0132	-0.0153	-0.0085	-0.0042	-0.0045	-0.0156	0.0000	0.0000	-0.0083	0.0003
90	19152	-0.0131	-0.0153	-0.0085	-0.0042	-0.0045	-0.0156	0.0000	0.0000	-0.0086	0.0003
92.5	19088	-0.0132	-0.0153	-0.0084	-0.0042	-0.0045	-0.0156	0.0000	0.0000	-0.0086	0.0003
95	19027	-0.0132	-0.0153	-0.0083	-0.0042	-0.0045	-0.0156	0.0000	0.0000	-0.0085	0.0003
97.5	18968	-0.0132	-0.0153	-0.0083	-0.0042	-0.0046	-0.0156	0.0000	0.0000	-0.0090	0.0003
100	18926	-0.0131	-0.0153	-0.0082	-0.0042	-0.0046	-0.0156	0.0000	0.0000	-0.0093	0.0003
102.5	18884	-0.0131	-0.0153	-0.0082	-0.0042	-0.0049	-0.0156	0.0000	0.0000	-0.0085	0.0003
105	18865	-0.0130	-0.0153	-0.0082	-0.0042	-0.0048	-0.0158	0.0000	0.0000	-0.0082	0.0004
107.5	18882	-0.0132	-0.0153	-0.0082	-0.0042	-0.0048	-0.0157	0.0000	0.0000	-0.0086	0.0003
110	18936	-0.0132	-0.0153	-0.0082	-0.0042	-0.0048	-0.0157	0.0000	0.0000	-0.0082	0.0003
112.5	19418	-0.0132	-0.0153	-0.0082	-0.0042	-0.0048	-0.0159	0.0000	0.0000	-0.0083	0.0003
115	19912	-0.0135	-0.0156	-0.0084	-0.0042	-0.0047	-0.0157	0.0000	0.0000	-0.0082	0.0003
117.5	19928	-0.0136	-0.0157	-0.0086	-0.0044	-0.0048	-0.0156	0.0000	0.0000	-0.0082	0.0003
120	19849	-0.0135	-0.0157	-0.0085	-0.0045	-0.0048	-0.0156	0.0000	0.0000	-0.0082	0.0003
122.5	19781	-0.0138	-0.0157	-0.0088	-0.0045	-0.0048	-0.0157	0.0000	0.0000	-0.0088	0.0003
125	19713	-0.0141	-0.0157	-0.0092	-0.0049	-0.0049	-0.0158	0.0000	0.0000	-0.0090	0.0001
127.5	19648	-0.0142	-0.0157	-0.0096	-0.0052	-0.0050	-0.0156	0.0000	0.0000	-0.0086	-0.0002
130	19581	-0.0153	-0.0163	-0.0110	-0.0057	-0.0057	-0.0168	0.0000	0.0000	-0.0076	-0.0021
132.5	19519	-0.0156	-0.0164	-0.0113	-0.0062	-0.0058	-0.0175	0.0000	0.0000	-0.0077	-0.0027
135	19455	-0.0156	-0.0164	-0.0113	-0.0062	-0.0057	-0.0175	0.0000	0.0000	-0.0083	-0.0027



Table A.13: Tabulated Results from 11 Nov 2005, Field Load Test #13 (continued)

Test # 13		Notes: -- Linear Pot #3 was determined to be damaged at the outset of these tests -- The data gathered from Linear Pot #4 was discarded due to excessive scatter -- Each Telltale is labeled by the same notation: (LP# (Depth) I/O)									
Date: 11-Nov-05		Interior Telltales (I)					Perimeter Telltales (O)				
Time	Load	LP7 (surf) I	LP6 (6") I	LP8 (12") I	LP10 (18") I	LP12 (30") I	LP1 (surf) O	LP4 (6") O	LP3 (12") O	LP9 (18") O	LP2 (30") O
(sec)	(lbs)	(in)	(in)	(in)	(in)	(in)	(in)	(in)	(in)	(in)	(in)
137.5	19392	-0.0157	-0.0164	-0.0113	-0.0062	-0.0054	-0.0175	0.0000	0.0000	-0.0087	-0.0027
140	19337	-0.0157	-0.0165	-0.0113	-0.0062	-0.0052	-0.0175	0.0000	0.0000	-0.0080	-0.0027
142.5	19276	-0.0158	-0.0164	-0.0110	-0.0062	-0.0055	-0.0169	0.0000	0.0000	-0.0064	-0.0027
145	19221	-0.0159	-0.0167	-0.0109	-0.0062	-0.0060	-0.0172	0.0000	0.0000	-0.0069	-0.0027
147.5	19142	-0.0159	-0.0168	-0.0109	-0.0062	-0.0061	-0.0174	0.0000	0.0000	-0.0072	-0.0028
150	18996	-0.0159	-0.0168	-0.0109	-0.0062	-0.0060	-0.0173	0.0000	0.0000	-0.0077	-0.0030
152.5	18834	-0.0159	-0.0168	-0.0109	-0.0062	-0.0058	-0.0171	0.0000	0.0000	-0.0071	-0.0030
155	18636	-0.0159	-0.0168	-0.0109	-0.0062	-0.0057	-0.0168	0.0000	0.0000	-0.0082	-0.0030
157.5	17649	-0.0159	-0.0168	-0.0109	-0.0062	-0.0058	-0.0167	0.0000	0.0000	-0.0062	-0.0030
160	15615	-0.0155	-0.0162	-0.0107	-0.0062	-0.0056	-0.0163	0.0000	0.0000	-0.0073	-0.0030
162.5	13800	-0.0150	-0.0157	-0.0102	-0.0062	-0.0059	-0.0155	0.0000	0.0000	-0.0073	-0.0030
165	12294	-0.0142	-0.0150	-0.0096	-0.0062	-0.0058	-0.0158	0.0000	0.0000	-0.0069	-0.0030
167.5	11025	-0.0137	-0.0141	-0.0091	-0.0059	-0.0056	-0.0152	0.0000	0.0000	-0.0070	-0.0025
170	9940	-0.0130	-0.0132	-0.0086	-0.0059	-0.0054	-0.0145	0.0000	0.0000	-0.0062	-0.0023
172.5	9000	-0.0128	-0.0124	-0.0082	-0.0059	-0.0048	-0.0135	0.0000	0.0000	-0.0066	-0.0023
175	8000	-0.0126	-0.0116	-0.0079	-0.0058	-0.0052	-0.0122	0.0000	0.0000	-0.0055	-0.0024
177.5	6382	-0.0113	-0.0107	-0.0074	-0.0054	-0.0049	-0.0111	0.0000	0.0000	-0.0059	-0.0024
180	5040	-0.0098	-0.0094	-0.0067	-0.0050	-0.0041	-0.0102	0.0000	0.0000	-0.0054	-0.0025
182.5	4113	-0.0085	-0.0082	-0.0058	-0.0046	-0.0032	-0.0091	0.0000	0.0000	-0.0047	-0.0023
185	3265	-0.0077	-0.0068	-0.0052	-0.0043	-0.0025	-0.0085	0.0000	0.0000	-0.0032	-0.0023
187.5	2680	-0.0069	-0.0057	-0.0047	-0.0038	-0.0018	-0.0080	0.0000	0.0000	-0.0016	-0.0023
190	1737	-0.0054	-0.0043	-0.0038	-0.0032	-0.0012	-0.0063	0.0000	0.0000	-0.0014	-0.0022
192.5	0	-0.0017	-0.0015	-0.0015	-0.0014	-0.0003	-0.0025	0.0000	0.0000	-0.0004	-0.0018
195	-1	-0.0014	-0.0011	-0.0012	-0.0011	-0.0002	-0.0021	0.0000	0.0000	-0.0004	-0.0014
197.5	0	-0.0014	-0.0011	-0.0013	-0.0011	0.0000	-0.0018	0.0000	0.0000	-0.0007	-0.0013
200	0	-0.0011	-0.0009	-0.0011	-0.0010	-0.0001	-0.0016	0.0000	0.0000	-0.0001	-0.0012
202.5	0	-0.0007	-0.0007	-0.0009	-0.0008	-0.0001	-0.0014	0.0000	0.0000	0.0000	-0.0009
205	0	-0.0008	-0.0007	-0.0007	-0.0004	0.0000	-0.0009	0.0000	0.0000	0.0008	-0.0007
207.5	0	-0.0005	-0.0004	-0.0006	-0.0003	0.0001	-0.0006	0.0000	0.0000	0.0015	-0.0003
210	0	-0.0003	-0.0002	-0.0003	-0.0001	0.0001	-0.0004	0.0000	0.0000	0.0014	0.0000
212.5	0	-0.0003	0.0000	-0.0001	0.0000	0.0001	-0.0002	0.0000	0.0000	0.0016	0.0002
215	0	0.0000	0.0000	0.0002	0.0002	-0.0001	0.0002	0.0000	0.0000	0.0017	0.0003
217.5	0	0.0000	0.0000	0.0003	0.0002	-0.0001	0.0003	0.0000	0.0000	0.0012	0.0003
220	0	0.0001	0.0000	0.0003	0.0004	0.0001	0.0007	0.0000	0.0000	0.0014	0.0004
222.5	0	0.0002	0.0000	0.0004	0.0006	0.0002	0.0012	0.0000	0.0000	0.0019	0.0007
225	0	0.0003	0.0000	0.0006	0.0006	0.0000	0.0011	0.0000	0.0000	0.0016	0.0006
227.5	0	0.0003	0.0000	0.0007	0.0006	0.0001	0.0011	0.0000	0.0000	0.0019	0.0007
230	0	0.0003	0.0000	0.0007	0.0006	0.0004	0.0012	0.0000	0.0000	0.0016	0.0004
232.5	0	0.0003	0.0000	0.0008	0.0006	0.0005	0.0010	0.0000	0.0000	0.0016	0.0003
235	0	0.0003	0.0000	0.0007	0.0006	0.0003	0.0010	0.0000	0.0000	0.0011	0.0003
237.5	-1	0.0003	0.0000	0.0009	0.0006	0.0002	0.0009	0.0000	0.0000	0.0020	0.0004
240	0	0.0006	0.0000	0.0010	0.0006	0.0004	0.0009	0.0000	0.0000	0.0015	0.0006
242.5	0	0.0006	0.0000	0.0010	0.0008	0.0005	0.0011	0.0000	0.0000	0.0018	0.0007
245	0	0.0007	0.0000	0.0010	0.0009	0.0004	0.0011	0.0000	0.0000	0.0013	0.0007
247.5	0	0.0007	0.0000	0.0010	0.0009	0.0005	0.0011	0.0000	0.0000	0.0012	0.0007
250	0	0.0007	0.0000	0.0010	0.0009	0.0004	0.0011	0.0000	0.0000	0.0010	0.0007
252.5	0	0.0007	0.0000	0.0010	0.0009	0.0004	0.0011	0.0000	0.0000	0.0009	0.0007
255	0	0.0007	0.0000	0.0010	0.0009	0.0004	0.0012	0.0000	0.0000	0.0020	0.0007

Table A.14: Tabulated Results from 11 Nov 2005, Field Load Test #14

Test # 14		Notes:									
Date: 11-Nov-05		-- Linear Pot #3 was determined to be damaged at the outset of these tests -- The data gathered from Linear Pot #4 was discarded due to excessive scatter -- Each Telltale is labeled by the same notation: (LP# (Depth) I/O)									
Time (sec)	Load (lbs)	Interior Telltales (I)					Perimeter Telltales (O)				
		LP7 (surf) I	LP6 (6") I	LP8 (12") I	LP10 (18") I	LP12 (30") I	LP1 (surf) O	LP4 (6") O	LP3 (12") O	LP9 (18") O	LP2 (30") O
		(in)	(in)	(in)	(in)	(in)	(in)	(in)	(in)	(in)	(in)
MAX	19949	-0.0164	-0.0168	-0.0119	-0.0069	-0.0058	-0.0171	0.0000	0.0000	-0.0123	-0.0032
0	-6	0.0001	0.0001	0.0001	0.0001	0.0001	0.0001	0.0000	0.0000	0.0001	0.0001
2.5	-2	0.0001	0.0001	0.0001	0.0002	0.0002	0.0000	0.0000	0.0000	0.0002	0.0002
5	-2	0.0001	0.0001	0.0001	0.0002	0.0001	0.0001	0.0000	0.0000	0.0002	0.0002
7.5	0	0.0001	0.0001	0.0001	0.0001	-0.0001	0.0001	0.0000	0.0000	0.0001	0.0001
10	0	0.0002	0.0002	0.0002	0.0002	0.0001	0.0000	0.0000	0.0000	0.0002	0.0002
12.5	4	0.0001	0.0001	0.0001	0.0001	-0.0002	-0.0002	0.0000	0.0000	0.0001	-0.0001
15	27	0.0001	0.0001	0.0001	0.0002	-0.0001	-0.0002	0.0000	0.0000	0.0001	-0.0001
17.5	563	0.0000	0.0000	0.0000	0.0000	0.0000	-0.0001	0.0000	0.0000	0.0000	0.0000
20	1668	-0.0001	-0.0004	-0.0003	0.0001	0.0002	0.0000	0.0000	0.0000	-0.0006	0.0000
22.5	2845	-0.0014	-0.0015	-0.0008	0.0001	0.0000	-0.0016	0.0000	0.0000	-0.0015	0.0000
25	4679	-0.0028	-0.0029	-0.0017	0.0001	0.0000	-0.0038	0.0000	0.0000	-0.0026	0.0001
27.5	6514	-0.0050	-0.0048	-0.0028	0.0000	-0.0001	-0.0057	0.0000	0.0000	-0.0032	-0.0001
30	8198	-0.0061	-0.0064	-0.0037	-0.0006	-0.0004	-0.0072	0.0000	0.0000	-0.0047	0.0000
32.5	9747	-0.0074	-0.0078	-0.0044	-0.0011	-0.0010	-0.0084	0.0000	0.0000	-0.0049	-0.0001
35	11169	-0.0087	-0.0094	-0.0053	-0.0014	-0.0018	-0.0092	0.0000	0.0000	-0.0075	-0.0003
37.5	12484	-0.0096	-0.0106	-0.0058	-0.0017	-0.0026	-0.0101	0.0000	0.0000	-0.0074	-0.0002
40	13697	-0.0105	-0.0115	-0.0065	-0.0026	-0.0028	-0.0110	0.0000	0.0000	-0.0085	-0.0003
42.5	14815	-0.0120	-0.0125	-0.0076	-0.0034	-0.0038	-0.0120	0.0000	0.0000	-0.0092	-0.0007
45	15847	-0.0133	-0.0135	-0.0085	-0.0042	-0.0049	-0.0134	0.0000	0.0000	-0.0099	-0.0010
47.5	16814	-0.0143	-0.0145	-0.0093	-0.0047	-0.0056	-0.0152	0.0000	0.0000	-0.0109	-0.0013
50	17724	-0.0145	-0.0147	-0.0095	-0.0051	-0.0054	-0.0158	0.0000	0.0000	-0.0112	-0.0013
52.5	18572	-0.0149	-0.0151	-0.0101	-0.0056	-0.0052	-0.0165	0.0000	0.0000	-0.0110	-0.0015
55	19370	-0.0153	-0.0153	-0.0102	-0.0056	-0.0051	-0.0163	0.0000	0.0000	-0.0093	-0.0014
57.5	19949	-0.0158	-0.0158	-0.0106	-0.0060	-0.0051	-0.0162	0.0000	0.0000	-0.0103	-0.0016
60	19874	-0.0159	-0.0162	-0.0110	-0.0064	-0.0058	-0.0163	0.0000	0.0000	-0.0114	-0.0020
62.5	19781	-0.0158	-0.0165	-0.0111	-0.0064	-0.0058	-0.0164	0.0000	0.0000	-0.0123	-0.0020
65	19690	-0.0157	-0.0166	-0.0111	-0.0063	-0.0058	-0.0166	0.0000	0.0000	-0.0115	-0.0021
67.5	19618	-0.0159	-0.0166	-0.0111	-0.0064	-0.0057	-0.0167	0.0000	0.0000	-0.0106	-0.0023
70	19557	-0.0158	-0.0166	-0.0111	-0.0063	-0.0056	-0.0166	0.0000	0.0000	-0.0103	-0.0023
72.5	19501	-0.0159	-0.0166	-0.0111	-0.0064	-0.0056	-0.0166	0.0000	0.0000	-0.0109	-0.0023
75	19446	-0.0159	-0.0167	-0.0112	-0.0064	-0.0056	-0.0167	0.0000	0.0000	-0.0106	-0.0024
77.5	19397	-0.0159	-0.0166	-0.0111	-0.0063	-0.0053	-0.0166	0.0000	0.0000	-0.0109	-0.0023
80	19351	-0.0159	-0.0166	-0.0111	-0.0064	-0.0052	-0.0167	0.0000	0.0000	-0.0114	-0.0023
82.5	19305	-0.0159	-0.0166	-0.0111	-0.0064	-0.0052	-0.0167	0.0000	0.0000	-0.0108	-0.0023
85	19260	-0.0159	-0.0166	-0.0111	-0.0064	-0.0052	-0.0167	0.0000	0.0000	-0.0117	-0.0023
87.5	19222	-0.0159	-0.0166	-0.0111	-0.0063	-0.0052	-0.0166	0.0000	0.0000	-0.0123	-0.0023
90	19182	-0.0159	-0.0167	-0.0111	-0.0064	-0.0052	-0.0167	0.0000	0.0000	-0.0111	-0.0023
92.5	19159	-0.0159	-0.0167	-0.0112	-0.0064	-0.0053	-0.0167	0.0000	0.0000	-0.0114	-0.0024
95	19192	-0.0159	-0.0166	-0.0111	-0.0064	-0.0052	-0.0166	0.0000	0.0000	-0.0116	-0.0023
97.5	19398	-0.0159	-0.0167	-0.0112	-0.0064	-0.0053	-0.0167	0.0000	0.0000	-0.0117	-0.0024
100	19781	-0.0159	-0.0167	-0.0111	-0.0064	-0.0052	-0.0168	0.0000	0.0000	-0.0101	-0.0024
102.5	19851	-0.0159	-0.0167	-0.0111	-0.0064	-0.0052	-0.0168	0.0000	0.0000	-0.0088	-0.0024
105	19765	-0.0159	-0.0167	-0.0111	-0.0064	-0.0054	-0.0168	0.0000	0.0000	-0.0101	-0.0023
107.5	19693	-0.0159	-0.0166	-0.0111	-0.0064	-0.0053	-0.0167	0.0000	0.0000	-0.0092	-0.0023
110	19621	-0.0159	-0.0166	-0.0111	-0.0064	-0.0052	-0.0166	0.0000	0.0000	-0.0099	-0.0023
112.5	19553	-0.0159	-0.0167	-0.0112	-0.0065	-0.0053	-0.0168	0.0000	0.0000	-0.0100	-0.0024
115	19487	-0.0159	-0.0167	-0.0111	-0.0064	-0.0053	-0.0164	0.0000	0.0000	-0.0095	-0.0024
117.5	19422	-0.0159	-0.0167	-0.0112	-0.0064	-0.0053	-0.0165	0.0000	0.0000	-0.0102	-0.0024
120	19359	-0.0159	-0.0167	-0.0111	-0.0064	-0.0052	-0.0165	0.0000	0.0000	-0.0104	-0.0024
122.5	19300	-0.0160	-0.0167	-0.0113	-0.0064	-0.0053	-0.0166	0.0000	0.0000	-0.0091	-0.0025
125	19244	-0.0163	-0.0167	-0.0115	-0.0065	-0.0058	-0.0168	0.0000	0.0000	-0.0105	-0.0027
127.5	19183	-0.0163	-0.0167	-0.0115	-0.0065	-0.0058	-0.0170	0.0000	0.0000	-0.0101	-0.0027
130	19124	-0.0162	-0.0167	-0.0115	-0.0065	-0.0055	-0.0170	0.0000	0.0000	-0.0103	-0.0027
132.5	19063	-0.0163	-0.0167	-0.0115	-0.0066	-0.0055	-0.0170	0.0000	0.0000	-0.0110	-0.0028
135	19005	-0.0163	-0.0167	-0.0115	-0.0065	-0.0057	-0.0169	0.0000	0.0000	-0.0104	-0.0027

Table A.14: Tabulated Results from 11 Nov 2005, Field Load Test #14 (continued)

Test # 14		Notes:									
Date: 11-Nov-05		-- Linear Pot #3 was determined to be damaged at the outset of these tests -- The data gathered from Linear Pot #4 was discarded due to excessive scatter -- Each Telltale is labeled by the same notation: (LP# (Depth) I/O)									
Time	Load	Interior Telltales (I)					Perimeter Telltales (O)				
		LP7 (surf) I	LP6 (6") I	LP8 (12") I	LP10 (18") I	LP12 (30") I	LP1 (surf) O	LP4 (6") O	LP3 (12") O	LP9 (18") O	LP2 (30") O
(sec)	(lbs)	(in)	(in)	(in)	(in)	(in)	(in)	(in)	(in)	(in)	(in)
137.5	18950	-0.0162	-0.0166	-0.0116	-0.0065	-0.0056	-0.0168	0.0000	0.0000	-0.0100	-0.0026
140	18894	-0.0162	-0.0167	-0.0118	-0.0067	-0.0054	-0.0169	0.0000	0.0000	-0.0100	-0.0027
142.5	18827	-0.0163	-0.0167	-0.0118	-0.0068	-0.0055	-0.0171	0.0000	0.0000	-0.0103	-0.0027
145	18700	-0.0163	-0.0168	-0.0119	-0.0069	-0.0055	-0.0171	0.0000	0.0000	-0.0108	-0.0029
147.5	18534	-0.0163	-0.0167	-0.0119	-0.0068	-0.0053	-0.0169	0.0000	0.0000	-0.0110	-0.0030
150	18380	-0.0164	-0.0168	-0.0119	-0.0068	-0.0053	-0.0169	0.0000	0.0000	-0.0106	-0.0030
152.5	18203	-0.0163	-0.0168	-0.0118	-0.0068	-0.0053	-0.0170	0.0000	0.0000	-0.0105	-0.0031
155	17842	-0.0163	-0.0168	-0.0117	-0.0069	-0.0054	-0.0167	0.0000	0.0000	-0.0114	-0.0032
157.5	16084	-0.0160	-0.0164	-0.0114	-0.0066	-0.0052	-0.0161	0.0000	0.0000	-0.0096	-0.0029
160	14403	-0.0159	-0.0159	-0.0113	-0.0066	-0.0053	-0.0163	0.0000	0.0000	-0.0099	-0.0030
162.5	12831	-0.0159	-0.0152	-0.0109	-0.0067	-0.0056	-0.0167	0.0000	0.0000	-0.0096	-0.0030
165	11347	-0.0157	-0.0147	-0.0104	-0.0068	-0.0058	-0.0161	0.0000	0.0000	-0.0088	-0.0030
167.5	10025	-0.0147	-0.0138	-0.0098	-0.0066	-0.0053	-0.0151	0.0000	0.0000	-0.0091	-0.0030
170	8866	-0.0142	-0.0127	-0.0094	-0.0063	-0.0047	-0.0128	0.0000	0.0000	-0.0093	-0.0030
172.5	7780	-0.0137	-0.0116	-0.0091	-0.0061	-0.0041	-0.0119	0.0000	0.0000	-0.0096	-0.0030
175	6604	-0.0125	-0.0107	-0.0087	-0.0058	-0.0033	-0.0116	0.0000	0.0000	-0.0071	-0.0030
177.5	5350	-0.0111	-0.0097	-0.0078	-0.0055	-0.0028	-0.0106	0.0000	0.0000	-0.0079	-0.0028
180	4331	-0.0099	-0.0085	-0.0070	-0.0051	-0.0026	-0.0094	0.0000	0.0000	-0.0076	-0.0027
182.5	3579	-0.0091	-0.0074	-0.0064	-0.0043	-0.0018	-0.0090	0.0000	0.0000	-0.0068	-0.0026
185	2972	-0.0085	-0.0065	-0.0059	-0.0040	-0.0017	-0.0086	0.0000	0.0000	-0.0055	-0.0026
187.5	2627	-0.0078	-0.0056	-0.0056	-0.0040	-0.0013	-0.0076	0.0000	0.0000	-0.0037	-0.0026
190	1028	-0.0050	-0.0033	-0.0038	-0.0026	-0.0005	-0.0045	0.0000	0.0000	-0.0034	-0.0022
192.5	-7	-0.0024	-0.0010	-0.0023	-0.0013	-0.0002	-0.0018	0.0000	0.0000	-0.0032	-0.0017
195	-7	-0.0023	-0.0007	-0.0021	-0.0013	-0.0003	-0.0017	0.0000	0.0000	-0.0023	-0.0017
197.5	-8	-0.0022	-0.0006	-0.0021	-0.0010	-0.0004	-0.0017	0.0000	0.0000	-0.0021	-0.0017
200	-8	-0.0023	-0.0006	-0.0019	-0.0009	-0.0003	-0.0017	0.0000	0.0000	-0.0029	-0.0016
202.5	-2	-0.0022	-0.0007	-0.0020	-0.0010	-0.0003	-0.0017	0.0000	0.0000	-0.0032	-0.0017
205	-1	-0.0021	-0.0007	-0.0019	-0.0011	-0.0003	-0.0016	0.0000	0.0000	-0.0037	-0.0016
207.5	-4	-0.0023	-0.0007	-0.0020	-0.0011	-0.0005	-0.0015	0.0000	0.0000	-0.0039	-0.0017
210	-2	-0.0021	-0.0007	-0.0020	-0.0011	-0.0005	-0.0015	0.0000	0.0000	-0.0038	-0.0015
212.5	-2	-0.0021	-0.0007	-0.0020	-0.0011	-0.0005	-0.0015	0.0000	0.0000	-0.0046	-0.0014
215	-1	-0.0020	-0.0007	-0.0019	-0.0010	-0.0004	-0.0014	0.0000	0.0000	-0.0048	-0.0014
217.5	0	-0.0020	-0.0007	-0.0019	-0.0010	-0.0004	-0.0014	0.0000	0.0000	-0.0050	-0.0014
220	0	-0.0021	-0.0007	-0.0020	-0.0010	-0.0005	-0.0014	0.0000	0.0000	-0.0034	-0.0014
222.5	-1	-0.0021	-0.0006	-0.0020	-0.0011	-0.0006	-0.0015	0.0000	0.0000	-0.0033	-0.0015
225	-4	-0.0021	-0.0004	-0.0019	-0.0011	-0.0003	-0.0012	0.0000	0.0000	-0.0035	-0.0015
227.5	-2	-0.0019	-0.0003	-0.0017	-0.0009	0.0002	-0.0011	0.0000	0.0000	-0.0024	-0.0014
230	0	-0.0017	-0.0003	-0.0015	-0.0006	0.0001	-0.0009	0.0000	0.0000	-0.0021	-0.0013
232.5	0	-0.0017	-0.0003	-0.0012	-0.0006	0.0001	-0.0009	0.0000	0.0000	-0.0013	-0.0011
235	-1	-0.0017	-0.0003	-0.0012	-0.0006	0.0000	-0.0008	0.0000	0.0000	-0.0022	-0.0010
237.5	-1	-0.0016	-0.0003	-0.0012	-0.0005	0.0002	-0.0007	0.0000	0.0000	-0.0031	-0.0010
240	0	-0.0013	-0.0003	-0.0009	-0.0003	0.0002	-0.0005	0.0000	0.0000	-0.0037	-0.0010
242.5	-3	-0.0015	-0.0003	-0.0010	-0.0004	0.0002	-0.0005	0.0000	0.0000	-0.0035	-0.0011
245	0	-0.0014	-0.0003	-0.0009	-0.0003	0.0001	-0.0004	0.0000	0.0000	-0.0020	-0.0010
247.5	0	-0.0014	-0.0003	-0.0009	-0.0004	0.0001	0.0004	0.0000	0.0000	-0.0013	-0.0009
250	-1	-0.0013	-0.0003	-0.0007	-0.0003	0.0003	0.0003	0.0000	0.0000	-0.0009	-0.0007
252.5	0	-0.0013	-0.0002	-0.0005	-0.0003	0.0006	0.0002	0.0000	0.0000	-0.0015	-0.0008
255	-2	-0.0013	-0.0002	-0.0005	-0.0002	0.0006	0.0002	0.0000	0.0000	-0.0015	-0.0007



Table A.15: Tabulated Results from 11 Nov 2005, Field Load Test #15

Test # 15		Notes:									
Date: 11-Nov-05		-- Linear Pot #3 was determined to be damaged at the outset of these tests -- The data gathered from Linear Pot #4 was discarded due to excessive scatter -- Each Telltale is labeled by the same notation: (LP# (Depth) I/O)									
Time (sec)	Load (lbs)	Interior Telltales (I)					Perimeter Telltales (O)				
		LP7 (surf) I	LP6 (6") I	LP8 (12") I	LP10 (18") I	LP12 (30") I	LP1 (surf) O	LP4 (6") O	LP3 (12") O	LP9 (18") O	LP2 (30") O
		(in)	(in)	(in)	(in)	(in)	(in)	(in)	(in)	(in)	(in)
MAX	19937	-0.0160	-0.0167	-0.0113	-0.0068	-0.0063	-0.0170	0.0000	0.0000	-0.0140	-0.0027
0	-3	0.0000	0.0000	0.0000	0.0000	0.0000	0.0000	0.0000	0.0000	0.0000	0.0000
2.5	-6	0.0000	0.0000	0.0000	0.0000	-0.0001	0.0000	0.0000	0.0000	0.0000	0.0000
5	-34	0.0000	0.0000	0.0000	0.0000	-0.0001	0.0000	0.0000	0.0000	0.0000	0.0000
7.5	-13	0.0000	0.0000	0.0000	0.0000	0.0000	0.0000	0.0000	0.0000	0.0000	0.0000
10	-10	0.0000	0.0000	0.0000	0.0000	0.0000	0.0000	0.0000	0.0000	0.0000	0.0000
12.5	-9	0.0000	0.0000	0.0000	0.0000	0.0000	0.0000	0.0000	0.0000	0.0000	0.0000
15	-9	0.0000	0.0000	0.0000	0.0000	0.0000	0.0000	0.0000	0.0000	0.0000	0.0000
17.5	909	0.0000	-0.0003	0.0000	0.0000	-0.0001	0.0000	0.0000	0.0000	0.0001	0.0000
20	3194	-0.0014	-0.0017	-0.0011	0.0000	-0.0003	-0.0022	0.0000	0.0000	-0.0012	0.0000
22.5	5240	-0.0037	-0.0033	-0.0023	0.0000	-0.0003	-0.0046	0.0000	0.0000	-0.0018	0.0000
25	7077	-0.0051	-0.0052	-0.0032	-0.0006	-0.0007	-0.0067	0.0000	0.0000	-0.0019	0.0001
27.5	8762	-0.0065	-0.0069	-0.0041	-0.0011	-0.0009	-0.0078	0.0000	0.0000	-0.0019	-0.0001
30	10309	-0.0079	-0.0082	-0.0048	-0.0014	-0.0013	-0.0091	0.0000	0.0000	-0.0062	-0.0003
32.5	11738	-0.0089	-0.0098	-0.0056	-0.0018	-0.0024	-0.0098	0.0000	0.0000	-0.0064	-0.0002
35	13053	-0.0096	-0.0111	-0.0060	-0.0024	-0.0029	-0.0107	0.0000	0.0000	-0.0064	-0.0003
37.5	14258	-0.0106	-0.0119	-0.0068	-0.0030	-0.0033	-0.0116	0.0000	0.0000	-0.0070	-0.0004
40	15375	-0.0117	-0.0125	-0.0073	-0.0037	-0.0037	-0.0123	0.0000	0.0000	-0.0077	-0.0006
42.5	16408	-0.0126	-0.0132	-0.0080	-0.0042	-0.0042	-0.0134	0.0000	0.0000	-0.0081	-0.0007
45	17369	-0.0133	-0.0140	-0.0087	-0.0044	-0.0051	-0.0153	0.0000	0.0000	-0.0088	-0.0007
47.5	18269	-0.0138	-0.0147	-0.0091	-0.0048	-0.0054	-0.0161	0.0000	0.0000	-0.0094	-0.0007
50	19112	-0.0145	-0.0153	-0.0098	-0.0055	-0.0057	-0.0165	0.0000	0.0000	-0.0093	-0.0010
52.5	19814	-0.0153	-0.0160	-0.0107	-0.0063	-0.0062	-0.0162	0.0000	0.0000	-0.0105	-0.0017
55	19819	-0.0153	-0.0163	-0.0110	-0.0064	-0.0060	-0.0164	0.0000	0.0000	-0.0085	-0.0020
57.5	19709	-0.0153	-0.0164	-0.0111	-0.0065	-0.0061	-0.0164	0.0000	0.0000	-0.0086	-0.0020
60	19618	-0.0153	-0.0164	-0.0113	-0.0065	-0.0062	-0.0165	0.0000	0.0000	-0.0103	-0.0020
62.5	19531	-0.0153	-0.0164	-0.0113	-0.0065	-0.0062	-0.0165	0.0000	0.0000	-0.0094	-0.0020
65	19450	-0.0153	-0.0164	-0.0113	-0.0066	-0.0062	-0.0167	0.0000	0.0000	-0.0099	-0.0024
67.5	19384	-0.0153	-0.0164	-0.0113	-0.0065	-0.0063	-0.0168	0.0000	0.0000	-0.0115	-0.0024
70	19322	-0.0153	-0.0164	-0.0113	-0.0066	-0.0063	-0.0168	0.0000	0.0000	-0.0119	-0.0024
72.5	19276	-0.0153	-0.0164	-0.0113	-0.0066	-0.0063	-0.0168	0.0000	0.0000	-0.0116	-0.0024
75	19450	-0.0153	-0.0164	-0.0113	-0.0067	-0.0062	-0.0168	0.0000	0.0000	-0.0123	-0.0024
77.5	19838	-0.0154	-0.0164	-0.0113	-0.0067	-0.0062	-0.0170	0.0000	0.0000	-0.0126	-0.0024
80	19937	-0.0153	-0.0167	-0.0113	-0.0067	-0.0061	-0.0169	0.0000	0.0000	-0.0123	-0.0024
82.5	19843	-0.0153	-0.0167	-0.0113	-0.0067	-0.0059	-0.0168	0.0000	0.0000	-0.0130	-0.0024
85	19756	-0.0153	-0.0166	-0.0113	-0.0067	-0.0059	-0.0168	0.0000	0.0000	-0.0131	-0.0024
87.5	19675	-0.0155	-0.0167	-0.0113	-0.0067	-0.0059	-0.0168	0.0000	0.0000	-0.0139	-0.0024
90	19596	-0.0157	-0.0166	-0.0113	-0.0068	-0.0058	-0.0168	0.0000	0.0000	-0.0140	-0.0024
92.5	19518	-0.0157	-0.0167	-0.0113	-0.0068	-0.0058	-0.0168	0.0000	0.0000	-0.0140	-0.0024
95	19437	-0.0157	-0.0167	-0.0113	-0.0068	-0.0058	-0.0168	0.0000	0.0000	-0.0140	-0.0024
97.5	19366	-0.0155	-0.0167	-0.0113	-0.0068	-0.0058	-0.0168	0.0000	0.0000	-0.0140	-0.0024
100	19308	-0.0157	-0.0167	-0.0113	-0.0068	-0.0058	-0.0168	0.0000	0.0000	-0.0140	-0.0024
102.5	19259	-0.0157	-0.0166	-0.0113	-0.0068	-0.0058	-0.0168	0.0000	0.0000	-0.0140	-0.0024
105	19465	-0.0157	-0.0165	-0.0113	-0.0068	-0.0058	-0.0168	0.0000	0.0000	-0.0140	-0.0024
107.5	19894	-0.0157	-0.0167	-0.0113	-0.0068	-0.0057	-0.0168	0.0000	0.0000	-0.0140	-0.0024
110	19825	-0.0157	-0.0166	-0.0113	-0.0068	-0.0057	-0.0168	0.0000	0.0000	-0.0140	-0.0024
112.5	19741	-0.0157	-0.0167	-0.0113	-0.0067	-0.0057	-0.0168	0.0000	0.0000	-0.0140	-0.0024
115	19663	-0.0157	-0.0165	-0.0113	-0.0068	-0.0055	-0.0168	0.0000	0.0000	-0.0140	-0.0024
117.5	19585	-0.0157	-0.0165	-0.0113	-0.0068	-0.0055	-0.0168	0.0000	0.0000	-0.0140	-0.0024
120	19511	-0.0157	-0.0165	-0.0113	-0.0068	-0.0055	-0.0168	0.0000	0.0000	-0.0140	-0.0024
122.5	19444	-0.0157	-0.0165	-0.0113	-0.0068	-0.0057	-0.0168	0.0000	0.0000	-0.0140	-0.0024
125	19379	-0.0157	-0.0165	-0.0113	-0.0068	-0.0055	-0.0168	0.0000	0.0000	-0.0140	-0.0024
127.5	19308	-0.0157	-0.0164	-0.0113	-0.0068	-0.0056	-0.0168	0.0000	0.0000	-0.0140	-0.0024
130	19233	-0.0157	-0.0164	-0.0113	-0.0068	-0.0056	-0.0168	0.0000	0.0000	-0.0132	-0.0024
132.5	19170	-0.0157	-0.0164	-0.0113	-0.0068	-0.0058	-0.0168	0.0000	0.0000	-0.0111	-0.0024
135	19101	-0.0157	-0.0164	-0.0113	-0.0067	-0.0058	-0.0168	0.0000	0.0000	-0.0117	-0.0024

Table A.15: Tabulated Results from 11 Nov 2005, Field Load Test #15 (continued)

Test # 15		Notes:									
Date: 11-Nov-05		-- Linear Pot #3 was determined to be damaged at the outset of these tests -- The data gathered from Linear Pot #4 was discarded due to excessive scatter -- Each Telltale is labeled by the same notation: (LP# (Depth) I/O)									
Time (sec)	Load (lbs)	Interior Telltales (I)					Perimeter Telltales (O)				
		LP7 (surf) I	LP6 (6") I	LP8 (12") I	LP10 (18") I	LP12 (30") I	LP1 (surf) O	LP4 (6") O	LP3 (12") O	LP9 (18") O	LP2 (30") O
		(in)	(in)	(in)	(in)	(in)	(in)	(in)	(in)	(in)	(in)
137.5	19032	-0.0157	-0.0164	-0.0113	-0.0067	-0.0058	-0.0168	0.0000	0.0000	-0.0122	-0.0024
140	18964	-0.0157	-0.0164	-0.0113	-0.0067	-0.0058	-0.0168	0.0000	0.0000	-0.0128	-0.0024
142.5	18885	-0.0157	-0.0164	-0.0113	-0.0067	-0.0058	-0.0168	0.0000	0.0000	-0.0127	-0.0024
145	18769	-0.0157	-0.0164	-0.0113	-0.0068	-0.0058	-0.0168	0.0000	0.0000	-0.0128	-0.0024
147.5	18613	-0.0157	-0.0164	-0.0113	-0.0068	-0.0058	-0.0168	0.0000	0.0000	-0.0128	-0.0024
150	18450	-0.0159	-0.0164	-0.0113	-0.0067	-0.0058	-0.0168	0.0000	0.0000	-0.0132	-0.0024
152.5	18265	-0.0160	-0.0164	-0.0113	-0.0066	-0.0058	-0.0167	0.0000	0.0000	-0.0131	-0.0024
155	17766	-0.0160	-0.0164	-0.0113	-0.0067	-0.0058	-0.0165	0.0000	0.0000	-0.0116	-0.0024
157.5	15708	-0.0158	-0.0160	-0.0113	-0.0067	-0.0058	-0.0163	0.0000	0.0000	-0.0087	-0.0024
160	12635	-0.0153	-0.0150	-0.0105	-0.0064	-0.0061	-0.0162	0.0000	0.0000	-0.0092	-0.0024
162.5	11196	-0.0150	-0.0142	-0.0101	-0.0065	-0.0059	-0.0158	0.0000	0.0000	-0.0086	-0.0025
165	9851	-0.0140	-0.0132	-0.0096	-0.0065	-0.0057	-0.0149	0.0000	0.0000	-0.0085	-0.0026
167.5	8649	-0.0135	-0.0124	-0.0092	-0.0064	-0.0055	-0.0126	0.0000	0.0000	-0.0079	-0.0025
170	7527	-0.0131	-0.0115	-0.0088	-0.0064	-0.0050	-0.0119	0.0000	0.0000	-0.0077	-0.0026
172.5	6593	-0.0122	-0.0107	-0.0085	-0.0061	-0.0042	-0.0118	0.0000	0.0000	-0.0068	-0.0026
175	5814	-0.0115	-0.0098	-0.0081	-0.0057	-0.0036	-0.0110	0.0000	0.0000	-0.0051	-0.0027
177.5	5052	-0.0105	-0.0091	-0.0076	-0.0054	-0.0033	-0.0105	0.0000	0.0000	-0.0058	-0.0027
180	4223	-0.0097	-0.0083	-0.0070	-0.0052	-0.0030	-0.0099	0.0000	0.0000	-0.0060	-0.0027
182.5	3167	-0.0086	-0.0068	-0.0062	-0.0046	-0.0024	-0.0088	0.0000	0.0000	-0.0050	-0.0027
185	2633	-0.0078	-0.0059	-0.0056	-0.0042	-0.0020	-0.0081	0.0000	0.0000	-0.0042	-0.0027
187.5	1182	-0.0052	-0.0036	-0.0042	-0.0032	-0.0013	-0.0054	0.0000	0.0000	-0.0025	-0.0023
190	-1	-0.0026	-0.0014	-0.0025	-0.0016	-0.0009	-0.0029	0.0000	0.0000	-0.0009	-0.0020
192.5	-1	-0.0024	-0.0011	-0.0025	-0.0016	-0.0008	-0.0024	0.0000	0.0000	-0.0008	-0.0020
195	0	-0.0023	-0.0011	-0.0022	-0.0014	-0.0010	-0.0021	0.0000	0.0000	-0.0018	-0.0018
197.5	0	-0.0023	-0.0011	-0.0021	-0.0013	-0.0010	-0.0021	0.0000	0.0000	-0.0019	-0.0018
200	-1	-0.0022	-0.0011	-0.0021	-0.0013	-0.0010	-0.0021	0.0000	0.0000	-0.0019	-0.0017
202.5	0	-0.0021	-0.0011	-0.0021	-0.0013	-0.0010	-0.0020	0.0000	0.0000	-0.0022	-0.0017
205	0	-0.0021	-0.0011	-0.0019	-0.0013	-0.0010	-0.0020	0.0000	0.0000	-0.0023	-0.0017
207.5	0	-0.0021	-0.0008	-0.0018	-0.0013	-0.0014	-0.0021	0.0000	0.0000	-0.0022	-0.0017
210	0	-0.0021	-0.0007	-0.0018	-0.0013	-0.0011	-0.0020	0.0000	0.0000	-0.0023	-0.0017
212.5	0	-0.0021	-0.0007	-0.0018	-0.0013	-0.0011	-0.0021	0.0000	0.0000	-0.0026	-0.0017
215	0	-0.0021	-0.0007	-0.0018	-0.0013	-0.0011	-0.0020	0.0000	0.0000	-0.0027	-0.0017
217.5	0	-0.0021	-0.0007	-0.0018	-0.0013	-0.0009	-0.0020	0.0000	0.0000	-0.0029	-0.0017
220	0	-0.0020	-0.0007	-0.0018	-0.0013	-0.0007	-0.0019	0.0000	0.0000	-0.0032	-0.0017
222.5	0	-0.0019	-0.0007	-0.0018	-0.0012	-0.0009	-0.0020	0.0000	0.0000	-0.0027	-0.0017
225	0	-0.0018	-0.0007	-0.0018	-0.0013	-0.0007	-0.0020	0.0000	0.0000	-0.0035	-0.0017
227.5	0	-0.0018	-0.0007	-0.0018	-0.0013	-0.0007	-0.0020	0.0000	0.0000	-0.0036	-0.0017
230	0	-0.0019	-0.0007	-0.0018	-0.0013	-0.0007	-0.0020	0.0000	0.0000	-0.0038	-0.0017
232.5	0	-0.0019	-0.0007	-0.0018	-0.0013	-0.0008	-0.0021	0.0000	0.0000	-0.0044	-0.0017
235	-3	-0.0021	-0.0007	-0.0018	-0.0013	-0.0010	-0.0018	0.0000	0.0000	-0.0039	-0.0018
237.5	-4	-0.0019	-0.0007	-0.0018	-0.0013	-0.0007	-0.0018	0.0000	0.0000	-0.0039	-0.0017
240	-1	-0.0019	-0.0007	-0.0018	-0.0013	-0.0010	-0.0020	0.0000	0.0000	-0.0035	-0.0017
242.5	-3	-0.0019	-0.0007	-0.0018	-0.0013	-0.0010	-0.0019	0.0000	0.0000	-0.0035	-0.0017
245	-6	-0.0021	-0.0007	-0.0018	-0.0013	-0.0010	-0.0018	0.0000	0.0000	-0.0036	-0.0017
247.5	-9	-0.0018	-0.0007	-0.0020	-0.0013	-0.0011	-0.0019	0.0000	0.0000	-0.0029	-0.0017
250	-9	-0.0018	-0.0007	-0.0018	-0.0012	-0.0011	-0.0018	0.0000	0.0000	-0.0029	-0.0017
252.5	-10	-0.0018	-0.0007	-0.0019	-0.0013	-0.0011	-0.0019	0.0000	0.0000	-0.0029	-0.0017
255	-10	-0.0018	-0.0007	-0.0018	-0.0012	-0.0011	-0.0020	0.0000	0.0000	-0.0028	-0.0017



**APPENDIX A**  
**SECTION 2**

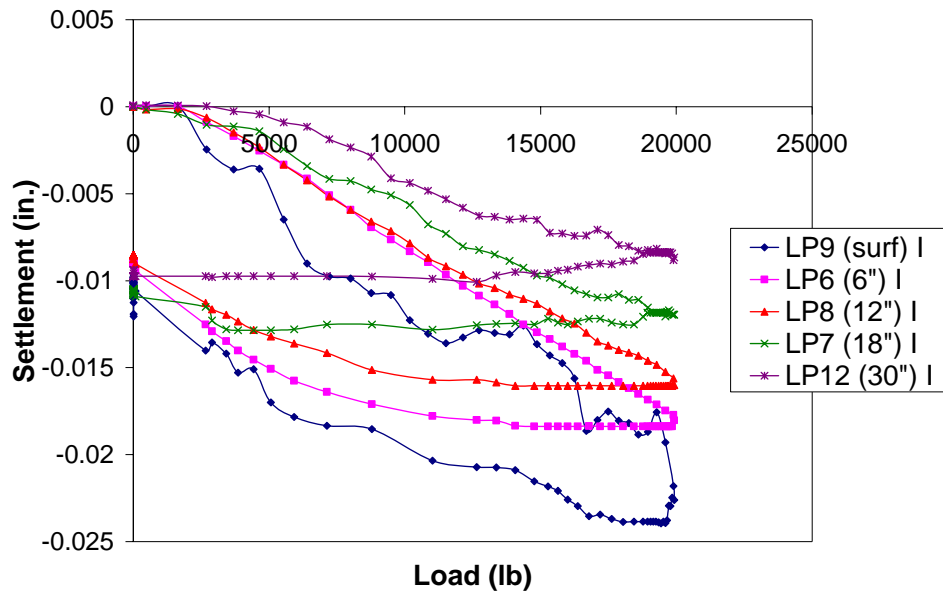


Figure A.1.1: Settlement Measurements of the Surface and the Telltales Beneath the Center of the Footing for 11 Nov 05, Field Load Test #1

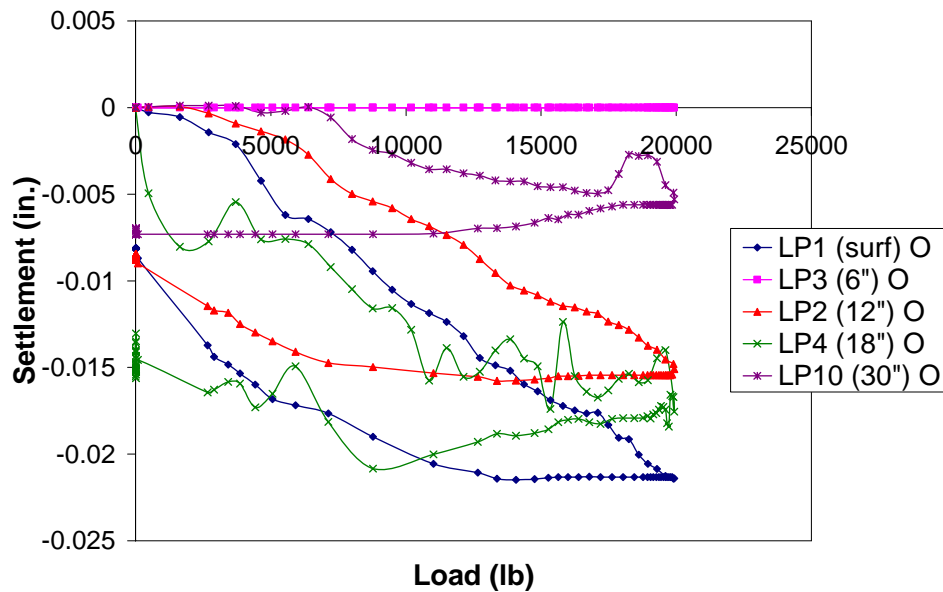


Figure A.1.2: Settlement Measurements of the Surface and the Telltales Beneath the Perimeter of the Footing for 11 Nov 05, Field Load Test #1

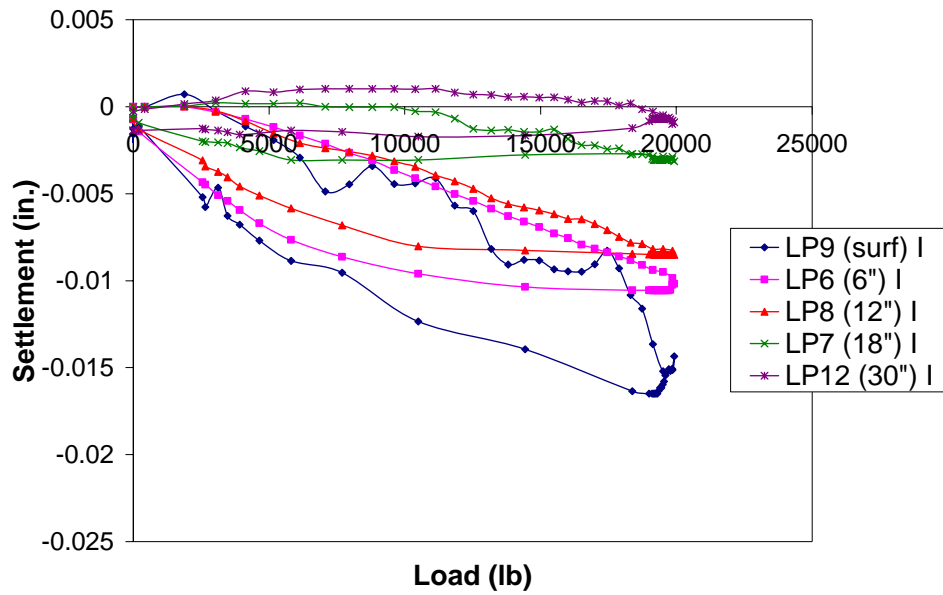


Figure A.2.1: Settlement Measurements of the Surface and the Telltales Beneath the Center of the Footing for 11 Nov 05, Field Load Test #2

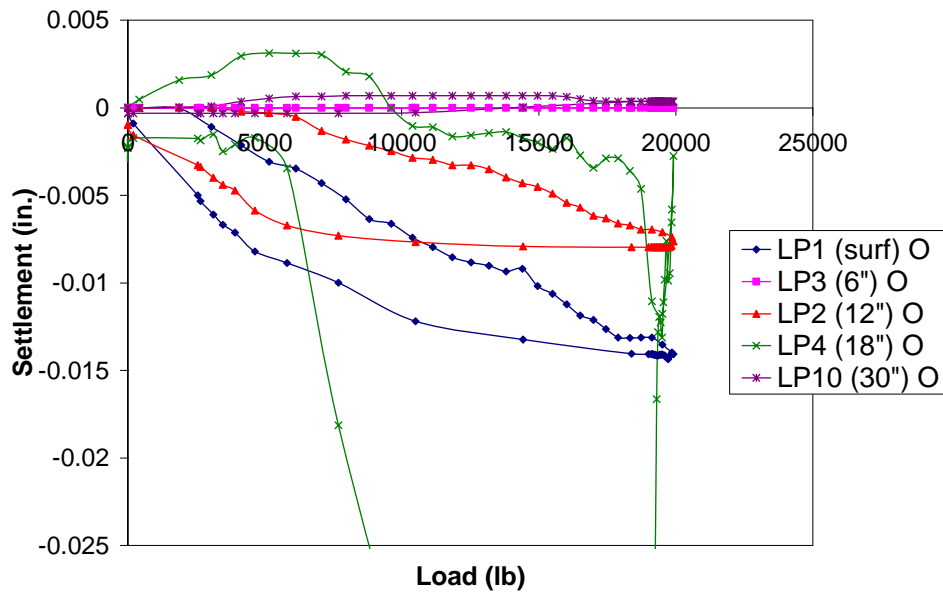


Figure A.2.2: Settlement Measurements of the Surface and the Telltales Beneath the Perimeter of the Footing for 11 Nov 05, Field Load Test #2

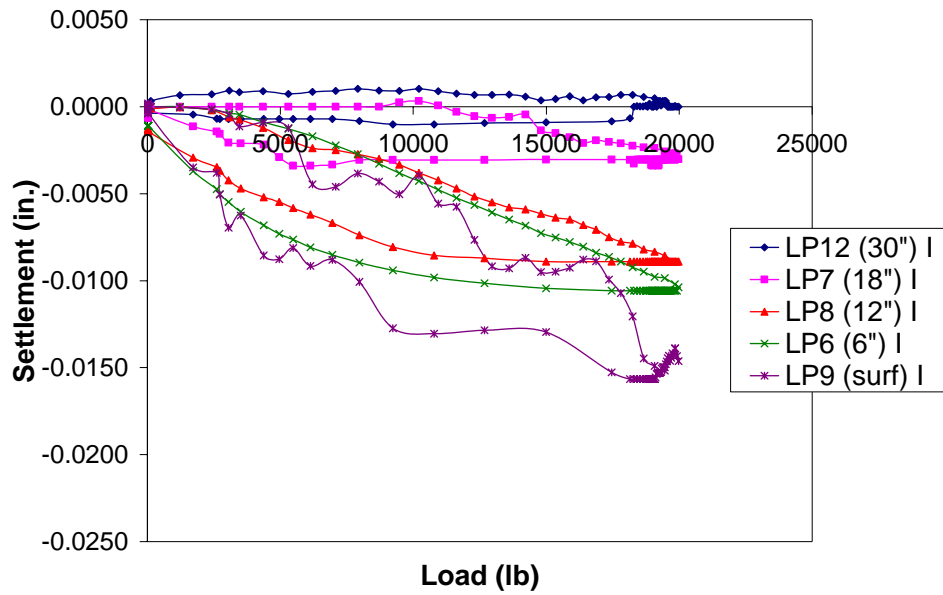


Figure A.3.1: Settlement Measurements of the Surface and the Telltales Beneath the Center of the Footing for 11 Nov 05, Field Load Test #3

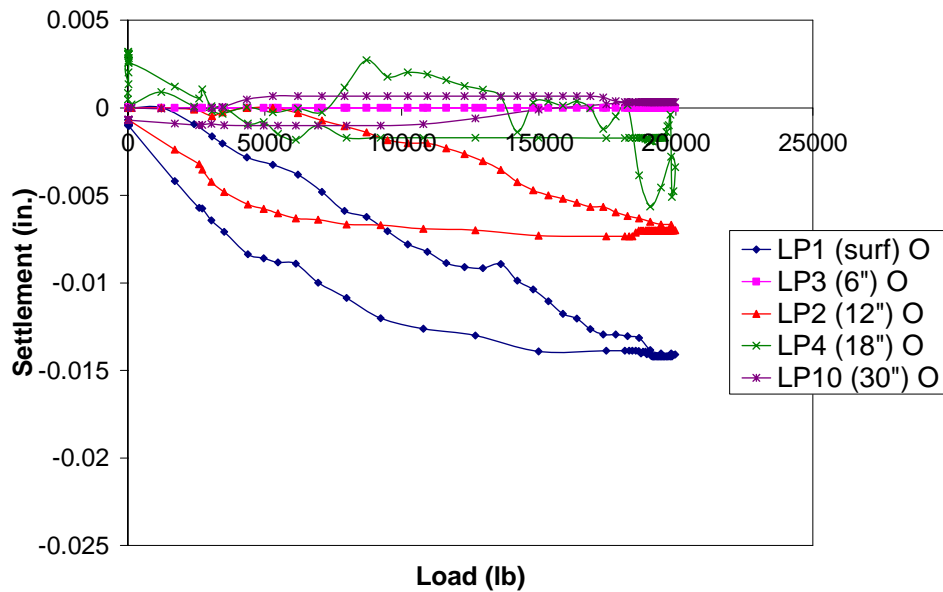


Figure A.3.2: Settlement Measurements of the Surface and the Telltales Beneath the Perimeter of the Footing for 11 Nov 05, Field Load Test #3

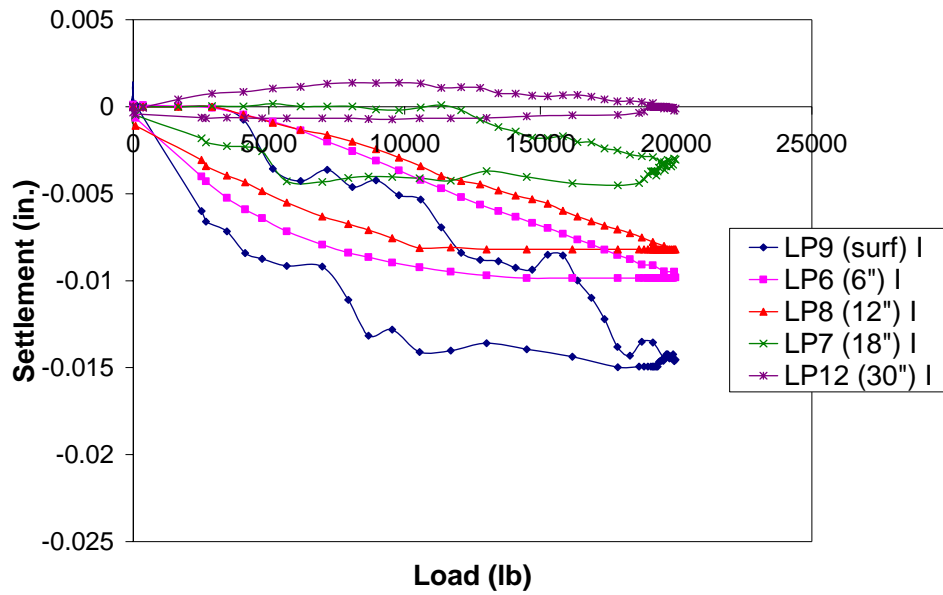


Figure A.4.1: Settlement Measurements of the Surface and the Telltales Beneath the Center of the Footing for 11 Nov 05, Field Load Test #4

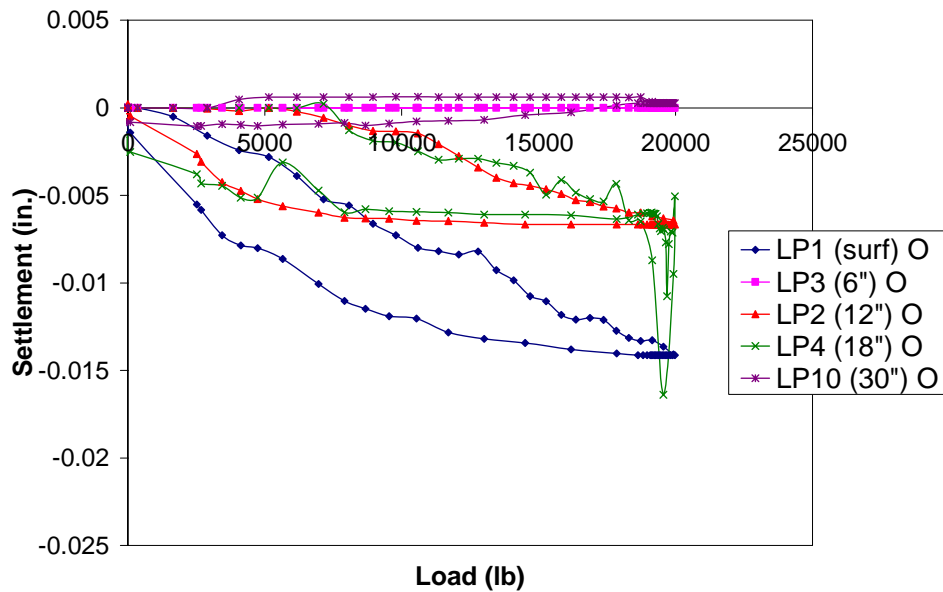


Figure A.4.2: Settlement Measurements of the Surface and the Telltales Beneath the Perimeter of the Footing for 11 Nov 05, Field Load Test #4

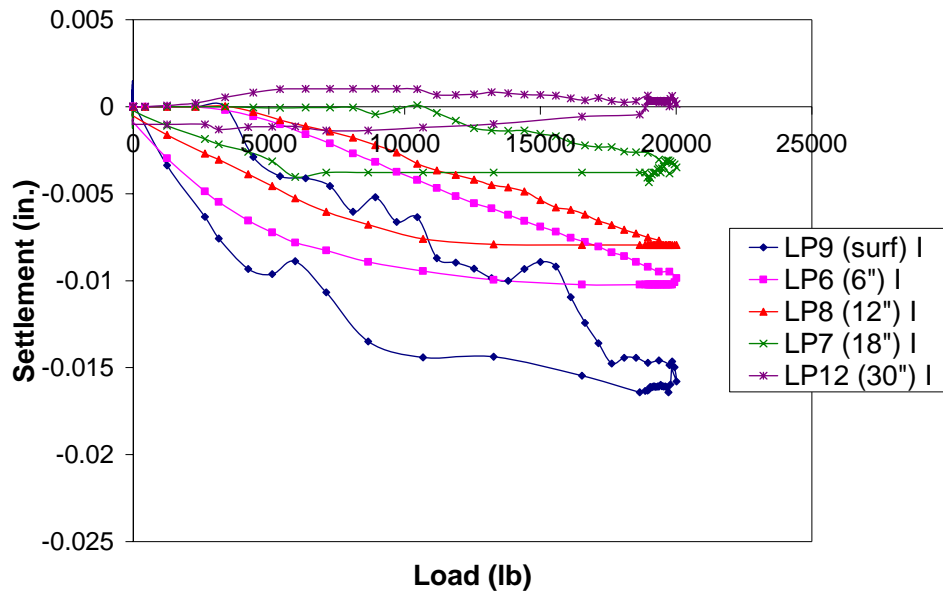


Figure A.5.1: Settlement Measurements of the Surface and the Telltales Beneath the Center of the Footing for 11 Nov 05, Field Load Test #5

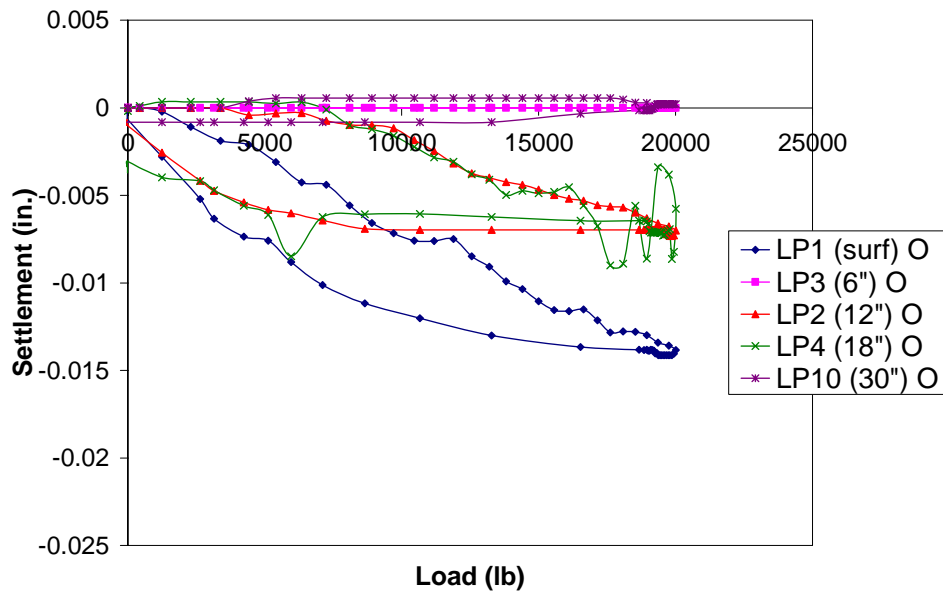


Figure A.5.2: Settlement Measurements of the Surface and the Telltales Beneath the Perimeter of the Footing for 11 Nov 05, Field Load Test #5

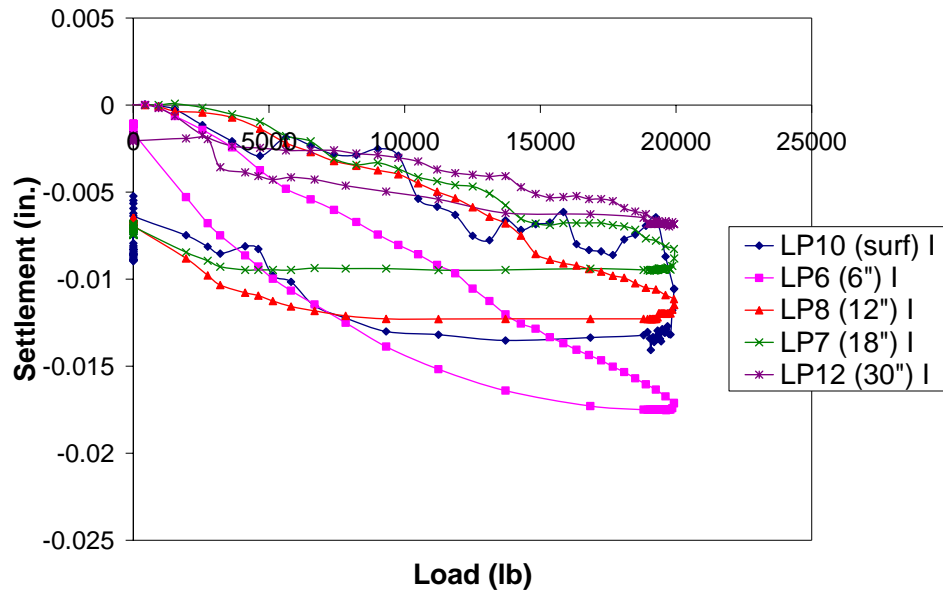


Figure A.6.1: Settlement Measurements of the Surface and the Telltales Beneath the Center of the Footing for 11 Nov 05, Field Load Test #6

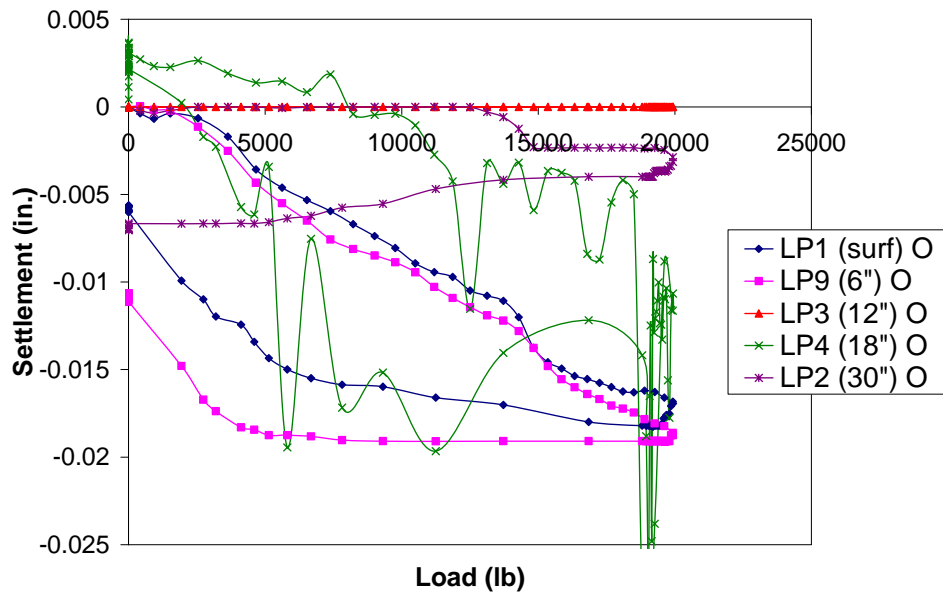


Figure A.6.2: Settlement Measurements of the Surface and the Telltales Beneath the Perimeter of the Footing for 11 Nov 05, Field Load Test #6

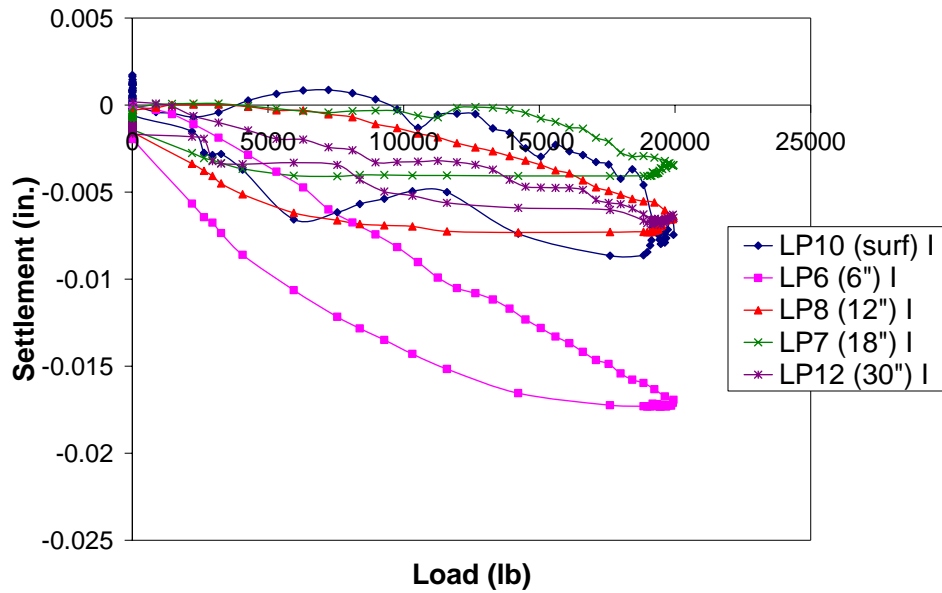


Figure A.7.1: Settlement Measurements of the Surface and the Telltales Beneath the Center of the Footing for 11 Nov 05, Field Load Test #7

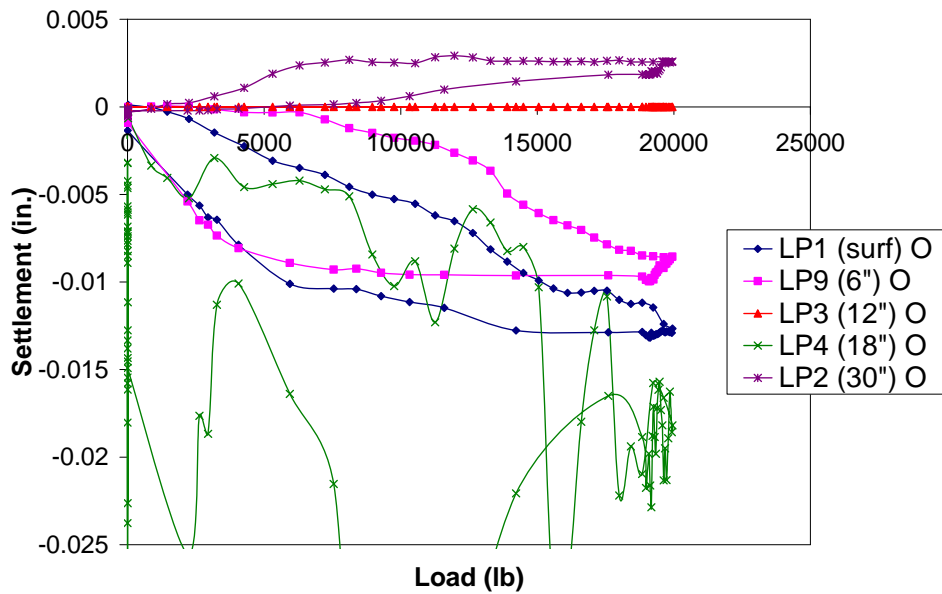


Figure A.7.2: Settlement Measurements of the Surface and the Telltales Beneath the Perimeter of the Footing for 11 Nov 05, Field Load Test #7



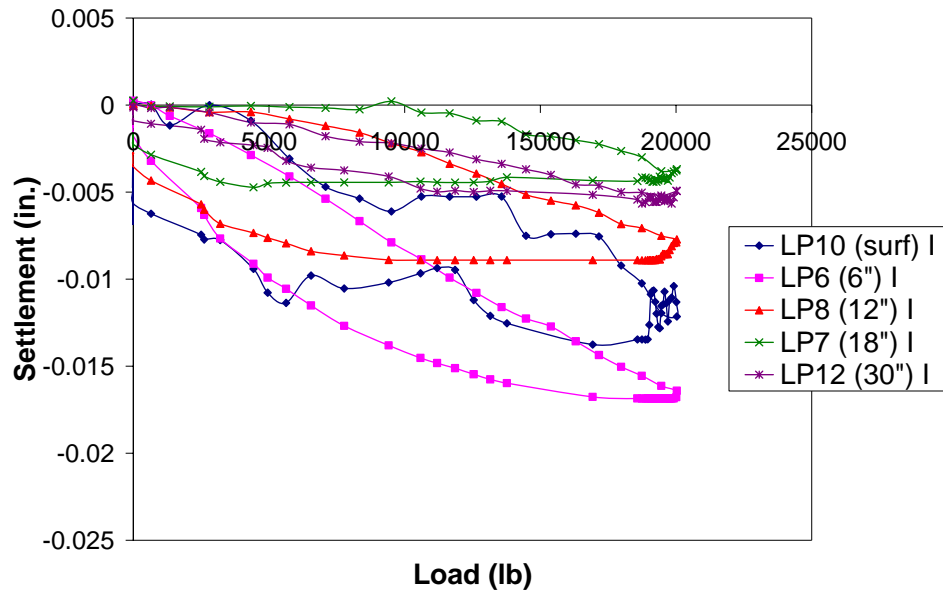


Figure A.8.1: Settlement Measurements of the Surface and the Telltales Beneath the Center of the Footing for 11 Nov 05, Field Load Test #8

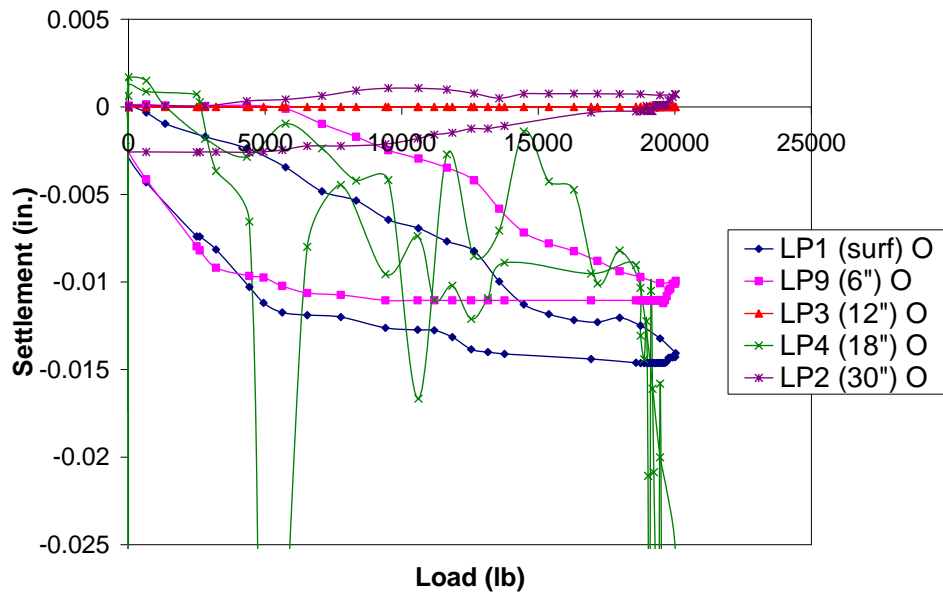


Figure A.8.2: Settlement Measurements of the Surface and the Telltales Beneath the Perimeter of the Footing for 11 Nov 05, Field Load Test #8

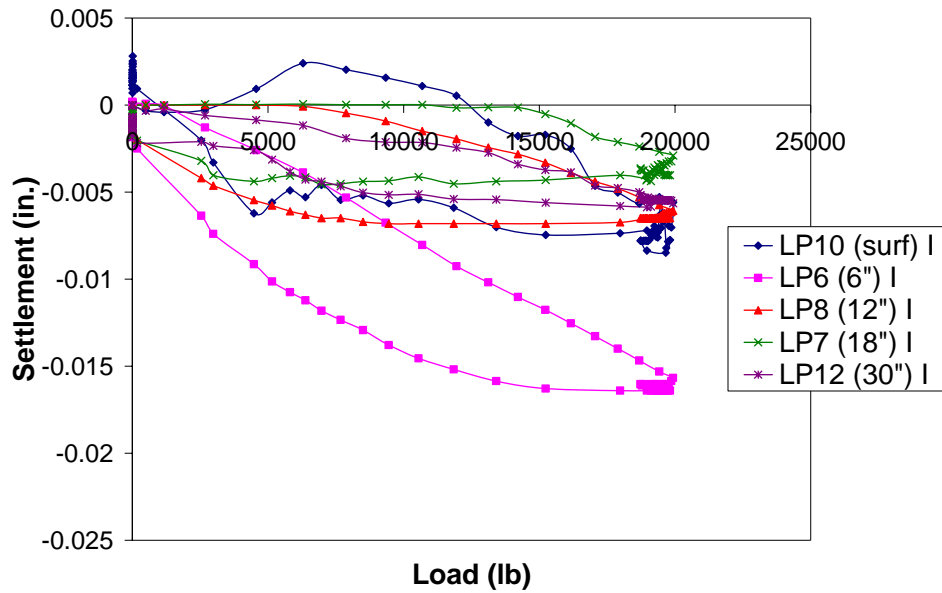


Figure A.9.1: Settlement Measurements of the Surface and the Telltales Beneath the Center of the Footing for 11 Nov 05, Field Load Test #9

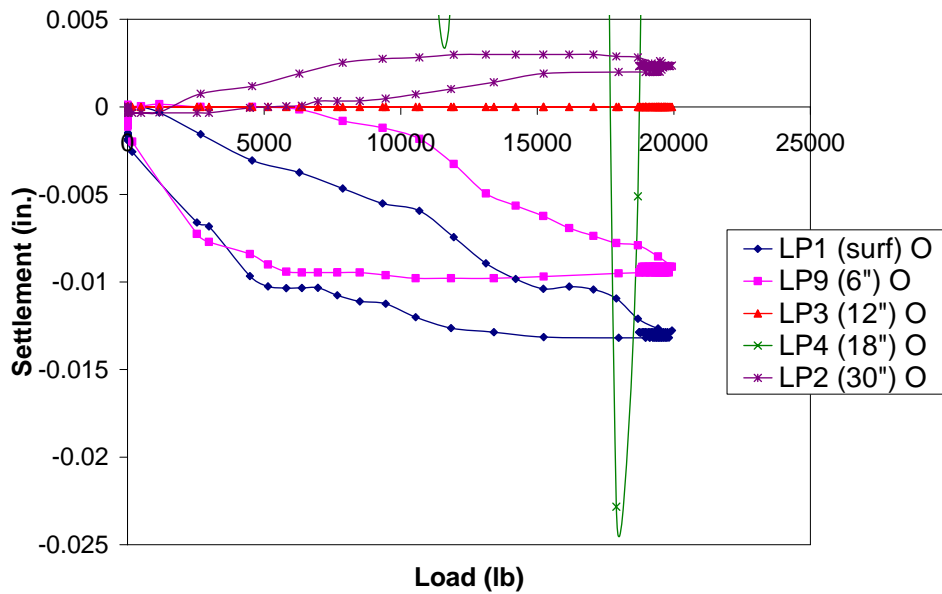


Figure A.9.2: Settlement Measurements of the Surface and the Telltales Beneath the Perimeter of the Footing for 11 Nov 05, Field Load Test #9

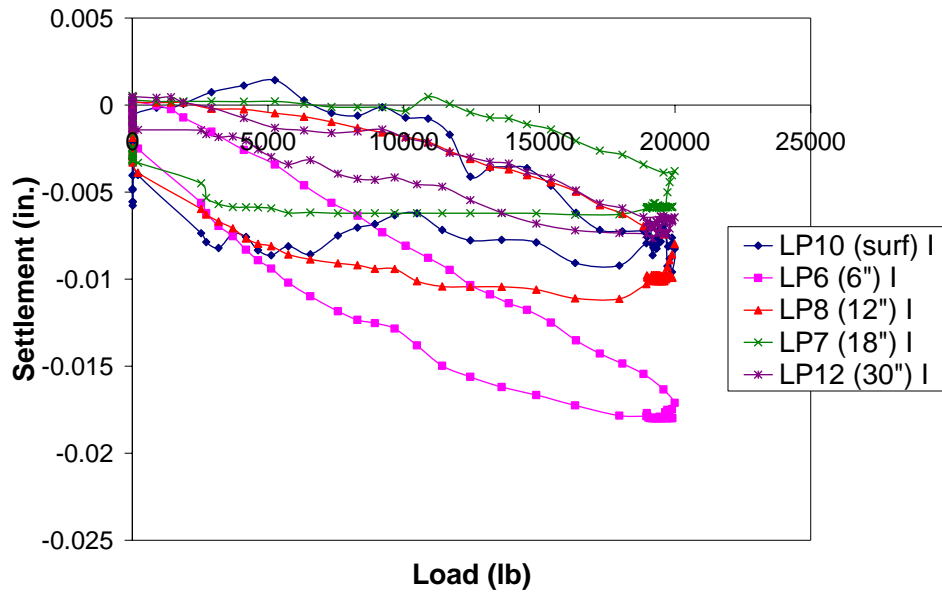


Figure A.10.1: Settlement Measurements of the Surface and the Telltales Beneath the Center of the Footing for 11 Nov 05, Field Load Test #10

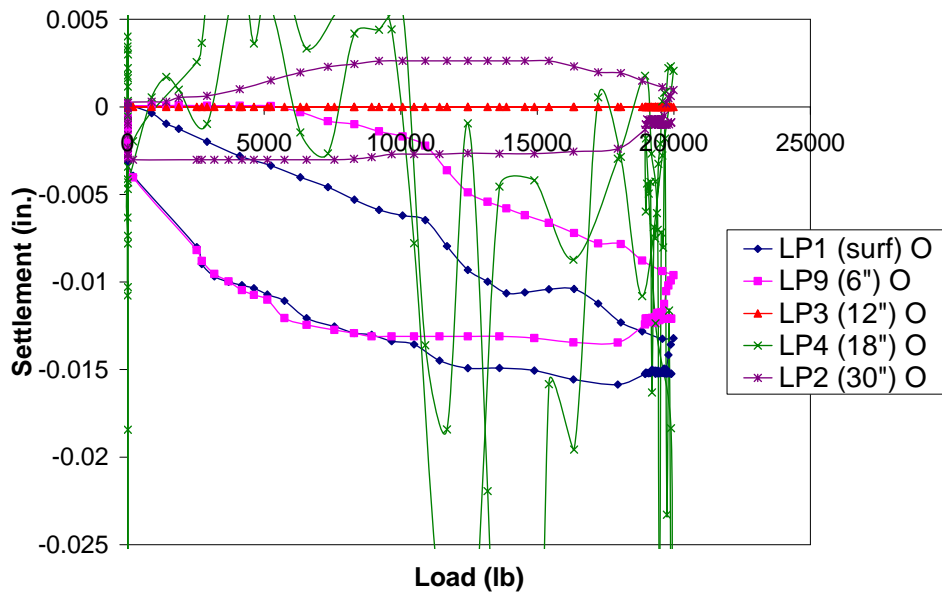


Figure A.10.2: Settlement Measurements of the Surface and the Telltales Beneath the Perimeter of the Footing for 11 Nov 05, Field Load Test #10

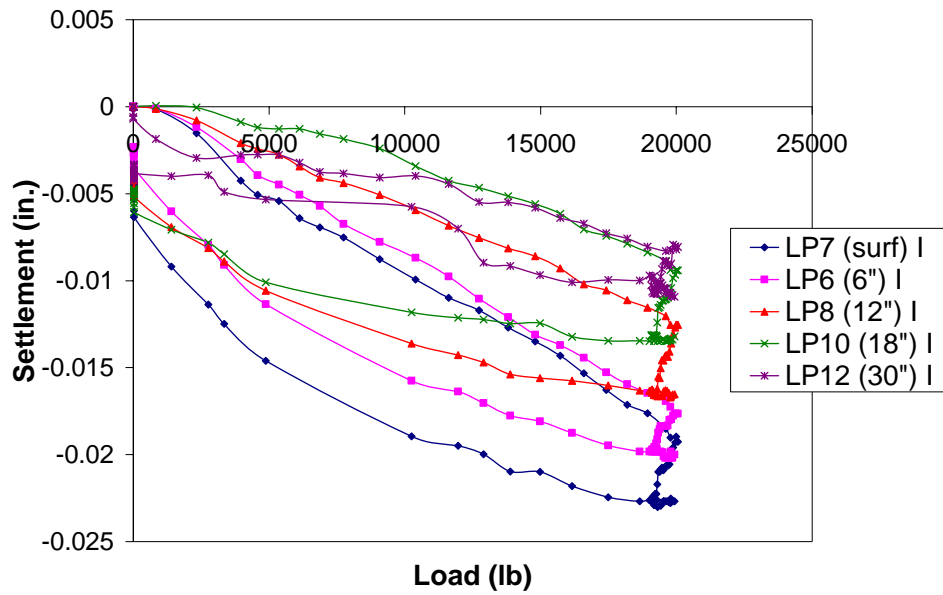


Figure A.11.1: Settlement Measurements of the Surface and the Telltales Beneath the Center of the Footing for 11 Nov 05, Field Load Test #11

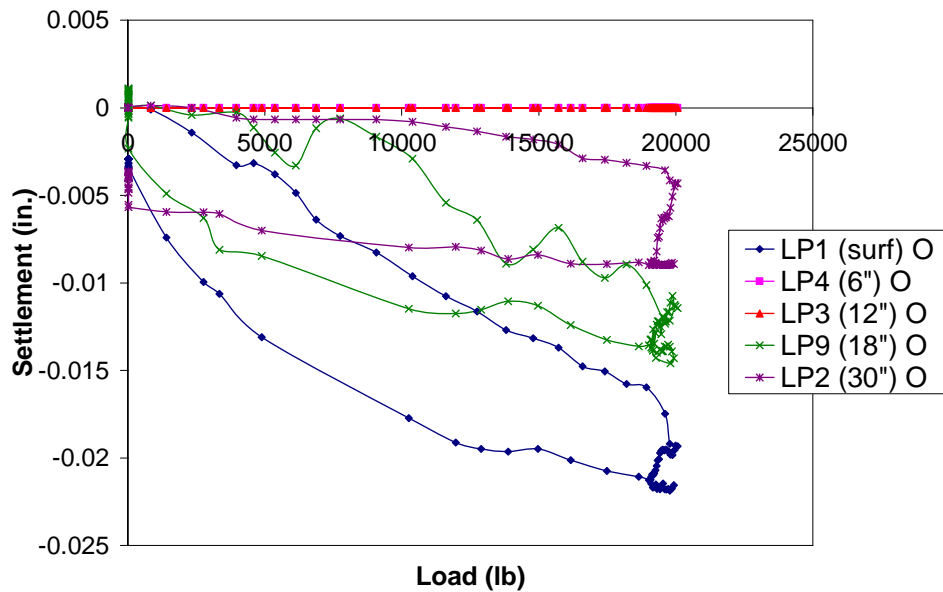


Figure A.11.2: Settlement Measurements of the Surface and the Telltales Beneath the Perimeter of the Footing for 11 Nov 05, Field Load Test #11

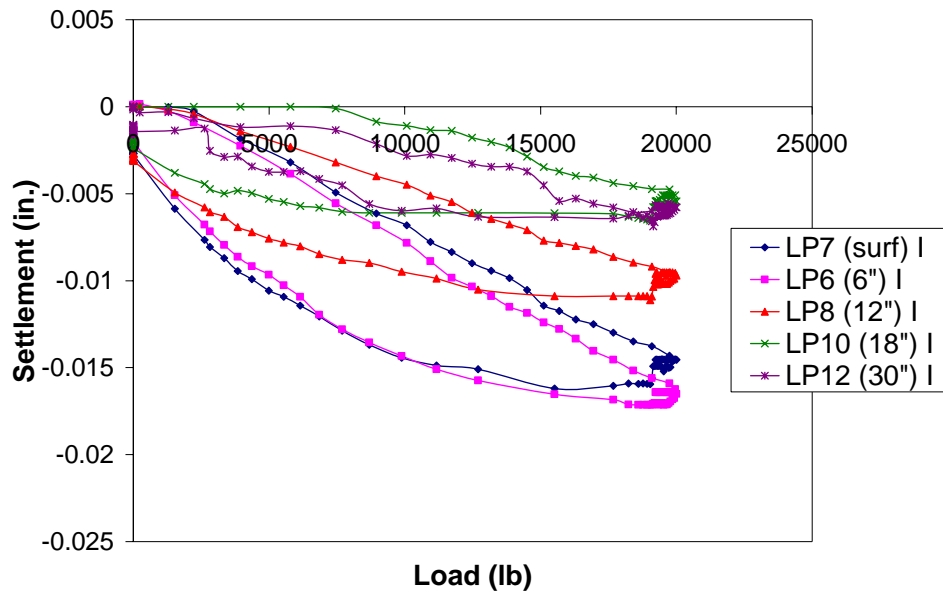


Figure A.12.1: Settlement Measurements of the Surface and the Telltales Beneath the Center of the Footing for 11 Nov 05, Field Load Test #12

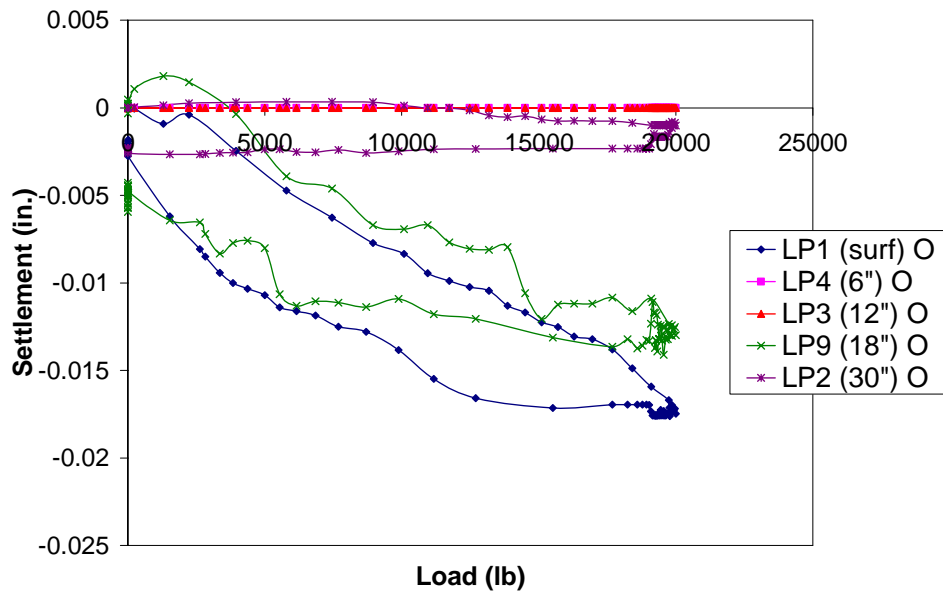


Figure A.12.2: Settlement Measurements of the Surface and the Telltales Beneath the Perimeter of the Footing for 11 Nov 05, Field Load Test #12

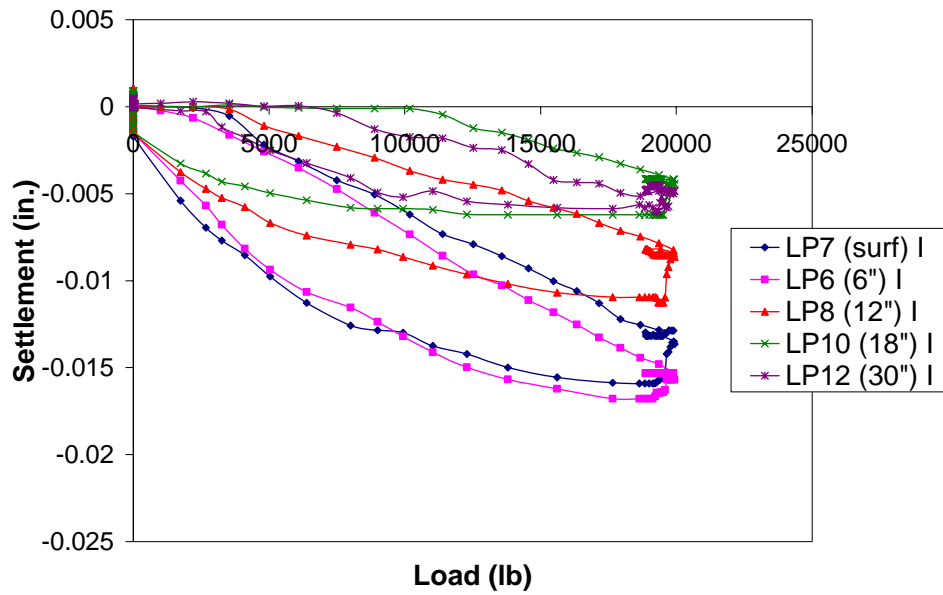


Figure A.13.1: Settlement Measurements of the Surface and the Telltales Beneath the Center of the Footing for 11 Nov 05, Field Load Test #13

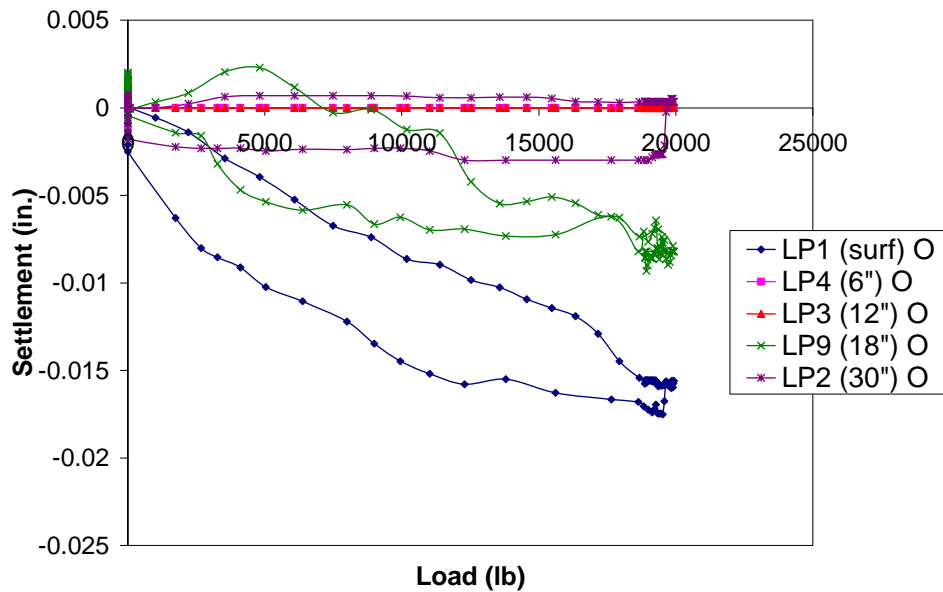


Figure A.13.2: Settlement Measurements of the Surface and the Telltales Beneath the Perimeter of the Footing for 11 Nov 05, Field Load Test #13

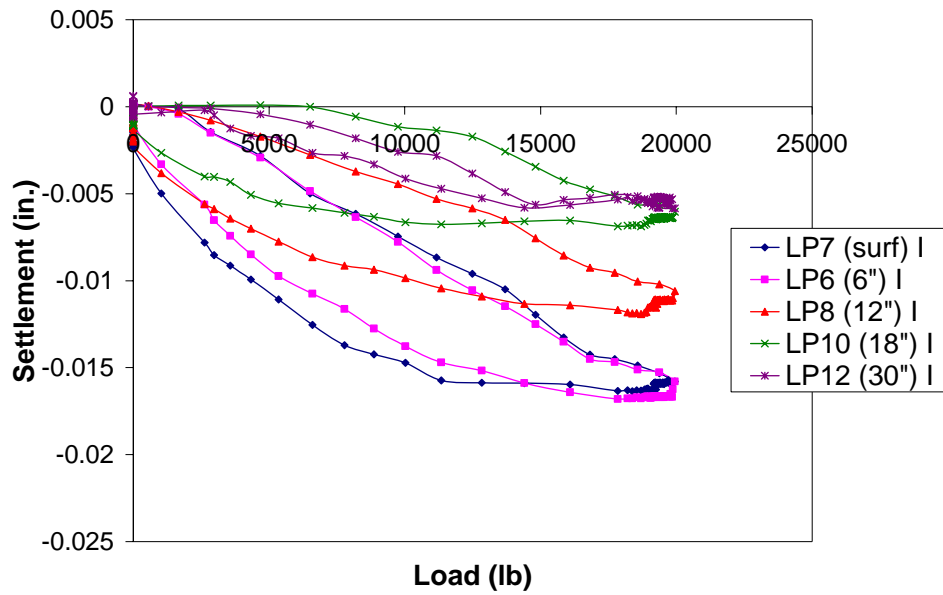


Figure A.14.1: Settlement Measurements of the Surface and the Telltales Beneath the Center of the Footing for 11 Nov 05, Field Load Test #14

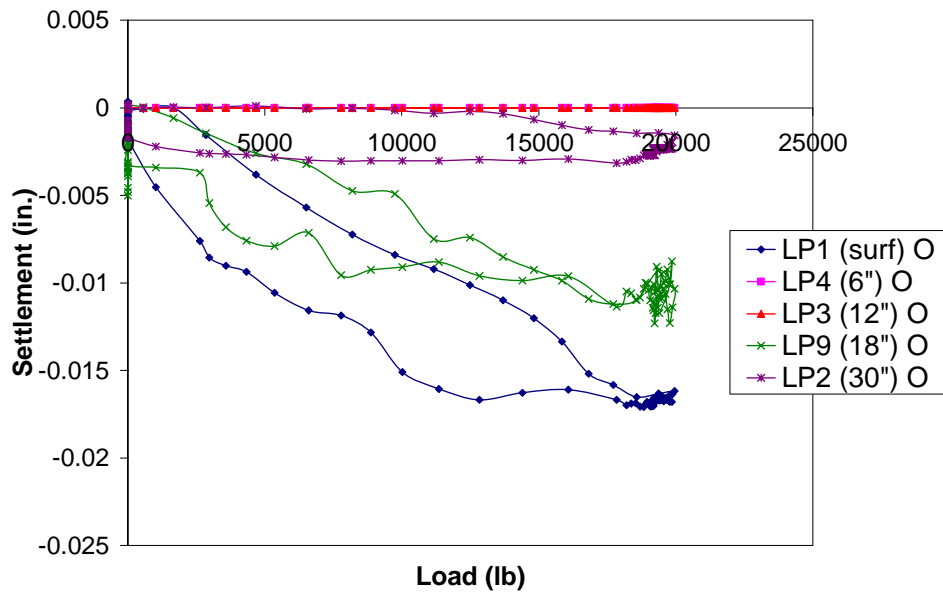


Figure A.14.2: Settlement Measurements of the Surface and the Telltales Beneath the Perimeter of the Footing for 11 Nov 05, Field Load Test #14

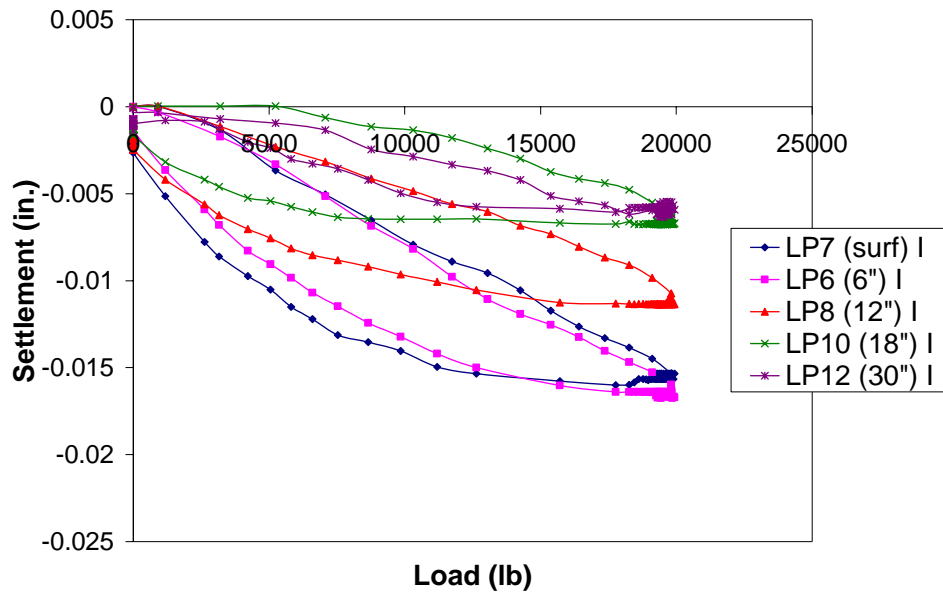


Figure A.15.1: Settlement Measurements of the Surface and the Telltales Beneath the Center of the Footing for 11 Nov 05, Field Load Test #15

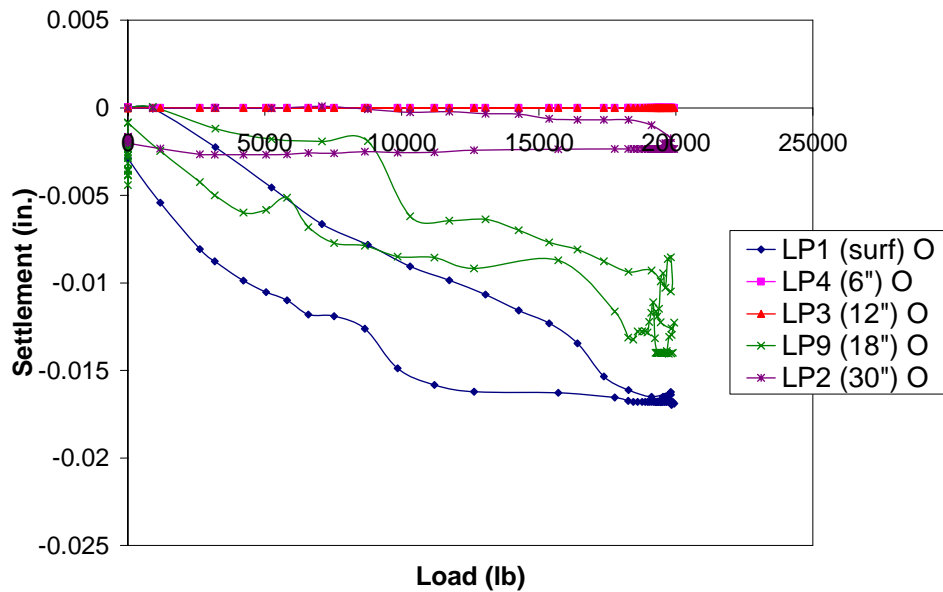


Figure A.15.2: Settlement Measurements of the Surface and the Telltales Beneath the Perimeter of the Footing for 11 Nov 05, Field Load Test #15



**APPENDIX A**  
**SECTION 3**

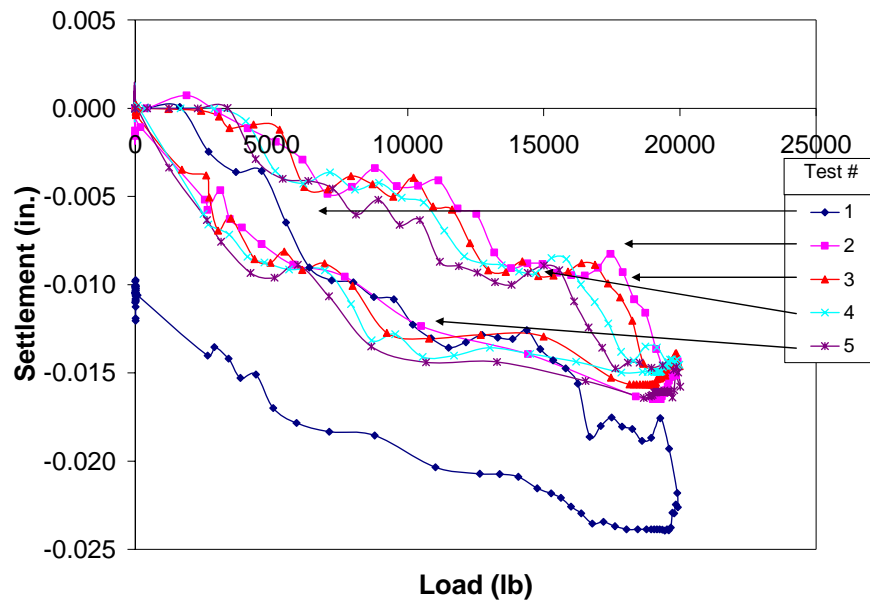


Figure A.16: Measured Settlements at the Center of the Surface of the Footing for Tests #1-5 on 11 Nov 05

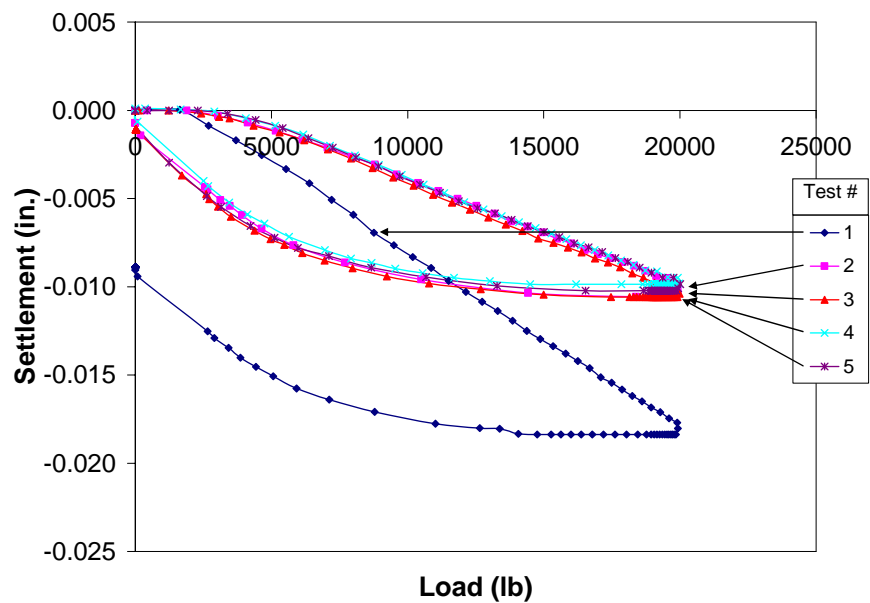


Figure A.17: Measured Settlements at 6 in. Beneath the Center of the Footing for Tests #1-5 on 11 Nov 05

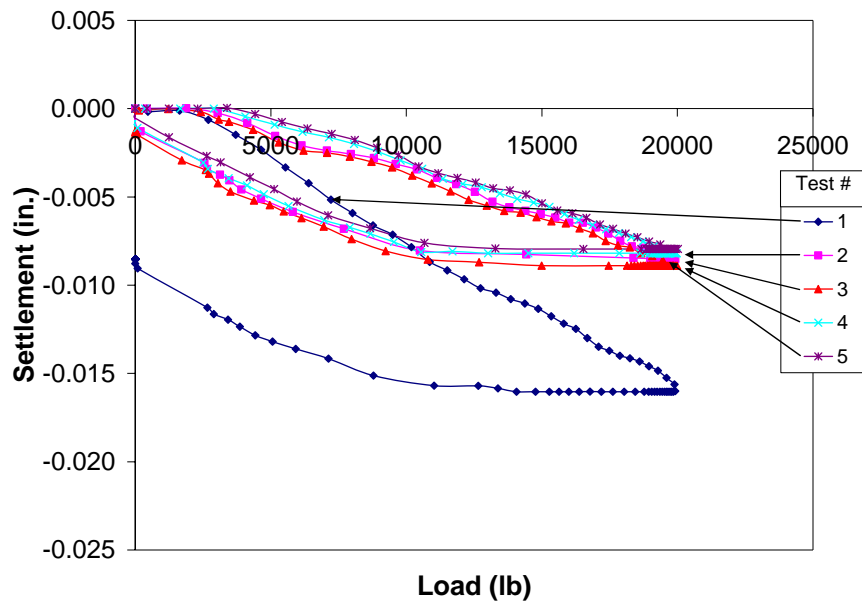


Figure A.18: Measured Settlements at 12 in. Beneath the Center of the Footing for Tests #1-5 on 11 Nov 05

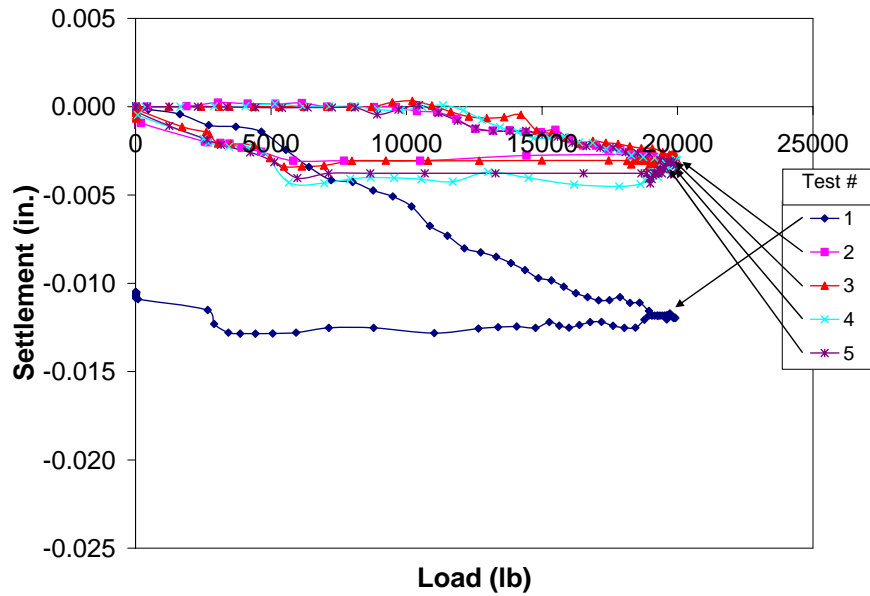


Figure A.19: Measured Settlements at 18 in. Beneath the Center of the Footing for Tests #1-5 on 11 Nov 05

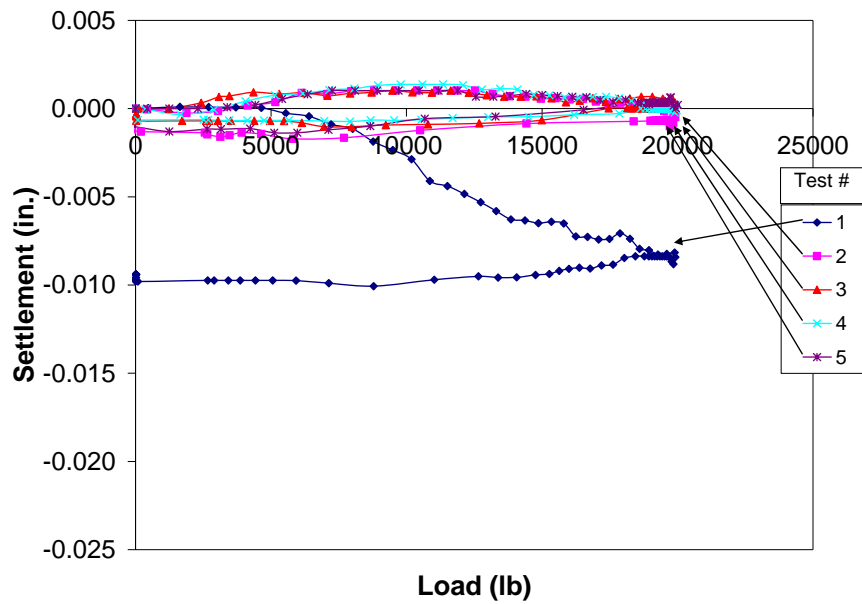


Figure A.20: Measured Settlements at 30 in. Beneath the Center of the Footing for Tests #1-5 on 11 Nov 05

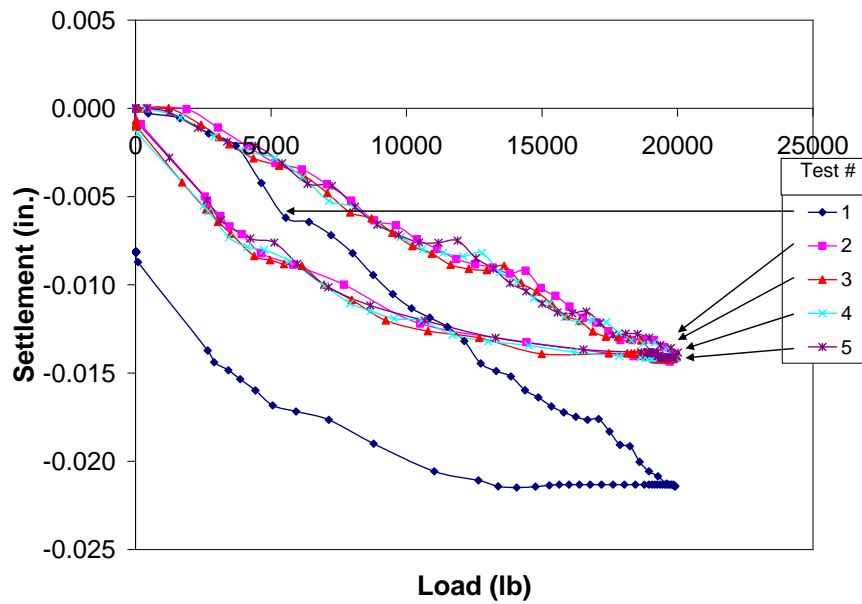


Figure A.21: Measured Settlements at the Perimeter of the Surface of the Footing for Tests #1-5 on 11 Nov 05

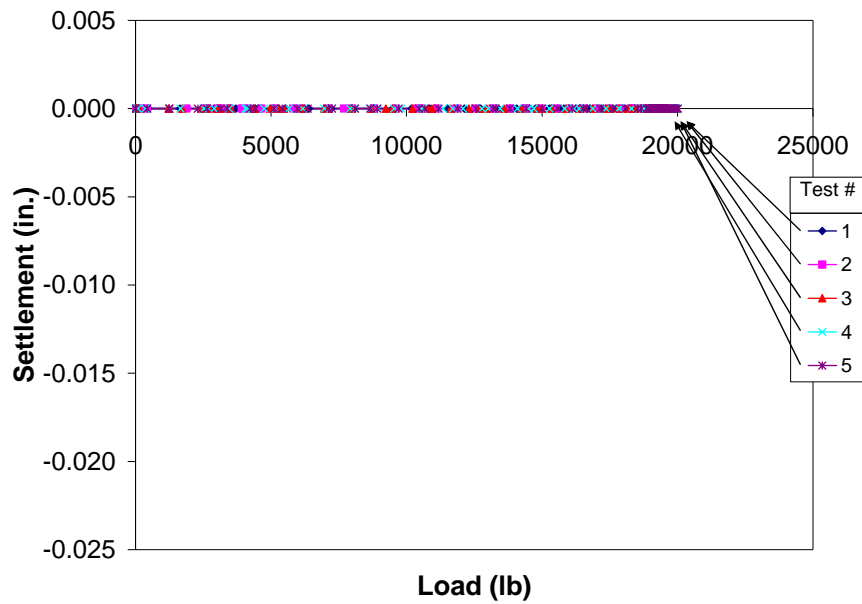


Figure A.22: Measured Settlements at 6 in. Beneath the Perimeter of the Footing for Tests #1-5 on 11 Nov 05

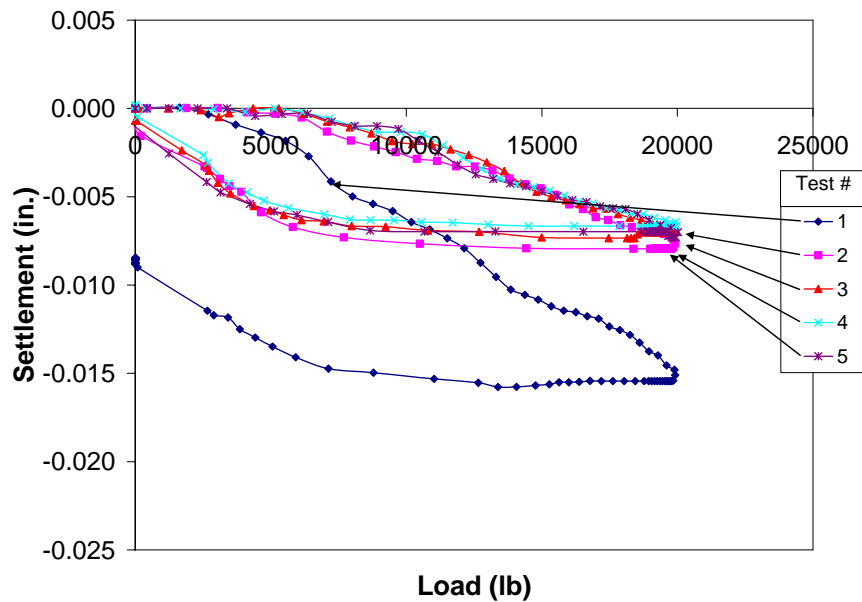


Figure A.23: Measured Settlements at 12 in. Beneath the Perimeter of the Footing for Tests #1-5 on 11 Nov 05

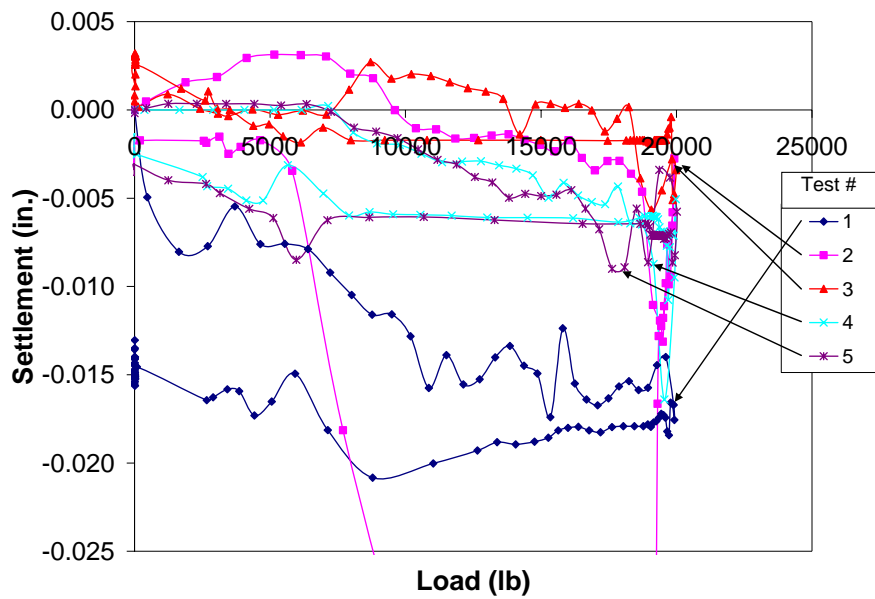


Figure A.24: Measured Settlements at 18 in. Beneath the Perimeter of the Footing for Tests #1-5 on 11 Nov 05

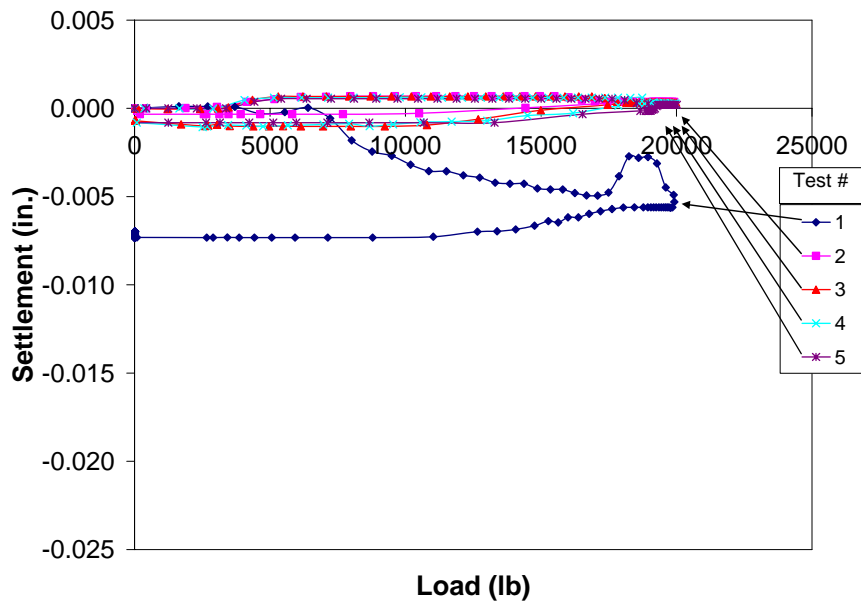


Figure A.25: Measured Settlements at 30 in. Beneath the Perimeter of the Footing for Tests #1-5 on 11 Nov 05

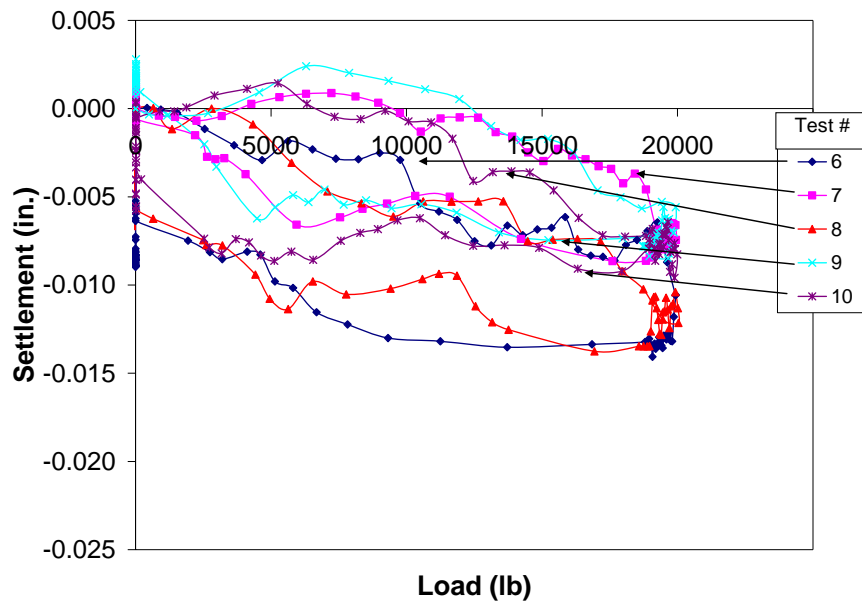


Figure A.26: Measured Settlements at the Center of the Surface of the Footing for Tests #6-10 on 11 Nov 05

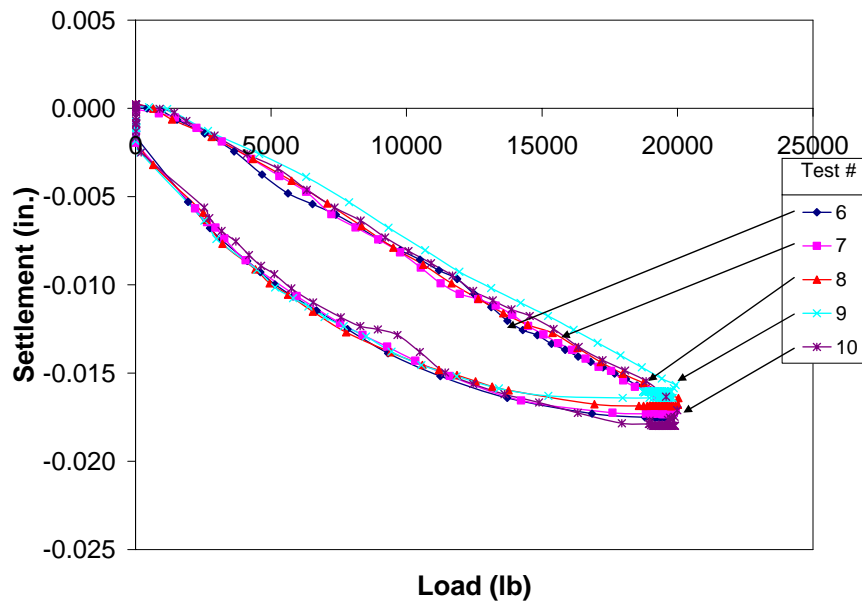


Figure A.27: Measured Settlements at 6 in. Beneath the Center of the Footing for Tests #6-10 on 11 Nov 05

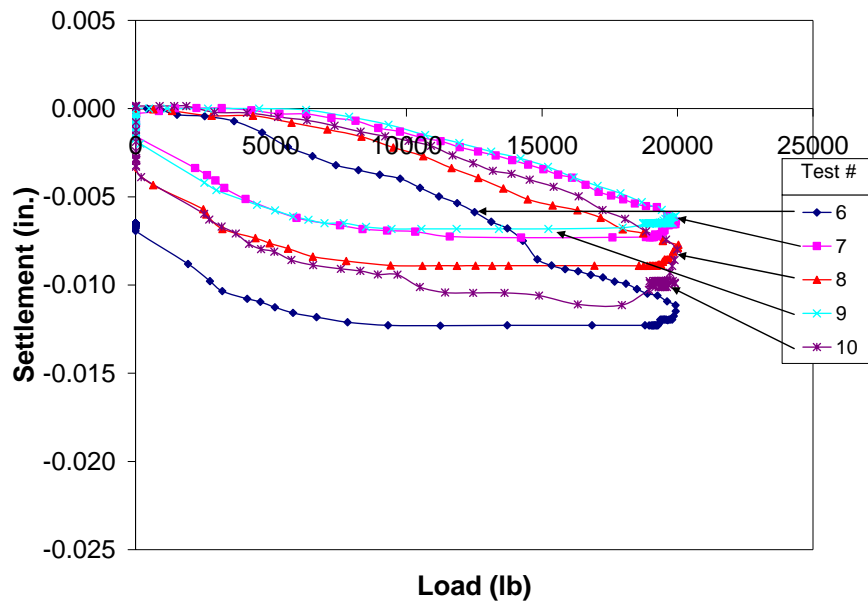


Figure A.28: Measured Settlements at 12 in. Beneath the Center of the Footing for Tests #6-10 on 11 Nov 05

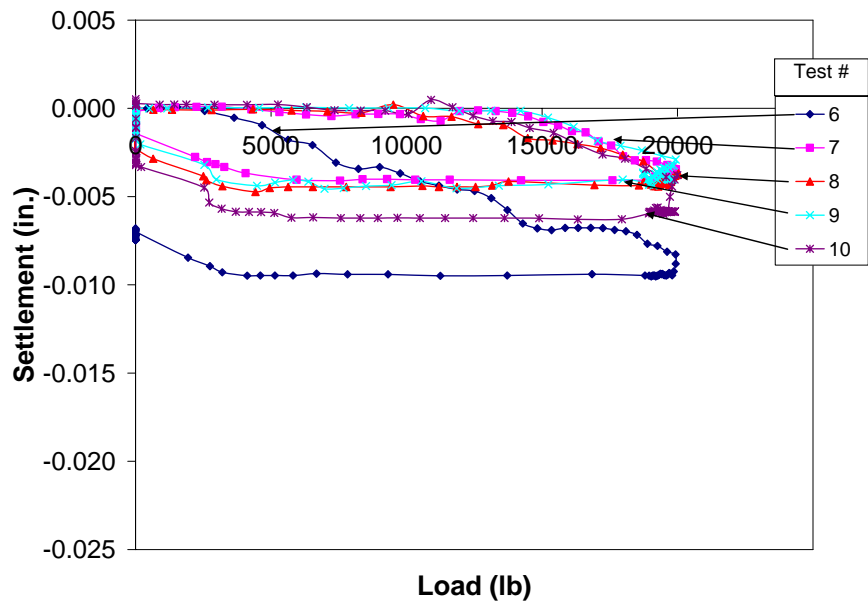


Figure A.29: Measured Settlements at 18 in. Beneath the Center of the Footing for Tests #6-10 on 11 Nov 05



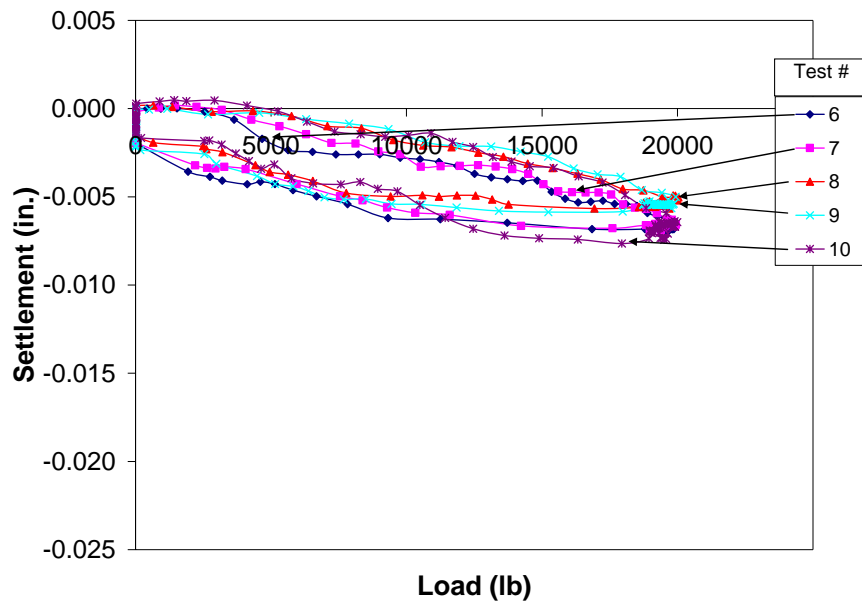


Figure A.30: Measured Settlements at 30 in. Beneath the Center of the Footing for Tests #6-10 on 11 Nov 05

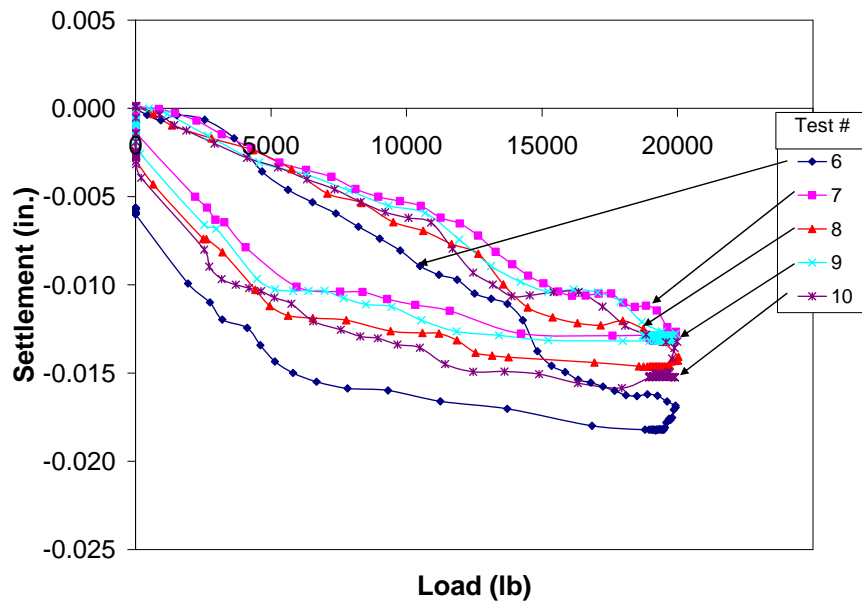


Figure A.31: Measured Settlements at the Perimeter of the Surface of the Footing for Tests #6-10 on 11 Nov 05

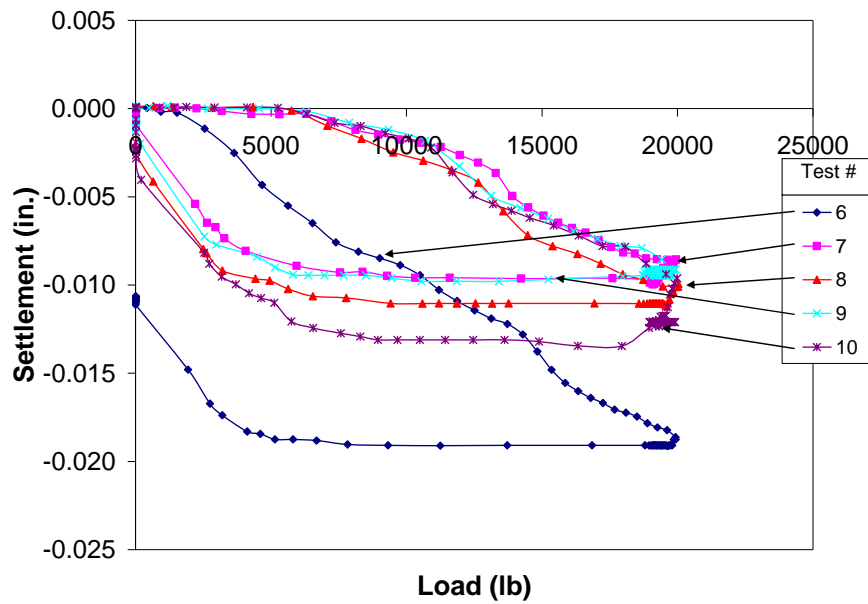


Figure A.32: Measured Settlements at 6 in. Beneath the Perimeter of the Footing for Tests #6-10 on 11 Nov 05

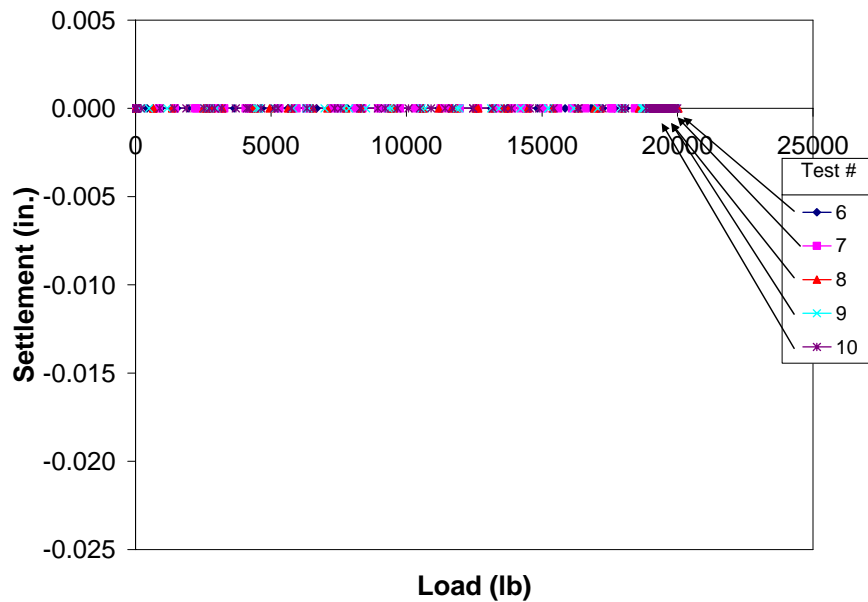


Figure A.33: Measured Settlements at 12 in. Beneath the Perimeter of the Footing for Tests #6-10 on 11 Nov 05

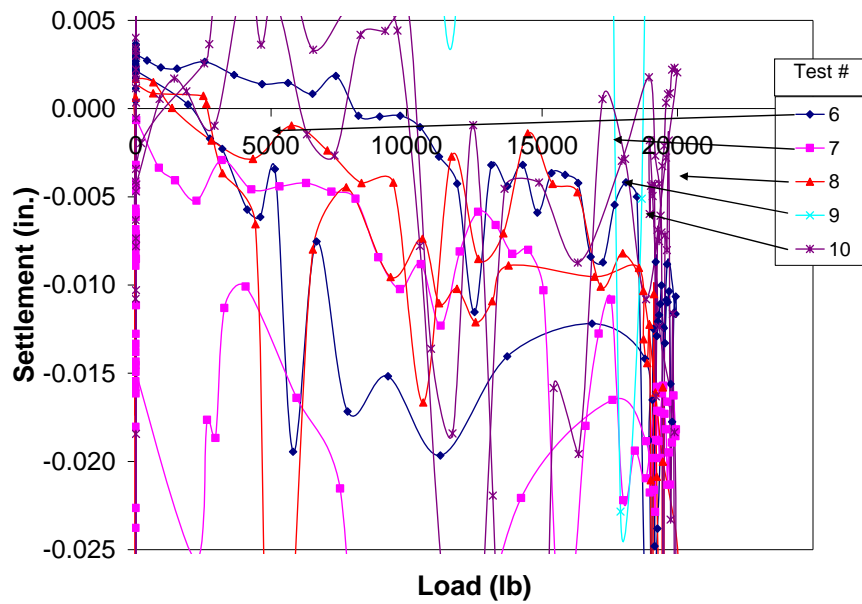


Figure A.34: Measured Settlements at 18 in. Beneath the Perimeter of the Footing for Tests #6-10 on 11 Nov 05

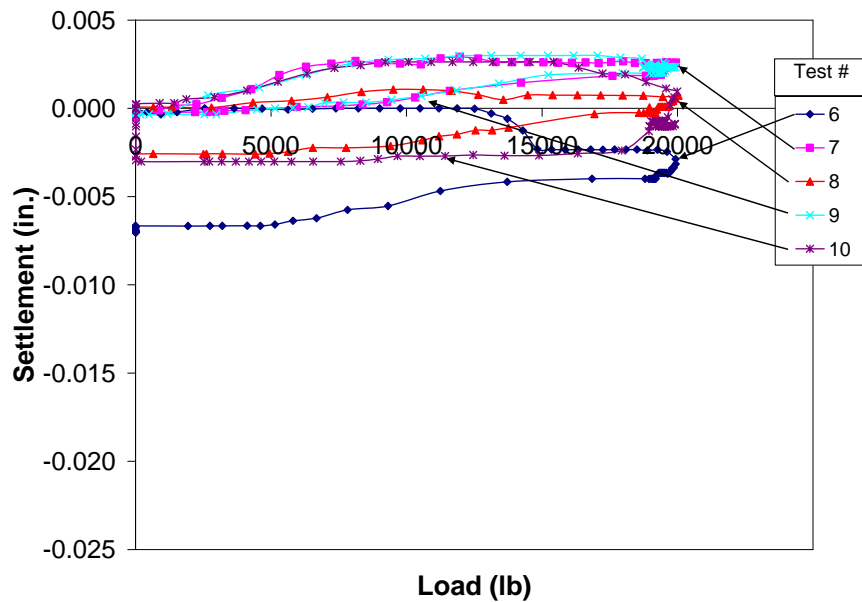


Figure A.35: Measured Settlements at 30 in. Beneath the Perimeter of the Footing for Tests #6-10 on 11 Nov 05

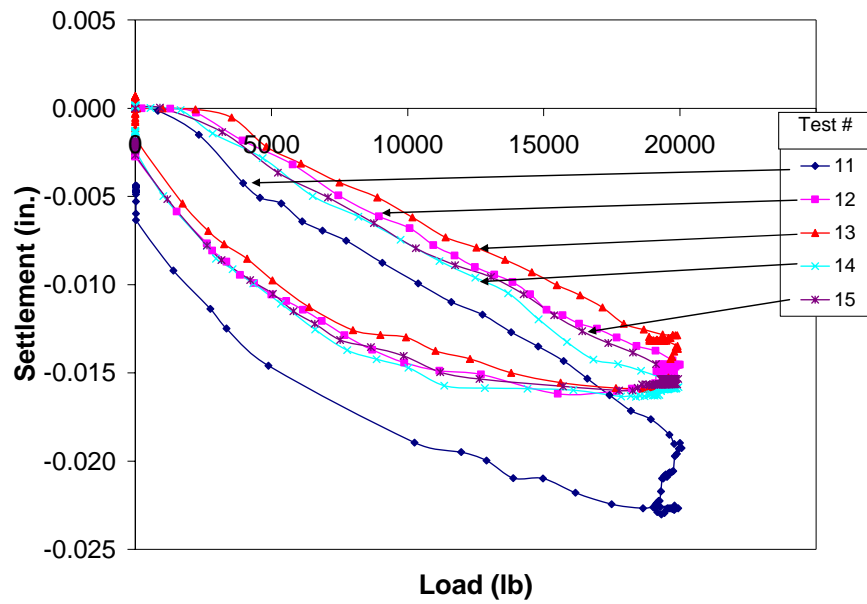


Figure A.36: Measured Settlements at the Center of the Surface of the Footing for Tests #11-15 on 11 Nov 05

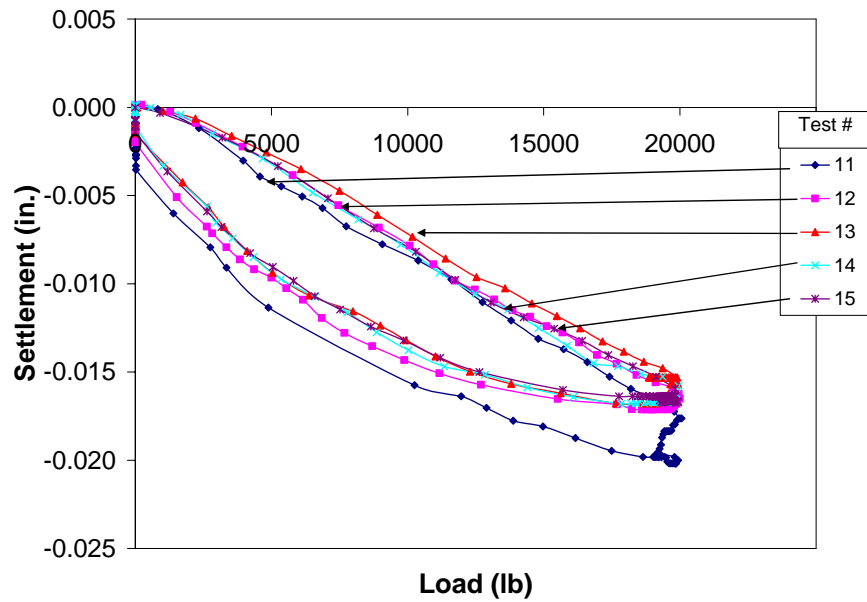


Figure A.37: Measured Settlements at 6 in. Beneath the Center of the Footing for Tests #11-15 on 11 Nov 05

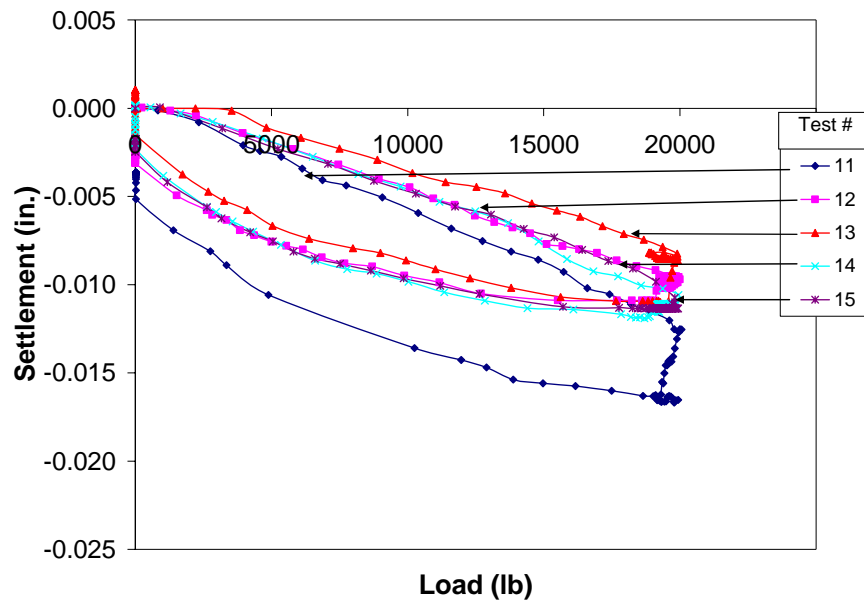


Figure A.38: Measured Settlements at 12 in. Beneath the Center of the Footing for Tests #11-15 on 11 Nov 05

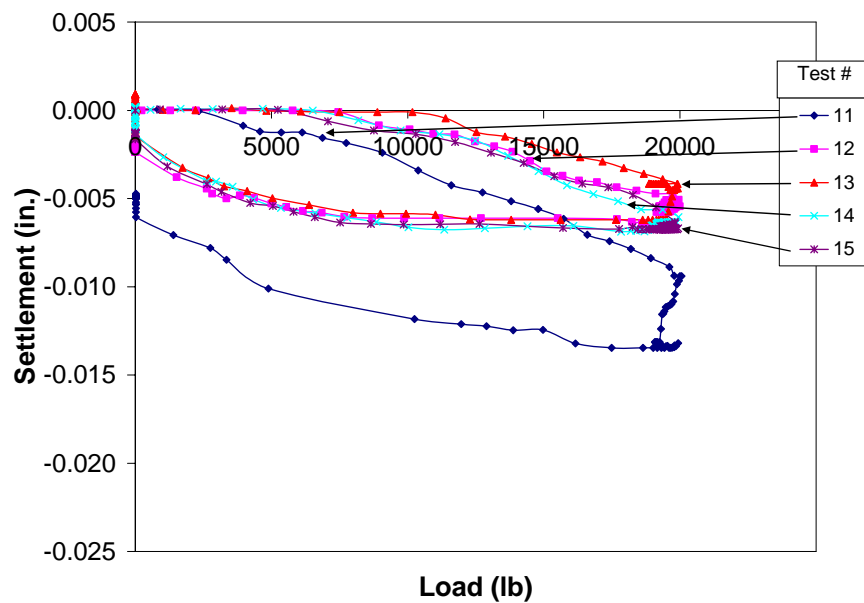


Figure A.39: Measured Settlements at 18 in. Beneath the Center of the Footing for Tests #11-15 on 11 Nov 05

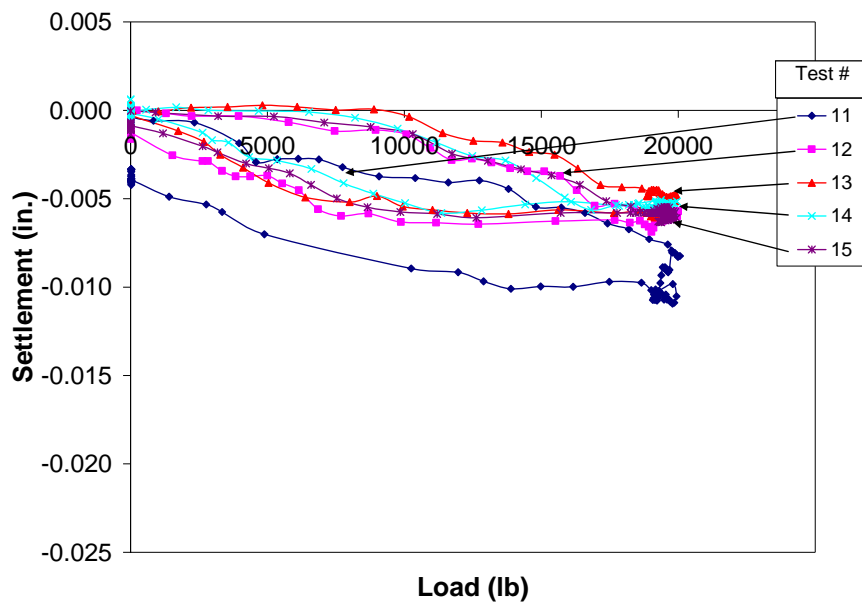


Figure A.40: Measured Settlements at 30 in. Beneath the Center of the Footing for Tests #11-15 on 11 Nov 05

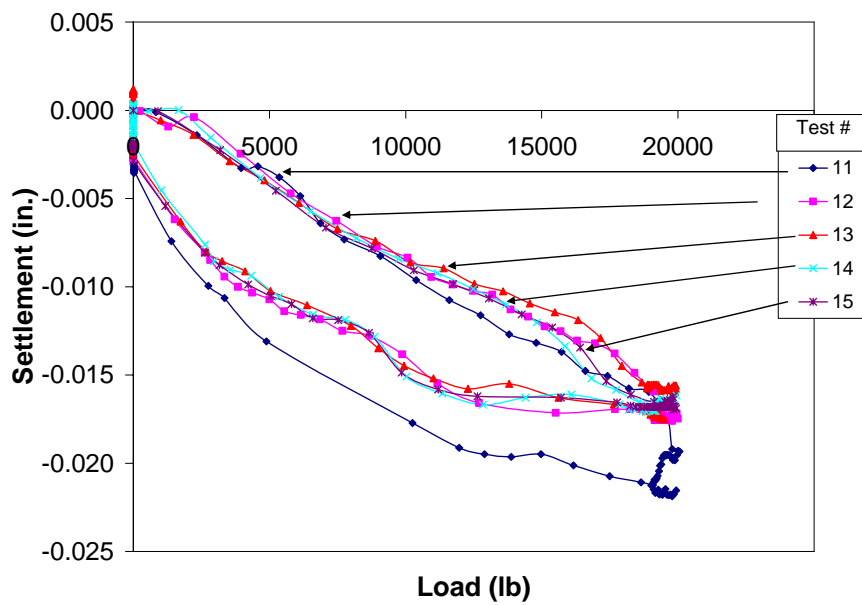


Figure A.41: Measured Settlements at the Perimeter of the Surface of the Footing for Tests #11-15 on 11 Nov 05

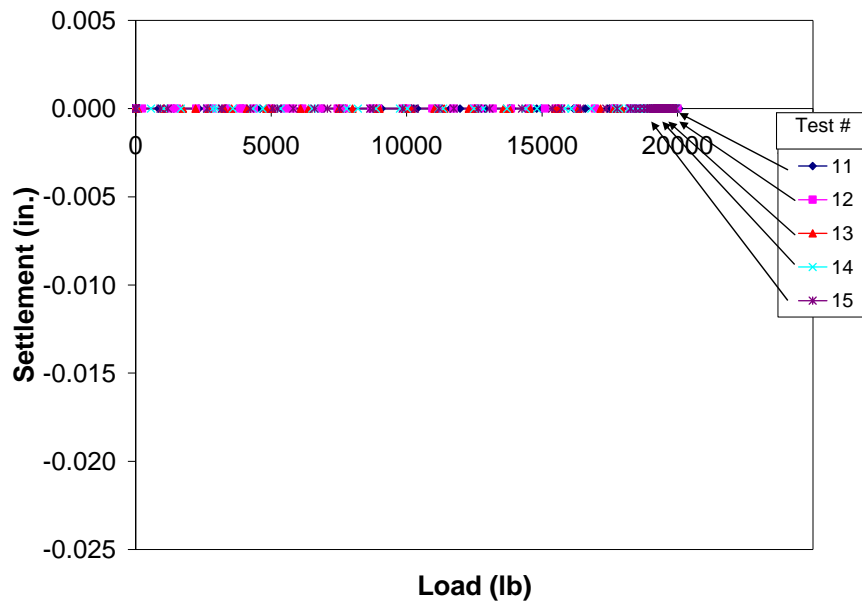


Figure A.42: Measured Settlements at 6 in. Beneath the Perimeter of the Footing for Tests #11-15 on 11 Nov 05

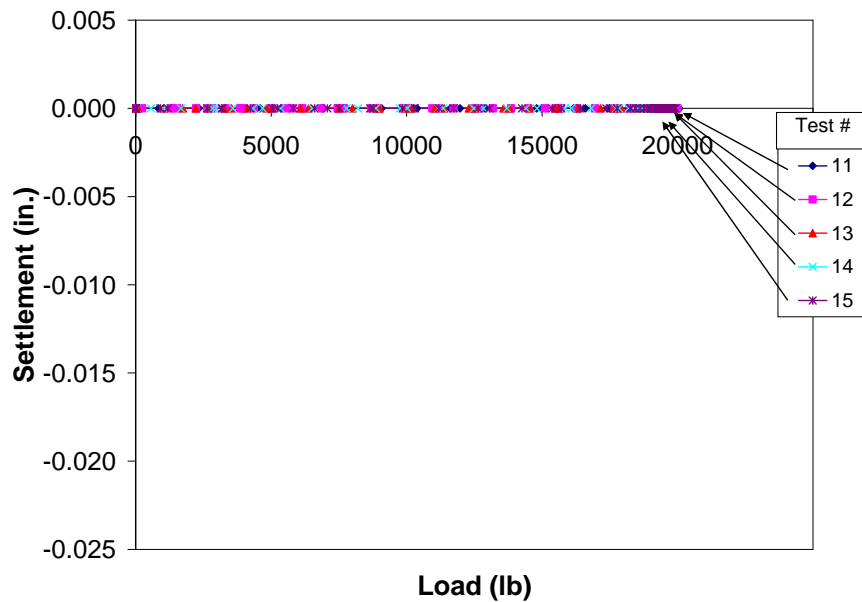


Figure A.43: Measured Settlements at 12 in. Beneath the Perimeter of the Footing for Tests #11-15 on 11 Nov 05

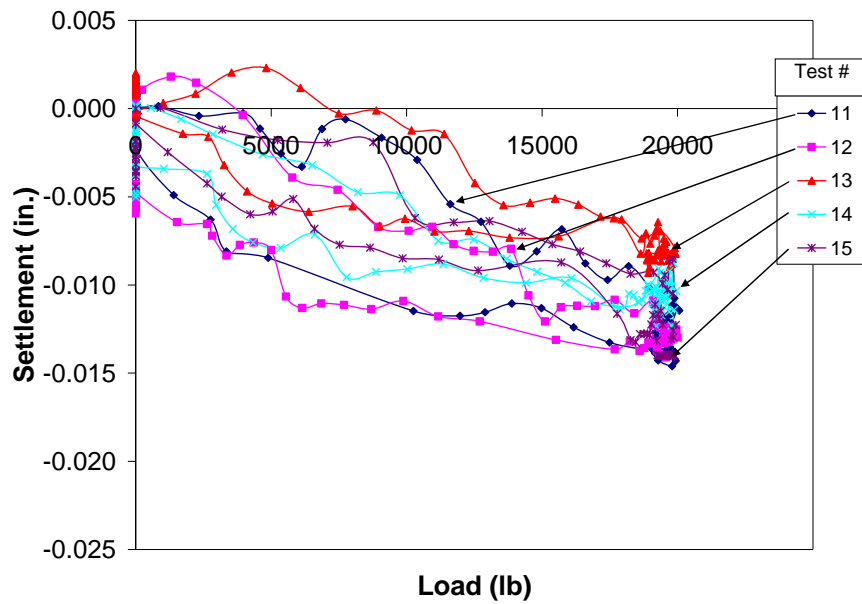


Figure A.44: Measured Settlements at 18 in. Beneath the Perimeter of the Footing for Tests #11-15 on 11 Nov 05

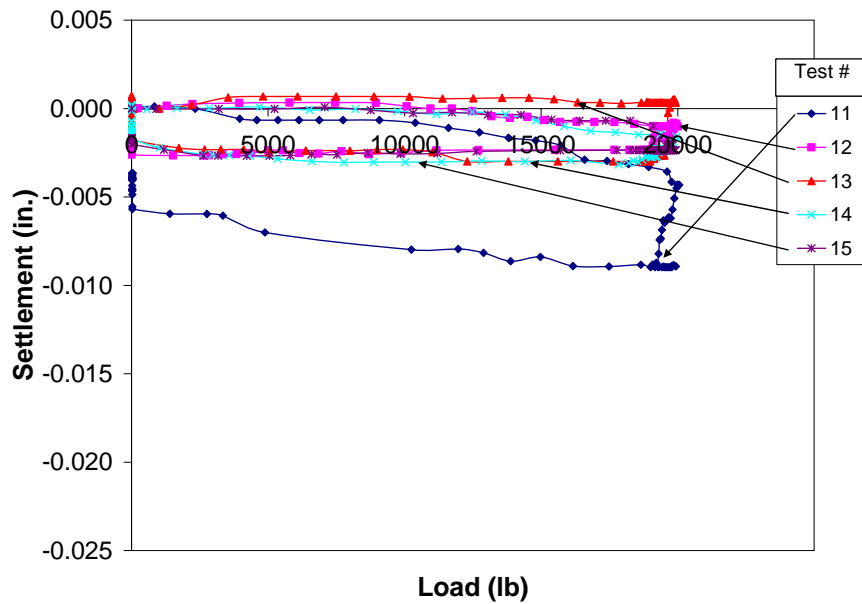


Figure A.45: Measured Settlements at 30 in. Beneath the Perimeter of the Footing for Tests #11-15 on 11 Nov 05



## **APPENDIX B**

### **INSTRUMENT CALIBRATION DATA**

#### **INTRODUCTION**

In this appendix, the calibration data is given for the load cell and linear potentiometers used in this study.

#### **SECTION 1- LOAD CELL**

The calibration factor for the 50-kip load cell used in this study is given. Additionally, the warranty information provided by the manufacturer is presented.

#### **SECTION 2- LINEAR POTENTIOMETERS**

Each Linear Potentiometer was calibrated twice, once before testing and once after testing. The data presented is from the calibration tests done after testing. Several linear potentiometers were damaged during the course of this project. The calibration data for those linear pots (i.e. linear pots #3 and #4) is not given since the data from those linear pots was not used.

Each linear potentiometer was calibrated with the VXI multi-channel analyzer and the power source used in the field. Further, one channel on the VXI was designated for each linear potentiometer. The linear pot was calibrated and used in the field on the same channel.

First, the results of each calibration test are presented graphically for each linear potentiometer. Then, the data gather during calibration is presented in tabular form.

## APPENDIX B

### SECTION 1

#### LOAD CELL

Interface Load Cell (Capacity 50-kips)  
Calibration Factor

Performance:

	Compression
Rated Output	- 4.1966 mV/V
SED Output	- 4.1959 mV/V

Shrunt:

	Compression
Output	-2.9048 mV/V

## TWO YEAR WARRANTY

Interface, Inc. hereby warrants all products of its manufacture as follows: Commencing with the date of shipment of each load cell to the original purchaser, and for a period expiring two years from said date, Interface, Inc. warrants that each unit shall remain free from defects in parts, materials, and workmanship.

The warranties herein shall not obligate Interface, Inc. in any manner whatsoever with respect to, and shall not be applicable to, any defects which after inspection by Interface, Inc. are not to Interface, Inc.'s reasonable satisfaction demonstrably the result of defective parts, materials or workmanship. Interface is not liable for consequential or contingent damages. Its liability is strictly limited to the original purchase price of the product or its repair or replacement at Interface's option. The factory should be immediately notified of suspected warranty claims. All transportation, handling, customs clearance and insurance charges for returned merchandise are to be prepaid and borne by customer.

The foregoing warranty is in lieu of any and all other warranties or guarantees expressed or implied and of all other obligations on the part of Interface, Inc. whether in contract or in tort. This warranty shall be void on any Interface product which has been subject to misuse, negligence or accident, or has been installed, adjusted or used otherwise than in accordance with the instructions furnished by Interface, Inc.

## CERTIFICATION

Interface, Inc. certifies that this load cell was thoroughly tested and inspected and found to meet its published specifications when shipped from the factory. Interface, Inc. further certifies that its calibration measurements are traceable to NIST.

## INSTALLATION

See Installation Information Sheet for instructions.

## WIRING

CONNECTOR		CABLE (ALL MODELS)	
PIN	FUNCTION	COLOR	FUNCTION
A	• Excitation	Red	• Excitation
B	• Output (positive reading)	Green	• Output
C	• Output (or tension)	White	• Output
D	Excitation	Black	Excitation
E	No Connection	White/Red	• Sense
F	No Connection	White/Black	• Sense
		White/Yellow	Shunt Cal
		Shield	No Connection

**RDD Truck**  
**LT 726006**  
**Interface**  
**Load Cell**

**CALIBRATION  
CERTIFICATION**

**WARRANTY**

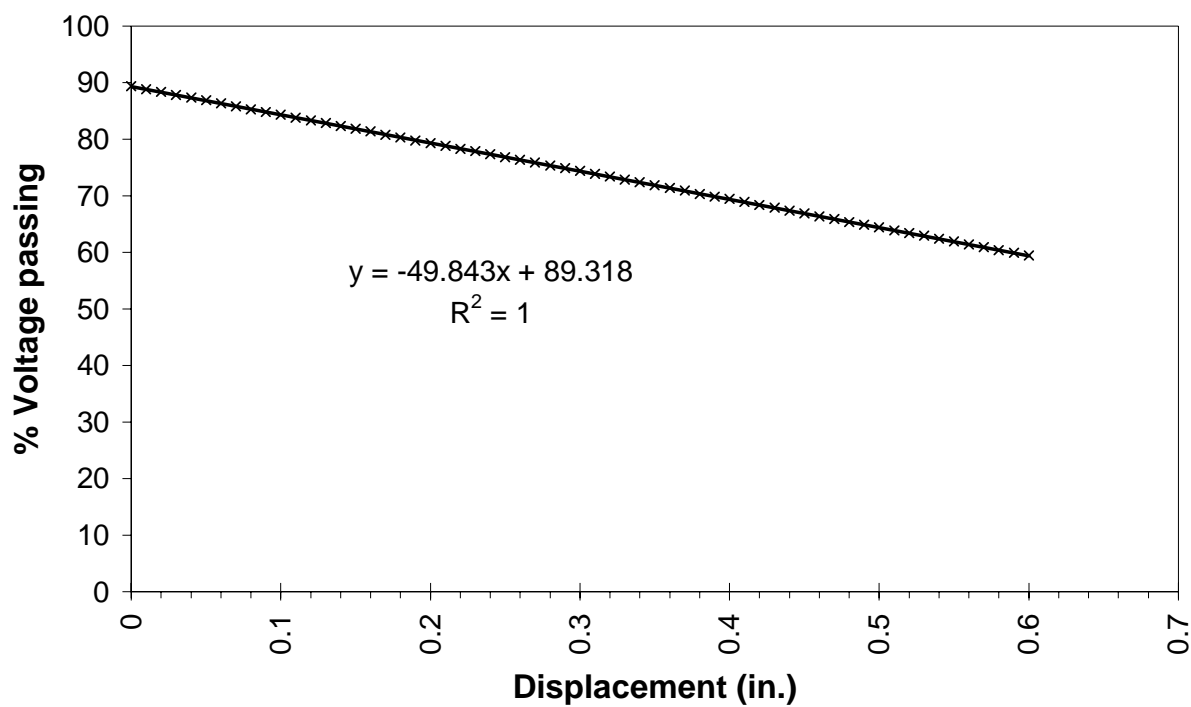
**INSTALLATION  
INFORMATION**

**APPENDIX B**

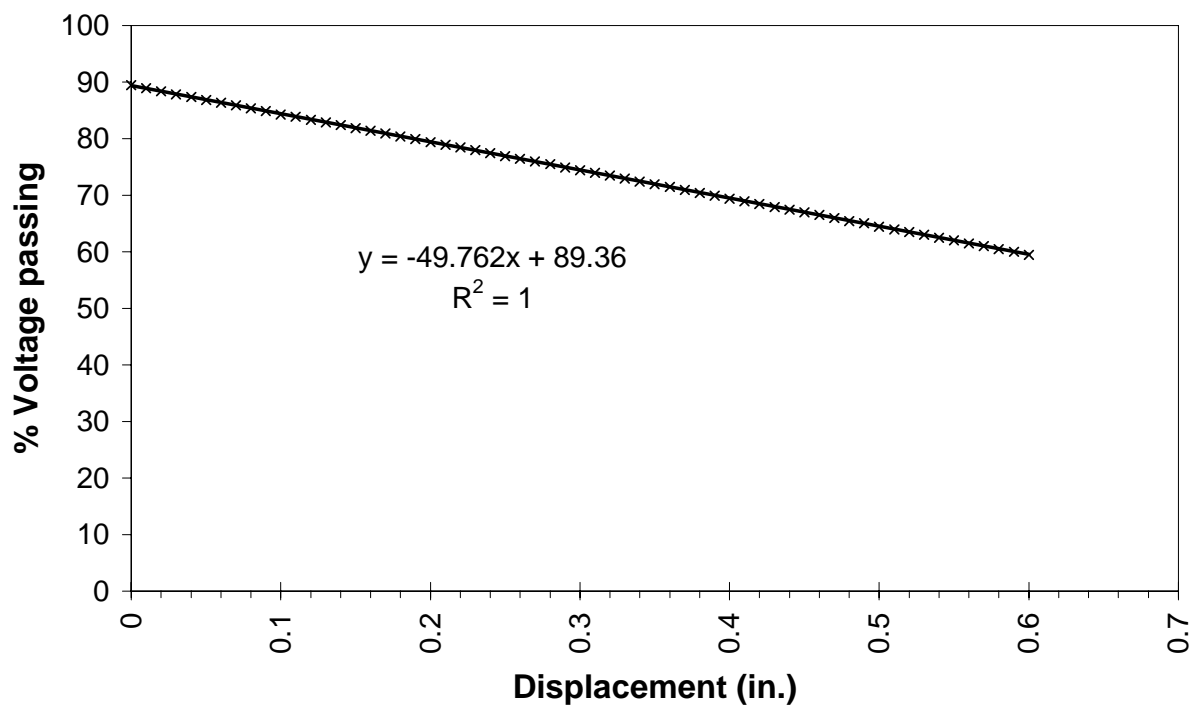
**SECTION 2**

**LINEAR POTENTIOMETERS**

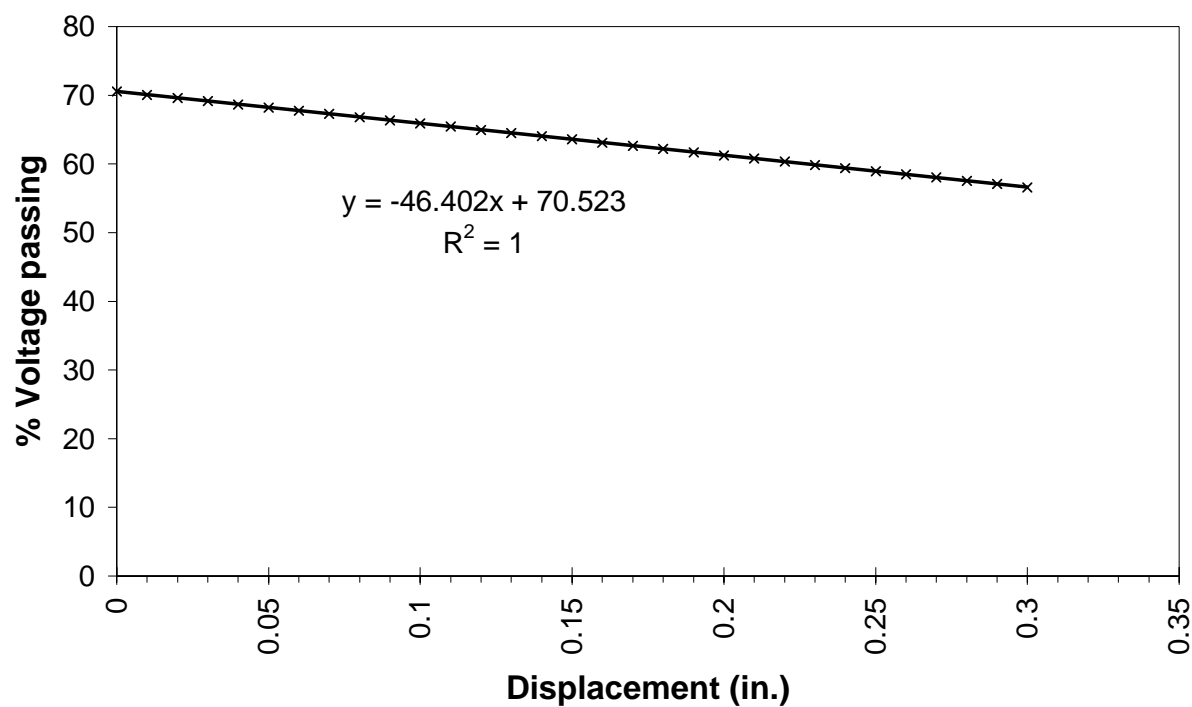
### Linear Pot Calibration (LP #1)



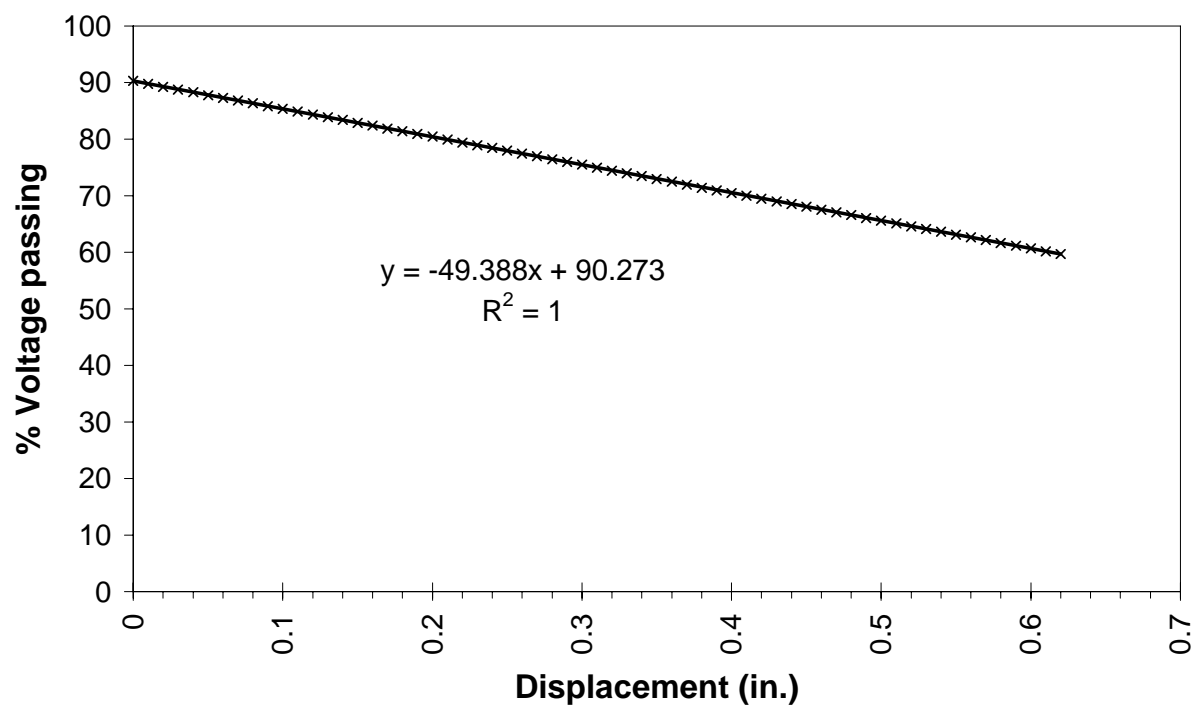
### Linear Pot Calibration (LP #2)



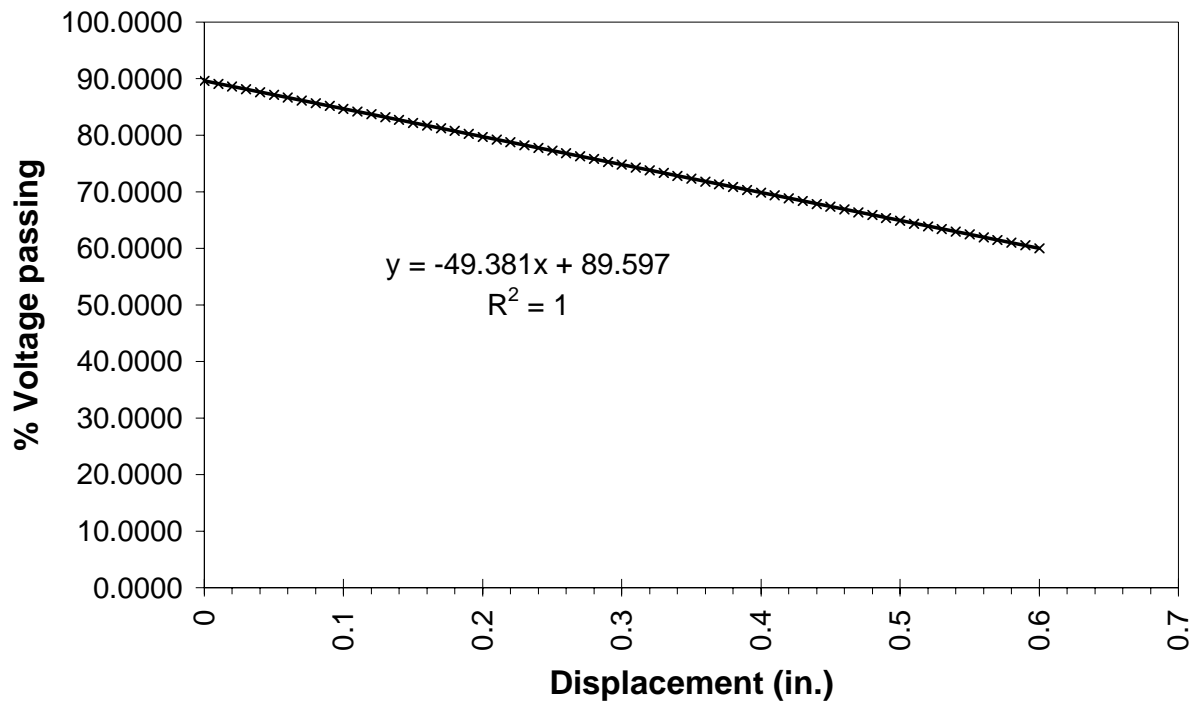
### Linear Pot Calibration (LP #6)



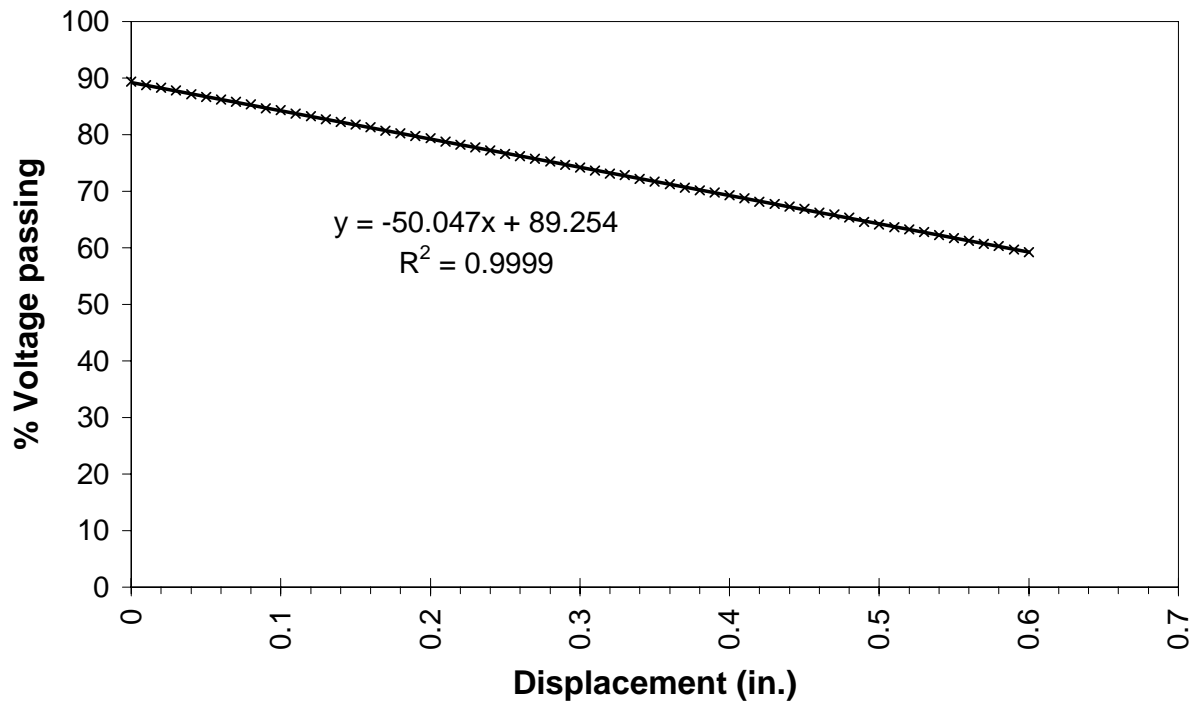
### Linear Pot Calibration (LP #7)



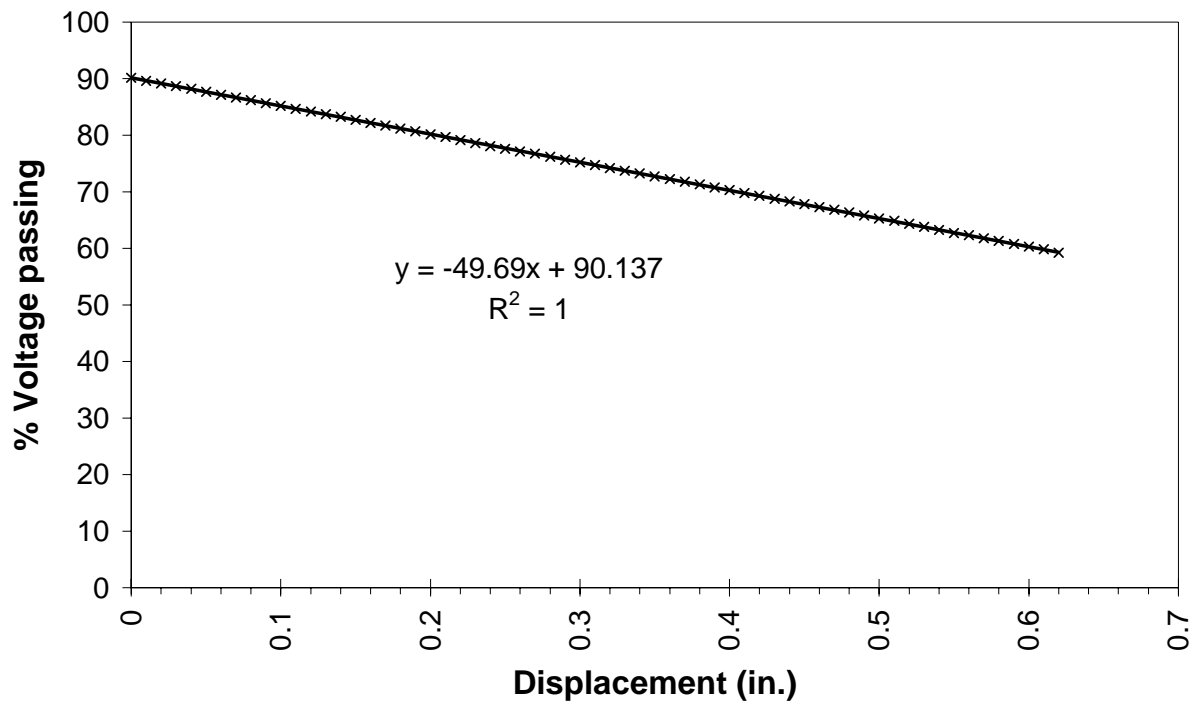
### Linear Pot Calibration (LP #8)



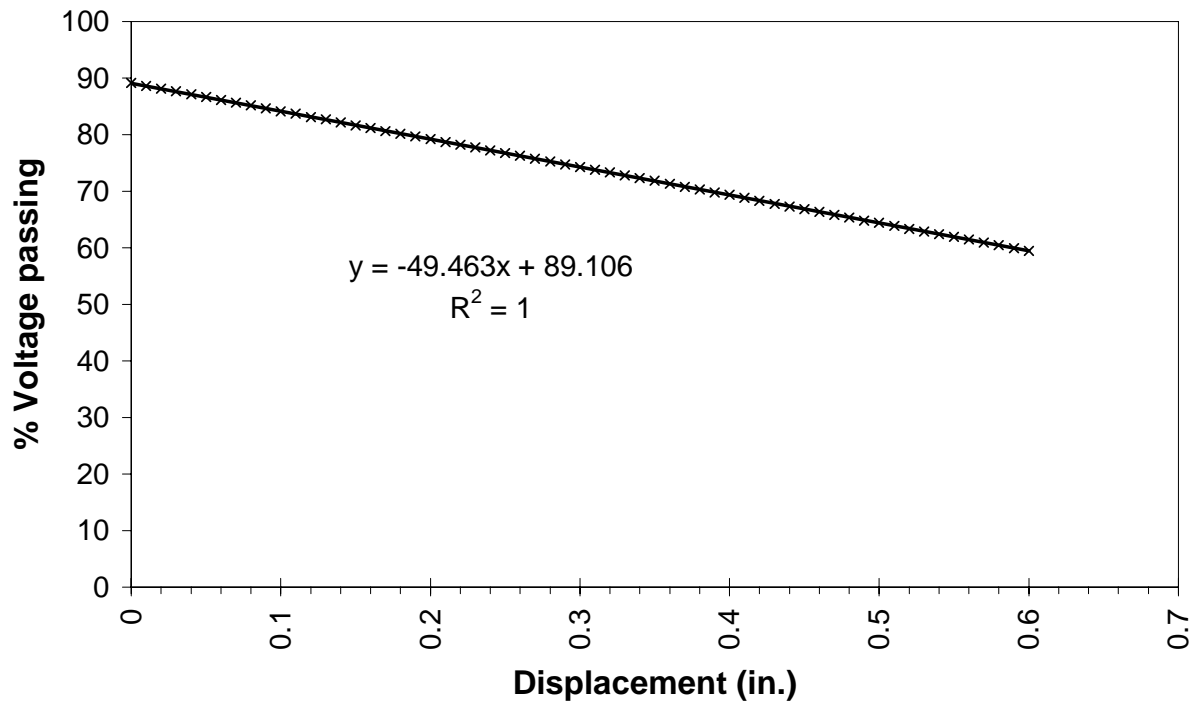
### Linear Pot Calibration (LP #9)



### Linear Pot Calibration (LP #10)



### Linear Pot Calibration (LP #12)





Linear Pot #	1						+/- in.	%
Channel #	50				AVG ERROR MAX ERROR		0.00053 0.0015	0.02630 0.0771
		Slope	49.843					
Micrometer Reading (in)	Power Source (Volts)	Linear Pot (Volts)	% of Source	% difference (in)	Calc pos. (in)	Delta (in)	Error (in)	Error (%)
0	10.099	9.0227	89.3425		0.00000			
				-0.4991		0.01001	0.00001	0.00071
0.01	10.107	8.9794	88.8434		0.01001			
				-0.5016		0.01006	0.00006	0.00322
0.02	10.119	8.9393	88.3417		0.02008			
				-0.5077		0.01019	0.00019	0.00929
0.03	10.111	8.8809	87.8340		0.03026			
				-0.4412		0.00885	0.00115	0.05738
0.04	10.122	8.8459	87.3928		0.03912			
				-0.5314		0.01066	0.00066	0.03305
0.05	10.132	8.8008	86.8614		0.04978			
				-0.5035		0.01010	0.00010	0.00512
0.06	10.137	8.7541	86.3579		0.05988			
				-0.5394		0.01082	0.00082	0.04109
0.07	10.226	8.7758	85.8185		0.07070			
				-0.5150		0.01033	0.00033	0.01663
0.08	10.231	8.7274	85.3035		0.08103			
				-0.4822		0.00967	0.00033	0.01632
0.09	10.242	8.6874	84.8213		0.09071			
				-0.4967		0.00996	0.00004	0.00175
0.1	10.239	8.634	84.3246		0.10067			
				-0.5057		0.01015	0.00015	0.00732
0.11	10.249	8.5906	83.8189		0.11082			
				-0.5126		0.01028	0.00028	0.01417
0.12	10.256	8.5439	83.3064		0.12110			
				-0.4723		0.00948	0.00052	0.02617
0.13	10.254	8.4938	82.8340		0.13058			
				-0.5117		0.01027	0.00027	0.01331
0.14	10.257	8.4438	82.3223		0.14085			
				-0.4872		0.00977	0.00023	0.01125
0.15	10.261	8.3971	81.8351		0.15062			
				-0.4651		0.00933	0.00067	0.03344
0.16	10.416	8.4755	81.3700		0.15995			
				-0.5599		0.01123	0.00123	0.06163
0.17	10.418	8.4188	80.8101		0.17118			
				-0.5040		0.01011	0.00011	0.00561
0.18	10.421	8.3687	80.3061		0.18130			
				-0.5027		0.01009	0.00009	0.00432
0.19	10.426	8.3203	79.8034		0.19138			
				-0.4697		0.00942	0.00058	0.02886
0.2	10.431	8.2753	79.3337		0.20081			
				-0.5108		0.01025	0.00025	0.01236
0.21	10.433	8.2236	78.8230		0.21105			
				-0.4927		0.00988	0.00012	0.00578
0.22	10.439	8.1769	78.3303		0.22094			
				-0.4562		0.00915	0.00085	0.04238
0.23	10.438	8.1285	77.8741		0.23009			
				-0.5338		0.01071	0.00071	0.03550
0.24	10.441	8.0751	77.3403		0.24080			
				-0.5319		0.01067	0.00067	0.03362
0.25	10.446	8.0234	76.8083		0.25147			
				-0.4772		0.00957	0.00043	0.02128

Linear Pot #	1						+/- in.	%
Channel #	50				AVG ERROR MAX ERROR		0.00053 0.0015	0.02630 0.0771
		Slope	49.843					
Micrometer Reading (in)	Power Source (Volts)	Linear Pot (Volts)	% of Source	% difference (in)	Calc pos. (in)	Delta (in)	Error (in)	Error (%)
0.26	10.461	7.985	76.3311		0.26105			
				-0.4566		0.00916	0.00084	0.04191
0.27	10.469	7.9433	75.8745		0.27021			
				-0.5407		0.01085	0.00085	0.04241
0.28	10.471	7.8882	75.3338		0.28106			
				-0.4441		0.00891	0.00109	0.05454
0.29	10.473	7.8432	74.8897		0.28997			
				-0.4672		0.00937	0.00063	0.03130
0.3	10.476	7.7965	74.4225		0.29934			
				-0.5753		0.01154	0.00154	0.07712
0.31	10.483	7.7414	73.8472		0.31088			
				-0.4328		0.00868	0.00132	0.06583
0.32	10.488	7.6997	73.4144		0.31957			
				-0.5356		0.01075	0.00075	0.03729
0.33	10.501	7.653	72.8788		0.33031			
				-0.4764		0.00956	0.00044	0.02205
0.34	10.494	7.5979	72.4023		0.33987			
				-0.5092		0.01022	0.00022	0.01078
0.35	10.501	7.5495	71.8932		0.35009			
				-0.4965		0.00996	0.00004	0.00189
0.36	10.504	7.4995	71.3966		0.36005			
				-0.4942		0.00991	0.00009	0.00427
0.37	10.516	7.4561	70.9024		0.36996			
				-0.5581		0.01120	0.00120	0.05989
0.38	10.514	7.396	70.3443		0.38116			
				-0.4774		0.00958	0.00042	0.02110
0.39	10.519	7.3493	69.8669		0.39074			
				-0.4426		0.00888	0.00112	0.05598
0.4	10.526	7.3076	69.4243		0.39962			
				-0.5029		0.01009	0.00009	0.00446
0.41	10.523	7.2526	68.9214		0.40971			
				-0.5626		0.01129	0.00129	0.06436
0.42	10.529	7.1975	68.3588		0.42100			
				-0.4855		0.00974	0.00026	0.01300
0.43	10.533	7.1491	67.8734		0.43074			
				-0.4912		0.00985	0.00015	0.00725
0.44	10.543	7.1041	67.3821		0.44059			
				-0.5069		0.01017	0.00017	0.00851
0.45	10.548	7.054	66.8752		0.45076			
				-0.5283		0.01060	0.00060	0.03000
0.46	10.539	6.9923	66.3469		0.46136			
				-0.4592		0.00921	0.00079	0.03931
0.47	10.539	6.9439	65.8877		0.47057			
				-0.5052		0.01013	0.00013	0.00675
0.48	10.549	6.8972	65.3825		0.48071			
				-0.4872		0.00978	0.00022	0.01124
0.49	10.551	6.8471	64.8953		0.49048			
				-0.5083		0.01020	0.00020	0.00991
0.5	10.554	6.7954	64.3870		0.50068			

Linear Pot #	1						+/- in.	%
Channel #	50				AVG ERROR		0.00053	0.02630
		Slope	49.843	MAX ERROR		0.0015		0.0771
Micrometer Reading (in)	Power Source (Volts)	Linear Pot (Volts)	% of Source	% difference (in)	Calc pos. (in)	Delta (in)	Error (in)	Error (%)
				-0.5010		0.01005	0.00005	0.00254
0.51	10.561	6.747	63.8860		0.51073			
				-0.4981		0.00999	0.00001	0.00031
0.52	10.573	6.702	63.3879		0.52073			
				-0.4795		0.00962	0.00038	0.01900
0.53	10.566	6.6469	62.9084		0.53035			
				-0.5289		0.01061	0.00061	0.03058
0.54	10.578	6.5985	62.3795		0.54096			
				-0.4332		0.00869	0.00131	0.06545
0.55	10.574	6.5502	61.9463		0.54965			
				-0.5604		0.01124	0.00124	0.06215
0.56	10.578	6.4934	61.3859		0.56089			
				-0.4542		0.00911	0.00089	0.04436
0.57	10.583	6.4484	60.9317		0.57001			
				-0.5279		0.01059	0.00059	0.02960
0.58	10.576	6.3883	60.4037		0.58060			
				-0.4529		0.00909	0.00091	0.04567
0.59	10.578	6.3416	59.9508		0.58968			
				-0.5137		0.01031	0.00031	0.01536
0.6	10.588	6.2932	59.4371		0.59999			

Linear Pot #	2						+/- in.	%
Channel #	51				AVG ERROR MAX ERROR		0.00052 0.0022	0.02607 0.1124
		Slope	49.762					
Micrometer Reading (in)	Power Source (Volts)	Linear Pot (Volts)	% of Source	% difference (in)	Calc pos. (in)	Delta (in)	Error (%)	Error (in)
0	10.042	8.981	89.4344		0.00000			
				-0.5325		0.01070	0.00070	0.03509
0.01	10.044	8.9293	88.9018		0.01070			
				-0.5147		0.01034	0.00034	0.01720
0.02	10.044	8.8776	88.3871		0.02105			
				-0.5317		0.01068	0.00068	0.03420
0.03	10.044	8.8242	87.8554		0.03173			
				-0.4973		0.00999	0.00001	0.00028
0.04	10.042	8.7725	87.3581		0.04172			
				-0.5577		0.01121	0.00121	0.06037
0.05	10.045	8.7191	86.8004		0.05293			
				-0.4404		0.00885	0.00115	0.05751
0.06	10.044	8.674	86.3600		0.06178			
				-0.4978		0.01000	0.00000	0.00019
0.07	10.044	8.624	85.8622		0.07179			
				-0.4819		0.00968	0.00032	0.01582
0.08	10.044	8.5756	85.3803		0.08147			
				-0.4903		0.00985	0.00015	0.00732
0.09	10.045	8.5272	84.8900		0.09132			
				-0.5895		0.01185	0.00185	0.09232
0.1	10.05	8.4722	84.3005		0.10317			
				-0.4404		0.00885	0.00115	0.05748
0.11	10.049	8.4271	83.8601		0.11202			
				-0.4899		0.00985	0.00015	0.00774
0.12	10.044	8.3737	83.3702		0.12186			
				-0.5230		0.01051	0.00051	0.02548
0.13	10.045	8.322	82.8472		0.13237			
				-0.4808		0.00966	0.00034	0.01692
0.14	10.049	8.277	82.3664		0.14204			
				-0.4823		0.00969	0.00031	0.01543
0.15	10.047	8.2269	81.8841		0.15173			
				-0.4815		0.00968	0.00032	0.01624
0.16	10.045	8.1769	81.4027		0.16140			
				-0.4988		0.01002	0.00002	0.00114
0.17	10.045	8.1268	80.9039		0.17142			
				-0.4969		0.00999	0.00001	0.00070
0.18	10.049	8.0801	80.4070		0.18141			
				-0.5086		0.01022	0.00022	0.01099
0.19	10.044	8.025	79.8984		0.19163			
				-0.4887		0.00982	0.00018	0.00899
0.2	10.047	7.9783	79.4098		0.20145			
				-0.4741		0.00953	0.00047	0.02364
0.21	10.044	7.9283	78.9357		0.21098			
				-0.5053		0.01015	0.00015	0.00772
0.22	10.047	7.8799	78.4304		0.22113			
				-0.4803		0.00965	0.00035	0.01737

Linear Pot #	2						+/- in.	%
Channel #	51				AVG ERROR MAX ERROR		0.00052 0.0022	0.02607 0.1124
		Slope	49.762					
Micrometer Reading (in)	Power Source (Volts)	Linear Pot (Volts)	% of Source	% difference (in)	Calc pos. (in)	Delta (in)	Error (%)	Error (in)
0.23	10.049	7.8332	77.9500		0.23079			
				-0.4734		0.00951	0.00049	0.02431
0.24	10.05	7.7864	77.4766		0.24030	0.01084	0.00084	0.04219
				-0.5396				
0.25	10.049	7.7314	76.9370		0.25114	0.00949	0.00051	0.02541
				-0.4723				
0.26	10.05	7.6847	76.4647		0.26063	0.01063	0.00063	0.03126
				-0.5287				
0.27	10.054	7.6346	75.9359		0.27126	0.00939	0.00061	0.03048
				-0.4673				
0.28	10.05	7.5846	75.4687		0.28065	0.01098	0.00098	0.04887
				-0.5463				
0.29	10.052	7.5312	74.9224		0.29163	0.00968	0.00032	0.01620
				-0.4815				
0.3	10.052	7.4828	74.4409		0.30130	0.00972	0.00028	0.01399
				-0.4837				
0.31	10.05	7.4327	73.9572		0.31102	0.01019	0.00019	0.00954
				-0.5071				
0.32	10.049	7.381	73.4501		0.32121	0.01000	0.00000	0.00006
				-0.4976				
0.33	10.049	7.331	72.9525		0.33121	0.01040	0.00040	0.02016
				-0.5177				
0.34	10.054	7.2826	72.4349		0.34162	0.01005	0.00005	0.00230
				-0.4999				
0.35	10.052	7.2309	71.9349		0.35166	0.00944	0.00056	0.02776
				-0.4700				
0.36	10.055	7.1858	71.4649		0.36111	0.01091	0.00091	0.04533
				-0.5427				
0.37	10.052	7.1291	70.9222		0.37201	0.01005	0.00005	0.00271
				-0.5003				
0.38	10.05	7.0774	70.4219		0.38207	0.00996	0.00004	0.00212
				-0.4955				
0.39	10.052	7.029	69.9264		0.39203	0.01029	0.00029	0.01467
				-0.5122				
0.4	10.054	6.9789	69.4142		0.40232	0.00979	0.00021	0.01041
				-0.4873				
0.41	10.055	6.9306	68.9269		0.41211	0.00935	0.00065	0.03233
				-0.4654				
0.42	10.055	6.8838	68.4615		0.42146	0.01054	0.00054	0.02683
				-0.5243				
0.43	10.054	6.8304	67.9371		0.43200	0.00933	0.00067	0.03329
				-0.4645				
0.44	10.054	6.7837	67.4726		0.44134	0.00979	0.00021	0.01060
				-0.4871				

Linear Pot #	2						+/- in.	%
Channel #	51				AVG ERROR		0.00052	0.02607
		Slope	49.762	MAX ERROR		0.0022		0.1124
Micrometer Reading (in)	Power Source (Volts)	Linear Pot (Volts)	% of Source	% difference (in)	Calc pos. (in)	Delta (in)	Error (%)	Error (in)
0.45	10.055	6.7354	66.9856		0.45112			
				-0.4784		0.00961	0.00039	0.01930
0.46	10.052	6.6853	66.5072		0.46074			
				-0.5481		0.01102	0.00102	0.05077
0.47	10.052	6.6302	65.9590		0.47175			
				-0.5131		0.01031	0.00031	0.01551
0.48	10.057	6.5819	65.4460		0.48206			
				-0.3858		0.00775	0.00225	0.11237
0.49	10.055	6.5418	65.0602		0.48982			
				-0.6064		0.01219	0.00219	0.10935
0.5	10.059	6.4834	64.4537		0.50200			
				-0.4716		0.00948	0.00052	0.02612
0.51	10.055	6.4334	63.9821		0.51148			
				-0.5066		0.01018	0.00018	0.00903
0.52	10.059	6.385	63.4755		0.52166			
				-0.4730		0.00951	0.00049	0.02473
0.53	10.055	6.3349	63.0025		0.53117			
				-0.5266		0.01058	0.00058	0.02912
0.54	10.057	6.2832	62.4759		0.54175			
				-0.4644		0.00933	0.00067	0.03343
0.55	10.057	6.2365	62.0115		0.55108			
				-0.5638		0.01133	0.00133	0.06648
0.56	10.057	6.1798	61.4477		0.56241			
				-0.4522		0.00909	0.00091	0.04561
0.57	10.055	6.1331	60.9955		0.57150			
				-0.4934		0.00991	0.00009	0.00425
0.58	10.057	6.0847	60.5021		0.58141			
				-0.5021		0.01009	0.00009	0.00454
0.59	10.055	6.033	60.0000		0.59150			
				-0.5101		0.01025	0.00025	0.01253
0.6	10.057	5.9829	59.4899		0.60175			

Linear Pot #	6						+/- in.	%
Channel #	55				AVG ERROR	MAX ERROR	0.00061	0.03056
		Slope	49.402					
Micrometer Reading (in)	Power Source (Volts)	Linear Pot (Volts)	% of Source	% difference (in)	Calc pos. (in)	Delta (in)	Error (in)	Error (%)
0	9.995071875	7.054425	70.5790		0.00000			
				-0.5300		0.01073	0.00073	0.03640
0.01	9.991246875	6.998773438	70.0490		0.01073			
				-0.4839		0.00979	0.00021	0.01028
0.02	9.991067188	6.950304688	69.5652		0.02052			
				-0.4505		0.00912	0.00088	0.04406
0.03	9.989678125	6.904335938	69.1147		0.02964			
				-0.4612		0.00934	0.00066	0.03319
0.04	9.992846875	6.860435938	68.6535		0.03898			
				-0.4455		0.00902	0.00098	0.04911
0.05	9.989567188	6.81368125	68.2080		0.04800			
				-0.4598		0.00931	0.00069	0.03463
0.06	9.992190625	6.769526563	67.7482		0.05730			
				-0.4684		0.00948	0.00052	0.02595
0.07	9.989884375	6.721173438	67.2798		0.06678			
				-0.4719		0.00955	0.00045	0.02238
0.08	9.991820313	6.675323438	66.8079		0.07634			
				-0.4576		0.00926	0.00074	0.03682
0.09	9.990960938	6.629026563	66.3502		0.08560			
				-0.4563		0.00924	0.00076	0.03813
0.1	9.993321875	6.584989063	65.8939		0.09484			
				-0.4791		0.00970	0.00030	0.01513
0.11	9.991296875	6.535789063	65.4148		0.10453			
				-0.4694		0.00950	0.00050	0.02487
0.12	9.992003125	6.48934375	64.9454		0.11404			
				-0.4598		0.00931	0.00069	0.03459
0.13	9.993660938	6.444465625	64.4855		0.12335			
				-0.4597		0.00930	0.00070	0.03477
0.14	9.99336875	6.398340625	64.0259		0.13265			
				-0.4626		0.00936	0.00064	0.03179
0.15	9.993320313	6.352079688	63.5633		0.14201			
				-0.4583		0.00928	0.00072	0.03614
0.16	9.99253125	6.30578125	63.1049		0.15129			
				-0.4664		0.00944	0.00056	0.02796
0.17	9.995476563	6.261021875	62.6386		0.16073			
				-0.4740		0.00960	0.00040	0.02023
0.18	9.996215625	6.2141	62.1645		0.17033			
				-0.4691		0.00950	0.00050	0.02522
0.19	9.988975	6.162740625	61.6954		0.17982			
				-0.4729		0.00957	0.00043	0.02139
0.2	9.9880875	6.114960938	61.2225		0.18939			
				-0.4530		0.00917	0.00083	0.04156
0.21	9.991692188	6.071909375	60.7696		0.19856			
				-0.4520		0.00915	0.00085	0.04252
0.22	9.990628125	6.026104688	60.3176		0.20771			
				-0.4671		0.00946	0.00054	0.02720

Linear Pot #		6				+/- in.		%	
Channel #		55				AVG ERROR		0.00061	
				Slope		49.402		0.03056	
						MAX ERROR		0.0010	
								0.0515	
Micrometer Reading (in)	Power Source (Volts)	Linear Pot (Volts)	% of Source	% difference (in)	Calc pos. (in)	Delta (in)	Error (in)	Error (%)	
0.23	9.992110938	5.980321875	59.8504		0.21717				
				-0.4505		0.00912	0.00088	0.04408	
0.24	9.9939	5.936373438	59.4000		0.22629				
				-0.4743		0.00960	0.00040	0.01991	
0.25	9.990470313	5.886946875	58.9256		0.23589				
				-0.4735		0.00958	0.00042	0.02080	
0.26	9.995485938	5.842576563	58.4522		0.24547				
				-0.4431		0.00897	0.00103	0.05149	
0.27	9.989590625	5.7948625	58.0090		0.25444				
				-0.4698		0.00951	0.00049	0.02454	
0.28	9.99374375	5.750323438	57.5392		0.26395				
				-0.4645		0.00940	0.00060	0.02989	
0.29	9.99276875	5.703346875	57.0747		0.27336				
				-0.4824		0.00977	0.00023	0.01175	
0.3	9.993553125	5.655584375	56.5923		0.28312				



Linear Pot #	7						+/- in.	%
Channel #	56				AVG ERROR MAX ERROR		0.00037 0.0016	0.01865 0.0819
		Slope	49.388					
Micrometer Reading (in.)	Power Source (Volts)	Linear Pot (Volts)	% of Source	% difference (in.)	Calc pos. (in.)	Delta (in.)	Error (in.)	Error (%)
0	10.009	9.0377	90.2957		0.00000			
				-0.5383		0.01090	0.00090	0.04499
0.01	10.017	8.991	89.7574		0.01090			
				-0.4939		0.01000	0.00000	0.00002
0.02	10.007	8.9326	89.2635		0.02090			
				-0.4940		0.01000	0.00000	0.00016
0.03	10.012	8.8876	88.7695		0.03090			
				-0.4841		0.00980	0.00020	0.00993
0.04	10.014	8.8409	88.2854		0.04070			
				-0.5035		0.01020	0.00020	0.00976
0.05	10.022	8.7975	87.7819		0.05090			
				-0.4926		0.00997	0.00003	0.00134
0.06	10.027	8.7525	87.2893		0.06087			
				-0.4602		0.00932	0.00068	0.03413
0.07	10.032	8.7107	86.8291		0.07019			
				-0.4981		0.01009	0.00009	0.00431
0.08	10.03	8.659	86.3310		0.08028			
				-0.4968		0.01006	0.00006	0.00300
0.09	10.022	8.6023	85.8342		0.09034			
				-0.4756		0.00963	0.00037	0.01847
0.1	10.027	8.5589	85.3585		0.09997			
				-0.4987		0.01010	0.00010	0.00483
0.11	10.027	8.5089	84.8599		0.11006			
				-0.5079		0.01028	0.00028	0.01423
0.12	10.03	8.4605	84.3519		0.12035			
				-0.4906		0.00993	0.00007	0.00332
0.13	10.025	8.4071	83.8613		0.13028			
				-0.4739		0.00959	0.00041	0.02026
0.14	10.034	8.3671	83.3875		0.13988			
				-0.5157		0.01044	0.00044	0.02206
0.15	10.032	8.3137	82.8718		0.15032			
				-0.4918		0.00996	0.00004	0.00215
0.16	10.025	8.2586	82.3800		0.16028			
				-0.5060		0.01025	0.00025	0.01232
0.17	10.032	8.2136	81.8740		0.17052			
				-0.4843		0.00981	0.00019	0.00966
0.18	10.024	8.1585	81.3897		0.18033			
				-0.4770		0.00966	0.00034	0.01706
0.19	10.015	8.1034	80.9126		0.18999			
				-0.4797		0.00971	0.00029	0.01434
0.2	10.025	8.0634	80.4329		0.19970			
				-0.5316		0.01076	0.00076	0.03822
0.21	10.029	8.0133	79.9013		0.21047			
				-0.4997		0.01012	0.00012	0.00586
0.22	10.027	7.9616	79.4016		0.22058			
				-0.4827		0.00977	0.00023	0.01132

Linear Pot #	7						+/- in.	%
Channel #	56				AVG ERROR MAX ERROR		0.00037 0.0016	0.01865 0.0819
		Slope		49.388				
Micrometer Reading (in.)	Power Source (Volts)	Linear Pot (Volts)	% of Source	% difference (in.)	Calc pos. (in.)	Delta (in.)	Error (in.)	Error (%)
0.23	10.027	7.9132	78.9189		0.23036			
				-0.4814		0.00975	0.00025	0.01265
0.24	10.029	7.8665	78.4375		0.24010			
				-0.4345		0.00880	0.00120	0.06008
0.25	10.025	7.8198	78.0030		0.24890			
				-0.5748		0.01164	0.00164	0.08194
0.26	10.024	7.7614	77.4282		0.26054			
				-0.4736		0.00959	0.00041	0.02057
0.27	10.025	7.7147	76.9546		0.27013			
				-0.5081		0.01029	0.00029	0.01438
0.28	10.024	7.663	76.4465		0.28042			
				-0.4589		0.00929	0.00071	0.03543
0.29	10.034	7.6246	75.9876		0.28971			
				-0.4682		0.00948	0.00052	0.02600
0.3	10.03	7.5746	75.5194		0.29919			
				-0.5294		0.01072	0.00072	0.03597
0.31	10.034	7.5245	74.9900		0.30991			
				-0.5428		0.01099	0.00099	0.04955
0.32	10.04	7.4745	74.4472		0.32090			
				-0.4821		0.00976	0.00024	0.01195
0.33	10.04	7.4261	73.9651		0.33066			
				-0.4990		0.01010	0.00010	0.00519
0.34	10.04	7.376	73.4661		0.34076			
				-0.5160		0.01045	0.00045	0.02240
0.35	10.047	7.3293	72.9501		0.35121			
				-0.4962		0.01005	0.00005	0.00231
0.36	10.049	7.2809	72.4540		0.36126			
				-0.5333		0.01080	0.00080	0.03996
0.37	10.054	7.2309	71.9206		0.37206			
				-0.4885		0.00989	0.00011	0.00544
0.38	10.055	7.1825	71.4321		0.38195			
				-0.4853		0.00983	0.00017	0.00871
0.39	10.065	7.1408	70.9468		0.39177			
				-0.4787		0.00969	0.00031	0.01541
0.4	10.06	7.0891	70.4682		0.40146			
				-0.4911		0.00994	0.00006	0.00286
0.41	10.059	7.039	69.9771		0.41141			
				-0.4881		0.00988	0.00012	0.00588
0.42	10.06	6.9906	69.4891		0.42129			
				-0.4748		0.00961	0.00039	0.01936
0.43	10.064	6.9456	69.0143		0.43090			
				-0.4966		0.01005	0.00005	0.00272
0.44	10.059	6.8922	68.5177		0.44096			
				-0.4822		0.00976	0.00024	0.01185

Linear Pot #	7						+/- in.	%
Channel #	56				AVG ERROR MAX ERROR		0.00037 0.0016	0.01865 0.0819
		Slope		49.388				
Micrometer Reading (in.)	Power Source (Volts)	Linear Pot (Volts)	% of Source	% difference (in.)	Calc pos. (in.)	Delta (in.)	Error (in.)	Error (%)
0.45	10.064	6.8471	68.0356		0.45072			
				-0.4836		0.00979	0.00021	0.01039
0.46	10.057	6.7937	67.5520		0.46051			
				-0.4936		0.00999	0.00001	0.00029
0.47	10.059	6.7454	67.0584		0.47051			
				-0.5044		0.01021	0.00021	0.01065
0.48	10.055	6.692	66.5540		0.48072			
				-0.4813		0.00975	0.00025	0.01272
0.49	10.05	6.6403	66.0726		0.49047			
				-0.5116		0.01036	0.00036	0.01789
0.5	10.052	6.5902	65.5611		0.50082			
				-0.4775		0.00967	0.00033	0.01655
0.51	10.054	6.5435	65.0835		0.51049			
				-0.4862		0.00984	0.00016	0.00782
0.52	10.047	6.4901	64.5974		0.52034			
				-0.4520		0.00915	0.00085	0.04235
0.53	10.045	6.4434	64.1453		0.52949			
				-0.4903		0.00993	0.00007	0.00367
0.54	10.049	6.3967	63.6551		0.53942			
				-0.5401		0.01094	0.00094	0.04680
0.55	10.045	6.3399	63.1150		0.55035			
				-0.4747		0.00961	0.00039	0.01941
0.56	10.052	6.2966	62.6403		0.55996			
				-0.4987		0.01010	0.00010	0.00487
0.57	10.044	6.2415	62.1416		0.57006			
				-0.4786		0.00969	0.00031	0.01550
0.58	10.03	6.1848	61.6630		0.57975			
				-0.5287		0.01071	0.00071	0.03529
0.59	10.024	6.1281	61.1343		0.59046			
				-0.4729		0.00958	0.00042	0.02121
0.6	10.025	6.0813	60.6613		0.60003			
				-0.5306		0.01074	0.00074	0.03721
0.61	10.022	6.0263	60.1307		0.61078			
				-0.4330		0.00877	0.00123	0.06159
0.62	10.022	5.9829	59.6977		0.61954			

Linear Pot #	8						+/- in.	%
Channel #	57				AVG ERROR		0.00038	0.01892
		Slope	49.381	MAX ERROR		0.0013		0.0652
Micrometer Reading (in)	Power Source (Volts)	Linear Pot (Volts)	% of Source	% difference (in)	Calc pos. (in)	Delta (in)	Error (in)	Error (%)
0	10.117	9.0628	89.5799		0.00000			
				-0.5346		0.01083	0.00083	0.04130
0.01	10.129	9.0194	89.0453		0.01083			
				-0.4516		0.00915	0.00085	0.04274
0.02	10.126	8.971	88.5937		0.01997			
				-0.4816		0.00975	0.00025	0.01233
0.03	10.117	8.9143	88.1121		0.02972			
				-0.4901		0.00993	0.00007	0.00373
0.04	10.126	8.8726	87.6220		0.03965			
				-0.5038		0.01020	0.00020	0.01010
0.05	10.129	8.8242	87.1182		0.04985			
				-0.4647		0.00941	0.00059	0.02952
0.06	10.139	8.7858	86.6535		0.05926			
				-0.5167		0.01046	0.00046	0.02323
0.07	10.134	8.7291	86.1368		0.06973			
				-0.5042		0.01021	0.00021	0.01051
0.08	10.141	8.684	85.6326		0.07994			
				-0.4668		0.00945	0.00055	0.02738
0.09	10.132	8.629	85.1658		0.08939			
				-0.5019		0.01016	0.00016	0.00820
0.1	10.131	8.5773	84.6639		0.09955			
				-0.4782		0.00968	0.00032	0.01576
0.11	10.137	8.5339	84.1857		0.10924			
				-0.5023		0.01017	0.00017	0.00857
0.12	10.132	8.4788	83.6834		0.11941			
				-0.5097		0.01032	0.00032	0.01610
0.13	10.146	8.4388	83.1737		0.12973			
				-0.4778		0.00968	0.00032	0.01622
0.14	10.134	8.3804	82.6959		0.13941			
				-0.5269		0.01067	0.00067	0.03354
0.15	10.134	8.327	82.1689		0.15008			
				-0.4686		0.00949	0.00051	0.02556
0.16	10.139	8.2836	81.7004		0.15957			
				-0.4839		0.00980	0.00020	0.01005
0.17	10.144	8.2386	81.2165		0.16937			
				-0.4795		0.00971	0.00029	0.01448
0.18	10.136	8.1835	80.7370		0.17908			
				-0.4915		0.00995	0.00005	0.00233
0.19	10.144	8.1401	80.2455		0.18903			
				-0.5286		0.01070	0.00070	0.03524
0.2	10.136	8.0801	79.7169		0.19973			
				-0.5166		0.01046	0.00046	0.02305
0.21	10.141	8.0317	79.2003		0.21019			
				-0.4294		0.00870	0.00130	0.06518
0.22	10.137	7.985	78.7708		0.21889			
				-0.5315		0.01076	0.00076	0.03815

Linear Pot #	8						+/- in.	%
Channel #	57				AVG ERROR MAX ERROR		0.00038 0.0013	0.01892 0.0652
		Slope	49.381					
Micrometer Reading (in)	Power Source (Volts)	Linear Pot (Volts)	% of Source	% difference (in)	Calc pos. (in)	Delta (in)	Error (in)	Error (%)
0.23	10.144	7.9366	78.2394		0.22965			
				-0.4867		0.00986	0.00014	0.00723
0.24	10.141	7.8849	77.7527		0.23951			
				-0.4849		0.00982	0.00018	0.00903
0.25	10.142	7.8365	77.2678		0.24933			
				-0.4490		0.00909	0.00091	0.04534
0.26	10.147	7.7948	76.8188		0.25842			
				-0.5580		0.01130	0.00130	0.06504
0.27	10.149	7.7397	76.2607		0.26972			
				-0.4769		0.00966	0.00034	0.01713
0.28	10.149	7.6913	75.7838		0.27938			
				-0.4993		0.01011	0.00011	0.00559
0.29	10.141	7.6346	75.2845		0.28949			
				-0.5004		0.01013	0.00013	0.00670
0.3	10.142	7.5846	74.7841		0.29963			
				-0.4898		0.00992	0.00008	0.00410
0.31	10.146	7.5379	74.2943		0.30954			
				-0.5105		0.01034	0.00034	0.01695
0.32	10.146	7.4861	73.7838		0.31988			
				-0.4843		0.00981	0.00019	0.00967
0.33	10.147	7.4377	73.2995		0.32969			
				-0.4846		0.00981	0.00019	0.00930
0.34	10.139	7.3827	72.8149		0.33950			
				-0.4947		0.01002	0.00002	0.00095
0.35	10.146	7.3376	72.3201		0.34952			
				-0.5166		0.01046	0.00046	0.02311
0.36	10.147	7.2859	71.8035		0.35999			
				-0.4717		0.00955	0.00045	0.02242
0.37	10.144	7.2359	71.3318		0.36954			
				-0.4943		0.01001	0.00001	0.00049
0.38	10.137	7.1808	70.8375		0.37955			
				-0.5252		0.01064	0.00064	0.03183
0.39	10.151	7.1374	70.3123		0.39018			
				-0.4592		0.00930	0.00070	0.03500
0.4	10.139	7.0824	69.8530		0.39948			
				-0.4934		0.00999	0.00001	0.00044
0.41	10.151	7.0407	69.3597		0.40947			
				-0.4989		0.01010	0.00010	0.00518
0.42	10.147	6.9873	68.8607		0.41958			
				-0.4858		0.00984	0.00016	0.00808
0.43	10.141	6.9339	68.3749		0.42942			
				-0.5141		0.01041	0.00041	0.02055
0.44	10.144	6.8838	67.8608		0.43983			
				-0.4894		0.00991	0.00009	0.00444

Linear Pot #	8						+/- in.	%
Channel #	57				AVG ERROR MAX ERROR		0.00038 0.0013	0.01892 0.0652
		Slope		49.381				
Micrometer Reading (in)	Power Source (Volts)	Linear Pot (Volts)	% of Source	% difference (in)	Calc pos. (in)	Delta (in)	Error (in)	Error (%)
0.45	10.146	6.8355	67.3714		0.44974			
				-0.5004		0.01013	0.00013	0.00665
0.46	10.147	6.7854	66.8710		0.45987			
				-0.5263		0.01066	0.00066	0.03286
0.47	10.147	6.732	66.3447		0.47053			
				-0.4900		0.00992	0.00008	0.00389
0.48	10.149	6.6836	65.8548		0.48045			
				-0.4904		0.00993	0.00007	0.00345
0.49	10.141	6.6286	65.3644		0.49038			
				-0.4773		0.00967	0.00033	0.01675
0.5	10.141	6.5802	64.8871		0.50005			
				-0.5113		0.01035	0.00035	0.01770
0.51	10.149	6.5335	64.3758		0.51040			
				-0.4895		0.00991	0.00009	0.00433
0.52	10.164	6.4934	63.8863		0.52031			
				-0.4775		0.00967	0.00033	0.01655
0.53	10.159	6.4417	63.4088		0.52998			
				-0.4597		0.00931	0.00069	0.03455
0.54	10.159	6.395	62.9491		0.53929			
				-0.4949		0.01002	0.00002	0.00107
0.55	10.162	6.3466	62.4542		0.54931			
				-0.4950		0.01002	0.00002	0.00121
0.56	10.157	6.2932	61.9592		0.55934			
				-0.5197		0.01052	0.00052	0.02621
0.57	10.156	6.2398	61.4395		0.56986			
				-0.4431		0.00897	0.00103	0.05136
0.58	10.156	6.1948	60.9965		0.57884			
				-0.4814		0.00975	0.00025	0.01258
0.59	10.154	6.1447	60.5151		0.58858			
				-0.5377		0.01089	0.00089	0.04446
0.6	10.156	6.0913	59.9774		0.59947			

Linear Pot #	9						+/- in.	%
Channel #	58				AVG ERROR		0.00163	0.08151
		Slope	50.047	MAX ERROR		0.0058		0.2890
Micrometer Reading (in)	Power Source (Volts)	Linear Pot (Volts)	% of Source	% difference (in)	Calc pos. (in)	Delta (in)	Error (in)	Error (%)
0	10.005	8.9426	89.3813		0.00000			
				-0.6553		0.01321	0.00321	0.16031
0.01	10	8.8726	88.7260		0.01321			
				-0.4187		0.00844	0.00156	0.07814
0.02	10.002	8.8325	88.3073		0.02164			
				-0.5163		0.01041	0.00041	0.02028
0.03	10	8.7791	87.7910		0.03205			
				-0.6417		0.01293	0.00293	0.14663
0.04	9.9971	8.7124	87.1493		0.04498			
				-0.4593		0.00926	0.00074	0.03722
0.05	10	8.669	86.6900		0.05424			
				-0.5000		0.01008	0.00008	0.00382
0.06	10	8.619	86.1900		0.06431			
				-0.3439		0.00693	0.00307	0.15345
0.07	10.005	8.5889	85.8461		0.07124			
				-0.5071		0.01022	0.00022	0.01095
0.08	10	8.5339	85.3390		0.08146			
				-0.6509		0.01312	0.00312	0.15591
0.09	10.002	8.4705	84.6881		0.09458			
				-0.3838		0.00773	0.00227	0.11328
0.1	10.004	8.4338	84.3043		0.10232			
				-0.5668		0.01142	0.00142	0.07110
0.11	10.004	8.3771	83.7375		0.11374			
				-0.4672		0.00941	0.00059	0.02927
0.12	10.002	8.3287	83.2703		0.12315			
				-0.5504		0.01109	0.00109	0.05464
0.13	10.004	8.2753	82.7199		0.13425			
				-0.4415		0.00890	0.00110	0.05512
0.14	10.007	8.2336	82.2784		0.14314			
				-0.4761		0.00960	0.00040	0.02024
0.15	10.004	8.1835	81.8023		0.15274			
				-0.4998		0.01007	0.00007	0.00362
0.16	10.004	8.1335	81.3025		0.16281			
				-0.6081		0.01225	0.00225	0.11275
0.17	10.009	8.0767	80.6944		0.17507			
				-0.4576		0.00922	0.00078	0.03889
0.18	10.01	8.0317	80.2368		0.18429			
				-0.4596		0.00926	0.00074	0.03688
0.19	10.007	7.9833	79.7772		0.19355			
				-0.3905		0.00787	0.00213	0.10647
0.2	10.01	7.9466	79.3866		0.20142			
				-0.6648		0.01340	0.00340	0.16990
0.21	10.014	7.8832	78.7218		0.21482			
				-0.5163		0.01040	0.00040	0.02022
0.22	10.014	7.8315	78.2055		0.22522			
				-0.4852		0.00978	0.00022	0.01106

Linear Pot #	9						+/- in.	%
Channel #	58				AVG ERROR		0.00163	0.08151
		Slope	50.047	MAX ERROR		0.0058	0.2890	
Micrometer Reading (in)	Power Source (Volts)	Linear Pot (Volts)	% of Source	% difference (in)	Calc pos. (in)	Delta (in)	Error (in)	Error (%)
0.23	10.01	7.7798	77.7203		0.23500			
				-0.5165		0.01041	0.00041	0.02043
0.24	10.01	7.7281	77.2038		0.24541			
				-0.5887		0.01186	0.00186	0.09322
0.25	10.015	7.673	76.6151		0.25727			
				-0.4427		0.00892	0.00108	0.05390
0.26	10.014	7.6279	76.1724		0.26620			
				-0.4191		0.00845	0.00155	0.07769
0.27	10.01	7.5829	75.7532		0.27464			
				-0.4986		0.01005	0.00005	0.00236
0.28	10.012	7.5345	75.2547		0.28469			
				-0.5717		0.01152	0.00152	0.07609
0.29	10.015	7.4795	74.6830		0.29621			
				-0.4821		0.00972	0.00028	0.01420
0.3	10.017	7.4327	74.2009		0.30593			
				-0.5843		0.01177	0.00177	0.08875
0.31	10.015	7.3727	73.6166		0.31770			
				-0.5332		0.01075	0.00075	0.03727
0.32	10.015	7.3193	73.0834		0.32845			
				-0.2094		0.00422	0.00578	0.28900
0.33	10.014	7.2976	72.8740		0.33267			
				-0.6882		0.01387	0.00387	0.19348
0.34	10.024	7.2359	72.1858		0.34654			
				-0.4657		0.00938	0.00062	0.03076
0.35	10.017	7.1842	71.7201		0.35592			
				-0.4501		0.00907	0.00093	0.04644
0.36	10.024	7.1441	71.2700		0.36499			
				-0.6330		0.01276	0.00276	0.13787
0.37	10.017	7.0757	70.6369		0.37775			
				-0.4872		0.00982	0.00018	0.00906
0.38	10.02	7.029	70.1497		0.38757			
				-0.3493		0.00704	0.00296	0.14803
0.39	10.02	6.994	69.8004		0.39461			
				-0.4962		0.01000	0.00000	0.00001
0.4	10.017	6.9422	69.3042		0.40461			
				-0.5674		0.01143	0.00143	0.07174
0.41	10.022	6.8888	68.7368		0.41604			
				-0.5997		0.01209	0.00209	0.10433
0.42	10.027	6.8321	68.1370		0.42813			
				-0.4015		0.00809	0.00191	0.09543
0.43	10.02	6.7871	67.7355		0.43622			
				-0.4472		0.00901	0.00099	0.04938
0.44	10.027	6.747	67.2883		0.44523			
				-0.3686		0.00743	0.00257	0.12856



Linear Pot #	9						+/- in.	%
Channel #	58				AVG ERROR		0.00163	0.08151
		Slope	50.047	MAX ERROR		0.0058	0.2890	
Micrometer Reading (in)	Power Source (Volts)	Linear Pot (Volts)	% of Source	% difference (in)	Calc pos. (in)	Delta (in)	Error (in)	Error (%)
0.45	10.025	6.7087	66.9197		0.45266			
				-0.6993		0.01409	0.00409	0.20459
0.46	10.025	6.6386	66.2204		0.46676			
				-0.3463		0.00698	0.00302	0.15105
0.47	10.027	6.6052	65.8741		0.47373			
				-0.5528		0.01114	0.00114	0.05700
0.48	10.02	6.5452	65.3214		0.48487			
				-0.7311		0.01473	0.00473	0.23671
0.49	10.03	6.4784	64.5902		0.49961			
				-0.4592		0.00925	0.00075	0.03728
0.5	10.029	6.4317	64.1310		0.50886			
				-0.4889		0.00985	0.00015	0.00732
0.51	10.03	6.3833	63.6421		0.51872			
				-0.4171		0.00841	0.00159	0.07968
0.52	10.025	6.3383	63.2249		0.52712			
				-0.4081		0.00822	0.00178	0.08878
0.53	10.029	6.2999	62.8168		0.53535			
				-0.5387		0.01086	0.00086	0.04278
0.54	10.03	6.2465	62.2782		0.54620			
				-0.5422		0.01093	0.00093	0.04634
0.55	10.029	6.1915	61.7360		0.55713			
				-0.4633		0.00934	0.00066	0.03317
0.56	10.034	6.1481	61.2727		0.56647			
				-0.5917		0.01192	0.00192	0.09624
0.57	10.03	6.0863	60.6810		0.57839			
				-0.3429		0.00691	0.00309	0.15444
0.58	10.029	6.0513	60.3380		0.58530			
				-0.6789		0.01368	0.00368	0.18405
0.59	10.034	5.9862	59.6592		0.59898			
				-0.4038		0.00814	0.00186	0.09314
0.6	10.032	5.9445	59.2554		0.60712			

Linear Pot #	10						+/- in.	%
Channel #	59				AVG ERROR MAX ERROR		0.00068 0.0020	0.03395 0.0997
		Slope	49.69					
Micrometer Reading (in)	Power Source (Volts)	Linear Pot (Volts)	% of Source	% difference (in)	Calc pos. (in)	Delta (in)	Error (in)	Error (%)
0	10.055	9.0678	90.1820		0.00000			
				-0.5587		0.01124	0.00124	0.06222
0.01	10.06	9.0161	89.6233		0.01124			
				-0.4545		0.00915	0.00085	0.04264
0.02	10.057	8.9677	89.1687		0.02039			
				-0.4813		0.00969	0.00031	0.01574
0.03	10.057	8.9193	88.6875		0.03008			
				-0.4748		0.00955	0.00045	0.02228
0.04	10.06	8.8742	88.2127		0.03963			
				-0.5467		0.01100	0.00100	0.05013
0.05	10.06	8.8192	87.6660		0.05063			
				-0.5158		0.01038	0.00038	0.01898
0.06	10.064	8.7708	87.1502		0.06101			
				-0.4809		0.00968	0.00032	0.01608
0.07	10.064	8.7224	86.6693		0.07069			
				-0.4895		0.00985	0.00015	0.00746
0.08	10.065	8.674	86.1798		0.08054			
				-0.5548		0.01117	0.00117	0.05829
0.09	10.064	8.6173	85.6250		0.09171			
				-0.4217		0.00849	0.00151	0.07567
0.1	10.059	8.5706	85.2033		0.10020			
				-0.5233		0.01053	0.00053	0.02658
0.11	10.062	8.5205	84.6800		0.11073			
				-0.5046		0.01016	0.00016	0.00777
0.12	10.059	8.4672	84.1754		0.12088			
				-0.4812		0.00968	0.00032	0.01584
0.13	10.059	8.4188	83.6942		0.13057			
				-0.4643		0.00934	0.00066	0.03284
0.14	10.059	8.3721	83.2299		0.13991			
				-0.5058		0.01018	0.00018	0.00899
0.15	10.062	8.3237	82.7241		0.15009			
				-0.5302		0.01067	0.00067	0.03346
0.16	10.064	8.272	82.1940		0.16076			
				-0.5228		0.01052	0.00052	0.02608
0.17	10.065	8.2202	81.6711		0.17128			
				-0.5056		0.01018	0.00018	0.00875
0.18	10.064	8.1685	81.1655		0.18145			
				-0.4471		0.00900	0.00100	0.05007
0.19	10.064	8.1235	80.7184		0.19045			
				-0.5545		0.01116	0.00116	0.05799
0.2	10.069	8.0717	80.1639		0.20161			
				-0.4840		0.00974	0.00026	0.01300
0.21	10.059	8.015	79.6799		0.21135			
				-0.5546		0.01116	0.00116	0.05810
0.22	10.06	7.96	79.1252		0.22251			
				-0.5293		0.01065	0.00065	0.03256

Linear Pot #	10						+/- in.	%
Channel #	59				AVG ERROR MAX ERROR		0.00068 0.0020	0.03395 0.0997
		Slope		49.69				
Micrometer Reading (in)	Power Source (Volts)	Linear Pot (Volts)	% of Source	% difference (in)	Calc pos. (in)	Delta (in)	Error (in)	Error (%)
0.23	10.064	7.9099	78.5960		0.23317			
				-0.5465		0.01100	0.00100	0.04991
0.24	10.064	7.8549	78.0495		0.24416			
				-0.4867		0.00979	0.00021	0.01030
0.25	10.069	7.8098	77.5628		0.25396			
				-0.4141		0.00833	0.00167	0.08327
0.26	10.069	7.7681	77.1487		0.26229			
				-0.4098		0.00825	0.00175	0.08764
0.27	10.064	7.723	76.7389		0.27054			
				-0.5213		0.01049	0.00049	0.02454
0.28	10.065	7.6713	76.2176		0.28103			
				-0.5239		0.01054	0.00054	0.02715
0.29	10.062	7.6163	75.6937		0.29157			
				-0.4979		0.01002	0.00002	0.00102
0.3	10.062	7.5662	75.1958		0.30159			
				-0.4536		0.00913	0.00087	0.04356
0.31	10.065	7.5228	74.7422		0.31072			
				-0.5284		0.01063	0.00063	0.03170
0.32	10.067	7.4711	74.2138		0.32136			
				-0.4808		0.00968	0.00032	0.01622
0.33	10.067	7.4227	73.7330		0.33103			
				-0.4520		0.00910	0.00090	0.04522
0.34	10.07	7.3794	73.2810		0.34013			
				-0.5424		0.01092	0.00092	0.04577
0.35	10.067	7.3226	72.7387		0.35104			
				-0.4854		0.00977	0.00023	0.01155
0.36	10.07	7.2759	72.2532		0.36081			
				-0.4592		0.00924	0.00076	0.03789
0.37	10.067	7.2275	71.7940		0.37005			
				-0.4993		0.01005	0.00005	0.00242
0.38	10.072	7.1808	71.2947		0.38010			
				-0.5278		0.01062	0.00062	0.03111
0.39	10.067	7.1241	70.7669		0.39073			
				-0.4689		0.00944	0.00056	0.02813
0.4	10.07	7.079	70.2979		0.40016			
				-0.4946		0.00995	0.00005	0.00228
0.41	10.065	7.0257	69.8033		0.41012			
				-0.5115		0.01029	0.00029	0.01472
0.42	10.067	6.9756	69.2917		0.42041			
				-0.4981		0.01002	0.00002	0.00117
0.43	10.072	6.9289	68.7937		0.43043			
				-0.4839		0.00974	0.00026	0.01313
0.44	10.07	6.8788	68.3098		0.44017			
				-0.4797		0.00965	0.00035	0.01728

Linear Pot #	10						+/- in.	%
Channel #	59				AVG ERROR		0.00068	0.03395
		Slope			MAX ERROR		0.0020	0.0997
Micrometer Reading (in)	Power Source (Volts)	Linear Pot (Volts)	% of Source	% difference (in)	Calc pos. (in)	Delta (in)	Error (in)	Error (%)
0.45	10.065	6.8271	67.8301		0.44983			
				-0.5404		0.01088	0.00088	0.04377
0.46	10.069	6.7754	67.2897		0.46070			
				-0.4807		0.00967	0.00033	0.01632
0.47	10.069	6.727	66.8090		0.47038			
				-0.4368		0.00879	0.00121	0.06047
0.48	10.075	6.687	66.3722		0.47917			
				-0.5770		0.01161	0.00161	0.08064
0.49	10.067	6.6236	65.7952		0.49078			
				-0.5002		0.01007	0.00007	0.00336
0.5	10.07	6.5752	65.2949		0.50085			
				-0.4285		0.00862	0.00138	0.06879
0.51	10.067	6.5301	64.8664		0.50947			
				-0.4990		0.01004	0.00004	0.00208
0.52	10.07	6.4818	64.3674		0.51951			
				-0.5736		0.01154	0.00154	0.07718
0.53	10.069	6.4234	63.7938		0.53106			
				-0.5347		0.01076	0.00076	0.03799
0.54	10.067	6.3683	63.2592		0.54182			
				-0.5260		0.01059	0.00059	0.02930
0.55	10.069	6.3166	62.7331		0.55240			
				-0.4310		0.00867	0.00133	0.06629
0.56	10.069	6.2732	62.3021		0.56108			
				-0.5027		0.01012	0.00012	0.00585
0.57	10.07	6.2232	61.7994		0.57119			
				-0.4479		0.00901	0.00099	0.04934
0.58	10.07	6.1781	61.3515		0.58021			
				-0.5592		0.01125	0.00125	0.06273
0.59	10.072	6.123	60.7923		0.59146			
				-0.4637		0.00933	0.00067	0.03345
0.6	10.072	6.0763	60.3286		0.60079			
				-0.4964		0.00999	0.00001	0.00048
0.61	10.072	6.0263	59.8322		0.61078			
				-0.5959		0.01199	0.00199	0.09966
0.62	10.069	5.9645	59.2363		0.62278			

Linear Pot #	12						+/- in.	%
Channel #	54				AVG ERROR MAX ERROR		0.00060 0.0016	0.03023 0.0821
		Slope	49.463					
Micrometer Reading (in)	Power Source (Volts)	Linear Pot (Volts)	% of Source	% difference (in)	Calc pos. (in)	Delta (in)	Error (in)	Error (%)
0	10.035	8.946	89.1480		0.00000			
				-0.5505		0.01113	0.00113	0.05649
0.01	10.039	8.8943	88.5975		0.01113			
				-0.4909		0.00992	0.00008	0.00377
0.02	10.04	8.8459	88.1066		0.02105			
				-0.4651		0.00940	0.00060	0.02981
0.03	10.04	8.7992	87.6414		0.03046			
				-0.5058		0.01023	0.00023	0.01133
0.04	10.037	8.7458	87.1356		0.04068			
				-0.4653		0.00941	0.00059	0.02967
0.05	10.037	8.6991	86.6703		0.05009			
				-0.5214		0.01054	0.00054	0.02703
0.06	10.057	8.664	86.1490		0.06063			
				-0.4885		0.00988	0.00012	0.00618
0.07	10.054	8.6123	85.6604		0.07051			
				-0.4887		0.00988	0.00012	0.00595
0.08	10.047	8.5572	85.1717		0.08039			
				-0.5060		0.01023	0.00023	0.01152
0.09	10.05	8.5089	84.6657		0.09062			
				-0.5235		0.01058	0.00058	0.02914
0.1	10.055	8.4605	84.1422		0.10120			
				-0.4485		0.00907	0.00093	0.04660
0.11	10.055	8.4154	83.6937		0.11027			
				-0.5720		0.01156	0.00156	0.07825
0.12	10.062	8.3637	83.1216		0.12184			
				-0.4399		0.00889	0.00111	0.05529
0.13	10.057	8.3153	82.6817		0.13073			
				-0.5297		0.01071	0.00071	0.03545
0.14	10.065	8.2686	82.1520		0.14144			
				-0.4978		0.01006	0.00006	0.00318
0.15	10.059	8.2136	81.6542		0.15150			
				-0.4819		0.00974	0.00026	0.01285
0.16	10.057	8.1635	81.1723		0.16125			
				-0.5214		0.01054	0.00054	0.02701
0.17	10.062	8.1151	80.6510		0.17179			
				-0.4810		0.00972	0.00028	0.01379
0.18	10.06	8.0651	80.1700		0.18151			
				-0.5149		0.01041	0.00041	0.02050
0.19	10.06	8.0133	79.6551		0.19192			
				-0.4563		0.00923	0.00077	0.03870
0.2	10.059	7.9666	79.1987		0.20115			
				-0.5362		0.01084	0.00084	0.04199
0.21	10.064	7.9166	78.6626		0.21199			
				-0.4640		0.00938	0.00062	0.03093
0.22	10.064	7.8699	78.1985		0.22137			
				-0.4559		0.00922	0.00078	0.03919

Linear Pot #	12						+/- in.	%
Channel #	54				AVG ERROR MAX ERROR		0.00060 0.0016	0.03023 0.0821
		Slope	49.463					
Micrometer Reading (in)	Power Source (Volts)	Linear Pot (Volts)	% of Source	% difference (in)	Calc pos. (in)	Delta (in)	Error (in)	Error (%)
0.23	10.065	7.8248	77.7427		0.23058			
				-0.5060		0.01023	0.00023	0.01148
0.24	10.064	7.7731	77.2367		0.24081			
				-0.4700		0.00950	0.00050	0.02488
0.25	10.067	7.7281	76.7667		0.25031			
				-0.5128		0.01037	0.00037	0.01838
0.26	10.069	7.678	76.2538		0.26068			
				-0.5096		0.01030	0.00030	0.01514
0.27	10.064	7.6229	75.7442		0.27099			
				-0.4368		0.00883	0.00117	0.05846
0.28	10.067	7.5812	75.3074		0.27982			
				-0.5578		0.01128	0.00128	0.06389
0.29	10.064	7.5228	74.7496		0.29109			
				-0.4513		0.00912	0.00088	0.04384
0.3	10.069	7.4811	74.2983		0.30022			
				-0.4638		0.00938	0.00062	0.03116
0.31	10.069	7.4344	73.8345		0.30959			
				-0.5135		0.01038	0.00038	0.01903
0.32	10.069	7.3827	73.3211		0.31997			
				-0.5024		0.01016	0.00016	0.00783
0.33	10.072	7.3343	72.8187		0.33013			
				-0.4742		0.00959	0.00041	0.02061
0.34	10.062	7.2793	72.3445		0.33972			
				-0.5196		0.01050	0.00050	0.02524
0.35	10.072	7.2342	71.8249		0.35022			
				-0.5063		0.01024	0.00024	0.01180
0.36	10.064	7.1775	71.3186		0.36046			
				-0.5517		0.01115	0.00115	0.05769
0.37	10.067	7.1241	70.7669		0.37161			
				-0.4499		0.00910	0.00090	0.04519
0.38	10.065	7.0774	70.3169		0.38071			
				-0.5483		0.01109	0.00109	0.05427
0.39	10.07	7.0257	69.7686		0.39180			
				-0.4134		0.00836	0.00164	0.08208
0.4	10.065	6.9806	69.3552		0.40015			
				-0.5446		0.01101	0.00101	0.05054
0.41	10.072	6.9306	68.8106		0.41116			
				-0.4974		0.01006	0.00006	0.00282
0.42	10.072	6.8805	68.3131		0.42122			
				-0.5293		0.01070	0.00070	0.03504
0.43	10.067	6.8238	67.7838		0.43192			
				-0.4839		0.00978	0.00022	0.01080
0.44	10.07	6.7771	67.2999		0.44171			
				-0.4776		0.00966	0.00034	0.01720

Linear Pot #	12						+/- in.	%
Channel #	54				AVG ERROR MAX ERROR		0.00060 0.0016	0.03023 0.0821
		Slope	49.463					
Micrometer Reading (in)	Power Source (Volts)	Linear Pot (Volts)	% of Source	% difference (in)	Calc pos. (in)	Delta (in)	Error (in)	Error (%)
0.45	10.067	6.727	66.8223		0.45136			
				-0.4645		0.00939	0.00061	0.03043
0.46	10.057	6.6736	66.3578		0.46075			
				-0.5507		0.01113	0.00113	0.05668
0.47	10.055	6.6169	65.8071		0.47189			
				-0.4774		0.00965	0.00035	0.01738
0.48	10.057	6.5702	65.3296		0.48154			
				-0.4993		0.01009	0.00009	0.00474
0.49	10.047	6.5135	64.8303		0.49163			
				-0.4209		0.00851	0.00149	0.07450
0.5	10.04	6.4667	64.4094		0.50014			
				-0.5065		0.01024	0.00024	0.01203
0.51	10.044	6.4184	63.9028		0.51038			
				-0.5340		0.01080	0.00080	0.03976
0.52	10.039	6.3616	63.3689		0.52118			
				-0.4699		0.00950	0.00050	0.02499
0.53	10.045	6.3182	62.8990		0.53068			
				-0.5148		0.01041	0.00041	0.02036
0.54	10.037	6.2615	62.3842		0.54109			
				-0.4468		0.00903	0.00097	0.04838
0.55	10.034	6.2148	61.9374		0.55012			
				-0.4960		0.01003	0.00003	0.00142
0.56	10.039	6.1681	61.4414		0.56015			
				-0.5076		0.01026	0.00026	0.01316
0.57	10.035	6.1147	60.9337		0.57041			
				-0.4955		0.01002	0.00002	0.00086
0.58	10.04	6.068	60.4382		0.58043			
				-0.5468		0.01106	0.00106	0.05278
0.59	10.037	6.0113	59.8914		0.59148			
				-0.4410		0.00892	0.00108	0.05423
0.6	10.044	5.9712	59.4504		0.60040			

**APPENDIX C**

**SITE CHARACTERIZATION OF**

**THE CAPITOL AGGREGATES FIELD SITE**





## **SUMMARY REPORT**

### **Site Characterization of Capital Aggregates Test Site**

by

Asli Kurtulus, M.S., Graduate Research Assistant

Jung Jae Lee, M.S., Graduate Research Assistant

Kenneth H. Stokoe, II, Ph.D., P.E., Jennie C. and Milton T. Graves Chair in Engineering  
University of Texas at Austin

#### **Introduction**

This report summarizes the results of a site characterization study for the Capitol Aggregates test site. Capitol Aggregates is a local quarry located in the south of Austin. A 50 ft by 50 ft natural soil area was selected as a test site for this pre-NEESR project. The location of the site relative to the location of The University of Texas at Austin is illustrated in Figure 1. Figure 2, shows a picture from the test site. A plan view of the test site is shown in Figure 3.

Two, Standard Penetration Test (SPT) boreholes (each 36 ft deep) and two 3-in. O.D. Shelby-tube sampling boreholes (14.5 ft and 9.5 ft deep) were drilled at the site to characterize the soil profile. The locations of these boreholes are shown in Figure 3. Disturbed and undisturbed samples were collected from the boreholes and were tested in the laboratory at The University of Texas at Austin. Information about the soil classification, fines content, water content, unit weight, degree of saturation and void ratio were obtained from the laboratory tests. A consolidated undrained triaxial test and two combined resonant column and torsional shear (RCTS) tests were conducted on undisturbed specimens. These tests were used to evaluate the strength and nonlinear properties, respectively, of the soil at the site. Additionally, Spectral-Analysis-of-Surface-Waves (SASW) tests were performed at the test site to obtain shear wave velocity profiles in the field. All resulting information is discussed below.

#### **Standard Penetration Tests**

SPT profiling was conducted in two boreholes situated in the vicinity of the selected test area on December 14, 2004. The locations of these boreholes (D1 and D2) are shown in Figure 3. The boreholes were drilled to a depth of 36 feet using a 7-in. O.D. hollow stem auger. The profiling was stopped at the 36-ft depth because a layer of shale was encountered. SPT blow counts were obtained at 2.5-ft depth intervals up to a 25 ft depth and at 5-ft depth intervals thereafter. A Model CME-75 drill rig that is equipped with an automatic drive hammer was used to conduct the SPT tests. A picture of the SPT equipment is given in Figure 4. At each sampling depth, a standard split spoon sampler was used to obtain representative disturbed samples. SPT testing and soil sampling were performed in accordance with ASTM D 1586. Corrected SPT

blow count values,  $N_{1,60}$  were calculated as recommended by NCEER-97-0022 (1997) and the resulting SPT profiles are plotted in Figure 5. Values of field and corrected blow counts for each borehole is given in Table 1. The static ground water level was found to be at a depth of 21.5 ft.

During the process of testing, representative water content samples were taken at each depth as soon as the split spoon sampler was received. Samples were weighed immediately on the site and kept secure for oven drying in the laboratory. Variation of the water content with depth at the time of the SPT tests (December 14, 2004) is shown in Figure 6.

### **Disturbed Samples from SPT Boreholes**

Disturbed soil samples obtained using the split spoon sampler were used to classify the soil at the site. Grain size analyses with wet sieving and Atterberg limit tests (in accordance with ASTM D 2217, and ASTM D 4318, respectively) were performed on samples obtained from the top 14 ft of soil. Grain size distribution curves obtained by wet sieving of soil samples using sieve sizes that are greater than ASTM No.200 sieve (0.075 mm) are shown in Figure 7. The variation of the fines content (percentage by weight of particles passing ASTM No. 200 sieve) with depth is illustrated in Figure 8. Results from Atterberg limit tests indicated that the fine grained material is composed of non-plastic silt.

Results from grain size and Atterberg limit tests were used to classify the soil according to the Unified Soil Classification System (USCS) (ASTM D 2487). Based on the available information, the top 14 ft of soil at the site is comprised of non-plastic silt (ML) with some silty sand (SM) layers at the top 1.5 ft and bottom 1.5 ft of the 14-feet deep profile. USCS soil classification for the top 14 ft of soil material is given in Table 2.

### **Undisturbed Samples from Shelby Tube Sampling**

Representative undisturbed samples were obtained from two sampling boreholes (S1 which was 14.5 ft and S2 which was 9.5 ft deep) using 3-in. O.D. ASTM thin-walled Shelby tubes. The undisturbed sampling was performed on the same day that SPT testing was performed. The locations of the sampling boreholes are shown in Figure 3. Shelby tube samples were obtained at 2.5-ft intervals and the sampling procedure was in accordance with ASTM D 1587. The Shelby tubes were sealed with wax in the field and transported to the laboratory.

In the laboratory, the Shelby tubes were cut into ~6-in. sections with a four wheel cutter and weighed immediately after cutting to calculate approximate unit weight values. To ensure minimum disturbance, each section of the tube was cut lengthwise on two opposite sides such that it was possible to split the steel tube into two pieces. An intact soil sample was then carefully removed from the tube pieces without any need for extrusion. Upon removal from the tube, samples were carefully trimmed in preparation for testing. Water content samples were taken from the trimmings of each specimen. Due to the fragile nature of the soil, it was not possible to get intact test specimens at every attempt. However, it was possible to obtain two, 2-in. diameter undisturbed test specimens for nonlinear dynamic testing (RCTS) and one, 1.5-in. diameter undisturbed triaxial test specimen. These specimens were used to gather information about water content, unit weight, and dry unit weight. Figures 6 and 8 include the water contents and fine contents, respectively, obtained from the undisturbed samples. A specific gravity value of 2.68 was assumed in calculating the void ratio and degree of saturation of each soil specimen. Table 3 gives the summary of available information obtained from undisturbed samples. A comprehensive summary of the index properties of the top 14 ft of soil as obtained from

disturbed and undisturbed samples is presented in Figure 9. SPT blow count values corrected for fines content (based on recommendations by NCEER-97-0022, 1997) are also included in the figure.

### **Triaxial Test**

One, 1.5-in. diameter triaxial test specimen was trimmed from an undisturbed soil sample obtained from Borehole S1 at an approximate depth of 10.6 ft. The initial size and index properties of the soil specimen are given in Table 4. In the triaxial cell, the specimen was allowed to come into equilibrium (compress/consolidate with drainage lines open) under an isotropic pressure equal to the assumed in-situ mean total stress (~5.6 psi). Upon equilibrating, the specimen was sheared under undrained conditions with a strain rate of %1 per hour. No pore pressure readings were taken since the specimen was unsaturated. The resulting stress-strain curve is presented in Figure 10. An estimate of the undrained shear strength in terms of total stresses was measured as 13.41 psi (~1931 psf) at about 9 % strain. The specimen failed in a bulging mode. The index properties of the specimen at failure are presented in Table 4.

### **Dynamic Laboratory Tests**

Two, 2-in. diameter specimens were trimmed from undisturbed soil samples from approximate depths of 6.0 ft and 9.2 ft. Each of the tests specimens was tested using the combined resonant column and torsional shear (RCTS) device to determine the variation of the shear modulus and material damping with the level of shearing strain. The effects of various parameters on the shear modulus and material damping are conveniently evaluated in the laboratory with a RCTS device as discussed by Stokoe et al. (1994).

RCTS test specimens were prepared with minimum disturbance as discussed previously. The sizes of the specimens and their initial index properties are summarized in Table 5. Upon preparation, specimens were tested in a fixed-free RCTS device. Five isotropic confining pressure levels were used in each test. These pressure levels were 1.5, 3, 6, 12 and 24 psi. At confining pressures of 1.5 psi, 3 psi and 12 psi, the specimens were excited only with low-amplitude ( $\gamma < 0.001\%$ ) dynamic loading. At confining pressures of 6 psi and 24 psi, after the low-amplitude testing was completed, each specimen was subjected to high-amplitude testing to determine nonlinear behavior.

The variation of the shear wave velocity, shear modulus, and material damping ratio at small strains ( $V_s$ ,  $G_{\max}$  and  $D_{\min}$ , respectively) with confining pressure are presented in Figures 11, 12 and 13, respectively, for the two specimens. The  $\log V_s - \log \sigma_o$  and  $\log G_{\max} - \log \sigma_o$  relationships for each specimen are composed of two linear segments, with intersection occurring at the maximum previous in-situ mean total stress. For both undisturbed specimens, the values of the confining stress at the intersection are higher (~6.5 psi for Specimen No.1 and ~8.8 psi for Specimen No.2) than the estimated in-situ mean stress, using a coefficient of earth pressure at-rest of 0.5 (~3.5 psi for Specimen No.1 and ~5.3 psi for Specimen No.2). This indicates that both specimens are overconsolidated. Figures 11 and 12, show that stiffness increases with decreasing void ratio. This is observed from Specimen No.1 ( $e=0.48$ ) having higher  $V_s$  (therefore  $G_{\max}$ ) values than the Specimen No.2 ( $e= 0.69$ ) at a given confining pressure. Figure 13 shows that Specimen No.1 has also higher material damping than Specimen No.2. This can be interpreted as material damping decreasing as void ratio increases (Hardin and Drenevich, 1972).

The effect of excitation frequency on  $V_s$ ,  $G_{\max}$  and  $D_{\min}$  is also evaluated using the information obtained in combined RCTS testing. Figures 14, 15 and 16 illustrate the variation of  $V_s$ ,  $G_{\max}$  and  $D_{\min}$ , respectively, with excitation frequency. The effect of excitation frequency is relatively small for both specimens.

The effect of shearing strain amplitude on the shear modulus,  $G$ , and normalized shear modulus  $G/G_{\max}$ , are shown in Figures 17 and 18, respectively. The maximum shearing strain level that was generated in the tests was 0.040% at confining pressure of 6 psi and 0.051% at confining pressure of 24 psi for Specimen No.1. For Specimen No.2, these values were 0.038% and 0.196%, respectively. The nonlinear behavior can be expressed by the reference strain,  $\gamma_r$ , which is simply the value of  $\gamma$  at  $G/G_{\max} = 0.5$  (Darendeli, 2001) and by the elastic threshold shearing strain,  $\gamma_t^e$ , which is the value of  $\gamma$  below which  $G$  is independent of strain amplitude and equal to  $G_{\max}$ . The value of the reference shearing strain, at  $\sigma_o = 6$  psi is about 0.04% and 0.05% for Specimens No.1 and No.2, respectively. At  $\sigma_o = 24$  psi,  $\gamma_r$  values are about 0.07% and 0.09% for Specimens No.1 and No.2, respectively. The value of the elastic threshold shearing strain, at 6 psi confining pressure level, is about 0.0007 % for Specimen No.1 and 0.0011% for Specimen No.2. At 24 psi confining pressure level, elastic threshold shearing strain values are about 0.0009% and 0.0014% for Specimen No.1 and No.2, respectively. Figure 18, also shows the effect of confining pressure on  $G/G_{\max}$ -log  $\gamma$  curves, which is the same for both specimens. As the confining pressure increases, the value of elastic threshold shearing strain increases and the  $G/G_{\max}$ -log  $\gamma$  relationship shifts to higher strains. To compare,  $G/G_{\max}$ -log  $\gamma$  curves obtained from RC tests are plotted together with the modulus reduction curves proposed by Seed et al. (1986) and Darendeli (2001). Figure 19 and 20 show the comparison at  $\sigma_o = 6$  psi and at  $\sigma_o = 24$  psi, respectively. Both figures show that RC test curves are close the upper bound curve for sands presented by Seed et. al. (1986) and plus one standard deviation of curves proposed by Darendeli (2001) for sands at 6 psi and 24 psi confining pressure levels.

The effect of shearing strain amplitude on the material damping ratio,  $D$ , is shown in Figure 21. The effect of confining pressure on  $D$ -log  $\gamma$  curves is the same for both specimens. As the confining pressure increases,  $D$ -log  $\gamma$  relationship shifts to higher strains while simultaneously shifting downward. Figures 22 and 23, show comparisons of the  $D$ -log  $\gamma$  curves from RC tests with those proposed by Seed et al. (1986) and Darendeli (2001). RC test curves are closer to the lower bound curve of Seed et. al. (1986) and minus one standard deviation of curves proposed by Darendeli (2001) at 6 psi and 24 psi confining pressure levels. The fact that the RC modulus curves match with the upper boundary curves of Seed et al. (1986) and Darendeli (2001) (as well as RC damping curves being closer to the lower boundary curves) can be explained by the presence of high percentage of fines in the materials tested.

To evaluate the effect of number of loading cycles,  $N$ , on  $G/G_{\max}$  and  $D$ , normalized modulus reduction curves and material damping ratio curves from combined RCTS test are plotted in Figures 24 through 27 and Figures 28 through 31, respectively. Figures 24 through 27 do not show any significant effect of  $N$ , on  $G/G_{\max}$ . However, it is possible to observe the effect of  $N$  on  $D$ , as shown in Figures 28 through 31. At large shearing strain values,  $D$ , decreases with increasing  $N$  at a constant  $\gamma$ .

After the RCTS tests were completed, specimens were air dried and complete particle size analysis tests (combination of sieve analysis and hydrometer analysis) were conducted in accordance with ASTM D 422. Resulting grain size distribution curves are shown in Figure 32.

## SASW Testing

Conventional SASW testing was performed at the Capitol Aggregates site during February 3, 2005 to evaluate the shear wave velocity profile. Testing was conducted along two perpendicular arrays that were centered within the 50 ft by 50 ft test area. The location of the corresponding arrays is shown in Figure 3.

The basic configuration of the source and receivers used in field testing at each array location is illustrated in Figure 33. One-dimensional Mark Products Model L-4 velocity transducers with a natural frequency of 1 Hz were used as receivers. Two types of sources were used to generate energy over the required frequency ranges. At shorter receiver spacings (2, 4 and 8 ft), a sledge hammer was employed as a source. At longer spacings (15, 30 and 60 ft), "Thumper" (the nees@UTexas mobile shaker) was used as the source of the surface wave energy. In the case of Thumper, the source was used in the stepped-sine mode. The data acquisition system was a VXI technology, 48-channel dynamic signal analyzer. The VXI system was used to collect the time records and to perform calculations in the frequency domain so that the relative phase of the cross-power spectrum was reviewed at each receiver spacing.

Two shear wave velocity profiles were obtained from the SASW testing. The composite experimental dispersion curves that were constructed from the data collected in the field at each SASW array are presented in Figures 34 and 35 for Lines A and B, respectively. The theoretical dispersion curves that were fitted to these experimental dispersion curves are also shown in the figures. The two shear wave velocity profiles are presented in Figure 36. Tabulated values describing the shear wave velocity profiles are given in Tables 6 and 7. The curves on Figure 36 indicate that the two arrays produced the same shear wave velocity profile except for slight differences in the top 7.0 ft of soil. The shear wave velocity of the top 1 ft is unusually low in both profiles due to the rainy weather conditions that existed at the day of testing. Both profiles agree well and indicate that the site has an increasing stiffness with depth. The significant increase (jump) in  $V_s$  at an average depth of about 38 ft is consistent with the shale layer encountered at about 36 ft during SPT profiling.

To have a better understanding of the properties of the top 15 ft of soil, the scatter in the composite field dispersion curves was studied further. Variability in the shear wave velocity due to scatter in the constructed field dispersion curves, was determined by fitting alternative theoretical dispersion curves to the data. These theoretical curves were fitted to the upper and lower boundaries of the observed scatter in the composite field dispersion curves. The resulting variability in shear wave velocity is shown in Figure 37, where the shear wave velocity profiles from two arrays were redrawn in an attempt to focus on the top 15 ft of soil material. The shear wave velocity values that are determined from boundary theoretical dispersion curves are listed in Tables 8 and 9. The boundary theoretical curves are shown in Figures 38 and 39 for Line A and Line B, respectively.

## Summary

Linear and nonlinear soil properties of the Capitol Aggregates test site are characterized by means of laboratory and field testing. Two, Standard Penetration Test (SPT) boreholes (each 36 ft deep) and two, 3-in. O.D. Shelby-tube sampling boreholes (14.5 ft and 9.5 ft deep) were drilled at the test site on December 14, 2005. The SPT profiles of the site are given in Figure 5. Disturbed and undisturbed samples collected from the boreholes were tested in the laboratory at

The University of Texas at Austin. Index property tests, conducted in accordance with ASTM standards, revealed that the top 14 ft of soil at the site is comprised of non-plastic silt (ML) with some silty sand (SM) layers in the top 1.5 ft and bottom 1.5 ft of the 14-foot deep profile. All information about the fines content, water content, unit weight, degree of saturation and void ratio of the top 14 ft of the soil material as obtained from the disturbed and undisturbed samples is plotted in Figure 9.

A consolidated undrained triaxial test was performed on an undisturbed specimen obtained from an approximate depth of 10.6 ft. The resulting stress-strain curve is presented in Figure 10. An estimate of the undrained shear strength in terms of total stresses was measured as 13.41 psi (~1931 psf) at about 9 % strain. The specimen failed in a bulging mode.

Two combined resonant column and torsional shear (RCTS) tests were conducted on undisturbed specimens obtained from approximate depths of 6.0 ft and 9.2 ft. These tests were used to evaluate linear and nonlinear dynamic properties of the soil at the site. The variation of dynamic properties in the linear strain range ( $V_s$ ,  $G_{max}$  and  $D_{min}$ ) with confining pressure are presented in Figures 11 through 13. Dynamic properties in the nonlinear strain range, represented by the variation of shear modulus,  $G$ , normalized shear modulus  $G/G_{max}$ , and material damping ratio,  $D$ , with shearing strain amplitude, are shown in Figures 17, 18 and 21, respectively. The value of the reference shearing strain,  $\gamma_r$ , at  $\sigma_o = 6$  psi is about 0.04% and 0.05% for Specimens No.1 and No.2, respectively. At  $\sigma_o = 24$  psi,  $\gamma_r$  values are about 0.07% and 0.09% for Specimens No.1 and No.2, respectively. The value of the elastic threshold shearing strain,  $\gamma_t^e$ , at 6 psi confining pressure level, is about 0.0007 % for Specimen No.1 and 0.0011% for Specimen No.2. At 24 psi confining pressure level,  $\gamma_t^e$  values are about 0.0009% and 0.0014% for Specimen No.1 and No.2, respectively.

The  $G/G_{max} - \log \gamma$  curves obtained from RC tests match with the upper bound curve for sands proposed by Seed et al. (1986) and plus one standard deviation curve for sands presented by Darendeli (2001) (see Figures 19 and 20). The  $D - \log \gamma$  curves obtained from RC tests, are close to the lower bound curve of Seed et al. (1986) and minus one standard deviation curve of Darendeli (2001) (see Figures 22 and 23). This can be explained by the presence of high percentage of fines in the materials tested.

Additionally, conventional SASW testing was performed at the Capitol Aggregates site (on February 3, 2005) to evaluate the shear wave velocity profile. Two SASW arrays were tested. The resulting shear wave velocity profiles are shown in Figure 36. The two shear wave velocity profiles agree well (except for slight differences in the top 7.0 ft of soil) and indicate that the site has an increasing stiffness with depth. The significant increase (jump) in  $V_s$  at an average depth of about 38 ft observed at the SASW shear wave velocity profiles is consistent with the shale layer encountered at about 36 ft during SPT profiling.

## References

- ASTM D 422 (2002) "Standard Test Method for Particle-Size Analysis of Soils", *Annual Book of ASTM Standards*, Vol 04.08.
- ASTM D 1586 (1999), "Standard Test Method for Penetration Test and Split-Barrel Sampling of Soils", *Annual Book of ASTM Standards*, Vol 04.08.

- ASTM D 1587 (2000), “Standard Practice for Thin-Walled Tube Sampling of Soils for Geotechnical Purposes”, *Annual Book of ASTM Standards*, Vol 04.08.
- ASTM D 2217 (2002), “Standard Practice for Wet Preparation of Soil Samples for Particle Size Analysis and Determination of Soil Constants”, *Annual Book of ASTM Standards*, Vol 04.08.
- ASTM D 2487 (2000), “Standard Practice for Classification of Soils for Engineering Purposes (Unified Soil Classification System)”, *Annual Book of ASTM Standards*, Vol 04.08.
- ASTM D 4318 (2000), “Standard Test Methods for Liquid Limit, Plastic Limit, and Plasticity Index of Soils”, *Annual Book of ASTM Standards*, Vol 04.08.
- Darendeli, M. B. (2001), “Development of a New Family of Normalized Modulus Reduction and Material Damping Curves”, Ph.D. Dissertation, The University of Texas at Austin, 362 pp.
- Hardin, B. O. and Drnevich, V. P. (1972), “Shear Modulus And Damping in Soils: Design Equations and Curves”, *Journal of the Soil Mechanics and the Foundations Division, ASCE*, Vol. 87, No.SM7, pp 667-692.
- NCEER-97-0022 (1997), “Proceedings of the NCEER Workshop on Evaluation of Liquefaction Resistance of Soils’, edited by L. Youd & I.M. Idriss, Technical Report, 276 pp.
- Seed, H.B., Wong, R.T., Idriss, I.M. and Tokimatsu, K. (1986), “Moduli and Damping Factors for Dynamic Analyses of Cohesionless Soils”, *Journal of the Soil Mechanics and the Foundations Division, ASCE*, Vol. 112, No. SM11, pp.1016-1032.
- Stokoe, K. H., Hwang, S. K., Lee, J. N. and Andrus, R. D. (1994) “Effect of Various Parameters on the Stiffness and Damping of Soils at Small to Medium Strains”, *Invited Keynote Lecture, Int. Symposium on Pre-failure Deformation Characteristics of Geomaterials*, Shibuya, Mitachi and Miura, eds., Sapporo, Japan, pp. 785-816.

Table 1. Values of Field and Corrected Standard Penetration Blow Counts obtained at Capitol Aggregates Site on December 14, 2005

<b>Borehole No.</b>	<b>Depth, ft</b>	<b>Field N, bpf</b>	<b>N<sub>60</sub>, bpf</b>	<b>N<sub>1,60</sub>, bpf</b>
<b>D1</b>	1.0	13	15	29
	3.5	8	9	18
	6.0	8	9	16
	8.5	14	16	24
	11.0	12	15	20
	13.5	19	24	29
	16.0	19	27	30
	18.5	6	9	9
	21.0	2	3	3
	23.5	22	31	28
	26.0	11	16	13
	31.0	13	19	15
	36.0	100	shale	shale
<b>D2</b>	1.0	12	13	27
	3.5	6	7	13
	6.0	8	9	16
	8.5	5	6	8
	11.0	10	13	17
	13.5	13	17	20
	16.0	9	13	14
	18.5	8	11	12
	21.0	10	14	14
	23.5	14	20	18
	26.0	6	9	7
	31.0	18	27	21
	36.0	100	shale	shale



Table 2. USCS Soil Classification for Top 14 ft of Soil Material at Capitol Aggregates

<b>Borehole No.</b>	<b>Depth Range, ft</b>	<b>Fines Content, %</b>	<b>Soil Classification, USCS</b>
<b>D1</b>	0- 1.5	28	SM
	2.5-4.0	58	ML
	5.0- 6.5	65	ML
	7.5- 9.0	82	ML
	10.0- 11.5	83	ML
	12.5- 14.0	25	SM
<b>D2</b>	0- 1.5	14	SM
	2.5-4.0	51	ML
	5.0- 6.5	61	ML
	7.5- 9.0	84	ML
	10.0- 11.5	80	ML
	12.5- 14.0	23	SM

Table 3. Summary of Soil Index Properties Determined from Undisturbed Samples

<b>Depth, ft</b>	<b>Water Content, %</b>	<b>Total Unit Weight, pcf</b>	<b>Dry Unit Weight, pcf</b>	<b>Void Ratio*</b>	<b>Degree of Saturation*, %</b>
5.6	8	NA	NA	NA	NA
6.0	16	131.1	113.0	0.5	89
6.5	NA	112.3	NA	NA	NA
8.4	22	118.3	97.1	0.7	81
8.8	25	110.7	88.6	0.9	75
9.2	24	122.7	99.1	0.7	93
10.6	18	107.3	90.9	0.8	57
11.1	8	96.1	89.1	0.9	24
11.6	10	99.7	90.7	0.8	31

\*Specific Gravity,  $G_s$ , is assumed to be 2.68.

Table 4. Index Properties of the Undisturbed Triaxial Test Specimen

<b>Soil Index Property</b>	<b>Initial</b>	<b>After consolidation/ compression</b>	<b>Failure</b>
<b>Diameter, D, inch</b>	1.50	1.48	1.56
<b>Height, H, inch</b>	3.00	2.87	2.56
<b>Total Unit Weight, <math>\gamma_t</math>, pcf</b>	107.3	111.1	112.8
<b>Water Content, w, %</b>	18	18	18
<b>Dry Unit Weight, <math>\gamma_d</math>, pcf</b>	90.9	94.3	95.7
<b>Void Ratio, <math>e^*</math></b>	0.84	0.77	0.75
<b>Degree of Saturation, <math>S_r^*</math>, %</b>	57	62	64

\*Specific Gravity,  $G_s$ , is assumed to be 2.68.

Table 5. Initial Properties of the Undisturbed RCTS Test Specimens

<b>Specimen No.</b>	<b>1</b>	<b>2</b>
<b>Specimen Depth, ft</b>	6.0	9.2
<b>Soil Classification, USCS</b>	ML	ML
<b>Fines Content, %</b>	67	83
<b>Diameter, D, inch</b>	2.00	2.015
<b>Height, H, inch</b>	4.00	3.70
<b>Total Unit Weight, <math>\gamma_t</math>, pcf</b>	131.1	122.7
<b>Water Content, w, %</b>	16	24
<b>Dry Unit Weight, <math>\gamma_d</math>, pcf</b>	113.0	99.1
<b>Void Ratio, e*</b>	0.48	0.69
<b>Degree of Saturation, <math>S_r</math>*, %</b>	89	93

\*Specific Gravity,  $G_s$ , is assumed to be 2.68.

Table 6. Tabulated Values of Best-Fit Wave Velocity Profile (Figure 36) from SASW Testing at Capitol Aggregates Test Site; SASW- Line A

<b>Depth to Top of Layer, ft</b>	<b>Layer Thickness, ft</b>	<b>Compression Wave Velocity*, fps</b>	<b>Shear Wave Velocity, fps</b>	<b>Assumed Poisson's Ratio</b>	<b>Assumed Total Unit Weight, pcf</b>
0	1	635	320	0.33	110
1	1.5	834	420	0.33	110
2.5	4.5	1072	540	0.33	110
7	7	1310	660	0.33	110
14	7.5	1390	700	0.33	110
21.5	17	5000	750	0.49	125
38.5	half-space	5000	2200	0.38	125

\*Based on the shear wave velocity and assumed value of Poisson's ratio above the water table. Below the water table,  $V_p$  was assumed equal to 5000 fps.

Table 7. Tabulated Values of Best-Fit Wave Velocity Profile (Figure 36) from SASW Testing at Capitol Aggregates Test Site; SASW- Line B

<b>Depth to Top of Layer, ft</b>	<b>Layer Thickness, ft</b>	<b>Compression Wave Velocity*, fps</b>	<b>Shear Wave Velocity, fps</b>	<b>Assumed Poisson's Ratio</b>	<b>Assumed Total Unit Weight, pcf</b>
0	1	675	340	0.33	110
1	1.5	953	480	0.33	110
2.5	4.5	1013	510	0.33	110
7	7	1310	660	0.33	110
14	7.5	1390	700	0.33	110
21.5	17	5000	750	0.49	125
38.5	half-space	5000	2200	0.38	125

\*Based on the shear wave velocity and assumed value of Poisson's ratio above the water table. Below the water table,  $V_p$  was assumed equal to 5000 fps.

Table 8. Tabulated Values of Boundary Wave Velocity Profiles (Figure 37) from SASW Testing at Capitol Aggregates Test Site; SASW- Line A

Depth to Top of Layer, ft	Layer Thickness, ft	Upper and Lower Bound Compression Wave Velocity*, fps	Upper and Lower Bound Shear Wave Velocity, fps	Assumed Poisson's Ratio	Assumed Total Unit Weight, pcf
0	1	635	320	0.33	110
1	1.5	834	420	0.33	110
2.5	4.5	993, 1132	500, 570	0.33	110
7	7	1271, 1350	640, 680	0.33	110
14	7.5	1390	700	0.33	110
21.5	17	5000	750	0.49	125
38.5	half-space	5000	2200	0.38	125

\*Based on the shear wave velocity and assumed value of Poisson's ratio above the water table. Below the water table,  $V_p$  was assumed equal to 5000 fps.

Table 9. Tabulated Values of Boundary Wave Velocity Profiles (Figure 37) from SASW Testing at Capitol Aggregates Test Site; SASW- Line B

Depth to Top of Layer, ft	Layer Thickness, ft	Upper and Lower Bound Compression Wave Velocity*, fps	Upper and Lower Bound Shear Wave Velocity, fps	Assumed Poisson's Ratio	Assumed Total Unit Weight, pcf
0	1	675	340	0.33	110
1	1.5	933, 973	470, 490	0.33	110
2.5	4.5	953, 1112	480, 560	0.33	110
7	7	1310	660	0.33	110
14	7.5	1390	700	0.33	110
21.5	17	5000	750	0.49	125
38.5	half-space	5000	2200	0.38	125

\*Based on the shear wave velocity and assumed value of Poisson's ratio above the water table. Below the water table,  $V_p$  was assumed equal to 5000 fps

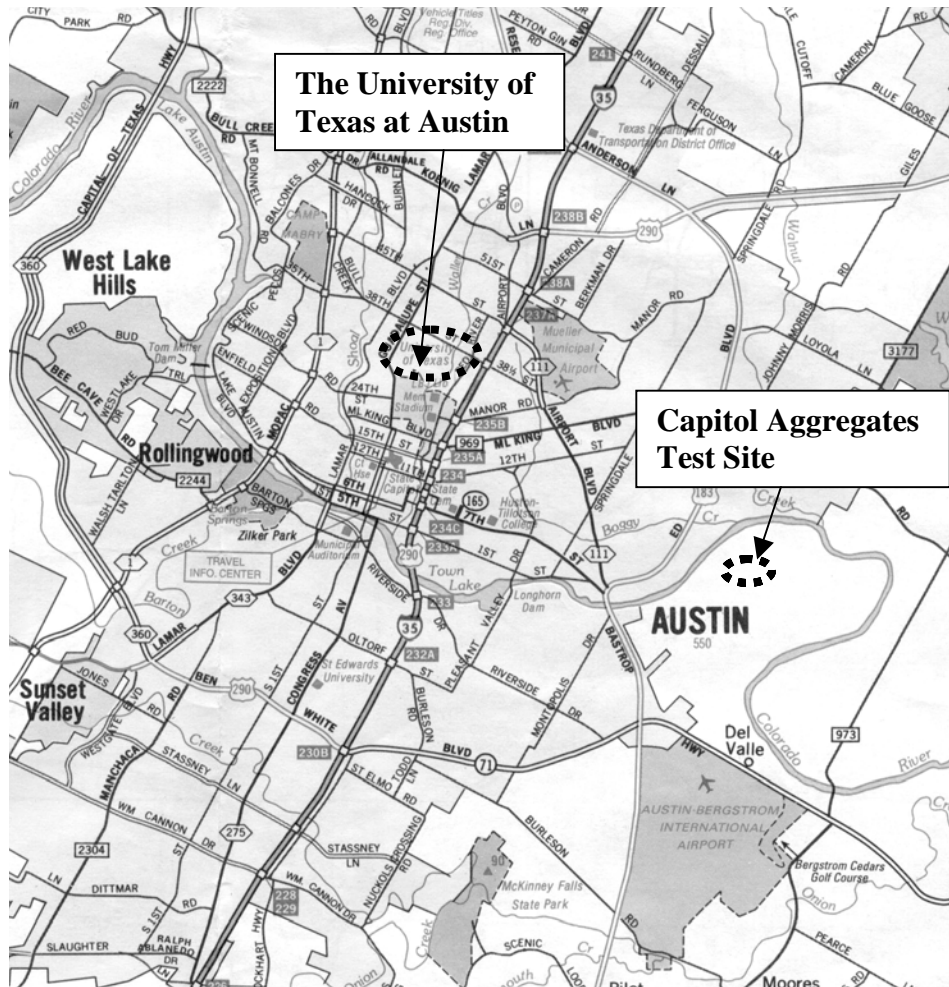


Figure 1. Location of the Capitol Aggregates Test Site in Austin, Texas



Figure 2. Capitol Aggregates Test Site

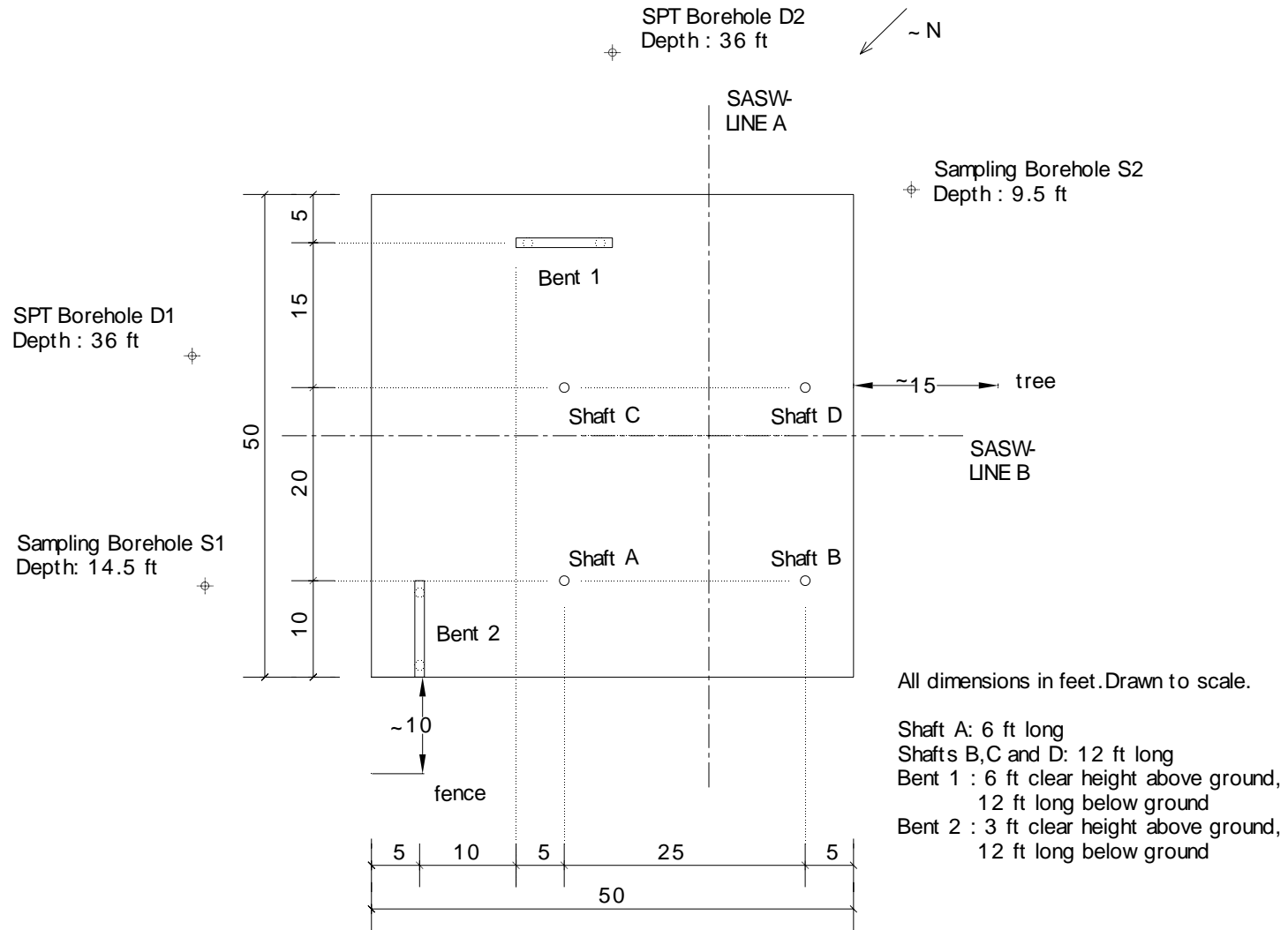


Figure 3. Plan View of Capitol Aggregates Test Site



Figure 4. Drill Rig used in Standard Penetration Tests at Capitol Aggregates Site, December 14, 2004

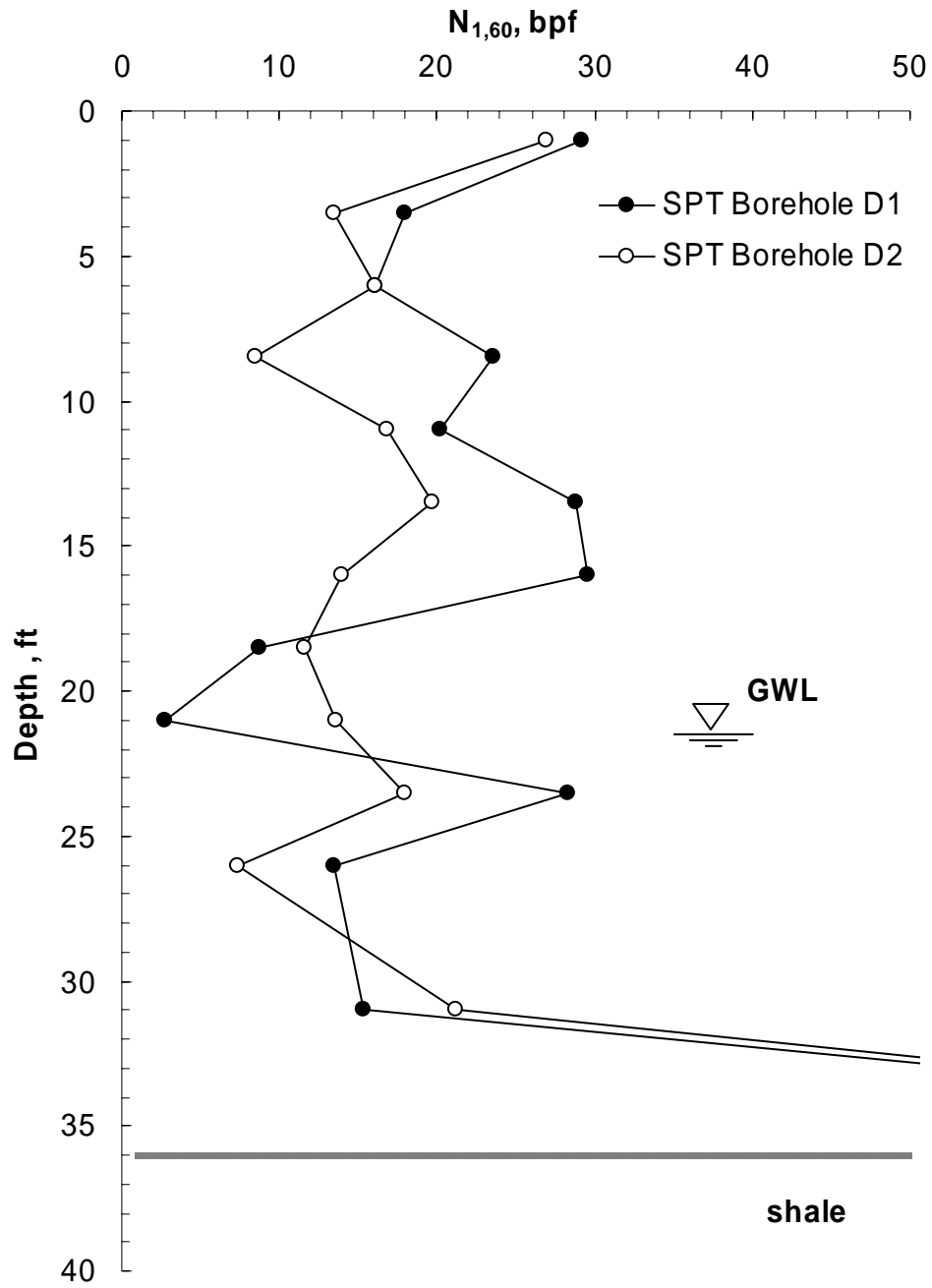


Figure 5. Variation of Corrected SPT Blow Count Values with Depth Obtained from SPT Testing at Capitol Aggregates Test Site on December 14, 2004



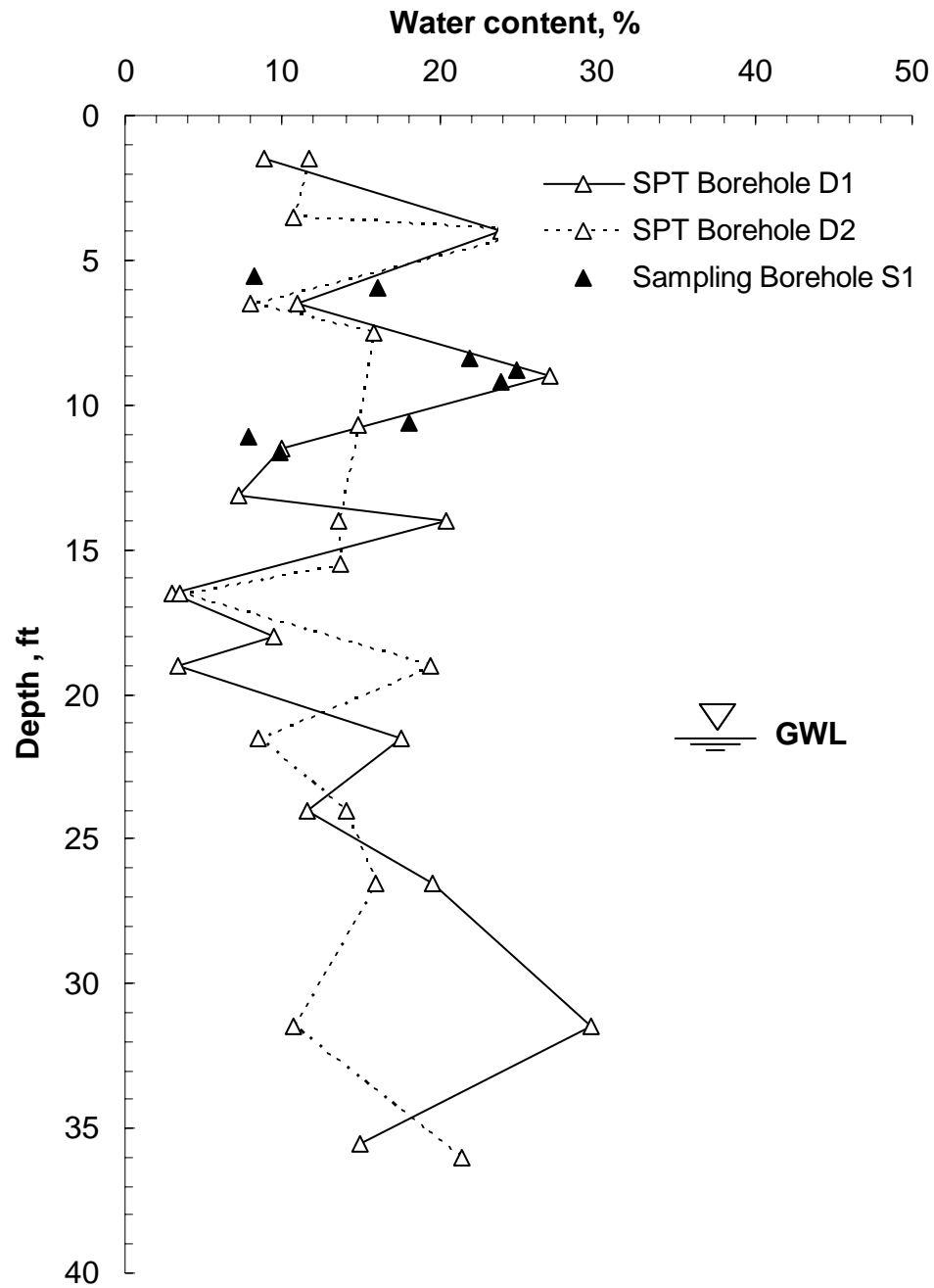


Figure 6. Variation of Water Content of Soil with Depth Obtained from SPT Samples at Capitol Aggregates Test Site on December 14, 2004

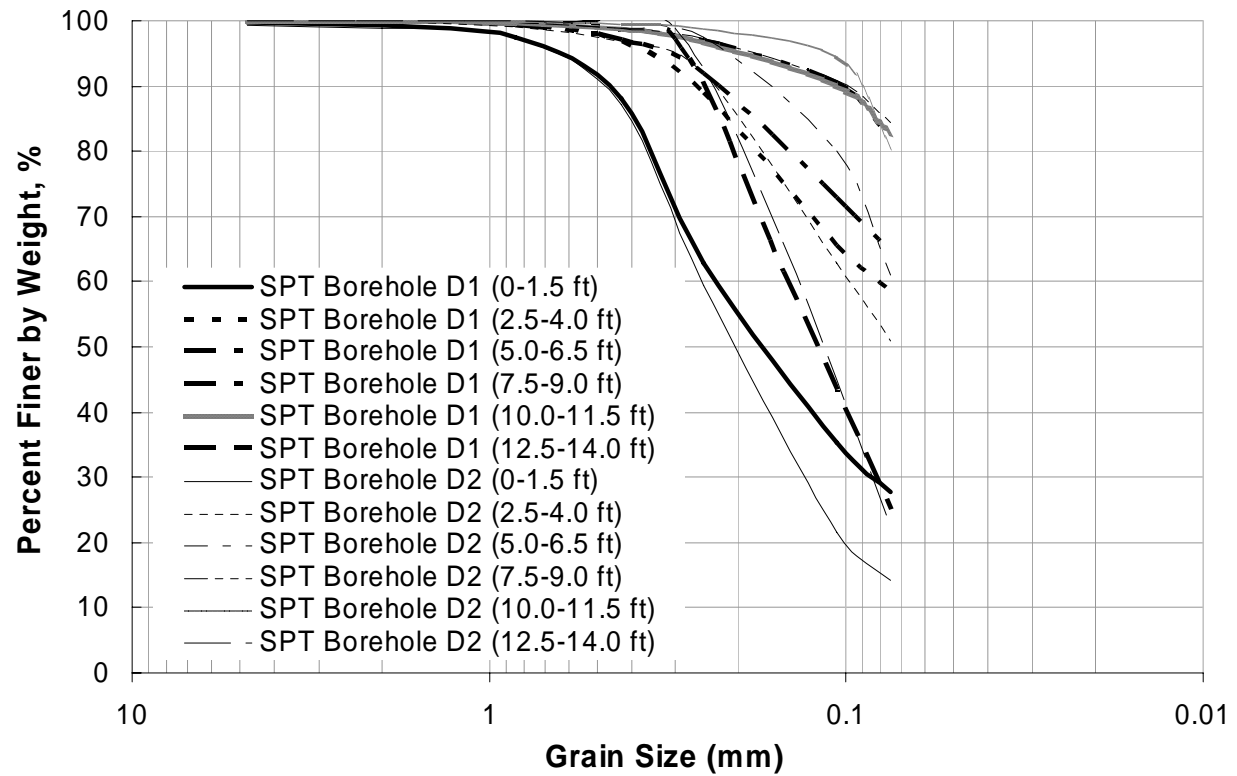


Figure 7. Grain Size Distribution Curves (for Particle Size Larger than 0.075 mm) Determined from Disturbed Samples Representing Top 14 ft of Soil Material at Capitol Aggregates Test Site

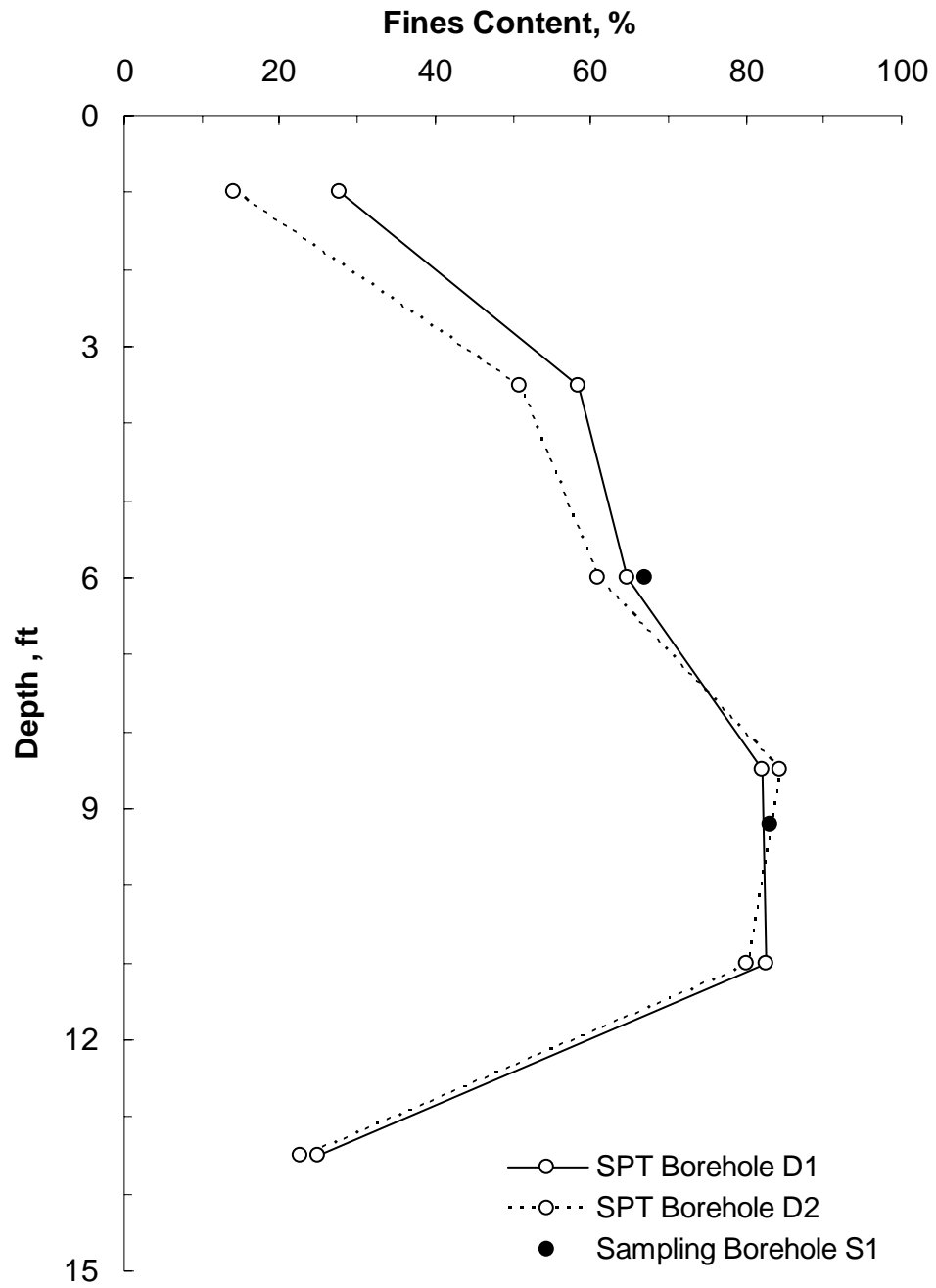


Figure 8. Variation of Fines Content with Depth for Top 14 ft of Soil Material at Capitol Aggregates Test Site

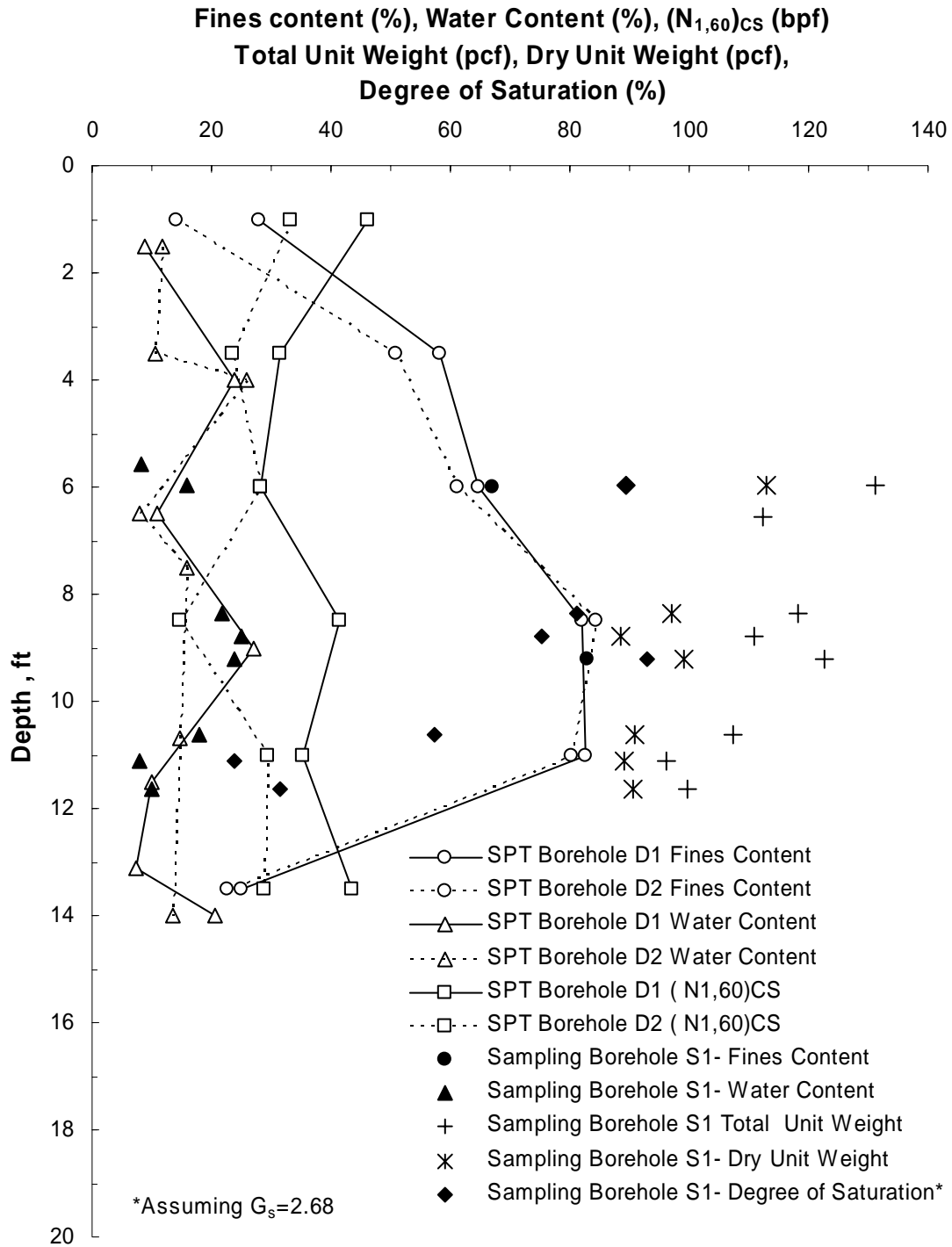


Figure 9. Index Properties of the Top 14 ft of Soil as Obtained from the Disturbed and Undisturbed Samples

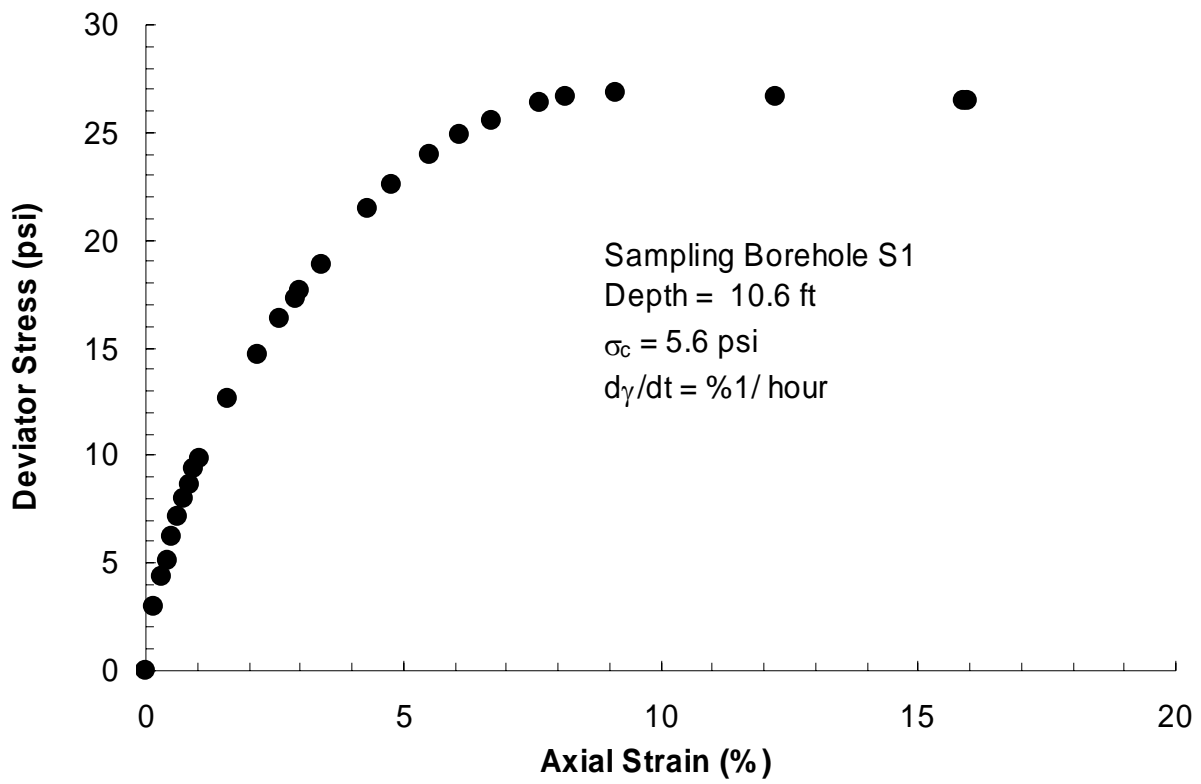


Figure 10. Total Stress-Strain Curve Determined from Undrained Shearing of Triaxial Specimen Trimmed from an Undisturbed Sample from a Depth of 10.6 ft

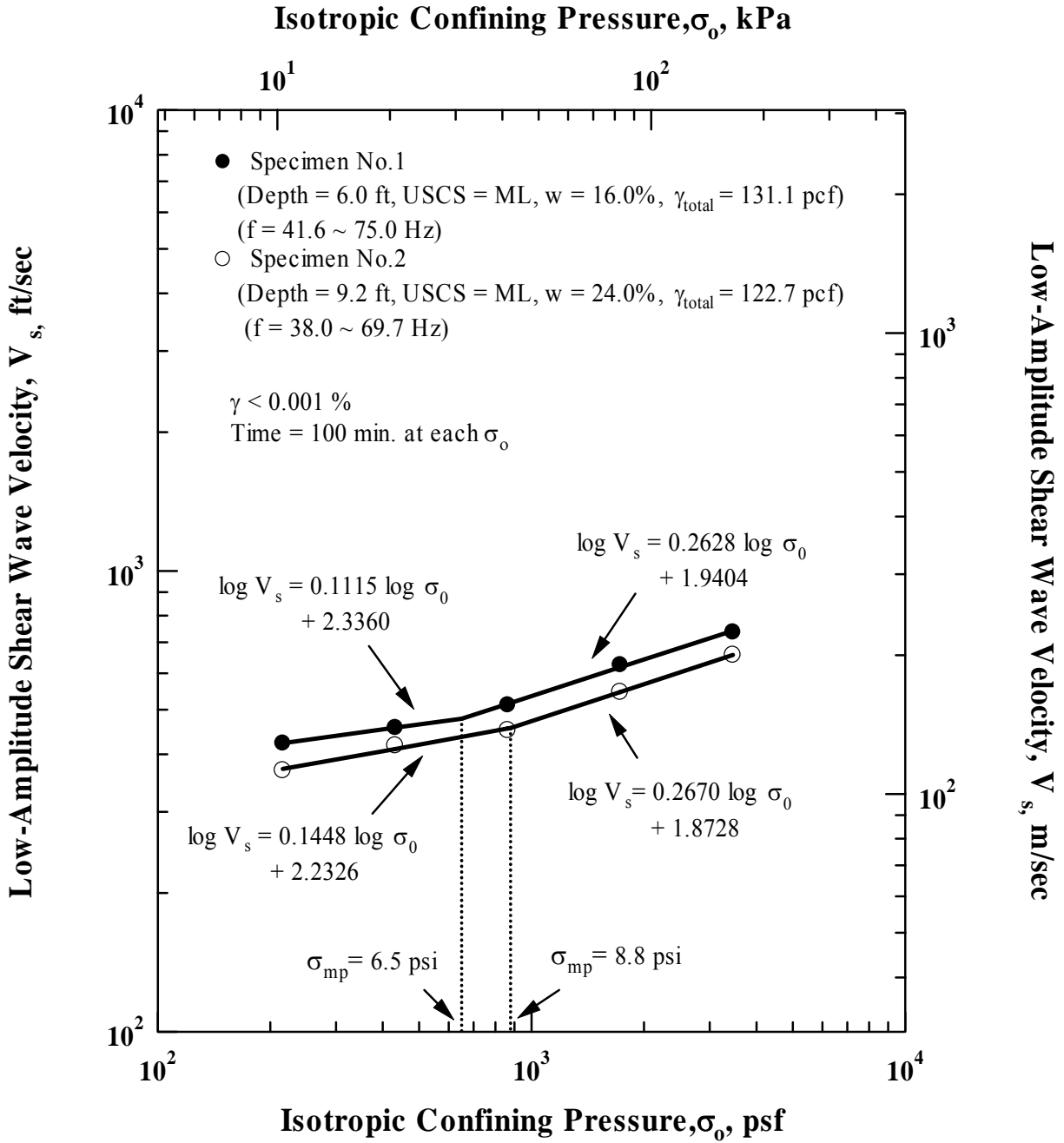


Figure 11. Variation in Low-Amplitude Shear Wave Velocity with Isotropic Confining Pressure from Resonant Column Tests

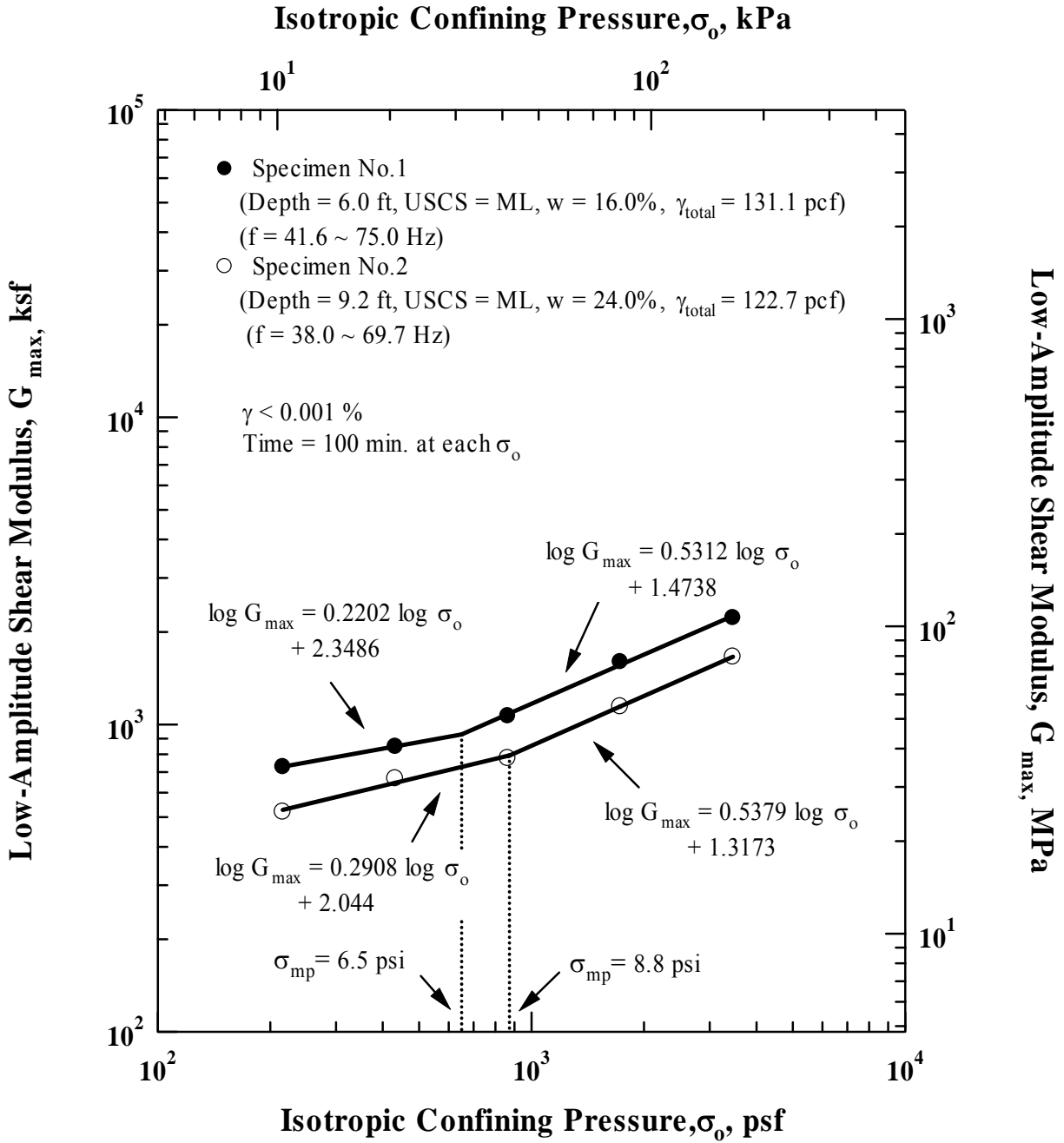


Figure 12. Variation in Low-Amplitude Shear Modulus with Isotropic Confining Pressure from Resonant Column Tests

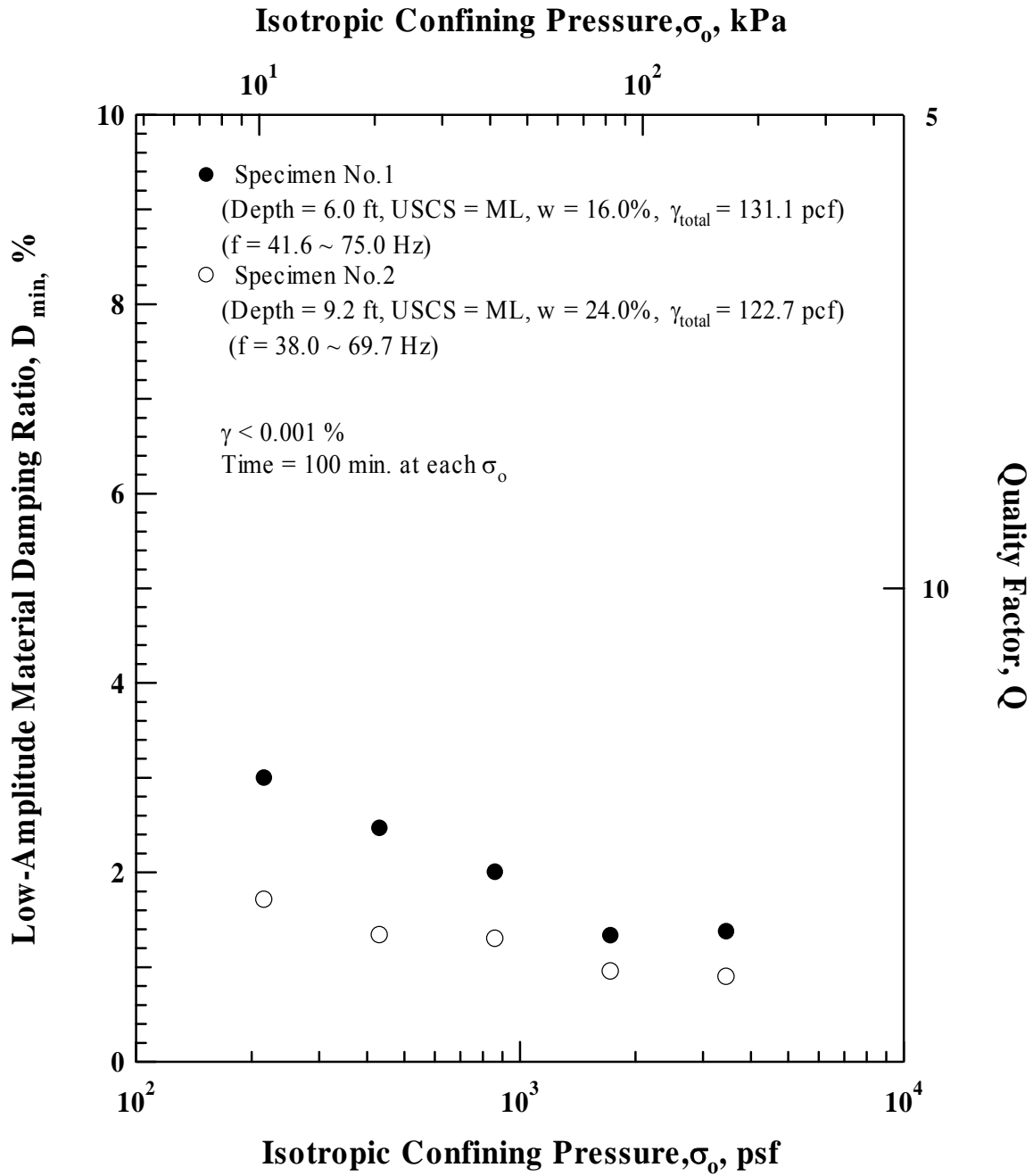


Figure 13. Variation in Low-Amplitude Material Damping Ratio with Isotropic Confining Pressure from Resonant Column Tests



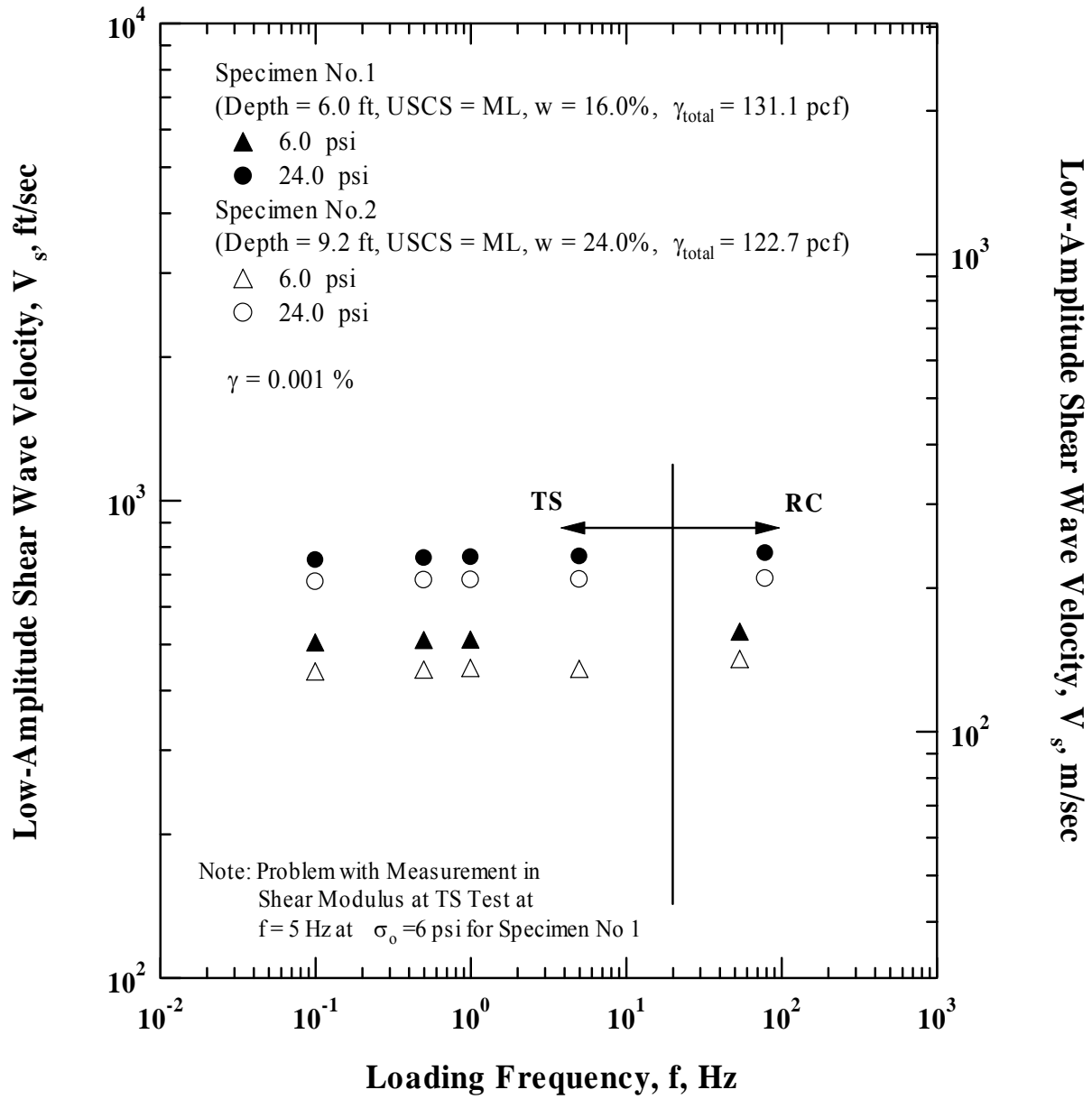


Figure 14. Variation in Low-Amplitude Shear Wave Velocity with Loading Frequency from Combined RCTS Tests

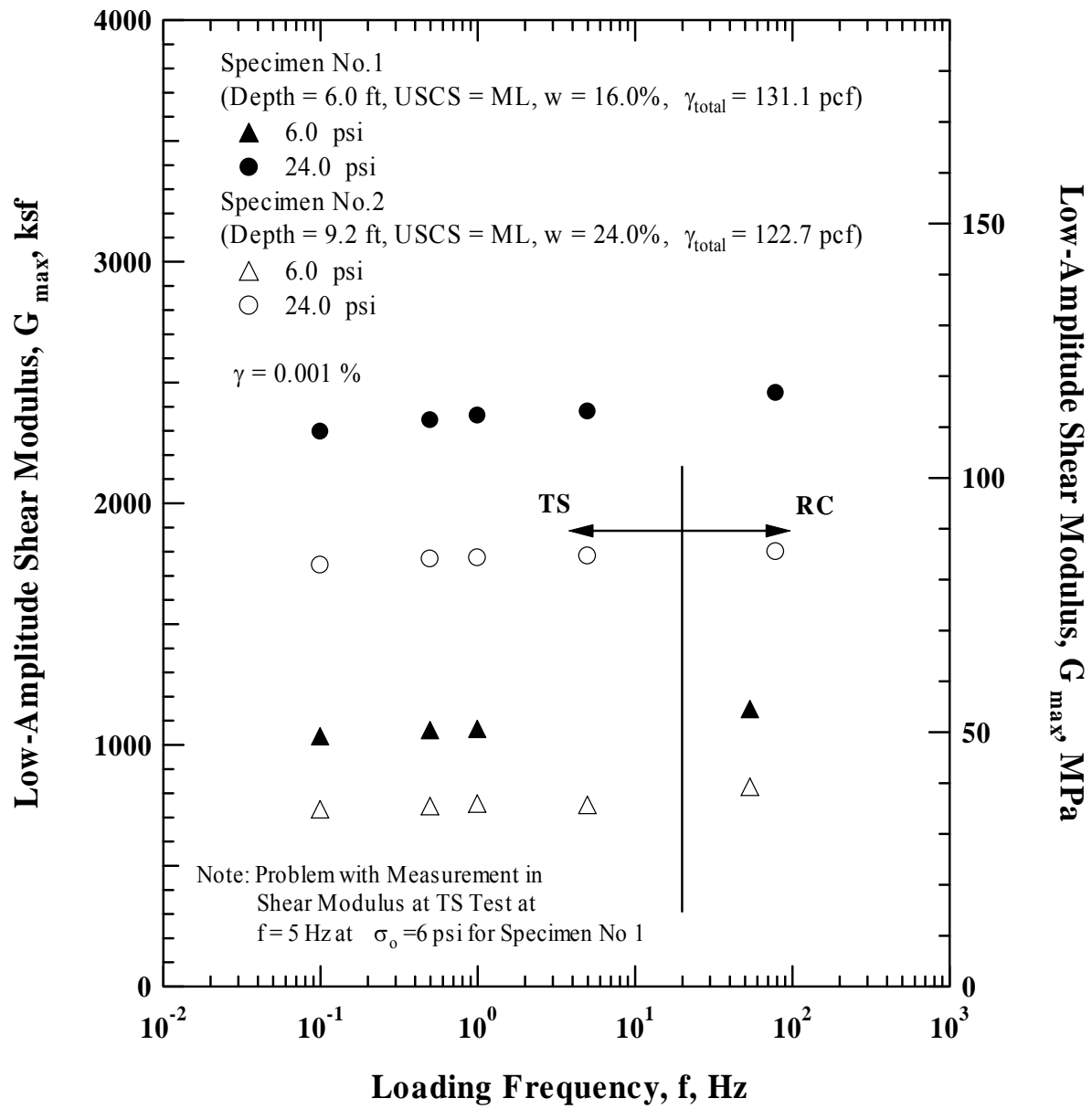


Figure 15. Variation in Low-Amplitude Shear Modulus with Loading Frequency from Combined RCTS Tests

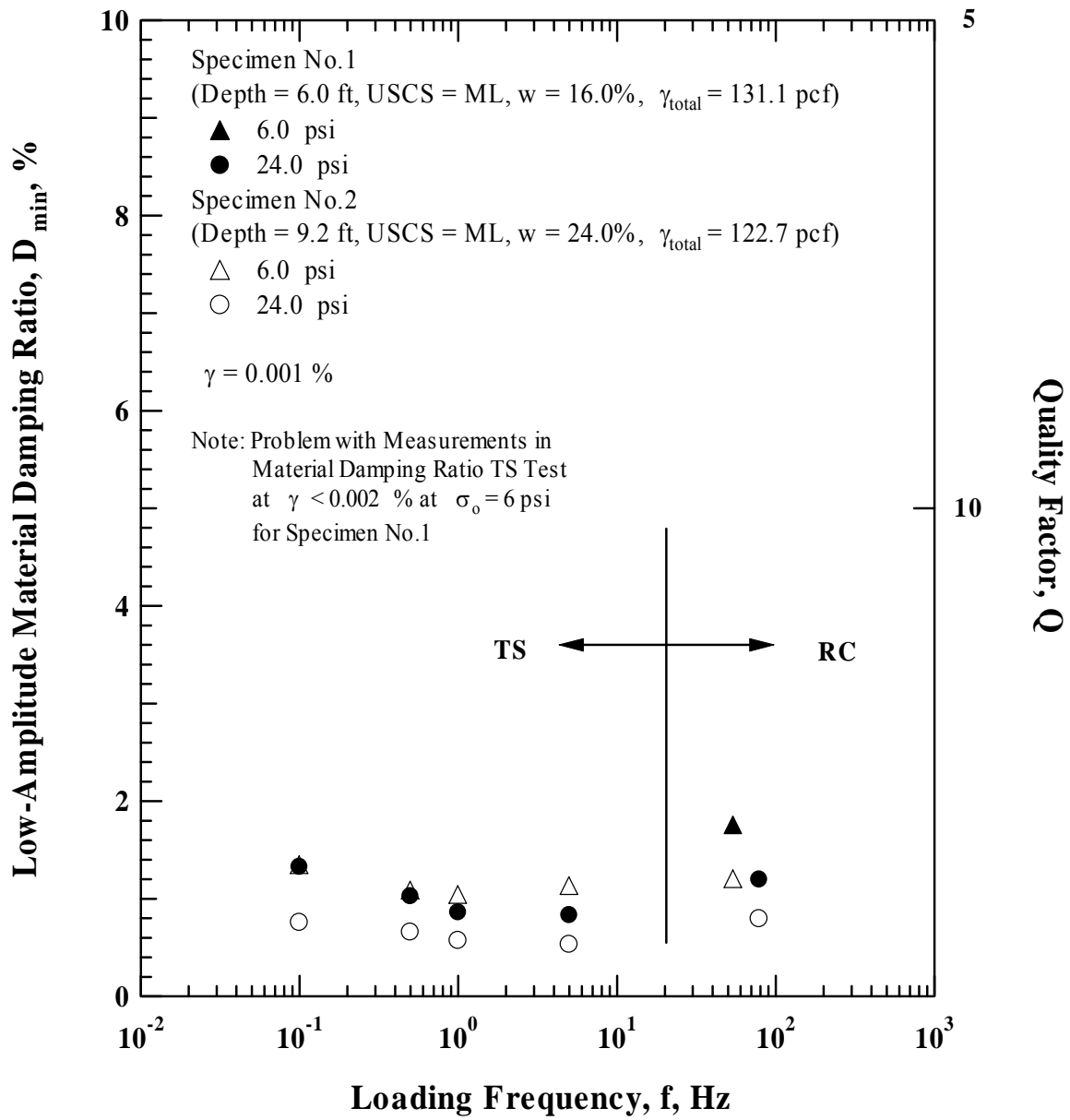


Figure 16. Variation in Low-Amplitude Material Damping Ratio with Loading Frequency from Combined RCTS Tests

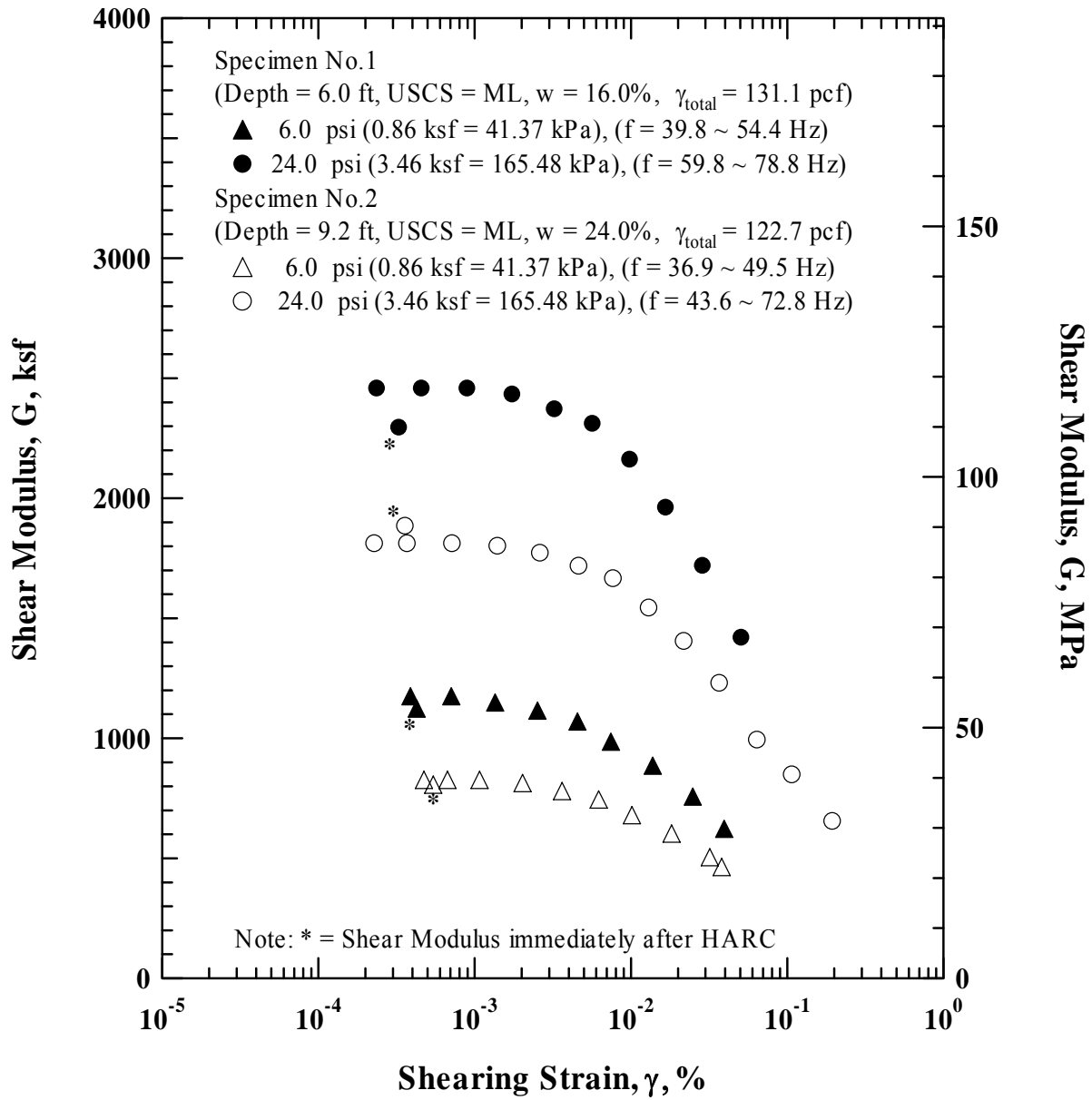


Figure 17. Comparison of the Variation in Shear Modulus with Shearing Strain at Two Isotropic Confining Pressures from the Resonant Column Tests

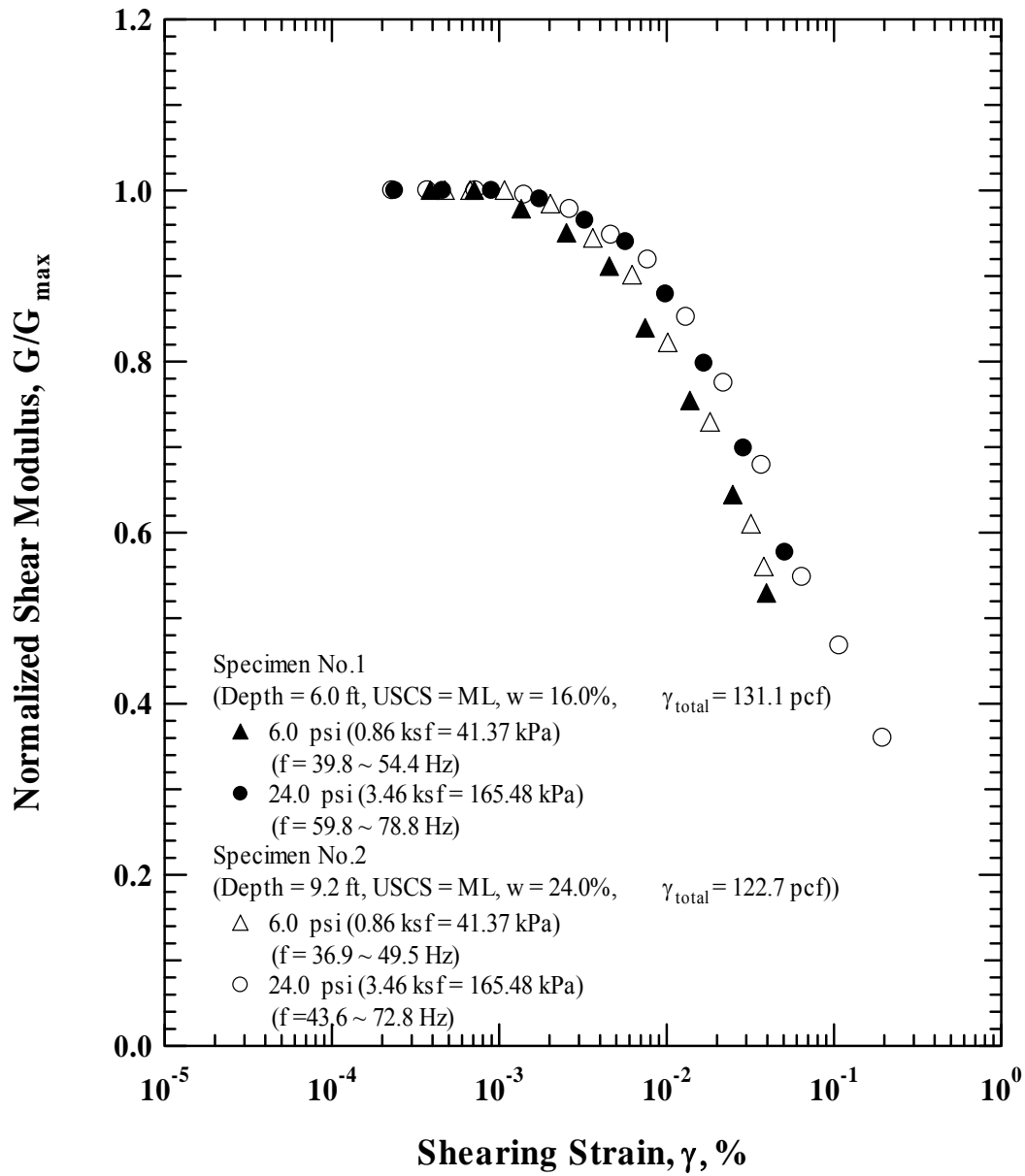


Figure 18. Comparison of the Variation in Normalized Shear Modulus with Shearing Strain at Two Isotropic Confining Pressures from the Resonant Column Tests

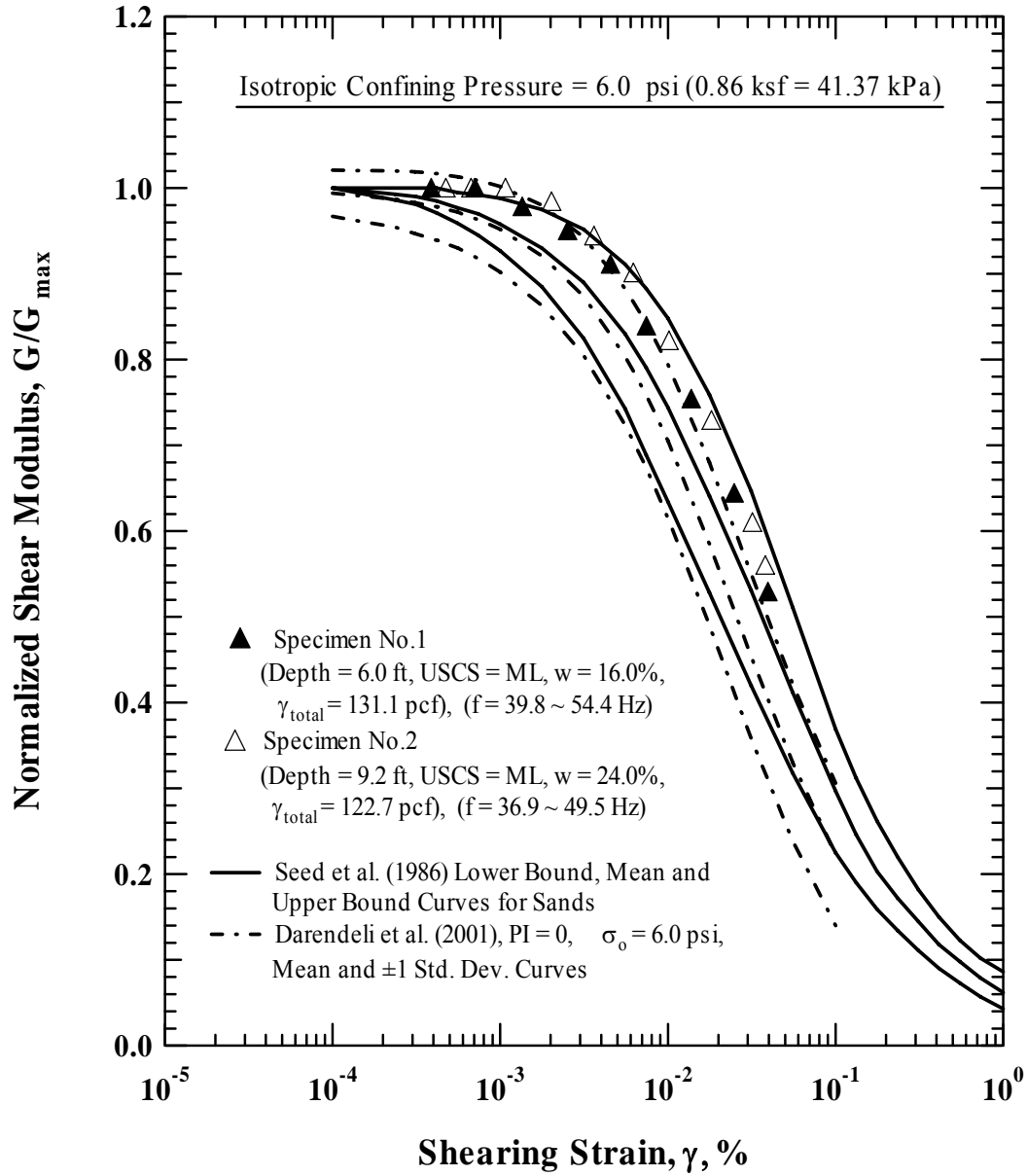


Figure 19. Comparison of the Variation in Normalized Shear Modulus with Shearing Strain at Isotropic Confining Pressure of 6 psi (0.86 ksf = 41.37 kPa) from the Resonant Column Tests with Modulus Reduction Curves proposed by Seed et al. (1986) and Darendeli (2001)

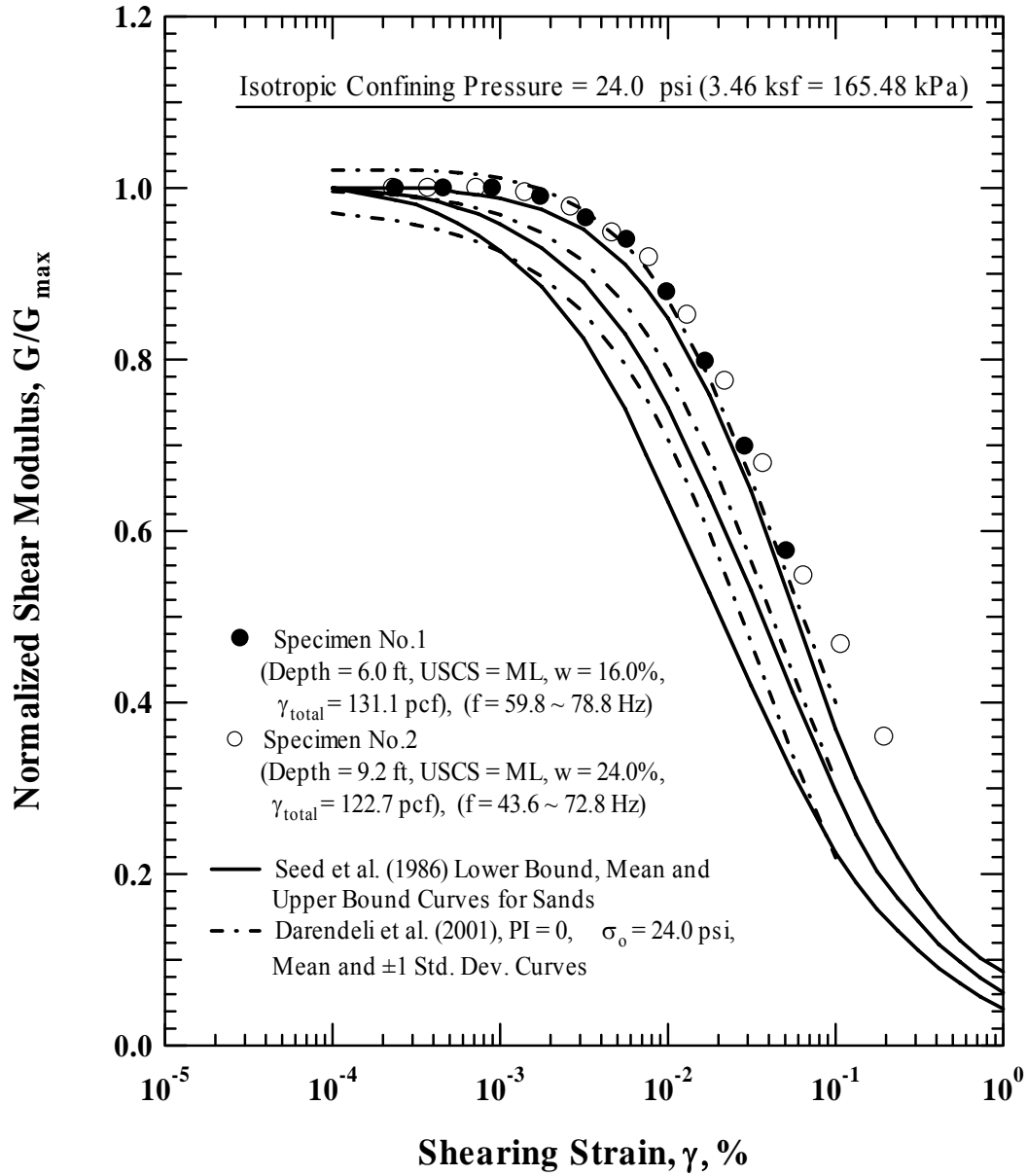


Figure 20. Comparison of the Variation in Normalized Shear Modulus with Shearing Strain at Isotropic Confining Pressure of 24 psi (3.46 ksf = 165.48 kPa) from the Resonant Column Tests with Modulus Reduction Curves proposed by Seed et al. (1986) and Darendeli (2001)

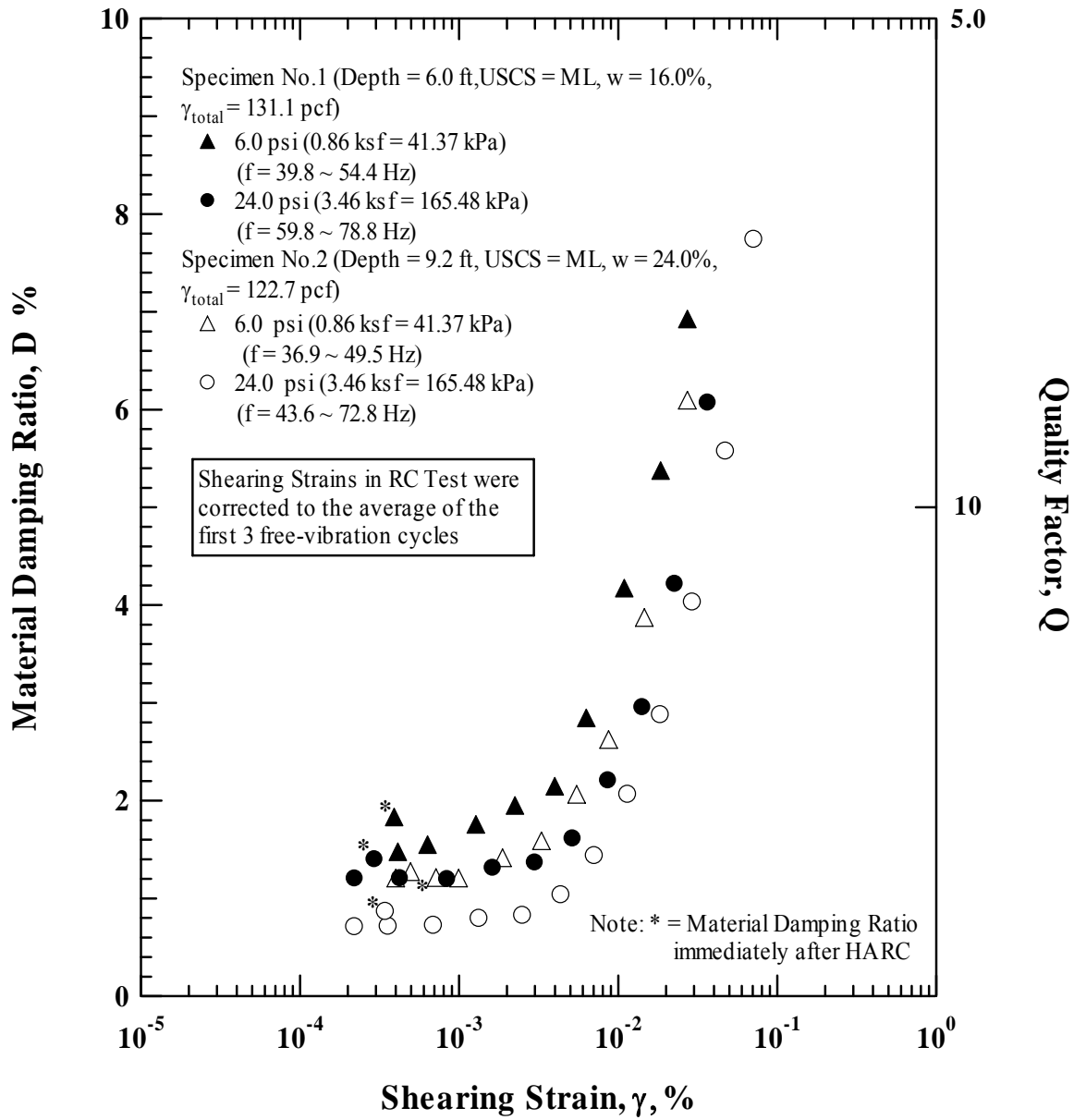


Figure 21. Comparison of the Variation in Material Damping Ratio with Shearing Strain and Isotropic Confining Pressures from the Resonant Column Tests



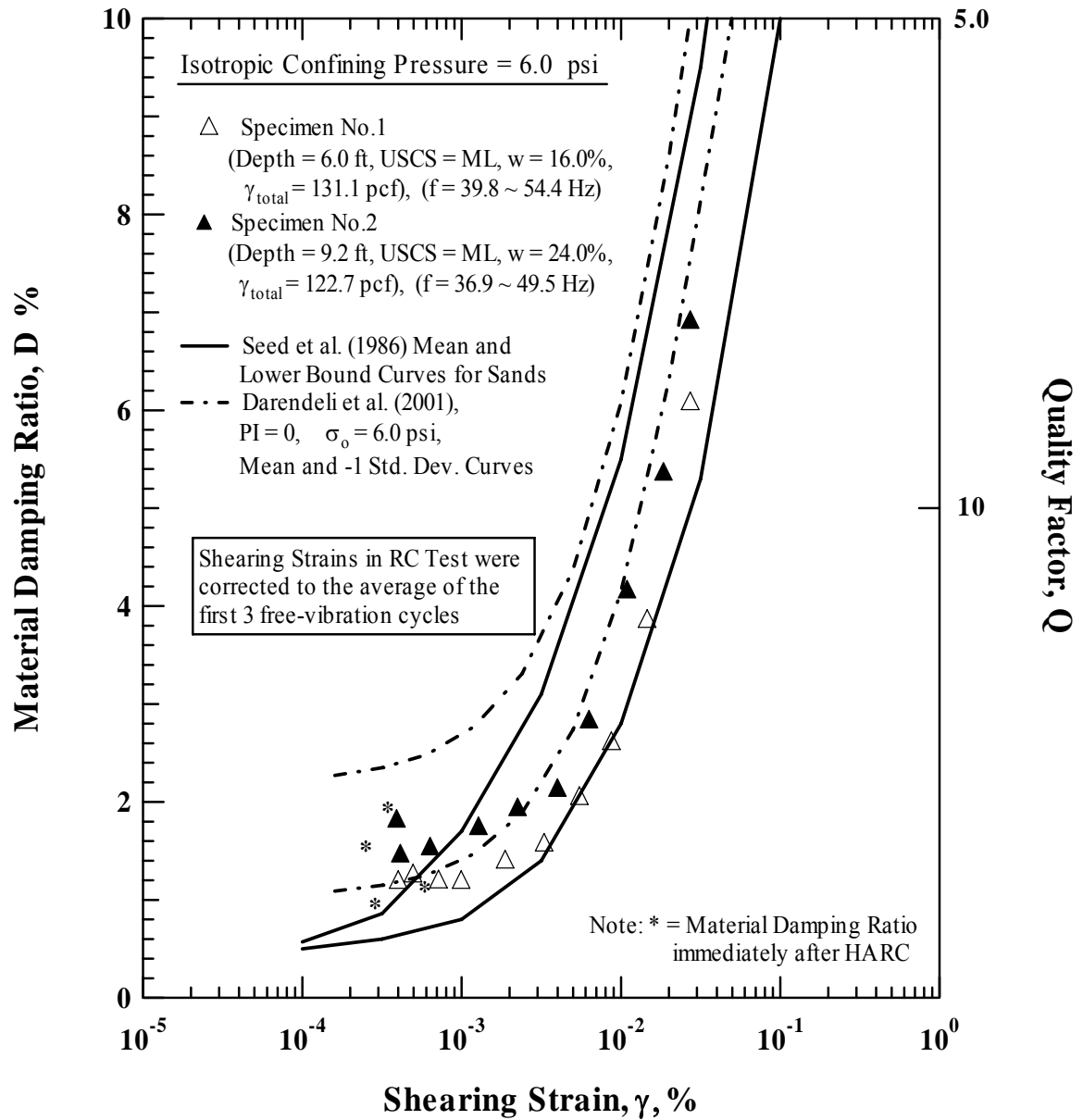


Figure 22. Comparison of the Variation in Material Damping Ratio with Shearing Strain at Isotropic Confining Pressure of 6 psi (0.86 ksf = 41.37 kPa) from the Resonant Column Tests with Material Damping Curves proposed by Seed et al. (1986) and Darendeli (2001)

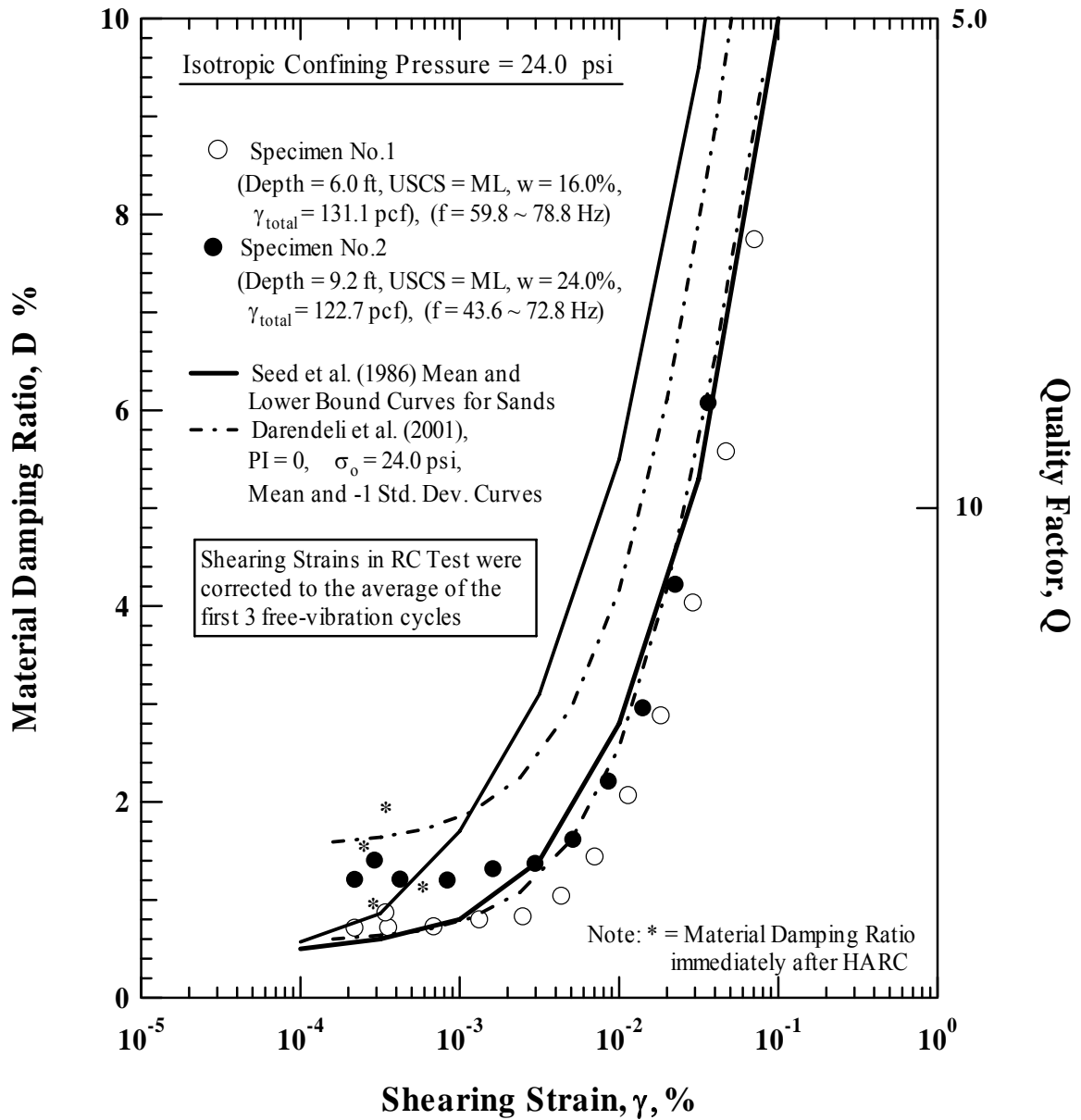


Figure 23. Comparison of the Variation in Material Damping Ratio with Shearing Strain at Isotropic Confining Pressure of 24 psi (3.46 ksf = 165.48 kPa) from the Resonant Column Tests with Material Damping Curves proposed by Seed et al. (1986) and Darendeli (2001)

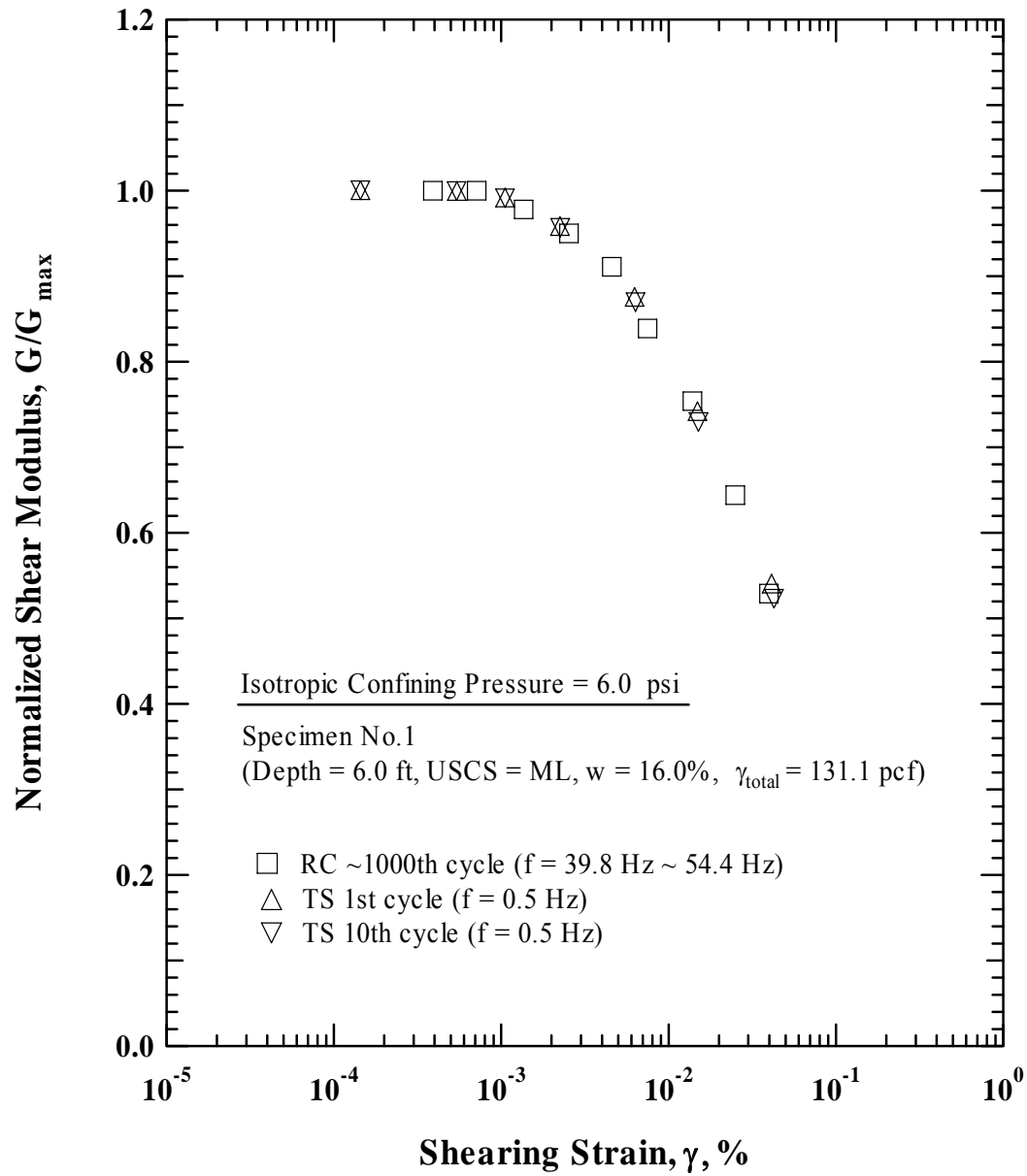


Figure 24. Comparison of the Variation in Normalized Shear Modulus with Shearing Strain at Isotropic Confining Pressure of 6 psi (0.86 ksf = 41.37 kPa) from Combined RCTS Tests of Specimen No. 1

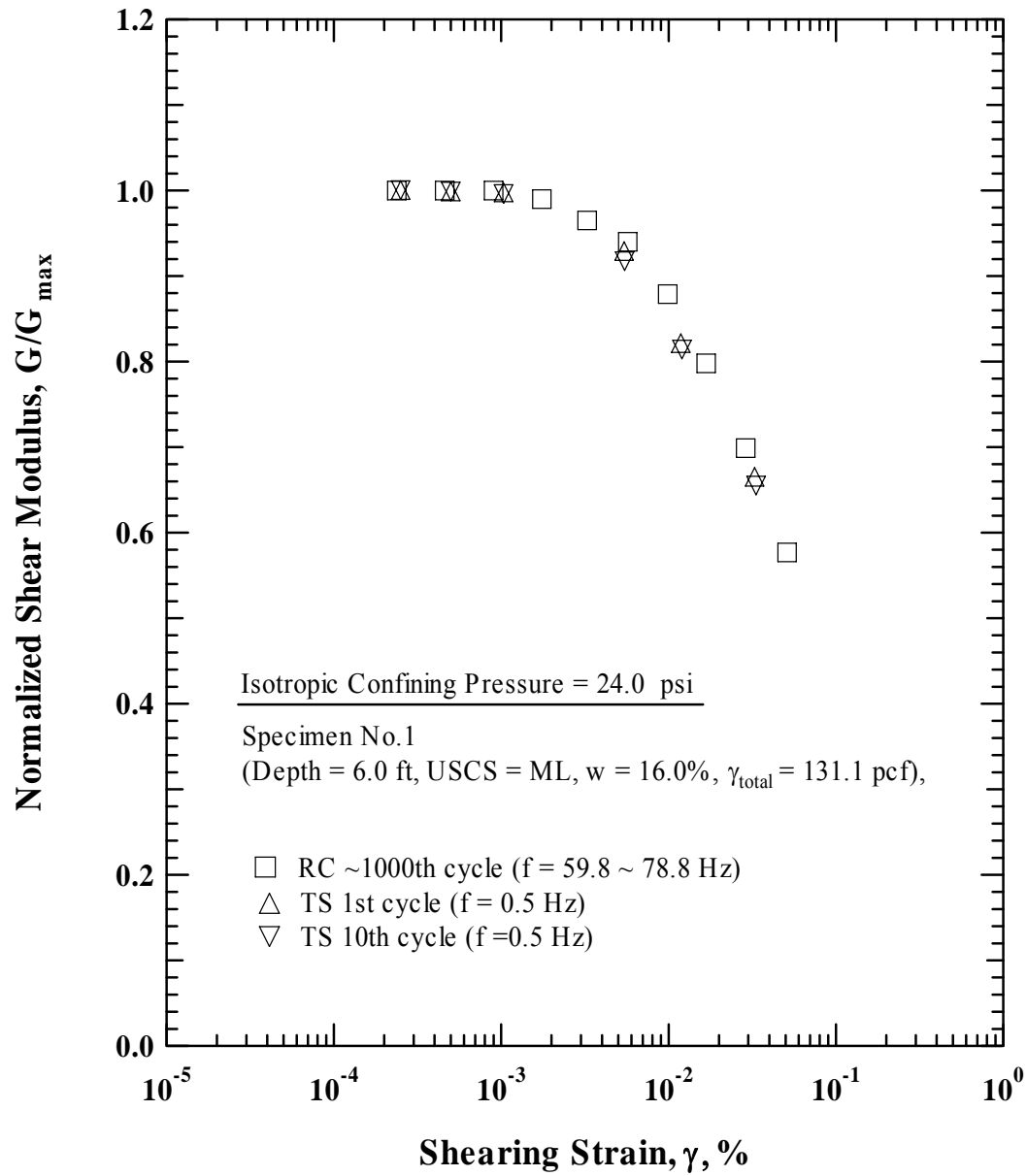


Figure 25. Comparison of the Variation in Normalized Shear Modulus with Shearing Strain at Isotropic Confining Pressure of 24 psi (3.46 ksf = 165.48 kPa) from Combined RCTS Tests of Specimen No. 1

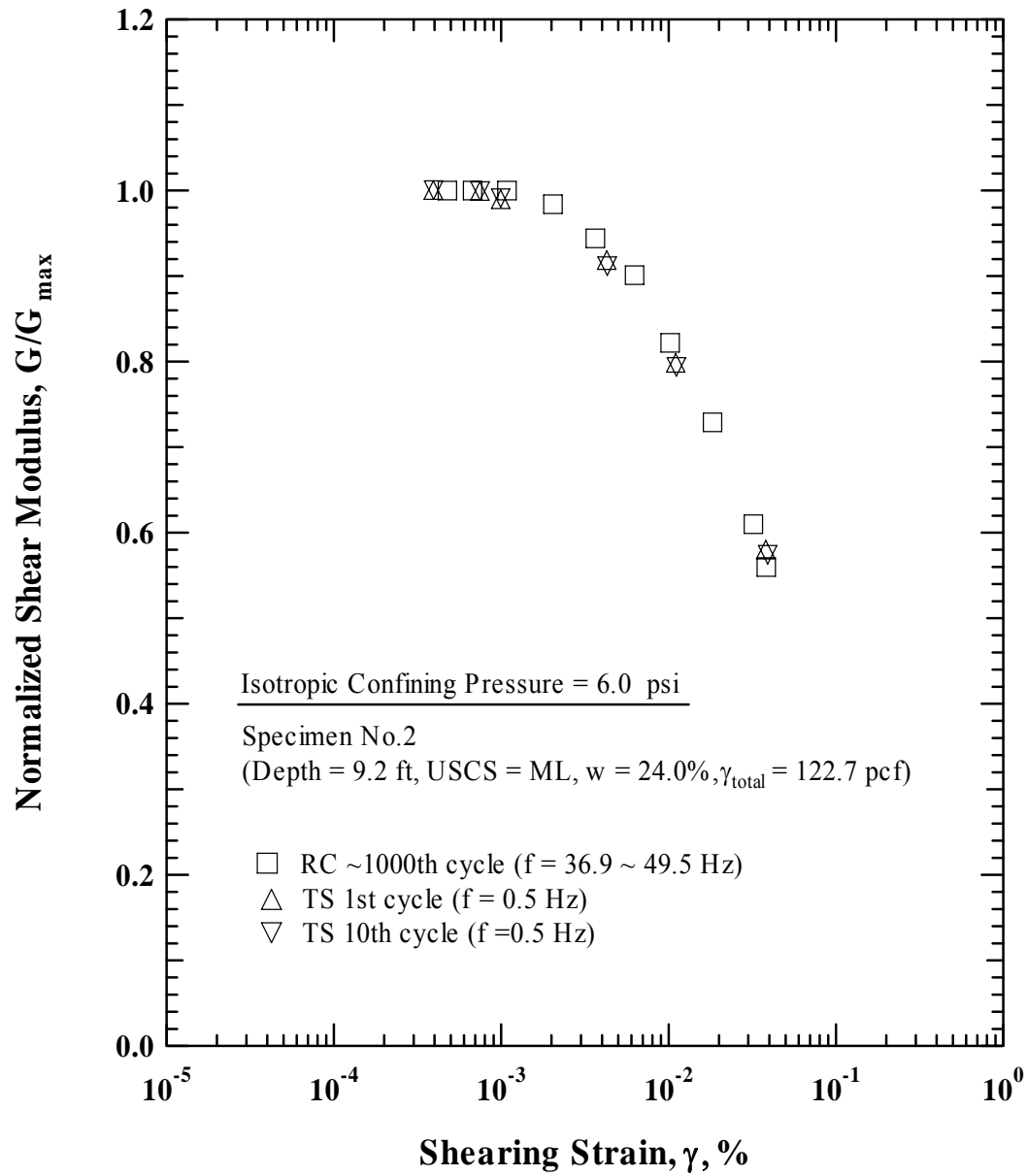


Figure 26. Comparison of the Variation in Normalized Shear Modulus with Shearing Strain at Isotropic Confining Pressure of 6 psi (0.86 ksf = 41.37 kPa) from Combined RCTS Tests of Specimen No. 2

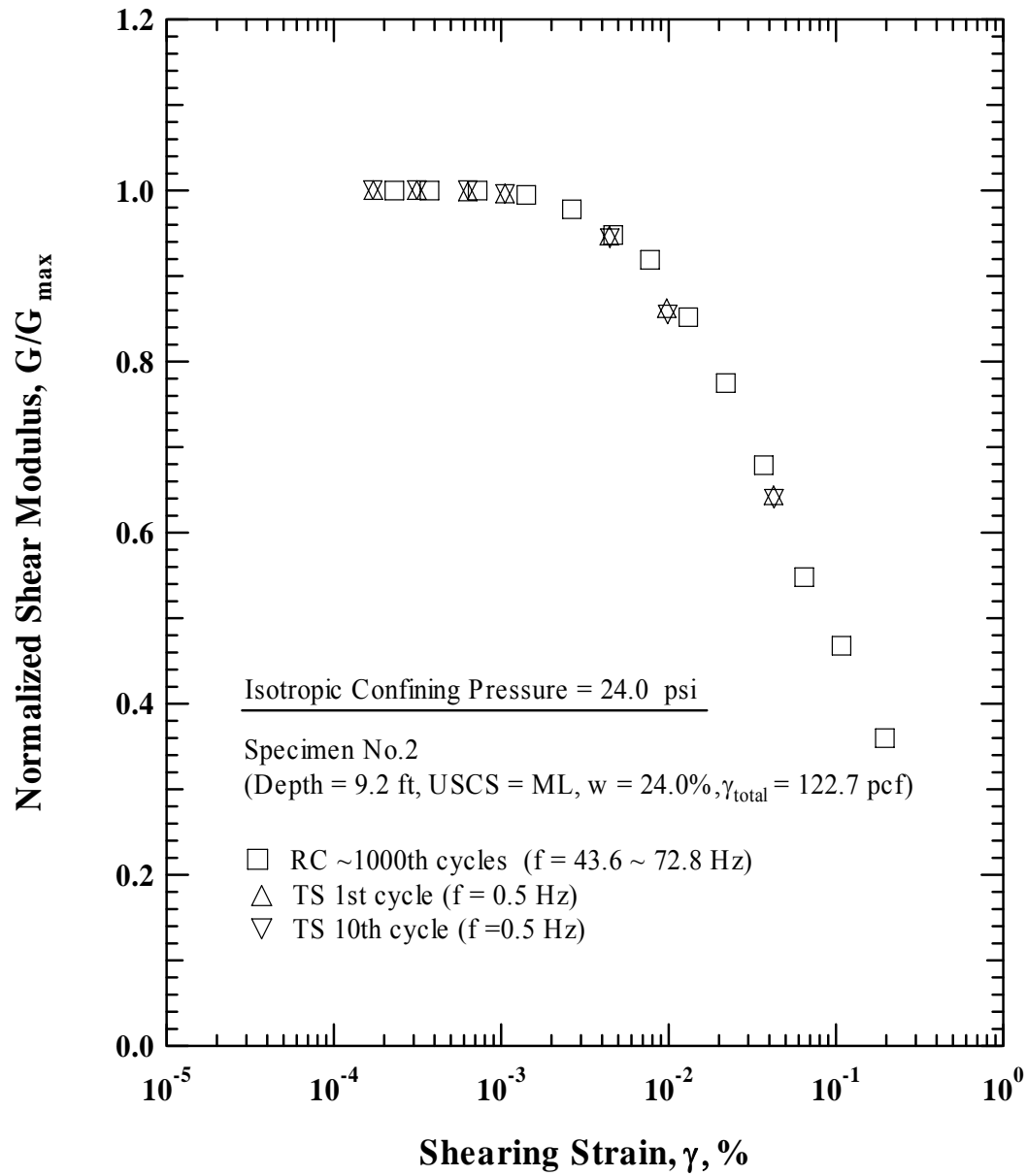


Figure 27. Comparison of the Variation in Normalized Shear Modulus with Shearing Strain at Isotropic Confining Pressure of 24 psi (3.46 ksf = 165.48 kPa) from Combined RCTS Tests of Specimen No. 2

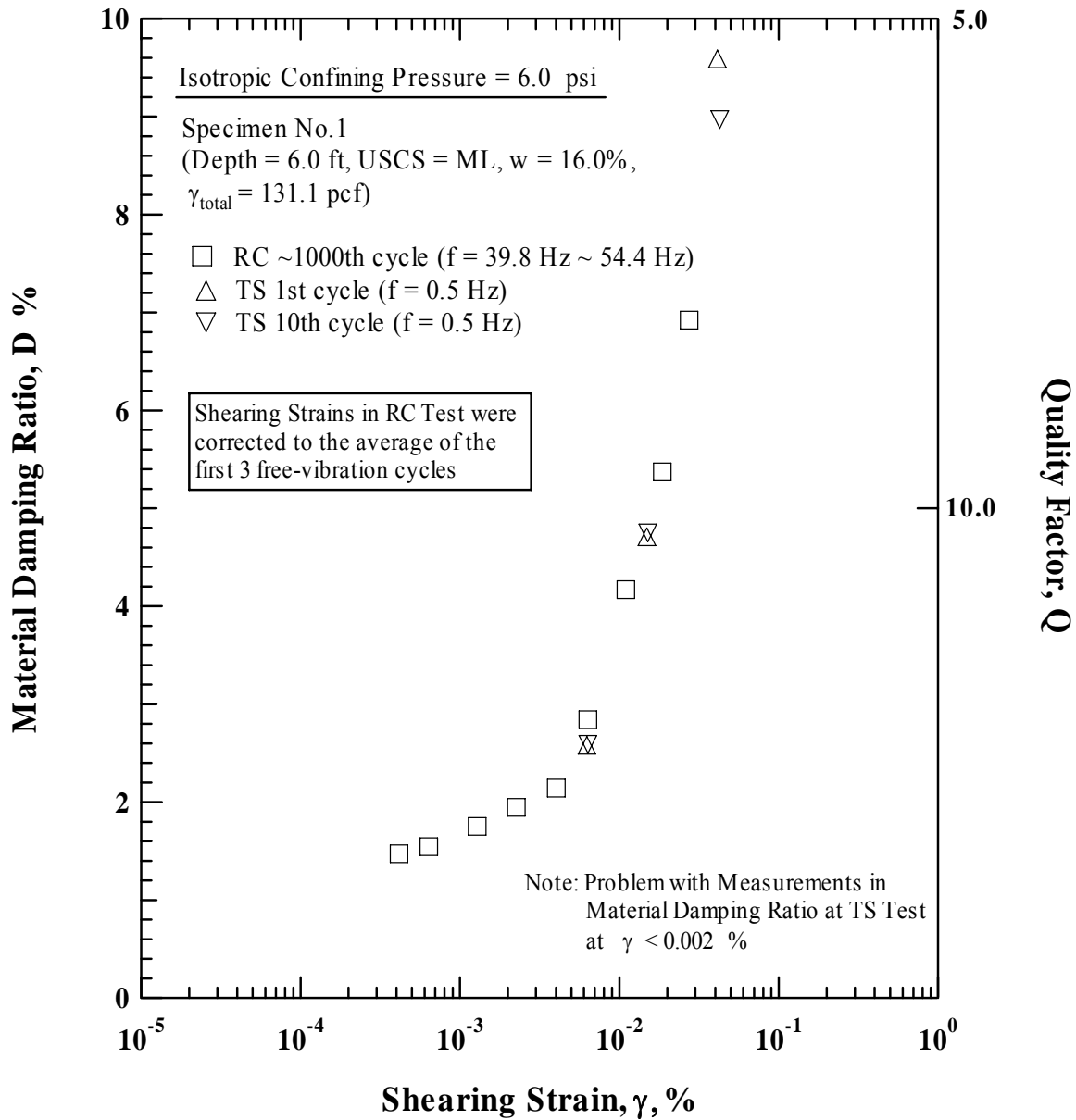


Figure 28. Comparison of the Variation in Material Damping Ratio with Shearing Strain at Isotropic Confining Pressure of 6 psi (0.86 ksf = 41.37 kPa) from Combined RCTS Tests of Specimen No. 1

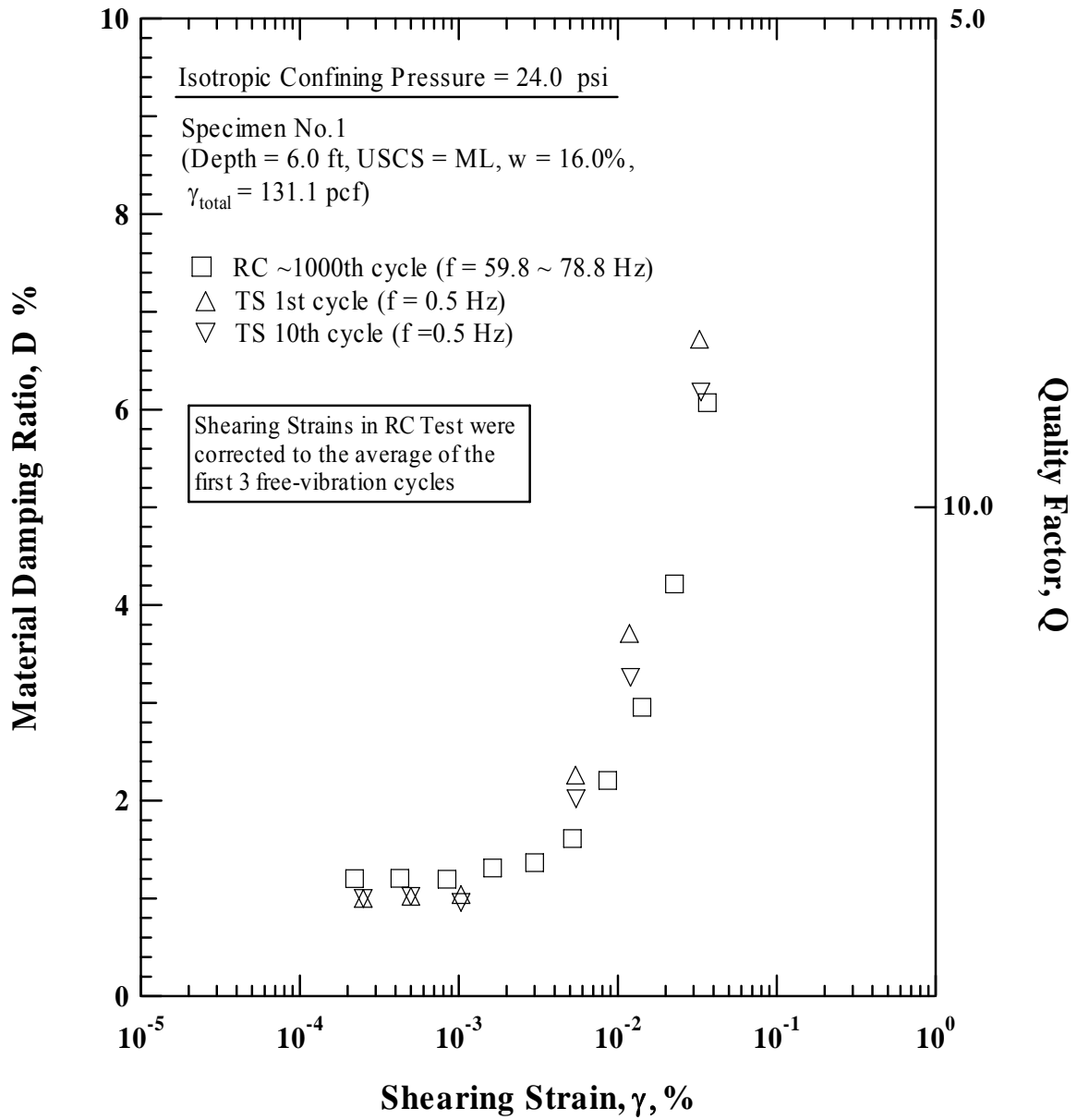


Figure 29. Comparison of the Variation in Material Damping Ratio with Shearing Strain at Isotropic Confining Pressure of 24 psi (3.46 ksf = 165.48 kPa) from Combined RCTS Tests of Specimen No. 1



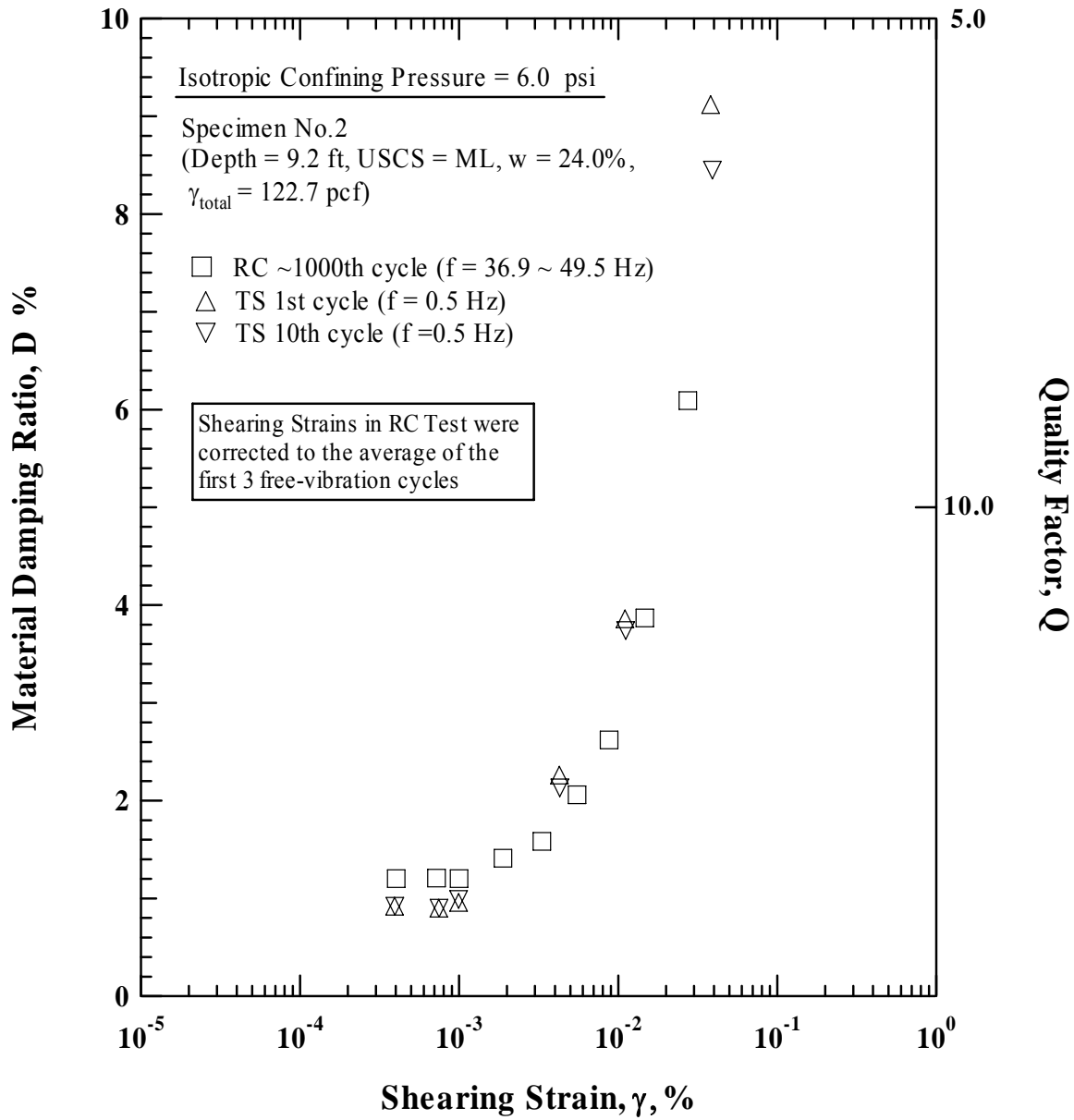


Figure 30. Comparison of the Variation in Material Damping Ratio with Shearing Strain at Isotropic Confining Pressure of 6 psi (0.86 ksf = 41.37 kPa) from Combined RCTS Tests of Specimen No. 2

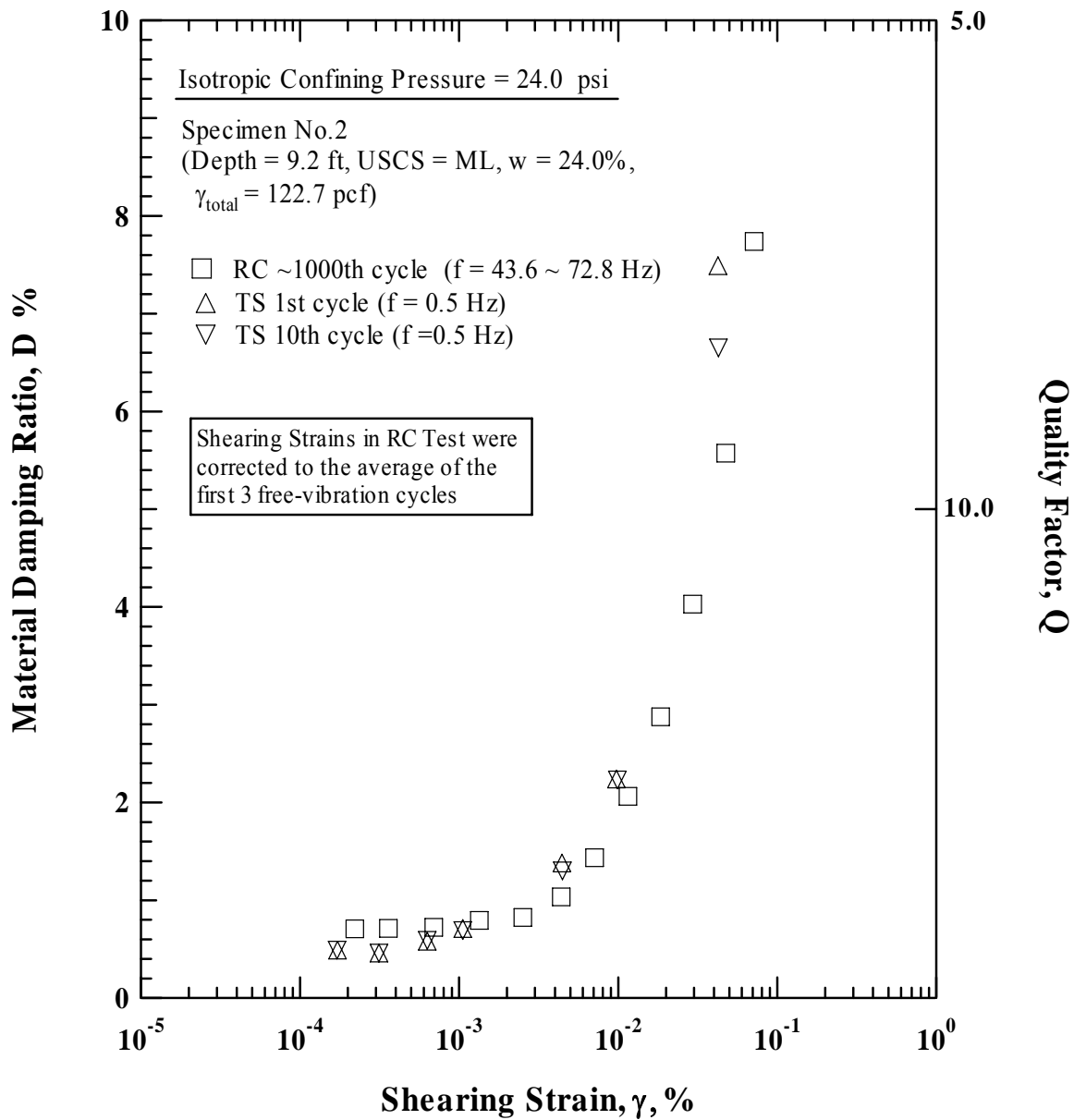


Figure 31. Comparison of the Variation in Material Damping Ratio with Shearing Strain at Isotropic Confining Pressure of 24 psi (3.46 ksf = 165.48 kPa) from Combined RCTS Tests of Specimen No. 2

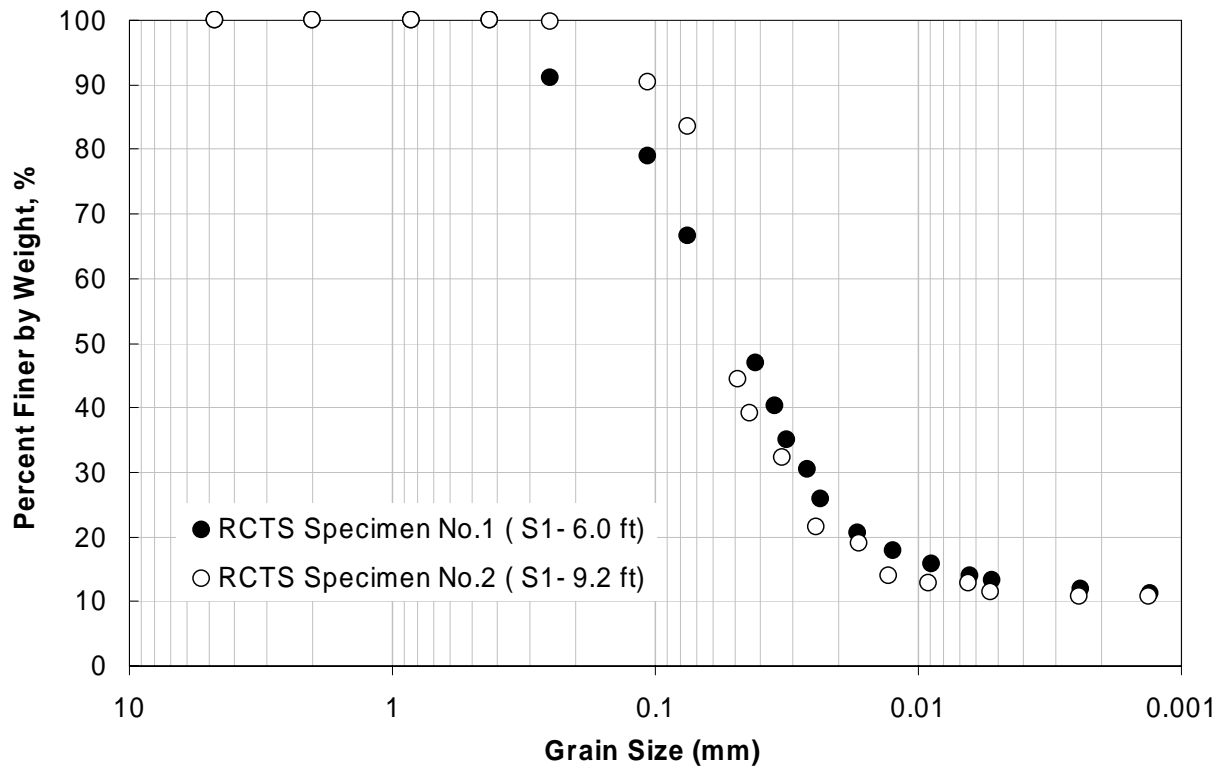


Figure 32. Grain Size Distribution Curves of Specimens Tested in the RCTS device.

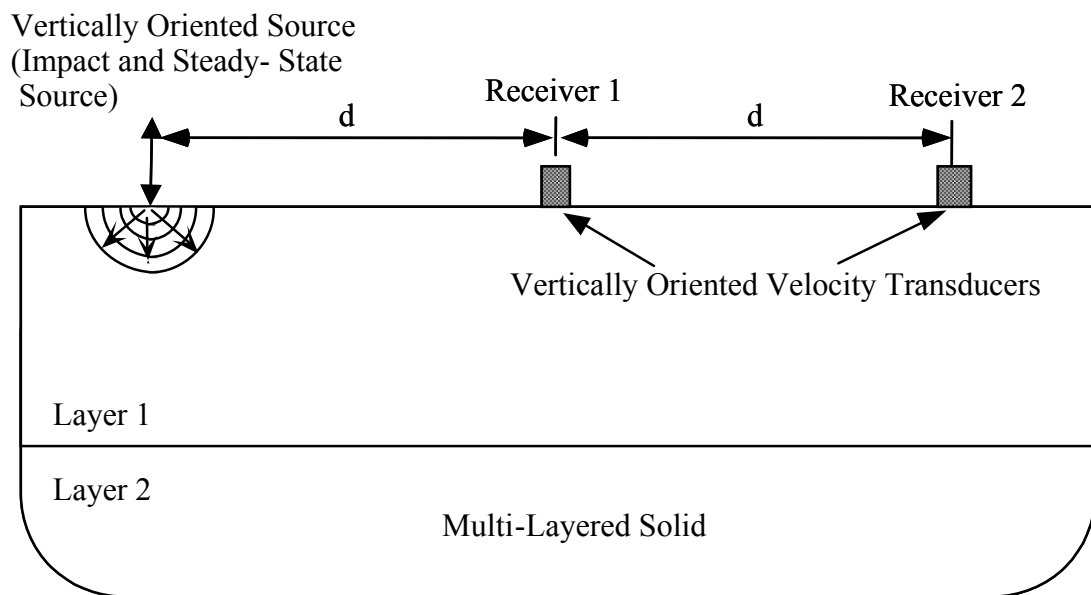


Figure 33. Schematic Diagram of the Generalized Equipment Arrangement used in Spectral-Analysis-of-Surface-Waves (SASW) Testing

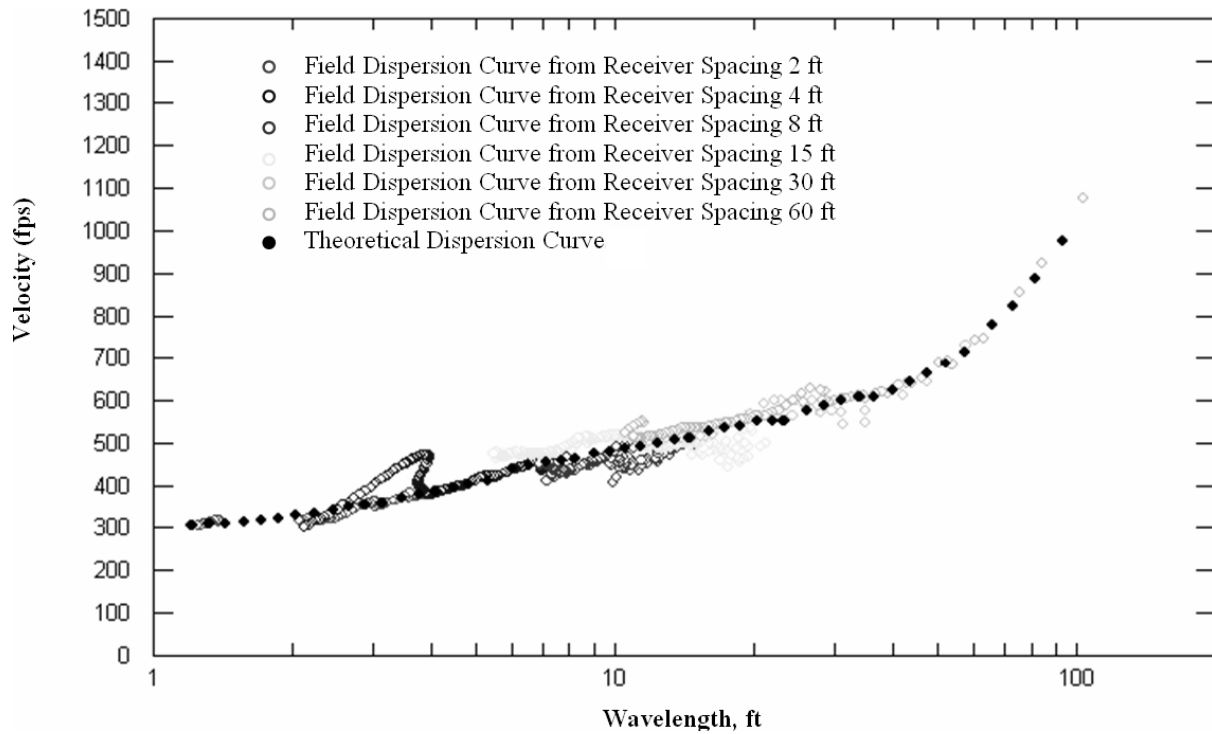


Figure 34. Theoretical Dispersion Curve Fit to the Composite Experimental Dispersion Curve at SASW-Line A

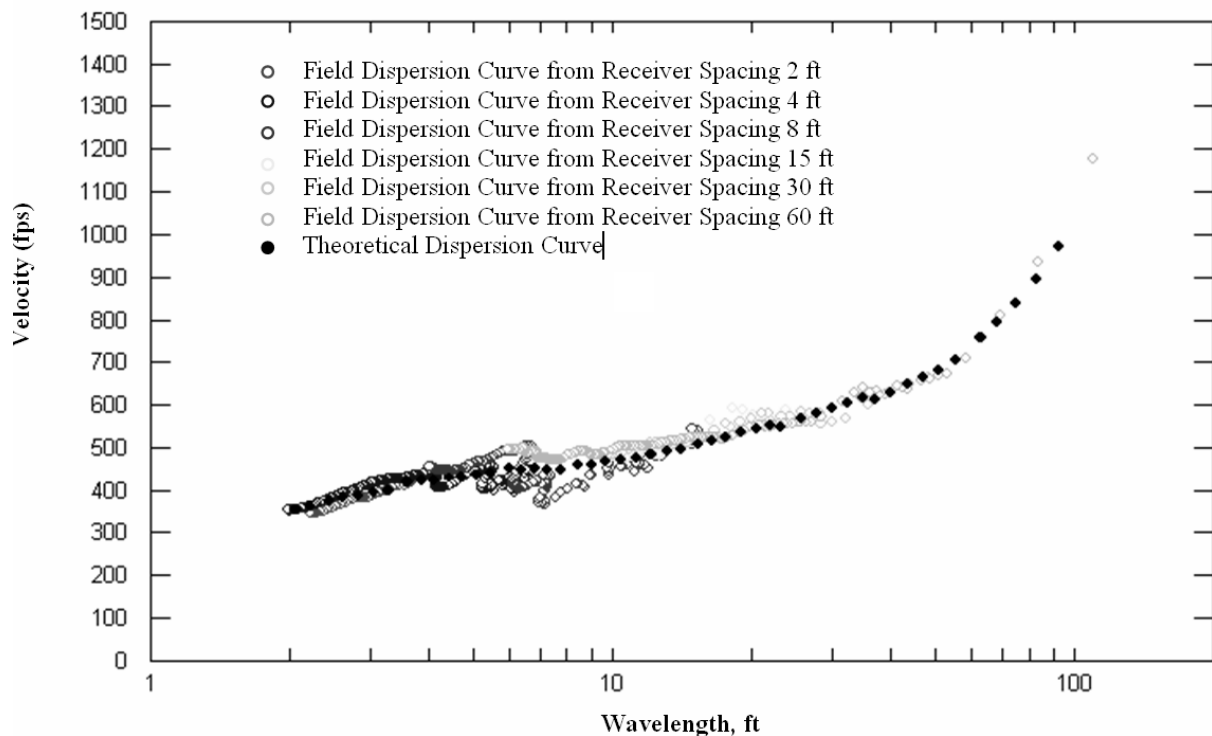


Figure 35. Theoretical Dispersion Curve Fit to the Composite Experimental Dispersion Curve at SASW-Line B

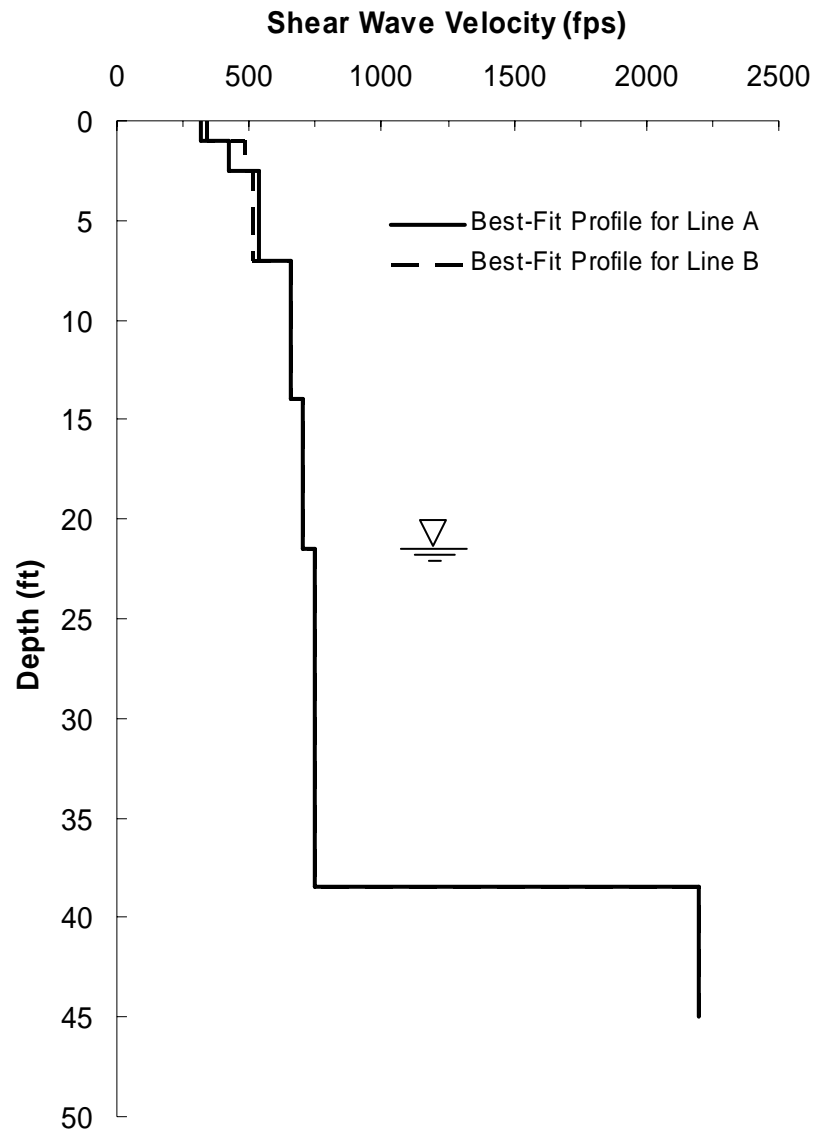


Figure 36. Shear Wave Velocity Profiles determined from SASW Testing at Capitol Aggregates Test Site on February 3, 2005

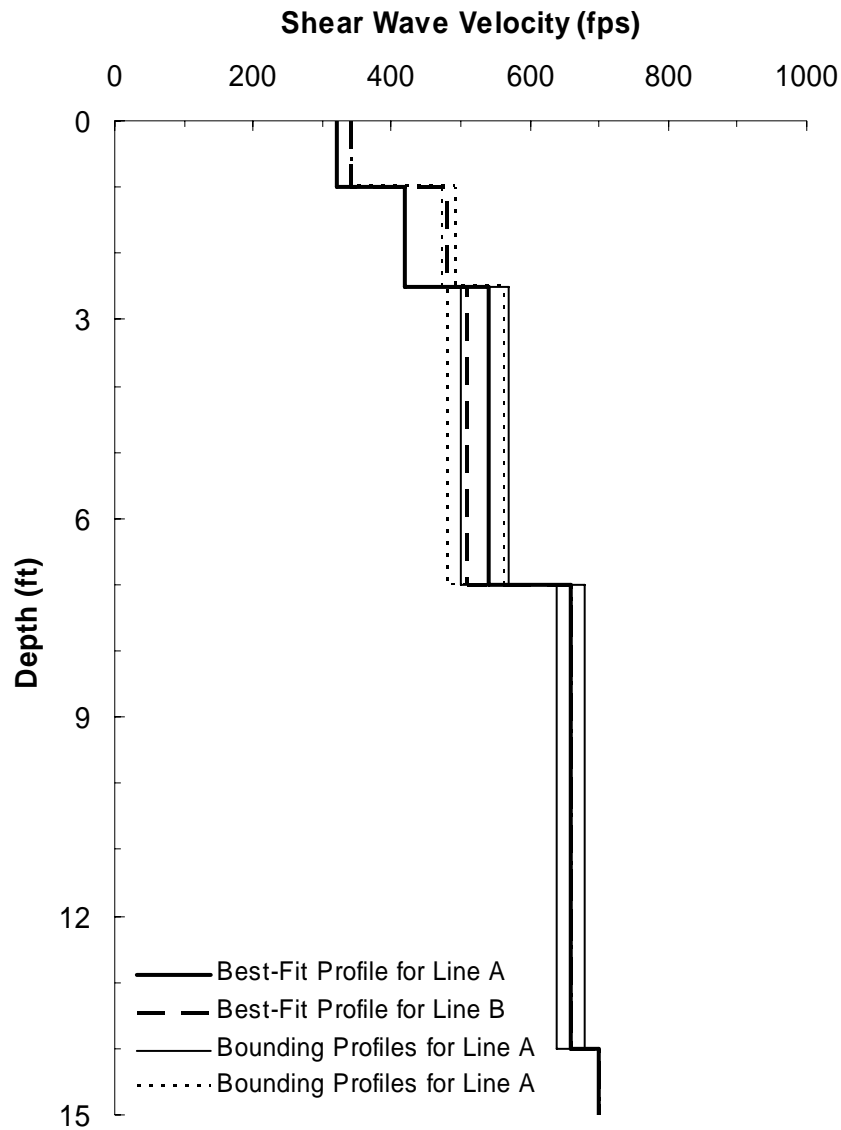


Figure 37. Shear Wave Velocity Profile of the Top 15 ft of Soil Material at Capitol Aggregates Test Site Determined from SASW Testing on February 3, 2005 (Variability of the Shear Wave Velocity due to the Scatter in the Composite Field Dispersion Curve is Taken into Account)

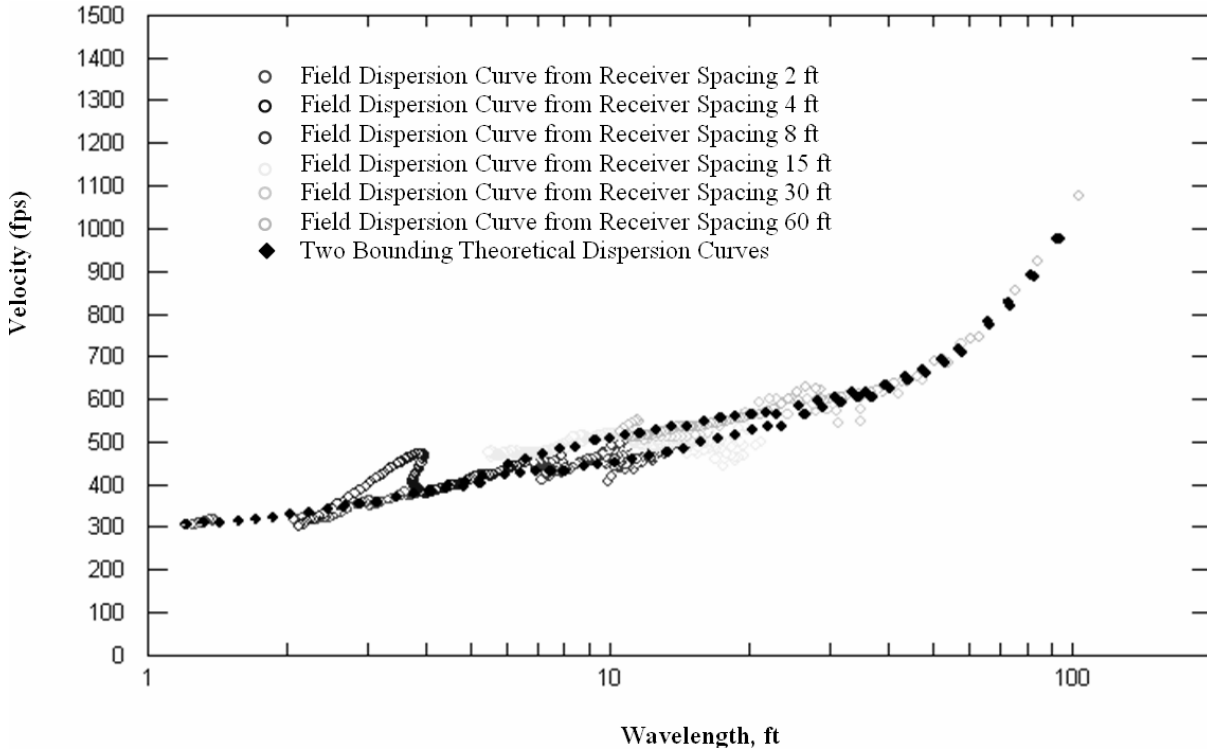


Figure 38. Two Bounding Theoretical Dispersion Curves Fit to the Composite Experimental Dispersion Curve at SASW-Line A

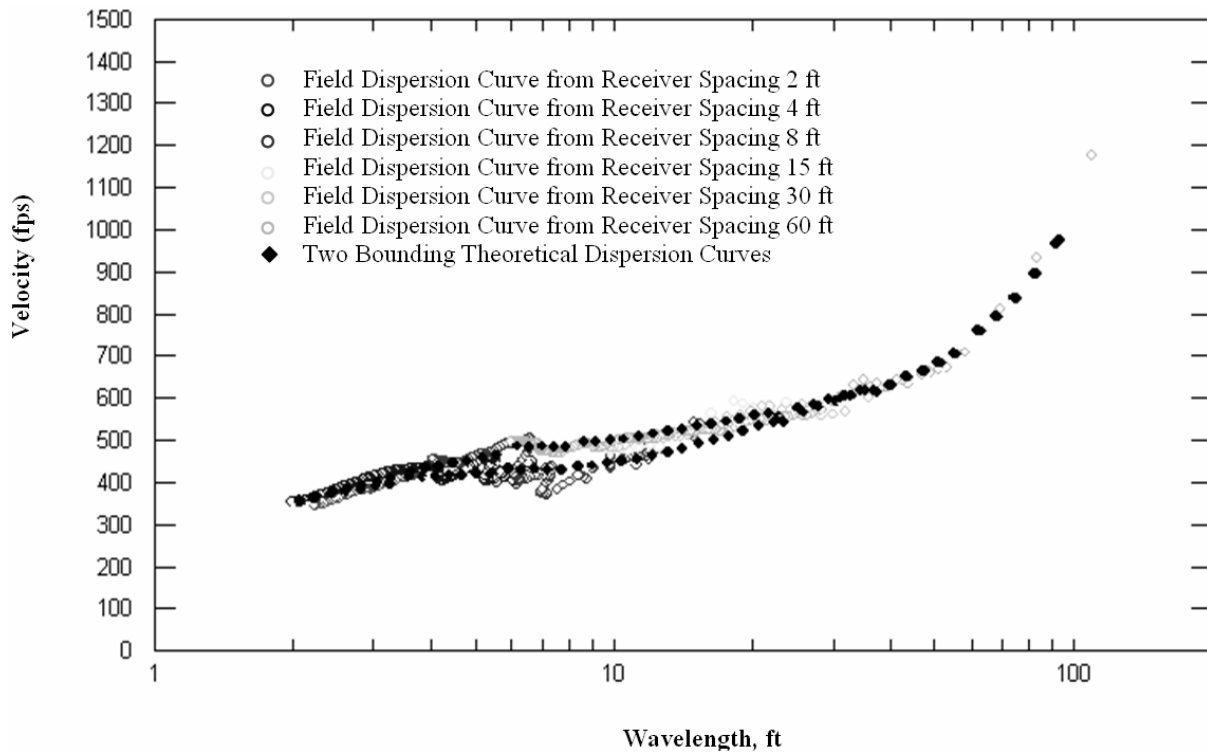


Figure 39. Two Bounding Theoretical Dispersion Curves Fit to the Composite Experimental Dispersion Curve at SASW-Line B

## REFERENCES

- Burland, J. B., and Burbidge, M. C. (1985). "Settlement of foundations on sand and gravel." *Proc., Inst. Civ. Engrs.*, 78, Part 1, 1325-1381.
- Burland, J.B., and Hancock, R.J.R. (1977) "Underground carpark at the House of Commons, London: geotechnical aspects." *Structural Engineer*, 55(2): 87-100.
- Coduto, Donald P., (2001) *Foundation Design: Principles and Practices*, Second Edition, Prentice Hall, Inc. Upper Saddle River, New Jersey.
- Clayton C.R.I., Edwards A., Webb M.J., (1991). "Displacements within the London Clay during construction." *Proceedings of the 10th European Conference on Soil Mechanics and Foundation Engineering*, Florence., vol ii, 791 – 796.
- Clayton C.R.I., Gunn J.M.F., Hope V.S., (1993). "The prediction of ground geometry and stiffness using seismic tomography." *Proceedings of the Wroth Memorial Symposium*, Oxford, Thomas Telford, London, July 1992, 173 – 185.
- Darendeli, M. B. (2001) "Development of a new family of normalized modulus reduction and material damping curves." Ph.D. dissertation, University of Texas.
- Gibbens, J.B., and Briaud, J-L, (1994) "Predicted and Measured Behavior of Five Spread Footings on Sand", *Results of Prediction Symposium Sponsered by FHWA, Geotechnical Special Publication No. 41*, ASCE.
- Gordon, M.A., Clayton, C.R.I., Thomas, T.C. & Matthews, M.C. (1995) "The selection and interpretation of seismic geophysical methods for site investigation." *Proc. ICE Conf. on Advances in Site Investigation Practice*, March 1995.
- Kupholt, T., (2003) "Potentiometer as a voltage divider." [http://www.allaboutcircuits.com/vol\\_6/chpt\\_3/6.html](http://www.allaboutcircuits.com/vol_6/chpt_3/6.html)



- Kurtulus, A., Lee, J. J.; and Stokoe, K. H. (2005), "Summary Report: Site Characterization of the Capitol Aggregates Test site." Part of Ph.D. dissertation, University of Texas.
- Matthews, M. C., (1993) Mass Compressibility of Fractured Chalk. PhD Thesis, University of Surrey.
- Matthews, M.C., Hope, V.S., and Clayton, C.R.I., (1996) The use of surface waves in the determination of ground stiffness profiles. Proceedings of the Institution of Civil Engineers, Geotechnical Engineering 1996, 119, Apr., 84-95.
- Maugeri, M., Castelli, F., Massimino, M.R. and Verona, G. (1998); "Observed and Computed Settlements of Two Shallow Foundations on Sand." *Journal of Geotechnical and Geoenvironmental Engineering* 124, 595-605.
- Menzies, B., (2001) "Near-surface site characterization by ground stiffness profiling using surface waver geophysics." *Instrumentation in Geotechnical Engineering. H.C.Verma Commemorative Volume*. Eds. K.R. Saxena and V.M. Sharma. Oxford & IBH Publishing Co. Pvt. Ltd., New Delhi, Calcutta. pp 43-71.  
[http://www.gdsinstruments.com/technical\\_papers/india\\_paper/indiapaper.htm](http://www.gdsinstruments.com/technical_papers/india_paper/indiapaper.htm)
- Meyerhoff, G., (1951) "The Ultimate Bearing Capacity of Foundations," *Geotechnique*, Vol. 2, No. 4, pp. 301-331.
- Peck, R. B., Hansen, W.E., and Thornburn, T. H., (1974) *Foundation Engineering*, 2nd Edition John Wiley and Sons, Inc., New York.
- PLAXIS 2D version 8.1, PLAXIS b.v, Delft, Netherlands, A.A Balkema Publishers, [www.balkema.nl](http://www.balkema.nl)
- Schmertmann, J.H.; "Static Cone to Compute Static Settlement Over Sand," *Journal of Soil Mechanics and Foundations Division, ASCE*, Vol. 96, No.SM3, Proc. Paper 7302, May, 1970, pp.1011-1043.
- Schmertmann, J.H., Hartman, J.P., and Brown, P.R.; "Improved Strain Influence Factor Diagrams," *Journal of Soil Mechanics and Foundations Division, ASCE*, Vol. 104, No.GT8, August, 1978, pp.1131-1135.

- Stokoe, K.H., Joh, Sung-Ho, and Woods, R.D; “Some Contributions of In Situ Geophysical Measurements to solving Geotechnical Engineering Problems,” Proceedings of the 2nd International Conference on Site Characterization, ISC’2 , Porto, 19-22 September 2004.
- Stokoe, K. H., II and Santamarina, J.C. (2000) “Seismic-wave-based testing in geotechnical engineering.” Plenary Paper, International Conference on Geotechnical and Geological Engineering, GeoEng 2000, Melbourne, Australia, pp. 1490-1536.
- Terzaghi, K., Peck, R., and Mesri, G., (1996) *Soil Mechanics in Engineering Practice, 3<sup>rd</sup> Edition*. John Wiley & Sons, Inc., New York, New York
- Richart, F.E., Jr., Hall, J.R. and Woods, R.D. (1970) *Vibrations of Soils and Foundations*, Prentice Hall, Englewood Cliffs, New Jersey.
- Weber, Richard P; “Settlement of Shallow Footings.” <http://www.weta-llc.com/settlement.html>

## **VITA**

Andrew J. Sheehan was born in Dayton, Ohio, the son of John and Deborah Sheehan. After completing his study at Severna Park High School, Severna Park, Maryland, in 1994, he entered Purdue University in West Lafayette Indiana. In May, 1998, he received the degree of Bachelor of Science in Civil Engineering from Purdue University and was commissioned as a Second Lieutenant in the United States Air Force. In April 2002, he graduated from the United States Air Force Squadron Officer School as a distinguished graduate. He has served as a US Air Force Officer for seven years. In September, 2004, he entered The Graduate School at The University of Texas. Upon graduation, he will be assigned to Ramstein AB, Germany, where he will continue his career in the US Air Force.

This thesis was typed by Andrew Sheehan